Chemistry of Water-Soluble N-Heterocyclic Carbene Platinum Complexes

Edwin Arley Baquero Velasco

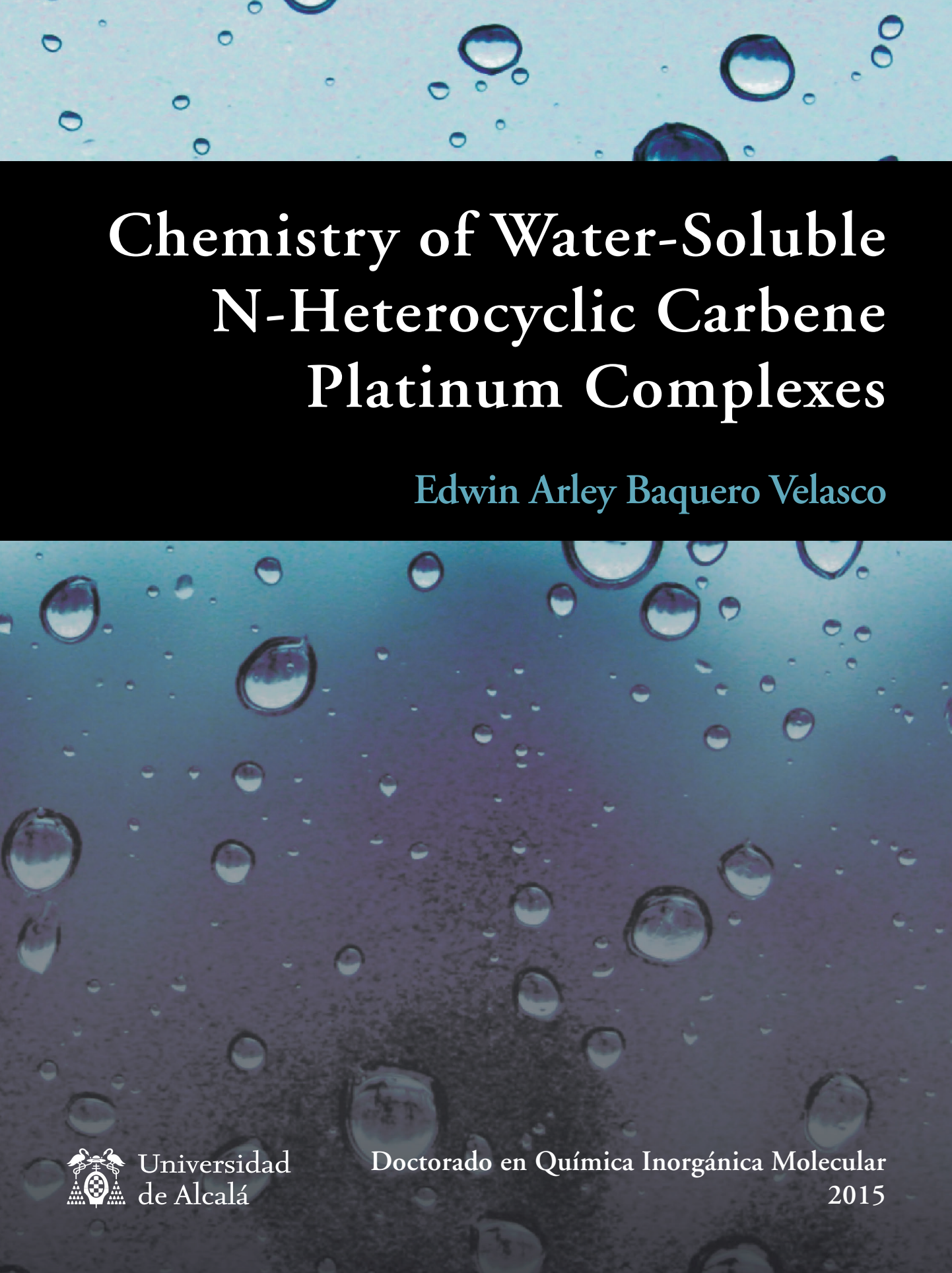

Universidad de Alcalá

Doctorado en Química Inorgánica Molecular
2015

UNIVERSIDAD DE ALCALÁ

FACULTAD DE QUÍMICA

Departamento de Química Orgánica y Química Inorgánica
Unidad Docente de Química Inorgánica

TESIS DOCTORAL

CHEMISTRY OF WATER-SOLUBLE N-HETEROCYCLIC CARBENE PLATINUM COMPLEXES

Edwin Arley Baquero Velasco

Alcalá de Henares 2015

UNIVERSIDAD DE ALCALÁ

FACULTAD DE QUÍMICA

Departamento de Química Orgánica y Química Inorgánica
Unidad Docente de Química Inorgánica

TESIS DOCTORAL

CHEMISTRY OF WATER-SOLUBLE N-HETEROCYCLIC CARBENE PLATINUM COMPLEXES

Memoria presentada en la Universidad de Alcalá por el Magister en Química **Edwin Arley Baquero Velasco** para optar al grado de Doctor en Química

Directores:
Prof. Dr. Ernesto de Jesús Alcañiz
Dr. Juan Carlos Flores Serrano

Universidad de Alcalá

ERNESTO DE JESÚS ALCAÑIZ, Catedrático de Universidad del Departamento de Química Orgánica y Química Inorgánica (Unidad Docente de Química Inorgánica) de la Universidad de Alcalá,

y

JUAN CARLOS FLORES SERRANO, Profesor Titular del Departamento de Química Orgánica y Química Inorgánica (Unidad Docente de Química Inorgánica) de la Universidad de Alcalá,

CERTIFICAN:

Que la presente Memoria Titulada "**Chemistry of Water-Soluble N-Heterocyclic Carbene Platinum Complexes**" ha sido realizada por Edwin Arley Baquero Velasco en el Departamento de Química Orgánica y Química Inorgánica (Unidad Docente de Química Inorgánica) de la Universidad de Alcalá con nuestra inmediata dirección y autorizamos su presentación para que sea calificada como Tesis Doctoral.

Alcalá de Henares, a 22 de Diciembre de 2014

Fdo. Prof. Dr. Ernesto de Jesús Alcañiz

Fdo. Dr. Juan Carlos Flores Serrano

Universidad de Alcalá

MANUEL GÓMEZ RUBIO, Catedrático de Universidad y Director del Departamento de Química Orgánica y Química Inorgánica de la Universidad de Alcalá,

CERTIFICA:

Que la presente Memoria Titulada "**Chemistry of Water-Soluble N-Heterocyclic Carbene Platinum Complexes**" ha sido realizada por Edwin Arley Baquero Velasco en el Departamento de Química Orgánica y Química Inorgánica (Unidad Docente de Química Inorgánica) de la Universidad de Alcalá, dirigida por el Prof. Dr. Ernesto de Jesús Alcañiz y el Dr. Juan Carlos Flores Serrano y cumple todos los requisitos para su presentación como Tesis Doctoral.

Alcalá de Henares, a 22 de Diciembre de 2014

Fdo. Prof. Dr. Manuel Gómez Rubio.

Agradecimientos

Terminando esta importante etapa de mi vida, llega el momento de inmortalizar mi agradecimiento a todos aquellos que me acompañaron, apoyaron y que han sido siempre motivo principal, para cumplir este sueño de niño de ser Doctor en el antiguo continente muy lejos de casa.

Primero que todo, quiero agradecer a toda mi familia quienes han sido siempre el pilar más importante en mi vida y quienes son mi motivación principal para salir adelante. Les doy gracias por siempre haberme apoyado a cumplir mis sueños y aunque hemos estado separados durante los últimos años, siempre han estado ahí desde la distancia para todo. Principalmente, agradezco a mi papá, pues a él le debo todo lo que soy, además de nunca haber dejado de creer en mí dándome siempre sus mejores consejos. A mis dos hermanitas, Nelcy y Mireya, quienes me han brindado su ayuda siempre que la he necesitado y que nunca me han dejado de apoyar. A mis sobrinos Juan David, Nicolás y Valentina quienes tanto quiero y a mis cuñados Fernando y Carlos por toda su ayuda. Este trabajo está especialmente dedicado a la memoria de mi mamá, a quien extrañamos demasiado, y por quien daría todo para que estuviera con nosotros y poder compartir este logro con ella, ya que gracias a todo su esfuerzo junto con el de mi papá, pudimos estudiar para cumplir nuestros objetivos. Estoy seguro que ella se ha convertido en nuestro ángel guardián.

Agradezco a Brillyt, por ser ese ángel guardián hecho persona, por siempre haber estado ahí y apoyarme durante todo este camino, pues sabes que sin tu ayuda, amor y comprensión, esto nunca hubiera sido posible. Gracias por estar en mi vida, por tus enseñanzas y por ser la luz que siempre mi camino necesitó. Este logro es completamente tuyo y me gustaría dedicarte muchos más. Gracias a tu familia por toda la ayuda que siempre me brindaron.

Quiero expresar mi agradecimiento a mis directores de tesis, Ernesto y Juan Carlos, quienes fueron personas fundamentales en mi formación y a su vez han sido los autores principales para que este trabajo de investigación haya salido adelante. Les doy las gracias por haber creído en mí y por haberme acogido en su grupo de investigación, además de brindarme muchas enseñanzas y consejos. Gracias!.

A Carmen y a Román por su ayuda y aportes a lo largo de este trabajo, además de sus consejos en los group meetings.

A Mikhail Galakhov por su ayuda con los experimentos de RMN.

A Javi y a Juan del Instituto "Rocasolano" por su completa colaboración con los experimentos llevados a cabo en fase gas en el ICR y en el triple cuadrupolo. Aprendí mucho con ustedes.

A Manuel Temprado por su ayuda con los cálculos DFT, además de sus excelentes aportes en nuestra investigación.

I would also like to express my acknowledgements to Bruno Chaudret not only for giving me the opportunity to carry out the "nano-research" in his group, but also for his outstanding lessons of nanochemistry. I have learnt a lot about this topic. Besides, I want to thank' Simon Tricard for his invaluable help during my two internships in Toulouse. You perfectly know that it would not have been the same without your collaboration. It was an excellent experience for me and I am pretty sure that I will enjoy my Post-doc stay there.

Quiero expresar mi más sincero agradecimiento al grupo CoñazoPanchitadas: Anita, Cris, Jairo, Lina Orrego y el paisis (Miguel) por todos los excelentes momentos que pasamos juntos en diferentes sitios de España y Europa, además de haberse convertido en mi familia en este continente. A mis españolas favoritas, Anita y Cris, por siempre hacernos más leve el factor distancia Panchilandia–España con los detalles que tuvieron siempre en Navidad y cumpleaños para con nosotros los panchitos, además de adoptar palabras y costumbres autóctonas de nuestras regiones. Por todas las risas viendo pelis de terror, las conversaciones y anécdotas al son de buena música. Las voy a extrañar mucho!. A Lina Orrego y a Jairo por ser simplemente una chimba!, por todas las risas que compartimos, las comidas y las fiestas. Ya saben que en Bogotá tienen casa y que no todos los rolos son aburridos. A el paisis por estos casi cuatro años de excelente convivencia (cero discusiones). Sabes que sos y serás siempre para mí un hermano. Realmente agradezco haber dado con alguien como vos, pues estos años han sido muy bacanos y muy bien llevaderos, además de compartir muchas anécdotas e historias charras, así como el gusto por el cine Danés!. A todos ustedes muchachos, los voy a extrañar muchísimo y de sobra saben que tienen una casa esperando tanto en Toulouse como en Bogotá. Éxitos para lo que les queda de doctorado que es ná!.

A mis compañeros del grupo de investigación DENDROCAT, por todos los buenos momentos dentro y fuera del laboratorio: Ana, Andrea, Camino, Fran, JuanMa y Marina; y a quienes ya se han ido, Anderson, Gustavo, Paulo Sergio, Pili y Roberto. Fue muy bueno haber dado con gente como ustedes para hacer agradable mi estancia en E'paña y les deseo lo mejor para el futuro.

Quiero dar mi agradecimiento especial a Gustavo Silbestri por haber sido mi mentor y un muy buen amigo. Gracias por los consejos, enseñanzas y toda esa ayuda incondicional en este trabajo.

A mis compañeros del departamento (los que siguen y los que se han ido): Adrián, Alberto, Carlos (Charlie Bond), Gema, Gonzalo, Jorge, María García, María Ventura y Silvia por los buenos momentos y las risas compartidas durante los almuerzos y fuera del

laboratorio, además de haber comprendido en general mis panchi-cosas. A los demás compañeros de otros departamentos que de una u otra manera han contribuido en este trabajo.

A Roberto por la gran amistad que me ha brindado siempre durante estos años, además de toda la ayuda y apoyo incondicional que he recibido por parte suya. Por todas las risas compartidas tanto en el laboratorio, como en los congresos y vacaciones. Te deseo lo mejor NOI!, y sabes que en Colombia tienes una casa (no olvidar las flechas). La taza que me diste, la llevaré como un buen recuerdo de E'paña.

A Charlie y a Camino por siempre tener una risa disponible en todo momento, por hacer el esfuerzo siempre de entender mi idioma y mi manera de decir las palabras. Además de las buenas conversaciones que tuvimos sobre las diferencias Panchi-E'pañolas.

A Marina por su bonita amistad y por su manera de ver la vida. Ha sido un placer haberte conocido y estoy seguro que nos volveremos a ver muy pronto porque me prometiste que irías a Colombia, además tendré también que venir para tu tesis para ver como deslumbras a todos con "tenacitas". Te deseo lo mejor para lo que queda. A JuanMa por todos los buenos momentos que pasamos tanto en los laboratorios de Alcalá y Toulouse, así como en los bares de la ciudad entendiendo los puntos de vista de "los extranjeros", claro, siempre y cuando no generalicemos! jejeje. Espero que vuelvas más tiempo por Toulouse!.

A Troski Katroski por todos los buenos momentos compartidos y las risas. Por su manera de ser y sobre todo, porque siempre tuvo una risa para mí cuando siempre la necesitaba. Kocham cię.

I also thank my friends in Toulouse who made my internships really funny and very fruitful. I would like to give my special thanks to Sergio, Tere and Floran, Udishnu, Dominikus, Justine, Lia, and Benoit. I have no doubt that my Post-doc stay there will be awesome with all of you.

A mi hermano del alma Danielin Pingüin, por toda esta amistad que ha perdurado años y porque siempre ha estado ahí en todos los momentos, además de siempre compartir mis alegrías igual o más, como yo las suyas. Parce, este logro hace parte suya también y ya sabe, a montar nuestro grupo de Organometálica en Colombia!.

A mi otro hermano del alma Fercho (Pony), por su amistad incondicional. Por ser familia para mí y que a pesar de la distancia, siempre estuvo disponible para todo. Parce, tenemos que hacer el tour por Europa. Acá lo espero!.

A Harold, por los buenos momentos que pasamos juntos durante mi primer año de estadía en España. Por todas las risas y los viajes hechos. Parce, es muy grato ser el padrino de su hija AnaLu y ya celebraremos este logro muy pronto junto a Marcela!.

A todos mis amigos de la Universidad Nacional de Colombia (la nacho), con los que compartí años maravillosos durante toda mi carrera y con los que pude compartir navidades y/u otras ocasiones en Alcalá. A la ComUNidad del Árbol por todas las risas y buenos momentos, a la paisita por sus chistes únicos y momentos en el llarbi. A mi Aleyda que tanto quiero. A Carlos Alarcón, Ingrid y Mikel, Genhli, Jorge Ivan (el patrón), Paulo Sergio, Vida y Maycoll, por la buena amistad y momentos por estas tierras. A James y Pili por las buenas navidades que pasamos juntos al buen sabor de un buñuelo con natilla. A Alejo, Choco, Felipe y Pipeta por las risas en el laboratorio de Macromoléculas, A Laurita y a Lore por las fiestas y las tomatas en las rocolas y el billar. Quiero agradecer especialmente al cromador Alex Silva, pues sin él las risas en la nacho hubieran sido pocas.

A mis amigos del colegio y con los que aun la amistad perdura, a Corzo, Marlon y Jhon Fredy y Carito Sánchez por todos los buenos momentos, fiestas, viajes y risas. Espero que nos podamos ver pronto para celebrar.

Quiero dar un especial agradecimiento a mi *alma mater*, Universidad Nacional de Colombia y su profesorado por haberme brindado una formación profesional en Química excepcional, especialmente a los profesores Marco Fidel, Luca y Rodolfo por todas sus enseñanzas y quienes jugaron un papel muy importante en mi formación académica. A la Universidad de Alcalá y su programa de becas FPI-UAH para realizar el doctorado, así como la Fundación Carolina quien gracias a ella, pude iniciar mis estudios de postgrados en España.

A todos GRACIAS!…

A mi mamá quien tanto extraño y a mi papá por sus enseñanzas

"Imagination is more important than knowledge.
Knowledge is limited; imagination encircles the world"
Albert Einstein

Table of Contents

Chapter I. Introduction and Objectives

I.1. Introduction

I.1.1. General Features of N-Heterocyclic Carbenes

N-Heterocyclic Carbenes (NHCs) were first reported by Wanzlick[1] and Öfele[2] in 1968. However, it was after the isolation of the first stable and crystalline NHC [1,3-bis(adamantyl)imidazole-2-ylidene] by Arduengo[3] in 1991 (Scheme I.1), when they became very attractive compounds for the scientific community. Subsequently, the potential of NHCs as spectator ligands in catalysis was discovered by Herrmann and co-workers[4] in 1995, thus triggering a wide-spread research interest in catalytic processes involving such compounds. The plethora of work in the field has led to major advances in the development of a large variety of NHC ligands[5] and their transition metal complexes, in which those derived from imidazolium or 4,5-dihydroimidazolium salts are the most widely applied in homogeneous catalysis. A remarkable example of complexes of this type concerns the ruthenium catalysts developed by Grubbs and co-workers for metathesis reactions.[6]

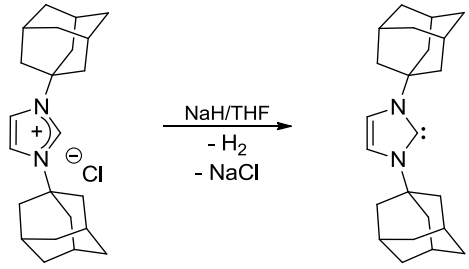

Scheme I.1. Synthesis of the first stable N-Heterocyclic Carbene.

NHCs are singlet carbenes with a nucleophilic character, as it can be deduced from the resonance structures **a** and **c** depicted in Scheme I.2 for an imidazole-2-ylidene. The electron pair is located in a sp^2 molecular orbital, which can be stabilized by the presence of the two adjacent nitrogen atoms.[7] This stability is explained by mesomeric and inductive effects working in a synergic way. The electron pair is stabilized by the inductive effect of the heteroatoms, at the same time that π-donation from their non-bonding electrons to the empty *p*-orbital located at the carbenic carbon in the single state, reduces its electron deficiency (Scheme I.3).

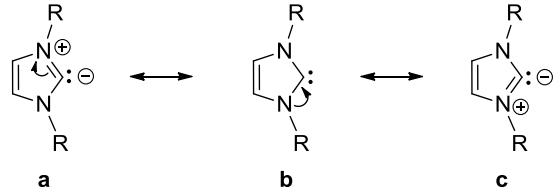

Scheme I.2. Resonance structures for an imidazol-2-ylidene.

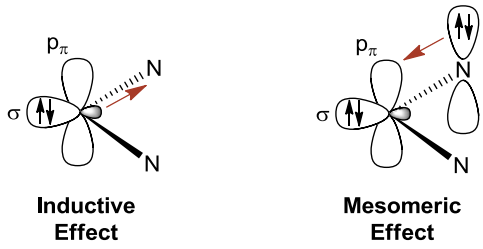

Scheme I.3. Mesomeric and inductive effects in the diaminecarbenes.

A large number of NHCs have been described in the literature (Scheme I. 4), ranging from four membered to seven membered rings, including imidazolium (**L1**), imidazolinium (**L2**, **L8**),[8] triazolium (**L3**),[9] oxazolium (**L4**),[10] thiazolium (**L5**),[7,11] pyrrolidium (**L6**),[12] benzimidazolium (**L7**),[13] bisoxazoline (**L9**),[14] quinoxaline (**L10a**),[15] naphtha annulated imidazolium (**L10b**),[16] diazaphosphetidin amine (**L11**),[17] pyrimidine (**L12**),[18] perimidine (**L13**),[19] dibenzo(1,3)diazepine (**L14**),[20] imidazo[1,5-a]pyridine (**L15**, **L16**),[21] 2,2'-bipyridine derived imidazolium (**L17**),[22] or bisimidazolium with arene backbone (**L18**).[23]

Non-coordinated NHC ligands are among the strongest neutral Brønsted bases known (pKa > 23 in the gas-phase).[24] Therefore, their isolation requires extremely anhydrous conditions.[25] In their coordination to transition metals, they are generally considered strong two-electrons sigma-donors with poor π back-donation ability.[26] These features together with their thermal stability, make them an attractive alternative to phosphane ligands, which customarily find many uses in catalysis. Despite of their important applications, phosphanes have shown different drawbacks such as their facile redox degradation.[27]

The way in which steric and electronic effects are controlled in NHC and phosphane ligands has some differences. Electronic effects are more dependent of the substituents in phosphane ligands compared with NHCs. This can be explained by the structural features of each ligand; in phosphanes the substituents are bound to the phosphorous atom, whereas they are not directly attached to the donor atom in NHCs, and are more often substituting the adjacent atoms. Therefore, steric constrains can be modulated with no remarkable consequences on the electronic effects in the latter compared to that found in the former. Moreover, the fundamental topology of each type of ligand result in quite different steric

impact on the metal center. Whilst the three substituents in phosphanes point back away from the metal, the N-substituents of a coordinated NHC ligand are directed to the metal, imposing higher protection. The latter also contributes to a more restricted rotation around the NHC-Metal bond compared to that in phosphanes.[27b,28]

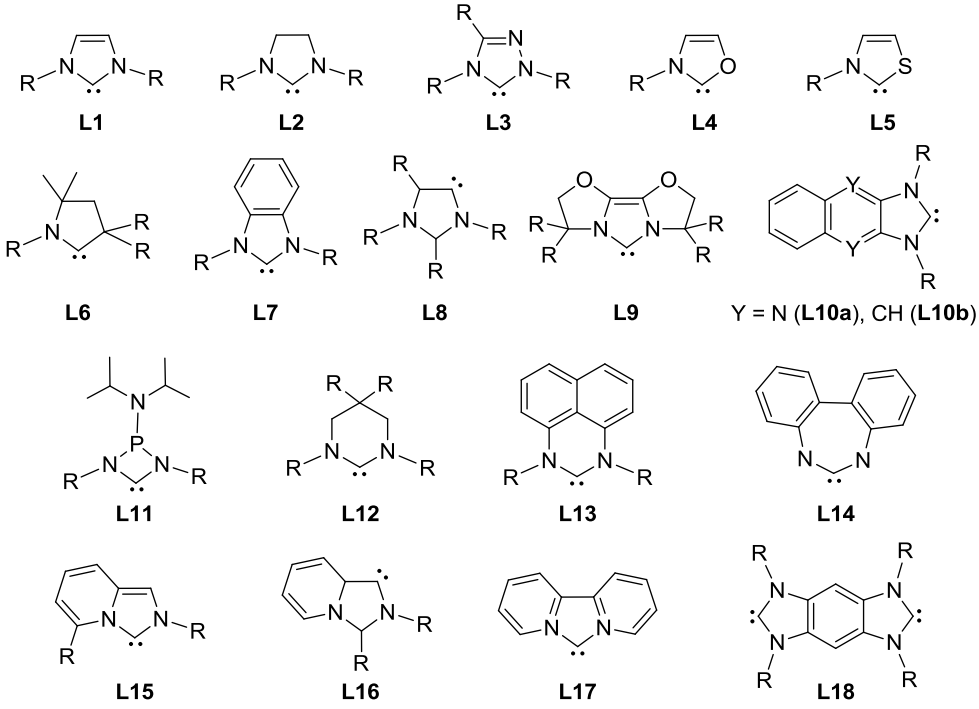

Scheme I.4. Different types of NHCs (R = alkyl or aryl groups).

The differences in ligand arrangement make the classic Tolman cone angle unsuitable to parametrize the shape influence of NHC ligands. The first effort to model their steric effects was made by Nolan in 1999, introducing the A_H and A_L angles for coordinated NHC ligands (Figure I.1).[29]

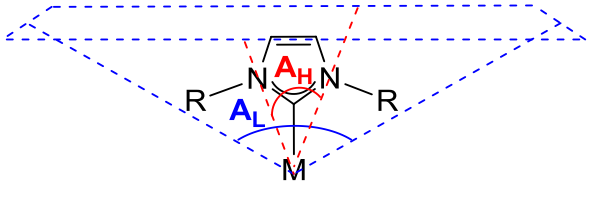

Figure I.1. A_H and A_L angles parameters defined by Nolan to describe the steric effects of the NHC ligands.

In 2003, Nolan and Cavallo introduced the percentage of buried volume $\%V_{bur}$ (Figure I.2)[30] as a more convincing parameter for the evaluation of the steric pressure of the ligand on the metal center. It consisted on the determination of volume occupied by the NHC ligand in a sphere of 3 Å of radius centered at the metal, which is located at 2 Å from the carbenic carbon.

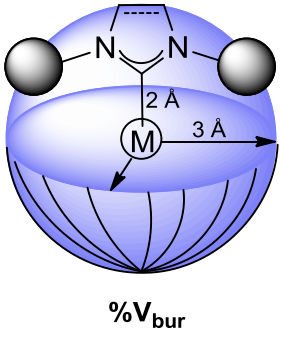

Figure I.2. Schematic representation of the sphere used for $\%V_{bur}$ determinations.

Currently, the $\%V_{bur}$ is under discussion because it does not describe properly the occupancy distribution of such sphere. Tolman cone angle provides a good idea of that distribution for phosphane ligands because of their conical rather homogeneous structure. In contrast, this is not the case for NHC ligands, and the $\%V_{bur}$ has begun to be complemented, for instance, by contour maps,[31] or more recently, by the eccentricity of the buried volume.[32]

I.1.2. General procedures for the synthesis of NHC ligands and their transition metal complexes

Imidazole-based NHC ligands are commonly obtained by deprotonating the corresponding imidazolium salts with a suitable base. Those starting materials can be prepared following several synthetic pathways, in which symmetric and asymmetric N,N'-substitution of the heterocyclic ring with different groups is achievable (Scheme I.5).[26]

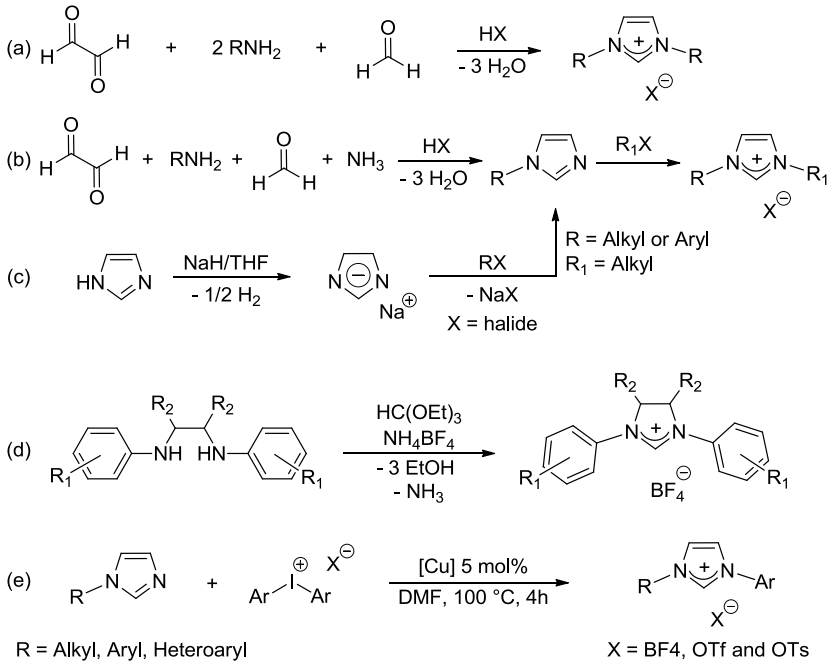

Scheme I.5. a-e) Some common synthetic pathways for the synthesis of imidazolium salts.

The free NHCs are fairly reactive species that undergoes different processes such as dimerization,[33] hydrogenation,[34] bond insertion,[35] protonation through hydrolysis processes, or hydrolytic cleavage of the heterocycle ring (Scheme I.6).[34,36] Dimerization and other undesired side reactions that make difficult the isolation of some free NHCs can be avoided by the coordination of the NHC ligand to a metal centre or by bulky *N*-substituents.

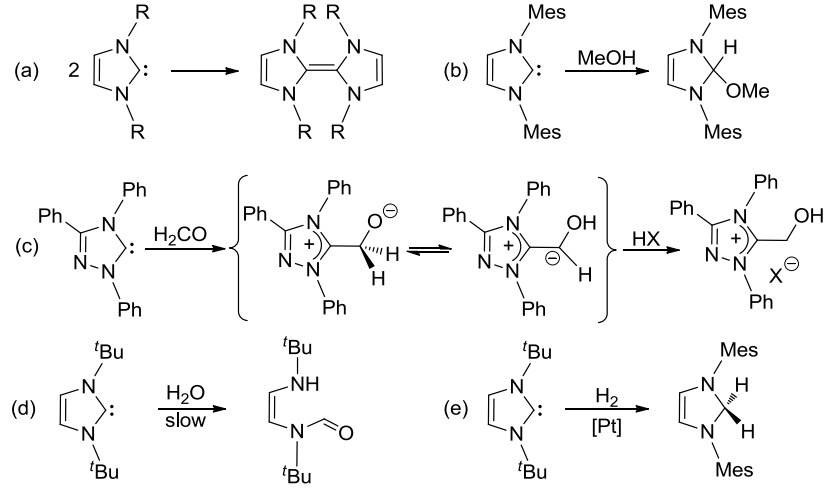

Scheme I.6. Examples of the reactivity shown by free NHCs. (a) Dimerization, (b) O-H bond insertion, (c) C=O bond insertion, (d) hydrolysis with ring opening, and (e) hydrogenation.

As a consequence of the flexibility in stereoelectronic features of NHC ligands, NHC complexes are known for alkaline,[37] and alkaline earth metals,[38] as well as for most of the transition,[26] and inner transition metals.[39] Their synthesis often involves the use of the free NHC previously isolated (if stable) or generated *in situ* in the presence of the metal precursor (Scheme I.7).

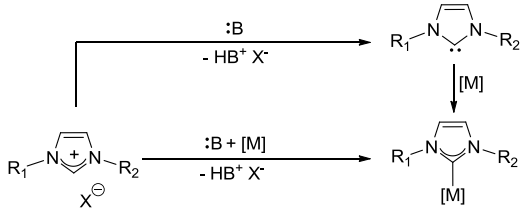

Scheme I.7. Synthesis of NHC metal complexes by direct reaction of a metal precursor with the free carbene previously isolated or generated *in situ*.

Another useful strategy for the preparation of NHC metal complexes, particularly when the free NHC cannot be isolated and/or the metal precursor is base sensitive consists in the transfer of the NHC ligand from a carbene adduct with easily removable groups (Scheme I.8).[40] Silver(I) complexes are widely used because of their easy preparation, high stability, and great efficiency as transmetallation agents, even in the presence of bulky N-substituents on the imidazolic ring.[41]

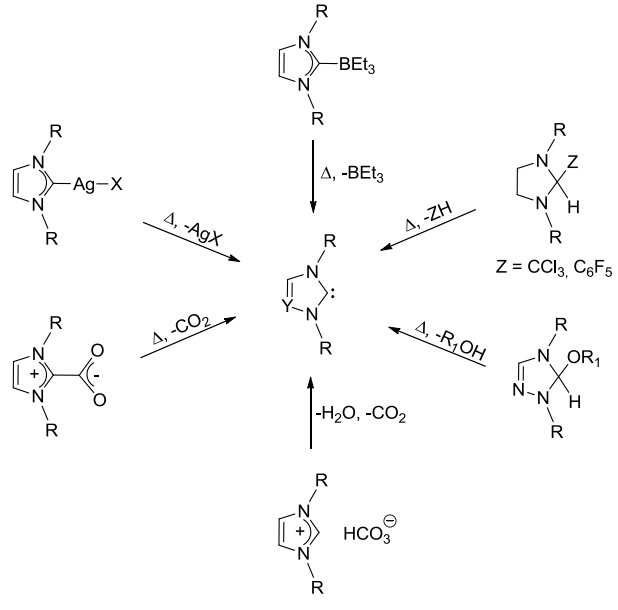

Scheme I.8. Carbene adducts with triethylborane,[42] hydrogencarbonate,[43] carbon dioxide,[43b,44] pentafluorobenzyl,[40,45] trichloromethyl,[40,46] or alkoxides[47] used as NHC ligands transfer agents.

Silver(I) complexes must be highlighted among the carbene adducts showed in the Scheme I.8. They are of widespread use because of their easy preparation, high stability, and great efficiency as transmetallation agent, even in the presence of bulky N-substituents on the imidazolic ring.[48]

The simplest method to synthesize NHC Ag(I) complexes was described by Lin in 1998,[48] and consists in the treatment of an imidazolium salt with Ag_2O, which acts as both metal precursor and deprotonating agent. Mono or bis(NHC) silver(I) complexes form depending on the counterion, solvent and other conditions, which can be in a rapid and reversible equilibrium in solution as it is depicted in the illustrative example of Scheme I.9. These transformations are in agreement with a labile NHC–Ag bond and explain the high efficiency showed by silver complexes as carbene transfer agents to metals such as Au(I), Cu(I), Cu(II), Ni(II), Pd(II), Pt(II), Rh(I), Rh(III), Ir(III), Ru(II), Ru(III), Ru(IV), and Os(II), among others.[48b,49]

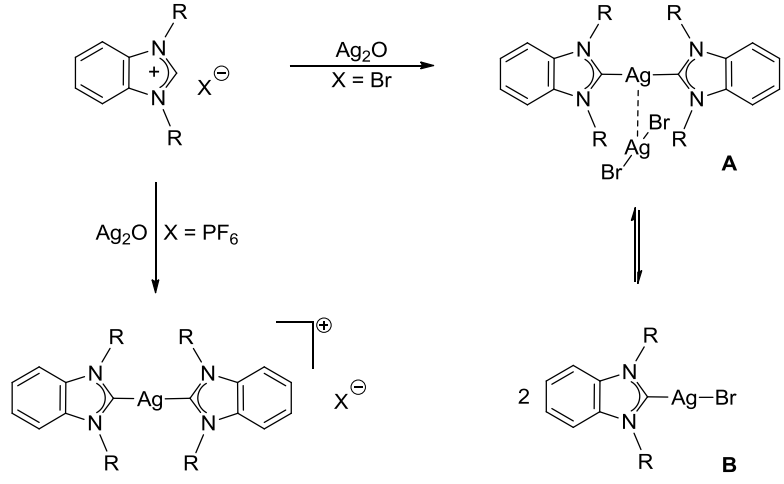

Scheme I.9. NHC silver(I) complexes derived from a benzimidazole.

I.1.3. NHC Pt(II) and Pt(0) complexes

NHC platinum complexes have been usually synthesized following the general synthetic methods mentioned above: *a)* ligand substitution at the metal center using free or *in situ* carbene generation in the presence of a strong or weak base, or *b)* via NHC silver(I) intermediates (see section I.1.2). Hashmi and co-workers prepared in good yields challenging unsymmetrically substituted imidazolidene NHC-Pt(II) complexes from coordinated isonitrile ligands, through an intermolecular nucleophilic addition of β-chloroammonium salts (Scheme I.10). This metal template controlled synthesis procedure[50] has been extended later to the synthesis of other NHC ligands and metal complexes.[51]

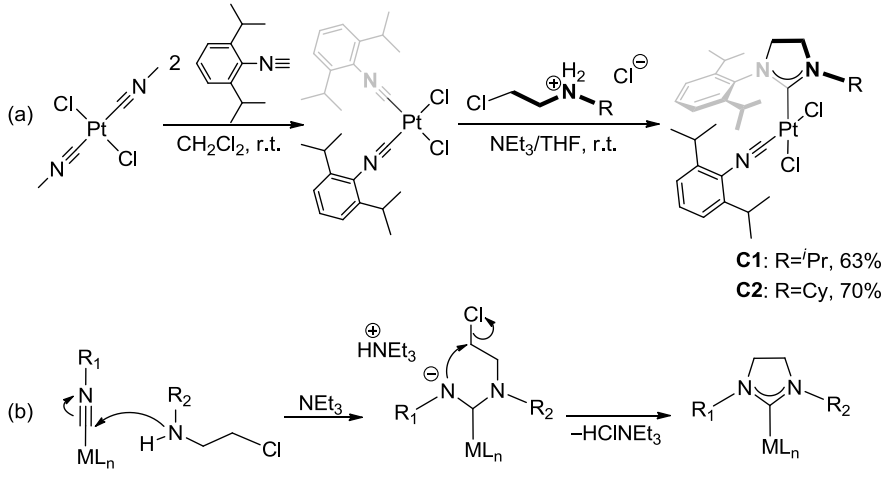

Scheme I.10. (a) Metal template controlled synthesis of unsymmetrically substituted NHC Pt(II) complexes. (b) Possible mechanism for the carbene formation.

As for structural features, platinum complexes reported similar to those described in this work are depicted in Scheme I.11. Pt(II) complexes have been reported containing more conventional monodentate mono (**C3**–**C14**),[52] bis,[52e,52f,53] tetra,[53c] or chelating[52f,54] NHC ligands. These complexes have proven to be useful as catalysts in the reductive cyclization of diynes and enynes in organic solvents,[55] and also as metal-based chemotherapeutic agents.[56] On the other hand, Pt(0) complexes containing NHC ligands (**C15**–**C28**), have been reported mainly as mono carbene species in which the presence of a π-back donating ligand such as diolefins helps to stabilize the electron rich platinum complex.[52f,53d,57] These complexes have been used as catalysts in the diboration of unsaturated molecules,[58] tandem hydroboration-cross coupling,[57g] and the hydrosilylation of unsaturated carbon-carbon bonds such as olefin and alkynes.[52f,57a-f]

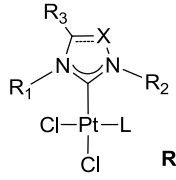

Ref. 52a, d-e

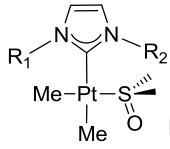

Ref. 52g

C3: R_1=R_2=Mes, R_3=H, X=CH, L=DMSO, Im=sat.
C4: R_1=R_2=Mes, R_3=H, X=CH, L=DMSO, Im=unsat.
C5: R_1=R_2=2,6-di-^{i}Pr-Ph, R_3=H, X=CH, L=DMSO, Im=sat.
C6: R_1=R_2=2,6-di-^{i}Pr-Ph, R_3=H, X=CH, L=DMSO, Im=unsat.
C7: R_1=R_2=2,6-di-^{i}Pr-Ph, R_3=H, X=CH, L=$CH_2CH(CH_2)_2CHCH_2$, DMSO, Im=unsat.
C8: R_1=R_2=Ph, R_3=Ph, X=N, L=DMSO, Im=unsat.
C9: R_1=Me, R_2=CH_2-4-FPh R_3=H, X=CH, L=DMSO, Im=unsat.
C10: R_1=Me, R_2=CH_2-4-FPh, R_3=H, X=CH, L=PPh_3, Im=unsat.

C11: R_1=Me, R_2=4-FPh
C12: R_1=R_2=4-FPh
C13: R_1=4-FPh, R_2=CH_2-4-FPh
C14: R_1=Me, R_2=CH_2-4-FPh

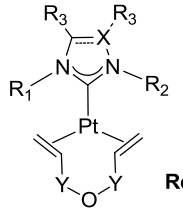

Ref. 57c, f-g

C15: R_1=R_2=Ad., R_3=H, X=C, Y=$SiMe_2$, Im=unsat.
C16: R_1=R_2=Mes, R_3=H, X=C, Y=$SiMe_2$, Im=unsat.
C17: R_1=R_2=Mes, R_3=H, X=C, Y=$SiMe_2$, Im=sat.
C18: R_1=R_2=2,6-di-^{i}Pr-Ph, R_3=H, X=C, Y=$SiMe_2$, Im=unsat.
C19: R_1=R_2=2,6-di-^{i}Pr-Ph, R_3=H, X=C, Y=$SiMe_2$, Im=sat.
C20: R_1=R_2=2,6-di-^{i}Pr-Ph, R_3=H, X=C, Y=$SiMe_2$, Im=unsat.
C21: R_1=R_2=2,6-di-^{i}Pr-Ph, R_3=H, X=C, Y=CH_2, Im=unsat.
C22: R_1=R_2=*n*-Bu, R_3=H, X=N, Y=$SiMe_2$, Im=unsat.
C23: R_1=R_2=*n*-Bu, R_3=Cl, X=C, Y=$SiMe_2$, Im=unsat.
C24: R_1=R_2=*n*-Bu, R_3=H, X=C, Y=$SiMe_2$, Im=unsat.
C25: R_1=R_2=*n*-Bu, R_3=Me, X=C, Y=$SiMe_2$, Im=unsat.
C26: R_1=R_2=Me, R_3=H, X=C, Y=$SiMe_2$, Im=unsat.
C27: R_1=R_2=Cy, R_3=H, X=C, Y=$SiMe_2$, Im=unsat.
C28: R_1=R_2=^{t}Bu, R_3=H, X=C, Y=$SiMe_2$, Im=unsat.

Scheme I.11. Examples of reported NHC Pt(II) and Pt(0) complexes.

I.1.4. Synthesis of water-soluble NHC ligands and their related organometallic complexes

As a reaction medium for chemical transformations, water is the greenest and most abundant solvent, not only supported by Green Chemistry,[59] but also of great interest for the chemical industry. "Volatile organic compounds" (VOCs), currently involved as solvents in most industrial processes, are associated to enormous safety and health risks, and ensuing costs, since most organic solvents are harmful, if not toxic, carcinogenic, flammable, or explosive. In contrast, and besides to its low toxicity, water offers exceptional chemical reactivity due to its unique properties, such as its ability to solvate salts and polar compounds or its high dielectric constant. Thanks to the combination of this distinctive set of features and those mentioned for NHC compounds, the design of tailor made carbene ligands modified by hydrophilic substituents has gained great interest during the past few years. A convenient way to render water-solubility to these kind of ligands involves the attachment to

the ligand of ionic or non-ionic modifiers such as carbonate, carboxylate, ester, sulfonate, amine, ammonium, alcohol or ether groups (Scheme I.12).[60] Additionally, this approach has been extended by the functionalization of carbene precursors with water-soluble polymeric or natural product moieties.[52c,60l,61]

The synthesis of the first example of water-soluble NHC-metal complexes was reported by Herrmann and co-workers in a patent filed in 1995, with the preparation in water of sulfonated bis(NHC) platinum(ii) complexes **C29–C31** (Scheme I.13 a). They were synthesized by reacting K_2PtCl_4 with the imidazolium salts **L23–L25** in absence of an external base, thus, most likely throughout a concerted mechanism pathway because free carbene species cannot exist in water. It should be noted that characterization data of such compounds were not provided.[60e] Six years later, Özdemir and co-workers reported the first aqueous-phase catalyzed reaction using water-soluble NHC complexes. Specifically, they performed the synthesis of 2,3-dimethylfuran catalyzed by a water-soluble NHC ruthenium complex **C32** (Scheme I.13 b).[62] The ruthenium compound was prepared starting from the corresponding tetraaminoethylene **L48** and $[RuCl(\mu\text{-}Cl)(\eta^6\text{-}C_6Me_6)]_2$ as metal source, affording the neutral diamine-substituted imidazolin-2-ylidene complex, which after protonation upon treatment with anhydrous HCl in ether led to the desired complex **C32** in high yields (87% after two steps reaction). Complex **C32** was found to be recyclable (at least five runs) and more active catalyst than its analogue without hydrophilic substituents in organic solvents for the intramolecular cyclization of (*Z*)-3-methylpenten-2-en-4-yn-1-ol into 2,3-dimethylfuran at 80 °C, in a biphasic toluene–H_2O system (Scheme I.13 c).[62]

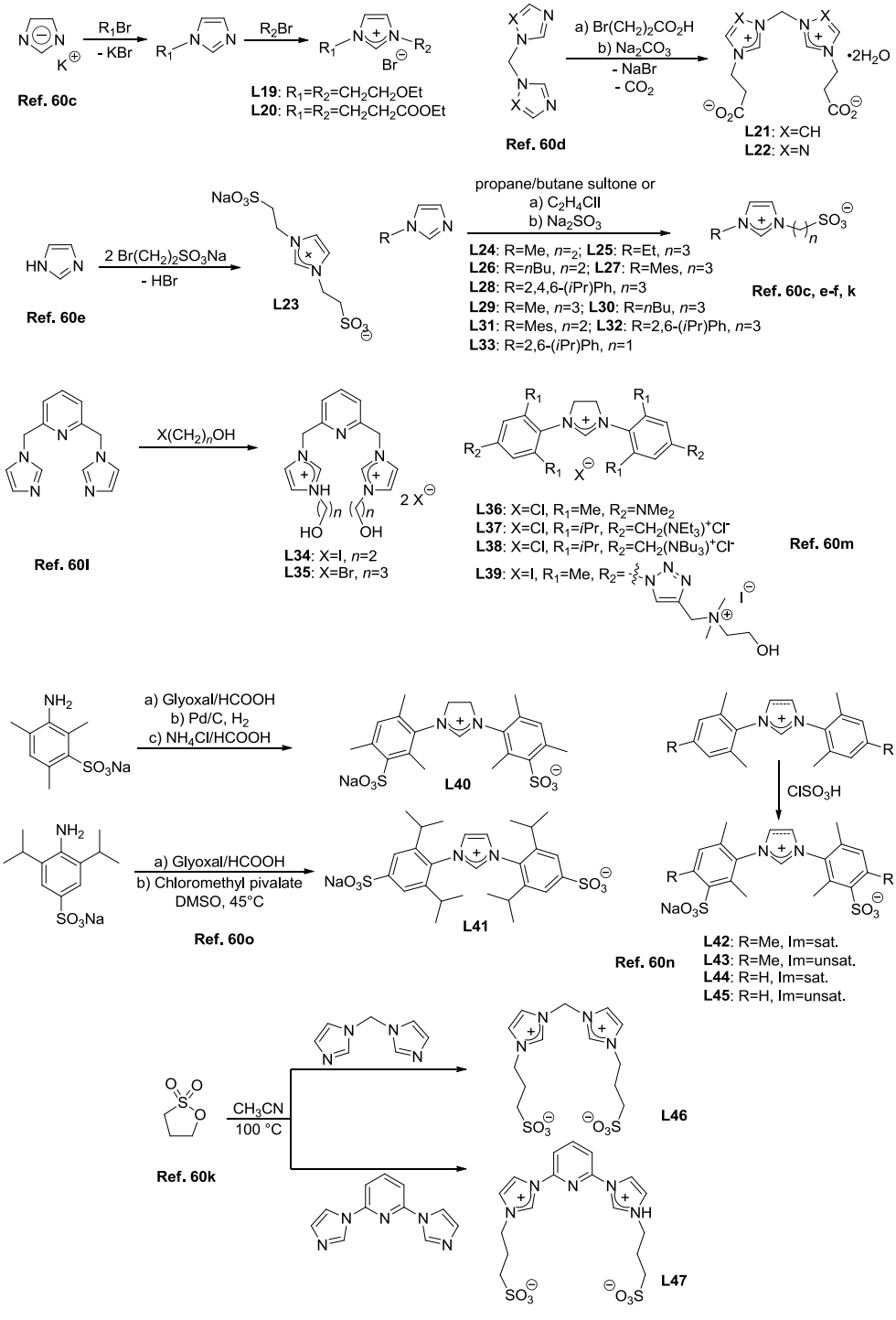

Scheme I.12. Synthesis of representative water-soluble NHC ligand precursors.

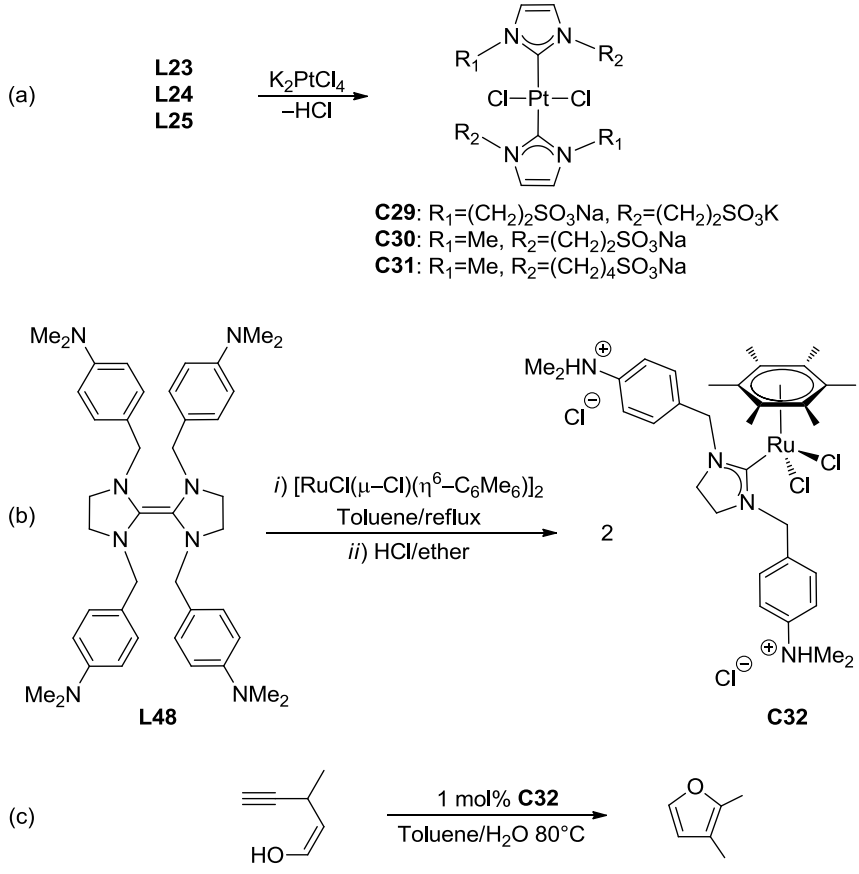

Scheme I.13. Synthesis of the first water-soluble NHC-Metal complexes of (a) Pt(II)[60e] and (b) Ru(II)[62] and (c) the application in biphasic catalysis of the latter complex.

In the last few years, the number of papers involving water-soluble NHC-Metal complexes has rapidly grown. These kind of systems have been reported to be efficient catalysts in several aqueous-phase processes, including ruthenium complexes in olefin metathesis,[63] allylic alcohol isomerizations,[64] or acetophenone hydrogenations,[60i] palladium complexes in cross-coupling reactions,[60k,60n,60o,61,65] or double carbonylation of aryl iodides with amines,[66] gold complexes in alkyne hydrations,[60j,67] or cycloisomerization of *γ*-alkynoic acids,[68] iridium complexes in transfer hydrogenations,[69] or copper complexes in click reactions.[60m] Recently, two reviews concerning the synthesis and applications of water-soluble NHC transition-metal complexes in catalysis have been published.[60b,70]

I.2. Objectives

Although examples of water-soluble (NHC)Pt(II) complexes were first reported in 1998 by Herrmann and co-workers (see Scheme I.13a),[60e] the characterization data of such class of complexes remained unknown until recently. Our research group has reported the synthesis of the first fully-characterized water-soluble (NHC)Pt(0) complexes **C33–C34** (Scheme I.14).[71]

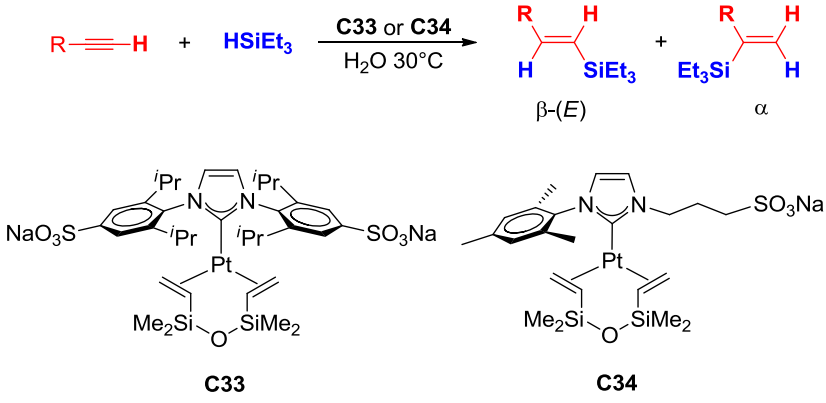

Scheme I.14. The first example of catalytic systems based on water-soluble (NHC)Pt(0) complexes for the hydrosilylation of alkynes in water.[71]

Furthermore, complexes **C33–C34** were found to be highly active and recoverable catalysts for the hydrosilylation of alkynes in water at room temperature. The study also revealed that the Pt–NHC bond was hydrolytically stable under catalysis conditions. This remarkable result encouraged us to get a deeper insight on the hydrolytic stability of such bond. By looking at the literature we realized that, for NHC metal systems, there is as yet not available information concerning stability and reactivity of Pt–C bonds in water, including the limits of the hydrolytic stability of metal–NHC bonds.

The broad aim set out for this PhD dissertation is the synthesis of new water-soluble Pt(II) (**1** and **2** in Scheme I.15) and Pt(0) complexes (**3**) bearing sulfonated NHC ligands as model systems, and the study of their chemical behavior in aqueous-phase under different conditions, particularly focused on the stability of the NHC–metal bond and the transformations that might affect other coligands, which are relevant for the understanding of their role in processes such as catalysis.

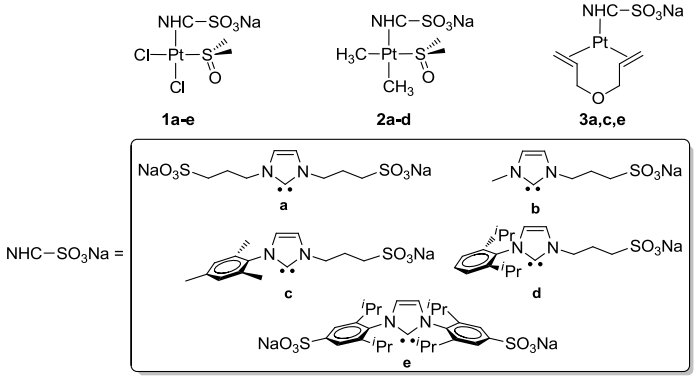

Scheme I.15. Targeting complexes for this PhD dissertation.

I.3. PhD dissertation structure

After **Chapter I**, which collects the introduction and objectives of this work, the dissertation is divided into the next chapters, according to either papers already published or manuscripts in the process to be published.

- **Chapter II**: The improved syntheses for the valuable starting materials *cis*-[Pt(dmso)$_2$Me$_2$] and *trans*-[Pt(dmso)$_2$MeCl], which were used in several subsequent studies, are reported here.

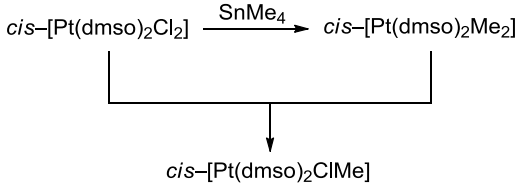

- **Chapter III**: This section concerns the synthesis of water-soluble (NHC)Ag(I) complexes, their behavior in aqueous medium and their capability as carbene transfer agents to Pt(II). The synthesis of *cis*-[(NHC)PtCl$_2$(dmso)] complexes, and their catalytic performance in the hydration of alkynes in water, is reported here as well.

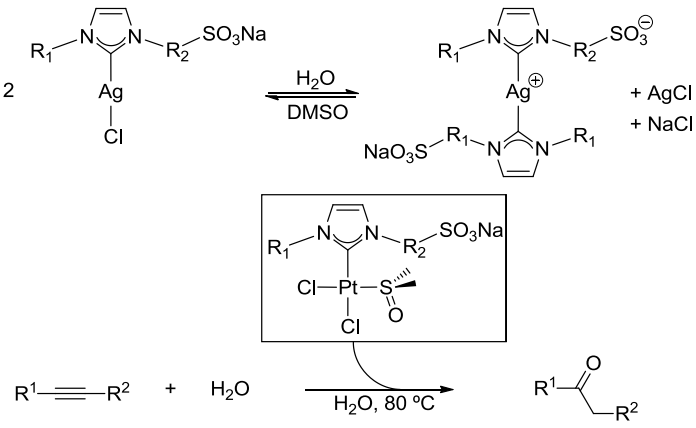

- **Chapter IV**: The preparation of mono and dimethyl (NHC)Pt(II) complexes **2** are disclosed in these chapters, together fundamental studies on the reactivity and hydrolytic stability of the platinum complexes.

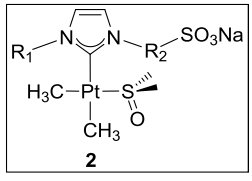

2

Aqueous-phase Reactivity

The outcomes collected in the reactivity of platinum complexes **2** have encouraged us to explore their use as suitable precursors for the controlled formation of water-soluble platinum nanoparticles (PtNPs), as well as to study C(sp^3)–H bond activations observed in complexes **2** in the gas-phase.

- **Chapter V**: This section gathers preliminary results concerning the reactivity of water-soluble (NHC)Pt(0) complex **3e** in oxidative addition reactions for the synthesis of water-soluble hydrides Pt(II) complexes and their behavior in aqueous medium.

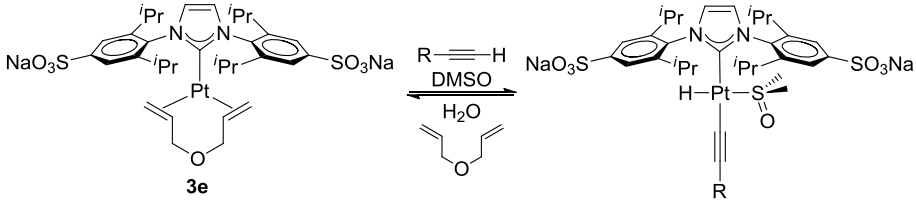

3e

- **Chapters VI** and **VII**: The main results concerning the preparation of water-soluble PtNPs by different methods using complexes **2** and **3** as metal precursors are collected in these two chapters.

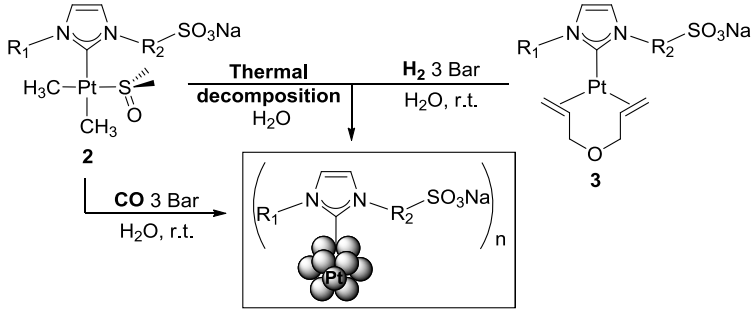

- **Chapter VIII**: The last part of the PhD dissertation is devoted to experimental and theoretical studies on the activation of C(sp^3)–H bonds of complexes $\mathbf{2}^{-}$ in the gas-phase.

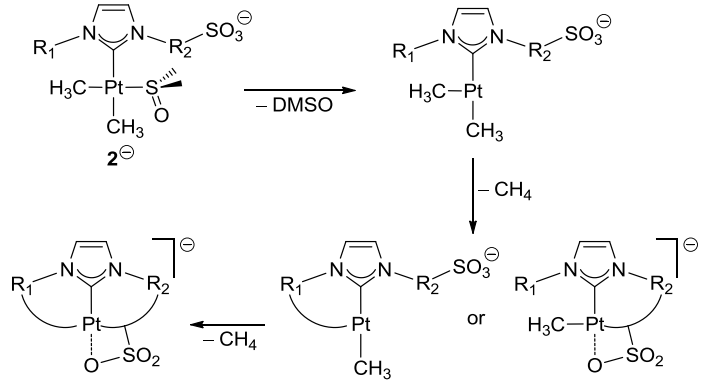

- **Chapter IX**: A summary of most relevant findings and conclusions is presented in this last section in the Spanish Language.

I.4. References

(1) H. W. Wanzlick, H. J. Schoenherr, *Angew. Chem., Int. Ed.* **1968**, *7*, 141-142.

(2) K. Öfele, *J. Organometal. Chem.* **1968**, *12*, P42-P43.

(3) A. J. Arduengo, III, R. L. Harlow, M. Kline, *J. Am. Chem. Soc.* **1991**, *113*, 361-363.

(4) W. A. Herrmann, M. Elison, J. Fischer, C. Köcher, G. R. J. Artus, *Angew. Chem., Int. Ed.* **1995**, *34*, 2371-2374.

(5) F. E. Hahn, *Angew. Chem., Int. Ed.* **2006**, *45*, 1348-1352.

(6) R. H. Grubbs, *Angew. Chem., Int. Ed.* **2006**, *45*, 3760-3765.

(7) R. W. Alder, M. E. Blake, L. Chaker, J. N. Harvey, F. Paolini, J. Schuetz, *Angew. Chem., Int. Ed.* **2004**, *43*, 5896-5911.

(8) a) A. J. Arduengo, III, J. R. Goerlich, W. J. Marshall, *J. Am. Chem. Soc.* **1995**, *117*, 11027-11028; b) M. K. Denk, A. Thadani, K. Hatano, A. J. Lough, *Angew. Chem., Int. Ed.* **1997**, *36*, 2607-2609.

(9) D. Enders, T. Balensiefer, *Acc. Chem. Res.* **2004**, *37*, 534-541.

(10) a) A. Fekete, L. Nyulaszi, *J. Organomet. Chem.* **2002**, *643-644*, 278-284; b) W. W. Schoeller, D. Eisner, *Inorg. Chem.* **2004**, *43*, 2585-2589.

(11) A. J. Arduengo, III, J. R. Goerlich, W. J. Marshall, *Liebigs Ann./Recl.* **1997**, 365-374.

(12) a) S. Solet, H. Gornitzka, W. W. Schoeller, D. Bourissou, G. Bertrand, *Science* **2001**, *292*, 1901-1903; b) X. Cattoeen, H. Gornitzka, D. Bourissou, G. Bertrand, *J. Am. Chem. Soc.* **2004**, *126*, 1342-1343; c) V. Lavallo, J. Mafhouz, Y. Canac, B. Donnadieu, W. W. Schoeller, G. Bertrand, *J. Am. Chem. Soc.* **2004**, *126*, 8670-8671; d) V. Lavallo, Y. Canac, C. Prasang, B. Donnadieu, G. Bertrand, *Angew. Chem., Int. Ed.* **2005**, *44*, 5705-5709.

(13) a) F. E. Hahn, L. Wittenbecher, R. Boese, D. Blaser, *Chem. Eur. J.* **1999**, *5*, 1931-1935; b) F. E. Hahn, L. Wittenbecher, D. Le Van, R. Frohlich, *Angew. Chem., Int. Ed.* **2000**, *39*, 541-544.

(14) G. Altenhoff, R. Goddard, C. W. Lehmann, F. Glorius, *Angew. Chem., Int. Ed.* **2003**, *42*, 3690-3693.

(15) S. Saravanakumar, M. K. Kindermann, J. Heinicke, M. Koeckerling, *Chem. Commun. (Cambridge, U. K.)* **2006**, 640-642.

(16) S. Saravanakumar, A. I. Oprea, M. K. Kindermann, P. G. Jones, J. Heinicke, *Chem. Eur. J.* **2006**, *12*, 3143-3154.

(17) E. Despagnet-Ayoub, R. H. Grubbs, *J. Am. Chem. Soc.* **2004**, *126*, 10198-10199.

(18) a) M. Mayr, K. Wurst, K.-H. Ongania, M. R. Buchmeiser, *Chem. Eur. J.* **2004**, *10*, 1256-1266; b) J. Yun, E. R. Marinez, R. H. Grubbs, *Organometallics* **2004**, *23*, 4172-4173.

(19) P. Bazinet, G. P. A. Yap, D. S. Richeson, *J. Am. Chem. Soc.* **2003**, *125*, 13314-13315.

(20) C. C. Scarborough, M. J. W. Grady, I. A. Guzei, B. A. Gandhi, E. E. Bunel, S. S. Stahl, *Angew. Chem., Int. Ed.* **2005**, *44*, 5269-5272.

(21) M. Alcarazo, S. J. Roseblade, A. R. Cowley, R. Fernandez, J. M. Brown, J. M. Lassaletta, *J. Am. Chem. Soc.* **2005**, *127*, 3290-3291.

(22) R. Weiss, S. Reichel, M. Handke, F. Hampel, *Angew. Chem., Int. Ed.* **1998**, *37*, 344-347.

(23) A. J. Boydston, C. W. Bielawski, *Dalton Trans.* **2006**, 4073-4077.

(24) H. Chen, D. R. Justes, R. G. Cooks, *Org. Lett.* **2005**, *7*, 3949-3952.

(25) M. Hargittai, *Struct. Chem.* **2003**, *14*, 239.

(26) W. A. Herrmann, *Angew. Chem., Int. Ed.* **2002**, *41*, 1290-1309.

(27) a) A. R. Chianese, X. Li, M. C. Janzen, J. W. Faller, R. H. Crabtree, *Organometallics* **2003**, *22*, 1663-1667; b) R. Dorta, E. D. Stevens, N. M. Scott, C. Costabile, L. Cavallo, C. D. Hoff, S. P. Nolan, *J. Am. Chem. Soc.* **2005**, *127*, 2485-2495.

(28) a) L. Cavallo, A. Correa, C. Costabile, H. Jacobsen, *J. Organomet. Chem.* **2005**, *690*, 5407-5413; b) C. A. Tolman, *Chem. Rev.* **1977**, *77*, 313-348.

(29) J. Huang, H.-J. Schanz, E. D. Stevens, S. P. Nolan, *Organometallics* **1999**, *18*, 2370-2375.

(30) A. C. Hillier, W. J. Sommer, B. S. Yong, J. L. Petersen, L. Cavallo, S. P. Nolan, *Organometallics* **2003**, *22*, 4322-4326.

(31) a) A. Chartoire, M. Lesieur, L. Falivene, A. M. Z. Slawin, L. Cavallo, C. S. J. Cazin, S. P. Nolan, *Chem. Eur. J.* **2012**, *18*, 4517-4521; b) A. Collado, J. Balogh, S. Meiries, A. M. Z. Slawin, L. Falivene, L. Cavallo, S. P. Nolan, *Organometallics* **2013**, *32*, 3249-3252; c) P. Liu, J. Montgomery, K. N. Houk, *J. Am. Chem. Soc.* **2011**, *133*, 6956-6959.

(32) A. M. Ortiz, P. Gomez-Sal, J. C. Flores, E. de Jesus, *Organometallics* **2014**, *33*, 600-603.

(33) a) A. Poater, F. Ragone, S. Giudice, C. Costabile, R. Dorta, S. P. Nolan, L. Cavallo, *Organometallics* **2008**, *27*, 2679-2681; b) I. Alkorta, J. Elguero, *Struct. Chem.* **2011**, *22*, 1087-1094.

(34) M. K. Denk, J. M. Rodezno, S. Gupta, A. J. Lough, *J. Organomet. Chem.* **2001**, *617-618*, 242-253.

(35) a) A. J. Arduengo, III, J. C. Calabrese, F. Davidson, H. V. R. Dias, J. R. Goerlich, R. Krafczyk, W. J. Marshall, M. Tamm, R. Schmutzler, *Helv. Chim. Acta* **1999**, *82*, 2348-2364; b) A. G. Tskhovrebov, E. Solari, M. D. Wodrich, R. Scopelliti, K. Severin, *Angew. Chem., Int. Ed.* **2012**, *51*, 232-234; c) W. Kirmse, *Eur. J. Org. Chem.* **2005**, 237-260; d) N. Kuhn, A. Al-Sheikh, *Coord. Chem. Rev.* **2005**, *249*, 829-857.

(36) a) O. Holloczki, P. Terleczky, D. Szieberth, G. Mourgas, D. Gudat, L. Nyulaszi, *J. Am. Chem. Soc.* **2011**, *133*, 780-789; b) F. Bonnette, T. Kato, M. Destarac, G. Mignani, F. P. Cossio, A. Baceiredo, *Angew. Chem., Int. Ed.* **2007**, *46*, 8632-8635; c) C. Segarra, E. Mas-Marza, M. Benitez, J. A. Mata, E. Peris, *Angew. Chem., Int. Ed.* **2012**, *51*, 10841-10845; d) G.-F. Wang, X.-J. Song, F. Chen, Y.-Z. Li, X.-T. Chen, Z.-L. Xue, *Dalton Trans.* **2012**, *41*, 10919-10922; e) W. Zuo, P. Braunstein, *Dalton Trans.* **2012**, *41*, 636-643; f) S. K. Gupta, D. Ghorai, J. Choudhury, *Organometallics* **2014**, *33*, 3215-3218.

(37) R. W. Alder, M. E. Blake, C. Bortolotti, S. Bufali, C. P. Butts, E. Linehan, J. M. Oliva, A. G. Orpen, M. J. Quayle, *Chem. Commun.* **1999**, 241-242.

(38) a) N. Froehlich, U. Pidun, M. Stahl, G. Frenking, *Organometallics* **1997**, *16*, 442-448; b) W. A. Herrmann, O. Runte, G. Artus, *J. Organomet. Chem.* **1995**, *501*, C1-C4.

(39) P. L. Arnold, S. A. Mungur, A. J. Blake, C. Wilson, *Angew. Chem., Int. Ed.* **2003**, *42*, 5981-5984.

(40) G. W. Nyce, S. Csihony, R. M. Waymouth, J. L. Hedrick, *Chem. Eur. J.* **2004**, *10*, 4073-4079.

(41) a) A. J. Arduengo, III, H. V. R. Dias, F. Davidson, R. L. Harlow, *J. Organomet. Chem.* **1993**, *462*, 13-18; b) D. S. McGuinness, K. J. Cavell, *Organometallics* **2000**, *19*, 741-748; c) O. Guerret, S. Sole, H. Gornitzka, M. Teichert, G. Trinquier, G. Bertrand, *J. Am. Chem. Soc.* **1997**, *119*, 6668-6669; d) O. Guerret, S. Sole, H. Gornitzka, G. Trinquier, G. Bertrand, *J. Organomet. Chem.* **2000**, *600*, 112-117.

(42) a) Y. Yamaguchi, T. Kashiwabara, K. Ogata, Y. Miura, Y. Nakamura, K. Kobayashi, T. Ito, *Chem. Commun. (Cambridge, U. K.)* **2004**, 2160-2161; b) K. Ogata, Y. Yamaguchi, T. Kashiwabara, T. Ito, *J. Organomet. Chem.* **2005**, *690*, 5701-5709.

(43) a) M. Fevre, J. Pinaud, A. Leteneur, Y. Gnanou, J. Vignolle, D. Taton, K. Miqueu, J.-M. Sotiropoulos, *J. Am. Chem. Soc.* **2012**, *134*, 6776-6784; b) M. Smiglak, C. C. Hines, R. D. Rogers, *Green Chem.* **2010**, *12*, 491-501.

(44) a) J. D. Holbrey, W. M. Reichert, I. Tkatchenko, E. Bouajila, O. Walter, I. Tommasi, R. D. Rogers, *Chem. Commun. (Cambridge, U. K.)* **2003**, 28-29; b) A. M. Voutchkova, M. Feliz, E. Clot, O. Eisenstein, R. H. Crabtree, *J. Am. Chem. Soc.* **2007**, *129*, 12834-12846.

(45) A. P. Blum, T. Ritter, R. H. Grubbs, *Organometallics* **2007**, *26*, 2122-2124.

(46) T. M. Trnka, J. P. Morgan, M. S. Sanford, T. E. Wilhelm, M. Scholl, T.-L. Choi, S. Ding, M. W. Day, R. H. Grubbs, *J. Am. Chem. Soc.* **2003**, *125*, 2546-2558.

(47) a) O. Coulembier, A. P. Dove, R. C. Pratt, A. C. Sentman, D. A. Culkin, L. Mespouille, P. Dubois, R. M. Waymouth, J. L. Hedrick, *Angew. Chem., Int. Ed.* **2005**, *44*, 4964-4968; b) K. Denk, P. Sirsch, W. A. Herrmann, *J. Organomet. Chem.* **2002**, *649*, 219-224; c) S. Csihony, D. A. Culkin, A. C. Sentman, A. P. Dove, R. M. Waymouth, J. L. Hedrick, *J. Am. Chem. Soc.* **2005**, *127*, 9079-9084; d) O. Coulembier, B. G. G. Lohmeijer, A. P. Dove, R. C. Pratt, L. Mespouille, D. A. Culkin, S. J. Benight, P. Dubois, R. M. Waymouth, J. L. Hedrick, *Macromolecules* **2006**, *39*, 5617-5628.

(48) a) H. M. J. Wang, I. J. B. Lin, *Organometallics* **1998**, *17*, 972-975; b) I. J. B. Lin, C. S. Vasam, *Coord. Chem. Rev.* **2007**, *251*, 642-670.

(49) J. C. Garrison, W. J. Youngs, *Chem. Rev.* **2005**, *105*, 3978-4008.

(50) a) M. Tamm, F. E. Hahn, *Coord. Chem. Rev.* **1999**, *182*, 175-209; b) R. A. Michelin, A. J. L. Pombeiro, M. F. C. Guedes da Silva, *Coord. Chem. Rev.* **2001**, *218*, 75-112; c) F. E. Hahn, C. G. Plumed, M. Muender, T. Luegger, *Chem. Eur. J.* **2004**, *10*, 6285-6293; d) M. Basato, R. A. Michelin, M. Mozzon, P. Sgarbossa, A. Tassan, *J. Organomet. Chem.* **2005**, *690*, 5414-5420; e) U. Belluco, R. A. Michelin, P. Uguagliati, B. Crociani, *J. Organomet. Chem.* **1983**, *250*, 565-587; f) M. Basato, F. Benetollo, G. Facchin, R. A. Michelin, M. Mozzon, S. Pugliese, P. Sgarbossa, S. M. Sbovata, A. Tassan, *J. Organomet. Chem.* **2004**, *689*, 454-462; g) G. Facchin, R. A. Michelin, M. Mozzon, P. Sgarbossa, A. Tassan, *Inorg. Chim. Acta* **2004**, *357*, 3385-3389.

(51) a) A. S. K. Hashmi, C. Lothschütz, K. Graf, T. Häffner, A. Schuster, F. Rominger, *Adv. Synth. Catal.* **2011**, *353*, 1407-1412; b) A. S. K. Hashmi, C. Lothschütz, C. Böhling, T. Hengst, C. Hubbert, F. Rominger, *Adv. Synth. Catal.* **2010**, *352*, 3001-3012.

(52) a) S. Fantasia, H. Jacobsen, L. Cavallo, S. P. Nolan, *Organometallics* **2007**, *26*, 3286-3288; b) D. Brissy, M. Skander, P. Retailleau, G. Frison, A. Marinetti, *Organometallics* **2008**, *28*, 140-151; c) J. J. Hu, S.-Q. Bai, H. H. Yeh, D. J. Young, Y. Chi, T. S. A. Hor, *Dalton Trans.* **2011**, *40*, 4402-4406; d) S. Fantasia, J. L. Petersen, H. Jacobsen, L. Cavallo, S. P. Nolan, *Organometallics* **2007**, *26*, 5880-5889; e) C. P. Newman, R. J. Deeth, G. J. Clarkson, J. P. Rourke, *Organometallics* **2007**, *26*, 6225-6233; f) J. J. Hu, F. Li, T. S. A. Hor, *Organometallics* **2009**, *28*, 1212-1220; g) G. L. Petretto, M. Wang, A. Zucca, J. P. Rourke, *Dalton Trans.* **2010**, *39*, 7822-7825.

(53) a) O. Rivada-Wheelaghan, B. Donnadieu, C. Maya, S. Conejero, *Chem. Eur. J.* **2010**, *16*, 10323-10326; b) O. Rivada-Wheelaghan, M. A. Ortuno, J. Diez, A. Lledos, S. Conejero, *Angew. Chem., Int. Ed.* **2012**, *51*, 3936-3939; c) V. Blase, A. Flores-Figueroa, C. Schulte to Brinke, F. E. Hahn, *Organometallics* **2014**, *33*, 4471-4478; d) M. A. Duin, N. D. Clement, K. J. Cavell, C. J. Elsevier, *Chem. Commun.* **2003**, 400-401.

(54) a) D. Meyer, S. Ahrens, T. Strassner, *Organometallics* **2010**, *29*, 3392-3396; b) S. Jamali, D. Milic, R. Kia, Z. Mazloomi, H. Abdolahi, *Dalton Trans.* **2011**, *40*, 9362-9365; c) M. Frøseth, K. A. Netland, C. Rømming, M. Tilset, *J. Organomet. Chem.* **2005**, *690*, 6125-6132; d) K. A. Netland, A. Krivokapic, M. Tilset, *J. Coord. Chem.* **2010**, *63*, 2909-2927; e) P. Nägele, U. Herrlich, F. Rominger, P. Hofmann, *Organometallics* **2012**, *32*, 181-191; f) B. Pan, S. Pierre, M. W. Bezpalko, J. W. Napoline, B. M. Foxman, C. M. Thomas, *Organometallics* **2013**, *32*, 704-710.

(55) I. G. Jung, J. Seo, S. I. Lee, S. Y. Choi, Y. K. Chung, *Organometallics* **2006**, *25*, 4240-4242.

(56) a) G. Alves, L. Morel, M. El-Ghozzi, D. Avignant, B. Legeret, L. Nauton, F. Cisnetti, A. Gautier, *Chem. Commun.* **2011**, *47*, 7830-7832; b) M. Skander, P. Retailleau, B. Bourrié, L. Schio, P. Mailliet, A. Marinetti, *J. Med. Chem.* **2010**, *53*, 2146-2154; c) E. Chardon, G. Dahm, G. Guichard, S. Bellemin-Laponnaz, *Organometallics* **2012**, *31*, 7618-7621.

(57) a) I. E. Marko, S. Sterin, O. Buisine, G. Mignani, P. Branlard, B. Tinant, J.-P. Declercq, *Science* **2002**, *298*, 204-207; b) O. Buisine, G. Berthon-Gelloz, J.-F. Briere, S. Sterin, G. Mignani, P. Branlard, B. Tinant, J.-P. Declercq, I. E. Marko, *Chem. Commun.* **2005**, 3856-3858; c) G. Berthon-Gelloz, O. Buisine, J.-F. Briere, G. Michaud, S. Sterin, G. Mignani, B.

Tinant, J.-P. Declercq, D. Chapon, I. E. Marko, *J. Organomet. Chem.* **2005**, *690*, 6156-6168; d) J. W. Sprengers, M. J. Mars, M. A. Duin, K. J. Cavell, C. J. Elsevier, *J. Organomet. Chem.* **2003**, *679*, 149-152; e) G. De Bo, G. Berthon-Gelloz, B. Tinant, I. E. Marko, *Organometallics* **2006**, *25*, 1881-1890; f) G. Berthon-Gelloz, J.-M. Schumers, G. De Bo, I. E. Marko, *J. Org. Chem.* **2008**, *73*, 4190-4197; g) V. Lillo, J. A. Mata, A. M. Segarra, E. Peris, E. Fernandez, *Chem. Commun.* **2007**, 2184-2186.

(58) V. Lillo, J. Mata, J. Ramírez, E. Peris, E. Fernandez, *Organometallics* **2006**, *25*, 5829-5831.

(59) P. Anastas, N. Eghbali, *Chem. Soc. Rev.* **2010**, *39*, 301-312.

(60) a) K. H. Shaughnessy, *Chem. Rev.* **2009**, *109*, 643-710; b) H. D. Velazquez, F. Verpoort, *Chem. Soc. Rev.* **2012**, *41*, 7032-7060; c) W. A. Herrmann, L. J. Goossen, M. Spiegler, *J. Organomet. Chem.* **1997**, *547*, 357-366; d) J. Cure, R. Poteau, I. C. Gerber, H. Gornitzka, C. Hemmert, *Organometallics* **2012**, *31*, 619-626; e) W. A. Herrmann, M. Elison, J. Fischer, C. Köcher, K. Öfele, US Patent 5,728,839, **1998**; f) G. Papini, M. Pellei, G. Gioia Lobbia, A. Burini, C. Santini, *Dalton Trans.* **2009**, 6985-6990; g) Y. Nagai, T. Kochi, K. Nozaki, *Organometallics* **2009**, *28*, 6131-6134; h) J. Mesnager, P. Lammel, E. Jeanneau, C. Pinel, *Appl. Catal., A* **2009**, *368*, 22-28; i) H. Syska, W. A. Herrmann, F. E. Kuehn, *J. Organomet. Chem.* **2012**, *703*, 56-62; j) A. Almassy, C. E. Nagy, A. C. Benyei, F. Joo, *Organometallics* **2010**, *29*, 2484-2490; k) F. Godoy, C. Segarra, M. Poyatos, E. Peris, *Organometallics* **2011**, *30*, 684-688; l) A. Melaiye, R. S. Simons, A. Milsted, F. Pingitore, C. Wesdemiotis, C. A. Tessier, W. J. Youngs, *J. Med. Chem.* **2004**, *47*, 973-977; m) W. Wang, J. Wu, C. Xia, F. Li, *Green Chem.* **2011**, *13*, 3440-3445; n) S. Roy, H. Plenio, *Adv. Synth. Catal.* **2010**, *352*, 1014-1022; o) C. Fleckenstein, S. Roy, S. Leuthaeusser, H. Plenio, *Chem. Commun.* **2007**, 2870-2872.

(61) F.-T. Luo, H.-K. Lo, *J. Organomet. Chem.* **2011**, *696*, 1262-1265.

(62) İ. Özdemir, B. Yiğit, B. Çetinkaya, D. Ülkü, M. N. Tahir, C. Arıcı, *J. Organomet. Chem.* **2001**, *633*, 27-32.

(63) a) J. P. Gallivan, J. P. Jordan, R. H. Grubbs, *Tetrahedron Lett.* **2005**, *46*, 2577-2580; b) S. H. Hong, R. H. Grubbs, *J. Am. Chem. Soc.* **2006**, *128*, 3508-3509; c) J. P. Jordan, R. H. Grubbs, *Angew. Chem. Int. Ed.* **2007**, *46*, 5152-5155; d) S. L. Balof, B. Yu, A. B. Lowe, Y. Ling, Y. Zhang, H.-J. Schanz, *Eur. J. Inorg. Chem.* **2009**, *2009*, 1717-1722.

(64) A. Azua, S. Sanz, E. Peris, *Organometallics* **2010**, *29*, 3661-3664.

(65) a) D. Schönfelder, O. Nuyken, R. Weberskirch, *J. Organomet. Chem.* **2005**, *690*, 4648-4655; b) M. Meise, R. Haag, *ChemSusChem* **2008**, *1*, 637-642; c) C.-C. Yang, P.-S. Lin, F.-C. Liu, I. J. B. Lin, G.-H. Lee, S.-M. Peng, *Organometallics* **2010**, *29*, 5959-5971; d) B. Karimi, P. Fadavi Akhavan, *Chem. Commun.* **2011**, *47*, 7686-7688; e) L. Li, J. Wang, C. Zhou, R. Wang, M. Hong, *Green Chem.* **2011**, *13*, 2071-2077; f) D. Yuan, Q. Teng, H. V. Huynh, *Organometallics* **2014**, *33*, 1794-1800; g) R. Zhong, A. Pothig, Y. Feng, K. Riener, W. A. Herrmann, F. E. Kuhn, *Green Chem.* **2014**, *16*, 4955-4962.

(66) Y. Wang, X. Yang, C. Zhang, J. Yu, J. Liu, C. Xia, *Adv. Synth. Catal.* **2014**, *356*, 2539-2546.

(67) a) C. E. Czégéni, G. Papp, Á. Kathó, F. Joó, *J. Mol. Catal. A: Chem.* **2011**, *340*, 1-8; b) C. Wetzel, P. C. Kunz, I. Thiel, B. Spingler, *Inorg. Chem.* **2011**, *50*, 7863-7870; c) G. A. Fernández, A. S. Picco, M. R. Ceolín, A. B. Chopa, G. F. Silbestri, *Organometallics* **2013**, *32*, 6315-6323.

(68) a) E. Tomás-Mendivil, P. Y. Toullec, J. Díez, S. Conejero, V. Michelet, V. Cadierno, *Org. Lett.* **2012**, *14*, 2520-2523; b) E. Tomás-Mendivil, P. Y. Toullec, J. Borge, S. Conejero, V. Michelet, V. Cadierno, *ACS Catal.* **2013**, *3*, 3086-3098.

(69) A. Azua, S. Sanz, E. Peris, *Chem. Eur. J.* **2011**, *17*, 3963-3967.

(70) L.-A. Schaper, S. J. Hock, W. A. Herrmann, F. E. Kühn, *Angew. Chem. Int. Ed.* **2013**, *52*, 270-289.

(71) G. F. Silbestri, J. C. Flores, E. de Jesus, *Organometallics* **2012**, *31*, 3355-3360.

Chapter II. Improved synthesis of *cis*-[Pt(dmso)$_2$Me$_2$] and *trans*-[Pt(dmso)$_2$MeCl]

Edwin A. Baquero, Juan C. Flores, and Ernesto de Jesús, *Manuscript In Preparation*, **2015**.

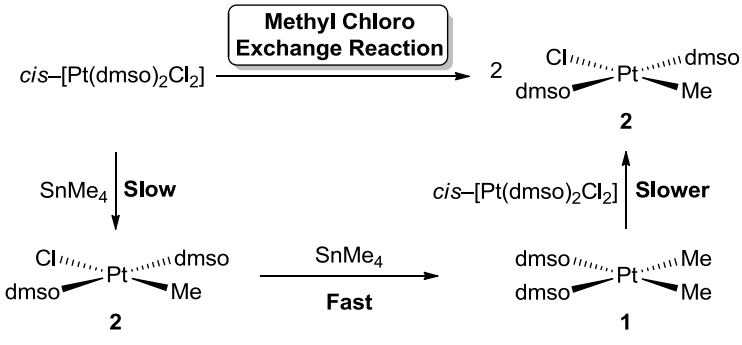

Improved synthesis of *cis*-[Pt(dmso)$_2$Me$_2$] and *trans*-[Pt(dmso)$_2$MeCl]

Edwin A. Baquero*, Juan C. Flores,* and Ernesto de Jesús**

Departamento de Química Inorgánica, Campus Universitario, Universidad de Alcalá, 28871 Alcalá de Henares, Madrid, Spain.

ABSTRACT

An improved procedure for the preparation of *cis*-[Pt(dmso)$_2$Me$_2$] and *trans*-[Pt(dmso)$_2$MeCl] (dmso = dimethylsulfoxide) complexes, which is based on the study of their formation reactions from SnMe$_4$ and *cis*-[Pt(dmso)$_2$Cl$_2$] as starting materials, is described. The reaction of SnMe$_4$ with *cis*-[Pt(dmso)$_2$Cl$_2$] forms *trans*-[Pt(dmso)$_2$MeCl], but quickly reacts to *cis*-[Pt(dmso)$_2$Me$_2$] due to the kinetic *trans*-effect of the methyl group that makes the second methylation more favorable than the first one. A distribution reaction between *cis*-[Pt(dmso)$_2$Me$_2$] and *cis*-[Pt(dmso)$_2$Cl$_2$] is the key step to lead the reaction back to the formation of *trans*-[Pt(dmso)$_2$MeCl]. The thermal stability of *cis*-[Pt(dmso)$_2$Me$_2$] in the presence of SnMe$_4$ greatly affects the yield in its preparation.

INTRODUCTION

The synthesis of *cis*-[Pt(dmso)$_2$Me$_2$] (**1**) and *trans*-[Pt(dmso)$_2$MeCl] (**2**) was first reported by Eaborn and coworkers in 1979,[1] and described in more detail for **2** by Romeo and Scolaro two decades later.[2] Complexes **1** and **2** are relatively stables and they have been used as suitable precursors for the preparation of numerous organoplatinum compounds by substitution of the labile ligand dmso by other donor ligands, such as N-heterocyclic carbenes,[3] phosphanes,[4] thioxamides,[5] CN-chelates,[6] CNN-[7] or CNC-pincers,[8] N-, S-, or P-chelates,[9] imines,[10] etc. The preparative approaches for other valuable Pt-synthon sources of the same type, namely [Pt(cod)Me$_2$], [Pt(cod)MeCl] (cod = 1,5-cyclooctadiene),[11] [Pt(SMe$_2$)Me$_2$]$_2$, and [Pt(SMe$_2$)$_2$MeCl],[12] involve the use of methyllithium,[11c,12] trimethylaluminium,[11a] or Grignard reagents[11b] and, in many cases, delicate steps.

The synthetic procedure described by Eaborn appears to be a simpler one, and is appealing because of the wide range of accessible organotin compounds.[13] It makes use of stable and easy to handle starting materials (*cis*-[Pt(dmso)$_2$Cl$_2$] and SnMe$_4$, Scheme 1), and leads to complexes **1** and **2** in a single step in warm dmso, although in reported yields of 55% and 26%

for **1** and **2**, respectively,[1] or 56% for **2** according to Romeo's description.[2] This method works better with more reactive $SnMe_3R$ derivatives (*e.g.*, R = aryl), which are also able to react with $[Pt(cod)Cl_2]$ in chlorinated solvents.[14] Nevertheless, Eaborn pointed that reactions with $[Pt(dmso)_2Cl_2]$ in dmso appeared to be superior because they were faster, and the formed complexes were more stable in dmso than in chlorinated solvents at the working temperatures probably because the dissociation of the coordinated dmso is suppressed.[1b] At this point, it is worth to mention that Vrieze and coworkers have described the preparation of [Pt(cod)MeCl] with 79% yield by reaction of $[Pt(cod)Cl_2]$ and $SnMe_4$ (1:1) in CH_2Cl_2/MeOH (1:1) at room temperature for 24 h.[15]

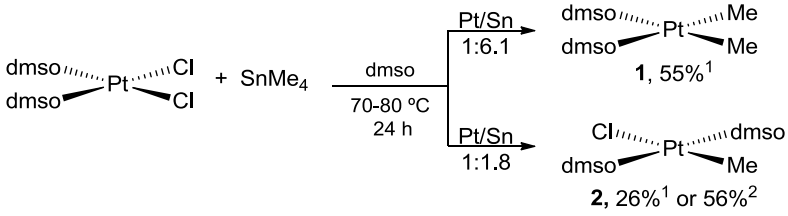

Scheme 1. Reported synthesis for complexes **1** and **2** from *cis*-$[Pt(dmso)_2Cl_2]$ and $SnMe_4$.

Due to our research interest in complexes **1** and **2**,[16] we have studied with some detail their formation reaction from *cis*-$[Pt(dmso)_2Cl_2]$ and $SnMe_4$. The results presented here have allowed the optimization of the procedures and revealed details of their mechanism of formation.

RESULTS AND DISCUSSION

In our attempts to obtain **2** from *cis*-$[Pt(dmso)_2Cl_2]$ and $SnMe_4$ following Romeo's method (Scheme 1a),[2] in most instances no reaction took place, or the *trans* complex was obtained with, as much, 9% yield after the work up procedure. As reported, the operation was carried out by heating the dmso mixture at 80 ºC in a flask equipped with a condenser, and under an inert atmosphere.

Since $SnMe_4$ is a volatile compound (b.p. 74-75 °C at 1 atm) and might be essentially present in the gas phase at 80 ºC, we envisioned that the success of this reaction must be very sensitive to the experimental set up. Thus, the reaction was repeated in a closed system (ampule tube with a PTFE valve) under otherwise identical conditions (*i.e.*, dmso, 80 ºC, 24 h, 1:1.8 molar ratio). The reaction proceeded leading to the formation of the dimethyl complex **1**, instead of **2,** as the sole product in nearly 50% yield together with around a 50% of unreacted *cis*-$[Pt(dmso)_2Cl_2]$. The unexpected result barely changes using a 1:1 molar ratio of starting materials. Consequently, an eventual formation of **1** caused by the excess of $SnMe_4$ (*i.e.*, 0.8 equiv) may be ruled out. Instead, a feasible alternative explanation is that the Pt–Cl bond in

trans-[Pt(dmso)$_2$MeCl] (**2**) is kinetically more reactive toward $SnMe_4$ than those in *cis*-[Pt(dmso)$_2$Cl$_2$], due to the large *trans* effect of the opposite methyl group in **2** as compared to that of dmso in the dichloride.[17] Under this hypothesis the formation of **1** and **2** was experimentally examined.

According to Eaborn, the yield found for these reactions reflected the efficiency of isolation of purified compounds rather than the efficiency of the reactions themselves, which showed to be notably superior in studies performed in syntheses of aryl derivatives, but no attempts were made to optimize their reaction time. Thus, the yield reported for **1** was 55%, using a Pt/Sn molar ratio of 1:6.1, and a reaction time of 24 h (Scheme 1b).[1b] However, we have observed, in a closed set up, darkening of the solutions as the reaction with $SnMe_4$ progresses, followed by the appearance of significant amounts of platinum black after 24 h. We have monitored the reaction by ^{1}H-NMR spectroscopy, although combining the reactants with a much smaller excess of $SnMe_4$ (1:2.5) in dmso-d_6. Gratifyingly, the formation of the dimethyl complex **1** is quantitative after 3 h at 80 °C, and no darkening of the solution or Pt(0) precipitate is observed. Also, it is noteworthy that the monomethyl compound **2** is detected (*ca.* 20% combined with **1**) at 1 h of the start of the experiment, and that reproduction of these operational conditions at preparative scale renders **1** with up to 82% after work up.[18] Therefore, long reaction times and large excess of $SnMe_4$ in the synthesis of **1** are counterproductive, since they promote the product decomposition. In fact, no deterioration of **1** in dmso-d_6 is appreciable after 48 h at 80 ºC, but decomposition to Pt(0) is perceptible after 10 h in the presence of 3 equiv of $SnMe_4$ at that temperature. Additionally, and as noticed by Romeo in the work up for **2**,[2] after the formation of **1** and upon removal of dmso under vacuum at 80 ºC, we have observed some decomposition, which seems to accelerate with the concentration of the solution. Since an intermolecular reductive elimination leading to Pt(0) and ethane might be responsible of such a result, and heating during solvent elimination would favor it, the reaction was attempted in a different solvent at room temperature. In CH_2Cl_2 the reaction took place, but leading to a mixture of compounds, and noting slow darkening over time, whereas in CH_2Cl_2/MeOH (1:1) no alkylation was observed probably because of *cis*-[Pt(dmso)$_2$Cl$_2$] insolubility.

Due to our difficulties to prepare the monomethyl complex **2** by the reported and modified methods,[1,2] we have tested to adapt that described by Puddephatt for the synthesis of [Pt(SMe$_2$)$_2$MeCl],[12,19] and related complexes,[20] consisting in methyl-chloro exchange process between the dimethyl and the dichloro platinum complexes –a transformation also noted by Eaborn for [Pt(cod)$_2$RCl] (R = aryl) complexes.[14] Thus, we have examined the reaction between *cis*-[Pt(dmso)$_2$Cl$_2$] and **1**, in a molar ratio 1:1, at a NMR tube scale using dmso-d_6 as solvent. The reaction occurs at 80 °C, only the reagents are observed at lower temperatures, and the total conversion into *trans*-[Pt(dmso)$_2$MeCl] (**2**) is completed after 24 h. Regrettably,

under these conditions the best yield at preparative scale was 30%. Once more, the formation of large amounts of platinum black was observed during the work up (*i.e.*, upon removal of the dmso under vacuum at 80 ºC), and despite of the confirmed stability of isolated **2** in warm dmso (no decomposition detected after 48 h at 80 ºC). However, the reaction proceeds smoothly at room temperature in CH_2Cl_2, after 24 h, and affording complex **2** in a 65% yield after work-up. Although again, the moderate yield obtained can be explained by the low amounts of platinum black observed during reaction.

The set of outcomes, lead us to understand these reactions as schematically represented in Scheme 2. Starting with Pt/Sn molar ratios of 1:2, or higher, the reaction in dmso evolves to **1** as expected. For a molar ratio of 1:1, the reaction is kinetically controlled. Dimethyl complex **1** forms rapidly after the first methylation because compound **2** is more prone to react with $SnMe_4$ than the starting dichloride due to the strong *trans* effect of its methyl group. Finally, the remaining *cis*-[Pt(dmso)$_2$Cl$_2$] reacts slowly with **1**, formed *in situ*, through a methyl-chloro exchange process, which selectively leads back to the monomethyl complex **2**.

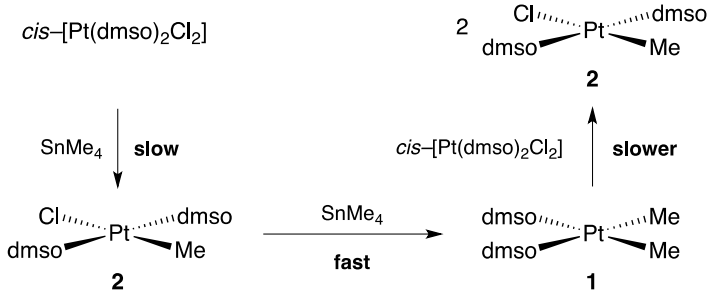

Scheme 2. Formation of **2** through methyl-chloro exchange between **1** formed *in situ* and *cis*-[Pt(dmso)$_2$Cl$_2$].

The role of the reaction solvent appears to be related to the intimate mechanism of the reactions and the stability of complexes **1** and **2** against decomposition to Pt(0). The fact that heating is required for methylation reactions in dmso, whereas they progress at room temperature in CH_2Cl_2, suggests a dissociative mechanism through mono-dmso species, facilitated in the latter solvent and hampered in the former. Dissociation and exchange of dmso has been evidenced for [Pt(dmso)$_2$RCl] and [Pt(dmso)$_2$R$_2$] compounds (R = Me, aryl),[1b] and in phosphane-dmso substitution reactions.[4b] Likewise, a SMe_2 dissociative pathway was deduced for the synthesis of [Pt(SMe$_2$)$_2$MeCl] by the methyl-chloro exchange approach.[10] At the same time, dmso seems to stabilize the tetracoordinate methylated complexes preventing their decomposition, which is significant only in concentrated warm solutions, while dissociation of coordinated dmso in CH_2Cl_2 might favor the intermolecular degradation of the methyl complexes, which occurs even at room temperature.

CONCLUSIONS

In this work, we have shown that the synthesis of *trans*-[Pt(dmso)$_2$MeCl], using *cis*-[Pt(dmso)$_2$Cl$_2$] and $SnMe_4$ as starting materials and dmso as the solvent, involves a process where the formation of *cis*-[Pt(dmso)$_2$Me$_2$] is kinetically faster than the formation of the corresponding chloromethylplatinum derivative. Thus, with the aim to obtain *trans*-[Pt(dmso)$_2$MeCl] as a sole product, the distribution reaction between *cis*-[Pt(dmso)$_2$Cl$_2$] and *cis*-[Pt(dmso)$_2$Me$_2$] is the key step to improve the yield of *trans*-[Pt(dmso)$_2$MeCl] up to 65%. At the same time, the synthesis of *cis*-[Pt(dmso)$_2$Me$_2$] has also been improved by shortening the reaction time and the excess of $SnMe_4$ previously reported.[1b]

EXPERIMENTAL SECTION

General Procedures. All reactions were performed under an argon atmosphere using standard Schlenk techniques. Unless otherwise stated, reagents and solvents were used as received from commercial sources. The complex *cis*-dichlorobis(dimethyl sulfoxide)platinum(II) was prepared as described in the literature.[2] All solvents were deoxygenated prior to use. Dimethyl sulfoxide was distilled under argon over calcium hydride and then was passed through a basic Alumina column. NMR spectra experiments were done in a Varian Mercury 300, Unity 300, or Unity 500 Plus spectrometer. Compounds **1** and **2** were characterized by comparison with their previously reported NMR data.[1,2]

Synthesis of *cis*-[Pt(dmso)$_2$Me$_2$] (1). In a 25 mL ampoule with TPFE valve, *cis*-[Pt(dmso)$_2$Cl$_2$] (2.015 g, 4.776 mmol), $SnMe_4$ (1.60 mL, 11.6 mmol) and dmso (6 mL) were completely submerged into an oil bath and stirred under an argon atmosphere at 80 °C until a colorless solution was formed (2 – 4 h). Then, dmso was removed to dryness at 80 °C under vacuum (2 mbar) as fast as possible in order to avoid decomposition of product. The brown solid crude was washed with Et_2O (3 × 20 mL), dissolved in 50 mL of CH_2Cl_2 and stirred with activated charcoal (2 g) at room temperature for 30 min. After filtration, the colorless solution was dried under vacuum (30 °C, 300 mbar) to obtained complex **1** as a white solid (1.476 g, 82%).

Synthesis of *trans*-[Pt(dmso)$_2$MeCl] (2). In a 50 mL Schlenck flask, *cis*-[Pt(dmso)$_2$Cl$_2$] (0.650 g, 1.54 mmol), *cis*-[Pt(dmso)$_2$Me$_2$] (0.588 g, 1.54 mmol) and CH_2Cl_2 (10 mL) were stirred under an argon atmosphere at room temperature for 24 h. Then, activated charcoal (1 g) was added and the solution was stirred at room temperature during 30 minutes. After filtration, the colorless solution was dried under vacuum (30 °C, 300 mbar), and the resulting solid was extracted with EtOH, filtered off and dried under vacuum (30 °C, 50 mbar) to give **2** as a white solid (0,804 g, 65%).

AUTHOR INFORMATION

Corresponding Authors

*Email: juanc.flores@uah.es (J.C.F.), ernesto.dejesus@uah.es (E.d.J).

ACKNOWLEDGMENT

This work was supported by the Spanish Ministerio de Economía y Competitividad (project CTQ2011-24096). E.A.B. is grateful to the Universidad de Alcalá for an FPI Doctoral Fellowship.

REFERENCES

(1) a) C. Eaborn, K. Kundu, A. Pidcock, *J. Organomet. Chem.* **1979**, *170*, C18-C20; b) C. Eaborn, K. Kundu, A. Pidcock, *J. Chem. Soc., Dalton Trans.* **1981**, 933-938.

(2) R. Romeo, L. M. Scolaro, *Inorg. Synth.* **1998**, *32*, 153-158.

(3) a) G. L. Petretto, M. Wang, A. Zucca, J. P. Rourke, *Dalton Trans.* **2010**, *39*, 7822-7825; b) V. Khlebnikov, M. Heckenroth, H. Mueller-Bunz, M. Albrecht, *Dalton Trans.* **2013**, *42*, 4197-4207.

(4) a) C. G. Arena, G. Bruno, M. G. De, E. Rotondo, D. Drommi, F. Faraone, *Inorg. Chem.* **1993**, *32*, 1601-1606; b) R. Romeo, S. L. Monsu, M. R. Plutino, d. B. F. Fabrizi, G. Bottari, A. Romeo, *Inorg. Chim. Acta* **2003**, *350*, 143-151; c) R. Romeo, G. D'Amico, *Organometallics* **2006**, *25*, 3435-3446; d) R. Romeo, M. R. Plutino, A. Romeo, *Helv. Chim. Acta* **2005**, *88*, 507-522; e) R. Romeo, G. Alibrandi, *Inorg. Chem.* **1997**, *36*, 4822-4830.

(5) a) S. Lanza, F. Nicolo, G. Tresoldi, *Eur. J. Inorg. Chem.* **2002**, 1049-1055; b) S. Lanza, S. L. Monsu, G. Rosace, *Inorg. Chim. Acta* **1994**, *227*, 63-69.

(6) a) G. Minghetti, A. Doppiu, S. Stoccoro, A. Zucca, M. A. Cinellu, M. Manassero, M. Sansoni, *Eur. J. Inorg. Chem.* **2002**, 431-438; b) A. Zucca, G. L. Petretto, S. Stoccoro, M. A. Cinellu, M. Manassero, C. Manassero, G. Minghetti, *Organometallics* **2009**, *28*, 2150-2159; c) A. Zucca, D. Cordeschi, S. Stoccoro, M. A. Cinellu, G. Minghetti, G. Chelucci, M. Manassero, *Organometallics* **2011**, *30*, 3064-3074; d) L. Maidich, G. Zuri, S. Stoccoro, M. A. Cinellu, M. Masia, A. Zucca, *Organometallics* **2013**, *32*, 438-448.

(7) M. R. Plutino, L. Fenech, S. Stoccoro, S. Rizzato, C. Castellano, A. Albinati, *Inorg. Chem.* **2010**, *49*, 407-418.

(8) a) A. Zucca, G. L. Petretto, S. Stoccoro, M. A. Cinellu, G. Minghetti, M. Manassero, C. Manassero, L. Male, A. Albinati, *Organometallics* **2006**, *25*, 2253-2265; b) A. Zucca, A. Doppiu, M. A. Cinellu, S. Stoccoro, G. Minghetti, M. Manassero, *Organometallics* **2002**, *21*, 783-785.

(9) D. Minniti, G. Alibrandi, M. L. Tobe, R. Romeo, *Inorg. Chem.* **1987**, *26*, 3956-3958.

(10) M. C. Aversa, P. Bonaccorsi, M. Cusumano, P. Giannetto, D. Minniti, *J. Chem. Soc., Dalton Trans.* **1991**, 3431-3434.

(11) a) F. Wen, H. Boennemann, *Appl. Organomet. Chem.* **2005**, *19*, 94-97; b) E. Costa, P. G. Pringle, M. Ravetz, R. J. Puddephatt, *Inorg. Synth.* **1997**, 284-286; c) H. C. Clark, L. E. Manzer, *J. Organometal. Chem.* **1973**, *59*, 411-428.

(12) G. S. Hill, M. J. Irwin, C. J. Levy, L. M. Rendina, R. J. Puddephatt, *Inorg. Synth.* **1998**, *32*, 149-153.

(13) a) *Gmelin Handbook of Inorganic Chemistry, Supplementary Work, Vol. 29: Organotin Compounds, Pt. 2: Tetraorganyltin Compounds R3SnR'. 8th Ed*, Springer, **1975**; b) A. G. MacDiarmid, Editor, *Organometallic Compounds of the Group IV Elements, Vol. 1: The Bond to Carbon, Pt. 2*, Dekker, **1968**; c) W. P. Neumann, *The Organic Chemistry of Tin (Collection of Chemical and Chemical-Technology Contributions, New Series, No. 63)*, Enke Verlag, **1967**.

(14) C. Eaborn, K. J. Odell, A. Pidcock, *J. Chem. Soc., Dalton Trans.* **1978**, 357-368.

(15) G. P. C. M. Dekker, A. Buijs, C. J. Elsevier, K. Vrieze, P. W. N. M. Van Leeuwen, W. J. J. Smeets, A. L. Spek, Y. F. Wang, C. H. Stam, *Organometallics* **1992**, *11*, 1937-1948.

(16) a) E. A. Baquero, J. C. Flores, J. Perles, P. Gomez-Sal, E. de Jesus, *Organometallics* **2014**, *33*, 5470-5482; b) E. A. Baquero, S. Tricard, J. C. Flores, J. E. de, B. Chaudret, *Angew. Chem. Int. Ed.* **2014**, 13220-13224.

(17) R. Romeo, L. M. Scolaro, N. Nastasi, B. E. Mann, G. Bruno, F. Nicolo, *Inorg. Chem.* **1996**, *35*, 7691-7698.

(18) Similar yield in larger scale syntheses up to 2g of *cis*-[$Pt(dmso)_2Cl_2$].

(19) J. D. Scott, R. J. Puddephatt, *Organometallics* **1983**, *2*, 1643-1648.

(20) R. J. Puddephatt, P. J. Thompson, *J. Organomet. Chem.* **1976**, *120*, C51-C52.

Chapter III. Sulfonated Water-Soluble N-Heterocyclic Carbene Silver(I) Complexes: Behavior in Aqueous Medium and as NHC-Transfer Agents to Platinum(II)

Edwin A. Baquero, Gustavo F. Silbestri, Pilar Gómez-Sal, Juan C. Flores, and Ernesto de Jesús, *Organometallics*, **2013**, *32*, 2814–2826. *One of the most read articles in April 2013*.

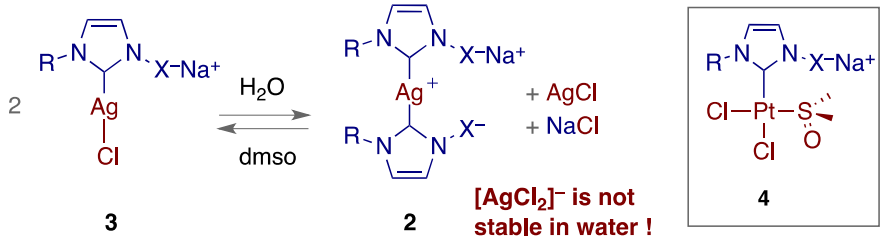

Sulfonated Water-Soluble N-Heterocyclic Carbene Silver(I) Complexes: Behavior in Aqueous Medium and as NHC-transfer Agents to Platinum(II)

Edwin A. Baquero*, Gustavo F. Silbestri, Pilar Gómez-Sal, Juan C. Flores,* and Ernesto de Jesús**

Departamento de Química Inorgánica, Campus Universitario, Universidad de Alcalá, 28871 Alcalá de Henares, Madrid, Spain.

ABSTRACT

This report describes the synthesis of water-soluble silver(I) and platinum(II) complexes bearing sulfonated mono- or dianionic N-heterocyclic carbene ligands. Thus, treatment of the corresponding zwitterionic imidazolium derivative with silver(I) oxide in water afforded the light-sensitive bis(carbene) complexes $Ag[Ag(NHC)_2]$ ($\mathbf{2}^{Ag+}$), which were transformed into the stable salts $Na[Ag(NHC)_2]$ (**2**) by addition of sodium chloride. In contrast, the same reaction in dmso afforded mono(carbenes) of general formula Na[AgCl(NHC)] (**3**). The solvent-dependence of the reaction product can be rationalized on the basis of the equilibrium $[AgCl_2]^- \leftrightarrow AgCl + Cl^-$. The precipitation of silver chloride is more favored in protic solvents than in aprotic solvents such as dmso, thus explaining the formation of bis(carbenes) in water. The formation of silver chloride may also promote the hydrolysis of silver NHC complexes under some conditions. The water-soluble platinum(II) complexes $Na[PtCl_2(dmso)(NHC)]$ were synthesized by using either mono(carbene) silver complexes **3** as carbene-transfer agents or by direct metalation of the imidazolium salt with *cis*-$[PtCl_2(dmso)_2]$ in the presence of $NaHCO_3$ as base. The (NHC)Pt(II) complexes were tested as catalysts for the hydration of alkynes in the aqueous phase and found to be active in neat water without the need for acidic co-catalysts.

INTRODUCTION

In terms of coordination versatility and stability, N-heterocyclic carbenes (NHCs) have proven to be a superb class of ancillary ligands in modern day organometallic chemistry.[1,2] In particular, those derived from imidazole are characterized by their very robust bonds to metals and their strong σ-donor capabilities,[3] forming excellent catalysts for a broad number of homogenous processes.[4] Applications outside catalysis have led to recent developments in the fields of medicinal, luminescent, or functional materials.[5] The advantages of using water-soluble metal complexes for some of these applications are evident, and a convenient way to

render metal NHC complexes water-soluble involves the attachment of hydrophilic substituents to the NHC ligand (sulfonates, carbonates, ammonium groups, sugar moieties, polyethers…).[6] Herrmann and coworkers published the first examples of such water-soluble NHC complexes in a patent filed in 1995.[7] Several years later, Özdemir and coworkers reported the synthesis of 2,3-dimethylfuran catalyzed by a water-soluble NHC ruthenium catalyst.[8] In the last few years, new water-soluble NHC metal complexes have been reported as catalysts in aqueous-phase processes, including ruthenium complexes in olefin metathesis,[9] allylic alcohol isomerizations,[10] or acetophenone hydrogenations,[11] palladium complexes in cross-coupling reactions,[12,13] gold complexes in alkyne hydrations,[14-16] iridium complexes in transfer hydrogenations,[17] or copper complexes in click reactions.[18] Two recent reviews concerning the synthesis and applications of water-soluble NHC transition-metal complexes in catalysis have appeared in the last few months.[19]

Platinum(II) complexes containing conventional monodentate[20,21-23] or chelating[23,24] NHC ligands have proven to be useful in a variety of catalytic processes in organic solvents, such as for the diboration of unsaturated molecules,[25] tandem hydroboration-cross coupling,[26] or reductive cyclation of diynes and enynes,[27] and also as metal-based chemotherapeutic agents.[28] However, platinum complexes containing hydrophilic NHC ligands were unknown until recently, when we reported the synthesis of water-soluble (NHC)Pt(0) complexes that could be used as recoverable catalysts for the hydrosilylation of alkynes in water at room temperature.[29]

Although the applications of water-soluble NHC complexes are progressing rapidly, there is as yet little information available concerning basic aspects of the chemical reactivity of these complexes in water, including the limits of the hydrolytic stability of the metal-NHC bonds. However, water offers exceptional chemical reactivity due to its unique properties, such as its ability to solvate salts and polar compounds or its high dielectric constant. Our aim with this work was to undertake a study of water-soluble NHC platinum complexes and their aqueous-phase chemical reactivity. In this first report, we discuss the synthesis of water-soluble complexes of silver(I) and platinum(II) with the sulfonated NHC ligands **a**–**e** shown in Figure 1. The platinum(II) complexes have been tested in the catalytic hydration of alkynes in aqueous phase. Special emphasis has been paid to understanding the effects of water on the formation of silver(I) NHC complexes.

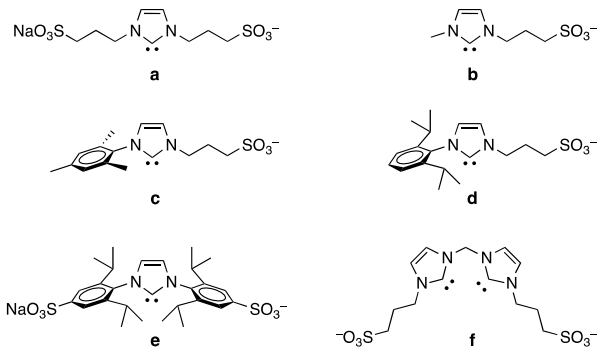

Figure 1. Sulfonate NHC ligands used in this work

RESULTS AND DISCUSSION

Synthesis and Characterization of Mono and Bis(carbene) Silver(I) Complexes. The preparation of water-soluble NHC Pt(II) complexes was initially attempted by way of silver intermediates. Silver NHC complexes are excellent agents for the transfer of carbenes to a variety of other metals in straightforward reactions and, at the same time, are readily synthesized by treating imidazolium salts with silver(I) oxide.[30-33] To this end, complexes **2b–d** of general formula $Na[Ag(NHC)_2]$ (Scheme 1(a)) were prepared by the procedure reported in the literature based on the addition of sodium chloride to a mixture of silver(I) oxide and the corresponding imidazolium salt **1b–d** in water.[15,28] The new complex **2e** was similarly obtained starting from the imidazolium **1e**.[13] As discussed below, transformation of imidazolium salt **1a** into complex **2a** invariably stopped when the molar ratio of both compounds reached a value of approximately 40-60%. The role played by the sodium halide is outlined in Scheme 1(b). Imidazolium derivatives **1** are zwitterionic compounds, with the cationic charge internally balanced by one sulfonate. As such, their deprotonation with silver oxide results in compounds $\mathbf{2}^{\mathbf{Ag+}}$, which contain an argentate anion $[Ag(NHC)_2]^-$ and a *naked* Ag^+ counterion. The latter is replaced by Na^+ upon addition of sodium chloride. This pathway has been demonstrated by the stepwise isolation of compounds $\mathbf{2e}^{\mathbf{Ag+}}$ and **2e**, whose structures have been confirmed by X-ray diffraction studies (vide infra). The sensitivity of the resulting compound to light is significantly affected by the nature of the cation. Thus, the darkening of $\mathbf{2e}^{\mathbf{Ag+}}$ in the presence of light is appreciable in the solid state as well as in solution, whereas the sodium salt **2e** is stable for an indeterminate period of time under both conditions.

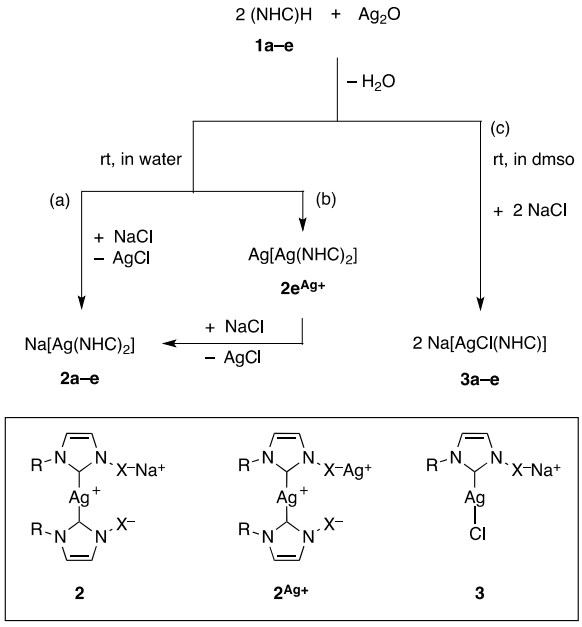

Scheme 1. Formation of Bis (**2**) and Mono(carbene) (**3)** Complexes of Silver(I) with Sulfonated NHC Ligands.

Mono(carbene) complexes with sulfonated NHC ligands of general formula $[AgX(NHC)]^-$ were previously unknown. In the above procedure to synthesize bis(carbene) complexes **2**, NaCl was added after formation of the $Ag[Ag(NHC)_2]$ ($\mathbf{2^{Ag+}}$) intermediates. It might be reasonable to infer that the precipitation of silver chloride after the addition of NaCl could preclude the rearrangement required to afford mono(carbene) complexes. However, the fact is that bis(carbene) complexes were likewise obtained when NaCl was added to the imidazolium salts **1** in water before silver oxide. Instead, the solvent was found to be fundamental in determining the final compound, with the mono(carbene) complexes **3a–e** being obtained in good yields (>80%) when the reactions were performed in dimethyl sulfoxide instead of water (Scheme 1(c)).

As would be expected, mono(carbenes) **3b–e** evolved into the corresponding bis(carbenes) **2b–e** in water at room temperature (Scheme 2). At this point it is important to note that the conversion of mono- into bis(carbenes) was accompanied by the precipitation of silver chloride instead of the usual formation of the ion $[AgCl_2]^-$ in solution. The conversion **3** → **2** were found to be reversible, with complexes **2b–e** affording mono(carbenes) **3b–e** in the presence of AgCl and NaCl when water was replaced by dmso. The transformations were fast in both directions at room temperature except for the complexes with the most sterically demanding NHC ligand (**2e** and **3e**). These results unequivocally show that the outcome of

the reaction of imidazolium salts **1** with Ag_2O is governed by the (solvent-dependent) thermodynamic stability of the reaction products.

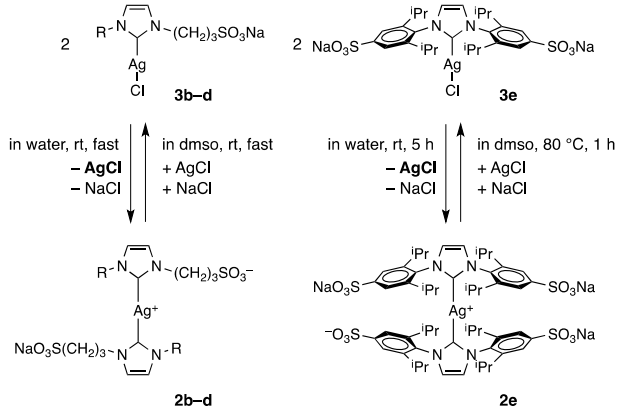

Scheme 2. Solvent-dependent and Reversible Transformation of Mono- (**3**) into Bis(carbene) Silver(I) Complexes (**2**).

Imidazolium halides are known to afford NHC-silver complexes of stoichiometry AgX(NHC) (X = halide), which adopt neutral mono- (**I**) or ionic bis(carbene) (**II**) architectures[30] that are often in equilibrium in solution (Scheme 3).[34,35] The formation of bis(carbene) complexes of type **III**, where the counterion is X^- instead of AgX_2^-, is usually associated with imidazolium salts containing non-coordinating anions, although it has also been reported with imidazolium halides.[36] Note that the NHC ligands in the chemical formulas of **I**–**III** are considered neutral for generalization purposes. The fact that the silver complexes reported here are negatively charged is irrelevant for the following discussion.

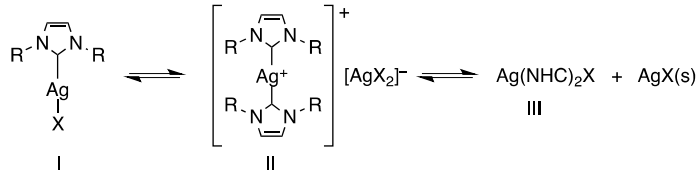

Scheme 3. Equilibria involving Different Structures found for Silver(I) NHC Complexes.

It has been noted previously that the neutral mono(carbene) form **I** is, in general, favored with regard to the ionic bis(carbene) form **II** by bulkier NHCs and less polar solvents.[34] Despite this, our understanding of the formation of bis(carbenes) in protic solvents is incomplete without taking into account the equilibrium between **II** and **III**. The thermodynamics of this equilibrium is mainly determined by the stability of the dihalidoargentate(1–) anions with regard to the precipitation of silver halide. The constant *K*

for the equilibrium $[AgX_2]^- \leftrightarrow AgX + X^-$ (X^- = halide) can be determined from the overall formation constant of the complex AgX_2^- (β_2) and the solubility constant of the silver halide (K_s).[37] A clear picture emerges from the values shown in Table 1. Complexes $[AgX_2]^-$ are quite stable in dimethyl sulfoxide, acetonitrile, or dimethylformamide ($K \sim 10^{-1} - 10^{-2}$) whereas the precipitation of silver halides is strongly favored in water or methanol ($K \sim 10^4 - 10^5$). This is because the halides are less solvated in aprotic than in protic solvents, whereas the opposite occurs with the $[AgX_2]^-$ ions.[37] The equilibria in Scheme 3 are therefore expected to be shifted towards the formation of bis(carbenes) of type **III** in protic solvents due to the poor stability of the AgX_2^- anions in these solvents irrespective of the factors governing the mono(carbene)-bis(carbene) equilibrium **I** ↔ **II**.

Table 1. Constants for Equilibria involving Silver(I) Ions and Halides at 25 °C

equilibrium	X	water	methanol	dmso	acetonitrile	dmf
$Ag^+ + 2\,X^- \rightleftharpoons [AgX_2]$, $p\beta_2$[a]	Cl	-5.4	-7.9	-11.7	-13.4	-16.3
	Br	-7.6	-10.6	-11.4	-13.7	-16.6
	I	-11.2	-14.8	-12.5	--	-17.8
$AgX \rightleftharpoons Ag^+ + X^-$, pK_s[a]	Cl	9.8	13.1	10.4	12.9	14.5
	Br	12.3	15.2	10.6	12.9	15.0
	I	16.0	18.3	11.4	--	15.8
$[AgX_2]^- \rightleftharpoons AgX + X^-$, pK[b]	Cl	-4.4	-5.2	1.3	0.5	1.8
	Br	-4.7	-4.6	0.8	0.8	1.6
	I	-4.8	-3.5	1.1	--	2.0

[a] Data from ref 37. [b] Determined as $pK = -(p\beta_2 + pK_s)$

To support the above hypothesis, a sample of the mono(carbene) complex **3e** was dissolved in methanol-d_4 and monitored by ^{1}H NMR spectroscopy. As expected, the transformation of **3e** into **2e** was accompanied by AgCl precipitation, although the process was quite slow, taking more than one day at 90 °C to go to completion. On the other hand, a look at the literature confirmed that water-soluble NHC silver complexes obtained by the reaction of imidazolium salts with silver oxide in the presence of halide anions have always been obtained in the form of bis(carbene) complexes in water.[14,38-41] It should be noted that Cazin and coworkers reported the preparation of mono(carbene) silver complexes of general formula [(NHC)AgCl] in

water.[42] However, these reactions involved the formation of complexes containing hydrophobic NHC ligands (IPr, IMes, or ICy), whose insolubility in water is most likely responsible for displacing the equilibria in Scheme 3 towards the mono(carbene) form **I**.

The hydrolytic stability of the NHC silver complexes merits a comment. Bis(carbene) complexes **2b**-**e** were found to be indefinitely stable in air in the solid-state, whereas mono(carbenes) **3a**–**e** were extensively hydrolyzed under the same conditions and had to be stored under an inert atmosphere. The stability in solution is, however, more complex to describe because it depends on numerous factors, some of which are discussed below. Bis(carbenes) **2b**-**e** again showed significant hydrolytic stability in pure water and their aqueous solutions did not show any noticeable degradation (as evidenced by ^{1}H NMR spectroscopy) when heated for hours or even days at 90 °C. Complex **2e** was particularly stable in water and remained unaltered for at least 24 h at 100 °C, and two days at 130 °C, with only 3% hydrolysis. The behavior of complex **2a**, in contrast, is quite remarkable. This complex has previously been described to be unstable in water.[14] Indeed, we have discussed above that all attempts to synthesize this complex pure failed as it was always obtained as an approximately 40-60% mixture with the corresponding imidazolium salt **1a**. In an attempt to understand this result, two NMR tubes containing a D_2O solution of the mixture of **2a** and **1a** (previously separated from the silver oxide/silver chloride precipitate) were prepared. One of these samples was heated for 24 h at 90 °C and showed no apparent changes in the composition of the **2a**/**1a** mixture. This result clearly indicates that **2a** is intrinsically stable towards hydrolysis. In a different experiment, in which sodium chloride (10 equiv. with respect to silver) was added to the second sample, complex **2a** was completely hydrolyzed in less than one hour at room temperature. Acceleration of the hydrolysis upon addition of NaCl was also observed for other bis(carbene) complexes, although the effect was less marked with NHC ligands that are hydrolyzed more slowly.[43] The same effect was observed when bis(carbenes) were heated in dmso with a small amount of added water. For instance, the percentage of hydrolysis of **2c** after 15 h at 90 °C rose from 3% to approximately 30% in the presence of NaCl. Interestingly, the formation of small amounts of the mono(carbene) **3c** was observed in the last process.

Any analysis of the hydrolytic stability of mono(carbene) complexes **3** is necessarily complicated by the fact discussed above, namely that they evolve to the corresponding bis(carbenes) in water. Nevertheless, the behavior of complex **3a** was unique because it was completely hydrolyzed in water instead of evolving to the corresponding bis(carbene). This result does not necessarily mean that **3a** is intrinsically more reactive with water than the other mono(carbenes) but only that hydrolysis of the NHC-Ag bond occurs faster than the transfer of NHC ligands between Ag centers in this case. Another important point in respect to mono(carbenes) is the reversibility of the hydrolysis observed in the solid state (Scheme 4(a)). Thus, when a hydrolyzed solid sample of **3a** containing 24% of the NHC ligand in the form

of the Ag complex (and 76% as imidazolium salt) was heated in dmso at 90 °C, the percentage of the mono(carbene) complex increased to 80% after 15 h. Similar transformations were observed for other complexes, although they were in general slower as the steric demand of the NHC ligand increased.

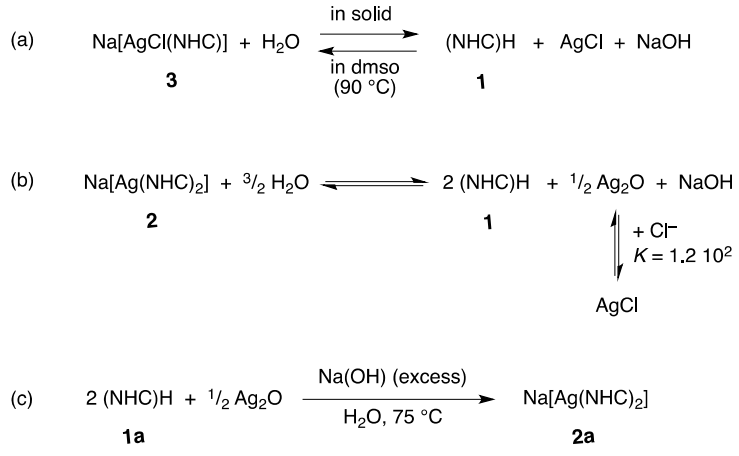

Scheme 4. Hydrolysis of the Silver NHC Complexes.

Although the hydrolysis of silver NHC complexes is a complex phenomenon in which both thermodynamics and kinetics play an important role, we can nevertheless extract several simple ideas. First, we should assume that solvation plays an important role in the thermodynamics of this hydrolysis to explain the differences found between mono(carbenes) in the solid state and in solution. Second, hydrolysis of the complexes containing two sulfonatopropyl substituents (**2a** and **3a**) is quite interesting because forward (hydrolysis) and reverse processes are fast and therefore controlled by the thermodynamics. Third, the effect of the addition of sodium chloride on the hydrolysis of bis(carbenes) is likely thermodynamic in nature and might be motivated by displacement of the equilibrium shown in Scheme 4(b) from the bis(carbene) **2** to the imidazolium salt **1** due to the favorable formation of silver chloride from silver oxide (K = 1.2 10^2 in water).[44] Indeed, the bis(carbene) complex **2a** was obtained spectroscopically pure by reaction of the imidazolium salt **1a** with silver oxide in the presence of an excess of sodium hydroxide (Scheme 4(c)).

The new NHC silver complexes **2e**, **2e**$^{Ag+}$ and **3a–e** were characterized by electrospray mass spectrometry and ^{1}H and ^{13}C NMR spectroscopy. These complexes were isolated as spectroscopically pure solids which afforded inaccurate C, H, and N elemental analyses due to the presence of solvent molecules trapped within their structures (see X-ray structures below) and the likely contamination with inorganic salts. The narrow range in which carbenic C^2 resonances are found (176.8–182.7 ppm, Table 2) is characteristic of N-alkyl and N-aryl silver

imidazolylidene complexes but cannot be used to differentiate between mono- and bis(carbene) structures.[33,45] The coupling constant of the C^2 resonance with $^{107,109}Ag$ is, in contrast, very informative when the intermolecular exchange of NHC ligands between silver centers is slow enough to observe splitting of the signal.[32,35] The $^1J(^{13}C–Ag)$ constants of neutral mono(carbenes) are, in general, 50-60 Hz larger than those of their corresponding ionic bis(carbenes) (values in the range 275-255 Hz for ^{109}Ag and 235-220 Hz for ^{107}Ag in mono(carbenes) versus 220-190 Hz for ^{109}Ag and 190-165 Hz for ^{107}Ag in bis(carbenes)).[31,33,35,45] The constants measured for complexes **2e** and **3e**, which bear the same NHC ligand, are within the expected ranges for their proposed structures (Table 2). In contrast, the C^2 resonances of the less encumbered complexes in Table 2 were observed as singlets (no $^1J(^{13}C–Ag)$ coupling), thereby suggesting that these complexes undergo intermolecular NHC ligand exchange that is fast on the NMR time scale. It is important to note that some of the bis(carbene) complexes listed in Table 2 undergo fast NHC exchange even in the absence of $[AgCl_2]^-$ counterions (or NaCl/AgCl).

Table 2. Chemical Shifts and Coupling Constants for the Carbenic C^2 Carbon in Silver NHC Complexes **2** and **3**

complex	δ (C^2, ppm)	$^1J(^{109}Ag\text{-}^{13}C)$, $^1J(^{107}Ag\text{-}^{13}C)$ in Hz
	Bis(carbene) complexes, $Na[Ag(NHC)_2]$ in D_2O	
2a	178.4 (singlet)	
2b[a]	179.7 (singlet)	
2c[b]	180.6 (two doublets)	208, 180
2d[b]	182.7 (broad doublet)	193.9
2e	181.2 (two doublets)	217, 188
	Mono(carbene) complexes, Na[AgX(NHC)] in dmso-d_6	
3a	176.8 (broad singlet)	--
3b	177.8 (singlet)	--
3c	not observed	--
3d	not observed	--
3e	181.4	268, 232

[a] From ref [14]. [b] From ref [38].

The ESI mass spectra of the silver complexes, recorded in methanol, further supported the proposed structures. Thus, in the case of the bis(carbene) complexes **2e** and **2e^{Ag+}**, the most intense peaks correspond to the whole molecular fragment ionized by the loss of one or more cations (Na^+ or Ag^+) in negative mode, or by addition of a hydrogen ion, probably from the solvent, in positive mode. The same anion $[M - Na]^-$ was also observed in the case of the monocarbene complexes **3a–e**, although the most intense peaks were those corresponding to bis(carbene) fragments, probably due to the rearrangement of these complexes in protic solvents (Scheme 2). Conversely, the ESI mass spectra of **3c** recorded in acetonitrile showed intense peaks for the mono(carbene) ions $[M - Na]^-$ and $[M - Na - Cl + CN]^-$. Acetonitrile appears to be the most likely source of CN^- in the latter fragment.[46]

X-ray Crystal Structures of the Silver(I) Complexes 2e, 2e^{Ag+}, and 3a. The crystal structures of the NHC silver complexes **2e, 2e^{Ag+}**, and **3a** have been determined by X-ray diffraction methods. In the case of complex **2e**, X-ray determinations were performed on two different crystalline samples, one obtained from dichloromethane/methanol solvent mixtures (**2e**•6MeOH) and the other from acetone/dmso (**2e**•5dmso•H_2O). The structures of **2e**•6MeOH, **2e**•5dmso•H_2O, and **2e^{Ag+}** contain similar $[Ag(NHC)_2]^{3-}$ moieties packed in different arrangements together with counterions and solvent molecules.

Figure 2 shows the molecular structure of the $[Ag(NHC)_2]^{3-}$ unit in **2e**•6MeOH together with a selection of distances and angles found in the three structures that contain this unit. The two carbene ligands are almost linearly coordinated to Ag in all three structures, with C_{NHC}-Ag-C_{NHC} angles ranging from 178.3(4)° to 179.8(4)°. The NHC rings are twisted with respect to each other by between 40.2° and 45.5°, thereby avoiding the steric hindrance that would otherwise arise between the bulky 2,6-diisopropylphenyl groups. The Ag-C_{NHC} distances are in the narrow range 2.090(12)–2.111(5) Å. These parameters can be compared with those found in $[Ag(IPr)_2][SbF_6]$ [180° for the C_{NHC}-Ag-C_{NHC} angle, 37.8° for the angle between the NHC rings, and 2.13(2) Å for the Ag-C_{NHC} distances].[47]

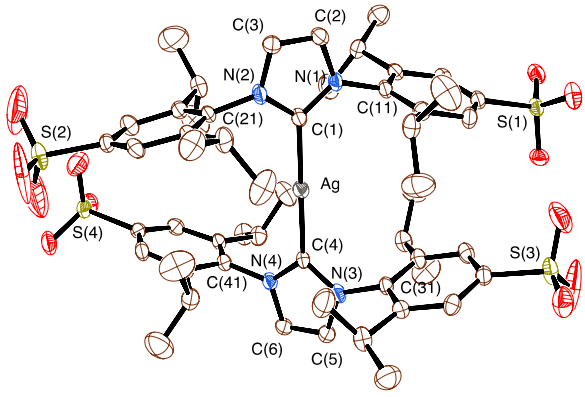

Figure 2. ORTEP diagram (50% probability ellipsoids) of the organometallic moiety of **2e**•6MeOH (H and Na atoms omitted for clarity). Essentially identical $[Ag(NHC)_2]^{3-}$ moieties are present in the crystal structures of **2e**•5Me_2SO•H_2O and $\mathbf{2e^{Ag+}}$. Selected bond lengths (Å) and angles (º) for **2e**•6MeOH: Ag–C(1), 2.115(5); Ag–C(4), 2.109(5); C(1)–Ag–C(4), 178.3(2); N(1)-C(1)-N(2), 103.2(4); N(3)-C(4)-N(4), 103.5(4). Selected bond lengths (Å) and angles (º) for **2e**•5Me_2SO•H_2O: Ag–C(1), 2.090(12); Ag–C(28), 2.101(12); C(1)-Ag-C(28), 178.3(4); N(1)-C(1)-N(1), 102.6(9); N(3)–C(28)–N(4), 103.5(10). Selected bond lengths (Å) and angles (º) for $\mathbf{2e^{Ag+}}$: Ag(1)–C(1), 2.111(7); C(1)–Ag(1)–C(1'), 179.8(4); N(1)-C(1)-N(2), 103.9(6) [both NHCs are related by a crystallographic two fold axis].

The extended structure of $\mathbf{2e^{Ag+}}$ consists of one-dimensional chains assembled by bridging Ag^+ counterions lying in a pseudotetrahedral environment between the sulfonate groups of two adjacent $[Ag(NHC)_2]^{3-}$ moieties, with mean short $Ag^+\cdots{}^-OSO_2R$ contacts of 2.59 Å (Figure 3). These negatively charged chains are aligned along the crystallographic *b* axis and stacked along the *a* axis via the sodium cations, which complete their coordination spheres with two water molecules (mean $Na^+\cdots O$ distance of 2.33 Å for sulfonate and 2.40 Å for water). The $[Ag(NHC)_2]^{3-}$ moieties in **2e**•6MeOH are distributed along the crystallographic *a* and *b* axes in a similar manner to that described for $\mathbf{2e^{Ag+}}$, although they are packed together exclusively by sodium cations bridging two or three sulfonate groups (mean $Na^+\cdots{}^-OSO_2R$ distance of 2.45 Å). The coordination sphere of these Na^+ ions is completed with methanol molecules (mean $Na^+\cdots O(H)Me$ distance of 2.34 Å). The crystal packing is markedly different in the case of **2e**•5Me_2SO•H_2O. In this case, the biscarbene moieties are organized centrosymmetrically around a cluster of six sodium ions arranged in a chair-type disposition with intermetallic distances in the range 3.42–3.93 Å (Figure 4a). This hexanuclear cluster of sodium ions is supported by coordination of the oxygen atoms from the eight sulfonate groups, four molecules of dmso, and two molecules of water, most of which bridge the edges and the triangular or square-planar faces of the cluster (Figure 4b).

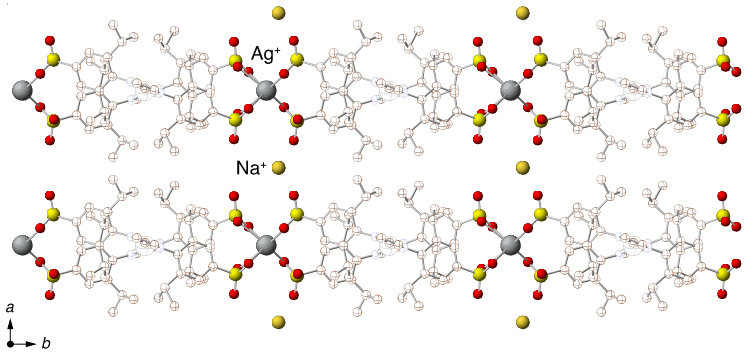

Figure 3. View of the crystal structure of **2e**$^{Ag+}$ along the crystallographic *c* axis highlighting the enchainment of $[Ag(NHC)_2]^{3-}$ moieties by interaction of the sulfonate groups with the Ag^+ counterions, and the position of the Na^+ counterions between the chains.

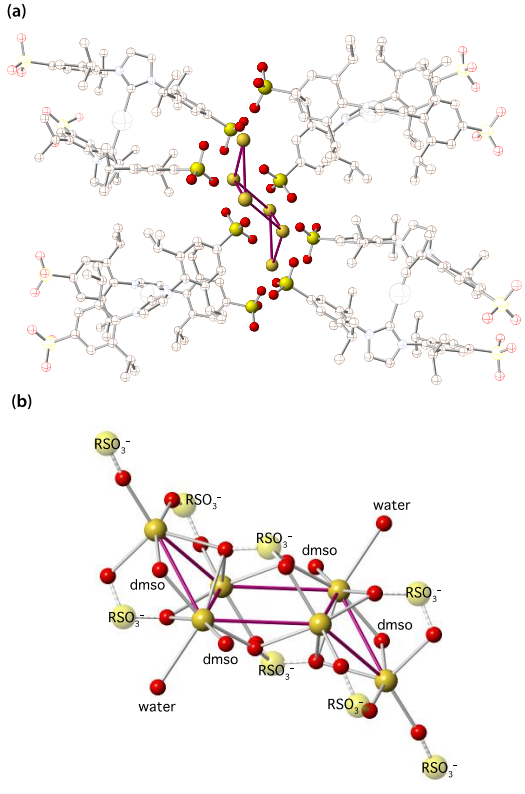

Figure 4. (a) Packing diagram showing the arrangement of $[Ag(NHC)_2]^{3-}$ moieties in **2e**•5Me_2SO•H_2O around a chair-like hexanuclear cluster of sodium ions. Solvent molecules have been omitted for clarity. (b) A detail of the hexanuclear cluster of sodium ions and its coordination sphere formed by oxygen atoms from sulfonate groups, dmso, and water.

Figure 5(a) shows a view of the crystal structure of **3e** whereas Figure 5(b) shows the molecular structure of an isolated moiety $[AgCl(NHC)]^{2-}$. The organometallic silver anions and the sodium counterions are arranged in layers. The coordination spheres of the Na^+ ions are composed by the oxygen atoms of two (Na(2)) or three (Na(1)) sulfonates from different silver moieties and one or two dmso molecules in tetrahedral environments (mean distances $Na^+\cdots{}^-OSO_2R$ = 2.27 Å, $Na^+\cdots OSMe_2$ = 2.31 Å). The C(1)–Ag–Cl angle (176.6(2)°) and the Ag–C(1) ((2.064(7) Å) and Ag–Cl(1) (2.297(4) Å) distances are very similar to those found in the nonsulfonated analogue [AgCl(IPr)] (175.2°, 2.056 Å, and 2.316 Å, respectively).[34]

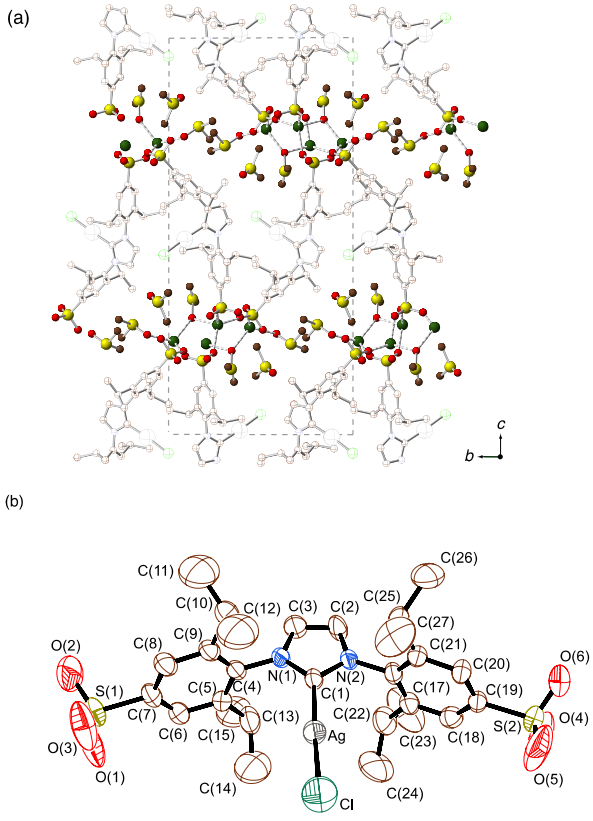

Figure 5. (a) View of the crystal structure of **3e** along the crystallographic *a* axis highlighting the interactions of Na^+ ions with the sulfonate groups of the $[AgCl(NHC)]^{2-}$ moieties and with the dmso molecules. (b) ORTEP diagram (50% probability ellipsoids) of the organometallic moiety of **3e** (H and Na atoms omitted for clarity). Selected bond lengths (Å) and angles (º): Ag–C(1), 2.063(7); Ag–Cl, 2.298(3); C(1)–N(2), 1.354(8); C(1)–N(1), 1.344(8); C(2)–N(2), 1.359(9); C(3)–N(1), 1.377(9); C(2)–C(3), 1.351(10); C(1)–Ag–Cl, 176.6(2); N(1)–C(1)–N(2), 104.3(5).

Synthesis of Platinum(II) NHC Complexes. No reaction was observed between the silver bis(carbenes) **2b–e** and the precursor *cis*-[$PtCl_2(dmso)_2$] when a mixture of both was heated in water at 90 °C for 12-14 h (Scheme 5(a)). Although the platinum precursor is poorly soluble in water, the same lack of reactivity was found in mixtures of water and dimethyl sulfoxide (50%-50%), in which the platinum precursor is soluble. In contrast, the reaction of one equivalent of the mono(carbene) silver complexes **3a–d** with the above Pt precursor in dimethyl sulfoxide led to complexes of general formula Na[$PtCl_2(dmso)$(NHC)] (**4a–d**) after heating at 80 °C for several hours (Scheme 5(b)). No transmetallation was observed with the most sterically hindered silver complex **3e** under the same conditions. These reactions took place with formation of the *cis* isomers of **4a–d** as the only Pt complexes. However, hydrolysis of the silver mono(carbenes) with traces of water, which are difficult to remove from the dmso solvent, resulted in concomitant formation of variable amounts of the corresponding imidazolium salt. The observation of hydrolysis under these conditions is not surprising given that the platinum precursor can be a source of the chlorides that favor the hydrolysis of silver NHC complexes, as we have shown above. The lack of an efficient method for separation of the platinum complexes and the imidazolium salts prompted us to search for an alternative approach to the synthesis of complexes **4**.

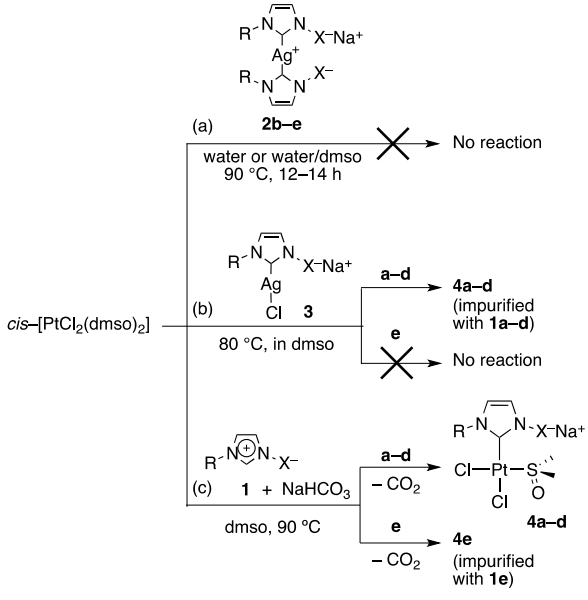

Scheme 5. Synthesis of the NHC Platinum(II) Complexes Na[$PtCl_2(dmso)$(NHC)] (**4**).

An improved procedure for the synthesis of complexes **4** consisted in the direct reaction of *cis*-[$PtCl_2(dmso)_2$] with imidazolium compounds **1** in dimethyl sulfoxide at 90 ºC in the presence of sodium hydrogencarbonate as the deprotonating agent (Scheme 5(c)). This

procedure afforded complexes **4a–d** as analytically pure solids in good to high yields (60–90%), with carbon dioxide being generated as the only by-product. Reaction times ranged from 17 to 25 h, with longer times being required for the more sterically demanding NHC ligands. Indeed, pure samples of the complex with the IPr-like NHC ligand **4e** could not be isolated due to the low conversion (65% after 10 days at 90 ºC). A similar result was obtained when replacing sodium hydrogencarbonate with sodium *tert*-butoxide as the base. Despite this, complex **4e** could still be characterized by ^{1}H and ^{13}C NMR spectroscopy and mass spectrometry. A similar procedure was used to synthesize the chelate complex **5**, which was isolated analytically pure in 76% yield from the zwitterionic bisimidazolium salt **1f** (Scheme 6).

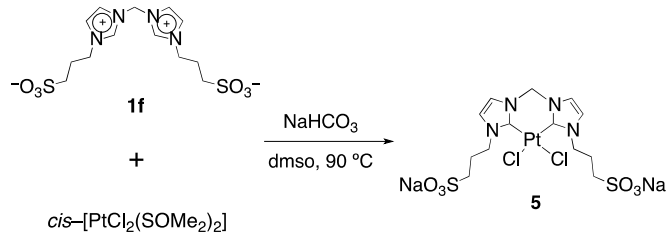

Scheme 6. Synthesis of the Bis(NHC) Platinum(II) Complex **5**.

The new water-soluble (NHC)Pt(II) complexes were characterized by ^{1}H, ^{13}C, and ^{195}Pt NMR spectroscopy, mass spectrometry, and elemental analysis. The ESI-TOF mass spectra of platinum complexes **4a–e** and **5** were recorded in methanol in negative mode and showed intense peaks corresponding to the fragments $[M - Na]^-$, with isotopic distributions matching the calculated patterns. The only clearly observed ^{195}Pt satellites in their $^{13}C\{^{1}H\}$ NMR spectra, recorded in dmso-d_6, were those of the carbenic carbon of complex **4b** ($^{1}J(^{13}C_{NHC}\text{-}^{195}Pt)$ = 1378 Hz). Solvents of relatively high viscosity, such as dimethyl sulfoxide, increase the contribution of chemical shift anisotropy to the ^{195}Pt relaxation, thereby often resulting in the broadening or disappearance of ^{195}Pt satellites.[48] Nevertheless, coordination of the NHC ligands to platinum was supported by the chemical shifts of the carbenic carbons (144.1–140.8 ppm). The ^{195}Pt chemical shifts ranged from -3474 to -3529 ppm in mono(carbenes) **4a–d**, whereas the resonance of the bis(carbene) **5** was shifted slightly to higher field (-3572 ppm). The above ^{13}C and ^{195}Pt chemical shifts are in agreement with those previously reported for *cis*-[$PtCl_2$(dmso)(NHC)] complexes.[21,22,49] The ^{1}H and $^{13}C\{^{1}H\}$ NMR spectra recorded in dimethyl sulfoxide revealed the existence of some asymmetry in mono(carbenes) **4a–d**, as seen by the lack of equivalence between (a) the two methylene protons α to the imidazole nitrogen in the sulfonatepropyl chains of **4a–d**; (b) the proton and carbon-13 nuclei in the *ortho* and *meta* positions of the mesityl or 2,6-bis(isopropyl)phenyl groups in **4c–e**; and (c) the two methyl groups of the dmso molecule coordinated to Pt in the case of complexes with asymmetrically substituted NHCs. These observations can only be explained by assuming a *cis* stereochemistry

of the square-planar metal environment, with a chloride *trans* to the carbene ligand, and with the NHC ring arranged perpendicularly to the coordination plane rotating slowly around the Pt-NHC bond on the NMR time scale.[22] The fact that this rotation is faster in water means that the α-methylene protons of the sulfonatepropyl chains and the coordinated dmso of **4a**,**b** appear as single resonances in this solvent. On the other hand, the chelate coordination in complex **5** is confirmed by the chemical nonequivalence of the two protons of the methylene bridge in the ^{1}H NMR spectrum, as would be expected for a boat conformation of the six-membered metallacycle with a slow boat-to-boat exchange of conformers on the NMR time scale.

The crystal structure of **4a** has been determined by X-ray diffraction methods. The asymmetric unit contains the organometallic dianion $[PtCl_2(dmso)(NHC)]^{2-}$ (Figure 6), together with two (disordered) sodium counterions and water molecules (not shown in Figure 6). Each sodium ion is adjacent to one sulfonate, with $RS(O_2)O^{-}\cdots Na^{+}$ distances in the range of 2.8 to 2.9 Å, whereas the nearest oxygen atoms of the other surrounding sulfonates are at 3.8-4.2 Å. The square-planar environment of the Pt atom is almost regular, with the metal lying 0.01 Å out the coordination plane defined by atoms S(3), C(1), Cl(1), and Cl(2), and the angles between cis bonds ranging from 88.1° to 91.1°. The dmso is coordinated to the metal center via the sulfur atom with the sulfur-oxygen moiety lying parallel to the Pt–C bond and pointing towards the NHC ligand. This arrangement presumably reduces any steric interactions between the methyl groups of the dmso and the heterocyclic ligand. The imidazolium ring is tilted 75.2(4)° relative to the platinum coordination plane. The Pt-C(1) distance of 1.975(16) Å is in the range of those reported for neutral *cis*-$[PtCl_2(dmso)(NHC)]$ complexes (1.88-1.99 Å).[21,22,49] The chlorine atoms are mutually arranged in a *cis* position, with the Pt-Cl distance of the chloride *trans* to the NHC ligand being significantly larger (2.360(5) versus 2.309(4) Å), as expected in light of the high sensitivity of Pt–Cl distances to the different influences of their *trans* ligands.[50]

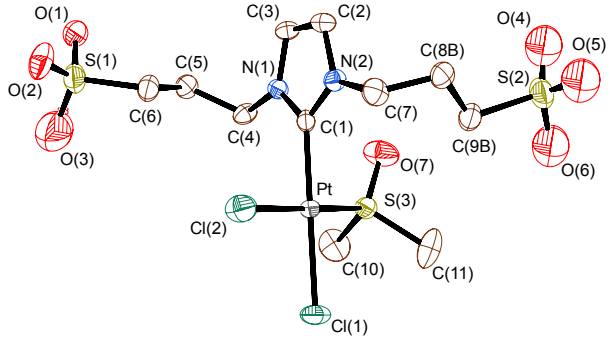

Figure 6. Molecular structure of the organometallic moiety of **4a** (50% probability ellipsoids). Selected bond lengths (Å) and angles (º): Pt–C(1), 1.975(16); Pt-Cl(1), 2.360(5); Pt–

Cl(2), 2.309(4); Pt–S(3), 2.209(4); C(1)–Pt–Cl(1), 177.8(5); S(3)–Pt–Cl(2), 177.2(2); C(1)–Pt–S(3), 91.1(5); C(1)–Pt–Cl(2), 88.1(5); Cl(1)–Pt–Cl(2), 90.38(17); S(3)–Pt–Cl(1), 90.46(16).

Hydration of Terminal Alkynes in Water. The hydration of alkynes is an important reaction for the synthesis of aldehydes or ketones. As such, major efforts have been made over the last few decades to develop new transition-metal catalysts for this reaction to replace traditional and highly toxic mercury-based catalysts.[51] Important developments in this area have included the discovery of the first anti-Markovnikov addition that yielded aldehydes from terminal alkynes, which is catalyzed by ruthenium(II) complexes,[52] or the publication of gold complexes that are highly active in acidic media.[53] In addition to gold(I) and gold(III), platinum(II) complexes are amongst the best metal catalysts for Markovnikov-selective alkyne hydration. Chatt and Duncanson reported the first platinum(II)-catalyzed hydration of alkynes using $Na_2PtCl_4 \cdot H_2O$ in ethanolic solution.[54] Subsequently, Jennings and coworkers showed that Zeise's dimer and Pt(II) halides were efficient catalysts for the addition of water to inactivated (electron-rich) terminal and internal alkynes in THF. These authors noted that the addition of acid was neither necessary nor advantageous in this case.[55] More recently, Atwood and coworkers used platinum(II) complexes with water-soluble sulfonated phosphines to hydrate alkynols in this solvent.[56] To the best of our knowledge, although NHC-Pt complexes have not been studied in this reaction, notable decreases in catalyst loadings were achieved when NHC ligands were involved with gold complexes.[57] More recently, Joó and coworkers have reported the hydration of alkynes with water-soluble sulfonated NHC gold(I) complexes in methanol/water mixtures.[14,15]

The NHC complexes **4a-d** and **5** were found to be active catalysts for the hydration of alkynes in water in the absence of an acid co-catalyst. The hydration of phenylacetylene was initially used as a benchmark reaction to compare the different Pt catalysts and to optimize the reaction conditions (Table 3). The activity of mono(carbene) complexes **4** was rather similar, reaching conversions of phenylacetylene to benzophenone of around 90% at 80 °C in 1 h (Table 3, entries 1, 8, and 15) and 100% in 3-4 h (Table 3, entries 3, 10, and 17) using Pt loadings of 2.0 mol %. The only exception was complex **4b**, which required 9 h for complete conversion (Table 3, entry 7). The bis(carbene) complex **5** also showed a similar activity to that observed for **4a,c,d**, completing the reaction in 4 h under the same conditions (Table 3, entry 19). The reaction also progressed at room temperature with catalyst **4d**, although the reaction time had to be prolonged to 24 h for completion (Table 3, entry 12).

Table 3. Hydration of Phenylacetylene Catalyzed by Complexes **4a–d** and **5** in Water[a]

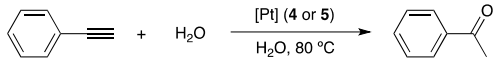

entry	catalyst	[Pt] (mol %)	time (h)	conversion (%)[b]
1	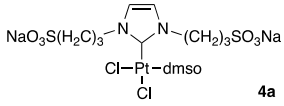 **4a**	2	1	91
2		2	2	93
3		2	4	100
4	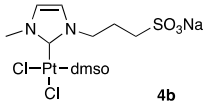 **4b**	2	1	20
5		2	2	32
6		2	3	48
7		2	9	100
8	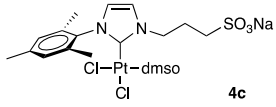 **4c**	2	1	90
9		2	2	98
10		2	3	100
11		2	8 (rt)[c]	44
12		2	24 (rt)[c]	100
13		1	3	47
14		0.5	3	30
15	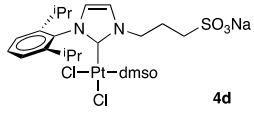 **4d**	2	1	91
16		2	2	95
17		2	4	100
18	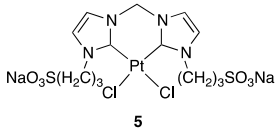 **5**	2	3	97
19		2	4	100

[a] Standard reaction conditions: 0.455 mmol phenylacetylene; 2 mL H_2O. [b] Conversions determined by ^1H NMR spectroscopy. [c] Reaction at room temperature.

We subsequently studied the hydration of selected terminal and internal alkynes catalyzed by **4c** in neat water at 80 °C (Table 4). The activity of **4c** in the addition of water to *para*-substituted phenylacetylenes decreased in the order -H > -OMe > $-CF_3$ > NO_2 (Table 3, entry

10, and Table 4, entries 1-3) thus correlating with the trend of electron-richness of the alkynes. The heterogeneous nature of the catalytic reaction cannot, however, be ignored when interpreting these results. Indeed, the limited reactivity of 3-nitrophenylacetylene may well be linked to the insolubility of this solid compound in the reaction medium (all the other phenylacetylenes tested are liquids under the same conditions). This may well also explain the lack of reactivity observed for diphenylacetylene.

Table 4. Hydration of Selected Alkynes in Water Catalyzed by Complex **4c**[a]

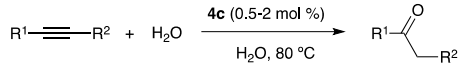

entry	R^1	R^2	[Pt] mol %	time (h)	conversion (%)[b]
1	4-MeO-Ph	H	2	5	100
2	4-CF_3-Ph	H	2	24	100
3	3-NO_2-Ph	H	2	24	2
4	HO$(CH_2)_3$-	H	0.5	0.3	100
5	HO$(CH_2)_2$-	CH_3	0.5	0.3	100
6	HOCH_2-	H	0.5	24	100 (43[c])
7	HOCH_2CH_2-	H	0.5	24	80 (23[c])

[a] Standard reaction conditions: 1 mmol alkyne; 2 mL H_2O. [b] Conversions determined by ^{1}H NMR spectroscopy. [c] Ketone yield measured by ^{1}H NMR spectroscopy using NEt_4I as internal standard.

Taking the hydration of phenylacetylene as a reference, the conversions obtained with **4c** can be compared with those reported for water-soluble NHC gold(I) complexes using the same metal loadings (2.0 mol %). Although a sulfoalkyl-substituted NHC-Au complex provided conversions of only 17% after 3 h in refluxing water (compared with 100% for **4c** in the same time period at 80 °C, entry 10, Table 3),[14] the reported activities are similar to those observed with the use of a bulky IMes-like NHC ligand (90% in 1 h at reflux; cf. entry 8, Table 3).[15] Another reference reaction for **4c** is Atwood's hydration of water-soluble alkynols with Pt(II) complexes of sulfonated phosphines.[56] Thus, in agreement with Atwood's findings, complex **4c** directs the hydration of either 3- or 4-pentynol exclusively to the formation of 5-hydroxy-2-pentanone, irrespective of the starting alkynol (Table 4, entries 4 and 5). For these reactions,

Atwood and coworkers proposed an anchimeric assistance of the unsaturated bond by the hydroxyl group of the substrate once the alkyne coordinates to the Pt center.[56] All reactions involving **4c** were complete in only 18 minutes at 80 °C with Pt loadings as low as 0.5 mol % (compared with 1 h for the sulfonated phosphine complexes). In agreement with the mechanism proposed above, the disfavored participation of the neighboring hydroxyl group explains the much slower kinetics found for the hydration of propargyl alcohol and 3-butyn-1-ol under the same conditions (Table 4, entries 6 and 7). As a consequence, extensive competitive polymerization was found with the latter alkynes.

CONCLUSIONS

Despite their increasing interest in catalytic or biomedical applications, the chemistry of water-soluble NHC complexes in water has barely been studied. One of the aspects considered in this report is the influence of an aqueous medium on the preparation and stability of sulfonated NHC silver complexes. In this respect, we have shown that precipitation of silver halides makes the difference between protic (such as water and alcohols) and aprotic solvents. In simple thermodynamic terms, the sequence of equilibria 2 [AgCl(NHC)] ↔ $[Ag(NHC)_2][AgCl_2]$ ↔ $[Ag(NHC)_2]Cl$ + AgCl is shifted to the right in protic solvents, partly because hydrogen bonds are involved in solvation of the chloride anion. This explains why the literature (and this work) reports the exclusive formation of bis(carbene) species when water-soluble Ag-NHC complexes are prepared in this solvent. In addition, we have shown that the sulfonated mono(carbenes) Na[AgCl(NHC)] (**3**), which can be prepared in aprotic solvents such as dmso, evolve reversibly to their bis(carbene) analogues $Na[Ag(NHC)_2]$ (**2**) when dissolved in water. The NHC-Ag bonds in these bis(carbene) complexes are very resistant to hydrolysis, even in refluxing water. However, hydrolysis is favored under some conditions and we can especially highlight the fact that the promotion of hydrolysis by chlorides might explain the problems found in the literature as regards the synthesis of various NHC silver complexes in water. Although water is the most natural solvent for the preparation of water-soluble NHC complexes, the use of silver complexes for this purpose can prove problematic, as shown in the synthesis of the water-soluble platinum(II) NHC complexes **4**. Thus, the most suitable procedure for the synthesis of these complexes was direct metallation of the corresponding imidazolium salts in dmso as silver(I) NHC intermediates failed to transfer their NHC ligands to the Pt centers in water (but not in dmso). Nevertheless, the transfer of NHC ligands from Ag to Au, Ru or Os centers has been reported to happen in water,[14,41,58] and NHC exchange between Ag centers also occurs rapidly in water on the NMR scale of time in the case of **2a**,**b**. However, steric hindrance makes bis(carbene) complexes kinetically worse transfer agents and water makes them thermodynamically more stable. From our point of view, this means that NHC transfer from silver complexes is generally expected to be disfavored by water. Finally, we have shown that *cis*-$[PtCl_2(dmso)(NHC)]$ complexes are active catalysts for the hydration

of alkynes in aqueous media, although their activity is currently comparable to that reported with platinum(II) complexes of sulfonated phosphines.

EXPERIMENTAL SECTION

General Procedures. All reactions were performed under an argon atmosphere using standard Schlenk techniques. Unless otherwise stated, reagents and solvents were used as received from commercial sources. The complex *cis*-dichlorobis(dimethyl sulfoxide)platinum(II)[59] and the imidazolium salts **1a**,[14] **1b**,[60] **1c**,**d**,[38] **1e**,[13] and **1f**,[39] were prepared as described in the literature. All solvents were deoxygenated prior to use. Dimethyl sulfoxide was distilled under argon over calcium hydride. Deionized water (type II quality) was obtained using a Millipore Elix 10 UV Water Purification System. ^{1}H, ^{13}C, ^{15}N, and ^{195}Pt NMR spectra were recorded with a Varian Mercury 300, Unity 300, or Unity 500 Plus spectrometer. Chemical shifts (δ, parts per million) are quoted relative to $SiMe_4$ (^{1}H, ^{13}C), CH_3NO_2 (^{15}N), and K_2PtCl_6 in water (^{195}Pt). They were measured by internal referencing to the ^{13}C or residual ^{1}H resonances of the deuterated solvents, or by the substitution method in the case of ^{15}N and ^{195}Pt. Coupling constants (J) are given in Hertz. When required, two-dimensional ^{1}H-^{13}C HSQC and HMBC experiments were carried out for the unequivocal assignment of ^{1}H and ^{13}C resonances. The Analytical Services of the Universidad de Alcalá performed the C, H, and N analyses using a Heraeus CHN-O-Rapid microanalyzer, and the mass spectra using an Agilent G3250AA LC/MSD TOF Multi (MALDI and ESI) mass spectrometer.

Synthesis of the Biscarbene Silver Complexes (2). The silver NHCs **2b**[14] and **2c,d**[38] were prepared according to published procedures and characterized by comparison of their NMR spectra with those previously described for all complexes.

*Trisodium [1,3-bis(3-sulfonatepropyl)imidazol-2-ylidene]argentate(3–) (**2a**).* A spectroscopically pure sample of **2a** was prepared by heating a mixture of the imidazolium salt **1a** (0.1632 g, 0.483 mmol), silver oxide (0.0684 mg, 0.295 mmol), and an excess of sodium hydroxide (0.0911 g, 2.28 mmol) in water (3 mL) for 36 h at 75 °C. ^{1}H NMR (300 MHz, D_2O): δ 7.19 (s, 1H, Imz), 4.12 (t, $^{3}J_{HH}$ = 6.3, 2H, NCH_2), 2.71 (t, $^{3}J_{HH}$ = 7.2, 2H, CH_2S), 2.13 (m, 2H, $CH_2CH_2CH_2$). ^{13}C{^{1}H} NMR (125 MHz, D_2O): δ 178.4 (s, Imz C^2), 121.3 (s, Imz $C^{4,5}$), 49.7 (s, NCH_2), 47.2 (s, CH_2S), 26.4 (s, $CH_2CH_2CH_2$). ESI-MS (negative ion, MeOH) m/z: 772.9449 [M–Na]$^-$ (calcd. 772.9438) 87%; 750.9629 [M+H-2Na]$^-$ (calcd. 750.9619) 85%; 728.9821 [M+2H–3Na]$^-$ (calcd. 728.9799) 100%.

*Silver Disodium Bis[1,3-bis(2,6-diisopropyl-4-sulfonatophenyl)imidazol-2-ylidene]argentate(3–) (**2e**$^{Ag+}$).* An excess of silver oxide (0.072 g, 0.31 mmol) was added to a solution of the imidazolium salt **1e** (0.191 g, 0.335 mmol) in water (7 mL). The mixture was stirred for 4 h at room temperature,

then centrifuged and filtered through a plug of kieselguhr. The resulting solution was evaporated to dryness under vacuum (4 h, 80 ºC, 4 mbar). Compound **2e^{Ag+}** was isolated as a light-sensitive white solid (0.415 g, 90%). ^{1}H NMR (300 MHz, D_2O): δ 7.44 (s, 2H, Ar), 7.25 (s, 1H, Imz), 2.13 (m, 2H, C*H*Me$_2$), 0.86 (d, $^{3}J_{HH}$ = 6.8, 6H, CH*Me*$_2$), 0.58 (d, $^{3}J_{HH}$ = 6.8, 6H, CH*Me*$_2$). ^{1}H NMR (300 MHz, dmso-d_6): δ 7.75 (s, 1H, Imz), 7.54 (s, 2H, Ar), 2.14 (m, 2H, C*H*Me$_2$), 0.99 (d, $^{3}J_{HH}$ = 6.8, 6H, CH*Me*$_2$), 0.69 (d, $^{3}J_{HH}$ = 6.8, 6H, CH*Me*$_2$). ^{13}C{^{1}H} NMR (75 MHz, D_2O): δ 181.2 (two d with $^{1}J(^{13}C\text{-}^{109}Ag)$ = 217 and $^{1}J(^{13}C\text{-}^{107}Ag)$ = 188, respectively, Imz C^2), 146.8 (s, Ar C^3), 144.8 (s, Ar C^1), 136.7 (s, Ar C^4), 125.1 (d, Imz C^{4,5}, ^{3}J(Ag-^{13}C) = 5.6), 121.7 (s, Ar C^2), 28.6 (s, *C*HMe$_2$), 23.6 (s, CH*Me*$_2$), 22.5 (s, CH*Me*$_2$). ESI-MS (negative ion, MeOH) *m*/*z*: 1245.2563 [M–Ag]$^-$ (calcd. 1245.2563) 36%; 1201.2919 [M–Ag–2Na+2H]$^-$ (calcd. 1201.2929) 100%; 600.1414 [M–Ag–2Na+H]$^{2-}$ (calcd. 600.1428) 52%.

*Trisodium Bis[1,3-bis(2,6-diisopropyl-4-sulfonatephenyl)imidazol-2-ylidene]argentate(3–) (**2e**).* A solution of sodium chloride (0.0099 g, 0.170 mmol) in water (1 mL) was added dropwise to a solution of **2e^{Ag+}** (0.230 g, 0.170 mmol) in the same solvent (2 mL) in the dark. Formation of a silver chloride precipitate was observed immediately. Stirring was continued for 30 min at room temperature, then the solution was centrifuged and filtered through a plug of kieselguhr. The resulting solution was evaporated to dryness under vacuum (4 h, 80 ºC, 4 mbar). Compound **2e** was obtained as a white solid (0.230 g, 98%). The ^{1}H and ^{13}C NMR data for this compound are identical to those given above for **2e^{Ag+}**. ESI-MS (positive ion, MeOH) *m*/*z*: 1269.2538 [M+H]$^+$ (calcd. 1269.2539) 10%; 1247.2715 [M–Na +2H]$^+$ (calcd. 1247.2714) 46%; 1225.2858 [M–2Na+3H]$^+$ (calcd. 1225.2894) 88%; 1203.3044 [M–3Na+4H]$^+$ (calcd. 1203.3075) 100%. The negative ion ESI mass spectrum is similar to that found for **2e^{Ag+}**.

General Procedure for the Synthesis of Monocarbene Silver(I) Complexes (3). An excess of silver oxide (0.333 g, 1.44 mmol) was added to a solution of the corresponding imidazolium salt (1.19 mmol) and sodium chloride (0.070 g, 1.20 mmol) in dimethyl sulfoxide (5 mL). The mixture was stirred for the time and at the temperature indicated below for each complex. The precipitate was then separated by centrifugation and filtration through a plug of kieselguhr, and the resulting solution evaporated to dryness under vacuum (6 h, 90 ºC, 4 mbar) to give the corresponding NHC silver(I) complex.

*Chlorido[1,3-bis(3-sodiumsulfonatepropyl)imidazol-2-ylidene]silver(I) (**3a**).* Complex **3a** was obtained from **1a** (0.398 g, 1.19 mmol) as an off-white solid (0.547 g, 92%) after 17 h of reaction at 60 ºC. ^{1}H NMR (300 MHz, dmso-d_6): δ 7.46 (s, 1H, Imz), 4.15 (t, $^{3}J_{HH}$ = 6.7, 2H, NCH_2), 2.38 (t, $^{3}J_{HH}$ = 7.0, 2H, CH_2S), 2.03 (m, 2H, $CH_2CH_2CH_2$). ^{13}C{^{1}H} NMR (75 MHz, dmso-d_6): δ 176.8 (br, Imz C^2), 121.4 (s, Imz C^{4,5}), 49.6 (s, NCH_2), 47.6 (s, CH_2S), 27.1 (s, $CH_2CH_2CH_2$). ESI-MS (negative ion, MeOH) *m*/*z*: 474.8939 [M–Na]$^-$ (calcd. 474.8930) 35%; 750.9629 [M–Na–Cl+NHC+H]$^-$ (calcd. 750.9619) 100%.

Chlorido[1-methyl-3-(3-sodiumsulfonatepropyl)imidazol-2-ylidene]silver(I) ***(3b)***. Complex **3b** was obtained from **1b** (0.243 g, 1.19 mmol) as an off-white solid (0.422 g, 96%) after 17 h of reaction at 60 ºC. ^{1}H NMR (300 MHz, dmso-d_6): δ 7.46 (d, $^{3}J_{HH}$ = 2.0, 1H, Imz), 7.41 (d, $^{3}J_{HH}$ = 1.7, 1H, Imz), 4.16 (t, $^{3}J_{HH}$ = 6.9, 2H, NCH_2), 3.76 (s, 3H, NMe), 2.41 (t, $^{3}J_{HH}$ = 7.6, 2H, CH_2S), 2.03 (m, 2H, $CH_2CH_2CH_2$). ^{13}C{^{1}H} NMR (75 MHz, dmso-d_6): δ 177.8 (s, Imz C^2), 122.4 (s, Imz C^5), 121.4 (s, Imz C^4), 49.4 (s, NCH_2), 47.6 (s, CH_2S), 37.7 (s, NMe), 27.1 (s, $CH_2CH_2CH_2$). ESI-MS (negative ion, MeOH) *m/z*: 344.9243 [M–Na]$^-$ (calcd. 344.9230) 29%; 513.0041 [M–Na–Cl+NHC$^-$]$^-$ (calcd. 513.0037) 100%.

Chlorido[1-(3-sodiumsulfonatepropyl)-3-(2,4,6-trimethylphenyl)imidazol-2-ylidene]silver(I) ***(3c)***. Complex **3c** was obtained from **1c** (0.367g, 1.19 mmol) as a brown solid (0.552 g, 98%) after 20 h of reaction at 60 ºC. ^{1}H NMR (300 MHz, dmso-d_6): δ 7.74 (s, 1H, Imz), 7.46 (s, 1H, Imz), 7.05 (s, 2H, Ar), 4.26 (t, $^{3}J_{HH}$ = 2.0, 2H, NCH_2), 2.43 (t, $^{3}J_{HH}$ = 7.9, 2H, CH_2S), 2.30 (s, 3H, Ar *p-Me*), 2.11 (m, 2H, $CH_2CH_2CH_2$), 1.90 (s, 6H, Ar *o-Me*). ^{13}C{^{1}H} NMR (75 MHz, dmso-d_6): δ Imz C^2 not observed, 138.1 (s, Ar C^4), 135.3 (s, Ar C^2), 134.0 (s, Ar C^1), 128.5 (s, Ar C^3), 122.7 (s, Imz C^4), 121.9 (s, Imz C^5), 49.6 (s, NCH_2), 47.5 (s, CH_2S), 27.2 (s, $CH_2CH_2CH_2$), 20.2 (s, Ar *p-Me*), 16.7 (s, Ar *o-Me*). ESI-MS (negative ion, MeOH) *m/z*: 448.9832 [M–Na]$^-$ (calcd. 448.9856) 10%; 721.1278 [M–Na–Cl+NHC]$^-$ (calcd. 721.1289) 100%. ESI-MS (negative ion, acetonitrile) *m/z*: 440.0205 [M–Na–Cl+CN]$^-$ (calcd. 440.0204) 29%; 448.9862 [M–Na]$^-$ (calcd. 448.9856) 20%; 721.1293 [M–Na–Cl+NHC]$^-$ (calcd. 721.1289) 100%.

Chlorido[1-(2,6-diisopropylphenyl)-3-(3-sodiumsulfonatepropyl)imidazol-2-ylidene]silver(I) ***(3d)***. Complex **3d** was obtained from **1d** (0.417 g, 1.19 mmol) as a brown solid (0.602 g, 98%) after 20 h of reaction at 60 ºC. ^{1}H NMR (300 MHz, dmso-d_6): δ 7.78 (s, 1H, Imz), 7.63 (s, 1H, Imz), 7.50 (t, $^{3}J_{HH}$ = 7.6, 1H, Ar H^4), 7.34 (d, $^{3}J_{HH}$ = 7.6, 2H, Ar H^3), 4.28 (t, $^{3}J_{HH}$ = 6.4, 2H, NCH_2), 2.43 (t, $^{3}J_{HH}$ = 7.0, 2H, CH_2S), 2.28 (m, 2H, $CHMe_2$), 2.12 (m, 2H, $CH_2CH_2CH_2$), 1.14 (d, $^{3}J_{HH}$ = 6.7, 6H, $CHMe_2$), 1.09 (d, $^{3}J_{HH}$ = 6.7, 6H, $CHMe_2$). ^{13}C{^{1}H} NMR (75 MHz, dmso-d_6): δ Imz C^2 not observed, 144.9 (s, Ar C^2), 134.6 (s, Ar C^1), 129.6 (s, Ar C^4), 124.1 (s, Imz C^5), 123.4 (s, Ar C^3), 121.8 (s, Imz C^4), 49.6 (s, NCH_2), 47.5 (s, CH_2), 27.3 (s, $CH_2CH_2CH_2$), 27.2 (s, $CHMe_2$), 23.7 (s, $CHMe_2$), 23.3 (s, $CHMe_2$). ESI-MS (negative ion, MeOH) *m/z*: 491.0338 [M–Na]$^-$ (calcd. 491.0325) 7.9%; 805.2223 [M–Na–Cl+NHC]$^-$ (calcd. 805.2228) 100%.

Chlorido[1,3-bis(2,6-diisopropyl-4-sodiumsulfonate)phenylimidazol-2-ylidene]silver(I) ***(3e)***. Complex **3e** was obtained from **1e** (0.682 g, 1.19 mmol) as a white solid (0.701 g, 80%) after 48 h of reaction at room temperature. ^{1}H NMR (300 MHz, dmso-d_6): δ 8.01 (s, 1H, Imz), 7.59 (s, 2H, Ar), 2.45 (m, 2H, $CHMe_2$), 1.18 (t, J = 5.7, 12H, $CHMe_2$). ^{13}C{^{1}H} NMR (75 MHz, dmso-d_6): δ 181.4 (two d with ^{1}J(^{13}C-^{109}Ag) = 268 and ^{1}J(^{13}C-^{107}Ag) = 232, respectively, Imz C^2) 149.3 (s, Ar C^1), 144.3 (s, Ar C^3), 134.1 (s, Ar C^4), 124.5 (d, ^{3}J(^{13}C-Ag) = 6.8, Imz $C^{4,5}$), 120.6 (s, Ar C^2), 27.8 (s, $CHMe_2$), 23.7 (s, $CHMe_2$), 22.9 (s, $CHMe_2$). ESI-MS (negative ion, MeOH) *m/z*: 711.0483 [M–

Na]$^-$ (calcd. 711.0495) 1.5%; 653.0820 [M–2Na–Cl]$^-$ (calcd. 653.0915) 6%; 1201.2871 [M–2Na+NHC+2H]$^-$ (calcd. 1201.2929) 100%.

General Procedure for the Synthesis of Platinum(II) Complexes 4 and 5. Sodium hydrogencarbonate (0.160 g, 1.91 mmol) was added to a solution of *cis*-[$PtCl_2$(dmso)$_2$] (0.322 g, 0.764 mmol) and the corresponding imidazolium salt (0.764 mmol) in dimethyl sulfoxide (5 mL). The mixture was stirred at 90 ºC for the time indicated below, then filtered through a plug of kieselguhr and the solvent partially removed under vacuum to a remaining volume of 2–3 mL. The platinum complex was then precipitated with acetone (60 mL), separated by filtration, washed with acetone (3 × 20 mL), and dried under vacuum (2 h, 90 ºC, 4 mbar).

*Cis-dichlorido[1,3-bis(3-sodiumsulfonatepropyl)imidazol-2-ylidene](dimethyl sulfoxide)platinum(II) (**4a**).* Complex **4a** was obtained from **1a** (0.255 g, 0.764 mmol) as a white solid (0.401 g, 75%) after 17 h of reaction at 90 ºC. ^{1}H NMR (300 MHz, dmso-d_6): δ 7.39 (s, 1H, Imz), 4.51 (m, 1H, NCH_2), 4.21 (m, 1H, NCH_2), 3.49 (s, 3H, Me_2SO), 2.49 (m, 2H, CH_2S), 2.20 (m, 2H, $CH_2CH_2CH_2$). ^{1}H-NMR (300 MHz, D_2O): δ 7.18 (s, 1H, Imz), 4.37 (t, $^3J_{HH}$ = 7.3, 2H, NCH_2), 3.42 (s, 3H, Me_2SO), 2.84 (m, 2H, CH_2S), 2.24 (m, 2H, $CH_2CH_2CH_2$). ^{13}C{^{1}H} NMR (75 MHz, dmso-d_6): δ 140.4 (s, Imz C^2), 120.9 (s, Imz C^{4,5}), 48.6 (s, NCH_2), 47.7 (s, CH_2S), 25.6 (s, $CH_2CH_2CH_2$). ^{195}Pt NMR (107 MHz, dmso-d_6): δ -3518. ESI-MS (negative ion, MeOH) *m/z*: 675.9366 [M–Na]$^-$ (calcd. 675.9355) 73%. Anal. Calcd (%) for $C_{11}H_{20}Cl_2N_2Na_2O_7PtS_3$: C, 18.86; H, 2.88; N, 4.00. Found (%): C 18.90, H 3.66, N 3.84.

*Cis-dichlorido(dimethyl sulfoxide)[1-methyl-3-(3-sodiumsulfonatepropyl)imidazol-2-ylidene] platinum(II) (**4b**).* Complex **4b** was obtained from **1b** (0.156 g, 0.764 mmol) as a white solid (0.261 g, 60%) after 17 h of reaction at 90 ºC. ^{1}H NMR (500 MHz, dmso-d_6): δ 7.39 (d, $^3J_{HH}$ = 2.0, 1H, Imz), 7.35 (d, $^3J_{HH}$ = 2.0, 1H, Imz), 4.50 (m, 1H, NCH_2), 4.20 (m, 1H, NCH_2), 3.85 (s, 3H, NMe), 2.50 (m, 2H, CH_2S), 2.20 (m, 2H, $CH_2CH_2CH_2$). ^{1}H NMR (300 MHz, D_2O): δ 7.11 (d, $^3J_{HH}$ = 1.3, 1H, Imz), 7.05 (d, $^3J_{HH}$ = 1.6, 1H, Imz), 4.32 (t, $^3J_{HH}$ = 7.2, 2H, NCH_2), 3.78 (s, 3H, NMe), 3.38 (s with ^{195}Pt satellites, ^3J(^{1}H-^{195}Pt) = 26.4, 6H, Me_2SO), 2.79 (m, 2H, CH_2S), 2.20 (m, 2H, $CH_2CH_2CH_2$). ^{13}C{^{1}H} NMR (75 MHz, dmso-d_6): δ 140.8 (s with ^{195}Pt satellites, ^1J(^{13}C-^{195}Pt) = 1378, Imz C^2), 122.1 (s, Imz C^5), 120.9 (s, Imz C^4), 48.3 (s, NCH_2), 47.6 (s, CH_2S), 36.6 (s, NMe), 25.7 (s, $CH_2CH_2CH_2$). ^{13}C{^{1}H} NMR (75 MHz, D_2O): δ 138.0 (s, Imz C^2), 123.6 (s, Imz C^5), 121.8 (s, Imz C^4), 48.8 (s, NCH_2), 47.8 (s, CH_2S), 45.4 (s, Me_2SO), 44.9 (s, Me_2SO), 37.1 (s, NMe), 25.2 (s, $CH_2CH_2CH_2$). ^{15}N NMR (50 MHz, dmso-d_6): δ -194.0 (s, NCH_2), -206.3 (s, NMe). ^{195}Pt NMR (107 MHz, dmso-d_6): δ -3529. ESI-MS (negative ion, MeOH) *m/z*: 545.9673 [M–Na]$^-$ (calcd. 545.9655) 19%. Anal. Calcd (%) for $C_9H_{17}Cl_2N_2NaO_4PtS_2$: C, 18.95; H, 3.00; N, 4.91. Found (%): C, 18.53; H, 3.64; N, 4.76.

*Cis-dichlorido[1-(3-sodiumsulfonatepropyl)-3-(2,4,6-trimethylphenyl)imidazol-2-ylidene](dimethyl sulfoxide)platinum(II) (**4c**).* Complex **4c** was obtained from **1c** (0.236 g, 0.764 mmol) as a pale-yellow solid (0.479 g 93%) after 23 h of reaction at 90 ºC. The solid was isolated by evaporation of the dimethyl sulfoxide solution to dryness and drying the resulting solid for 24 h at 90 ºC and 4 mbar. ^{1}H NMR (500 MHz, dmso-d_6): δ 7.66 (d, $^{3}J_{HH}$ = 2.0, 1H, Imz), 7.42 (d, $^{3}J_{HH}$ = 2.0, 1H, Imz), 7.07 (s, 1H, Ar), 7.04 (s, 1H, Ar), 4.71 (m, 1H, NCH_2), 4.30 (m, 1H, NCH_2), 3.47 (s, 3H, Me_2SO), 2.86 (m, 2H, CH_2S), 2.81 (s, 3H, Me_2SO), 2.33 (m, 2H, $CH_2CH_2CH_2$), 2.31 (s, 3H, Ar *p*-Me), 2.18 (s, 3H, Ar *o*-Me), 2.03 (s, 3H, Ar *o*-Me). ^{13}C{^{1}H} NMR (125 MHz, dmso-d_6): δ 141.7 (s, Imz C^2), 138.2 (s, Ar C^4), 135.5 (s, Ar C^2), 135.2 (s, Ar C^2), 134.1 (s, Ar C^1), 128.7 (s, Ar C^3), 128.3 (s, Ar C^3), 123.3 (s, Imz C^4), 121.4 (s, Imz C^5), 49.0 (s, NCH_2), 47.9 (s, CH_2S), 45.0 (s, Me_2SO), 44.0 (s, Me_2SO), 25.7 (s, $CH_2CH_2CH_2$), 20.1 (s, Ar *p*-Me), 18.7 (s, Ar *o*-Me), 17.7 (s, Ar *o*-Me). ^{15}N NMR (50 MHz, dmso-d_6): δ -190.9 (s, NCH_2), -192.0 (s, NAr). ^{195}Pt NMR (107 MHz, dmso-d_6): δ -3478. ESI-MS (negative ion, MeOH) *m/z*: 650.0301 $[M–Na]^-$ (calcd. 650.0281) 100%. Anal. Calcd (%) for $C_{17}H_{25}Cl_2N_2NaO_4PtS_2$: C, 30.27; H, 3.74; N, 4.15. Found (%): C, 30.00; H, 3.92; N, 3.62.

*Cis-dichlorido[1-(2,6-diisopropylphenyl)-3-(3-sodiumsulfonatepropyl)imidazol-2-ylidene](dimethyl sulfoxide)platinum(II) (**4d**).* Complex **4d** was obtained from **1d** (0.268 g, 0.764 mmol) as a pale-yellow solid (0.492 g, 90%) after 25 h of reaction at 90 ºC. The solid was isolated by evaporation of the dmso solution to dryness and drying the resulting solid for 24 h at 90 ºC and 4 mbar. ^{1}H NMR (500 MHz, dmso-d_6): δ 7.67 (d, $^{3}J_{HH}$ = 2.0, 1H, Imz), 7.545 (d, $^{3}J_{HH}$ = 2.0, 1H, Imz), 7.541 (t, $^{3}J_{HH}$ = 7.8, 1H, Ar H^4), 7.40 (d, $^{3}J_{HH}$ = 7.9, 1H, Ar H^3), 7.35 (d, $^{3}J_{HH}$ = 7.9, 1H, Ar H^3), 4.83 (m, 1H, NCH_2), 4.28 (m, 1H, NCH_2), 3.43 (s, 3H, Me_2SO), 3.14 (m, 1H, $CHMe_2$), 2.64 (s, 3H, Me_2SO), 2.59 (m, 2H, CH_2S), 2.53 (m, 1H, $CHMe_2$), 2.33 (m, 2H, $CH_2CH_2CH_2$), 1.29 (d, J = 6.6, 3H, $CHMe_2$), 1.20 (d, J = 6.6, 3H, $CHMe_2$), 1.04 (d, J = 6.6, 3H, $CHMe_2$), 0.88 (d, J = 6.6, 3H, $CHMe_2$). ^{13}C{^{1}H} NMR (125 MHz, dmso-d_6): δ 146.6 (s, Ar C^2), 145.9 (s, Ar C^2), 142.7 (s, Imz C^2), 133.7 (s, Ar C^1), 129.7 (s, Ar C^4), 124.6 (s, Imz C^5), 123.6 (s, Ar C^3), 123.3 (s, Ar C^3), 120.9 (s, Imz C^4), 49.2 (s, NCH_2), 47.7 (s, CH_2S), 27.4 (s, $CHMe_2$), 27.3 (s, $CHMe_2$), 26.4 (s, $CH_2CH_2CH_2$), 25.9 (s, $CHMe_2$), 25.7 (s, $CHMe_2$), 22.2 (s, $CHMe_2$), 22.0 (s, $CHMe_2$). ^{15}N NMR (50 MHz, dmso-d_6): δ -190.5 (s, NCH_2), -193.7 (s, NAr). ^{195}Pt NMR (107 MHz, dmso-d_6): δ -3474. ESI-MS (negative ion, MeOH) *m/z*: 692.0782 $[M–Na]^-$ (calcd. 692.0750) 100%. Anal. Calcd (%) for $C_{20}H_{31}Cl_2N_2NaO_4PtS_2$: C, 33.52; H, 4.36; N, 3.91. Found (%): C, 32.45; H, 4.69; N, 3.80.

*Cis-dichlorido[1,3-bis(2,6-diisopropyl-4-sodiumsulfonate-phenyl)imidazol-2-ylidene](dimethyl sulfoxide)platinum(II) (**4e**).* Using the above procedure, only 65% of the imidazolium salt **1e** was converted into **4e** after 10 days of reaction at 90 ºC (^{1}H NMR analysis). All attempts to isolate pure samples of complex **4e** failed. The characterization data are nevertheless given: ^{1}H NMR (300 MHz, dmso-d_6): δ 7.81 (s, 1H, Imz), 7.62 (d, $^{3}J_{HH}$ = 1.6, 1H, Ar), 7.59 (d, $^{3}J_{HH}$ = 1.6, 1H,

Ar), 3.14 (hept, $^3J_{HH}$ = 6.6, 1H, C*H*Me$_2$), 2.97 (hept, $^3J_{HH}$ = 6.6, 1H, C*H*Me$_2$), 1.33 (d, $^3J_{HH}$ = 6.6, 3H, CH*Me*$_2$), 1.30 (d, $^3J_{HH}$ = 6.6, 3H, CH*Me*$_2$), 1.05 (d, J = 6.6, 3H, CH*Me*$_2$), 1.01 (d, $^3J_{HH}$ = 6.6, 3H, CH*Me*$_2$). ^{13}C{^{1}H} NMR (75 MHz, dmso-d_6): δ 149.0 (s, Ar C^4), 146.0 (s, Ar C^2), 144.9 (s, Ar C^2), 144.1 (s, Imz C^2), 134.2 (s, Ar C^1), 124.8 (s, Imz C^{4,5}), 120.8 (s, Ar C^3), 120.3 (s, Ar C^3), 28.1 (s, *C*HMe$_2$), 27.6 (s, *C*HMe$_2$), 25.6 (s, two CH*Me*$_2$ overlapping), 22.5 (s, CH*Me*$_2$), 22.0 (s, CH*Me*$_2$). ESI-MS (negative ion, MeOH) *m*/*z*: 912.0954 [M–Na]$^-$ (calcd. 912.0920) 1.6%; 444.5531 [M–2Na]$^{2-}$ (calcd. 444.5516) 100%.

*Cis-dichlorido{bis[3-(3-sodiumsulfonatepropyl)imidazol-2-ylidene]methane}platinum(II) (**5**).* Complex **5** was obtained from **1f** (0.300 g, 0.764 mmol) as a white solid (0.408 g, 76%) after 34 h of reaction at 90 ºC. ^{1}H NMR (500 MHz, dmso-d_6): δ 7.51 (d, J = 1.9, 2H, Imz), 7.34 (d, $^3J_{HH}$ = 1.9, 1H, Imz), 6.13 (d, $^2J_{HH}$ = 13.2, 1H, NCH$_2$N), 5.91 (d, $^2J_{HH}$ = 12.9, 1H, NCH$_2$N), 4.75 (m, 2H, NCH$_2$), 4.18 (m, 2H, NCH$_2$), 2.46 (m, 2H, CH$_2$S), 2.27 (m, 2H, CH$_2$S), 2.06 (m, 4H, CH$_2$C*H*$_2$CH$_2$). ^{13}C{^{1}H} NMR (75 MHz, dmso-d_6): δ 143.6 (s, Imz C^2), 121.9 (s, Imz C^5), 121.0 (s, Imz C^4), 62.3 (s, NCH$_2$N), 48.5 (s, CH$_2$S), 48.5 (s, NCH$_2$), 27.2 (s, CH$_2$*C*H$_2$CH$_2$). ^{15}N NMR (50 MHz, dmso-d_6): δ -190.0 (s, NCH$_2$), -200.0 (s, NCH$_2$N). ^{195}Pt NMR (107 MHz, dmso-d_6): δ -3572. ESI-MS (negative ion, MeOH) *m*/*z*: 677.9590 [M–Na]$^-$ (calcd. 677.9590) 7.3 %; 620.0033 [M–2Na–Cl]$^-$ (calcd. 620.0010) 24 %. Anal. Calcd (%) for $C_{13}H_{18}Cl_2N_4Na_2O_6PtS_2$: C, 22.23; H, 2.58; N, 7.98. Found (%): C, 22.39; H, 3.09; N, 7.46.

General Method for the Hydration of Alkynes in Water. The reaction of phenylacetylene and water is given as an example. Phenylacetylene (0.05 mL g, 0.455 mmol), the corresponding platinum complex (9.1 μmol, 2 mol %), and water (2 mL), were introduced into an ampoule tube equipped with a PTFE valve. The mixture was vigorously stirred at the temperature and for the time specified in Tables 3 and 4. After cooling to room temperature, sodium chloride (1 g) was added to the resulting emulsion to facilitate the separation of layers, and the organics were extracted with diethyl ether (3 × 15 mL). The combined ethereal layers were dried over $MgSO_4$ and the solvent removed under vacuum (25 °C and 500 mbar). Conversions were determined by integration of the ^{1}H NMR spectra.

X-ray Crystallographic Studies. Suitable single crystals were obtained by slow diffusion of diethyl ether into a dmso solution (**2e**$^{Ag+}$), dichloromethane into a methanol solution (**2e**•6MeOH), acetone into a dmso solution (**2e**•5Me$_2$SO•H$_2$O and **3e**), or acetone into an aqueous solution (**4a**). A summary of crystal data, data collection, and refinement parameters for the structural analyses is given in Table S1 (Supporting Information). Crystals were glued to a glass fiber using an inert polyfluorinated oil and mounted in the low temperature N_2 stream (200 K) of a Bruker-Nonius Kappa-CCD diffractometer equipped with an area detector and an Oxford Cryostream 700 unit (**2e**•6MeOH and **2e**$^{Ag+}$) or at 100 K (**2e**•5Me$_2$SO•H$_2$O) or 296 K (**3e**, and **4a**) in a Bruker Kappa Apex II diffractometer.

Intensities were collected using graphite-monochromated Mo-$K\alpha$ radiation (λ = 0.71073 Å). Data were measured with exposure times of 19 s per frame for **2e**•6MeOH (13 sets; 599 frames; phi/omega scans; 1.9° scan-width), 120 s per frame for **2e**•5Me_2SO•H_2O (3 sets; 592 frames; phi/omega scans; 0.5° scan-width), 171 s per frame (4 sets; 288 frames; phi/omega scans; 1.9° scan-width) for $\mathbf{2e^{Ag+}}$, 10 s per frame for **3e** (5 sets; 1662 frames; phi/omega scans; 0.5° scan-width), and 5 s per frame for **4a** (10 sets; 3812 frames; phi/omega scans; 0.5° scan-width). Raw data were corrected for Lorenz and polarization effects. The structures were solved by direct methods, completed by subsequent difference Fourier techniques and refined by full-matrix least squares on F^2 (SHELXL-97).[61] Anisotropic thermal parameters were used in the last cycles of refinement for the non-hydrogen atoms. Absorption correction procedures were carried out using the multiscan SORTAV (semi-empirical from equivalent, **2e**•6MeOH and $\mathbf{2e^{Ag+}}$),[62] or SADABS programs (**2e**•5dmso•H_2O, **3e**, and **4a**).[63] Hydrogen atoms were included in the last cycle of refinement from geometrical calculations and refined using a riding model. All the calculations were made using the WINGX system.[64] In the case of **2e**•6MeOH, the disorder observed for O(21), O(22), and O(23) and for O(56) was modeled in two positional sets with occupancy factors of 0.54 and 0.46, and 0.81 and 0.19, respectively. In the case of $\mathbf{2e^{Ag+}}$, the disorder observed for O(1), O(2), and O(3) was modeled in two sets with occupancy factors of 0.85 and 0.15. In this compound, it was not possible to model some remaining electronic density found in the difference Fourier map and due to disordered solvent molecules. The Squeeze procedure[65] was used to remove this contribution to the structure factors.

ASSOCIATED CONTENT

Supporting Information

Crystallographic data for compounds **2e**•6MeOH, **2e**•5Me_2SO•H_2O, $\mathbf{2e^{Ag+}}$, **3e**, and **4a** in CIF format. This material is available free of charge via the Internet at http://pubs.acs.org.

AUTHOR INFORMATION

Corresponding Authors

*Email: juanc.flores@uah.es (J.C.F.), ernesto.dejesus@uah.es (E.d.J).

ACKNOWLEDGMENT

This work was supported by the Spanish Ministerio de Economía y Competitividad (project CTQ2011-24096) and the Factoria de Cristalización (CSD2006-00015). E.A.B. is grateful to the Fundación Carolina for an M. Sc. Fellowship and to the Universidad de Alcalá for a FPI

Doctoral Fellowship. G.F.S. is grateful to the Spanish Ministerio de Educación for a Postdoctoral Fellowship.

REFERENCES

(1) For recent revisions, see: *N-Heterocyclic Carbenes: From Laboratory Curiosities to Efficient Synthetic Tools*; Diez-Gonzalez, S., Ed.; RSC Catalysis Series; The Royal Society of Chemistry, **2011**. Jahnke, M. C.; Hahn, F. E. In *Transition Metal Complexes of Neutral eta1-Carbon Ligands*; Chauvin, R., Canac, Y., Eds.; Topics in Organometallic Chemistry 30; Springer: Berlin Heidelberg, 2010, p 95-129. Hahn, F. E.; Jahnke, M. C. *Angew. Chem., Int. Ed.* **2008**, *47*, 3122-3172. Kühl, O. *Chem. Soc. Rev.* **2007**, *36*, 592-607.

(2) For themed or special issues devoted to NHCs or carbenes in general: N-Heterocyclic Carbenes (Special issue, Hahn, F. E., Ed.) *Dalton Trans.* **2009** (35), 6893-7313. Carbenes (Special issue, Arduengo, A. J., Bertrand, G., Eds.) *Chem. Rev.* **2009**, *109* (8), 3209-3884. Recent Development in the Organometallic Chemistry of N-Heterocyclic Carbenes (Special issue, Crabtree, R. H., Ed.) *Coord. Chem. Rev.* **2007**, *251* (5–6), 595-896. For recent and leading general revisions in catalysis, see for instance: Carbene Chemistry (Special issue, Bertrand, G., Ed.) *J. Organomet. Chem.* **2005**, *690* (24-25), 5397-6252.

(3) Kelly III, R. A.; Clavier, H.; Giudice, S.; Scott, N. M.; Stevens, E. D.; Bordner, J.; Samardjiev, I.; Hoff, C. D.; Cavallo, L.; Nolan, S. P. *Organometallics* **2008**, *27*, 202-210.

(4) For recent revisions devoted to NHC metal complexes in catalysis, see for instance: Díez-González, S.; Marion, N.; Nolan, S. P. *Chem. Rev.* **2009**, *109*, 3612-3676. Poyatos, M.; Mata, J. A.; Peris, E. *Chem. Rev.* **2009**, *109*, 3677-3707. *N-Heterocyclic Carbenes in Transition Metal Catalysis*; Glorius, F., Ed.; Topics in Organometallic Chemistry 21; Springer: Berlin Heidelberg, 2007. *N-Heterocyclic Carbenes in Synthesis*; Nolan, S. P., Ed.; Wiley-VCH: Weinheim, 2006. Herrmann, W. A. *Angew. Chem., Int. Ed.* **2002**, *41*, 1290-1309.

(5) Mercs, L.; Albrecht, M. *Chem. Soc. Rev.* **2010**, *39*, 1903-1912. Liu, W.; Gust, R. *Chem. Soc. Rev.* **2013**. Gautier, A.; Cisnetti, F. *Metallomics* **2012**, *4*, 23-32. Teyssot, M.-L.; Jarrousse, A.-S.; Manin, M.; Chevry, A.; Roche, S.; Norre, F.; Beaudoin, C.; Morel, L.; Boyer, D.; Mahiou, R.; Gautier, A. *Dalton* Trans. **2009**, 6894-6902. Hindi, K. M.; Panzner, M. J.; Tessier, C. A.; Cannon, C. L.; Youngs, W. J. *Chem. Rev.* **2009**, *109*, 3859-3884. Kascatan-Nebioglu, A.; Panzner, M. J.; Tessier, C. A.; Cannon, C. L.; Youngs, W. J. *Coord. Chem. Rev.* **2007**, *251*, 884-895.

(6) Shaughnessy, K. H. Chem. *Rev.* **2009**, *109*, 643-710.

(7) Herrmann, W. A.; Elison, M.; Fisher, J.; Kocher, C.; Ofele, K. Metal complexes with heterocycles carbenes, US Patent 5,728,839, 1998. Herrmann, W. A.; Gooβen, L. J.; Spiegler, M. *J. Organomet. Chem.* **1997**, *547*, 357-366.

(8) Özdemir, İ.; Yiğit, B.; Çetinkaya, B.; Ülkü, D.; Tahir, M. N.; Arıcı, C. *J. Organomet. Chem.* **2001**, *633*, 27-32.

(9) Gallivan, J. P.; Jordan, J. P.; Grubbs, R. H. *Tetrahedron Lett.* **2005**, *46*, 2577-2580. Hong, S. H.; Grubbs, R. H. *J. Am. Chem. Soc.* **2006**, *128*, 3508-3509. Jordan, J. P.; Grubbs, R. H. *Angew. Chem., Int. Ed.* **2007**, *46*, 5152-5155. Balof, S. L.; Yu, B.; Lowe, A. B.; Ling, Y.; Zhang, Y.; Schanz, H.-J. *Eur. J. Inorg. Chem.* **2009**, 1717-1722.

(10) Azua, A.; Sanz, S.; Peris, E. *Organometallics* **2010**, *29*, 3661-3664.

(11) Syska, H.; Herrmann, W. A.; Kühn, F. E. *J. Organomet. Chem.* **2012**, *703*, 56-62.

(12) Schönfelder, D.; Nuyken, O.; Weberskirch, R. *J. Organomet. Chem.* **2005**, *690*, 4648-4655. Meise, M.; Haag, R. *ChemSusChem* **2008**, *1*, 637-642. Roy, S.; Plenio, H. *Adv. Synth. Catal.* **2010**, *352*, 1014-1022. Yang, C.-C.; Lin, P.-S.; Liu, F.-C.; Lin, I. J. B.; Lee, G.-H.; Peng, S.-M. *Organometallics* **2010**, *29*, 5959-5971. Godoy, F.; Segarra, C.; Poyatos, M.; Peris, E. *Organometallics* **2011**, *30*, 684-688. Karimi, B.; Fadavi Akhavan, P. *Chem. Commun.* **2011**, 7686-7688. Li, L. Y.; Wang, J. Y.; Zhou, C. S.; Wang, R. H.; Hong, M. C. *Green Chemistry* **2011**, *13*, 2071-2077. Luo, F.-T.; Lo, H.-K. *J. Organomet. Chem.* **2011**, *696*, 1262-1265.

(13) Fleckenstein, C.; Roy, S.; Leuthäußer, S.; Plenio, H. *Chem. Commun.* **2007**, 2870-2872.

(14) Almássy, A.; Nagy, C. E.; Bényei, A. C.; Joó, F. *Organometallics* **2010**, *29*, 2484-2490.

(15) Czégéni, C. E.; Papp, G.; Kathó, Á.; Joó, F. *J. Mol. Catal. A: Chem.* **2011**, *340*, 1-8.

(16) Wetzel, C.; Kunz, P. C.; Thiel, I.; Spingler, B. *Inorg. Chem.* **2011**, *50*, 7863-7870.

(17) Azua, A.; Sanz, S.; Peris, E. *Chem.—Eur. J.* **2011**, *17*, 3963-3967.

(18) Wang, W.; Wu, J.; Xia, C.; Li, F. *Green Chemistry* **2011**, *13*, 3440-3445.

(19) Velazquez, H. D.; Verpoort, F. *Chem. Soc. Rev.* **2012**, *41*, 7032. Schaper, L.-A.; Hock, S. J.; Herrmann, W. A.; Kühn, F. E. *Angew. Chem., Int. Ed.* **2013**, *52*, 270–289.

(20) Fantasia, S.; Jacobsen, H.; Cavallo, L.; Nolan, S. P. *Organometallics* **2007**, *26*, 3286-3288. Brissy, D.; Skander, M.; Retailleau, P.; Frison, G.; Marinetti, A. *Organometallics* **2008**, *28*, 140-151. Hu, J. J.; Bai, S. Q.; Yeh, H. H.; Young, D. J.; Chi, Y.; Hor, T. S. A. *Dalton Trans.* **2011**, *40*, 4402-4406.

(21) Fantasia, S.; Petersen, J. L.; Jacobsen, H.; Cavallo, L.; Nolan, S. P. *Organometallics* **2007**, *26*, 5880-5889.

(22) Newman, C. P.; Deeth, R. J.; Clarkson, G. J.; Rourke, J. P. *Organometallics* **2007**, *26*, 6225-6233.

(23) Hu, J. J.; Li, F.; Hor, T. S. A. *Organometallics* **2009**, *28*, 1212-1220.

(24) Meyer, D.; Ahrens, S.; Strassner, T. *Organometallics* **2010**, *29*, 3392-3396. Jamali, S.; Milic, D.; Kia, R.; Mazloomi, Z.; Abdolahi, H. *Dalton Trans.* **2011**, *40*, 9362-9365.

(25) Lillo, V.; Mata, J.; Ramírez, J.; Peris, E.; Fernandez, E. *Organometallics* **2006**, *25*, 5829-5831.

(26) Lillo, V.; Mata, J. A.; Segarra, A. M.; Peris, E.; Fernandez, E. *Chem. Commun.* **2007**, 2184-2186.

(27) Jung, I. G.; Seo, J.; Lee, S. I.; Choi, S. Y.; Chung, Y. K. *Organometallics* **2006**, *25*, 4240-4242.

(28) Alves, G.; Morel, L.; El-Ghozzi, M.; Avignant, D.; Legeret, B.; Nauton, L.; Cisnetti, F.; Gautier, A. *Chem. Commun.* **2011**, *47*, 7830-7832. Skander, M.; Retailleau, P.; Bourrié, B.; Schio, L.; Mailliet, P.; Marinetti, A. *J. Med. Chem.* **2010**, *53*, 2146-2154. Chardon, E.; Dahm, G.; Guichard, G.; Bellemin-Laponnaz, S. *Organometallics* **2012**, *31*, 7618-7621.

(29) Silbestri, G. F.; Flores, J. C.; de Jesús, E. *Organometallics* **2012**, *31*, 3355-3360.

(30) Lin, I. J. B.; Vasam, C. S. *Coord. Chem. Rev.* **2007**, *251*, 642-670.

(31) Lin, J. C. Y.; Huang, R. T. W.; Lee, C. S.; Bhattacharyya, A.; Hwang, W. S.; Lin, I. J. B. *Chem. Rev.* **2009**, *109*, 3561-3598.

(32) Wang, H. M. J.; Lin, I. J. B. *Organometallics* **1998**, *17*, 972-975.

(33) Garrison, J. C.; Youngs, W. J. *Chem. Rev.* **2005**, *105*, 3978-4008.

(34) de Frémont, P.; Scott, N. M.; Stevens, E. D.; Ramnial, T.; Lightbody, O. C.; Macdonald, C. L. B.; Clyburne, J. A. C.; Abernethy, C. D.; Nolan, S. P. *Organometallics* **2005**, *24*, 6301-6309.

(35) Su, H.-L.; Pérez, L. M.; Lee, S.-J.; Reibenspies, J. H.; Bazzi, H. S.; Bergbreiter, D. E. *Organometallics* **2012**, *31*, 4063-4071.

(36) McGuinness, D. S.; Cavell, K. J. *Organometallics* **2000**, *19*, 741-748. Wang, X.; Liu, S.; Weng, L.-H.; Jin, G.-X. *Organometallics* **2006**, *25*, 3565-3569. Newman, C. P.; Clarkson, G. J.; Rourke, J. P. *J. Organomet. Chem.* **2007**, *692*, 4962-4968.

(37) Alexander, R.; Ko, E. C. F.; Mac, Y. C.; Parker, A. J. *J. Am. Chem. Soc.* **1967**, *89*, 3703-3712.

(38) Moore, L. R.; Cooks, S. M.; Anderson, M. S.; Schanz, H.-J.; Griffin, S. T.; Rogers, R. D.; Kirk, M. C.; Shaughnessy, K. H. *Organometallics* **2006**, *25*, 5151-5158.

(39) Papini, G.; Pellei, M.; Gioia Lobbia, G.; Burini, A.; Santini, C. *Dalton Trans.* **2009**, 6985-6990.

(40) Kascatan-Nebioglu, A.; Panzner, M. J.; Garrison, J. C.; Tessier, C. A.; Youngs, W. J. *Organometallics* **2004**, *23*, 1928-1931. Melaiye, A.; Simons, R. S.; Milsted, A.; Pingitore, F.; Wesdemiotis, C.; Tessier, C. A.; Youngs, W. J. *J. Med. Chem.* **2004**, *47*, 973-977. Quezada, C. A.; Garrison, J. C.; Panzner, M. J.; Tessier, C. A.; Youngs, W. J. *Organometallics* **2004**, *23*, 4846-4848. Lee, C.-S.; Pal, S.; Yang, W.-S.; Hwang, W.-S.; Lin, I. J. B. *J. Mol. Catal. A: Chem.* **2008**, *280*, 115-121. Pellei, M.; Gandin, V.; Marinelli, M.; Marzano, C.; Yousufuddin, M.; Dias, H. V. R.; Santini, C. *Inorg. Chem.* **2012**, *51*, 9873-9882.

(41) Cure, J.; Poteau, R.; Gerber, I. C.; Gornitzka, H.; Hemmert, C. *Organometallics* **2012**, *31*, 619-626.

(42) Citadelle, C. A.; Nouy, E. L.; Bisaro, F.; Slawin, A. M. Z.; Cazin, C. S. J. *Dalton Trans.* **2010**, *39*, 4489-4491.

(43) For instance, the percentage of hydrolysis of **2d** after 3 d at 90 °C rose from 3% to 9% in the presence of NaCl.

(44) Biedermann, G.; Sillén, L. G. *Acta Chem. Scand.* **1960**, *14*, 717-725.

(45) Tapu, D.; Dixon, D. A.; Roe, C. *Chem. Rev.* **2009**, *109*, 3385-3407.

(46) Huang, W.; Zhang, R.; Zou, G.; Tang, J.; Sun, J. *J. Organomet. Chem.* **2007**, *692*, 3804-3809.

(47) Partyka, D. V.; Deligonul, N. *Inorg. Chem.* **2009**, *48*, 9463-9475.

(48) Lallemand, J.-Y.; Soulie, J.; Chottard, J.-C. *J. Chem. Soc., Chem. Commun.* **1980**, 436-438.

(49) Marshall, P.; Jenkins, R. L.; Clegg, W.; Harrington, R. W.; Callear, S. K.; Coles, S. J.; Fallis, I. A.; Dervisi, A. *Dalton Trans.* **2012**, *41*, 12839-12846.

(50) Kapoor, P. N.; Kakkar, R. *J. Mol. Struct. THEOCHEM* **2004**, *679*, 149-156.

(51) Alonso, F.; Beletskaya, I. P.; Yus, M. *Chem. Rev.* **2004**, *104*, 3079-3160. Hintermann, L.; Labonne, A. *Synthesis* **2007**, *2007*, 1121-1150.

(52) Tokunaga, M.; Wakatsuki, Y. *Angew. Chem., Int. Ed.* **1998**, *37*, 2867-2869.

(53) Mizushima, E.; Sato, K.; Hayashi, T.; Tanaka, M. *Angew. Chem., Int. Ed.* **2002**, *41*, 4563-4565. Casado, R.; Contel, M.; Laguna, M.; Romero, P.; Sanz, S. *J. Am. Chem. Soc.* **2003**, *125*, 11925-11935.

(54) Chatt, J.; Guy, R. G.; Duncanson, L. A. *J. Chem. Soc.* **1961**, 827-834.

(55) Hartman, J. W.; Hiscox, W. C.; Jennings, P. W. *J. Org. Chem.* **1993**, *58*, 7613-7614. Hiscox, W.; Jennings, P. W. *Organometallics* **1990**, *9*, 1997-1999. Jennings, P. W.; Hartman, J. W.; Hiscox, W. C. *Inorg. Chim. Acta* **1994**, *222*, 317-322.

(56) Francisco, L. W.; Moreno, D. A.; Atwood, J. D. *Organometallics* **2001**, *20*, 4237-4245. Lucey, D. W.; Atwood, J. D. *Organometallics* **2002**, *21*, 2481-2490.

(57) Marion, N.; Ramón, R. S.; Nolan, S. P. *J. Am. Chem. Soc.* **2008**, *131*, 448-449.

(58) Jantke, D.; Cokoja, M.; Pöthig, A.; Herrmann, W. A.; Kühn, F. E. *Organometallics* **2013**, *32*, 741-744

(59) Romeo, R.; Scolaro, L. M.; Catalano, V.; Achar, S. *Inorg. Synth.* **1998**, *32*, 153-158.

(60) Yoshizawa, M.; Ohno, H. *Ionics* **2002**, *8*, 267-271.

(61) Sheldrick, G. M. *Acta Crystallogr., Sect. A: Found. Crystallogr.* **2008**, *64*, 112-122.

(62) Blessing, R. H. *Acta Crystallogr., Sect. A: Found. Crystallogr.* **1995**, *51*, 33-38.

(63) Sheldrick, G. M. *SADABS: Program for Absorption Correction for Data from Area Detector Frames.*

(64) Farrugia, L. J. *J. Appl. Crystallogr.* **1999**, *32*, 837-838.

(65) van der Sluis, P.; Spek, A. L. *Acta Crystallogr., Sect. A: Found. Crystallogr.* **1990**, *46*, 194-201.

Supporting Information

Sulfonated Water-Soluble N-Heterocyclic Carbene Silver(I) Complexes: Behavior in Aqueous Medium and as NHC-transfer Agents to Platinum(II)

Edwin A. Baquero, Gustavo F. Silbestri, Pilar Gómez-Sal, Juan C. Flores,* and Ernesto de Jesús*

Departamento de Química Orgánica y Química Inorgánica, Campus Universitario, Universidad de Alcalá, 28871 Alcalá de Henares, Madrid, Spain.

Email: juanc.flores@uah.es, ernesto.dejesus@uah.es

Table of Contents

1. Crystallographic Data for Compounds 2e, 2e^{Ag+}, 3e, and 4a

Table S1. Crystallographic Data for Compounds **2e**, **2e^{Ag+}**, **3e**, and **4a**.

	2e•5dmso•H_2O	**2e**•6MeOH	**2e^{Ag+}**•2H_2O
empirical formula	$C_{64}H_{98}AgN_4Na_3O_{18}S_9$	$C_{60}H_{92}AgN_4Na_3O_{18}S_4$	$C_{54}H_{68}Ag_2N_4Na_2O_{15}S_4$
formula weight	1676.85	1462.46	1403.08
crystal size (mm)	0.05 × 0.18 × 0.20	0.7 × 0.64 × 0.24	0.4 × 0.3 × 0.3
color / habit	colorless / prismatic	colorless	colorless
temperature (K)	100(2)	200(2)	200(2)
wavelength (Å)	0.71073	0.71073	0.71073
crystal system	monoclinic	triclinic	monoclinic
space group	$P2_1/n$	P-1	$P2/c$
a (Å)	21.864(2)	11.0810(11)	11.119(2)
b (Å)	14.9797(19)	17.746(2)	17.365(4)
c (Å)	24.108(2)	19.4760(12)	18.3179(19)
α (deg)	90	83.536(5)	90
β(deg)	93.662(4)	73.590(7)	81.104(14)
γ (deg)	90	72.324(10)	90
volume (Å^3)	7879.6(15)	3498.9(6)	3494.4(11)
Z	4	2	2
calcd density (g/cm^3)	1.413	1.388	1.334
μ (mm^{-1})	0.576	0.494	0.750
F(000)	3512	1536	1440
θ range (deg)	1.22 to 20.91	3.01 to 27.50	3.09 to 27.58
limiting indices (h, k, l)	–19/21, –13/14, ±24	±14, ±23, ±25	±14, 0/22, 0/23
no. of reflns collected	34390	30781	7973
no. of reflns unique / R_{int}	8022 / 0.0510	16021 / 0.0665	7973 / 0.1053
no. of reflns observed [$I > 2\sigma(I)$]	6369	9107	4981
completeness to θ	96.1%	99.7%	98.4%
absorption correction	multi-scan	semi-empirical from equivalents	semi-empirical from equivalents
max. and min. transmission	0.9717 and 0.8934	0.906 and 0.727	0.746 and 0.505
refinement method	full-matrix least-squares on F^2		
no. of data / restraints / parameters	8022 / 0 / 892	16021 / 0 / 818	7973 / 0 / 367
goodness of fit on F^2	1.084	1.038	1.157
$R1$ / $wR2$ [$I > 2\sigma(I)$][a]	0.0835 / 0.2479	0.0729 / 0.1815	0.1119 / 0.3041
$R1$ / $wR2$ (all data)	0.1127 / 0.2973	0.1417 / 0.2036	0.1444 / 0.3280
largest diff. peak and hole (e/Å^3)	1.929 and –1.524	2.520 and –0.946	2.770 and –4.956

[a] $R1 = \Sigma(||F_o|-|F_c||)/\Sigma|F_o|$; $wR2 = \{[\Sigma w(F_o^2-F_c^2)]/[\Sigma w(F_o^2)^2]\}^{1/2}$.

Table S1 (cont.). Crystallographic Data for Compounds **2e**, **2e**$^{Ag+}$, **3e**, and **4a**.

	3e•2Me$_2$SO	**4a**•3.5H$_2$O
empirical formula	$C_{31}H_{49}AgClN_2Na_2O_8S_4$	$C_{11}H_{20}Cl_2N_2Na_2O_{10.5}PtS_3$
formula weight	895.26	756.45
crystal size (mm)	0.10 × 0.18 × 0.37	0.12 × 0.16 × 0.27
color / habit	pale yellow / prismatic	colorless / prismatic
temperature (K)	296(2)	296(2)
wavelength (Å)	0.71073	0.71073
crystal system	monoclinic	triclinic
space group	$P2_1/c$	P-1
a (Å)	10.2882(3)	8.2265(2)
b (Å)	14.4724(4)	10.4402(2)
c (Å)	31.0300(9)	16.4703(4)
α (deg)	90	96.1470(10)
β(deg)	91.9910(10)	93.5040(10)
γ (deg)	90	95.0300(10)
volume (Å^3)	4617.4(2)	1397.47(5)
Z (g/cm^3)	4	2
calcd density (g/mol)	1.288	1.798
μ (mm^{-1})	0.735	5.510
F(000)	1852	732
θ range (deg)	1.31 to 25.39	1.25 to 25.35
limiting indices (h, k, l)	–11/12, ±17, ±37	±9, ±12, ±19
no. of reflns collected	67891	35550
no. of reflns unique / R_{int}	67891	5064 / 0.0358
no. of reflns observed [$I > 2\sigma(I)$]	4984	4933
completeness to θ	98.6%	98.6%
absorption correction	multi-scan	multi-scan
max. and min. transmission	0.9301 and 0.7727	0.5577 and 0.3177
refinement method	full-matrix least-squares on F^2	
no. of data / restraints / parameters	8389 / 4 / 504	5064 / 0 / 271
goodness of fit on F^2	1.086	1.141
$R1$ / $wR2$ [$I > 2\sigma(I)$][a]	0.0773 / 0.2337	0.0801/0.2255
$R1$ / $wR2$ (all data)	0.1340 / 0.2863	0.0859/0.2428
largest diff. peak and hole (e/Å^3)	1.360 and –0.668	5.667 and –6.503

[a] $R1 = \Sigma||F_o|-|F_c||/\Sigma|F_o|$; $wR2 = \{[\Sigma w (F_o^2-F_c^2)]/[\Sigma w (F_o^2)^2]\}^{1/2}$.

2. ^{1}H and $^{13}C\{^{1}H\}$ NMR spectra of the new complexes (Figures S1–S13)

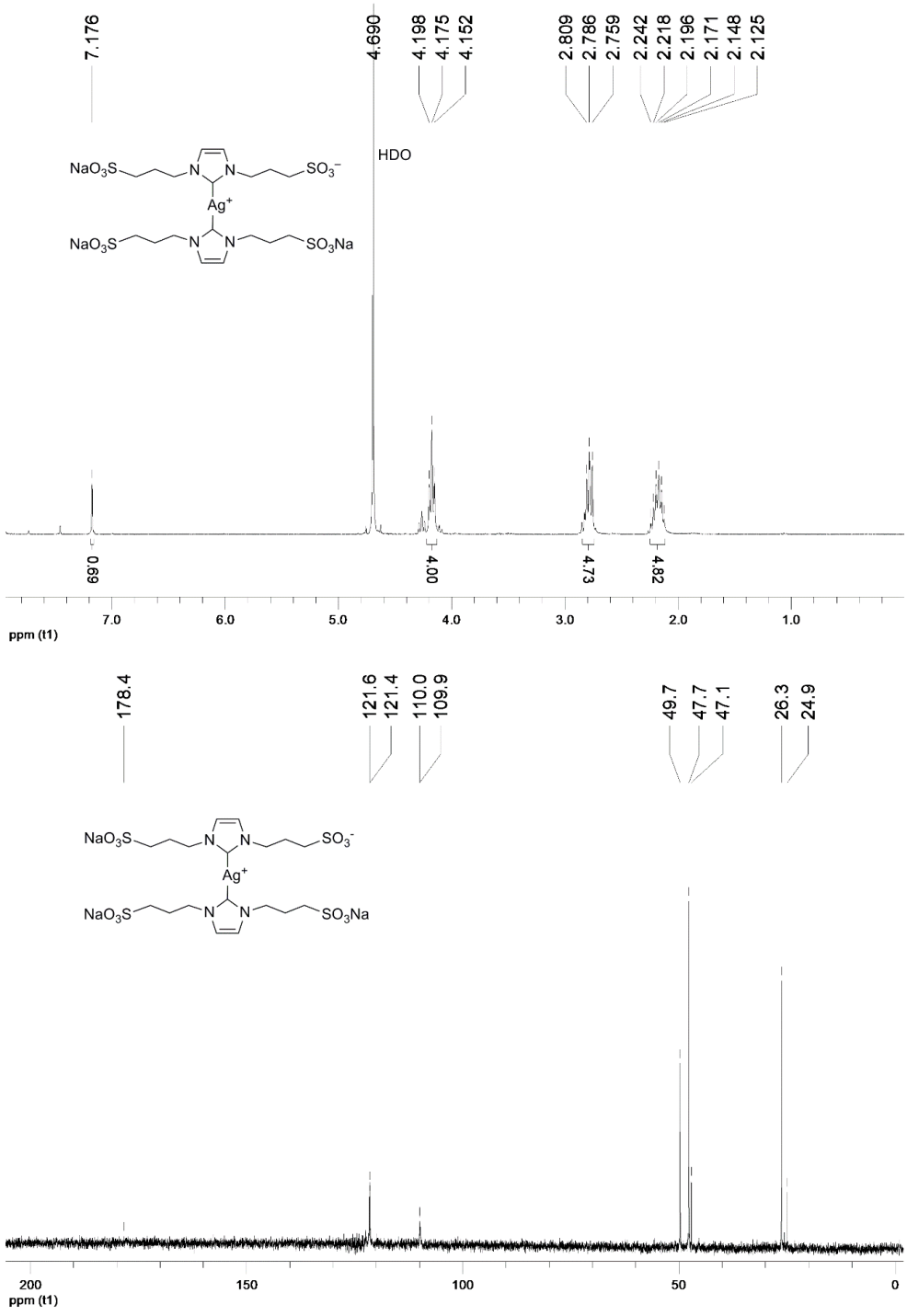

Figure S1. ^{1}H (300 MHz, D_2O) and $^{13}C\{^{1}H\}$ (75 MHz, D_2O) NMR Spectra for **2a**

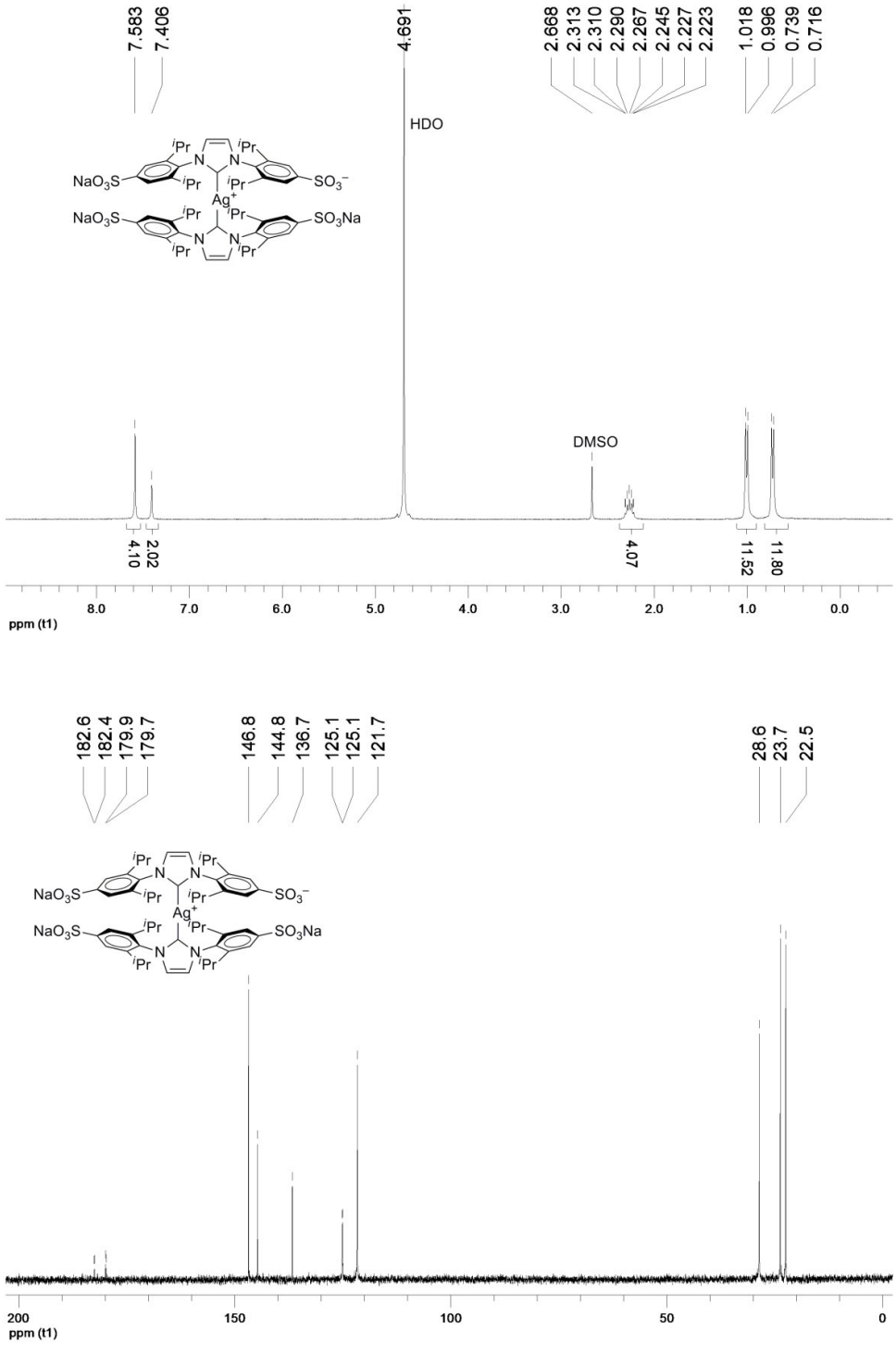

Figure S2. ^{1}H (300 MHz, D_2O) and $^{13}C\{^{1}H\}$ (75 MHz, D_2O) NMR Spectra for **2e**

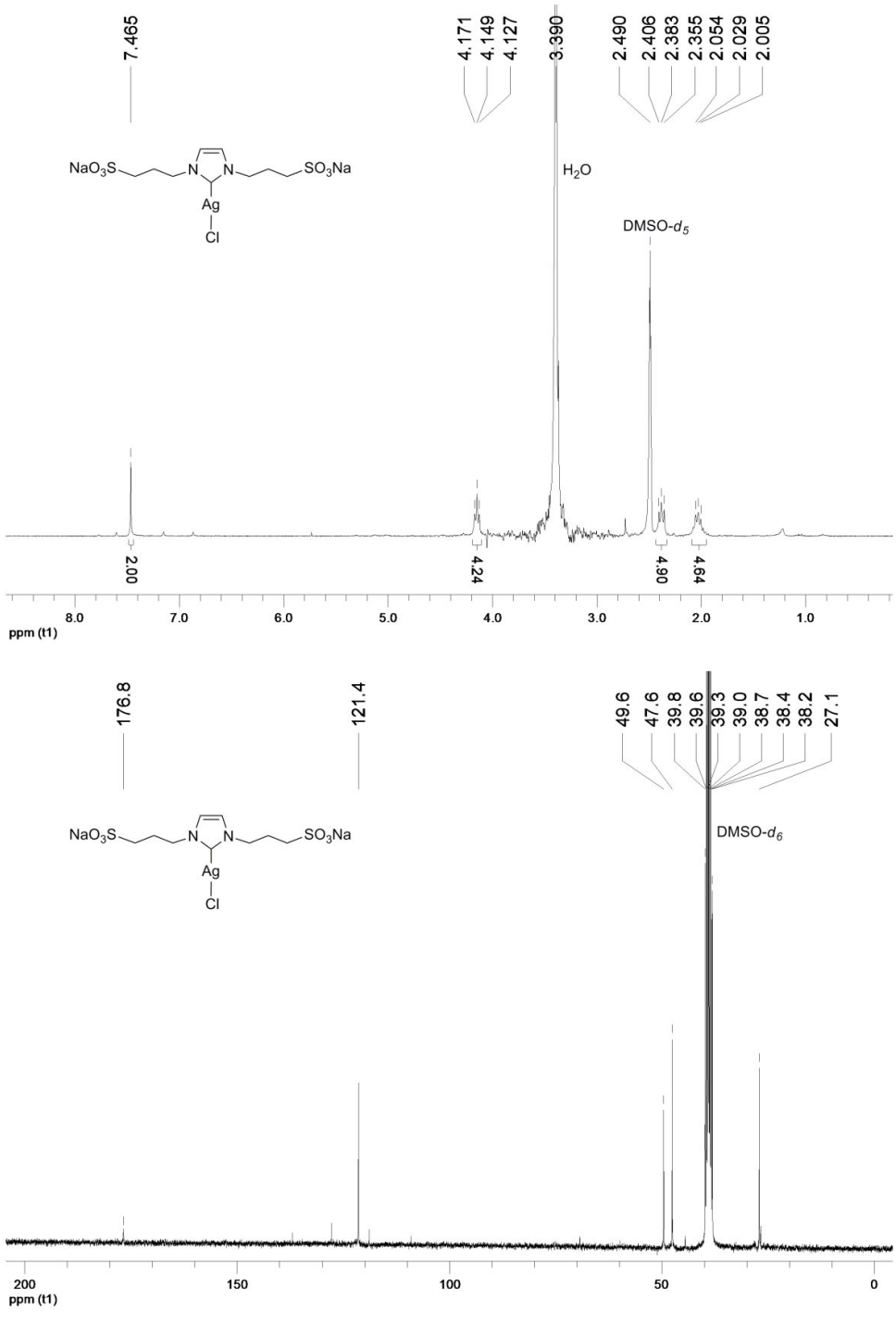

Figure S3. ^{1}H (300 MHz, DMSO-d_6) and $^{13}C\{^{1}H\}$ (75 MHz, DMSO-d_6) NMR Spectra for **3a**

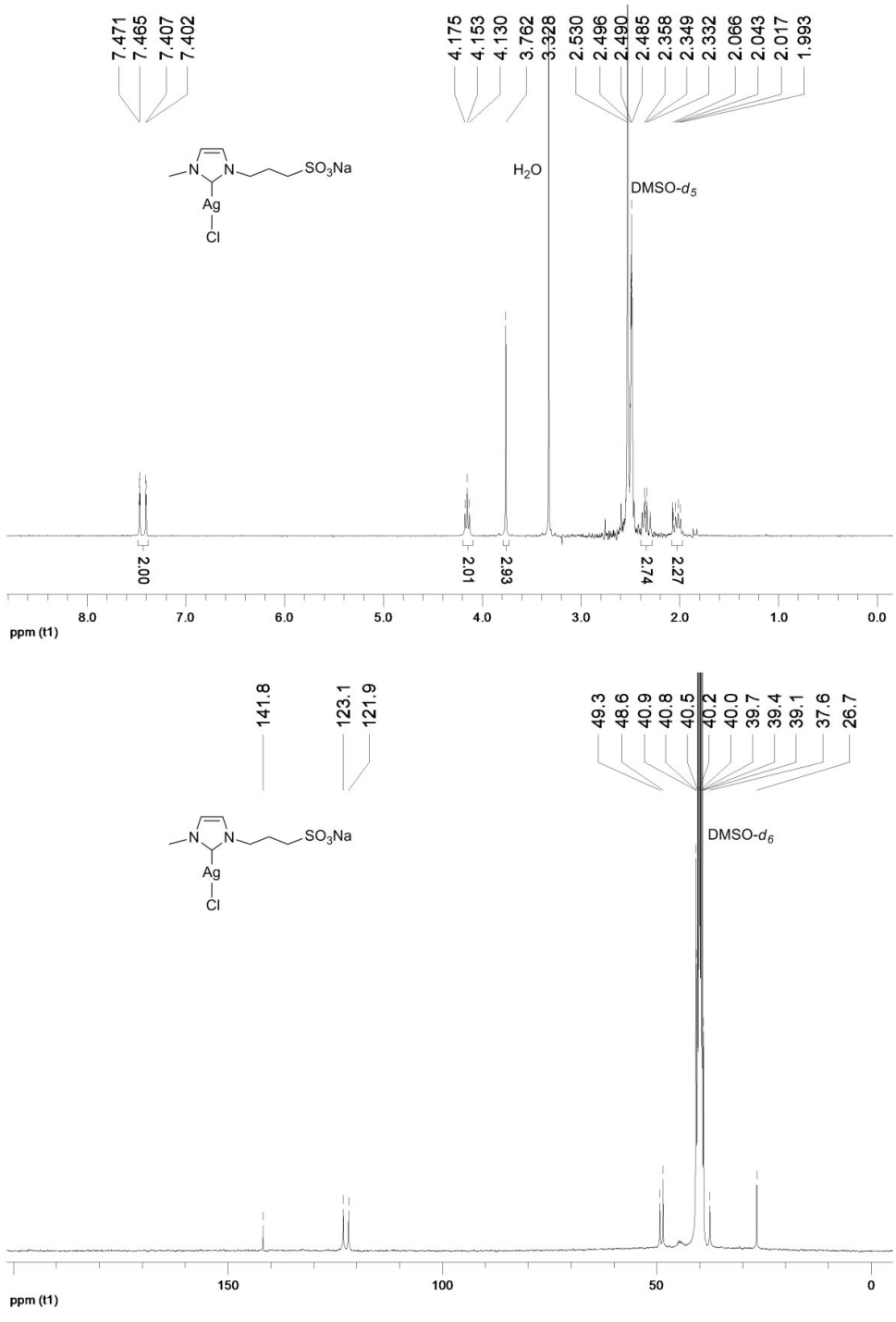

Figure S4. ^{1}H (300 MHz, DMSO-d_6) and $^{13}C\{^{1}H\}$ (75 MHz, DMSO-d_6) NMR Spectra for **3b**

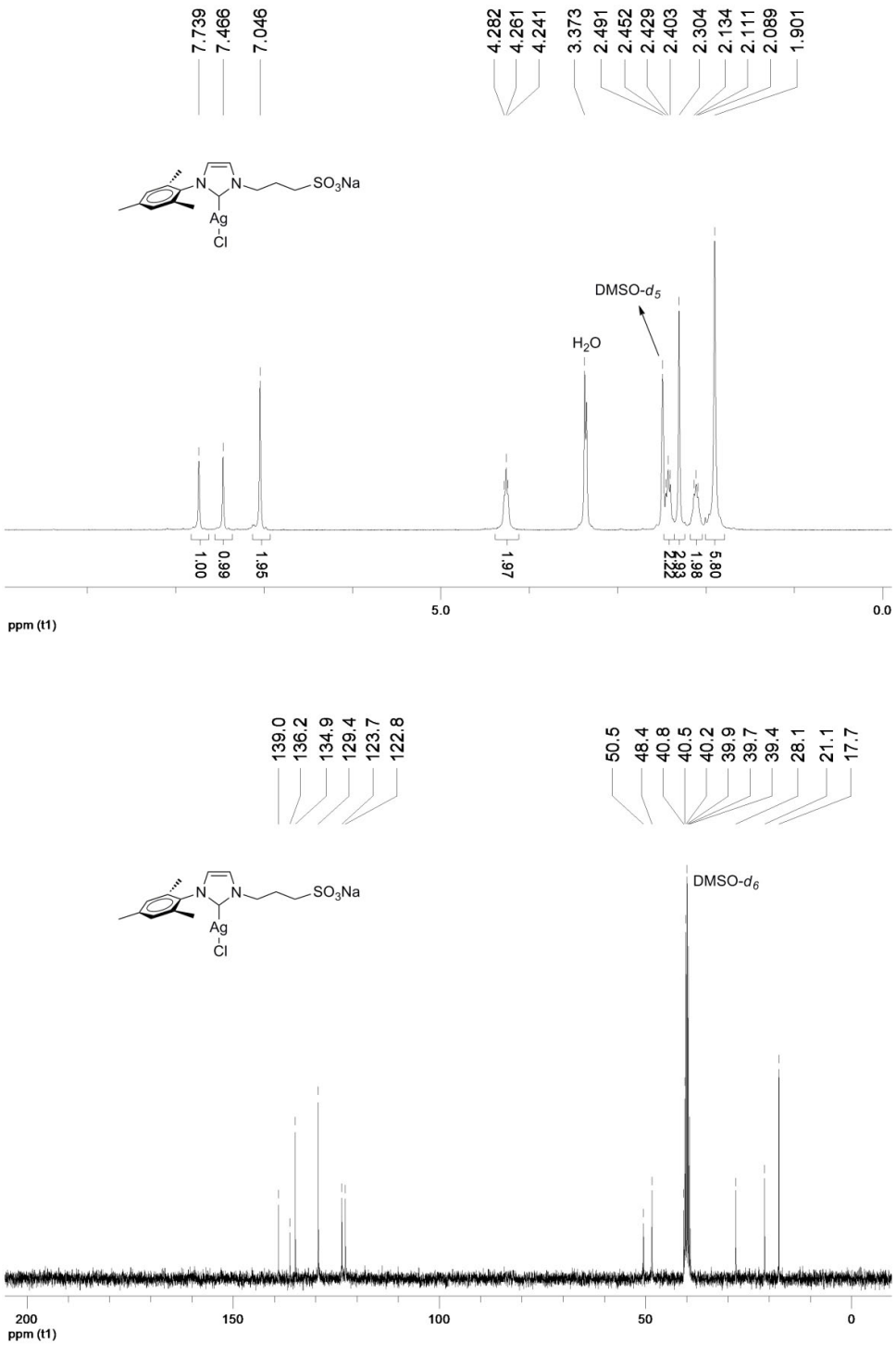

Figure S5. ^{1}H (300 MHz, DMSO-d_6) and $^{13}C\{^{1}H\}$ (75 MHz, DMSO-d_6) NMR Spectra for **3c**

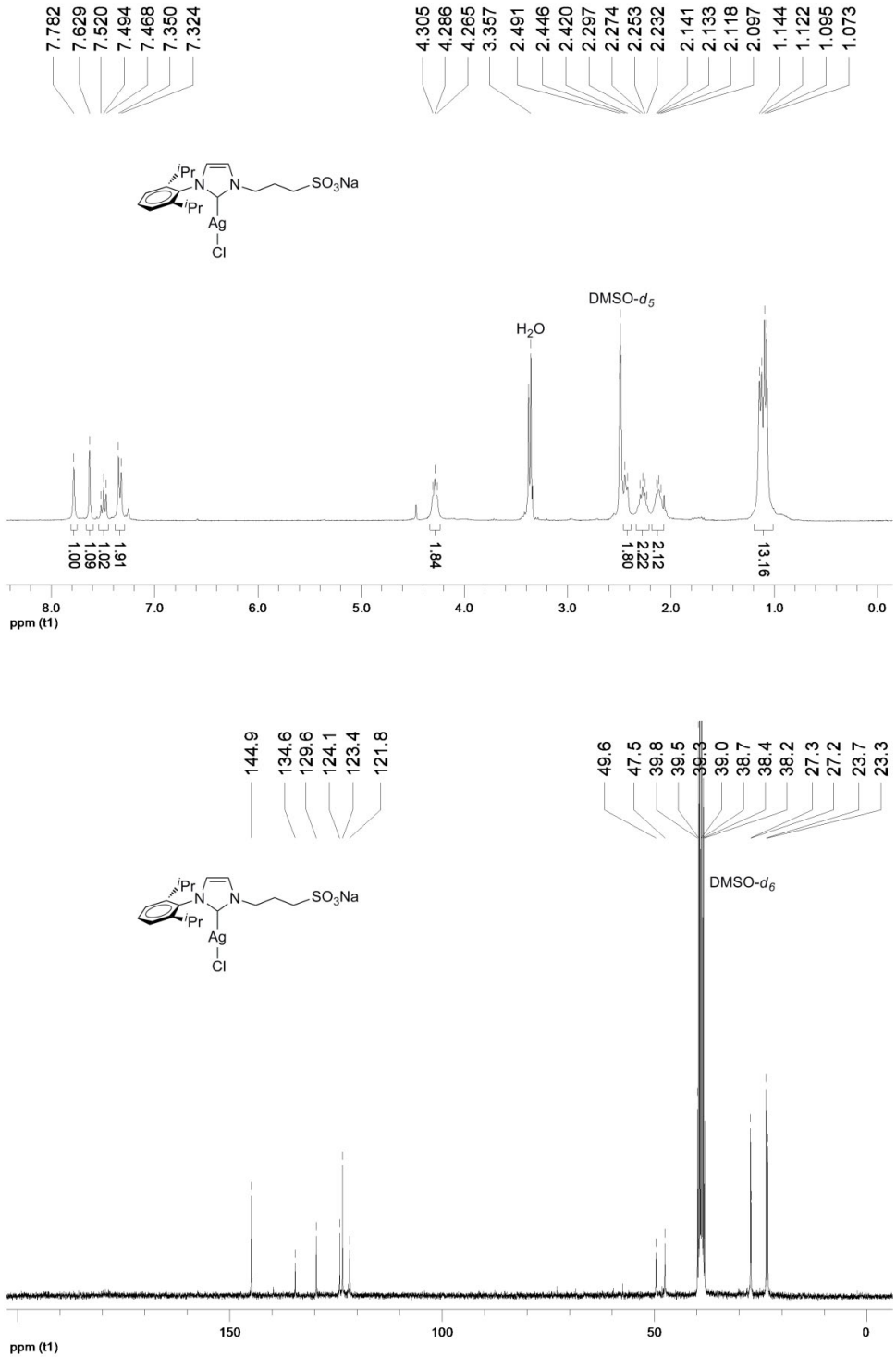

Figure S6. ^{1}H (300 MHz, DMSO-d_6) and $^{13}C\{^{1}H\}$ (75 MHz, DMSO-d_6) NMR Spectra for **3d**

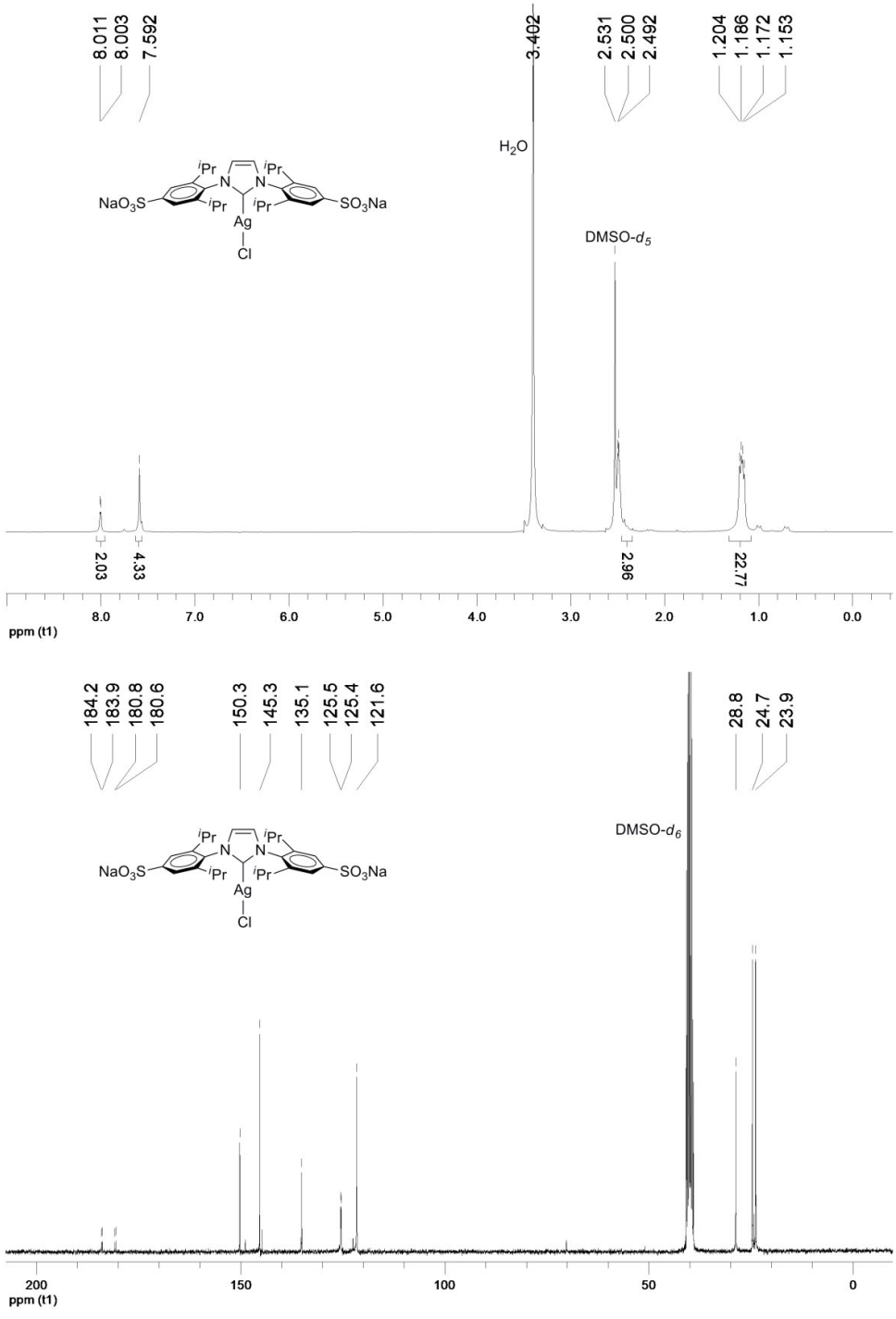

Figure S7. ^{1}H (300 MHz, DMSO-d_6) and $^{13}C\{^{1}H\}$ (75 MHz, DMSO-d_6) NMR Spectra for **3e**

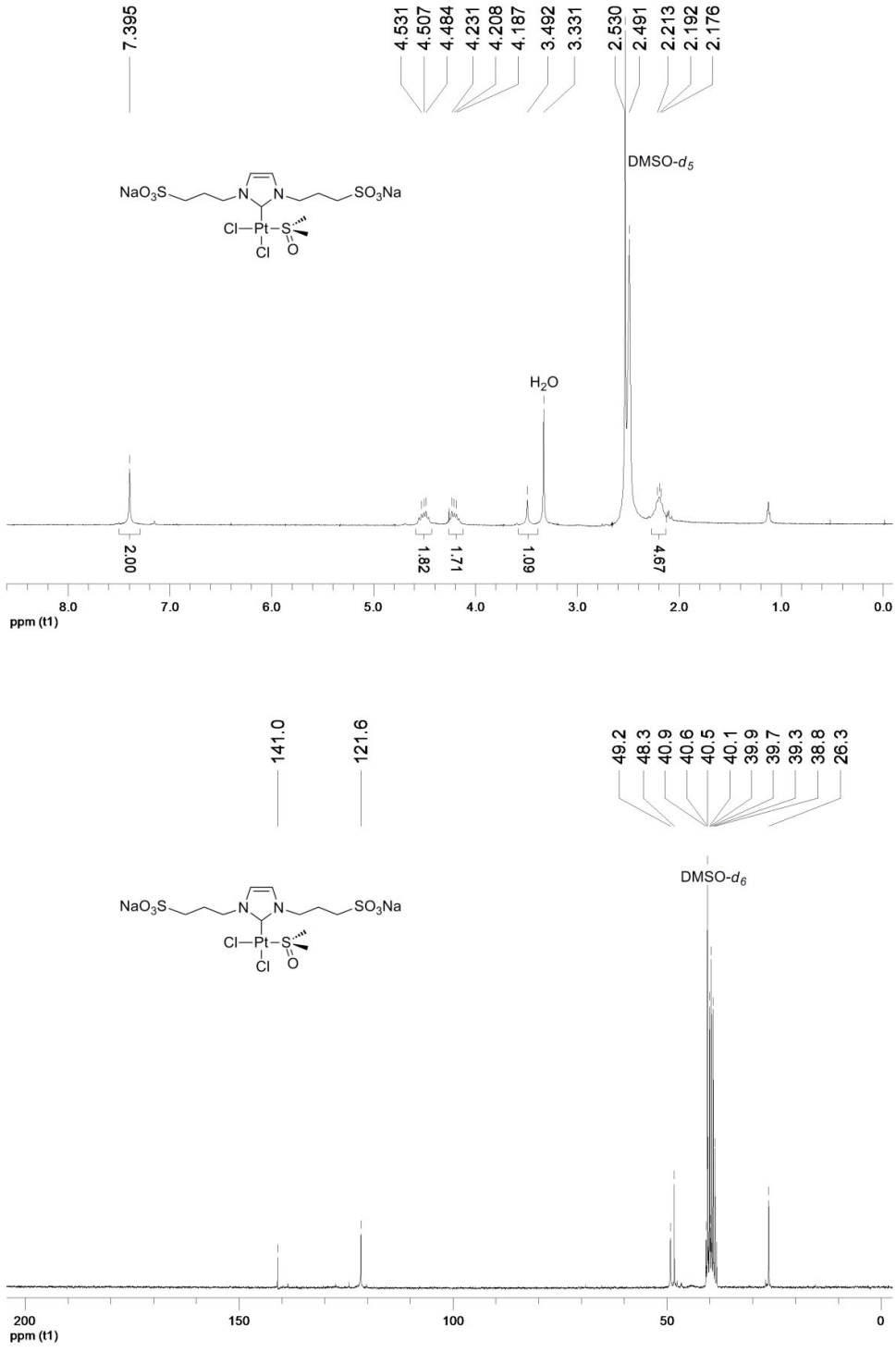

Figure S8. ^{1}H (300 MHz, DMSO-d_6) and $^{13}C\{^{1}H\}$ (75 MHz, DMSO-d_6) NMR Spectra for **4a**

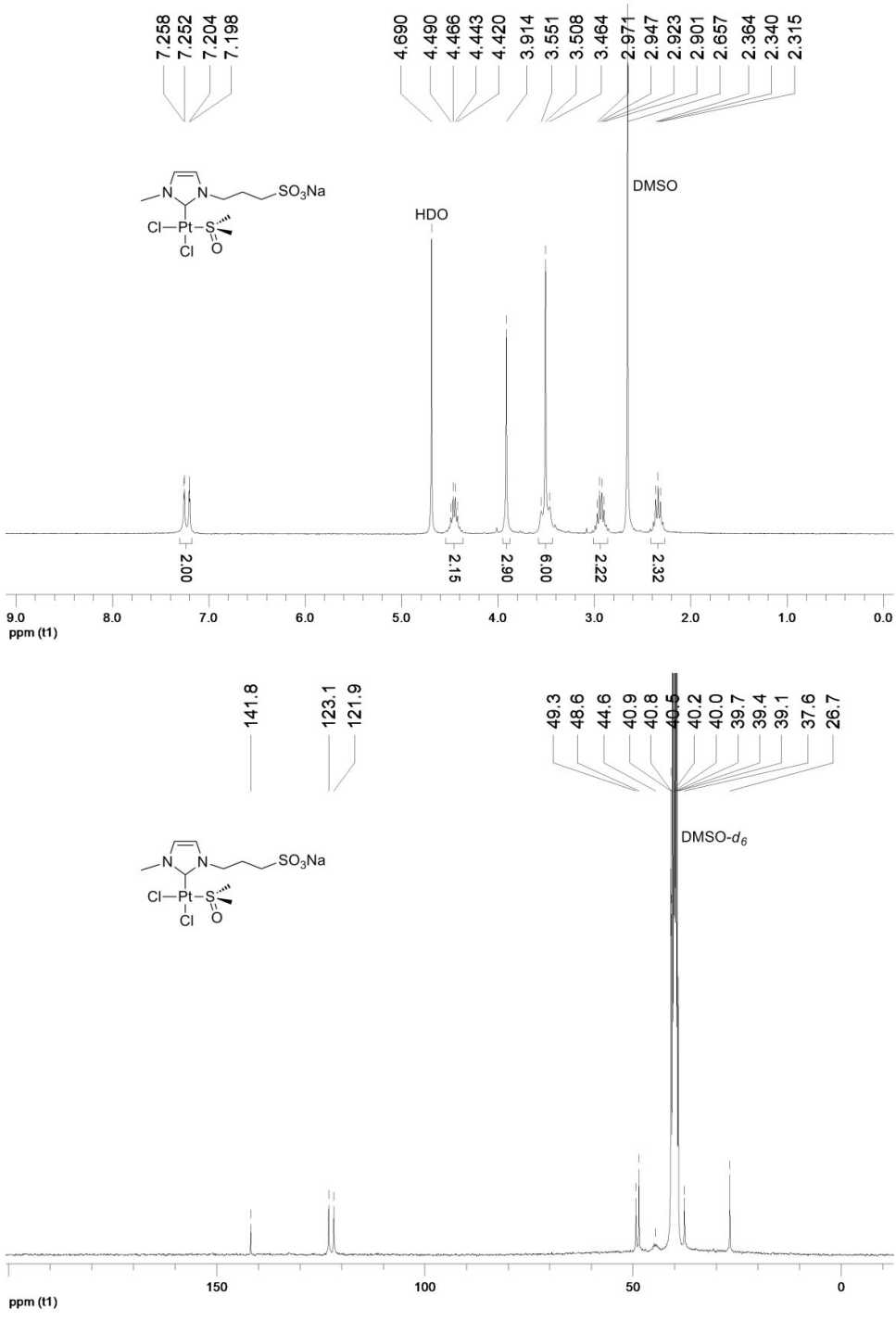

Figure S9. ^{1}H (300 MHz, D_2O) and $^{13}C\{^{1}H\}$ (75 MHz, DMSO-d_6) NMR Spectra for **4b**

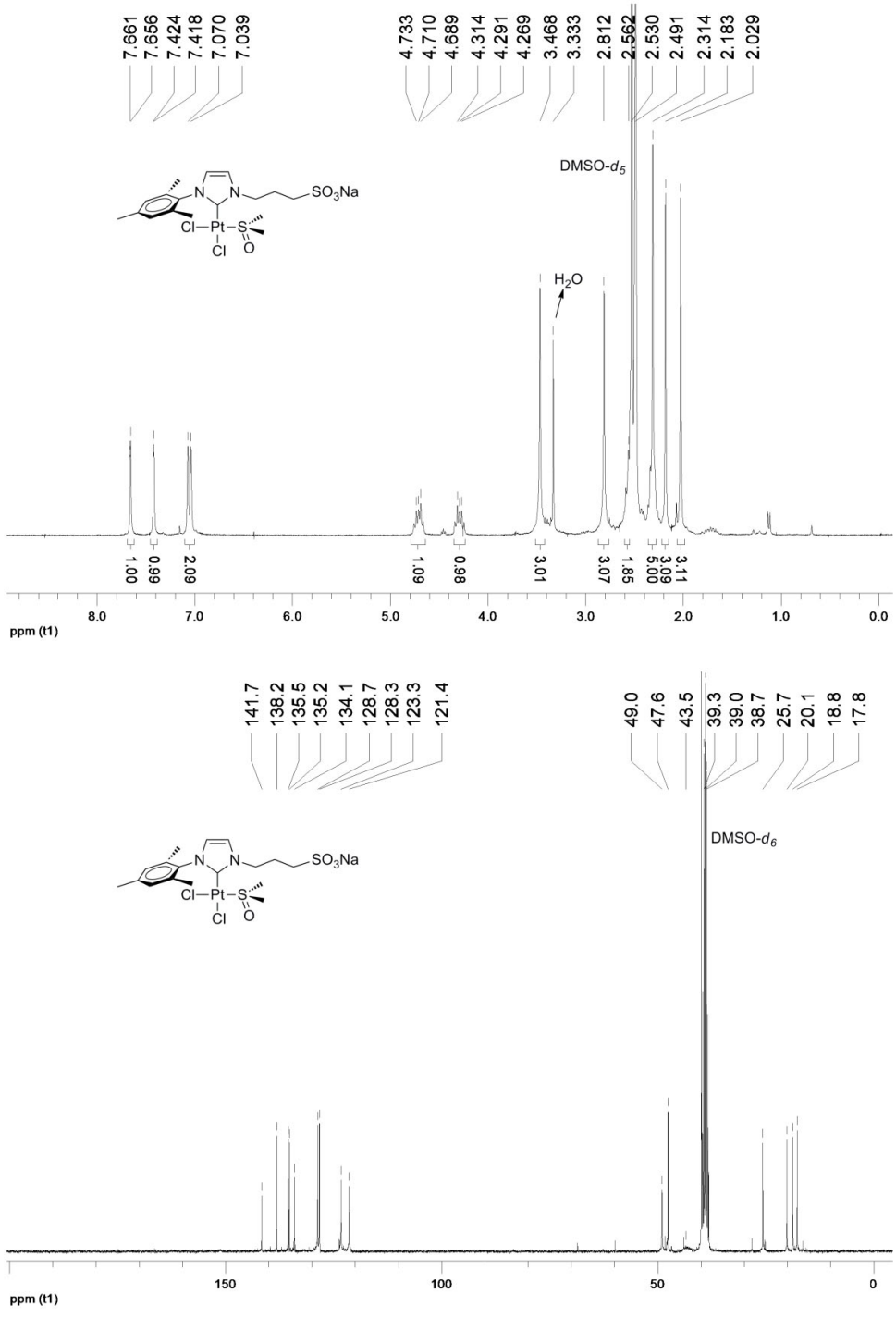

Figure S10. ^{1}H (300 MHz, DMSO-d_6) and $^{13}C\{^{1}H\}$ (75 MHz, DMSO-d_6) NMR Spectra for **4c**

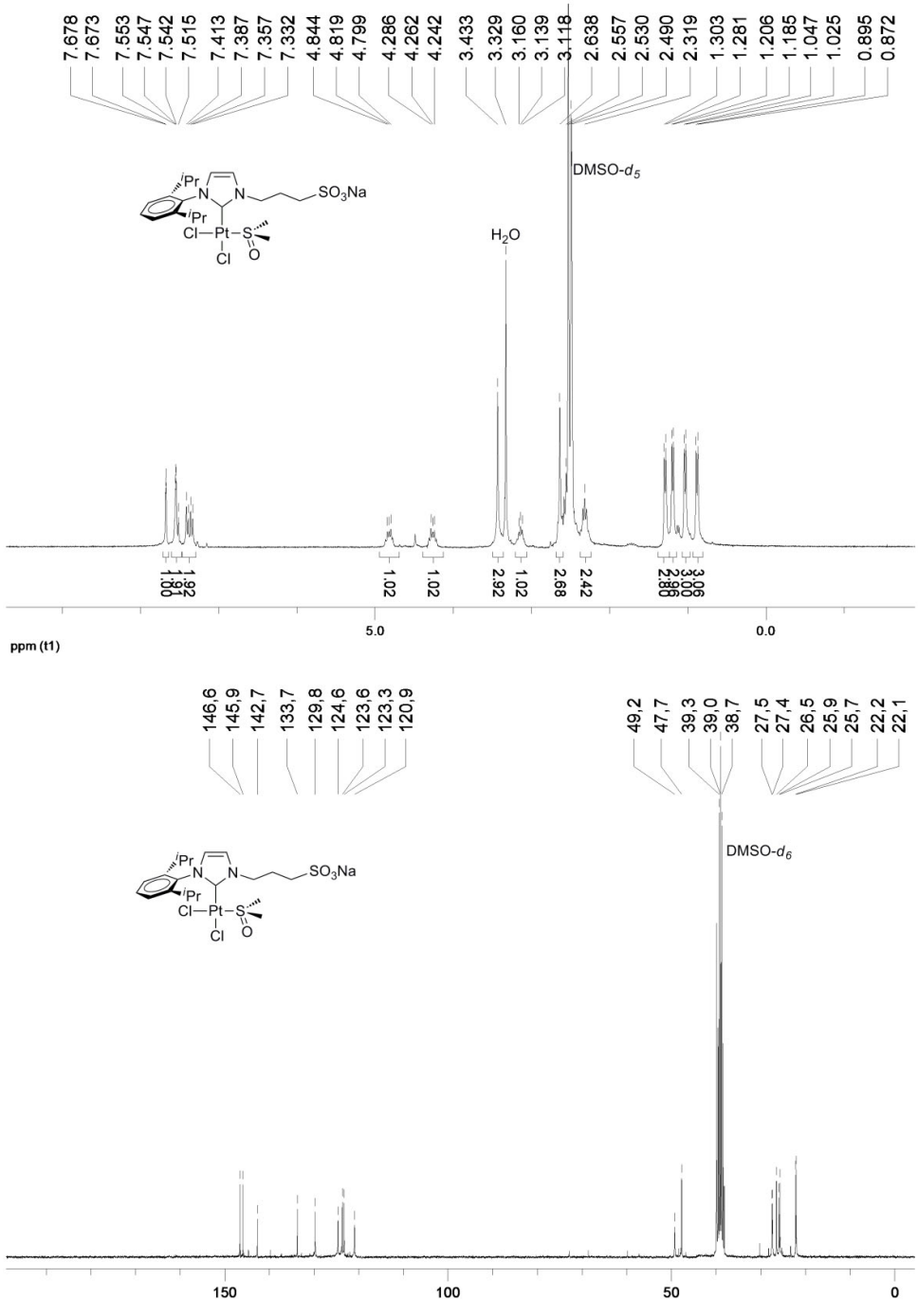

Figure S11. ^{1}H (300 MHz, DMSO-d_6) and $^{13}C\{^{1}H\}$ (75 MHz, DMSO-d_6) NMR Spectra for **4d**

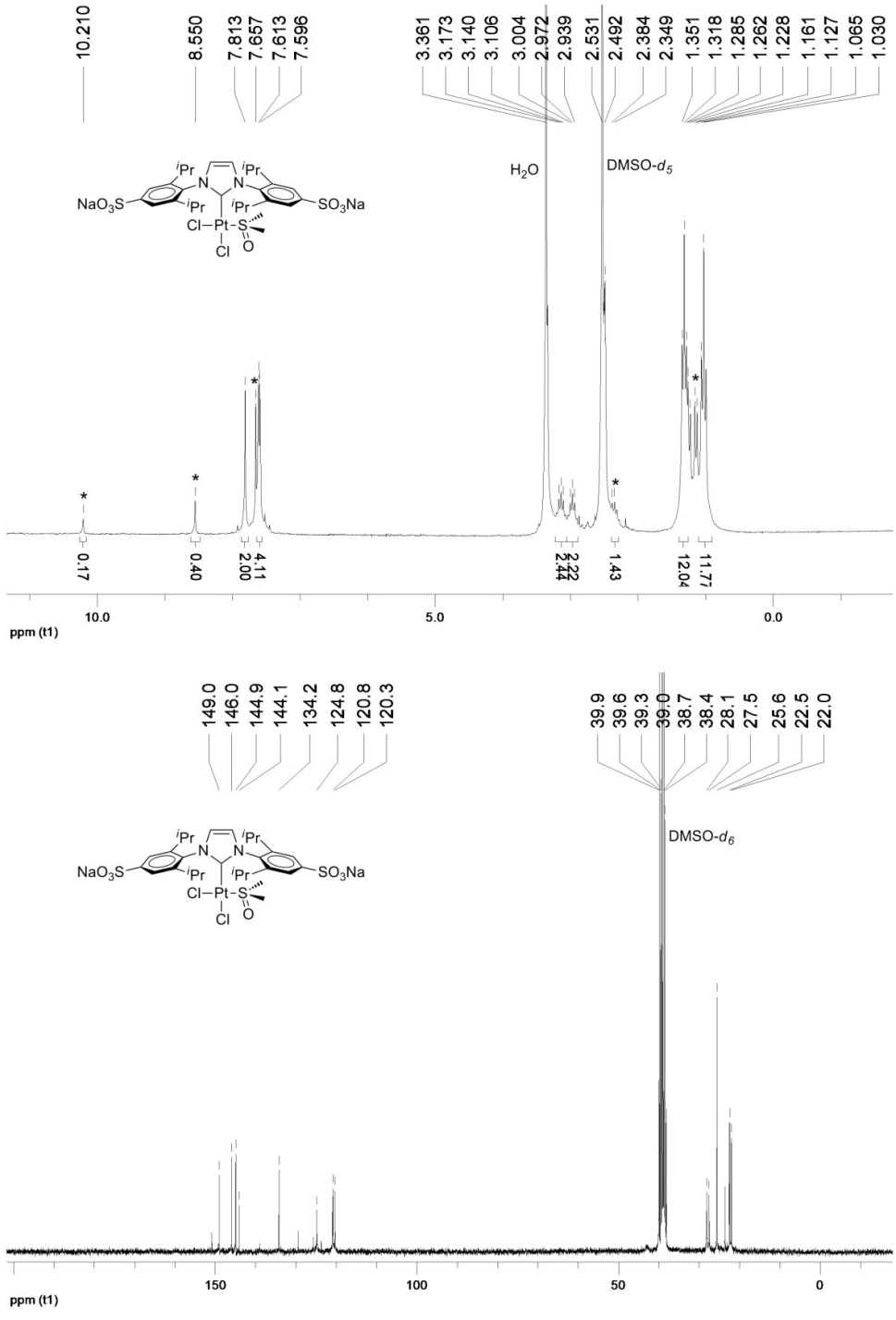

Figure S12. ^{1}H (300 MHz, DMSO-d_6) and $^{13}C\{^{1}H\}$ (75 MHz, DMSO-d_6) NMR Spectra for **4e** (The signals marked with an asterix, correspond to the imidazolium salt **e–H**)

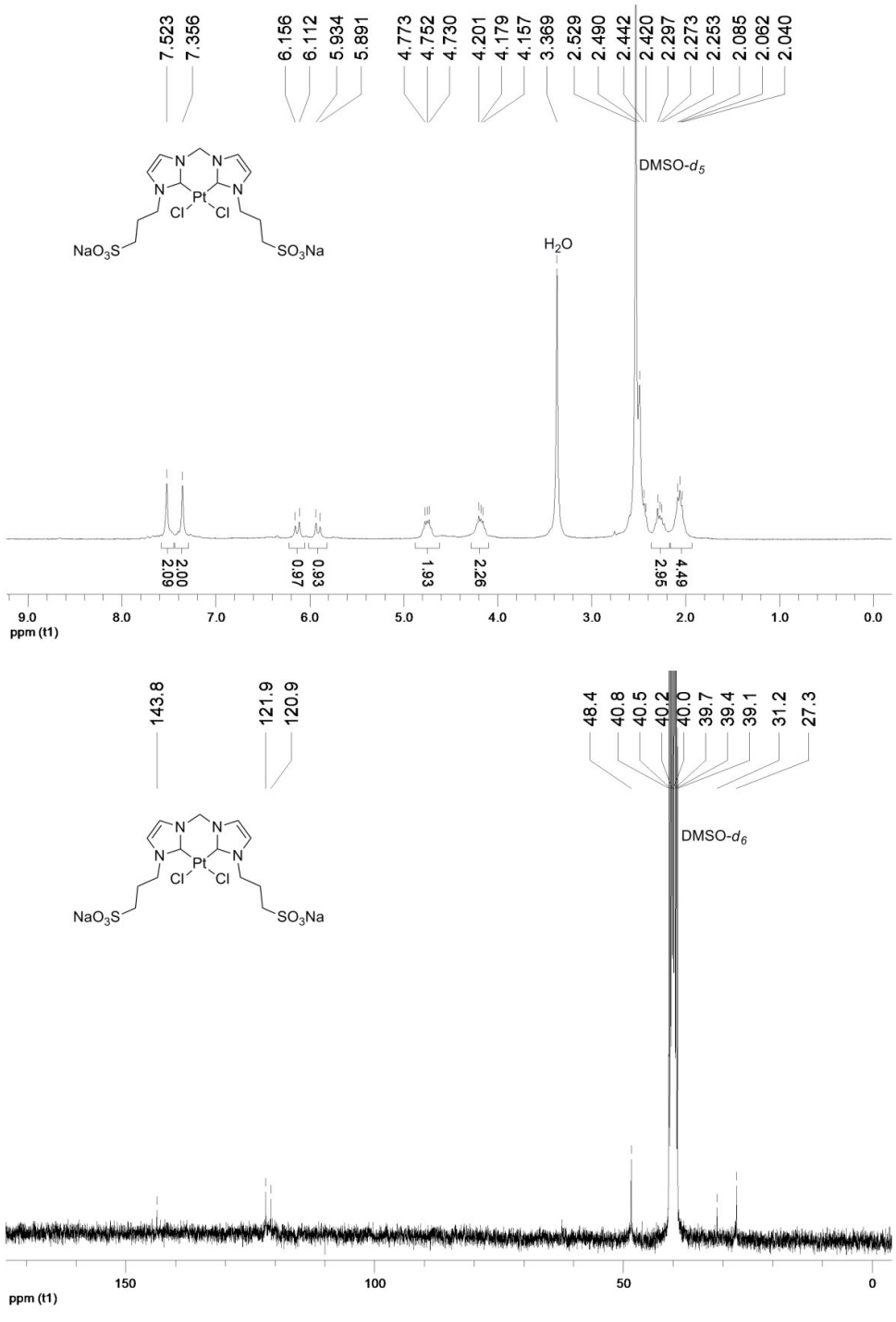

Figure S13. ^{1}H (300 MHz, DMSO-d_6) and $^{13}C\{^{1}H\}$ (75 MHz, DMSO-d_6) NMR Spectra for **5**

Chapter IV. Water-Soluble Mono- and Dimethyl N-Heterocyclic Carbene Platinum(II) Complexes: Synthesis and Reactivity

Edwin A. Baquero, Juan C. Flores, Josefina Perles, Pilar Gómez-Sal, and Ernesto de Jesús, *Organometallics*, **2014**, *33*, 5470–5482. *One of the most read articles in October 2014*

Aqueous-Phase Reactivity

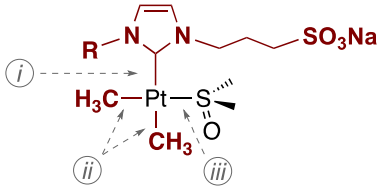

stable at room temperature in neutral water or alkaline media

(*i*) **inert bond**

(*ii*) **hydrolysis/reductive elimination, selective protonolysis**

(*iii*) **substitution reactions**

Water-Soluble Mono- and Dimethyl N-Heterocyclic Carbene Platinum(II) Complexes: Synthesis and Reactivity

Edwin A. Baquero,[†] Juan C. Flores,[†] Josefina Perles,[‡] Pilar Gómez-Sal[†] and Ernesto de Jesús*[†]*

[†]Departamento de Química Orgánica y Química Inorgánica, Campus Universitario, Universidad de Alcalá, 28871 Alcalá de Henares, Madrid, Spain

[‡]Servicio Interdepartamental de Investigación (SIDI), Universidad Autónoma de Madrid, Cantoblanco, 28049 Madrid, Spain

ABSTRACT

A family of water-soluble dimethyl complexes of formula *cis*-[$PtMe_2$(dmso)(NHC·Na)] (**2**), in which NHC is an anionic N-heterocyclic carbene bearing a sulfonatepropyl chain on one of the nitrogen atoms and a sulfonatepropyl (**a**), methyl (**b**), mesityl (**c**) or 2,6-diisopropylphenyl group (**d**) on the other, have been prepared. The hydrolytic stability of the Pt−C bonds in these complexes under different neutral, alkaline and acidic aqueous conditions has also been studied. Complexes **2** were found to be quite stable at room temperature in water under neutral or alkaline conditions. Degradation occurred at higher temperatures but involved Csp^3–H activation and C–C reductive elimination processes in addition to Pt–Me bond hydrolysis. Hydrolytic cleavage of the platinum-methyl bonds was favored by good nucleophiles. Thus, the addition of KCN to an aqueous solution of **2** resulted in formation of the monomethyl complexes K[$PtMe(CN)_2$(NHC·Na)] (**9**), whereas the dimethyl complexes K[$PtMe_2$(CNR)(NHC·Na)] (**10**) were formed with the isocyanide $CNCH_2COOK$. The addition of stoichiometric amounts of protic acids to aqueous solutions of **2** resulted in the clean cleavage of one or both platinum(II)−methyl bonds. Thus, the reaction of **2** with HCl afforded the complexes [PtClMe(dmso)(NHC·Na)] (**3**) and [$PtCl_2$(dmso)(NHC·Na)] (**4**), whereas [$PtMe(OH_2)$(dmso)(NHC)] (**5**) and [$Pt(OH_2)_2$(dmso)(NHC)][BF_4] were obtained upon treatment with HBF_4. The crystal structure of **9a** is remarkable in light of the longitudinal channels around 6 Å in diameter internally decorated with Pt–Me bonds.

INTRODUCTION

N-heterocyclic carbenes (NHCs)[1] derived from imidazole are characterized by their versatile substitution and outstanding features as ancillary ligands. Their strong σ-donor capabilities in conjunction with usual imposed steric protection tend to afford robust bonds to metals in

fairly stable complexes[2] that are able to catalyze a wide range of homogenous processes[3] and also have many other major applications.[4] Since water offers exceptional chemical reactivity due to its unique properties, such as its ability to solvate salts and polar compounds or its high dielectric constant, the interest in using water-soluble NHC metal complexes for some of their applications is evident. A convenient way to render NHC metal complexes water-soluble involves the attachment of ionic or non-ionic hydrophilic substituents to the NHC ligand.[5] Herrmann and coworkers patented the first examples of such NHC complexes in 1995,[6] which was followed by a report from Özdemir's group describing a water-soluble NHC-based ruthenium catalyst for the synthesis of 2,3-dimethylfuran.[7] In the last few years, the number of new complexes of this type has increased and, subsequently, the range of catalytic processes tested with them in the aqueous phase has widened. For instance, ruthenium complexes have been studied in olefin metathesis,[8] allylic alcohol isomerizations,[9] or acetophenone hydrogenations,[10] with palladium complexes being studied in cross-coupling reactions,[11,12] gold complexes in alkyne hydrations,[13,14] iridium complexes in transfer hydrogenations,[15] and copper complexes in click reactions.[16] The synthesis and application of water-soluble NHC transition-metal complexes in catalysis has recently been reviewed.[17]

Platinum(II) complexes containing more conventional monodentate[18,19,20] or chelating[20,21,22] NHC ligands have proven to be useful in a variety of catalytic processes in organic solvents, such as diboration of unsaturated molecules,[23] tandem hydroboration-cross coupling,[24] or reductive cyclization of diynes and enynes,[25] and also as metal-based chemotherapeutic agents.[26] However, platinum complexes containing hydrophilic NHC ligands were unknown until recently, when we reported the synthesis of water-soluble (NHC)Pt(0)[27] and Pt(II)[28] complexes that could be used as recoverable catalysts for the hydrosilylation of alkynes in water at room temperature in the former case, or for the hydration of alkynes in water in the latter.

Although the applications of water-soluble NHC complexes are progressing rapidly, there is as yet little information available concerning basic aspects of the chemical reactivity of these complexes in water, including the limits of the hydrolytic stability of the metal-NHC bonds. The aim of this work was to gain an understanding of the chemical behavior of water-soluble NHC platinum compounds containing alkyl ligands in the aqueous phase. Thus, herein we disclose the synthesis of methyl complexes of platinum(II) coordinated to sulfonated NHC ligands **a**−**d** (Figure 1) in a study that focuses on the hydrolytic stability of the Pt−C bonds in these complexes.

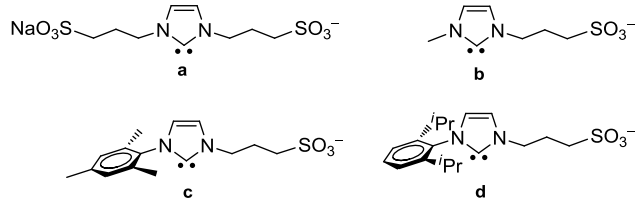

Figure 1. Anionic sulfonated NHC ligands used in this work.

RESULTS AND DISCUSSION

Synthesis and Characterization of the Dimethyl NHC Platinum(II) Complexes 2a−d. The mono(NHC) complexes *cis*-[$PtMe_2$(dmso)(NHC·Na)] (**2a−d**) were obtained by treating *cis*-[$PtMe_2(dmso)_2$] with a stoichiometric amount of the corresponding imidazolium salt **1a−d** using sodium *tert*-butoxide as the deprotonating agent (Scheme 1; the NHCs used in this work are anionic and the neutral formula unit will be abbreviated for convenience as NHC·Na). The transformations were completed in less than 1 h in dmso at room temperature and, after a simple work-up, the complexes were obtained as analytically pure solids in very high yields (>90%).

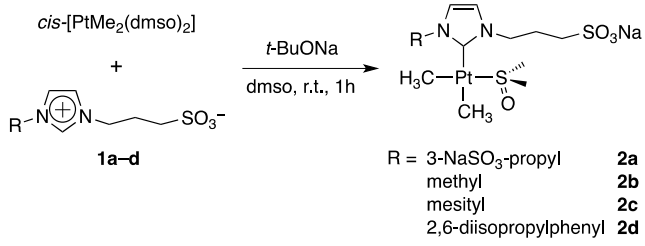

Scheme 1. Synthesis of the Complexes *cis*-[$PtMe_2$(dmso)(NHC·Na)] (**2**)

Complexes **2** were characterized by ^{1}H, ^{13}C and ^{195}Pt NMR spectroscopy, mass spectrometry (ESI-TOF), and elemental analysis, in addition to X-ray diffraction in the case of **2a**. Samples of **2a** and **2b** gave accurate C, H, and N analyses after being dried in vacuum for 12 h at 90 °C. In the case of **2c** and **2d**, the elemental analyses suggested the presence of water molecules, which were also observed in the ^{1}H NMR spectra obtained upon dissolving the solids in dry dmso-d_6. It should be noted that these compounds are hygroscopic in the solid state and quickly take up water from the air.

The fragments with the highest peaks in the ESI(−) mass spectra of **2** were those arising from the combined loss of a Na^+ cation and the coordinated dmso ($[M - Na - dmso]^-$) and, interestingly, from the additional elimination of methane ($[M - Na - dmso - 1 \text{ or } 2\ CH_4]^-$). The latter was the main fragment for the complexes with aryl substituents (**2c** and **2d**) and its

assignment was supported by the excellent agreement found between the experimental and calculated distributions of exact masses (with errors below 8 ppm). Methane evolution likely results from intramolecular Csp^3–H bond activations of the alkyl and aryl NHC substituents similar to those reported by the Nolan[29] and Conejero[30] groups in NHC platinum(II)−methyl complexes. Detection of the ion $[M - Na]^-$ in the mass spectra of **2a** and **2b** confirmed the coordination of the dmso molecule to the Pt center in these N-alkyl-substituted complexes. Further confirmation of this coordination was obtained by the observation, in D_2O, of the ^1H resonances corresponding to the coordinated dmso in the expected region of 2.7 to 3.0 ppm with $^3J(^1H-^{195}Pt) \approx 13–14$ Hz.

The ^{13}C chemical shifts of the carbene carbons (181 to 183 ppm) and the ^{195}Pt chemical shifts (−4023 to −3980 ppm) were comparable to those reported for other *cis*-[$PtMe_2$(L)(NHC)] complexes (176 to 191 ppm and –4002 to –3905 ppm, respectively, with L = dmso,[31] imine,[32,33] phosphane,[34] NHC and SMe_2[22]). The ^{195}Pt satellites of the ^{13}C resonances were undetectable, probably due to their broadening in solvents of relatively high viscosity.[48] The methyl groups *trans* to the dmso ligand resonated between 0.2 and 0.3 ppm (^1H), and −10 to −7 ppm (^{13}C), whereas those *trans* to NHC appeared in the range from −0.3 to 0.0 ppm (^1H), and from −4 to −1 ppm (^{13}C). The $^{195}Pt-^1H$ coupling constants were smaller for the methyl ligands *trans* to the carbene (≈60 Hz compared with ≈80 Hz), as might be expected in light of the larger trans influence of this ligand. The *cis* stereochemistry together with the slow rotation of the NHC ligand around the Pt−C bond on the NMR time scale explains the chemical nonequivalence observed in the ^1H and ^{13}C NMR spectra between both NCH_2 protons in **2a**−**2d** (and both aryl moieties in **2c**−**d**) and between the two dmso methyls in the complexes with asymmetrically substituted NHCs **2b**−**d**.[19,31]

Single crystals of **2a** suitable for X-ray diffraction analysis were obtained as an octahydrate (**2a**·$8H_2O$) by slow diffusion of acetone into an aqueous solution of the complex. It is worth mentioning that crystal structures containing sulfonated NHC metal complexes are rare,[13,28,35,36] probably due to the difficulties associated with the crystallization of this type of complexes. Figure 2a depicts one of the two crystallographically independent *cis*-$[PtMe_2(dmso)(NHC)]^{2-}$ moieties found in the crystal structure of **2a** together with a selection of distances and angles. The angles between the *cis* bonds in the square-planar coordination environment of the Pt atom range from 86.0(8)° to 94.0(5)° [from 84.1(7)° to 94.5(4)° for the second independent molecule]. The NHC ligand ring is almost perpendicular to the Pt coordination plane (86°) in both independent units and the Pt−C_{NHC} distance of 2.09(2) Å [2.04(2) Å] is within the range of those reported for *cis*-[$PtMe_2$(L)(NHC)] complexes with L = imine,[32,33] phosphane,[34] NHC or SMe_2[22] (2.03−2.09 Å). The *cis*-$[PtMe_2(dmso)(NHC)]^{2-}$ units are organized in the form of double layers parallel to the *ab* crystallographic plane in the three-dimensional structure of **2a**·$8H_2O$, with the methyl groups pointing inward and the sulfonates out of the layer (Figure

2b). These anionic double layers are stacked along the *c* axis and alternate with cationic layers of hydrated Na^+ cations (Figure S23, Supporting Information).

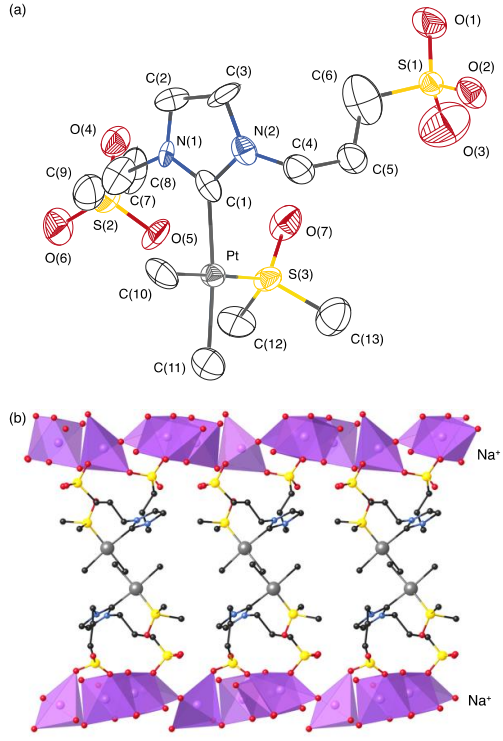

Figure 2. (a) ORTEP diagram (50% probability ellipsoids) of the anionic complex $[PtMe_2(dmso)(NHC)]^{2-}$ (**2a**). Hydrogen atoms have been omitted for clarity. Selected bond lengths (Å) and angles (deg) [the corresponding distances and angles for the second independent unit are given in brackets]: Pt−C(1), 2.09(2) [2.040(16)]; Pt−C(10), 2.062(18) [2.142(19)]; Pt−C(11), 2.08(2) [2.159(19)]; Pt−S(3), 2.237(4) [2.254(5)]; C(1)−Pt−C(10), 87.0(7) [84.1(7)]; C(10)−Pt−C(11), 86.0(8) [91.7(8)]; C(11)−Pt−S(3), 92.9(6) [94.5(4)]; C(1)−Pt−S(3), 94.0(5) [89.5(6)]; C(1)−Pt−C(11), 172.7(8) [175.7(8)]; C(10)−Pt−S(3), 178.9(6) [171.2(8)]. (b) View of the crystal structure of **2a** along the crystallographic *b* axis. The hydrated Na^+ cations are represented as polyhedra.

The ^1H NMR spectra of complexes **2** remained unaltered 8 days after being dissolved in D_2O under neutral or alkaline conditions (0.1 M NaOD) at room temperature. The stability of these complexes in water resembles that found by Atwood's group for Pt(II) dimethyl complexes with sulfonated phosphanes.[37] In contrast, it has been reported that $PtMe_2$ complexes with sulfonated iminopyridine ligands are quickly degraded under similar conditions by displacement of the didentate N,N-ligand by water.[38] At 80 °C and under neutral conditions, the decomposition of complexes **2** in D_2O is noticeable within hours, with the solutions

darkening and the evolution of gases. These gases were collected in chloroform-d_1 and their analysis by ^{1}H NMR showed the formation of comparable amounts of ethane, methane, and methane-d_1. In the case of **2a**, for instance, almost 50% of the methyl groups were transformed into ethane, more than 25% into methane and around 25% into methane-d_1. While the formation of methane-d_1 is easily explained by hydrolysis of the PtMe bonds, non-deuterated methane likely proceeds from the intramolecular Csp^3–H activation of the N-substituents discussed above (Scheme 2).[29,30] This preliminary study shows that hydrolysis of the Pt–Me bonds is only one of the routes involved in the thermally induced decomposition of complexes **2** in water.

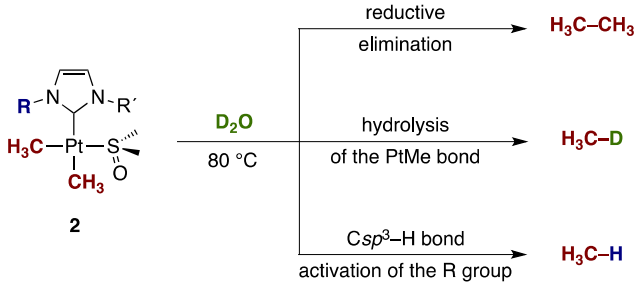

Scheme 2. Thermally Induced Decomposition of Complexes 2 in Water

Reactivity of the Dimethyl Complexes 2 with Brønsted Acids in Water. In light of these results, we examined the reactivity of complexes **2** in water with Brønsted acids derived from coordinating and non-coordinating anions (HCl and HBF_4, respectively). The reaction of **2** with hydrochloric acid is very fast at room temperature and occurs chemoselectively at the Pt-Me bonds in a stepwise manner. Thus, the addition of a first equivalent of a titrated hydrochloric acid solution results in protonolysis of only one of the Pt-Me bonds to give the monomethyl complexes [PtClMe(dmso)(NHC·Na)] (**3**, Scheme 3a), whereas reaction with a second equivalent of HCl affords the already known dichloride complexes *cis*-[$PtCl_2$(dmso)(NHC·Na)] (**4**, Scheme 3b).[28] The inertness of the Pt–NHC bond under these conditions, even when an excess of acid was used, is noteworthy. For instance, monitoring of a solution of **2b** and five equivalents of DCl in D_2O at room temperature by ^{1}H NMR spectroscopy for 7 days did not show the formation of any detectable amount of imidazolium salt. This resistance may be of interest as regards the application of these complexes under acidic aqueous conditions, for instance in the hydration of alkynes.[39]

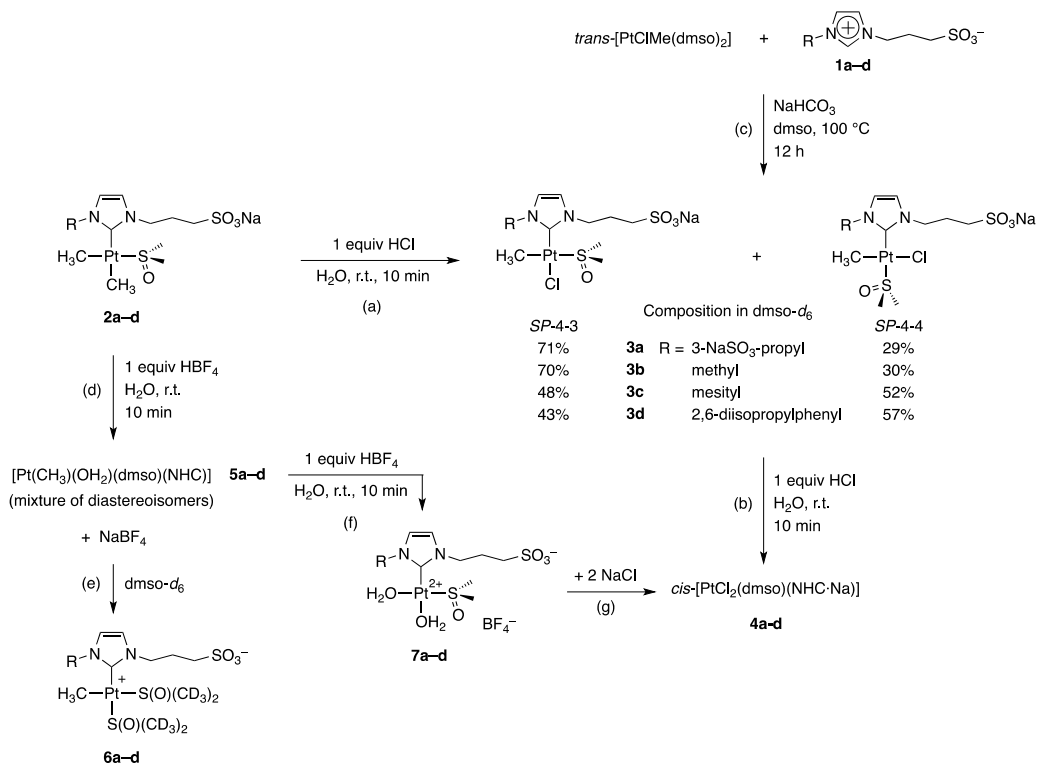

Scheme 3. Reactions of 2 with Hydrochloric and Tetrafluoroboric Acids

In solution, the monomethyl complexes **3** comprise a mixture of *SP*-4-3 and *SP*-4-4 diastereoisomers. These complexes can also be prepared by direct metalation of the corresponding imidazolium **1** with *trans*-[PtClMe(dmso)$_2$], using sodium hydrogencarbonate as the deprotonating base (Scheme 3c). To the best of our knowledge, the synthesis of haloalkyl mono(NHC) platinum(II) complexes has not been reported previously. As may be expected in light of the steric interactions, the isomer with the chlorido and carbene ligands in *cis* (*SP*-4-4) is favored by the most hindered NHCs (**3c** and **3d)** in both dmso-d_6 and D_2O (see Scheme 3 and Experimental Section). The composition of the mixture is also dependent on the solvent but independent of the method of preparation, thereby suggesting that both diastereoisomers are interconverting in solution. This isomerization is slow enough in dmso-d_6 at room temperature to observe sharp ^{1}H NMR resonances for the two isomers in all complexes, although a significant saturation transfer between the methyl ligands of both isomers was observed in a 1D EXSY experiment carried out for **3c** in dmso-d_6. Broadening of resonances was, however, observed in D_2O for **3c** and **3d**. The concurrence of isomerization processes in solution is well known for other square-planar haloalkyl platinum(II) complexes.[37,40]

The reaction of dimethyl complexes **2** with HBF_4 in water at room temperature also occurs rapidly and chemoselectively. After addition of the first equivalent of acid and subsequent removal of the aqueous solvent, the complexity of the ^1H NMR spectra obtained in D_2O was attributed to the formation of one major and one or two minor diastereoisomers of the "cationic" (more properly, zwitterionic) aquamethyl complexes [Pt(CH_3)(OH_2)(dmso)(NHC)] (**5**, Scheme 3d). In contrast, the spectra became drastically simplified in dmso-d_6, where displacement of the coordinated water (and the non-deuterated dmso) by the solvent resulted in formation of the *cis* complex **6** (Scheme 3e). The addition of a second equivalent of HBF_4 to complexes **2** afforded the "dicationic" complexes **7**, essentially as *cis* diastereoisomers (Scheme 3f). The formulation given to these diaqua complexes was supported by their clean transformation into the dichloride complexes **4** upon addition of sodium chloride (Scheme 3g).

Complexes **3**–**7** were obtained as spectroscopically pure solids and were characterized by ESI-TOF mass spectrometry and ^1H, ^{13}C and ^{195}Pt NMR spectroscopy. The elemental analyses found for complexes **3** were unsatisfactory, even taking into account the solvation by water molecules. Samples of the monomethyl (**5**–**6**) and diaqua complexes (**7**) were contaminated by the $NaBF_4$ formed as byproduct in the reaction. No purification was attempted. As was observed above for **2**, the most intense peaks detected in the mass spectra of these complexes were those associated with the decoordination of dmso or water ligands followed by the additional loss of methane in the case of the methyl complexes **3** and **5**. Coordination of a dmso molecule to the platinum center in **3** and **7** was confirmed by observation of the corresponding methyl protons in D_2O solution. The *cis* arrangement proposed for **6** and **7** was based on the number of ^2H or ^1H resonances observed for the methyl groups of the dmso ligands. When required, this assignment was corroborated by NOESY experiments that were also used to establish the stereochemistry of the two diastereoisomers found for **3** (see Experimental Section for details). The NCH_2 protons of the sulfonated chain were made equivalent by fast rotation of the NHC ligand around the Pt−NHC bond at room temperature in the case of some of the complexes bearing less hindered NHC ligands (**a** and **b**). The chemical shifts of the carbenic carbon (C^2) in the monomethyl complexes **3** (around 152 and 162 ppm for the *SP*-4-3 and *SP*-4-4 isomers, respectively) and **6** (156−158 ppm) were intermediate between those found in the dimethyl **2** (181−183 ppm) and dichloride complexes **4** (140−143 ppm). The values found for **6** were in excellent agreement with those previously reported for cationic [PtMeLL'(NHC)][X] complexes (L = L' = py, X = PF_6;[41] L = imine, L' = NCMe, X = OTf).[32 41]

Single crystals of **3a** were obtained in the form of the *SP*-4-3 isomer solvated with water and dmso molecules (*SP*-4-3-**3a**·$5H_2O$·0.5dmso). Figure 3a depicts one of the two crystallographically independent [PtMeCl(dmso)(NHC)]$^{2-}$ units together with a selection of

distances and angles found in both. These units are organized in the form of singly negatively charged layers between layers of sodium cations in the three-dimensional structure, with the sulfonate groups pointing towards the interface of both layers (Figure 3b). The NHC ring is almost perpendicular to the Pt coordination plane in both independent units (85.4° and 81.2°, respectively). The Pt−C_{NHC} distances of 1.945(8) and 1.966(8) Å are towards the low end of the range reported for (NHC)Pt(II) complexes (90% of Pt−C_{NHC} distances between 1.94 and 2.06 Å, mean 2.00 Å). This can be mostly ascribed to the influence of the chloride trans ligand, as can be deduced from a comparison with the distances found in the dichloride (**4a**)[28] and dimethyl (**2a**) analogues (1.97(2) and 2.04(2) [2.09(2)] Å, respectively), and with the typical distances for NHC–Pt(II) bonds with chloride in trans (from 1.94 to 2.00 Å, mean 1.97 Å). The Pt−CH_3 (2.095(7) [2.136(6)] Å) and Pt−Cl distances (2.359(2) [2.360(2)] Å) are comparable to those found for the corresponding bonds trans to the NHC ligand in **2a** (Pt−CH_3, 2.08(2) [2.16(2)] Å) and **4a** (Pt−Cl, 2.359(5) Å).[28]

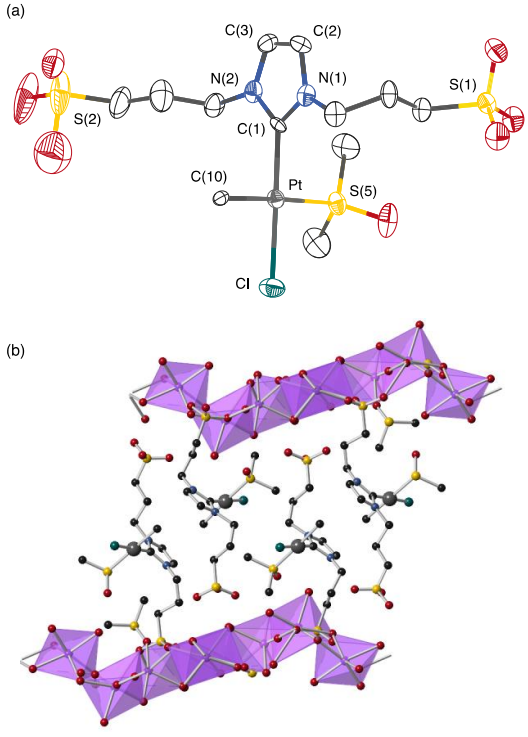

Figure 3. (a) ORTEP diagram (50% probability ellipsoids) of the anionic complex *SP*-4-3-[PtClMe(dmso)(NHC)]$^{2-}$ (*SP*-4-3-**3a**). Hydrogen atoms have been omitted for clarity. Selected bond lengths (Å) and angles (deg) [the corresponding distances and angles for the second independent unit are given between brackets]: Pt−C(1), 1.945(8) [1.966(8)]; Pt−C(10), 2.136(6) [2.095(7)]; Pt−Cl, 2.359(2) [2.360(2)]; Pt−S(5), 2.282(2) [2.305(2)]; C(1)−Pt−C(10), 88.7(3) [89.2(3)]; C(10)−Pt−Cl, 90.74(18) [88.5(2)]; Cl−Pt−S(5), 89.79(7) [89.04(8)]; C(1)−Pt−S(5),

90.9(2) [93.2(2)]; C(1)−Pt−Cl, 177.6(2) [177.3(2)]; C(10)−Pt−S(5), 177.06(16) [177.3(2)]. (b) View of the crystal structure of *SP*-4-3-**3a** along the crystallographic *a* axis. The solvated Na^+ cations are represented as polyhedra.

Hydrolysis of the Platinum−Methyl Bonds Promoted by Nucleophiles. In the course of our preliminary studies on the reactivity of the dimethyl complexes **2**, we observed that substitution of the coordinated dmso by ligands such as cyanide is accompanied by hydrolysis of the Pt-CH_3 bonds. After addition of one equivalent of potassium cyanide to a solution of **2a−c** in deuterated water, the expected substitution products K[$PtMe_2$(CN)(NHC·Na)] (**8a−c**) were slowly formed in the initial stages of the reaction (Scheme 4a). However, ligand exchange was incomplete (around 40% for **2a** after 4 h of reaction) and was accompanied by the formation of other minor byproducts. In addition, complexes **8a−c** evolved over time to give derivatives **9a−c**. Integration of the ^1H resonances for these derivatives and the observation of a small 1:1:1 triplet at 0.06 ppm (J_{HD} = 2.1 Hz), corresponding to CH_3D, suggested the involvement of hydrolysis of one of the Pt-CH_3 bonds in the formation of **9**. The formula K[$PtMe(CN)_2$(NHC·Na)] was corroborated when spectroscopically pure samples of **9a−c** were isolated by reaction of **2a−c** with two equivalents of KCN in water (Scheme 4b). Under these conditions, the reaction was almost quantitative in less than 3 h at room temperature. Complexes **9a−c** thus obtained were stable in water at room temperature for at least 8 d.

The notable acceleration of the transformations **2** → **8** → **9** with increasing cyanide concentration (compare the reactions with one and two equivalents of KCN) is to be expected for square-planar Pt(II) complexes involving associative substitution mechanisms. Thus, nucleophilic attack of the cyanide ligand to the platinum(II) center in **2** is followed by dissociation of the dmso ligand, whereas the alternative hydrolytic cleavage of the Pt−CH_3 bond does not occur to any observable extent in this complex. Cleavage of this bond likely involves two steps: nucleophilic attack of the cyanide to the platinum(II) center followed by electrophilic attack by the water protons to the methyl group. The balance between the two steps can tentatively explain the differences observed in the stability of the Pt–CH_3 bonds. The methyl probably becomes a better leaving group in **8** because replacement of the coordinated dmso by cyanide increases the electron-richness of the Pt(II) center, thus making the Pt–CH_3 bond more polar and susceptible to electrophilic attack by the water protons. It has to be assumed that the second cyanide ligand in **9** produces a notable reduction of the susceptibility of the Pt center to nucleophilic attack to explain the water stability of this complex.

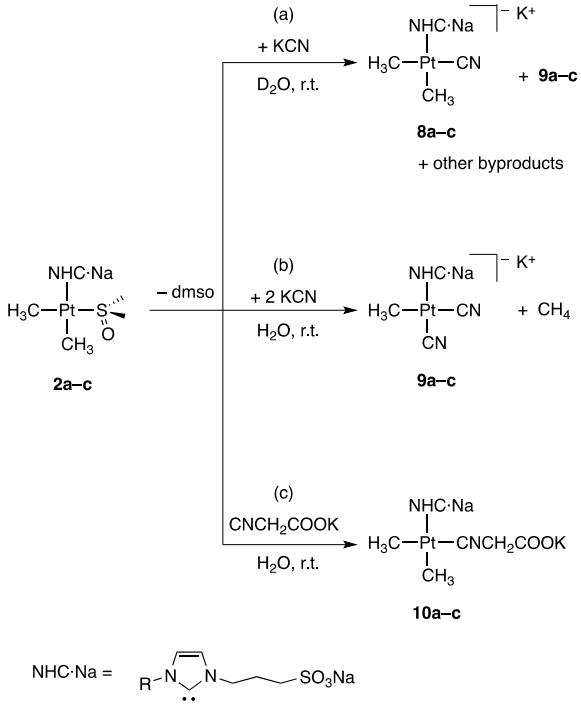

Scheme 4. Reactions of Dimethyl Complexes 2 with KCN and $CNCH_2COOK$ in Water

Since hydrolysis of the Pt−Me bond in the above complexes is promoted by nucleophiles, it is reasonable to propose that ligands displaying a lower nucleophilicity versus platinum(II) [42] than cyanide could stabilize the substitution product by inhibiting hydrolysis. The stability shown by complexes **2** under alkaline conditions might actually be considered to be a consequence of the lower nucleophilicity of the hydroxide ion, although substitution was not observed either. Unlike hydroxide, potassium 2-isocyanoacetate is a water-soluble isocyanide ligand that was able to displace the coordinated dmso ligand in **2a−c** to afford the dimethyl complexes **10a−c** in high yields (> 90%, Scheme 4c). The reaction occurs in water at room temperature without hydrolysis of the Pt–CH_3 bonds, even in the presence of an additional equivalent of the isocyanide.

The ESI−TOF mass spectra of **9** and **10** showed intense peaks corresponding to the loss of sodium(1+) or potassium(1+) ions from the neutral unit formula, in some instances accompanied by incorporation of a proton from the solvent (water or methanol). Fragments resulting from the additional loss of methane were also observed for all complexes. The coordination of two cyanide ligands in a *cis* disposition in **9** was inferred from observation of two IR absorptions corresponding to CN stretching vibrations (at *ca.* 2120 and 2100 cm^{-1}) and two NMR resonances for the cyanide carbons (at *ca.* 142 and 145 ppm). The carbenic and methyl carbons of **10** showed well-defined ^{195}Pt satellites with coupling constants of around

800 Hz for the carbene, 595 Hz for the methyl trans to the isocyanide, and 500 Hz for the methyl trans to the NHC. The *trans* influence of the NHC ligand probably causes the weaker coupling to ^{195}Pt of the methyl group trans to it.

Single crystals of **9a** suitable for X-ray diffraction analysis were obtained by slow diffusion of diethyl ether into a methanol solution of the complex. The solid-state structure contains two crystallographically independent $[PtMe(CN)_2(NHC)]^{3-}$ units together with their corresponding Na^+ and K^+ counterions, water molecules and, in addition, methanesulfonic acid of unknown origin (**9a**·1.5H_2O·0.5$MeSO_3H$). Figure 4a depicts one of the anionic organometallic Pt units together with a selection of bond distances and angles. The dihedral angle between the NHC ring and the metal coordination plane is equal to 72.1° in one and 85.8° in the other Pt unit. The average Pt−C_{NHC} (2.02 Å) and Pt−CH_3 distances (2.03 Å) are slightly shorter than the mean values found for (NHC)Pt(II) methyl complexes in the Cambridge Structural Database (2.036 Å and 2.084 Å, respectively). Nevertheless, the most remarkable feature is the three-dimensional arrangement of the structural units in a columnar honeycomb structure with cells of tetragonal symmetry and channels with an internal diameter of around 6 Å (Figure 4b). These channels are delimited by walls made of Pt complexes with their sulfonated groups pointing toward the Na^+ and K^+ cations arranged in the cell edges. In this way, the Pt−CH_3 bonds are facing onto the channel interior. This is interesting because activation of such bonds would result in exposure of the Pt centers to the interior of the enlarged channels (Figure 4c).

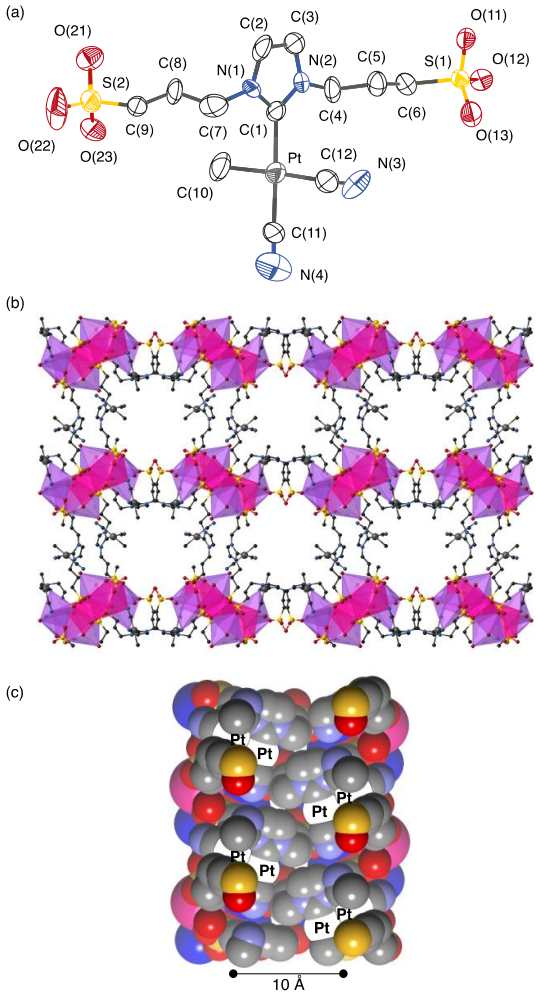

Figure 4. (a) ORTEP diagram (50% probability ellipsoids) for the complex $[PtMe(CN)_2(NHC)]^{3-}$ (**9a**). Hydrogen atoms have been omitted for clarity. Selected bond lengths (Å) and angles (deg) [the corresponding distances and angles for the second independent unit are given between brackets]: Pt−C(1), 1.993(16) [2.045(15)]; Pt−C(10), 2.05(2) [2.016(16)]; Pt−C(11), 1.990(19) [1.988(18)]; Pt−C(12), 1.94(2) [1.940(18)]; C(11)−N(4), 1.12(2) [1.117(19)]; C(12)−N(3), 1.13(2) [1.18(2)]; C(1)−Pt−C(10), 89.9(7) [87.3(7)]; C(10)−Pt−C(11), 87.3(8) [87.9(7)]; C(11)−Pt−C(12), 90.5(8) [94.2(6)]; C(1)−Pt−C(12), 92.3(7) [90.7(6)]; C(1)−Pt−C(11), 176.6(7) [174.4(6)]; C(10)−Pt−C(12), 177.6(8) [177.9(7)]; Pt−C(11)−N(4), 171(2) [176.6(17)]; Pt−C(12)−N(3), 174.9(19) [175.6(15)]. (b) View of the crystal structure of **9a** along the crystallographic *c* axis. The coordination spheres of the Na^+ and K^+ cations are represented as polyhedra. (c) Space-filling representation displaying a sectional view of one channel. Methyl groups have been removed to reveal the positions of the Pt center (shown as blank spheres in the picture).

CONCLUSIONS

We have developed an efficient method for the preparation of dimethyl derivatives of water-soluble NHC platinum(II) complexes and have studied the hydrolytic stability of their Pt−C bonds under different conditions. The platinum−methyl bonds of these derivatives are stable for days at room temperature in water under neutral or alkaline conditions. The degradation observed for these complexes at higher temperatures involves C–H activation and C–C reductive elimination processes in addition to Pt–Me bond hydrolysis. Nevertheless, we have shown that the reactivity of the platinum-methyl bonds with water increases significantly after addition of Lewis bases that are good nucleophiles toward the Pt(II) metal centers. The stoichiometric addition of protic acids to aqueous solutions of the above complexes results in the clean cleavage of one or both platinum(II)−methyl bonds. In contrast, the Pt−NHC bond remains unaltered under the above conditions. We have also shown the synthetic utility of selective protolysis of the Pt–Me bonds under acidic conditions by preparing several new neutral and cationic Pt(II) NHC derivatives. It is important to note that the reactivity trends observed in water for the hydrolysis of Pt–C bonds might be quite different in other solvents. As an example, the ring-opening hydrolysis of non-coordinated NHCs, which has been observed by several authors in organic solvents containing traces of moisture,[43] is disfavored in the presence of larger amounts of water because the solvation reduces the basicity of the hydroxide anion.[44]

In addition, we have reported the crystal structures of three complexes bearing sulfonatepropyl substituents at the nitrogen atoms of the NHC ligand. In these structures, the solvated sodium or potassium cations and the organometallic Pt complexes are arranged in separate domains, with the sulfonated groups of the NHC ligand located at the domain interface. In the case of complex **9a**, the three-dimensional arrangement is of special interest because of the longitudinal channels with a diameter of around 6 Å internally decorated with Pt–Me bonds.

Further efforts are underway in our laboratories with regard to the organometallic reactivity and applications of these water-soluble Pt(II) dimethyl complexes.

EXPERIMENTAL SECTION

General Procedures. All reactions were performed under an argon atmosphere using standard Schlenk techniques. Unless otherwise stated, reagents and solvents were used as received from commercial sources. The complexes *cis*-dimethylbis(dimethyl sulfoxide)platinum(II)[45] and *trans*-chloromethylbis(dimethyl sulfoxide)platinum(II)[46] and the imidazolium salts **1a**,[47] **1b**,[48] **1c**,[35] and **1d**[35] were prepared as described in the literature. All solvents were deoxygenated prior to use. Dimethyl sulfoxide was distilled under argon over calcium hydride. Deionized water (type II quality) was obtained using a Millipore Elix 10 UV

water purification system. ^{1}H, ^{13}C, and ^{195}Pt NMR spectra were recorded using a Varian Mercury 300, Unity 300, or Unity 500 Plus spectrometer. Chemical shifts (δ, parts per million) are quoted relative to $SiMe_4$ (^{1}H, ^{13}C) and K_2PtCl_6 in water (^{195}Pt). They were measured by internal referencing to the ^{13}C or residual ^{1}H resonances of the deuterated solvents (39.0 ppm for dmso-d_6 carbons; 2.49 ppm for dmso-d_5 protons and 4.69 ppm for HDO) or by the substitution method in the case of ^{195}Pt. Coupling constants (*J*) are given in hertz. When required, two-dimensional $^{1}H-^{13}C$ HSQC and HMBC experiments were carried out for the unequivocal assignment of ^{1}H and ^{13}C resonances. IR spectra were recorded for KBr pellets over the range 4000−400 cm^{-1} using a Perkin−Elmer Spectrum 2000 spectrophotometer. The Analytical Services of the Universidad de Alcalá performed the C, H, and N analyses using a LECO CHNS-932 microanalyzer, and the mass spectra were obtained using an Agilent G3250AA LC/MSD TOF Multi (MALDI and ESI) mass spectrometer in the electrospray ionization mode. The Analytical Services of the Universidad Autónoma de Madrid performed some of the mass spectra using an ABSciex QSTAR pulsar I QTOF mass spectrometer.

[$PtMe_2$(dmso)(NHC·Na)] (2). Sodium *tert*-butoxide (0.130 g, 1.35 mmol) was added to a solution of *cis*-[$PtMe_2(dmso)_2$] (0.515 g, 1.35 mmol) and the corresponding imidazolium salt (1.35 mmol) in dimethyl sulfoxide (10 mL). The mixture was stirred for 1 h at room temperature and then filtered through a plug of kieselguhr. The solvent was removed under high vacuum at 90 °C to dryness. The powdery solid thus obtained was dried under vacuum for 12 h at 90 ºC and 4 mbar of pressure.

cis-(Dimethyl sulfoxide)[1,3-bis(3-sodiumsulfonatepropyl)imidazol-2-ylidene]dimethylplatinum(II) ***(2a)***. Complex **2a** was obtained from **1a** (0.451 g, 1.35 mmol) as a white solid (0.864 g, 97%). ^{1}H NMR (300 MHz, D_2O): δ 7.13 (s, 2H, Imz), 4.31 (m, 2H, NCH_2), 4.14 (m, 2H, NCH_2), 2.95 (s with ^{195}Pt satellites, $^{3}J(^{1}H-^{195}Pt)$ = 13.2, 6H, Me_2SO), 2.82 (m, 4H, CH_2S), 2.17 (m, 4H, $CH_2CH_2CH_2$), 0.36 (s with ^{195}Pt satellites, $^{2}J(^{1}H-^{195}Pt)$ = 81.2, 3H, Me *cis* to NHC), 0.03 (s with ^{195}Pt satellites, $^{2}J(^{1}H-^{195}Pt)$ = 61.4, 3H, Me *trans* to NHC). ^{1}H NMR (300 MHz, dmso-d_6): δ 7.24 (s, 2H, Imz), 4.18 (m, 4H, NCH_2), 2.40 (m, 4H, CH_2S), 2.05 (m, 4H, $CH_2CH_2CH_2$), 0.16 (s with ^{195}Pt satellites, $^{2}J(^{1}H-^{195}Pt)$ = 78.6, 3H, Me *cis* to NHC), −0.06 (s with ^{195}Pt satellites, $^{2}J(^{1}H-^{195}Pt)$ = 60.0, 3H, Me *trans* to NHC). $^{13}C\{^{1}H\}$ NMR (75 MHz, D_2O): δ 181.5 (s, Imz C^2), 121.1 (s, Imz C^{4-5}), 48.4 (s, CH_2S), 48.4 (s, NCH_2), 43.7 (s, Me_2SO), 25.8 (s, $CH_2CH_2CH_2$), −3.8 (s, PtMe *trans* to NHC), −9.0 (s, PtMe *cis* to NHC). ^{195}Pt NMR (64 MHz, dmso-d_6): δ −4021. ESI-MS (negative ion, MeOH): *m/z* 636.0408 $[M - Na]^-$ (calcd 636.0453) 5%; 558.0279 $[M - Na - dmso]^-$ (calcd 558.0314) 100%; 541.9974 $[M - Na - dmso - CH_4]^-$ (calcd 542.0001) 44%; 525.9651 $[M - Na - dmso - 2CH_4]^-$ (calcd 525.9688) 31%; 503.9827 $[M + H - 2Na - dmso - 2CH_4]^-$ (calcd 503.9868) 52%. Anal. Calcd (%) for $C_{13}H_{26}N_2Na_2O_7PtS_3$: C, 23.67; H, 3.97; N, 4.25. Found (%): C, 23.45; H, 4.21; N, 4.05.

*cis-(Dimethyl sulfoxide)dimethyl[1-methyl-3-(3-sodiumsulfonatepropyl)imidazol-2-ylidene]platinum(II) (**2b**).* Complex **2b** was obtained from **1b** (0.276 g, 1.35 mmol) as a pale-yellow solid (0.686 g, 96%). ^{1}H NMR (300 MHz, D_2O): δ 7.08 (d, $^{3}J_{HH}$ = 2.1, 1H, Imz), 7.01 (d, $^{3}J_{HH}$ = 2.1, 1H, Imz), 4.27 (m, 1H, NCH_2), 4.13 (m, 1H, NCH_2), 3.64 (s, 3H, NMe), 2.94 (s with ^{195}Pt satellites, $^{3}J(^{1}H-^{195}Pt)$ = 13.8, 3H, Me_2SO), 2.93 (s with ^{195}Pt satellites, $^{3}J(^{1}H-^{195}Pt)$ = 13.8, 3H, Me_2SO), 2.81 (m, 2H, CH_2S), 2.15 (m, 2H, $CH_2CH_2CH_2$), 0.34 (s with ^{195}Pt satellites, $^{2}J(^{1}H-^{195}Pt)$ = 81.2, 3H, PtMe *cis* to NHC), 0.04 (s with ^{195}Pt satellites, $^{2}J(^{1}H-^{195}Pt)$ = 61.0, 3H, PtMe *trans* to NHC). ^{1}H NMR (300 MHz, dmso-d_6): δ 7.24 (d, $^{3}J_{HH}$ = 2.1, 1H, Imz), 7.19 (d, $^{3}J_{HH}$ = 2.1, 1H, Imz), 4.17 (m, 2H, NCH_2), 3.68 (s, 3H, NMe), 2.40 (m, 2H, CH_2S), 2.04 (m, 2H, $CH_2CH_2CH_2$), 0.17 (s with ^{195}Pt satellites, $^{2}J(^{1}H-^{195}Pt)$ = 82.6, 3H, PtMe *cis* to NHC), −0.04 (s with ^{195}Pt satellites, $^{2}J(^{1}H-^{95}Pt)$ = 62.7, 3H, PtMe *trans* to NHC). $^{13}C\{^{1}H\}$ NMR (75 MHz, D_2O): δ 181.3 (s, Imz-C^2), 122.6 (s, Imz-C^5), 120.6 (s, Imz-C^4), 48.4 (s, CH_2S), 48.2 (s, NCH_2), 43.9 (s, Me_2SO), 43.6 (s, Me_2SO), 36.8 (s, NMe), 25.8 (s, $CH_2CH_2CH_2$), −3.9 (s, PtMe *trans* to NHC), −9.7 (s, PtMe *cis* to NHC). ^{195}Pt NMR (64 MHz, dmso-d_6): δ −4023. ESI-MS (negative ion, MeOH): m/z 506.0758 $[M - Na]^-$ (calcd 506.0752) 2%; 428.0613 $[M - Na - dmso]^-$ (calcd 428.0613) 100%; 412.0298 $[M - Na - dmso - CH_4]^-$ (calcd 412.0300) 12%; 395.9987 $[M - Na - dmso - 2CH_4]^-$ (calcd 395.9987) 2%. Anal. Calcd (%) for $C_{11}H_{23}N_2NaO_4PtS_2$: C, 24.95; H, 4.38; N, 5.29. Found (%): C, 24.13; H, 4.54; N, 4.90.

*cis-(Dimethyl sulfoxide)dimethyl[1-(3-sodiumsulfonatepropyl)-3-(2,4,6-trimethylphenyl)imidazol-2-ylidene]platinum(II) (**2c**).* Complex **2c** was obtained from **1c** (0.416 g, 1.35 mmol) as a pale-brown solid (0.796 g, 93%). ^{1}H NMR (300 MHz, D_2O): δ 7.27 (d, $^{3}J_{HH}$ = 1.8, 1H, Imz), 6.93 (d, $^{3}J_{HH}$ = 1.8, 1H, Imz), 6.87 (s, 1H, Ar), 6.85 (s, 1H, Ar), 4.33 (m, 1H, NCH_2), 4.26 (m, 1H, NCH_2), 2.92 (s br, 3H, Me_2SO), 2.83 (m, 2H, CH_2S), 2.56 (s br, 3H, Me_2SO), 2.21 (m, 2H, $CH_2CH_2CH_2$), 2.15 (s, 3H, Ar-*p*-Me), 1.96 (s, 3H, Ar-*o*-Me), 1.90 (s, 3H, Ar-*o*-Me), 0.23 (s with ^{195}Pt satellites, $^{2}J(^{1}H-^{195}Pt)$ = 81.2, 3H, PtMe *cis* to NHC), −0.31 (s with ^{195}Pt satellites, $^{2}J(^{1}H-^{195}Pt)$ = 59.4, 3H, PtMe *trans* to NHC). ^{1}H NMR (300 MHz, dmso-d_6): δ 7.49 (d, $^{3}J_{HH}$ = 1.8, 1H, Imz), 7.13 (d, $^{3}J_{HH}$ = 1.8, 1H, Imz), 6.95 (s, 2H, Ar), 4.36 (m, 1H, NCH_2), 4.25 (m, 1H, NCH_2), 2.46 (m, 2H, CH_2S), 2.27 (s, 3H, Ar-*p*-Me), 2.16 (m, 2H, $CH_2CH_2CH_2$), 2.07 (s, 3H, Ar-*o*-Me), 1.99 (s, 3H, Ar-*o*-Me), 0.10 (s with ^{195}Pt satellites, $^{2}J(^{1}H-^{195}Pt)$ = 81.5, 3H, PtMe *cis* to NHC), −0.35 (s with ^{195}Pt satellites, $^{2}J(^{1}H-^{195}Pt)$ = 61.0, 3H, PtMe *trans* to NHC). $^{13}C\{^{1}H\}$ NMR (75 MHz, D_2O): δ 182.8 (s, Imz-C^2), 139.2 (s, Ar-C^4), 136.2 (s, Ar-C^2), 136.1 (s, Ar-C^1), 129.0 (s, Ar-C^3), 123.5 (s, Imz-C^4), 120.8 (s, Imz-C^5), 48.8 (s, NCH_2), 48.5 (s, CH_2S), 43.2 (s, Me_2SO), 42.5 (s, Me_2SO), 25.9 (s, $CH_2CH_2CH_2$), 20.6 (s, Ar-*p*-Me), 18.3 (s, Ar-*o*-Me), 18.2 (s, Ar-*o*-Me), −1.9 (s, PtMe *trans* to NHC), −7.3 (s, PtMe *cis* to NHC). ^{195}Pt NMR (64 MHz, dmso-d_6): δ −3985. ESI-MS (negative ion, MeOH): m/z 532.1192 $[M - Na - dmso]^-$ (calcd 532.1239) 3%; 516.0885 $[M - Na - dmso - CH_4]^-$ (calcd 516.0926) 100%; 500.0562 [M − Na

− dmso− $2CH_4$]$^-$ (calcd 500.0613) 18%. Anal. Calcd (%) for $C_{19}H_{36}N_2NaO_{6.5}PtS_2$ (**2c**·2.5H_2O): C, 33.62; H, 5.35; N, 4.13. Found (%): C, 33.50; H, 4.80; N, 4.36.

*cis-[1-(2,6-Diisopropylphenyl)-3-(3-sodiumsulfonatepropyl)imidazol-2-ylidene](Dimethyl sulfoxide)dimethylplatinum(II) (**2d**)*. Complex **2d** was obtained from **2d** (0.473 g, 1.35 mmol) as a pale-brown solid (0.830 g, 91%). ^{1}H NMR (300 MHz, D_2O): δ 7.37 (t, $^3J_{HH}$ = 6.9, 1H, Ar-H^4), 7.29 (s br, 1H, Imz), 7.24 (d, $^3J_{HH}$ = 6.6, 1H, Ar-H^3), 7.22 (d, $^3J_{HH}$ = 6.6, 1H, Ar-H^3), 7.09 (s br, 1H, Imz), 4.55 (m, 1H, NCH_2), 4.22 (m, 1H, NCH_2), 2.98 (s br, 3H, Me_2SO), 2.87 (m, 2H, CH_2S), 2.72 (s br, 3H, Me_2SO), 2.37 (m, 2H, C*H*Me_2), 2.25 (m, 2H, $CH_2CH_2CH_2$), 1.20 (d, $^3J_{HH}$ = 6.6, 3H, CH*Me*$_2$), 1.14 (d, $^3J_{HH}$ = 6.6, 3H, CH*Me*$_2$), 0.92 (d, $^3J_{HH}$ = 6.6, 3H, CH*Me*$_2$), 0.84 (d, $^3J_{HH}$ = 6.6, 3H, CH*Me*$_2$), 0.18 (s with ^{195}Pt satellites, $^2J(^1H-^{195}Pt)$ = 82.2, 3H, PtMe *cis* to NHC), −0.27 (s with ^{195}Pt satellites, $^2J(^1H-^{195}Pt)$ = 59.7, 3H, PtMe *trans* to NHC). ^{1}H NMR (300 MHz, dmso-d_6): δ 7.50 (d, $^3J_{HH}$ = 1.8, 1H, Imz), 7.41 (t, $^3J_{HH}$ = 7.6, 1H, Ar-H^4), 7.26 (d, $^3J_{HH}$ = 1.8, 1H, Imz), 7.25 (d, $^3J_{HH}$ = 7.6, 2H, Ar H^3), 4.45 (m, 1H, NCH_2), 4.30 (m, 1H, NCH_2), 2.97 (m, 1H, C*H*Me_2), 2.59 (m, 1H, C*H*Me_2), 2.48 (m, 2H, CH_2S), 2.17 (m, 2H, $CH_2CH_2CH_2$), 1.23 (d, $^3J_{HH}$ = 6.9, 3H, CH*Me*$_2$), 1.20 (d, $^3J_{HH}$ = 6.9, 3H, CH*Me*$_2$), 0.99 (d, $^3J_{HH}$ = 6.9, 3H, CH*Me*$_2$), 0.92 (d, $^3J_{HH}$ = 6.6, 3H, CH*Me*$_2$), 0.06 (s with ^{195}Pt satellites, $^2J(^1H-^{195}Pt)$ = 80.5, 3H, PtMe *cis* to NHC), −0.34 (s with ^{195}Pt satellites, $^2J(^1H-^{195}Pt)$ = 61.4, 3H, PtMe *trans* to NHC). ^{13}C{^{1}H} NMR (75 MHz, dmso-d_6): δ 183.1 (s, Imz-C^2), 145.6 (s, Ar-C^2), 145.5 (s, Ar-C^2), 135.7 (s, Ar-C^1), 128.6 (s, Ar-C^4), 123.9 (s, Imz-C^5), 122.9 (s, Ar-C^3), 122.7 (s, Ar-C^3), 119.3 (s, Imz-C^4), 48.5 (s, NCH_2), 48.1 (s, CH_2S), 27.3 (s, *C*HMe_2), 26.8 (s, *C*HMe_2), 26.0 (s, $CH_2CH_2CH_2$), 25.71 (s, CH*Me*$_2$), 25.67 (s, CH*Me*$_2$), 22.2 (s, CH*Me*$_2$), 21.9 (s, CH*Me*$_2$), −0.9 (s, PtMe *trans* to NHC), −8.4 (s, PtMe *cis* to NHC). ^{195}Pt NMR (64 MHz, dmso-d_6): δ −3980. ESI-MS (negative ion, MeOH): m/z 574.1738 [M − Na − dmso]$^-$ (calcd 574.1709) 47%; 558.1431 [M − Na − dmso − CH_4]$^-$ (calcd 558.1396) 100%; 542.1131 [M − Na − dmso −$2CH_4$]$^-$ (calcd 542.1083) 12%. Anal. Calcd (%) for $C_{22}H_{45}N_2NaO_8PtS_2$ (**2d**·4H_2O): C, 35.33; H, 6.07; N, 3.75. Found (%): C, 35.17; H, 5.51; N, 3.63.

[PtClMe(dmso)(NHC·Na)] (3). *Method (a).* A titrated aqueous solution of HCl (0.942 M, 150 μL, 0.141 mmol) was added dropwise to a solution of **2** (0.141 mmol) in water (2 mL). The mixture was stirred at room temperature until methane evolution ceased (*ca.* 5−10 min). The solvent was then removed under high vacuum at 50 °C and the solid thus obtained dried for 6 h at 70 ºC and 4 mbar of pressure.

Method (b). Sodium hydrogencarbonate (0.084 g, 1.0 mmol) was added to a solution of *trans*-[PtMeCl(dmso)$_2$] (0.101 g, 0.251 mmol) and the corresponding imidazolium salt (0.250 mmol) in dimethyl sulfoxide (3 mL). The mixture was stirred for 12 h at 100 ºC, cooled back to room temperature, and filtered through a plug of kieselguhr. After complete removal of the solvent, the resulting powdery solids were dried under vacuum (5 h, 90 ºC, 4 mbar).

Accurate elemental analyses could not be obtained for complexes **3a**−**d** probably due to their contamination with water and dmso molecules. They were characterized in solution as a mixture of two diastereoisomers. In the case of **3a**, the stereochemistry of these diastereoisomers was determined with a 2D NOESY experiment performed in D_2O. The methyl protons of both isomers showed cross peaks with the corresponding N-alkyl chain whereas the correlation between the dmso at 3.2 ppm and the methyl at 0.46 ppm, in one case, and the dmso at 3.0 ppm and one of the N-alkyl chains in the other, served to identify the *SP*-4-3 and *SP*-4-4 isomers, respectively. The assignment of stereoisomers for **3b**−**d** was based on the $^{1}H-^{195}Pt$ coupling constants found for the methyl groups in **3a**. Coupling constants of around 80-90 Hz (88 Hz in **3a**) were assigned to the isomer with the methyl and chloride ligands in trans (*SP*-4-4) whereas those around 60-70 Hz (66 Hz in **3a**) were assumed to be characteristic of the isomer with methyl and dmso in trans (*SP*-4-3).

Chlorido[1,3-bis(3-sodiumsulfonatepropyl)imidazol-2-ylidene](dimethyl sulfoxide)methylplatinum(II) ***(3a)***. Compound **3a** was obtained from **2a** (93.0 mg, 0.141 mmol) as a white, spectroscopically pure solid (93.0 mg, 97%). Ratio of diastereoisomers (*SP*-4-3/*SP*-4-4): 52:48 (D_2O), 71:29 (dmso-d_6). ^{1}H NMR (300 MHz, D_2O): δ [*SP*-4-3 and *SP*-4-4] 7.19 (s, 2H, Imz), 7.17 (s, 2H, Imz), 4.36 (m, 4H, NCH_2), 4.24 (m, 4H, NCH_2), 3.23 (s, 6H, Me_2SO), 3.03 (s, 6H, Me_2SO), 2.86 (t, $^{3}J_{HH}$ = 7.5, 8H, CH_2S, overlapped for both isomers) 2.25 (m, 8H, $CH_2CH_2CH_2$ overlapped for both isomers), 0.50 (s with ^{195}Pt satellites, 3H, $^{2}J(^{1}H-^{195}Pt)$ = 65.9, 3H, PtMe), 0.46 (s with ^{195}Pt satellites, $^{2}J(^{1}H-^{195}Pt)$ = 88.5, 3H, PtMe). ^{1}H NMR (300 MHz, dmso-d_6): δ [*SP*-4-3] 7.35 (s, 2H, Imz), 4.23 (t, $^{3}J_{HH}$ = 7.0, 4H, NCH_2), 2.47 (m, 4H, CH_2S), 2.11 (m, 4H, $CH_2CH_2CH_2$), 0.34 (s with ^{195}Pt satellites, $^{2}J(^{1}H-^{195}Pt)$ = 68.4, 3H, PtMe); [*SP*-4-4] 7.37 (s, 2H, Imz), 4.37 (m, 2H, NCH_2), 4.17 (m, 2H, NCH_2), 2.44 (m, 4H, CH_2S), 2.11 (m, 4H, $CH_2CH_2CH_2$), 0.32 (s, 3H, PtMe). $^{13}C\{^{1}H\}$ NMR (75 MHz, dmso-d_6): δ [*SP*-4-3] 151.8 (s, Imz-C^2), 120.4 (s, Imz-$C^{4,5}$), 48.5 (s, NCH_2), 47.8 (s, CH_2S), 25.7 (s, $CH_2CH_2CH_2$), −12.3 (s, PtMe); [*SP*-4-4] 161.7 (s, Imz-C^2), 120.6 (s, Imz-$C^{4,5}$), 48.2 (s, NCH_2), 47.8 (s, CH_2S), 25.9 (s, $CH_2CH_2CH_2$), −19.7 (s, PtMe). ^{195}Pt NMR (64 MHz, dmso-d_6): δ [*SP*-4-3] −3954; [*SP*-4-4] −4101. ESI-MS (negative ion, MeOH): *m*/*z* 656.0001 $[M - Na]^-$ (calcd 655.9907) 0.6%; 577.9896 $[M - Na - dmso]^-$ (calcd 577.9767) 21%; 556.0028 $[M - 2Na + H - dmso]^-$ (calcd 555.9948) 13%; 561.9588 $[M - Na - dmso - CH_4]^-$ (calcd 561.9454) 3.4%; 503.9981 $[M - 2Na - dmso - CH_4 - Cl]^-$ (calcd 503.9874) 100%.

Chlorido(dimethyl sulfoxide)methyl[1-methyl-3-(3-sodiumsulfonatepropyl)imidazol-2-ylidene] platinum(II) ***(3b)***. Compound **3b** was obtained from **2b** (74.7 mg, 0.141 mmol) as a white, spectroscopically pure solid (71.3 mg, 92%). Ratio of diastereoisomers (*SP*-4-3/*SP*-4-4): 53:47 (D_2O), 70:30 (dmso-d_6). ^{1}H NMR (300 MHz, D_2O): δ [*SP*-4-3 and *SP*-4-4] 7.15 (d, $^{3}J_{HH}$ = 1.8, 1H, Imz), 7.13 (s, $^{3}J_{HH}$ = 2.0, 1H, Imz), 7.10 (d, $^{3}J_{HH}$ = 1.8, 1H, Imz), 7.08 (d, $^{3}J_{HH}$ = 2.0, 1H, Imz), 4.38 (m, 2H, NCH_2), 4.21 (m, 2H, NCH_2), 3.75 (s, 3H, NMe), 3.73 (s, 3H, NMe), 3.22 (s with ^{195}Pt

satellites, $^{3}J(^{1}H\text{-}^{195}Pt)$ = 16.3, 6H, Me_2SO), 3.01 (s, 3H, Me_2SO), 2.99 (s, 3H, Me_2SO), 2.85 (t, $^{3}J_{HH}$ = 7.5, 4H, CH_2S overlapped for both isomers), 2.23 (m, 4H, $CH_2CH_2CH_2$ overlapped for both isomers), 0.45 (s with ^{195}Pt satellites, $^{2}J(^{1}H\text{-}^{195}Pt)$ = 70.2, 3H, PtMe), 0.33 (s with ^{195}Pt satellites, $^{2}J(^{1}H\text{-}^{195}Pt)$ = 87.6, 3H, PtMe). ^{1}H NMR (300 MHz, dmso-d_6): δ [*SP*-4-3] 7.35 (d, $^{3}J_{HH}$ = 2.0, 1H, Imz), 7.31 (d, $^{3}J_{HH}$ = 2.0, 1H, Imz), 4.22 (t, $^{3}J_{HH}$ = 6.9, 2H, NCH_2), 3.74 (s, 3H, NMe), 2.98 (s, 6H, Me_2SO), 2.44 (m, 2H, CH_2S), 2.10 (m, 2H, $CH_2CH_2CH_2$), 0.34 (s with ^{195}Pt satellites, $^{2}J(^{1}H\text{-}^{195}Pt)$ = 71.6, 3H, PtMe); [*SP*-4-4] 7.38 (d, $^{3}J_{HH}$ = 1.8, 1H, Imz), 7.32 (d, $^{3}J_{HH}$ = 1.8, 1H, Imz), 4.38 (m, 1H, NCH_2), 4.18 (m, 1H, NCH_2), 3.75 (s, 3H, NMe), 2.44 (m, 2H, CH_2S), 2.10 (m, 2H, $CH_2CH_2CH_2$), 0.33 (s, 3H, PtMe). $^{13}C\{^{1}H\}$ NMR (75 MHz, dmso-d_6): δ [*SP*-4-3] 152.0 (s, Imz-C^2), 121.2 (s, Imz-C^5), 120.0 (s, Imz-C^4), 48.0 (s, NCH_2), 47.5 (s, CH_2S), 41.3 (s, Me_2SO), 36.3 (s, NMe), 25.5 (s, $CH_2CH_2CH_2$), −13.1 (s, PtMe); [*SP*-4-4] 121.3 (s, Imz-C^5), 120.4 (s, Imz-C^4), 47.8 (s, NCH_2), 47.5 (s, CH_2S), 36.1 (s, NMe), 25.8 (s, $CH_2CH_2CH_2$), −20.4 (s, PtMe), Imz-C^2 not observed. ^{195}Pt NMR (64 MHz, dmso-d_6): δ [*SP*-4-3] −3964; [*SP*-4-4] −4104. ESI-MS (negative ion, MeOH): *m/z* 526.0146 $[M - Na]^-$ (calcd 526.0206) 2.4%; 448.0091 $[M - Na - dmso]^-$ (calcd 448.0067) 100%; 431.9780 $[M - Na - dmso - CH_4]^-$ (calcd 431.9754) 27%.

*Chlorido(dimethyl sulfoxide)methyl[1-(3-sodiumsulfonatepropyl)-3-(2,4,6-trimethylphenyl)imidazol-2-ylidene]platinum(II) (**3c**).* Compound **3c** was obtained from **2c** (89.3 mg, 0.141 mmol) as a white, spectroscopically pure solid (84.8 mg, 92%). Ratio of diastereoisomers (*SP*-4-3/*SP*-4-4): 32:68 (D_2O), 48:52 (dmso-d_6). Very broad resonances were observed in the ^{1}H NMR spectrum of **3c** in D_2O at room temperature; only selected resonances are given. ^{1}H NMR (300 MHz, D_2O): δ [*SP*-4-3] 3.05 (s br, 3H, Me_2SO), 2.87 (s br, 3H, Me_2SO), 0.42 (br, 3H, PtMe); [*SP*-4-4] 3.09 (s br, 3H, Me_2SO), 2.99 (s br, 3H, Me_2SO), 0.28 (s with ^{195}Pt satellites, $^{2}J(^{1}H\text{-}^{195}Pt)$ = 84.0, 3H, PtMe). ^{1}H NMR (500 MHz, dmso-d_6): δ [*SP*-4-3] 7.62 (d, $^{3}J_{HH}$ = 2.0, 1H, Imz), 7.30 (d, $^{3}J_{HH}$ = 2.0, 1H, Imz), 7.02 (s, 1H, Ar), 7.01 (s, 1H, Ar), 4.46 (m, 1H, NCH_2), 4.28 (m, 1H, NCH_2), 2.44 (m, 2H, CH_2S), 2.294 (s, 3H, Ar *p*-Me), 2.24 (m, 2H, $CH_2CH_2CH_2$), 2.10 (s, 3H, Ar-*o*-Me), 1.97 (s, 3H, Ar-*o*-Me), 0.28 (s with ^{195}Pt satellites, $^{2}J(^{1}H\text{-}^{195}Pt)$ = 61.2, 3H, PtMe); [*SP*-4-4] 7.64 (d, $^{3}J_{HH}$ = 2.0, 1H, Imz), 7.30 (d, $^{3}J_{HH}$ = 2.0, 1H, Imz), 6.99 (s, 1H, Ar), 6.98 (s, 1H, Ar), 4.76 (m, 1H, NCH_2), 4.21 (m, 1H, NCH_2), 2.44 (m, 2H, CH_2S), 2.29 (s, 3H, Ar-*p*-Me), 2.24 (m, 2H, $CH_2CH_2CH_2$), 2.18 (s, 3H, Ar-*o*-Me), 1.96 (s, 3H, Ar-*o*-Me), 0.14 (s with ^{195}Pt satellites, $^{2}J(^{1}H\text{-}^{195}Pt)$ = 81.0, 3H, PtMe). $^{13}C\{^{1}H\}$ NMR (75 MHz, dmso-d_6): δ [*SP*-4-3] 152.5 (s, Imz-C^2), 137.6 (s, Ar-C^4), 135.3 (s, Ar-C^2), 135.1 (s, Ar-C^2), 134.6 (s, Ar-C^1), 128.4 (s, Ar-C^3), 128.3 (s, Ar-C^3), 122.9 (s, Imz-C^4), 120.7 (s, Imz-C^5), 48.7 (s, NCH_2), 48.0 (s, CH_2S), 25.7 (s, $CH_2CH_2CH_2$), 20.1 (s, Ar-*p*-Me), 18.2 (s, Ar-*o*-Me), 17.8 (s, Ar-*o*-Me), −11.5 (s, PtMe); [*SP*-4-4] 162.0 (s, Imz-C^2), 137.5 (s, Ar-C^4), 135.1 (s, Ar-C^2), 135.0 (s, Ar-C^2), 134.0 (s, Ar-C^1), 128.4 (s, Ar-C^3), 127.9 (s, Ar-C^3), 122.7 (s, Imz-C^4), 121.3 (s, Imz-C^5), 49.1 (s, NCH_2), 47.9 (s, CH_2S), 26.1 (s, $CH_2CH_2CH_2$), 20.2 (s, Ar-*p*-Me), 17.7 (s, Ar-*o*-Me), 17.3 (s, Ar-*o*-Me), −19.8 (s, PtMe). ^{195}Pt

NMR (64 MHz, dmso-d_6): δ [*SP*-4-3] −3929; [*SP*-4-4] −4098. ESI-MS (negative ion, MeOH): m/z 630.0781 $[M-Na]^-$ (calcd 630.0832) 0.9%; 552.0718 $[M - Na - dmso]^-$ (calcd 552.0693) 100%; 536.0402 $[M - Na - dmso - CH_4]^-$ (calcd 536.0380) 54%.

*Chlorido[1-(2,6-diisopropylphenyl)-3-(3-sodiumsulfonatepropyl)imidazol-2-ylidene](dimethyl sulfoxide)methylplatinum(II) (**3d**).* Compound **3d** was obtained from **2d** (95.3 mg, 0.141 mmol) as a white, spectroscopically pure solid (92.3 mg, 94%). Ratio of diastereoisomers (*SP*-4-3/*SP*-4-4): 30:70 (D_2O), 43:57 (dmso-d_6). Very broad resonances were observed in the ^{1}H NMR spectrum of **3d** in D_2O at room temperature; only selected resonances are given. ^{1}H NMR (300 MHz, D_2O): δ [*SP*-4-3] 3.01 (s, 3H, Me_2SO), 2.84 (s, 3H, Me_2SO); [*SP*-4-4] 3.07 (s, 6H, Me_2SO), 2.95 (s, 6H, Me_2SO). ^{1}H NMR (500 MHz, dmso-d_6): δ [*SP*-4-3] 7.64 (d, $^3J_{HH}$ = 1.5, 1H, Imz), 7.47 (d, $^3J_{HH}$ = 3.0, 1H, Imz), 7.43 (m, 1H, Ar-H^4), 7.31 (d, $^3J_{HH}$ = 8.5, 1H, Ar-H^3), 7.307 (d, $^3J_{HH}$ = 8.5, 1H, Ar-H^3), 4.57 (m, 1H, NCH_2), 4.31 (m, 1H, NCH_2), 3.02 (m, 1H, C*H*Me_2), 2.36 (m, 1H, C*H*Me_2), 2.24 (m, 2H, CH_2S), 2.239 (m, 2H, $CH_2CH_2CH_2$), 1.29 (d, $^3J_{HH}$ = 6.5, 3H, CH*Me*$_2$), 1.21 (d, $^3J_{HH}$ = 6.5, 3H, CH*Me*$_2$), 1.04 (d, $^3J_{HH}$ = 7.0, 3H, CH*Me*$_2$), 0.91 (d, $^3J_{HH}$ = 6.5, 3H, CH*Me*$_2$), 0.25 (s, 3H, PtMe); [*SP*-4-4] 7.65 (d, $^3J_{HH}$ = 1.5, 1H, Imz), 7.44 (d, $^3J_{HH}$ = 1.5, 1H, Imz), 7.45 (m, 1H, Ar H^4), 7.29 (d, $^3J_{HH}$ = 8.0, 1H, Ar-H^3), 7.27 (d, $^3J_{HH}$ = 7.5, 1H, Ar-H^3), 4.84 (m, 1H, NCH_2); 4.20 (m, 1H, NCH_2), 3.15 (m, 1H, C*H*Me_2), 2.46 (m, 2H, CH_2S), 2.27 (m, 1H, C*H*Me_2), 2.24 (m, 2H, $CH_2CH_2CH_2$), 1.25 (d, $^3J_{HH}$ = 6.5, 3H, CH*Me*$_2$), 1.19 (d, $^3J_{HH}$ = 7.0, 3H, CH*Me*$_2$), 1.11 (d, $^3J_{HH}$ = 7.0, 3H, CH*Me*$_2$), 0.89 (d, $^3J_{HH}$ = 7.0, 3H, CH*Me*$_2$), 0.10 (s with ^{195}Pt satellites, $^2J(^1H-^{195}Pt)$ = 78.0, 3H, PtMe). $^{13}C\{^1H\}$ NMR (75 MHz, dmso-d_6): δ [*SP*-4-3] 145.7 (s, Ar-C^2), 145.6 (s, Ar-C^2), 135.4 (s, Ar-C^1), 129.21 (s, Ar-C^4), 124.41 (s, Imz-C^5), 123.24 (s, Ar-C^3), 123.0 (s, Ar-C^3), 120.9 (s, Imz-C^4), 48.0 (s, CH_2S), 47.1 (s, NCH_2), 27.6 (s, *C*HMe_2 isochronous for both isomers), 27.1 (s, *C*HMe_2), 26.3 (s, $CH_2CH_2CH_2$ isochronous for both isomers), 25.9 (s, CH*Me*$_2$), 25.5 (s, CH*Me*$_2$), 22.1 (s, CH*Me*$_2$), 21.8 (s, CH*Me*$_2$), −11.4 (s, PtMe), Imz-C^2 not observed; [*SP*-4-4] 162.7 (s, Imz-C^2), 146.0 (s, Ar-C^2), 144.8 (s, Ar-C^2), 134.5 (s, Ar-C^1), 129.17 (s, Ar-C^4), 124.36 (s, Imz-C^5), 123.17 (s, Ar-C^3), 122.9 (s, Ar-C^3), 120.8 (s, Imz-C^4), 48.9 (s, NCH_2), 47.9 (s, CH_2S), 27.6 (s, *C*HMe_2 isochronous for both isomers), 26.9 (s, *C*HMe_2), 26.3 (s, $CH_2CH_2CH_2$ isochronous for both isomers), 25.8 (s, CH*Me*$_2$), 25.2 (s, CH*Me*$_2$), 22.3 (s, CH*Me*$_2$), 22.0 (s, CH*Me*$_2$), −19.4 (s, PtMe). ^{195}Pt NMR (64 MHz, dmso-d_6): δ [*SP*-4-3] −3927; [*SP*-4-4] −4106. ESI-MS (negative ion, MeOH): m/z 672.1316 $[M - Na]^-$ (calcd 672.1302) 3.2%; 594.1179 $[M - Na - dmso]^-$ (calcd 594.1162) 100%; 578.0869 $[M - Na - dmso - CH_4]^-$ (calcd 578.0849) 4.4%.

[$PtCl_2$(dmso)(NHC·Na)] (4). A titrated aqueous solution of HCl (0.942 M, 150 μL, 0.141 mmol) was added dropwise to a solution of **2** (0.071 mmol) in water (2 mL). The mixture was stirred at room temperature until methane evolution ceased (*ca.* 5−10 min). The solvent was then removed under high vacuum at 50 °C and the solid thus obtained dried for 6 h at 70 °C

and 4 mbar of pressure. Complexes **4a**−**d** were characterized by comparison with their previously reported NMR data.[28]

[PtMe(OH$_2$)(dmso)(NHC)] (5). A 50% aqueous solution of HBF_4 (19 μL, 0.151 mmol) was added dropwise to a solution of **2** (0.151 mmol) in water (2 mL). The mixture was stirred at room temperature until methane evolution ceased (*ca.* 5−10 min). The solvent was then removed under high vacuum at 50 °C and the solid thus obtained dried for 6 h at 70 ºC and 4 mbar of pressure. Solid samples of **5** thus obtained are contaminated with $NaBF_4$.

*Sodium aqua[1,3-bis(3-sulfonatepropyl)imidazol-2-ylidene](dimethyl sulfoxide)methylplatinate(II) (**5a**).* Complex **5a** was obtained from **2a** (99.6 mg, 0.151 mmol) as a white solid (0.109 g). ESI-MS (positive ion, H_2O): *m*/*z* 644.0043 $[M + Na - H_2O]^+$ (calcd 644.0105) 100%; 618.0969 $[M - Na + 2H]^+$ (calcd 618.0572) 40%; 584.0052 $[M + Na - dmso]^+$ (calcd 584.0071) 45%; 565.9926 $[M + Na - H_2O - dmso]^+$ (calcd 565.9966) 83%; 549.9574 $[M + Na - H_2O - dmso - CH_4]^+$ (calcd 549.9653) 8.9%; 544.0088 $[M + H - H_2O - dmso]^+$ (calcd 544.0146) 10%; 527.9805 $[M + H - H_2O - dmso - CH_4]^+$ (calcd 527.9833) 4.3%. ESI-MS (negative ion, H_2O): *m*/*z* 598.0026 $[M - Na - H_2O]^-$ (calcd 598.0321) 4.5%; 519.9917 $[M - Na - H_2O - dmso]^-$ (calcd 520.0181) 2.3%; 503.9597 $[M - Na - H_2O - dmso - CH_4]^-$ (calcd 503.9868) 100%. ESI-MS (positive ion, H_2O:DMSO): *m*/*z* 722.02 $[M + Na - H_2O + dmso]^+$ (calcd 722.02) 11%; 644.01 $[M + Na - H_2O]^+$ (calcd 644.01) 100%.

*Aqua(dimethyl sulfoxide)methyl[1-methyl-3-(3-sulfonatepropyl)imidazol-2-ylidene]platinum(II) (**5b**).* Complex **5b** was obtained from **2b** (0.080 g, 0.151 mmol) as a white solid (0.092 g). ESI-MS (positive ion, H_2O): *m*/*z* 514.0268 $[M + Na - H_2O]^+$ (calcd 514.0404) 69%; 492.0506 $[M + H - H_2O]^+$ (calcd 492.0585) 83%; 436.0188 $[M + Na - H_2O - dmso]^+$ (calcd 436.0265) 25%; 419.9847 $[M + Na - H_2O - dmso - CH_4]^+$ (calcd 419.9952) 83%; 414.0386 $[M + H - H_2O - dmso]^+$ (calcd 414.0446) 9.6%; 398.0074 $[M + H - H_2O - dmso - CH_4]^+$ (calcd 398.0133) 100%.

*Aqua(dimethyl sulfoxide)methyl[1-(3-sulfonatepropyl)-3-(2,4,6-trimethylphenyl)imidazol-2-ylidene]platinum(II) (**5c**).* Complex **5c** was obtained from **2c** (95.7 mg, 0.151 mmol) as a pale-brown solid (0.105 g). ESI-MS (positive ion, H_2O): *m*/*z* 618.0936 $[M + Na - H_2O]^+$ (calcd 618.1030) 100%; 596.1119 $[M + H - H_2O]^+$ (calcd 596.1211) 35%; 540.0808 $[M + Na - H_2O - dmso]^+$ (calcd 540.0891) 4.9%; 524.0496 $[M + Na - H_2O - dmso - CH_4]^+$ (calcd 524.0578) 16%; 518.0957 $[M + H - H_2O - dmso]^+$ (calcd 518.1072) 1.4%; 502.0639 $[M + H - H_2O - dmso - CH_4]^+$ (calcd 502.0759) 5.5%.

*Aqua[1-(2,6-diisopropylphenyl)-3-(3-sulfonatepropyl)imidazol-2-ylidene](dimethyl sulfoxide)methylplatinum(II) (**5d**).* Complex **5d** was obtained from **2d** (0.102 g, 0.151 mmol) as a

pale-brown solid (0.105 g). ESI-MS (positive ion, H_2O): m/z 678.1622 $[M + Na]^+$ (calcd 678.1606) 1.0%; 660.1463 $[M + Na - H_2O]^+$ (calcd 660.1500) 100%; 638.1628 $[M + H - H_2O]^+$ (calcd 638.1680) 31%; 582.1331 $[M + Na - H_2O - dmso]^+$ (calcd 582.1361) 11%; 566.1012 $[M + Na - H_2O - dmso - CH_4]^+$ (calcd 566.1048) 3.4%; 560.1491 $[M + H - H_2O - dmso]^+$ (calcd 560.1541) 6.5%; 544.1241 $[M + H - H_2O - dmso - CH_4]^+$ (calcd 544.1228) 1.0%.

[PtMe(dmso-*d*$_6$)$_2$(NHC)] (6). These complexes were obtained by dissolution of **5** in dmso-*d*$_6$.

Complex ***6a***. ^{1}H NMR (300 MHz, dmso-*d*$_6$): δ 7.48 (s, 2H, Imz), 4.32 (t, $^3J_{HH}$ = 7.0, 4H, NCH_2), 2.53 (m, 4H, CH_2S), 2.12 (m, 4H, $CH_2CH_2CH_2$), 0.29 (s with ^{195}Pt satellites, $^1J(^1H\text{-}^{195}Pt)$ = 65.3, PtMe). $^{13}C\{^1H\}$ NMR (75 MHz, dmso-*d*$_6$): δ 156.2 (s, Imz-C^2), 121.7 (s, Imz-C^{4,5}), 48.8 (s, NCH_2), 47.6 (s, CH_2S), 26.0 (s, $CH_2CH_2CH_2$), −11.9 (s, PtMe). ^{195}Pt NMR (64 MHz, dmso-*d*$_6$): δ −4196.

Complex ***6b***. ^{1}H NMR (300 MHz, dmso-*d*$_6$): δ 7.51 (s, 1H, Imz), 7.45 (s, 1H, Imz), 4.34 (m, 2H, NCH_2), 3.78 (s, NMe), 2.52 (m, 2H, CH_2S), 2.11 (m, 2H, $CH_2CH_2CH_2$), 0.34 (s with ^{195}Pt satellites, $^1J(^1H\text{-}^{195}Pt)$ = 69.3, PtMe). $^{13}C\{^1H\}$ NMR (75 MHz, dmso-*d*$_6$): δ 156.0 (s, Imz-C^2), 123.0 and 121.7 (2 × s, Imz-C^{4,5}), 48.6 (s, NCH_2), 47.5 (s, CH_2S), 36.8 (s, NMe), 26.0 (s, $CH_2CH_2CH_2$), −12.4 (s, PtMe). ^{195}Pt NMR (64 MHz, dmso-*d*$_6$): δ −4192.

Complex ***6c***. ^{1}H NMR (300 MHz, dmso-*d*$_6$): δ 7.73 (s, 1H, Imz), 7.52 (s, 1H, Imz), 7.05 (s, 2H, Ar), 4.56 (m, 1H, NCH_2), 4.42 (m, 1H, NCH_2), 2.54 (m, 2H, CH_2S), 2.31 (s, 3H, Ar-*p*-Me), 2.20 (m, 2H, $CH_2CH_2CH_2$), 2.10 (s, 3H, Ar-*o*-Me), 2.01 (s, 3H, Ar-*o*-Me), 0.28 (s with ^{195}Pt satellites, $^2J(^1H\text{-}^{195}Pt)$ = 63.3, 3H, PtMe). ^{2}H NMR (77 MHz, dmso-*d*$_6$): δ 3.30 (broad s, 3D, $(CD_3)_2SO$), 2.99 (broad s, 3D, two $(CD_3)_2SO$ overlapping), 2.92 (broad s, 3D, $(CD_3)_2SO$). $^{13}C\{^1H\}$ NMR (75 MHz, dmso-d$_6$): δ 157.3 (s, Imz-C^2), 138.4 (s, Ar-C^4), 135.3 (s, Ar-C^2), 134.5 (s, Ar-C^2), 134.0 (s, Ar-C^1), 128.82 (s, Ar-C^3), 128.77 (s, Ar-C^3), 124.7 (s, Imz-C^4), 121.8 (s, Imz-C^5), 49.2 (s, NCH_2), 47.4 (s, CH_2S), 42.1 (s, Me_2SO), 26.3 (s, $CH_2CH_2CH_2$), 20.3 (s, Ar-*p*-Me), 18.1 (s, Ar-*o*-Me), 18.0 (s, Ar-*o*-Me), -10.1 (s, PtMe). ^{195}Pt NMR (64 MHz, dmso-*d*$_6$): δ −4174.

Complex ***6d***. ^{1}H NMR (300 MHz, dmso-*d*$_6$): δ 7.80 (s, 1H, Imz), 7.66 (s, 1H, Imz), 7.41 (t, $^3J_{HH}$ = 7.3, 1H, Ar-H^4), 7.39 (m, 2H, Ar-H^{3,5}), 4.65 (m, 1H, NCH_2), 4.49 (m, 1H, NCH_2), 2.76 (m, 1H, C*H*Me), 2.60 (m, 2H, CH_2S), 2.26 (m, 1H, C*H*Me), 2.19 (m, 2H, $CH_2CH_2CH_2$), 1.27 (d, $^3J_{HH}$ = 5.9, 3H, CH*Me*), 0.99 (d, $^3J_{HH}$ = 6.0, 3H, CH*Me*), 0.25 (s with ^{195}Pt satellites, $^2J(^1H\text{-}^{195}Pt)$ = 64.2, 3H, PtMe). $^{13}C\{^1H\}$ NMR (75 MHz, dmso-*d*$_6$): δ 157.8 (s, Imz-C^2), 145.6 (s, Ar-C^2), 145.5 (s, Ar-C^2), 133.7 (s, Ar-C^1), 130.0 (s, Ar-C^4), 126.1 (s, Imz-C^5), 123.6 (s, Ar-C^3), 121.3 (s, Imz-C^4), 49.3 (s, NCH_2), 47.1 (s, CH_2S), 27.7 (s, *C*HMe_2), 27.4 (s, *C*HMe_2), 26.6 (s,

$CH_2CH_2CH_2$), 26.2 (s, CH*Me*$_2$), 25.7 (s, CH*Me*$_2$), 22.2 (s, CH*Me*$_2$), 21.8 (s, CH*Me*$_2$), −10.1 (s, PtMe). ^{195}Pt NMR (64 MHz, dmso-d_6): δ −4173.

[Pt(OH$_2$)$_2$(dmso)(NHC)][BF$_4$] (7). A 50% aqueous solution of HBF_4 (67 μL, 0.53 mmol) was added dropwise to a solution of **2** (0.177 mmol) in water (2 mL). The mixture was stirred at room temperature until methane evolution ceased (*ca.* 5−10 min). The solvent was then removed under high vacuum at 50 °C and the solid thus obtained dried for 6 h at 70 ºC and 4 mbar of pressure. Solid samples of **7** thus obtained are contaminated with $NaBF_4$.

*cis-Diaqua[1,3-bis(3-sulfonatepropyl)imidazol-2-ylidene](dimethyl sulfoxide)platinum(II) (**7a**).* Complex **7a** was obtained from **2a** (116.8 mg, 0.177 mmol) as a white solid (0.119 g). ^{1}H NMR (300 MHz, D_2O): δ 7.32 (s, 2H, Imz), 4.57 (m, 2H, NCH_2), 4.45 (m, 2H, NCH_2), 3.45 (s, 6H, Me_2SO), 2.94 (t, $^3J_{HH}$ = 7.2, 4H, CH_2S), 2.28 (m, 4H, $CH_2CH_2CH_2$). ESI-MS (positive ion, H_2O): *m*/*z* 605.9920 $[M + Na - 2H_2O]^+$ (calcd 605.9973) 100%.

*cis-Diaqua(dimethyl sulfoxide)[1-methyl-3-(3-sulfonatepropyl)imidazol-2-ylidene]platinum(II) tetrafluoroborate(**7b**).* Complex **7b** was obtained from **2b** (93.7 mg, 0.177 mmol) as a pale-yellow solid (0.100 g). ^{1}H NMR (300 MHz, D_2O): δ 7.29 (d, $^3J_{HH}$ = 2.1, 1H, Imz), 7.23 (d, $^3J_{HH}$ = 1.8, 1H, Imz), 4.62 (m, 1H, NCH_2), 4.36 (m, 1H, NCH_2), 3.97 (s, 3H, NMe), 3.42 (s, 3H, Me_2SO), 3.41 (s, 3H, Me_2SO), 2.92 (m, 2H, CH_2S), 2.29 (m, 2H, $CH_2CH_2CH_2$). ESI-MS (positive ion, H_2O): *m*/*z* 476.0275 $[M - BF_4 - 2H_2O]^+$ (calcd 476.0272) 100%.

*cis-Diaqua(dimethyl sulfoxide)[1-(3-sulfonatepropyl)-3-(2,4,6-trimethylphenyl)imidazol-2-ylidene]platinum(II) tetrafluoroborate (**7c**).* Complex **7c** was obtained from **2c** (112.2 mg, 0.177 mmol) as a yellow solid (0.121 g). ^{1}H NMR (300 MHz, D_2O): δ 7.47 (d, $^3J_{HH}$ = 1.2, 1H, Imz), 7.32 (d, $^3J_{HH}$ = 1.5, 1H, Imz), 7.19 (s, 1H, Ar), 7.06 (s, 1H, Ar), 4.91 (m, 1H, NCH_2), 4.29 (m, 1H, NCH_2), 3.32 (s, 3H, Me_2SO), 2.92 (m, 2H, CH_2S), 2.55 (s, 3H, Me_2SO), 2.38 (m, 2H, $CH_2CH_2CH_2$), 2.25 (s, 3H, Ar-*p*-Me), 2.17 (s, 3H, Ar-*o*-Me), 1.86 (s, 3H, Ar-*o*-Me). ESI-MS (positive ion, H_2O): *m*/*z* 598.1071 $[M - BF_4 - H_2O]^+$ (calcd 598.1004) 20%, 580.0887 $[M - BF_4 - 2H_2O]^+$ (calcd 580.0898) 100%.

*cis-Diaqua[1-(2,6-diisopropylphenyl)-3-(3-sulfonatepropyl)imidazol-2-ylidene](dimethyl sulfoxide)platinum(II) (**7d**).* Complex **7d** was obtained from **2d** (119.6 mg, 0.177 mmol) as a yellow solid (0.125 g). ^{1}H NMR (300 MHz, D_2O): δ 7.46 (t, $^3J_{HH}$ = 7.8, 1H, Ar-H^4), 7.29 (s, 1H, Imz overlapped), 7.29 (m, 2H, Ar-H^{3,5} overlapped), 7.10 (d, $^3J_{HH}$ = 2.1, 1H, Imz), 4.53 (m, 1H, NCH_2), 4.33 (m, 1H, NCH_2), 3.00 (s, 3H, Me_2SO), 2.88 (m, 2H, CH_2S), 2.58 (s, 3H, Me_2SO), 2.35 (m, 2H, C*H*Me), 2.27 (m, 2H, $CH_2CH_2CH_2$), 1.17 (m, 6H, CH*Me*), 0.92 (m, 6H, CH*Me*). ESI-MS (positive ion, H_2O): *m*/*z* 622.1389 $[M - BF_4 - 2H_2O]^+$ (calcd 622.1367) 100%.

K[*cis*-PtMe$_2$(CN)(NHC·Na)] (8). Formation of these complexes was monitored by ^{1}H NMR spectroscopy. Potassium cyanide (2.3 mg, 0.035 mmol) was added to an NMR tube fitted with a J. Young valve containing a solution of the corresponding complex **2** (0.035 mmol) in D_2O (0.7 mL).

Complex ***8a***. ^{1}H NMR (300 MHz, D_2O): δ 7.05 (s, 2H, Imz), 4.21 (t, $^3J_{HH}$ = 6.6, 4H, NCH_2), 2.81 (m, 4H, CH_2S), 2.16 (m, 4H, $CH_2CH_2CH_2$), 0.03 (s with ^{195}Pt satellites, $^2J(^1H\text{-}^{195}Pt)$ = 62.4, 3H, PtMe *trans* to NHC), −0.23 (s with ^{195}Pt satellites, $^2J(^1H\text{-}^{195}Pt)$ = 69.4, 3H, PtMe *cis* to NHC).

Complex ***8b***. ^{1}H NMR (300 MHz, D_2O): δ 7.01 (d, $^3J_{HH}$ = 1.8, 1H, Imz), 6.95 (d, $^3J_{HH}$ = 1.8, 1H, Imz), 4.19 (t, $^3J_{HH}$ = 7.0, 2H, NCH_2), 3.59 (s, 3H, NMe), 2.80 (m, 2H, CH_2S), 2.16 (m, 2H, $CH_2CH_2CH_2$), 0.04 (s with ^{195}Pt satellites, $^2J(^1H\text{-}^{195}Pt)$ = 63.8, 3H, PtMe *trans* to NHC), −0.21 (s with ^{195}Pt satellites, $^2J(^1H\text{-}^{195}Pt)$ = 68.8, 3H, PtMe *cis* to NHC).

Complex ***8c***. ^{1}H NMR (300 MHz, D_2O): δ 7.26 (d, $^3J_{HH}$ = 1.8, 1H, Imz), 6.96 (s, 2H, Ar), 6.82 (d, $^3J_{HH}$ = 1.8, 1H, Imz), 4.36 (t, $^3J_{HH}$ = 6.7, 2H, NCH_2), 2.90 (t, $^3J_{HH}$ = 7.9, 2H, CH_2S), 2.26 (m, 2H, $CH_2CH_2CH_2$), 2.23 (s, 3H, Ar-*p*-Me), 1.99 (s, 3H, Ar-*o*-Me); −0.15 (s with ^{195}Pt satellites, $^2J(^1H\text{-}^{195}Pt)$ = 63.6, 3H, PtMe *trans* to NHC), −0.30 (s with ^{195}Pt satellites, $^2J(^1H\text{-}^{195}Pt)$ = 69.7, 3H, PtMe *cis* to NHC).

K[*cis*-PtMe(CN)$_2$(NHC·Na)] (9). Potassium cyanide (26.0 mg, 0.400 mmol) was added to a solution of the corresponding complex **2** (0.200 mmol) in water (3 mL). The mixture was stirred for 3 h at room temperature. The solvent was removed under vacuum and the solid thus obtained was dried for 5 h at 80 ºC and 4 mbar of pressure. No further purification was attempted.

Complex ***9a***. This complex was obtained from **2a** (0.132 g, 0.200 mmol) as a white solid (0.124 g). IR (cm^{-1}): ν (C≡N) 2118 (s), 2102 (s). ^{1}H NMR (300 MHz, D_2O): δ 7.13 (s, 2H, Imz), 4.18 (t, $^3J_{HH}$ = 6.8, 4H, NCH_2), 2.81 (m, 4H, CH_2S), 2.19 (m, 4H, $CH_2CH_2CH_2$), −0.02 (s with ^{195}Pt satellites, $^2J(^1H\text{-}^{195}Pt)$ = 67.1, 3H, PtMe). $^{13}C\{^1H\}$ NMR (75 MHz, D_2O): δ 168.5 (s, Imz-C^2), 145.2 (s, CN *cis* to NHC), 141.8 (s, CN *trans* to NHC), 121.4 (s with ^{195}Pt satellites, $^3J(^{13}C\text{-}^{195}Pt)$ = 30.9, Imz-$C^{4,5}$), 48.7 (s, NCH_2), 48.4 (s, CH_2S), 25.6 (s, $CH_2CH_2CH_2$), −18.2 (s with ^{195}Pt satellites, $^1J(^{13}C\text{-}^{195}Pt)$ = 508.6, PtMe). ESI-MS (negative ion, MeOH): m/z 633.9463 [M − Na]$^-$ (calcd 633.9777) 31%; 617.9711 [M − Na − CH_4]$^-$ (calcd 617.9464) 17%; 595.9322 [M − 2Na + H − CH_4]$^-$ (calcd 595.9645) 24%; 557.9776 [M − 2Na + 2H − K − CH_4]$^-$ (calcd 558.0086) 91%; 530.9663 [M − 2Na + H − KCN − CH_4]$^-$ (calcd 530.9977) 27%; 503.9581 [M − 2Na − KCN − CN − CH_4]$^-$ (calcd 503.9874) 100%.

*Complex (**9b**)*. This complex was obtained from **2b** (0.106 g, 0.200 mmol) as a pale-yellow solid (0.102 g). IR (cm^{-1}): ν (C≡N) 2119 (s), 2101 (s). ^{1}H NMR (300 MHz, D_2O): δ 7.08 (d, $^3J_{HH}$ = 1.8, 1H, Imz), 7.02 (d, $^3J_{HH}$ = 1.8, 1H, Imz), 4.16 (m, 2H, NCH_2), 3.60 (s, 3H, NMe), 2.80 (m, 2H, CH_2S), 2.16 (m, 2H, $CH_2CH_2CH_2$), −0.02 (s with ^{195}Pt satellites, $^2J(^1H\text{-}^{195}Pt)$ = 67.1, 3H, PtMe). $^{13}C\{^1H\}$ NMR (75 MHz, D_2O): δ 168.1 (s, Imz-C^2), 145.1 (s, CN *cis* to NHC), 141.9 (s, CN *trans* to NHC), 122.7 (s with ^{195}Pt satellites, $^3J(^{13}C\text{-}^{195}Pt)$ = 31.4, Imz-C^5), 120.8 (s with ^{195}Pt satellites, $^3J(^{13}C\text{-}^{195}Pt)$ = 31.8, Imz-C^4), 48.5 (s, NCH_2), 48.4 (s, CH_2S), 37.1 (s, NMe), 25.7 (s, $CH_2CH_2CH_2$), −18.6 (s, PtMe). ESI-MS (negative ion, MeOH): *m/z* 488.0342 [M − K]$^-$ (calcd 488.0338) 100%; 504.0078 [M − Na]$^-$ (calcd 504.0077) 93%; 439.0417 [M − Na − KCN]$^-$ (calcd 439.0409) 9.0%; 450.0200 [M − Na − K + H − CH_4]$^-$ (calcd 450.0205) 21%; 423.0087 [M − Na − KCN − CH_4]$^-$ (calcd 423.0096) 41%.

*Complex **9c***. This complex was obtained from **2c** (0.127 g, 0.200 mmol) as a yellow solid (0.120 g). IR (cm^{-1}): ν (C≡C) 2117 (s), 2102 (s). ^{1}H NMR (300 MHz, D_2O): δ 7.33 (d, $^3J_{HH}$ = 2.0, 1H, Imz), 6.99 (d, $^3J_{HH}$ = 2.0, 1H, Imz), 6.97 (s br, 2H, Ar), 4.31 (m, 2H, NCH_2), 2.84 (m, 2H, CH_2S), 2.26 (m, 2H, $CH_2CH_2CH_2$), 2.22 (s, 3H, Ar-*p*-Me), 2.00 (s, 3H, Ar-*o*-Me), 1.93 (s, 3H, Ar-*o*-Me), −0.13 (s with ^{195}Pt satellites, $^2J(^1H\text{-}^{195}Pt)$ = 67.1, 3H, PtMe). $^{13}C\{^1H\}$ NMR (75 MHz, D_2O): δ 169.4 (s, Imz-C^2), 145.5 (s, CN *cis* to NHC), 141.2 (s, CN *trans* to NHC), 139.4 (s, Ar-C^4), 136.0 (s, Ar-C^1), 135.6 (s, Ar-C^2), 135.5 (s, Ar-C^2), 129.0 (s, Ar-C^3), 128.9 (s, Ar-C^3), 123.4 (s with ^{195}Pt satellites, $^3J(^{13}C\text{-}^{195}Pt)$ = 27.0, Imz-C^4), 121.4 (s with ^{195}Pt satellites, $^3J(^{13}C\text{-}^{195}Pt)$ = 28.5, Imz-C^5), 48.4 (s, NCH_2), 48.0 (s, CH_2S), 25.3 (s, $CH_2CH_2CH_2$), 20.1 (s, Ar-*p*-Me), 17.6 (s, Ar-*o*-Me), 17.2 (s, Ar-*o*-Me), −18.0 (s, PtMe). ESI-MS (negative ion, MeOH): *m/z* 608.0708 [M − Na]$^-$ (calcd 608.0703) 17%; 592.0954 [M − K]$^-$ (calcd 592.0964) 27%; 554.0818 [M − Na − K + H − CH_4]$^-$ (calcd 554.0831) 100%; 543.1042 [M − Na − KCN]$^-$ (calcd 543.1035) 7.6%; 527.0723 [M − Na − KCN − CH_4]$^-$ (calcd 527.0727) 41%.

[$PtMe_2$(CNCH$_2$COOK)(NHC·Na)] (10). Potassium 2-isocyanoacetate (85% purity, 0.0217 g, 0.150 mmol) was added to a solution of the corresponding complex **2** (0.150 mmol) in water (5 mL) and the mixture stirred for 2 h at room temperature. The solvent was then removed under vacuum and the solid thus obtained dried for 5 h at 80 ºC and 4 mbar of pressure.

*cis-[1,3-Bis(3-sodiumsulfonatepropyl)imidazol-2-ylidene]dimethyl(potassium-2-isocyanidoacetate)platinum(II) (**10a**)*. This complex was obtained from **2a** (98.9 mg, 0.150 mmol) as a white solid (0.103 g, 97%). IR (cm^{-1}): ν (C≡N) 2167 (m). ^{1}H NMR (300 MHz, D_2O): δ 7.10 (s, 2H, Imz), 4.19 (t, $^3J_{HH}$ = 6.7, 4H, NCH_2), 2.78 (m, 4H, CH_2S), 2.14 (m, 4H, $CH_2CH_2CH_2$), 0.16 (s with ^{195}Pt satellites, $^2J(^1H\text{-}^{195}Pt)$ = 64.4, 3H, PtMe *trans* to NHC); −0.06 (s with ^{195}Pt satellites, $^2J(^1H\text{-}^{195}Pt)$ = 69.4, 3H, PtMe *cis* to NHC). $^{13}C\{^1H\}$ NMR (75 MHz, D_2O): δ 180.8 (s with ^{195}Pt satellites, $^1J(^{13}C\text{-}^{195}Pt)$ = 811.5, Imz-C^2), 171.3 (s, COOK), 142.8 (s,

Pt*C*NR), 121.0 (s with ^{195}Pt satellites, $^{3}J(^{13}C\text{-}^{195}Pt)$ = 20.1, Imz-C^{4,5}), 48.4 (s, CH_2S), 48.2 (s, CN*C*H_2COOK), 48.0 (s, NCH_2), 25.7 (s, $CH_2CH_2CH_2$), −6.1 (s, with ^{195}Pt satellites, $^{1}J(^{13}C\text{-}^{195}Pt)$ = 591.8, PtMe *cis* to NHC), −11.7 (s, with ^{195}Pt satellites, $^{1}J(^{13}C\text{-}^{195}Pt)$ = 498.8, PtMe *trans* to NHC). ESI-MS (negative ion, H_2O): *m*/*z* 621.0477 $[M - 2Na - K + 2H]^-$ (calcd 621.0658) 3.8%, 627.0263 $[M - Na - K + H - CH_4]^-$ (calcd 627.0164) 7.0%, 605.0263 $[M - 2Na - K + 2H - CH_4]^-$ (calcd 605.0345) 19%, 558.0356 $[M - Na - CNCH_2COOK]^-$ (calcd 558.0314) 3.5%, 536.0474 $[M - 2Na + H - CNCH_2COOK]^-$ (calcd 536.0494) 2.3%, 503.9894 $[M - 2Na + H - CNCH_2COOK - 2CH_4]^-$ (calcd 503.9868) 20%, 267.5213 $[M - 2Na - CNCH_2COOK]^{2-}$ (calcd 267.5210) 100%.

cis-Dimethyl[1-methyl-3-(3-sodiumsulfonatepropyl)imidazol-2-ylidene](potassium-2-isocyanidoacetate)platinum(II) (***10b***). This complex was obtained from **2b** (79.4 mg, 0.150 mmol) as a pale-yellow solid (84.5 mg, 98%). IR (cm^{-1}): ν (C≡N) 2168 (s). ^{1}H NMR (300 MHz, D_2O): δ 7.06 (d, $^{3}J_{HH}$ = 1.5, 1H, Imz), 7.00 (d, $^{3}J_{HH}$ = 1.5, 1H, Imz), 4.17 (t, $^{3}J_{HH}$ = 6.6, 2H, NCH_2), 3.99 (d, $^{3}J_{HH}$ = 5.7, 1H, $CNCH_2CO_2K$), 3.97 (d, $^{3}J_{HH}$ = 5.7, 1H, $CNCH_2CO_2K$), 3.60 (s, 3H, NMe), 2.79 (t, $^{3}J_{HH}$ = 6.9, 2H, CH_2S), 2.14 (q, $^{3}J_{HH}$ = 6.9, 2H, $CH_2CH_2CH_2$), 0.17 (s with ^{195}Pt satellites, $^{2}J(^{1}H\text{-}^{195}Pt)$ = 64.3, 3H, PtMe *trans* to NHC), −0.03 (s with ^{195}Pt satellites, $^{2}J(^{1}H\text{-}^{195}Pt)$ = 70.6, 3H, PtMe *cis* to NHC). $^{13}C\{^{1}H\}$ NMR (75 MHz, D_2O): δ 180.5 (s with ^{195}Pt satellites, $^{1}J(^{13}C\text{-}^{195}Pt)$ = 810.5, Imz-C^{2}), 171.3 (s, COOK), 142.7 (s, Pt*C*NR), 122.5 (s with ^{195}Pt satellites, $^{3}J(^{13}C\text{-}^{195}Pt)$ = 20.5, Imz-C^{5}), 120.3 (s with ^{195}Pt satellites, $^{3}J(^{13}C\text{-}^{195}Pt)$ = 20.0, Imz-C^{4}), 48.4 (s, CH_2S), 48.3 (s, CN*C*H_2COOK), 48.1 (s, NCH_2), 36.9 (s, NMe), 25.8 (s, $CH_2CH_2CH_2$), −6.5 (s, with ^{195}Pt satellites, $^{1}J(^{13}C\text{-}^{195}Pt)$ = 591.1, PtMe *cis* to NHC), −11.5 (s, with ^{195}Pt satellites, $^{1}J(^{13}C\text{-}^{195}Pt)$ = 496.4, PtMe *trans* to NHC). ESI-MS (negative ion, MeOH): *m*/*z* 551.0324 $[M - Na]^-$ (calcd 551.0336) 3.6%, 535.0596 $[M - K]^-$ (calcd 535.0596) 12%, 513.0770 $[M - Na - K + H]^-$ (calcd 513.0777) 100%, 497.0479 $[M - Na - K + H - CH_4]^-$ (calcd 497.0464) 2.7%, 428.0610 $[M - Na - CNCH_2COOK]^-$ (calcd 428.0613) 28%, 412.0286 $[M - Na - CNCH_2COOK - CH_4]^-$ (calcd 412.0300) 7.8%, 395.9987 $[M - Na - CNCH_2COOK - 2CH_4]^-$ (calcd 395.9987) 3.5%.

cis-Dimethyl(potassium-2-isocyanidoacetate)[1-(3-sodiumsulfonatepropyl)-3-(2,4,6-trimethylphenyl)imidazol-2-ylidene]platinum(II) (***10c***). This complex was obtained from **2c** (95.1 mg, 0.150 mmol) as a yellow solid (97.7 mg, 96%). IR (cm^{-1}): ν (C≡N) 2172 (m). ^{1}H NMR (300 MHz, D_2O): δ 7.31 (d, $^{3}J_{HH}$ = 1.8, 1H, Imz), 6.96 (s, 2H, Ar), 6.94 (d, $^{3}J_{HH}$ = 1.8, 1H, Imz), 4.28 (t, $^{3}J_{HH}$ = 6.9, 2H, NCH_2), 3.92 (d, $^{3}J_{HH}$ = 5.9, 1H, $CNCH_2CO_2K$), 3.90 (d, $^{3}J_{HH}$ = 5.9, 1H, $CNCH_2CO_2K$), 2.82 (m, 2H, CH_2S), 2.21 (m, 2H, $CH_2CH_2CH_2$), 2.21 (s, 3H, Ar-*p*-Me), 1.90 (s, 6H, Ar-*o*-Me), −0.05 (s with ^{195}Pt satellites, $^{2}J(^{1}H\text{-}^{195}Pt)$ = 64.6, 3H, PtMe *trans* to NHC), −0.08 (s with ^{195}Pt satellites, $^{2}J(^{1}H\text{-}^{195}Pt)$ = 70.9, 3H, PtMe *cis* to NHC). ^{1}H NMR (300 MHz, dmso-d_6): δ 7.49 (d, $^{3}J_{HH}$ = 1.8, 1H, Imz), 7.08 (d, $^{3}J_{HH}$ = 1.8, 1H, Imz), 6.92 (s, 2H, Ar), 4.29 (m, 2H, NCH_2), 3.61 (s, 2H, $CNCH_2CO_2K$), 2.45 (m, 2H, CH_2S), 2.26 (s, 3H, Ar-*p*-Me), 2.11

(m, 2H, $CH_2CH_2CH_2$), 1.94 (s, 6H, Ar-*o*-Me), −0.13 (s with ^{195}Pt satellites, $^2J(^1H\text{-}^{195}Pt)$ = 64.8, 3H, PtMe *trans* to NHC), −0.24 (s with ^{195}Pt satellites, $^2J(^1H\text{-}^{195}Pt)$ = 69.0, 3H, PtMe *cis* to NHC). $^{13}C\{^1H\}$ NMR (75 MHz, D_2O): δ 181.7 (s with ^{195}Pt satellites, $^1J(^{13}C\text{-}^{195}Pt)$ = 791.6, Imz-C^2), 170.6 (s, COOK), 142.9 (s, Pt*C*NR), 139.2 (s, Ar-C^4), 136.2 (s, Ar-C^1), 135.7 (s, Ar-C^2), 128.5 (s, Ar-C^3), 122.4 (s with ^{195}Pt satellites, $^3J(^{13}C\text{-}^{195}Pt)$ = 21.9, Imz-C^4), 120.7 (s with ^{195}Pt satellites, $^3J(^{13}C\text{-}^{195}Pt)$ = 17.8, Imz-C^5), 48.1 (s, CH_2S), 47.9 (s, CN*C*H_2COOK), 47.8 (s, NCH_2), 25.5 (s, $CH_2CH_2CH_2$), 20.1 (s, Ar-*p*-Me), 17.1 (s, Ar-*o*-Me), −5.3 (s with ^{195}Pt satellites, $^1J(^{13}C\text{-}^{195}Pt)$ = 595.8, PtMe *cis* to NHC), −11.8 (s with ^{195}Pt satellites, $^1J(^{13}C\text{-}^{195}Pt)$ = 496.9, PtMe *trans* to NHC). $^{13}C\{^1H\}$ NMR (75 MHz, dmso-d_6): δ 182.2 (s, Imz-C^2), 164.5 (s, COOK), 140.8 (s, Pt*C*NR), 136.6 (s, Ar-C^4), 136.3 (s, Ar-C^1), 134.5 (s, Ar-C^2), 127.9 (s, Ar-C^3), 121.3 (s, Imz-C^4), 120.1 (s, Imz-C^5), 47.9 (s, CH_2S), 47.6 (s, CN*C*H_2COOK), 47.0 (s, NCH_2), 25.9 (s, $CH_2CH_2CH_2$), 20.2 (s, Ar-*p*-Me), 17.2 (s, Ar-*o*-Me), −4.9 (s, PtMe *cis* to NHC), −9.0 (s, PtMe *trans* to NHC). ESI-MS (negative ion, MeOH): *m*/*z* 617.1402 $[M - Na - K + H]^-$ (calcd 617.1403) 68%, 557.1177 $[M - Na - K + H - CO_2 - CH_4]^-$ (calcd 557.1192) 100%, 541.0859 $[M - Na - K + H - CO_2 - 2CH_4]^-$ (calcd 541.0879) 64%, 516.0909 $[M - Na - CNCH_2COOK - CH_4]^-$ (calcd 516.0926) 97%, 500.0604 $[M - Na - CNCH_2COOK - 2CH_4]^-$ (calcd 500.0613) 33%.

X-ray Crystallographic Studies. Suitable single crystals were obtained by slow diffusion of acetone into an aqueous solution of **2a** or of diethyl ether into a methanol solution of **3a** or **9a**. A summary of crystal data, data collection, and refinement parameters for the structural analyses is given in Table S1 (Supporting Information). Crystals of **2a** were fitted on a MiTeGen micromount (**2a**) and mounted at room temperature (296 K) in a Bruker Kappa Apex II diffractometer (**2a**). Crystals of **3a** and **9a** were glued to a glass fiber using an inert polyfluorinated oil and mounted in the low temperature N_2 stream (200 K) of a Bruker-Nonius Kappa-CCD diffractometer equipped with an area detector and an Oxford Cryostream 700 unit.

Intensities were collected using graphite-monochromated Mo-*K*α radiation (λ = 0.71073 Å). Data were measured with exposure times of 10 s per frame for **2a** (5 sets; 1075 frames; phi/omega scans; 0.5° scan-width), 9 s per frame for **3a** (9 sets; 471 frames; phi/omega scans; 1.8° scan-width) and 63 s per frame for **9a** (5 sets; 811 frames; phi/omega scans; 0.9° scan-width). Raw data were corrected for Lorenz and polarization effects. The structures were solved by direct methods, completed by subsequent difference Fourier techniques, and refined by full-matrix least squares on F^2 (SHELXL-97).[49] Anisotropic thermal parameters were used in the last cycles of refinement for the non-hydrogen atoms, with the exception of **3a** for which a disorder was found and the sulfur S(7B) and Na(2) were refined isotropically. In compound **9a**, some disordered water was observed and some remaining electronic density due to another disordered solvent molecule was squeezed with Platon.[50] Absorption correction procedures

were carried out using the multi-scan SADABS (**2a**)[51] or SORTAV programs (semi-empirical from equivalent, **3a** and **9a**).[52] Hydrogen atoms were included in the last cycle of refinement from geometrical calculations and refined using a riding model. All calculations were performed using the SHELXTL Software Package (**2a**) or WINGX system (**3a** and **9a**).[53]

ASSOCIATED CONTENT

Supporting Information

NMR spectra of selected complexes, crystallographic data and CIF files for compounds **2a**, *SP*-4-3-**3a**, and **9a**. This material is available free of charge via the Internet at http://pubs.acs.org.

AUTHOR INFORMATION

Corresponding Authors

*Email: juanc.flores@uah.es (J.C.F.), ernesto.dejesus@uah.es (E.d.J).

ACKNOWLEDGMENT

This work was supported by the Spanish Ministerio de Economía y Competitividad (project CTQ2011-24096) and the Factoría de Cristalización (CSD2006-00015). E.A.B. is grateful to the Universidad de Alcalá for an FPI Doctoral Fellowship.

REFERENCES

(1) *N-Heterocyclic Carbenes: From Laboratory Curiosities to Efficient Synthetic Tools*; Diez-Gonzalez, S., Ed.; RSC Catalysis Series 6; The Royal Society of Chemistry, 2011. Jahnke, M. C.; Hahn, F. E. In *Transition Metal Complexes of Neutral η^1-Carbon Ligands*; Chauvin, R., Canac, Y., Eds.; Topics in Organometallic Chemistry 30; Springer: Berlin, 2010, pp. 95-129. Hahn, F. E.; Jahnke, M. C. *Angew. Chem., Int. Ed.* **2008**, *47*, 3122-3172. Kühl, O. *Chem. Soc. Rev.* **2007**, *36*, 592-607.

(2) Kelly III, R. A.; Clavier, H.; Giudice, S.; Scott, N. M.; Stevens, E. D.; Bordner, J.; Samardjiev, I.; Hoff, C. D.; Cavallo, L.; Nolan, S. P. *Organometallics* **2007**, *27*, 202-210.

(3) Díez-González, S.; Marion, N.; Nolan, S. P. *Chem. Rev.* **2009**, *109*, 3612-3676. Poyatos, M.; Mata, J. A.; Peris, E. *Chem. Rev.* **2009**, *109*, 3677-3707. *N-Heterocyclic Carbenes in Transition Metal Catalysis*; Glorius, F., Ed.; Topics in Organometallic Chemistry 21; Springer: Berlin Heidelberg, 2007. *N-Heterocyclic Carbenes in Synthesis*; Nolan, S. P., Ed.; Wiley-VCH: Weinheim, 2006. Herrmann, W. A. *Angew. Chem., Int. Ed.* **2002**, *41*, 1290-1309.

(4) Mercs, L.; Albrecht, M. *Chem. Soc. Rev.* **2010**, *39*, 1903-1912. Liu, W.; Gust, R. *Chem. Soc. Rev.* **2013**, *42*, 755-773. Gautier, A.; Cisnetti, F. *Metallomics* **2012**, *4*, 23-32. Teyssot, M.-L.; Jarrousse, A.-S.; Manin, M.; Chevry, A.; Roche, S.; Norre, F.; Beaudoin, C.; Morel, L.; Boyer,

D.; Mahiou, R.; Gautier, A. *Dalton Trans.* **2009**, 6894-6902. Hindi, K. M.; Panzner, M. J.; Tessier, C. A.; Cannon, C. L.; Youngs, W. J. *Chem. Rev.* **2009**, *109*, 3859-3884. Kascatan-Nebioglu, A.; Panzner, M. J.; Tessier, C. A.; Cannon, C. L.; Youngs, W. J. *Coord. Chem. Rev.* **2007**, *251*, 884-895.

(5) Shaughnessy, K. H. *Chem. Rev.* **2009**, *109*, 643-710.

(6) Herrmann, W. A.; Elison, M.; Fisher, J.; Kocher, C.; Ofele, K. Metal complexes with heterocycles carbenes, US Patent 5,728,839, 1998. Herrmann, W. A.; Goo β en, L. J.; Spiegler, M. *J. Organomet. Chem.* **1997**, *547*, 357-366.

(7) Özdemir, İ.; Yiğit, B.; Çetinkaya, B.; Ülkü, D.; Tahir, M. N.; Arıcı, C. *J. Organomet. Chem.* **2001**, *633*, 27-32.

(8) Gallivan, J. P.; Jordan, J. P.; Grubbs, R. H. *Tetrahedron Lett.* **2005**, *46*, 2577-2580. Hong, S. H.; Grubbs, R. H. *J. Am. Chem. Soc.* **2006**, *128*, 3508-3509. Jordan, J. P.; Grubbs, R. H. *Angew. Chem., Int. Ed.* **2007**, *46*, 5152-5155. Balof, S. L.; Yu, B.; Lowe, A. B.; Ling, Y.; Zhang, Y.; Schanz, H.-J. *Eur. J. Inorg. Chem.* **2009**, *2009*, 1717-1722.

(9) Azua, A.; Sanz, S.; Peris, E. *Organometallics* **2010**, *29*, 3661-3664.

(10) Syska, H.; Herrmann, W. A.; Kühn, F. E. *J. Organomet. Chem.* **2012**, *703*, 56-62.

(11) Schönfelder, D.; Nuyken, O.; Weberskirch, R. *J. Organomet. Chem.* **2005**, *690*, 4648-4655. Meise, M.; Haag, R. *ChemSusChem* **2008**, *1*, 637-642. Roy, S.; Plenio, H. *Adv. Synth. Catal.* **2010**, *352*, 1014-1022. Yang, C.-C.; Lin, P.-S.; Liu, F.-C.; Lin, I. J. B.; Lee, G.-H.; Peng, S.-M. *Organometallics* **2010**, *29*, 5959-5971. Godoy, F.; Segarra, C.; Poyatos, M.; Peris, E. *Organometallics* **2011**, *30*, 684-688. Karimi, B.; Fadavi Akhavan, P. *Chem. Commun.* **2011**, *47*, 7686-7688. Li, L.; Wang, J.; Zhou, C.; Wang, R.; Hong, M. *Green Chem.* **2011**, *13*, 2071-2077. Luo, F.-T.; Lo, H.-K. *J. Organomet. Chem.* **2011**, *696*, 1262-1265.

(12) Fleckenstein, C.; Roy, S.; Leuthau; Plenio, H. *Chem. Commun.* **2007**, 2870-2872.

(13) Almássy, A.; Nagy, C. E.; Bényei, A. C.; Joó, F. *Organometallics* **2010**, *29*, 2484-2490.

(14) Czégéni, C. E.; Papp, G.; Kathó, Á.; Joó, F. *J. Mol. Catal. A: Chem.* **2011**, *340*, 1-8. Wetzel, C.; Kunz, P. C.; Thiel, I.; Spingler, B. *Inorg. Chem.* **2011**, *50*, 7863-7870.

(15) Azua, A.; Sanz, S.; Peris, E. *Chem. Eur. J.* **2011**, *17*, 3963-3967.

(16) Wang, W.; Wu, J.; Xia, C.; Li, F. *Green Chem.* **2011**, *13*, 3440-3445.

(17) Velazquez, H. D.; Verpoort, F. *Chem. Soc. Rev.* **2012**, *41*, 7032-7060. Schaper, L.-A.; Hock, S. J.; Herrmann, W. A.; Kühn, F. E. *Angew. Chem., Int. Ed.* **2013**, *52*, 270-289.

(18) Fantasia, S.; Jacobsen, H.; Cavallo, L.; Nolan, S. P. *Organometallics* **2007**, *26*, 3286-3288. Brissy, D.; Skander, M.; Retailleau, P.; Frison, G.; Marinetti, A. *Organometallics* **2008**, *28*, 140-151. Hu, J. J.; Bai, S.-Q.; Yeh, H. H.; Young, D. J.; Chi, Y.; Hor, T. S. A. *Dalton Trans.* **2011**, *40*, 4402-4406. Fantasia, S.; Petersen, J. L.; Jacobsen, H.; Cavallo, L.; Nolan, S. P. *Organometallics* **2007**, *26*, 5880-5889.

(19) Newman, C. P.; Deeth, R. J.; Clarkson, G. J.; Rourke, J. P. *Organometallics* **2007**, *26*, 6225-6233.

(20) Hu, J. J.; Li, F.; Hor, T. S. A. *Organometallics* **2009**, *28*, 1212-1220.

(21) Meyer, D.; Ahrens, S.; Strassner, T. *Organometallics* **2010**, *29*, 3392-3396.

(22) Jamali, S.; Milic, D.; Kia, R.; Mazloomi, Z.; Abdolahi, H. *Dalton Trans.* **2011**, *40*, 9362-9365.

(23) Lillo, V.; Mata, J.; Ramírez, J.; Peris, E.; Fernandez, E. *Organometallics* **2006**, *25*, 5829-5831.

(24) Lillo, V.; Mata, J. A.; Segarra, A. M.; Peris, E.; Fernandez, E. *Chem. Commun.* **2007**, 2184-2186.

(25) Jung, I. G.; Seo, J.; Lee, S. I.; Choi, S. Y.; Chung, Y. K. *Organometallics* **2006**, *25*, 4240-4242.

(26) Alves, G.; Morel, L.; El-Ghozzi, M.; Avignant, D.; Legeret, B.; Nauton, L.; Cisnetti, F.; Gautier, A. *Chem. Commun.* **2011**, *47*, 7830-7832. Skander, M.; Retailleau, P.; Bourrié, B.; Schio, L.; Mailliet, P.; Marinetti, A. *J. Med. Chem.* **2010**, *53*, 2146-2154. Chardon, E.; Dahm, G.; Guichard, G.; Bellemin-Laponnaz, S. *Organometallics* **2012**, *31*, 7618-7621.

(27) Silbestri, G. F.; Flores, J. C.; de Jesús, E. *Organometallics* **2012**, *31*, 3355-3360.

(28) Baquero, E. A.; Silbestri, G. F.; Gómez-Sal, P.; Flores, J. C.; de Jesús, E. *Organometallics* **2013**, *32*, 2814-2826.

(29) Fortman, G. C.; Scott, N. M.; Linden, A.; Stevens, E. D.; Dorta, R.; Nolan, S. P. *Chem. Commun.* **2010**, *46*, 1050-1052.

(30) Rivada-Wheelaghan, O.; Donnadieu, B.; Maya, C.; Conejero, S. *Chem. Eur. J.* **2010**, *16*, 10323-10326. Rivada-Wheelaghan, O.; Ortuño, M. A.; Díez, J.; Lledós, A.; Conejero, S. *Angew. Chem., Int. Ed.* **2012**, *51*, 3936-3939.

(31) Petretto, G. L.; Wang, M.; Zucca, A.; Rourke, J. P. *Dalton Trans.* **2010**, *39*, 7822-7825.

(32) Netland, K. A.; Krivokapic, A.; Tilset, M. *J. Coord. Chem.* **2010**, *63*, 2909-2927.

(33) Frøseth, M.; Netland, K. A.; Rømming, C.; Tilset, M. *J. Organomet. Chem.* **2005**, *690*, 6125-6132.

(34) Nägele, P.; Herrlich, U.; Rominger, F.; Hofmann, P. *Organometallics* **2012**, *32*, 181-191.

(35) Moore, L. R.; Cooks, S. M.; Anderson, M. S.; Schanz, H.-J.; Griffin, S. T.; Rogers, R. D.; Kirk, M. C.; Shaughnessy, K. H. *Organometallics* **2006**, *25*, 5151-5158.

(36) Tomás-Mendivil, E.; Toullec, P. Y.; Díez, J.; Conejero, S.; Michelet, V.; Cadierno, V. *Org. Lett.* **2012**, *14*, 2520-2523. Tomás-Mendivil, E.; Toullec, P. Y.; Borge, J.; Conejero, S.; Michelet, V.; Cadierno, V. *ACS Catal.* **2013**, *3*, 3086-3098. Jantke, D.; Cokoja, M.; Pöthig, A.; Herrmann, W. A.; Kühn, F. E. *Organometallics* **2013**, *32*, 741-744. Yuan, D.; Teng, Q.; Huynh, H. V. *Organometallics* **2014**, *33*, 1794-1800.

(37) Lucey, D. W.; Helfer, D. S.; Atwood, J. D. *Organometallics* **2003**, *22*, 826-833.

(38) Britovsek, G. J. P.; Woo, G. Y. Y.; Assavathorn, N. *J. Organomet. Chem.* **2003**, *679*, 110-115.

(39) Hintermann, L.; Labonne, A. *Synthesis* **2007**, 1121-1150. Alonso, F.; Beletskaya, I. P.; Yus, M. *Chem. Rev.* **2004**, *104*, 3079-3160.

(40) Romeo, R.; Scolaro, L. M.; Nastasi, N.; Mann, B. E.; Bruno, G.; Nicolo, F. *Inorg. Chem.* **1996**, *35*, 7691-7698. Engelter, C.; Moss, J. R.; Nassimbeni, L. R.; Niven, M. L.; Reid, G.; Spiers, J. C. *J. Organomet. Chem.* **1986**, *315*, 255-268.

(41) Prokopchuk, E. M.; Puddephatt, R. J. *Organometallics* **2002**, *22*, 563-566.

(42) For a table of nucleophilic reactivity constants toward Pt(II) complexes, see for instance: Pearson, R. G.; Sobel, H. R.; Songstad, J. *J. Am. Chem. Soc.* **1968**, *90*, 319-326.

(43) Denk, M. K.; Rodezno, J. M.; Gupta, S.; Lough, A. J. *J. Organomet. Chem.* **2001**, *617-618*, 242-253. Bonnette, F.; Kato, T.; Destarac, M.; Mignani, G.; Cossio, F. P.; Baceiredo, A. *Angew. Chem., Int. Ed.* **2007**, *46*, 8632-8635. Segarra, C.; Mas-Marza, E.; Benitez, M.; Mata, J. A.; Peris, E. *Angew. Chem., Int. Ed.* **2012**, *51*, 10841-10845. Wang, G.-F.; Song, X.-J.; Chen, F.; Li, Y.-Z.; Chen, X.-T.; Xue, Z.-L. *Dalton Trans.* **2012**, *41*, 10919-10922. Zuo, W.; Braunstein, P. *Dalton Trans.* **2012**, *41*, 636-643. Gupta, S. K.; Ghorai, D.; Choudhury, J. *Organometallics* **2014**, *33*, 3215-3218.

(44) Holloczki, O.; Terleczky, P.; Szieberth, D.; Mourgas, G.; Gudat, D.; Nyulaszi, L. *J. Am. Chem. Soc.* **2011**, *133*, 780-789.

(45) Eaborn, C.; Kundu, K.; Pidcock, A. *J. Organomet. Chem.* **1979**, *170*, C18-C20. Eaborn, C.; Kundu, K.; Pidcock, A. *J. Chem. Soc., Dalton Trans.* **1981**, 933-938.

(46) Romeo, R.; Scolaro, L. M. *Inorg. Synth.* **1998**, *32*, 153-158.

(47) Almássy, A.; Nagy, C. E.; Bényei, A. C.; Joó, F. *Organometallics* **2010**, *29*, 2484-2490.

(48) Yoshizawa, M.; Ohno, H. *Ionics* **2002**, *8*, 267-271.

(49) Sheldrick, G. M. *Acta Crystallogr., Sect. A* **2008**, *64*, 112-122.

(50) van der Sluis, P.; Spek, A. L. *Acta Crystallogr., Sect. A* **1990**, *46*, 194-201.

(51) Sheldrick, G. M. *SADABS: Program for Absorption Correction for Data from Area Detector Frames*

(52) Blessing, R. H. *Acta Crystallogr., Sect. A* **1995**, *51*, 33-38.

(53) Farrugia, L. J. *J. Appl. Cryst.* **1999**, *32*, 837-838.

Supporting Information

Water-Soluble Mono- and Di-methyl(N-Heterocyclic Carbene) Platinum(II) Complexes: Synthesis and Reactivity

Edwin A. Baquero,[†] Juan C. Flores,*[,†] Josefina Perles,[‡] Pilar Gómez-Sal,[†] and Ernesto de Jesús*[,†]

[†]*Departamento de Química Orgánica y Química Inorgánica, Campus Universitario, Universidad de Alcalá, 28871 Alcalá de Henares, Madrid, Spain.*

[‡]*Servicio Interdepartamental de Investigación (SIDI), Universidad Autónoma de Madrid, Cantoblanco, 28049, Madrid, Spain*

Email: juanc.flores@uah.es, ernesto.dejesus@uah.es

Table of Contents

1. ^{1}H and ^{13}C{^{1}H} NMR spectra of the new compounds

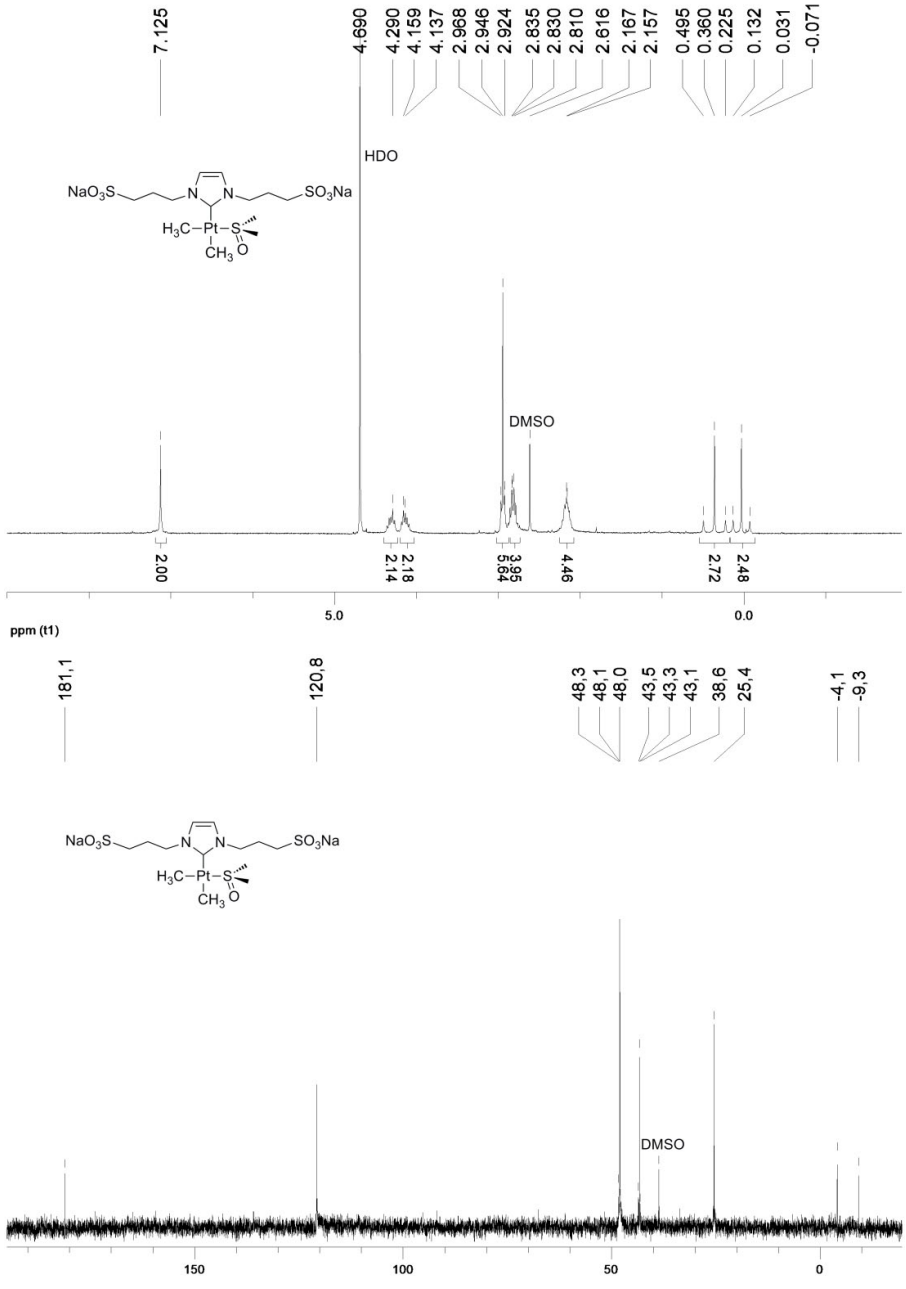

Figure S1. ^{1}H (300 MHz, D_2O) and ^{13}C{^{1}H} (75 MHz, D_2O) NMR spectra for **2a**.

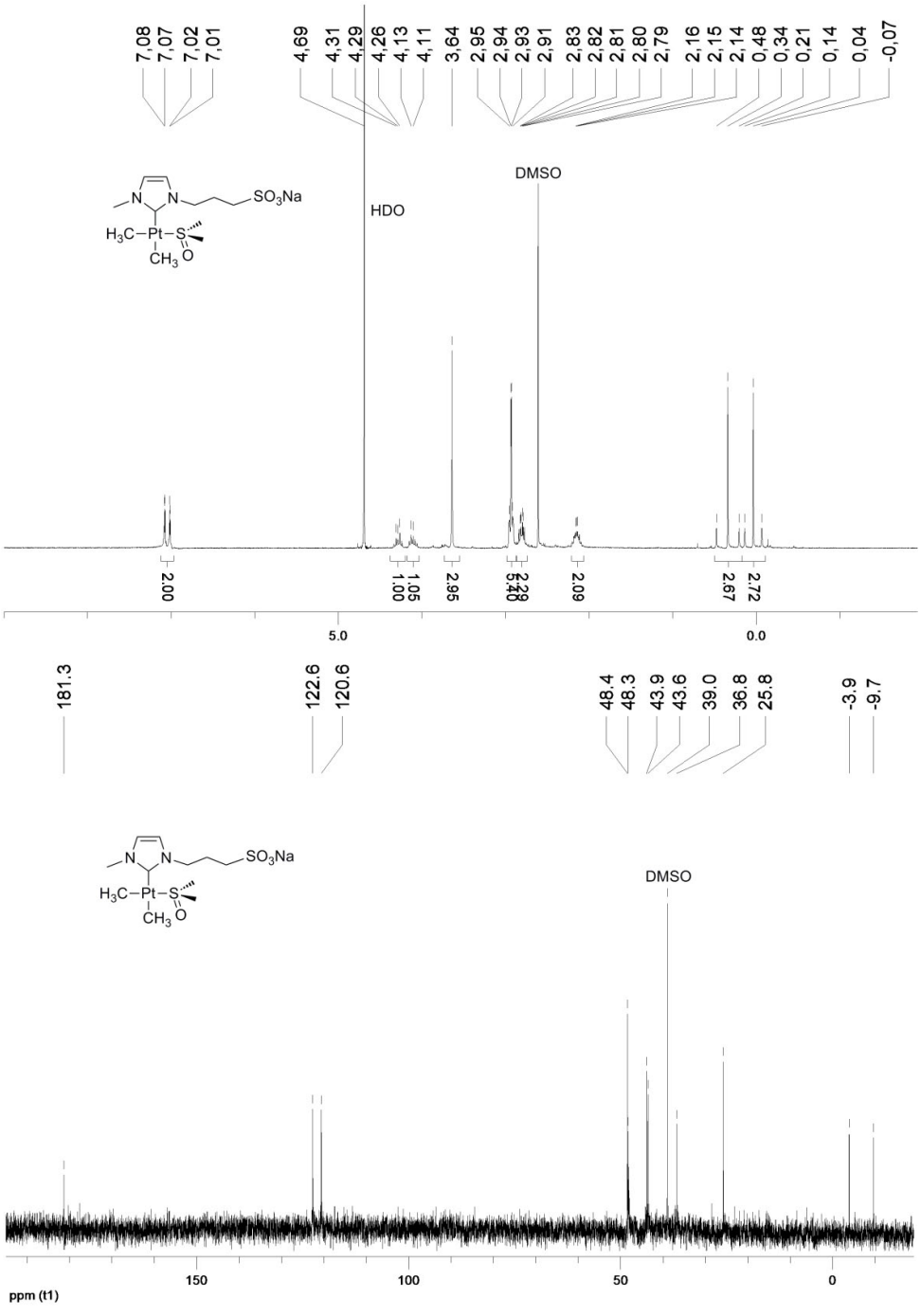

Figure S2. ^{1}H (300 MHz, D_2O) and $^{13}C\{^{1}H\}$ (75 MHz, D_2O) NMR spectra for **2b**.

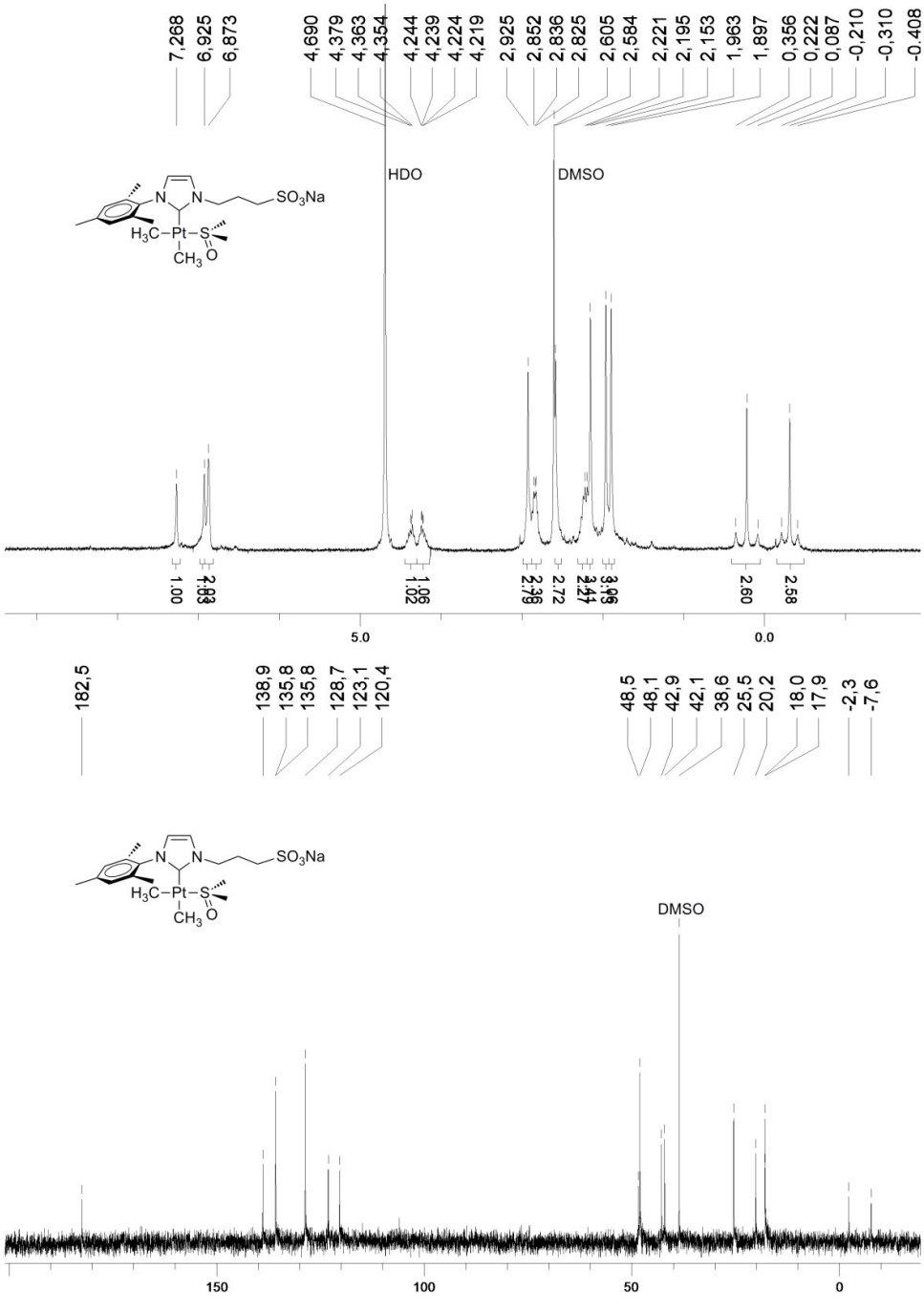

Figure S3. ^{1}H (300 MHz, D_2O) and $^{13}C\{^{1}H\}$ (75 MHz, D_2O) NMR spectra for **2c**.

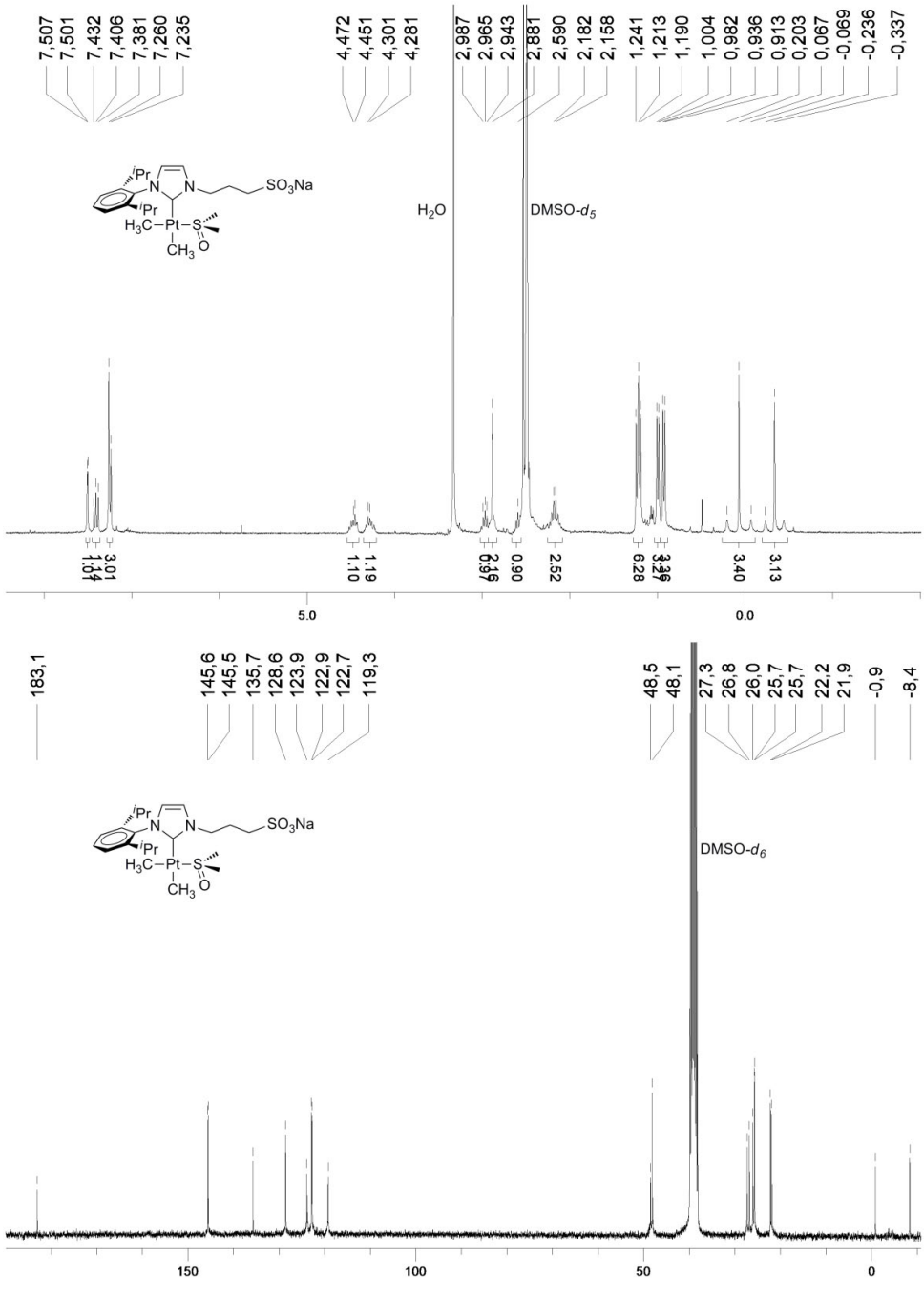

Figure S4. ^{1}H (300 MHz, dmso-d_6) and $^{13}C\{^{1}H\}$ (75 MHz, dmso-d_6) NMR spectra for **2d**.

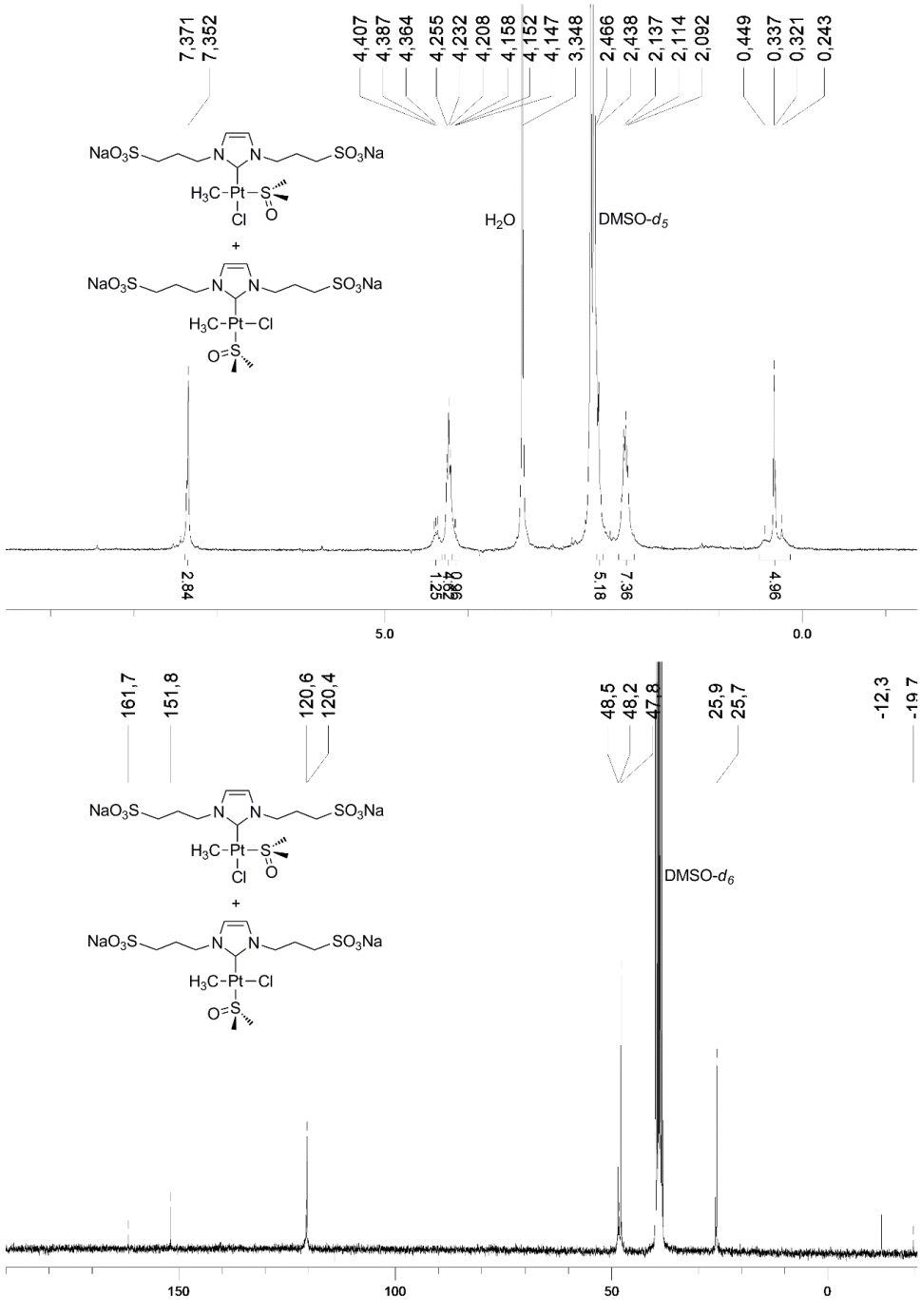

Figure S5. ^{1}H (300 MHz, dmso-*d*$_6$) and ^{13}C{^{1}H} (75 MHz, dmso-*d*$_6$) NMR spectra for **3a**.

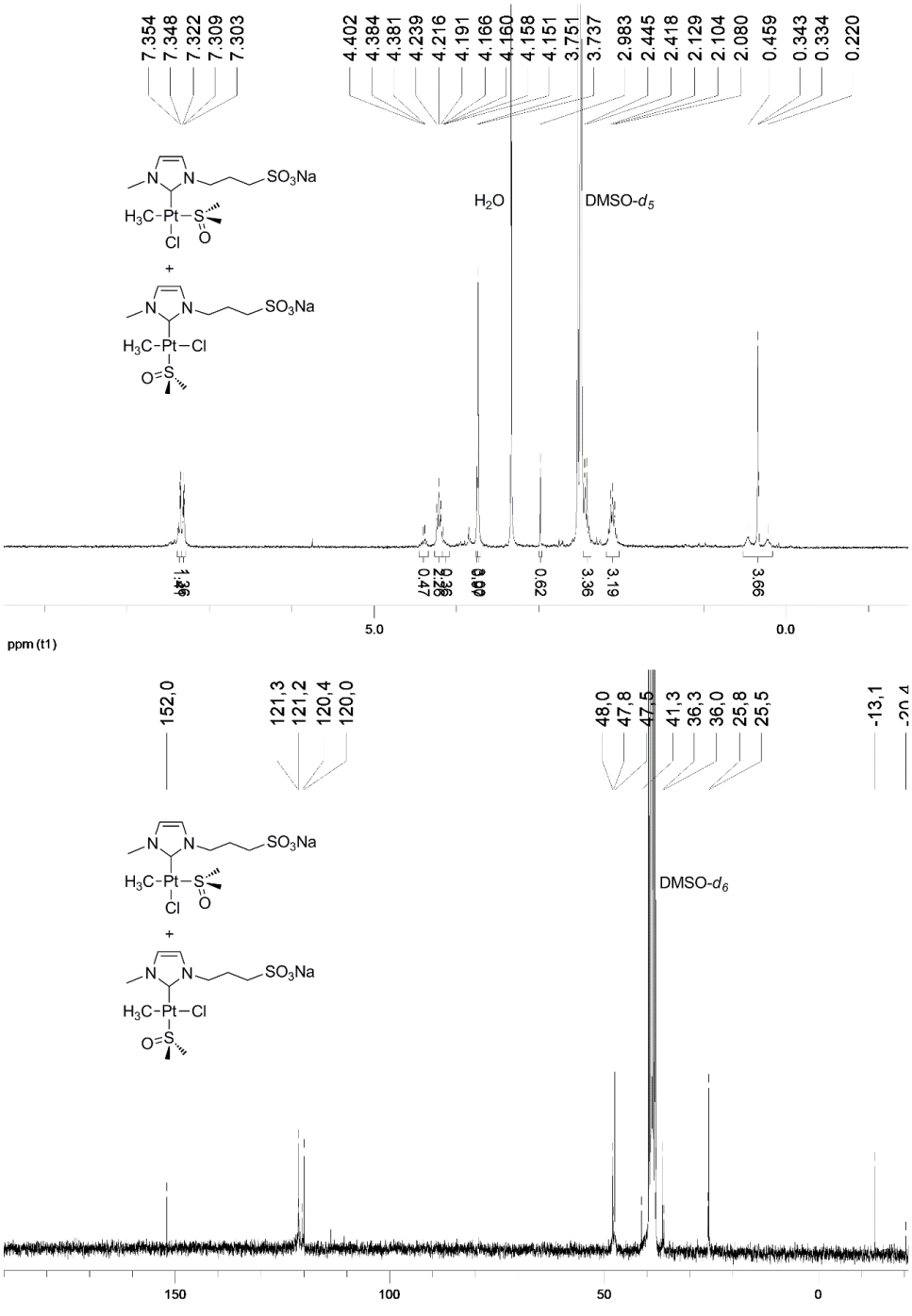

Figure S6. ^{1}H (300 MHz, dmso-d_6) and ^{13}C{^{1}H} (75 MHz, dmso-d_6) NMR spectra for **3b**.

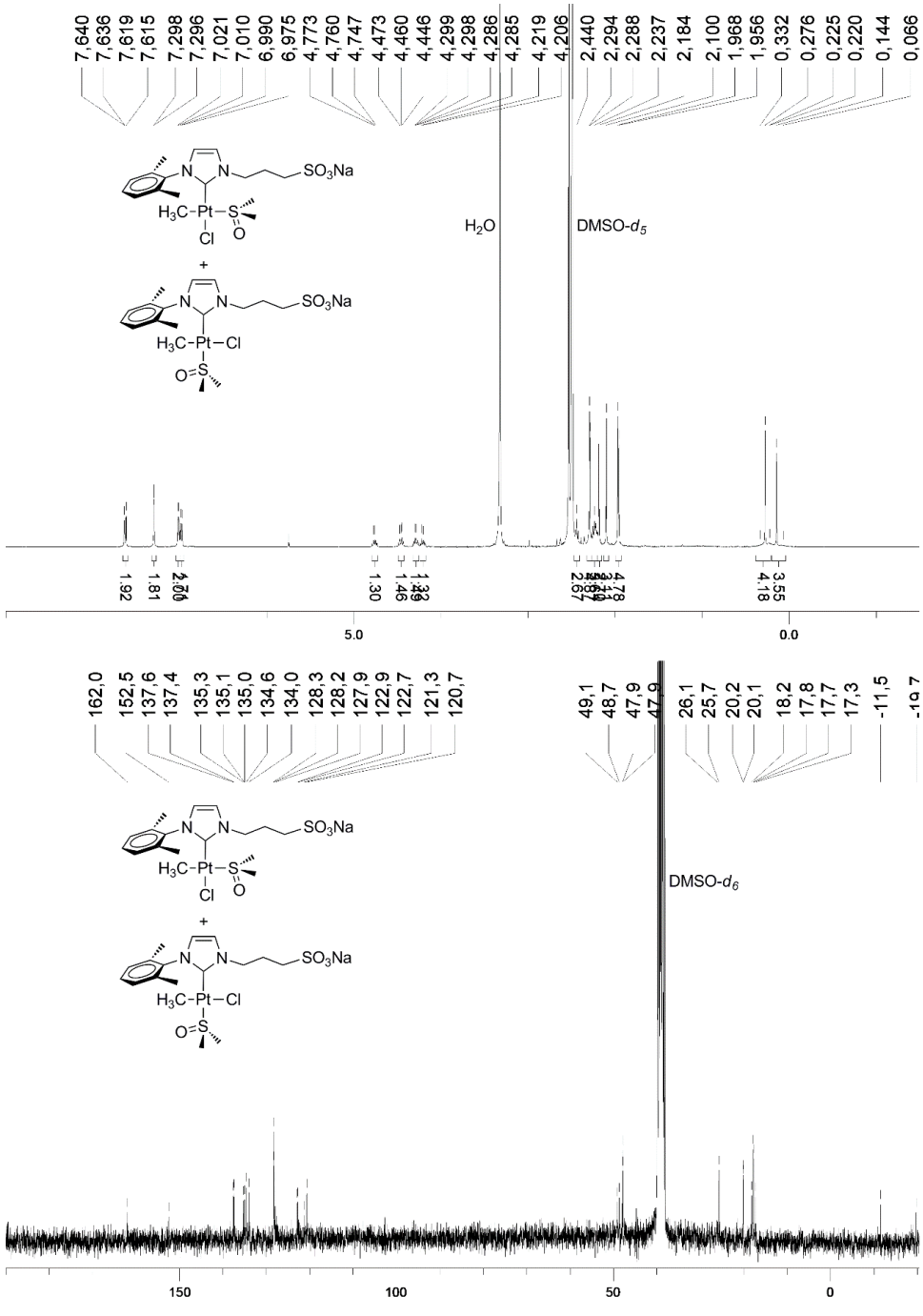

Figure S7. ^{1}H (500 MHz, dmso-*d*$_6$) and ^{13}C{^{1}H} (75 MHz, dmso-*d*$_6$) NMR spectra for **3c**.

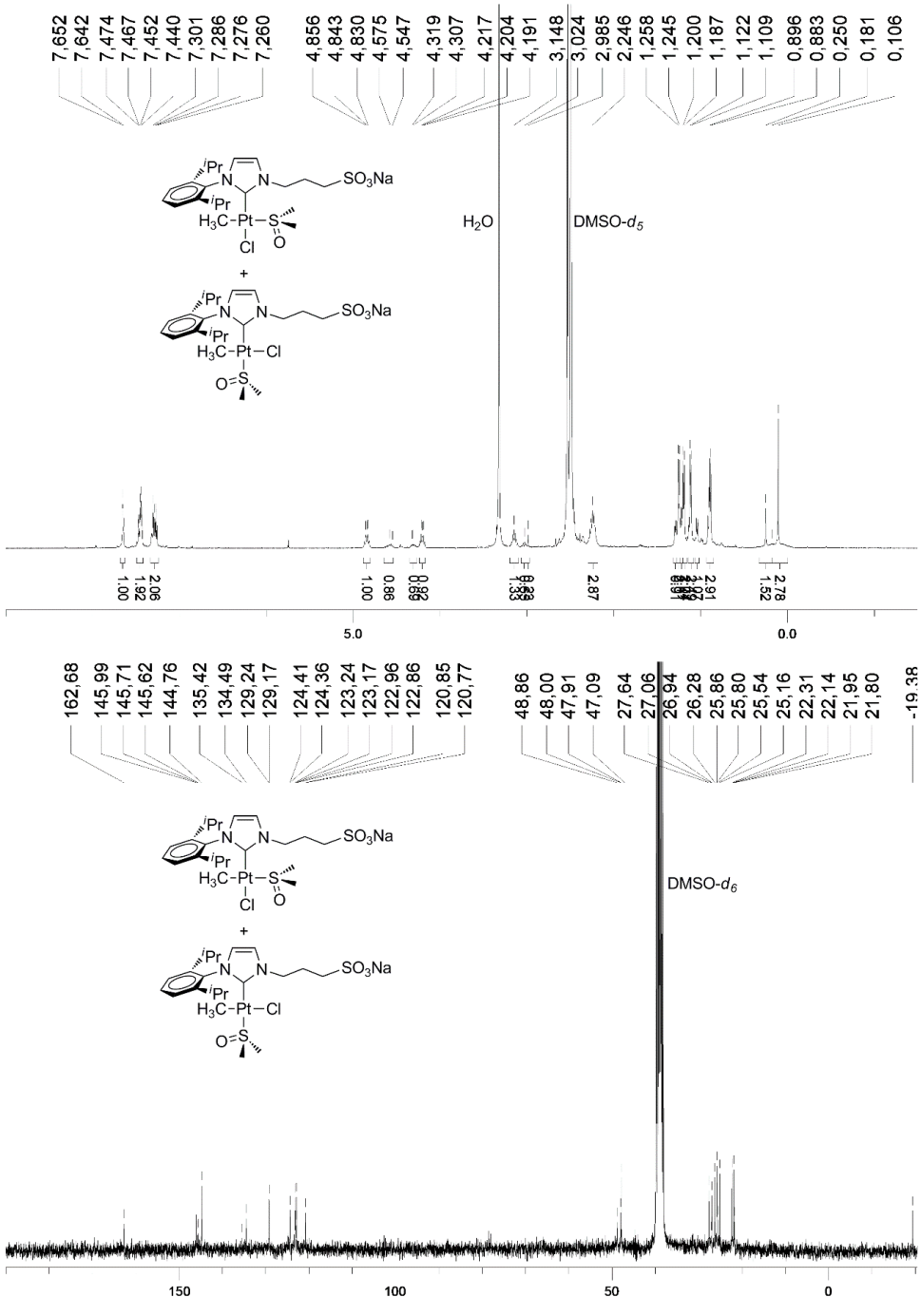

Figure S8. ^{1}H (500 MHz, dmso-d_6) and ^{13}C{^{1}H} (75 MHz, dmso-d_6) NMR spectra for **3d**.

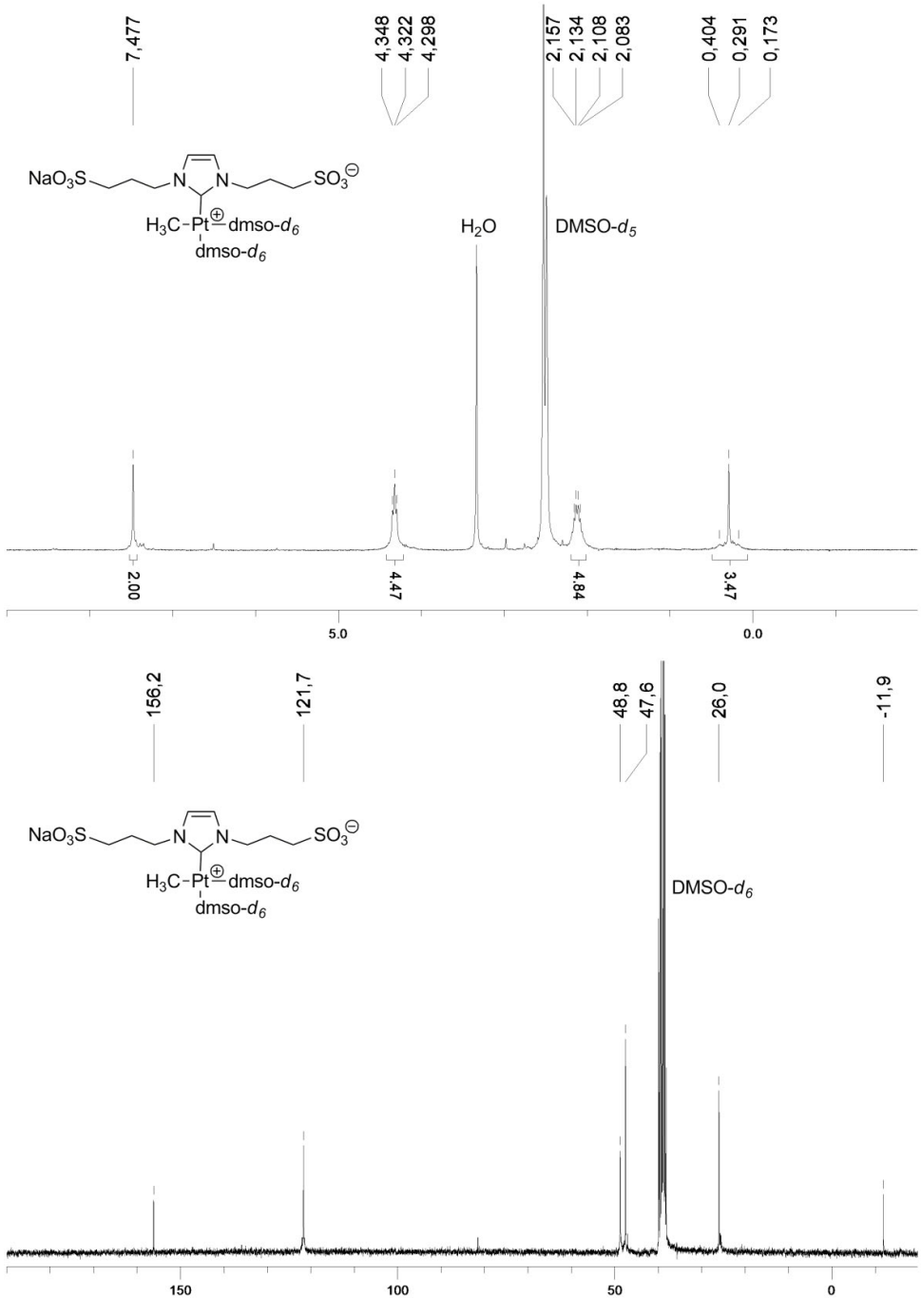

Figure S9. ^{1}H (300 MHz, dmso-d_6) and ^{13}C{^{1}H} (75 MHz, dmso-d_6) NMR spectra for **6a**.

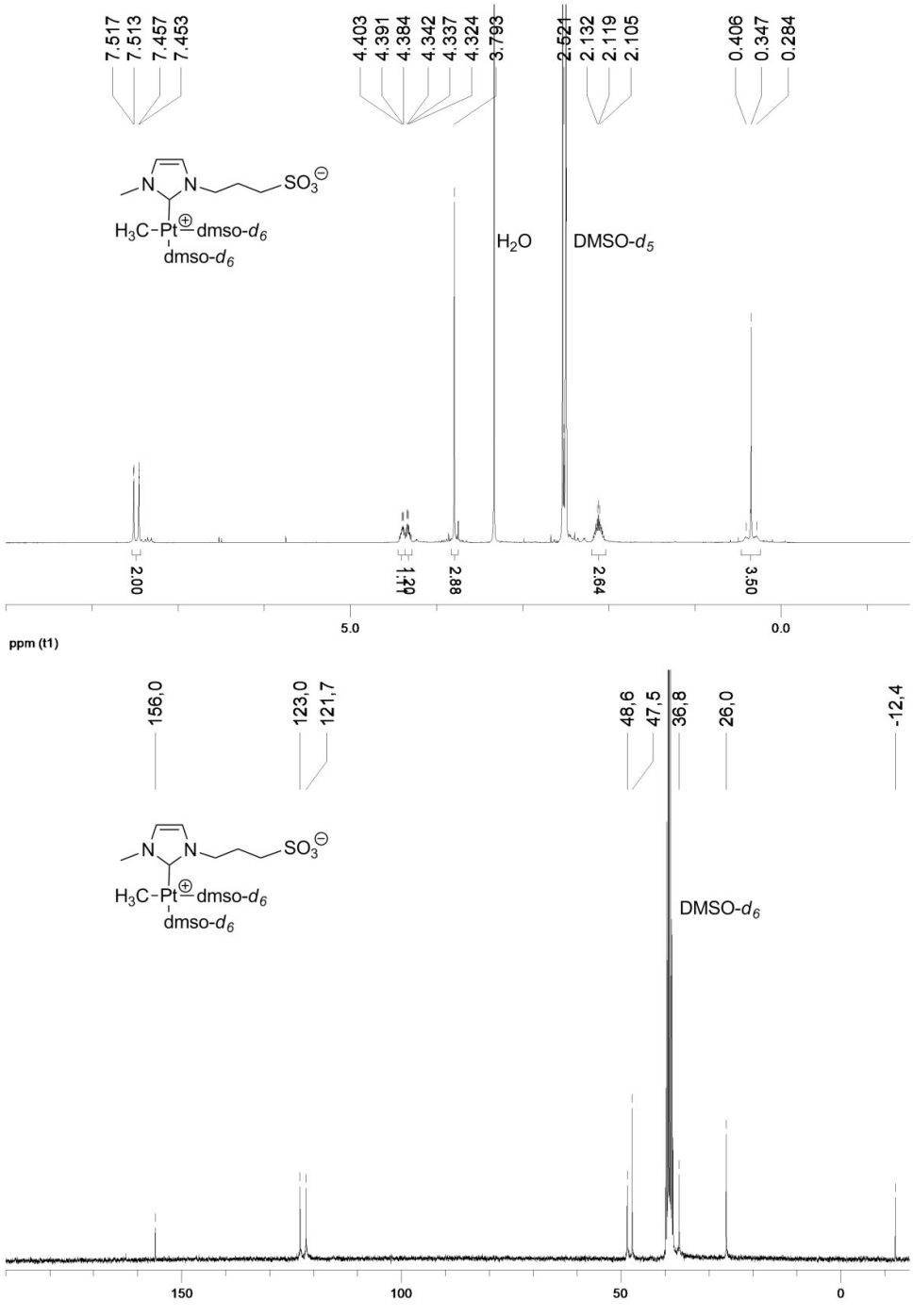

Figure S10. ^{1}H (500 MHz, dmso-d_6) and $^{13}C\{^{1}H\}$ (75 MHz, dmso-d_6) NMR spectra for **6b**.

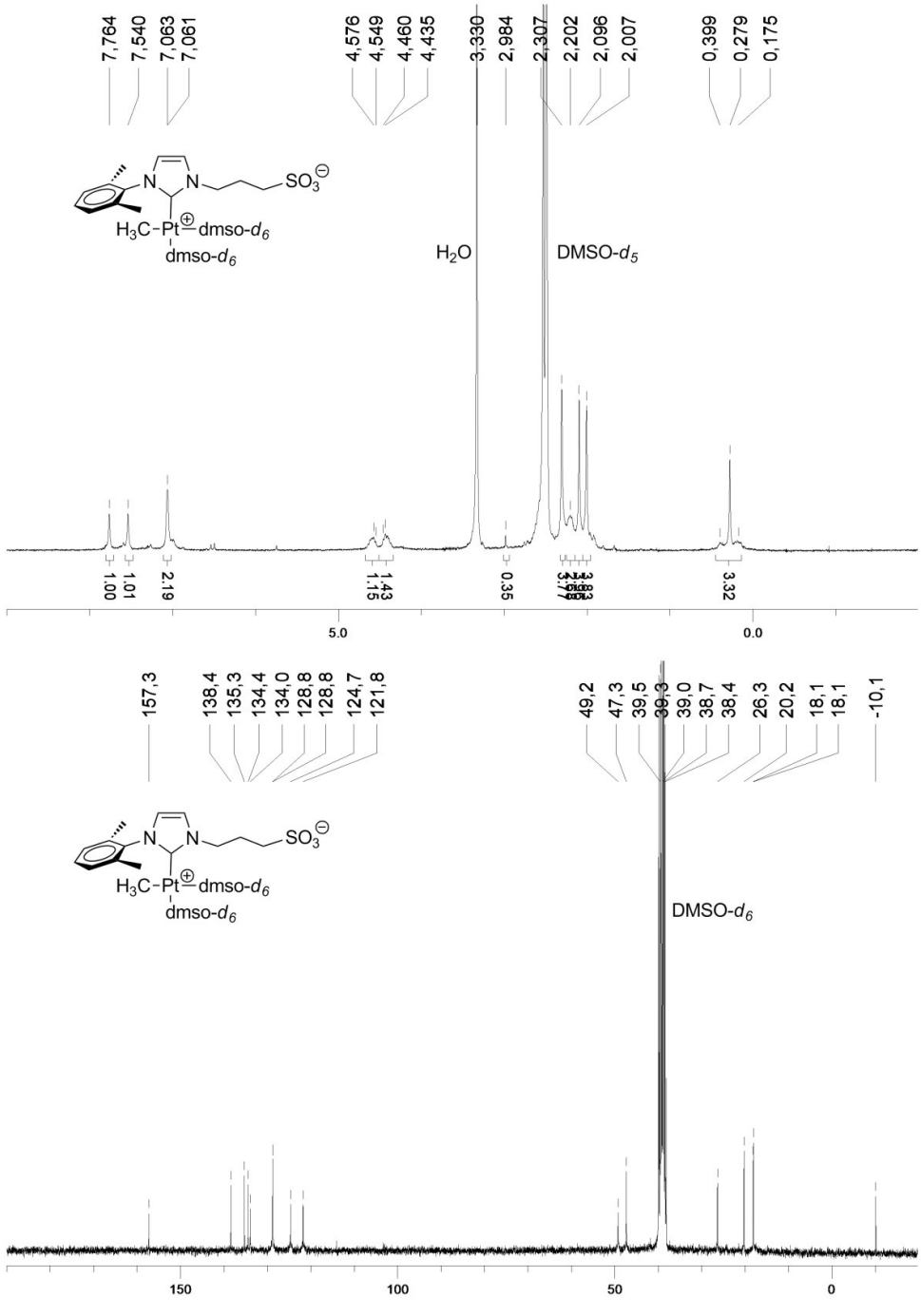

Figure S11. ^{1}H (300 MHz, dmso-d_6) and ^{13}C{^{1}H} (75 MHz, dmso-d_6) NMR spectra for **6c**.

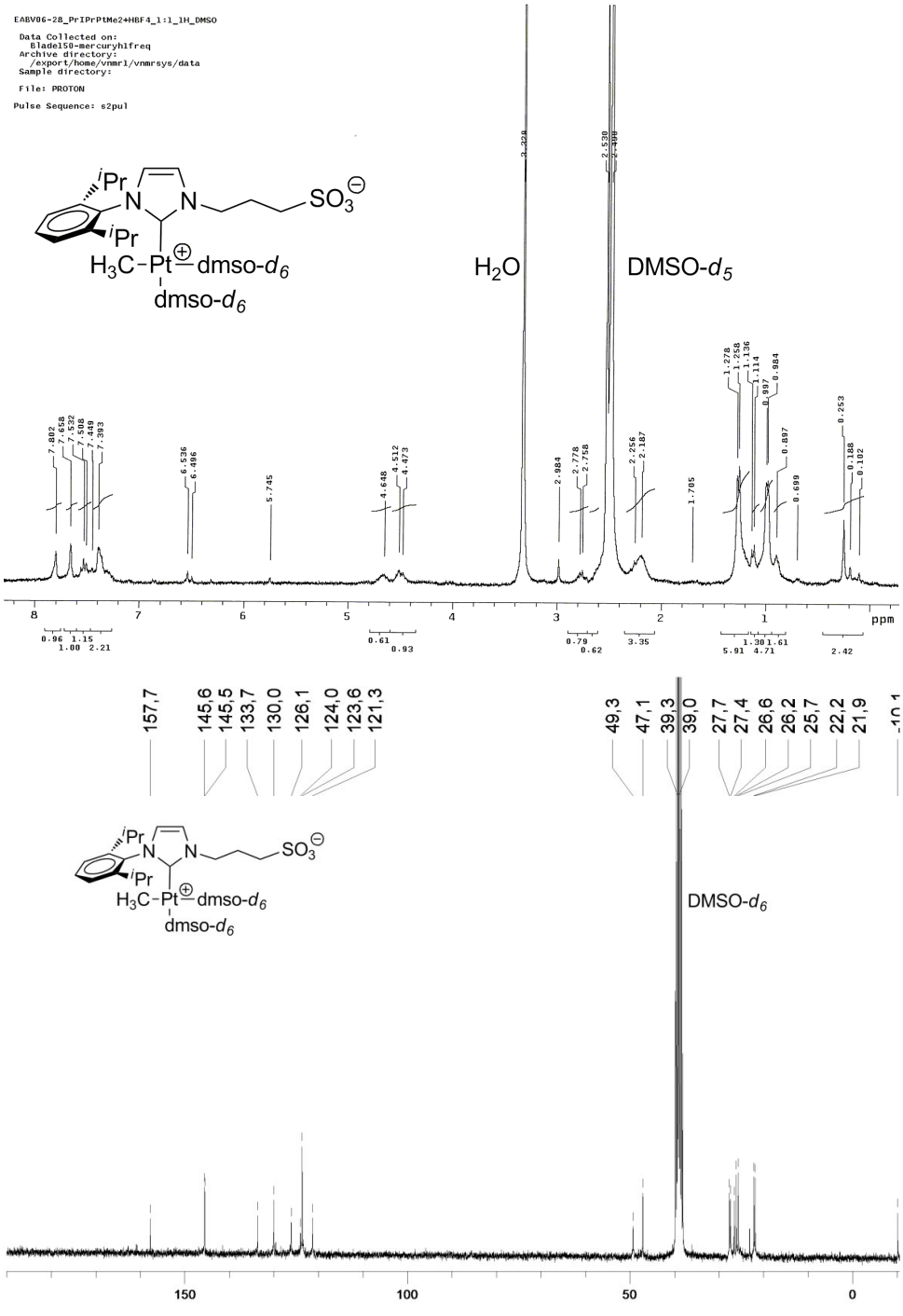

Figure S12. ^{1}H (300 MHz, dmso-d_6) and ^{13}C{^{1}H} (75 MHz, dmso-d_6) NMR spectra for **6d**.

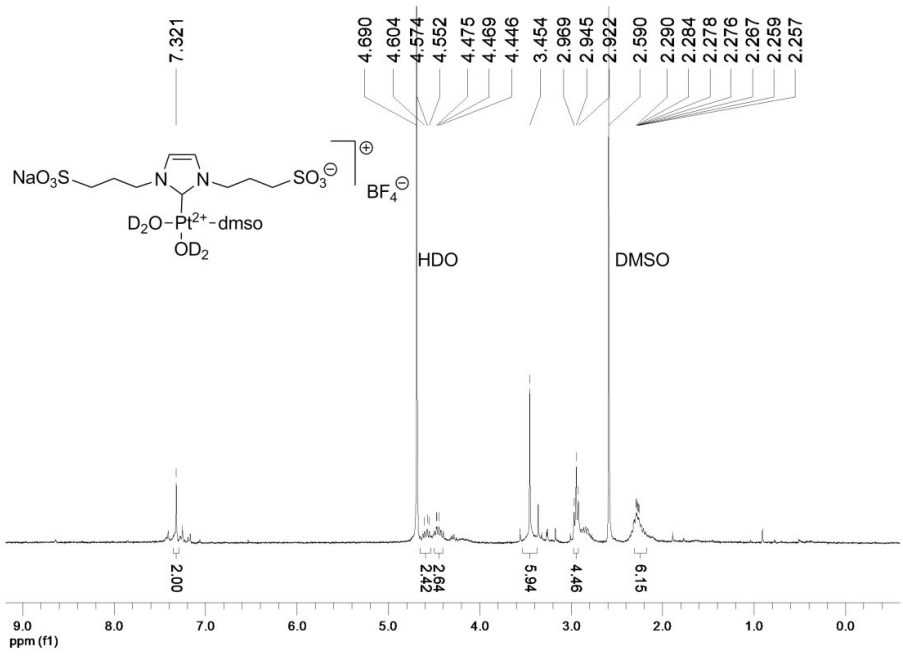

Figure S13. ^{1}H NMR spectrum (300 MHz, D_2O) for **7a**.

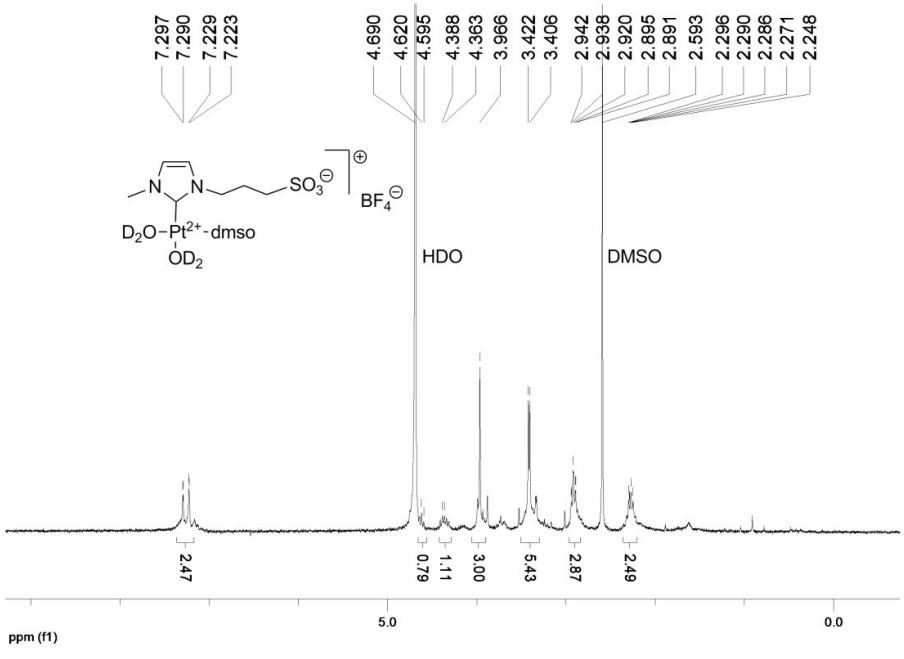

Figure S14. ^{1}H NMR spectrum (300 MHz, D_2O) for **7b**.

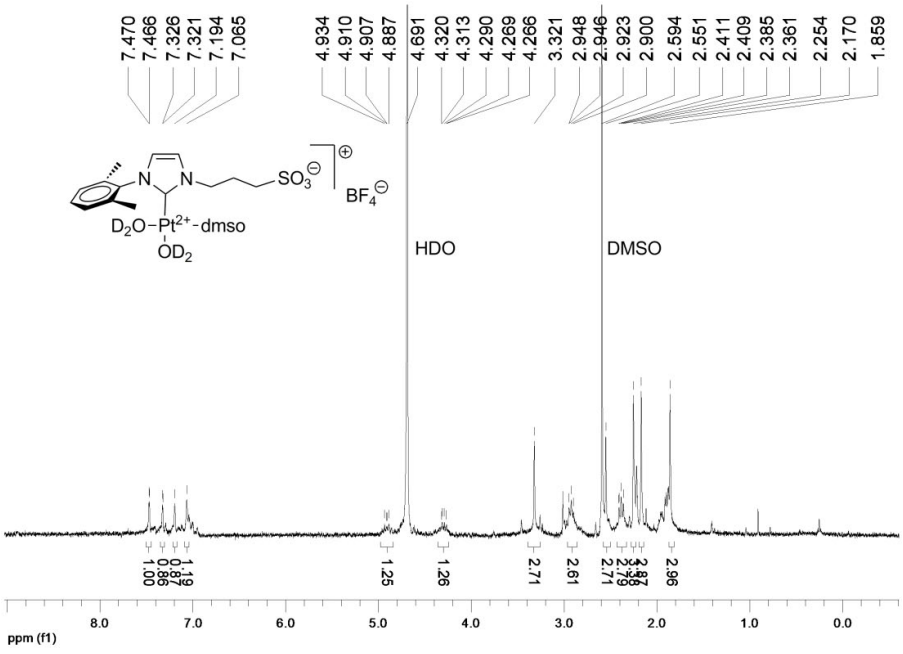

Figure S15. ^{1}H NMR spectrum (300 MHz, D_2O) for **7c**.

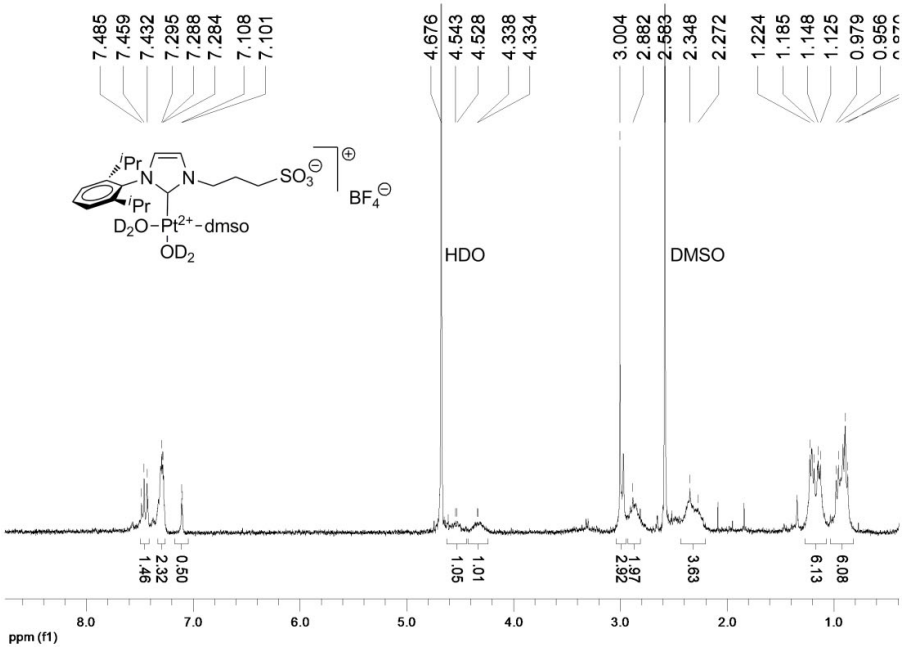

Figure S16. ^{1}H NMR spectrum (300 MHz, D_2O) for **7d**.

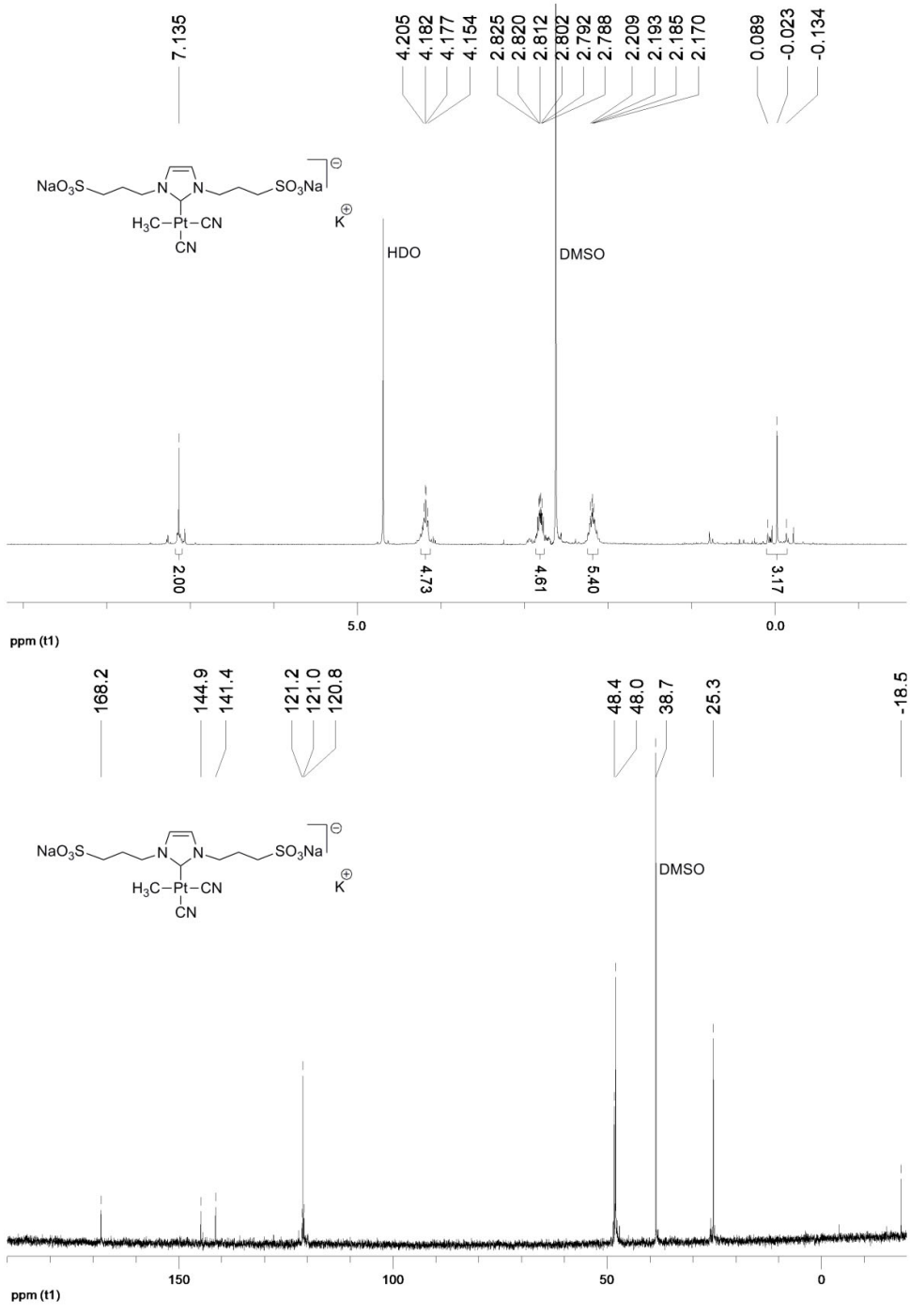

Figure S17. ^{1}H (300 MHz, D_2O) and $^{13}C\{^{1}H\}$ (75 MHz, D_2O) NMR spectra for **9a**.

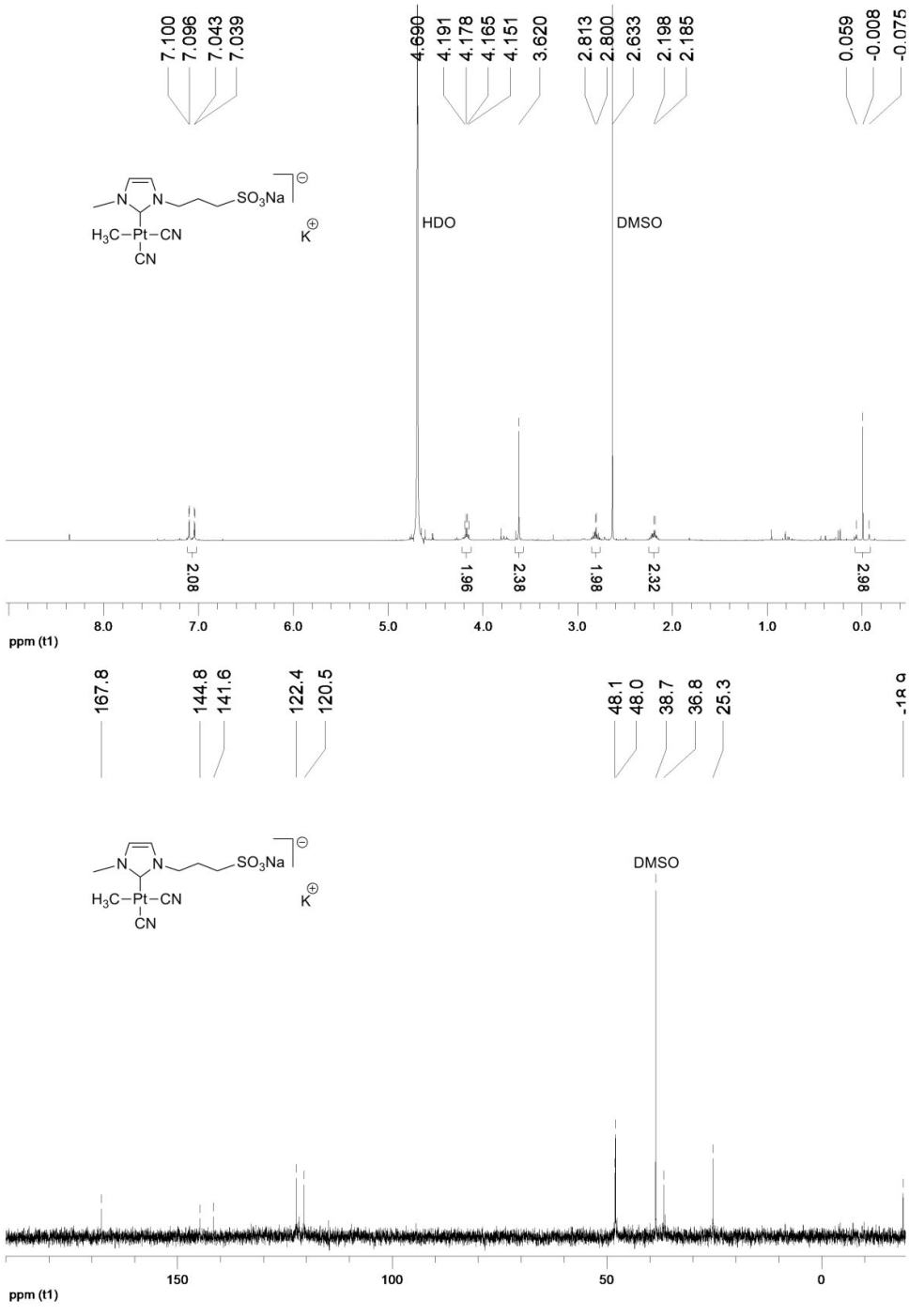

Figure S18. ^{1}H (300 MHz, D_2O) and $^{13}C\{^{1}H\}$ (75 MHz, D_2O) NMR spectra for **9b**.

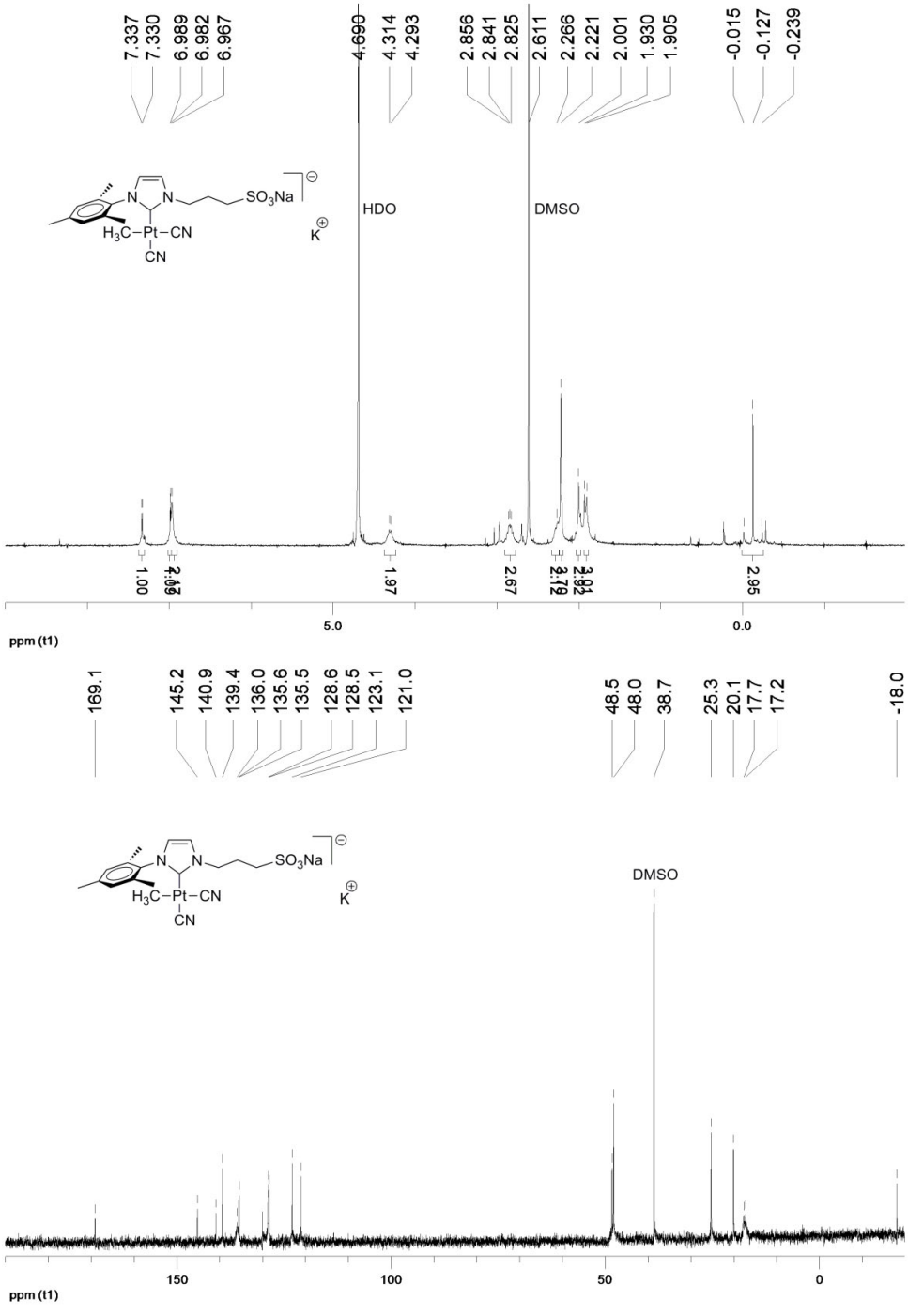

Figure S19. ^{1}H (300 MHz, D_2O) and $^{13}C\{^{1}H\}$ (75 MHz, D_2O) NMR spectra for **9c**.

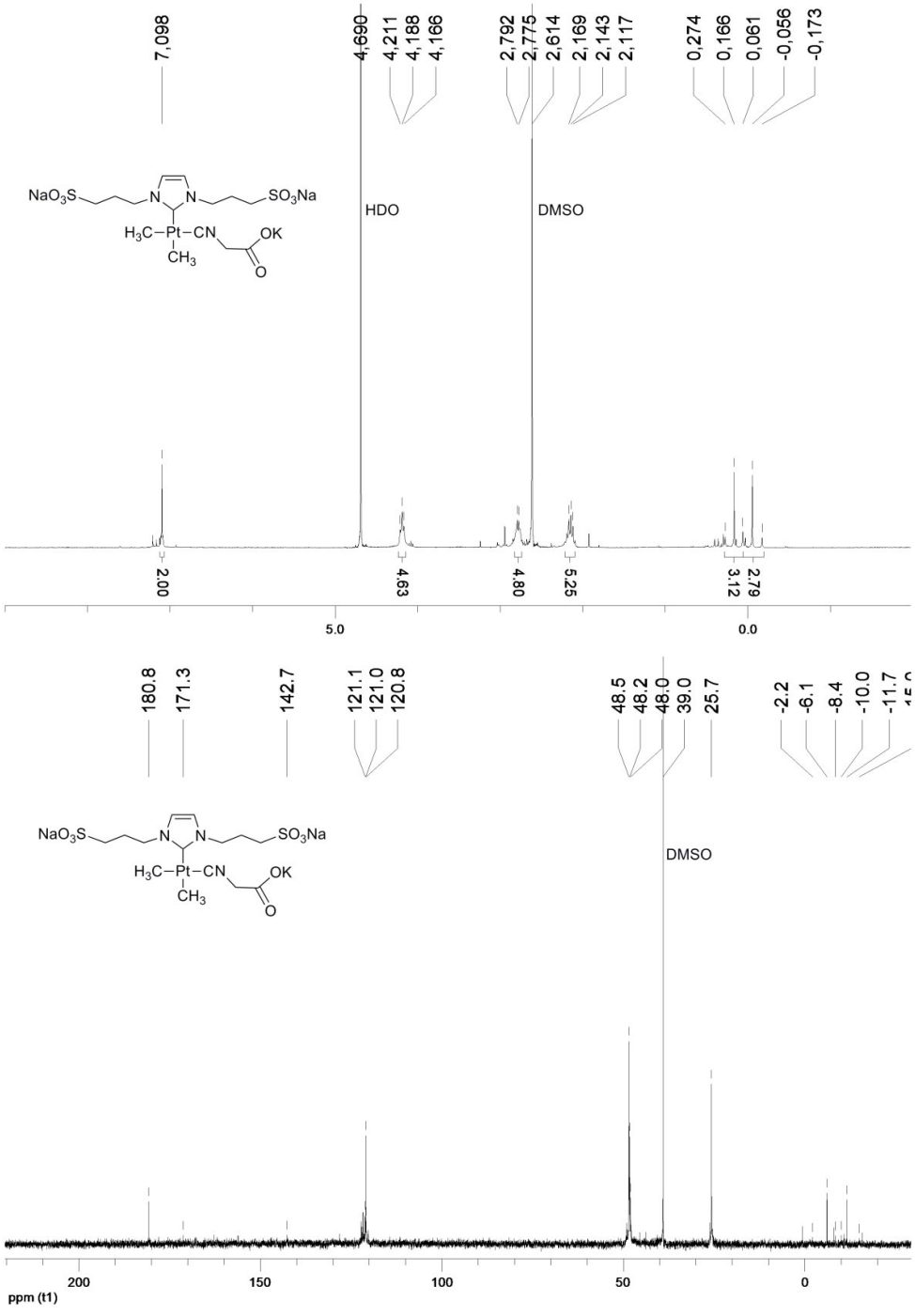

Figure S20. ^{1}H (300 MHz, D_2O) and $^{13}C\{^{1}H\}$ (75 MHz, D_2O) NMR spectra for **10a**.

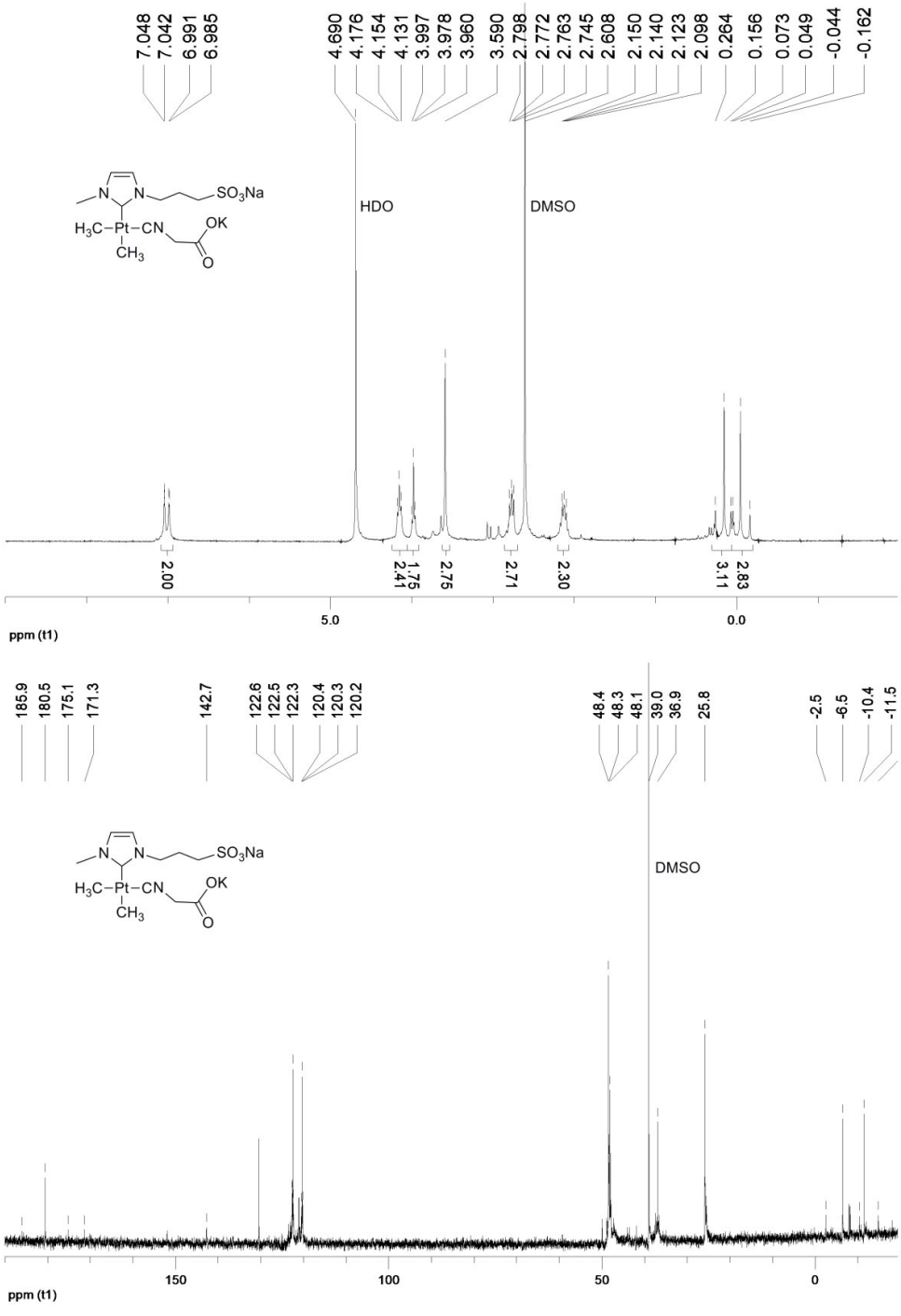

Figure S21. ^{1}H (300 MHz, D_2O) and $^{13}C\{^{1}H\}$ (75 MHz, D_2O) NMR spectra for **10b**.

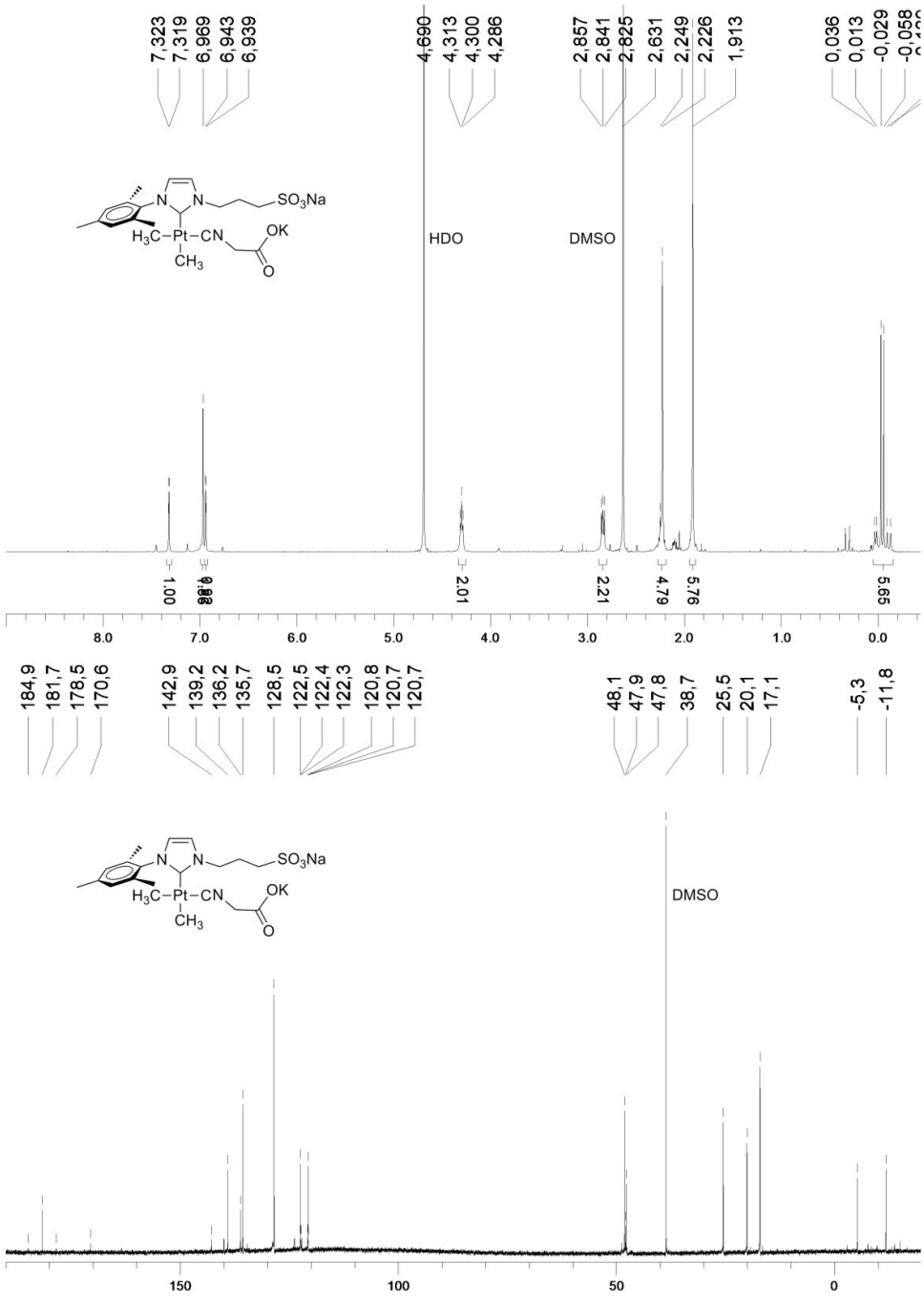

Figure S22. ^{1}H (500 MHz, D_2O) and $^{13}C\{^{1}H\}$ (125 MHz, D_2O) NMR spectra for **10c**.

2. X-ray Crystallographic studies (Table S1)

Table S1. Crystallographic Data for Compounds **2a**, **3a** and **9a**.

	2a·8H_2O	*SP*-4-3-**3a**·5H_2O·0.5dmso	**9a**·1.5H_2O·0.5$MeSO_3H$
empirical formula	$C_{13}H_{26}N_2Na_2O_{11}PtS_3$	$C_{26}H_{46}Cl_2N_4Na_4O_{25}Pt_2S_7$	$C_{25}H_{37}K_2N_8Na_4O_{18}Pt_2S_5$
formula weight	723.61	1592.13	1458.27
crystal size (mm)	0.10 × 0.10 × 0.40	0.3 × 0.35 × 0.4	0.2 × 0.31 × 0.32
color / habit	clear colorless needle	colorless	orange
temperature (K)	296(2)	293(2)	200(2)
wavelength (Å)	0.71073	0.71073	0.71073
crystal system	orthorhombic	triclinic	monoclinic
space group	*Pna*2_1	*P*-1	*P*$2_1/c$
a (Å)	17.7680(5)	8.1940(8)	17.146(3)
b (Å)	9.8038(4)	18.356(3)	34.756(7)
c (Å)	33.2663(11) Å	20.606(3)	10.6370(14)
α (deg)	90	66.934(10)	90.00
β(deg)	90	84.006(12)	96.595(17)
γ (deg)	90	81.200(10)	90.00
volume (Å^3)	5794.8(3)	2814.6(7)	6296.9(19)
Z	8	2	4
calcd density (g/cm^3)	1.659	1.879	1.538
μ (mm^{-1})	5.134	5.426	4.820
F(000)	2832	1552	2820
θ range (deg)	1.22 to 25.35	3.01 to 27.50	3.04 to 25.24
limiting indices (*h*, *k*, *l*)	-19/21, -8/11, -±40	–10/10, –23/23, –26/26	–20/20, 0/41, 0/12
no. of reflns collected	48498	23693	11374
no. of reflns unique / R_{int}	10325 / 0.0591	12853 / 0.0479	11374 / 0.0935
no. of reflns observed [$I > 2\sigma(I)$]	8227	8581	6156
completeness to θ	99.7%	99.3%	99.7%
absorption correction	multi-scan	multi-scan	multi-scan
max. and min. transmission	0.6277 and 0.2332	0.248 and 0.143	0.141 and 0.211
refinement method	Full-matrix least-squares on F^2		
no. of data / restraints / parameters	10325 / 4 / 519	12853 /0 / 629	11374 / 16 / 583
goodness of fit on F^2	1.096	1.055	0.997
*R*1 / *w*R2 [$I > 2\sigma(I)$][a]	0.0581 / 0.1660	0.0519 / 0.1297	0.0803 / 0.2177
*R*1 / *w*R2 (all data)	0.0822 / 0.2036	0.0914 / 0.1432	0.1390 / 0.2375
largest diff. peak and hole (e/Å^3)	3.019 and -1.659	3.964 and –1.952	2.071 and –1.662

[a] $R1 = \Sigma(||F_o|-|F_c||)/\Sigma|F_o|$; $wR2 = \{[\Sigma w(F_o^2-F_c^2)]/[\Sigma w(F_o^2)^2]\}^{1/2}$.

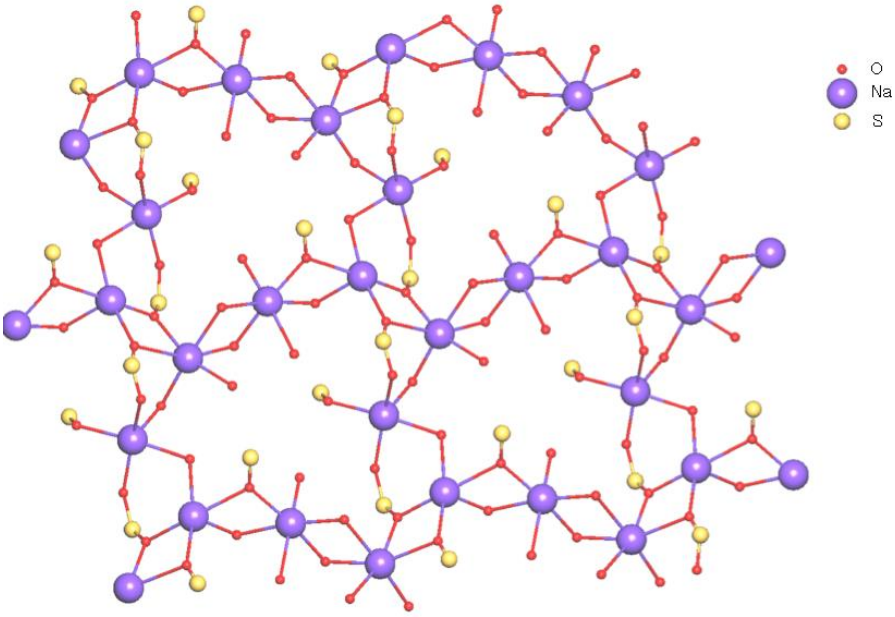

Figure S23. View of the layer of Na^+ cations coordinated to oxygen atoms from sulfonate groups and water molecules in the crystal structure of **2a**.

Chapter V. Synthesis of Water-Soluble Hydride(NHC)platinum(II) Complexes by Reversible Oxidative Addition of Alkynes to Pt(0) Complexes

Edwin A. Baquero, Gustavo F. Silbestri, Juan C. Flores, and Ernesto de Jesús, *Manuscript In Preparation*, **2015**.

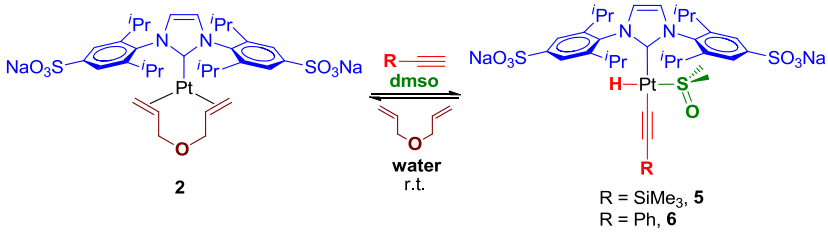

Synthesis of Water-Soluble Hydride(NHC)platinum(II) Complexes by Reversible Oxidative Addition of Alkynes to Pt(0) Complexes

Edwin A. Baquero*, Gustavo F. Silbestri, Juan C. Flores,* and Ernesto de Jesús**

Departamento de Química Orgánica y Química Inorgánica, Campus Universitario, Universidad de Alcalá, 28871 Alcalá de Henares, Madrid, Spain.

ABSTRACT

The reactivity of the platinum(0) complex (NHC)Pt(AE) **2**, where the NHC ligand is a sulfonated version of the IPr ligand [1,3-bis(2,6-diisopropylphenyl)imidazol-2-ylidene] and AE = allyl ether, towards oxidative addition of CH_3I and alkynes is reported. The reaction with the haloalkane affords the iodomethyl complex (NHC)Pt(II)MeI(dmso) **4**, whereas the addition of the alkynes via C(*sp*)–H bond activation leads to the new water-soluble hydride complexes (NHC)Pt(II)H(RCC)(dmso) **5** and **6**. Complexes **5** and **6** were found to be moderately stables in water, displaying an interesting behavior in this solvent. Thus, in the presence of the corresponding olefin, the reaction is reversible under mild conditions making possible the formation of diolefin(NHC)Pt(0) complexes **1**, **2** and **7**, with elimination of the alkyne.

INTRODUCTION

The activation of C–H bonds in alkynes has been of interest, mainly due to their implications in the alkyne/vinylidene tautomerization reaction, as well as in some catalytic processes involving platinum complexes.[1] Although NHCs (NHC = N-heterocyclic carbene) have proven to be an outstanding class of ancillary ligands,[2] the application of (NHC)Pt(II) complexes in C–H bond cleavage processes have been scarcely explored. In the last few years, some reports concerning the use of either mono(NHC)Pt(II) or bis(NHC)Pt(II) complexes for the activation of C(sp^2)–H,[3] or C(sp^3)–H bonds,[4] have appeared. Pt(0) complexes have been found to activate C–H bonds of imidazolium rings to yield either mono(NHC),[5] or bis(NHC)Pt(II) hydride compounds.[6] Contrastingly, no references dealing with C(*sp*)–H bond activation for the synthesis of hydride (NHC)Pt(II) complexes has been disclosed. Although, there has always been great interest for these kind of complexes as precursors or intermediates of catalytic processes, their behavior has been mainly studied in organic solvents.[7] Water offers

unique properties such as low toxicity, ability to solvate polar compounds and salts, as well as high dielectric constant, among others. Hydride complexes of platinum(IV) have been studied in aqueous mediums as key intermediates in the Shilov system for the oxidation of alkanes to alcohols in water. [7a,8] However, water-soluble hydride (NHC)Pt(II) complexes have not been reported to date.

After reporting the synthesis of the first water-soluble (NHC)Pt(0) complexes and their application as recoverable catalyst for the hydrosilylation of alkynes in water (Figure 1),[9] we started a research focusing on the synthesis and aqueous-phase reactivity of related compounds, including studies on their hydrolytic stability,[10] and their use as water-soluble platinum nanoparticles precursors.[11] Here, we communicate the reactivity of complex **2**[12] (Figure 1) towards the oxidative addition of CH_3I and, more interestingly, of terminal alkynes such as, trimethylsilylacetylene and phenylacetylene, leading to the formation of novel water-soluble hydride(NHC)Pt(II) complexes through the activation of C(*sp*)–H bonds. Reversibility of this reaction in water in the presence of different olefins to afford either (NHC)Pt(0)(η^2-olefine)$_2$ or (NHC)Pt(0)(η^2-η^2-olefine) complexes, is also reported.

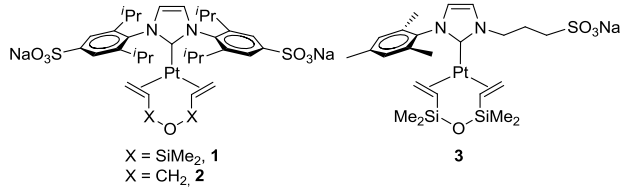

Figure 1. Reported water-soluble (NHC)Pt(0) complexes **1**, and **3**[9] and complex **2**[12] used in this study.

RESULTS AND DISCUSSION

Reactivity of Complex 2 with CH_3I. In order to test the propensity of complex **2** to undergo an oxidative addition, we initially tested the reaction with an excess of CH_3I at 50 °C in dmso. The reaction progressed in a straightforward way, and was completed after 1 h, according to analyses by ^{1}H NMR spectroscopy (Scheme 1). The haloalkyl complex **4** was obtained as a yellow solid, analytically pure and in high yield (90%) after a simple work-up. Compound **4** is stable in water, and its characterization was indicative of a stereoselective oxidative addition in **2**, leading solely to the *SP*-4-4 diastereoisomer of **4**, in sharp contrast with our earlier findings in the preparation of these type of compounds by protonolysis of dimethyl mono(NHC)Pt(II) complexes with HCl_{aq}, which showed to be chemoselective but gave mixtures of the two possible diastereoisomers for less hindered coordinated NHC ligands of the same class.[10b]

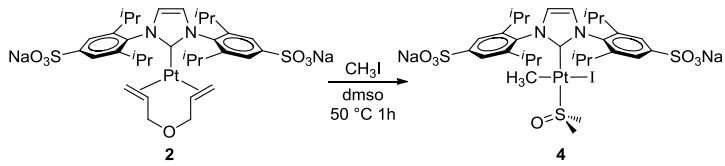

Scheme 1. Synthesis of complex **4** via oxidative addition.

Complex **4** was characterized by ^{1}H, and ^{13}C NMR spectroscopy, mass spectrometry (ESI-TOF), and elemental analysis. The elemental analysis suggested the presence of water molecules in the samples, which were also observed in the ^{1}H NMR spectra obtained upon dissolving **4** in dry dmso-d_6. It should be noted that this compound is hygroscopic in the solid state and quickly take up water from the air.

The fragment with the most intense peaks in the ESI(−) mass spectra of **4** was that arising from the combined loss of a Na^+ cation, the coordinated dmso and, interestingly, from the additional elimination of methane ($[M - Na - dmso - CH_4]^-$). Methane evolution has been previously observed in different NHC platinum(II)–methyl complexes in solution,[4,10b] and in the solid- and gas-phase,[13] as the results of intramolecular C(sp^3)–H bond activations at *ortho*-groups of *N*-aryl substituents of the NHC ligands. The presence of a dmso molecule in **4** was confirmed in D_2O by the observation of resonances for the protons corresponding to the coordinated ligand in the expected region (3.10 ppm). The ^{1}H NMR spectrum presented platinum satellites for the methyl group with a $^{3}J_{Pt-H}$ of 75 Hz.

The carbenic carbon resonates at 162.2 ppm, although the platinum satellites were undetectable in the ^{13}C NMR spectrum, probably due to their broadening in solvents of relatively high viscosity.[14] The chemical shift for the carbene carbon and the $^{3}J_{Pt-H}$ mentioned above for the methyl ligand are comparable to those found for *SP*-4–4-[PtMeCl(L)(NHC)] complexes (162-163 ppm, and 78-88 Hz, respectively).[10b] The stereochemistry in complex **4** was corroborated by a NOESY experiment, revealing proximity between the *N*-aryl substituents of the carbene and the methyl ligand. This configuration, together slow rotation of the NHC ligand around the Pt−C bond on the NMR time scale, explains the chemical nonequivalence observed in the ^{1}H and ^{13}C NMR spectra between the two aryl groups, and between the methine and methyl moieties of the isopropyl groups of each ring.[15]

Reactivity of Complex 2 with Alkynes. Subsequently, we decided to attempt oxidative addition reactions with terminal alkynes such as trimethylsilylacetylene and phenylacetylene. Thus, treatment of **2** with an excess of the corresponding alkyne in dmso at 50 °C, afforded hydride Pt(II) complexes **5** and **6**. These complexes were isolated in high yields (>90%) as

spectroscopically pure yellow solids after removal of the solvent (Scheme 2). The formation reaction of both complexes was stereoselective leading to *SP*-4-4 diastereoisomers.

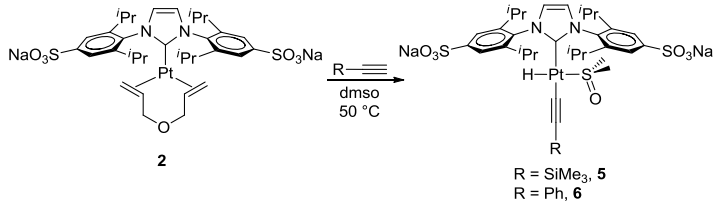

Scheme 2. Synthesis of water-soluble hydride (NHC)Pt(II) complexes **5** and **6**.

The hydride complexes **5** and **6** are moderately stables in water. Their decomposition was studied by ^{1}H NMR in D_2O. After 10 days at room temperature, the total disappearance of the hydride resonance at around – 12 ppm was observed. No deuteride resonances were observed in the ^{2}H NMR spectrum. The ^{1}H NMR spectrum showed also sharp resonances of an unidentified (NHC)Pt complex accompanied by broad resonances probably corresponding to NHC–Pt nanoparticles (in a 30:70 ratio, respectively). The corresponding alkyne RC≡CH was observed by ^{1}H NMR spectroscopy after extraction of the D_2O solution with $CDCl_3$. We hypothesized that this decomposition might be originated by the reductive elimination of the alkyne in water. With the aim to promote such a process, freshly prepared solutions of both compounds in this solvent were treated with olefins at room temperature (Scheme 3). Under these conditions, reductive elimination process took place towards the formation of the corresponding (NHC)Pt(0) di(olefin) or (η^2-η^2)diolefin complexes (**1**, **2** or **7**), with total conversion after 1 h in the presence of methyl acrylate (MA), or in 3 h with both allyl ether or divinyltetramethyldisiloxane, according to essays performed at NMR-tube scale (Scheme 3). Longer time reaction required for the latter is interpreted to be caused by the lower solubility of such olefins in water. Reactions at Schlenk-tube scale also proceeded straightforwardly in high yields (≥95%).

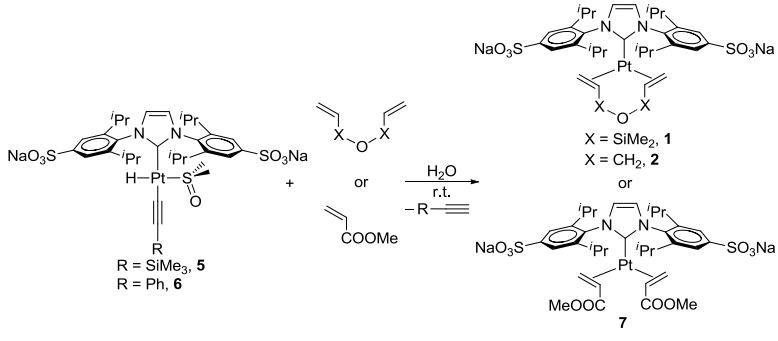

Scheme 3. Reductive elimination of acetylenes from complexes **5** and **6** in the presence of olefins in water.

The set of outcomes shown above demonstrates a clear influence of the nature of the solvent on the reversibility of these pair of complementary reactions, where oxidative addition of the terminal alkyne to Pt(0) is favored in dmso, whereas its reductive elimination from the hydridealkynylPt(II) complex is preferred in water (examples depicted in Scheme 4). To the best of our knowledge, no report has been disclosed for the synthesis of (NHC)Pt(0) complexes in water, therefore, the behavior described here widen the synthetic approaches available at the chemist's toolbox.

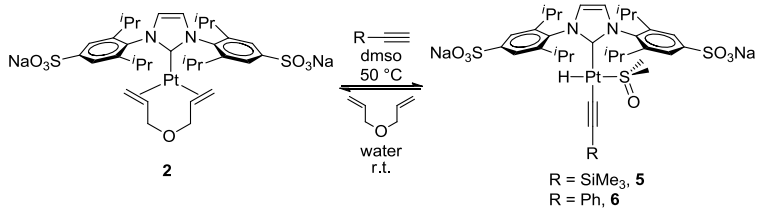

Scheme 4. Solvent effect promoting/reversing oxidative addition from complex **2** to **5** or **6**.

Complexes **5**-**7** were characterized by NMR, mass spectrometry, and IR spectroscopy in the case for **5** and **6**, whereas the NMR data for complex **1** were compared to those previously reported.[9] The infrared absorption for the C≡C group was found at a normal wavenumber (2037 and 2105 cm^{-1} for **5** and **6**, respectively) for terminal alkynyl ligands in platinum complexes (reported values within 2000–2100 cm^{-1}).[1a,16] The ESI-TOF(–) showed peaks corresponding the loss of a Na^+ ion for **5**, and $[M - Na - dmso]^-$ for **6**. Interestingly, the highest peak found appeared at m/z 368.5526 for both complexes, and was assigned to the dianion in which the alkaline cations, all ligands attached to the metal center and two molecules of H_2 were released (*i.e.*, $[M - 2Na - dmso - alkyne - 2H_2]^{2-}$). Taking into account our findings with related compounds in the activation of C–H bonds in the gas-phase under ESI MS conditions,[13] and the C(sp^3)–H bond activation at the isopropyl groups combined with β-hydride elimination described by Conejero *et al.* for (NHC)Pt(II) complexes (NHC = IPr ligand),[4a] a feasible species matching to the common and most intense ion-peak in the spectrum for both compounds is that of Pt(0) coordinated to a NHC ligand where one isopropyl of each aryl ring has converted to an 2-methylvinyl group, thus again resulting in a diolefin(NHC)Pt(0) complex. The ESI-TOF in positive mode for **7** showed only the fragments corresponding to $[M - 2Na + 3H]^+$ and $[M - 2Na + 3H - MA]^+$, whereas the most intense ion detected in negative mode was that assigned to dianion $[M - 2Na - MA]^{2-}$. The carbenic carbons for **5** and **6** were observed at around 175 ppm, whereas the hydride ligand appeared at – 12 ppm, displaying platinum satellites with a $^1J_{Pt-H}$ around 1400 Hz. Assignations for carbon atoms of the coordinated dmso, and the NHC and alkynyl ligands were based on ^1H-^{13}C HMBC experiments, in which cross peaks between the hydride ligand and the methyl groups of the dmso ligand, alkynyl moiety as well as the carbenic carbon, were detected (Figures S3 y S5 in

the Supporting Information). The *cis* positioning of the hydride and the NHC ligands was confirmed in NOESY experiments, carried out in dmso-d_6, showing cross peaks between the hydride ligand and the isopropyl (methyl and methine) protons. The equivalences found in the ^{1}H and ^{13}C NMR spectra for aryl, isopropyl, and methyl groups reveal a fast rotation of the Pt–NHC bond in both complexes on the NMR time scale. The ^{1}H and ^{13}C NMR spectra for complex **7** revealed the presence of two stereoisomers at a 70:30 ratio, as a consequence of the *re* or *si* enantioface that each methyl acrylate is able to display coordinated to platinum, which makes possible the presence of *racemic*- and *meso*-like diastereoisomers (enantiomers *re*/*re* and *si*/*si*, and isomer *re*/*si* = *re*/*si*, see Scheme 5a and 5b, respectively). As expected, the major compound was the less sterically hindered *rac*-isomer, on the basis of nonequivalences found in the ^{13}C and ^{1}H spectra for the aryl, methyl, and isopropyl moieties, in agreement with a C_2 symmetry in solution (Scheme 5a). Whilst the minor compound attributed to the *meso*-**7** stereoisomer displayed magnetic equivalence for the same moieties above mentioned, in concordance with a *Cs* symmetry in solution combined with a fast rotation of the NHC ligand around the Pt−C bond on the NMR time scale (Scheme 5b). This behavior together with the ^{13}C resonances found for the carbenic carbons (173 and 172 ppm for the major and minor product, respectively) resemble to those found for similar complexes (NHC)Pt(0)(DMFU) (DMFU = dimethylfumarate) previously reported.[6a,17]

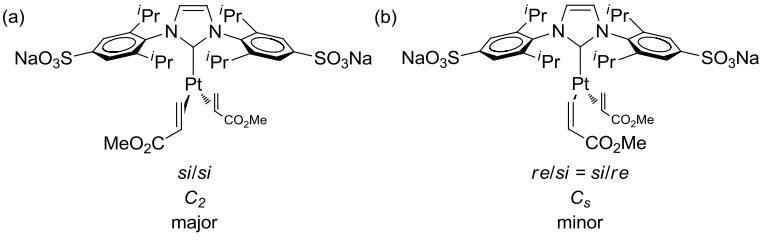

Scheme 5. Possible stereoisomers for complex **7** (enantiomer *re*, *re* not shown).

CONCLUSIONS

The studies on the reactivity starting from solutions of (NHC)Pt(0)(AE) complex **2** in dmso, where NHC is a sulfonated version of the IPr ligand,[18] illustrate two important reactions in organometallic chemistry, namely, oxidative addition and reductive elimination, which can be carried out under mild conditions. The stereoselective oxidative addition of CH_3I to that complex, leading to the iodomethyl(NHC)Pt(II) complex **4**, appears to be a synthetic methodology suitable for the preparation of complexes of such class. On the other hand, the same type of process involving a C(*sp*)–H bond activation of terminal alkynes gives access to new water-soluble hydridealkynyl(NHC)Pt(II) complexes, which are moderately stables in water. The investigation of the slow decomposition of these hydrides in water has provided signs of reversion of the oxidative addition, which has been confirmed in straightforward

reactions in the presence of alkenes where the complexes evolve back to diolefinic Pt(0) compounds. The full scheme of these transformations discloses a sharp solvent effect. The chemical equation shifts quite easily from a diolefin(NHC)Pt(0) to a hydridealkynyl(NHC)Pt(II) complex in the presence of a terminal alkyne in dmso, whereas reductive elimination of the latter readily takes place in water with liberation of the alkyne a "recoordination" of the olefins. We consider this finding relevant for synthetic purposes aiming to the preparation of (NHC)Pt(0) complexes in water, but also and for example, for the grafting of (NHC)Pt complexes on metallic surfaces modified with olefin groups by simple addition of hydridealkynyl(NHC)Pt(II) in water, such as in related approaches reported for gold.[19]

Further efforts to study the chemical behavior and possible applications of these water-soluble hydride(NHC)Pt(II) complexes are currently underway in our laboratories.

EXPERIMENTAL SECTION

General Procedures. All reactions were performed under an argon atmosphere using standard Schlenk techniques. Unless otherwise stated, reagents and solvents were used as received from commercial sources. The complex [1,3-bis(2,6-diisopropyl-4-sodiumsulfonatephenyl)imidazol-2-ylidene]diallyletherplatinum(0) **2**[12] was prepared as described in the literature. All solvents were deoxygenated prior to use. Dimethyl sulfoxide was distilled under argon over calcium hydride. Deionized water (type II quality) was obtained using a Millipore Elix 10 UV water purification system. ^{1}H, and ^{13}C spectra were recorded using a Varian Mercury 300, Unity 300, or Unity 500 Plus spectrometer. Chemical shifts (δ, parts per million) are quoted relative to $SiMe_4$ (^{1}H, ^{13}C). They were measured by internal referencing to the ^{13}C or residual ^{1}H resonances of the deuterated solvents (39.0 ppm for dmso-d_6 carbons; 2.49 ppm for dmso-d_5 protons and 4.69 ppm for HDO). Coupling constants (J) are given in hertz. When required, two-dimensional ^{1}H−^{13}C HMBC, HSQC or NOESY experiments were carried out for the unequivocal assignment of ^{1}H and ^{13}C resonances, or for discerning the stereochemistry of the complexes. IR spectra were recorded for KBr pellets over the range 4000−400 cm^{-1} using a Perkin−Elmer Spectrum 2000 spectrophotometer. The Analytical Services of the Universidad de Alcalá performed the C, H, and N analyses using a LECO CHNS-932 microanalyzer, and the mass spectra were obtained using an Agilent G3250AA LC/MSD TOF Multi (MALDI and ESI) mass spectrometer in the electrospray ionization mode.

Synthesis of (*SP*-4-4)-[(Dimethylsulfoxide)iodide{1,3-bis(2,6-diisopropyl-4-sodiumsulfonatophenyl)imidazol-2-ylidene}methylplatinum(II)] (4). Iodomethane (15 μL, 0.24 mmol) was added to a solution of complex **2** (0.101 g, 0.114 mmol) in dimethyl

sulfoxide (3 mL). The mixture was stirred at 50 °C for 1 h, and then filtered through a PTFE 0.22 μm filter. The solvent was partially removed under high vacuum at 90 °C to a remaining volume of 1 – 2 mL. The product was then precipitated with the addition of THF (50 mL), separated by filtration, washed with THF (3 × 15 mL), and dried under vacuum at 30 ºC and 4 mbar of pressure for 12 h to give the complex **4** as a yellow solid (0.104 g, 90%). ^{1}H NMR (500 MHz, D_2O): δ 7.69 (d, $^{4}J_{H\text{-}H}$ = 2.0, 2H, Ar); 7.67 (s, $^{4}J_{H\text{-}H}$ = 2.0, 2H, Ar); 7.60 (s, 2H, Imz); 3.16 (hept, $^{3}J_{H\text{-}H}$ = 7.0, 2H, C*H*Me$_2$); 3.10 (s, 6H, Me_2SO); 2.77 (hept, $^{3}J_{H\text{-}H}$ = 7.0, 2H, C*H*Me$_2$); 1.36 (d, $^{3}J_{H\text{-}H}$ = 6.5, 6H, CH*Me*$_2$); 1.30 (d, $^{3}J_{H\text{-}H}$ = 6.5, 6H, CH*Me*$_2$); 1.07 (d, $^{3}J_{H\text{-}H}$ = 6.5, 6H, CH*Me*$_2$); 1.04 (d, $^{3}J_{H\text{-}H}$ = 6.5, 6H, CH*Me*$_2$); 0.25 (s with ^{195}Pt satellites, $^{2}J_{H\text{-}Pt}$ = 75.1, 3H, PtMe). ^{1}H NMR (300 MHz, dmso-d_6): δ 7.72 (s, 1H, Imz); 7.50 (s, 2H, Ar); 3.30 (hept, $^{3}J_{H\text{-}H}$ = 6.9, 2H, C*H*Me$_2$); 2.78 (hept, $^{3}J_{H\text{-}H}$ = 6.9, 2H, C*H*Me$_2$); 1.34 (d, $^{3}J_{H\text{-}H}$ = 6.6, 6H, CH*Me*$_2$); 1.27 (d, $^{3}J_{H\text{-}H}$ = 6.6, 6H, CH*Me*$_2$); 1.08 (d, $^{3}J_{H\text{-}H}$ = 6.6, 6H, CH*Me*$_2$); 1.57 (d, $^{3}J_{H\text{-}H}$ = 6.6, 6H, CH*Me*$_2$); 0.25 (s with ^{195}Pt satellites, $^{2}J_{H\text{-}Pt}$ = 78.9, 3H, PtMe). ^{13}C{^{1}H} NMR (125 MHz, D_2O): δ 162.2 (s, Imz C^{2}), 148.0 (s, Ar-C^{4}), 147.8 (s, Ar-C^{2}), 144.3 (s, Ar-C^{2}), 137.6 (s, Ar-C^{1}), 125.5 (s, Imz-C^{4,5}), 121.6 (s, Ar-C^{3}), 121.4 (s, Ar-C^{3}), 43.8 (s, Me_2SO), 29.4 (s, *C*HMe$_2$), 29.2 (s, *C*HMe$_2$), 25.4 (s, CH*Me*$_2$), 25.3 (s, CH*Me*$_2$), 22.9 (s, CH*Me*$_2$), 22.0 (s, CH*Me*$_2$), –4.8 (s, PtMe). ESI-MS (negative ion, MeOH) *m*/*z*: 868.0626 [M – 2Na – dmso – CH_4 + H]$^-$ (calcd 868.0556) 1.8%; 740.1481 [M – 2Na – dmso –CH_4 – I]$^-$ (calcd 740.1433) 1%; 788.2069 [M – 2Na – dmso –I + CH_3OH]$^-$ (calcd 788.2008) 1%; 441.5327 [M – 2Na – dmso]$^{2-}$ (calcd 441.5398) 6.7%; 433.5208 [M – 2Na – dmso – CH_4]$^{2-}$ (calcd 433.5242) 100%. Anal. Calcd (%) for $C_{30}H_{59}IN_2Na_2O_{15}PtS_3$ (**3**•8H_2O): C, 31.28; H, 5.16; N, 2.43. Found (%): C, 30.93; H, 4.90; N, 2.25.

Synthesis of (*SP*-4-4)-[(dimethylsulfoxide)hydride{1,3-bis(2,6-diisopropyl-4-sodiumsulfonatophenyl)imidazol-2-ylidene}(trimethylsilylacetylide)platinum(II)] (5), and (*SP*-4-4)-[(dimethylsulfoxide)hydride{1,3-bis(2,6-diisopropyl-4-sodiumsulfonatophenyl)imidazol-2-ylidene}(phenylacetylide)platinum(II)] (6). The corresponding alkyne (0.180 mmol) was added to a solution of complex **2** (80.0 mg, 0.0903 mmol) in dimethyl sulfoxide (3 mL). The mixture was stirred for the time indicated below at 50 °C, and then filtered through a PTFE 0.22 μm filter. The solvent was removed under high vacuum at 90 °C to dryness. The powdery solid thus obtained was dried under vacuum at 90 ºC and 4 mbar of pressure for 12 h. Accurate elemental analysis could not be obtained for complexes **5** and **6** probably due to persistent retention of water and dmso molecules in the solid samples.

Complex **5** was obtained from ethynyltrimethylsilane (25 μL, 0.180 mmol) after 6 h of reaction as a yellow solid (82.7 mg, 95%). IR (cm^{-1}): ν (C≡C) 2037 (m). ^{1}H NMR (300 MHz, dmso-d_6): δ 7.72 (s, 2H, Imz); 7.54 (s, 4H, Ar); 2.82 (hept, $^{3}J_{H\text{-}H}$ = 7.0, 4H, C*H*Me$_2$); 1.26 (d, $^{3}J_{H\text{-}H}$ = 7.0, 12H, CH*Me*$_2$); 1.05 (d, $^{3}J_{H\text{-}H}$ = 6.6, 12H, CH*Me*$_2$); –0.13 (s, 9H, $SiMe_3$); –12.13 (s with ^{195}Pt satellites, $^{1}J_{H\text{-}Pt}$ = 1401.6, 1H, PtH). ^{1}H NMR (300 MHz, D_2O): δ 7.70 (s, 4H, Ar);

7.55 (s, 2H, Imz); 2.76 (hept, $^{3}J_{H\text{-}H}$ = 7.0, 4H, C*H*Me$_2$); 2.58 (s, 6H, Me$_2$SO); 1.27 (d, $^{3}J_{H\text{-}H}$ = 6.6, 12H, CH*Me*$_2$); 1.03 (d, $^{3}J_{H\text{-}H}$ = 6.6, 12H, CH*Me*$_2$); –0.15 (s, 9H, SiMe$_3$); –12.16 (s with ^{195}Pt satellites, $^{1}J_{H\text{-}Pt}$ = 1400.3, 1H, PtH). ^{13}C{^{1}H} NMR (75 MHz, dmso-d$_6$): δ 175.7 (s, Imz-C^2), 148.7 (s, Ar-C^4), 144.9 (s, Ar-C^2), 135.0 (s, Ar-C^1), 124.0 (s, Imz-C^{4,5}), 120.3 (s, Ar-C^3), 133.9 (s, *C*≡CSiMe$_3$), 108.8 (s, C≡*C* SiMe$_3$), 41.8 (s, Me$_2$SO), 27.6 (s, *C*HMe$_2$), 25.1 (s, CH*Me*$_2$), 22.2 (s, CH*Me*$_2$). 0.66 (s, SiMe$_3$). ^{13}C{^{1}H} NMR (75 MHz, D$_2$O): δ 174.1 (s, Imz-C^2), 147.9 (s, Ar-C^4), 144.1 (s, Ar-C^2), 137.4 (s, Ar-C^1), 129.3 (s, *C*≡CSiMe$_3$), 124.5 (s, Imz-C^{4,5}), 121.3 (s, Ar-C^3), 117.2 (s, C≡*C* SiMe$_3$), 42.9 (s, Me$_2$SO), 28.7 (s, *C*HMe$_2$), 24.7 (s, CH*Me*$_2$), 21.8 (s, CH*Me*$_2$). –0.38 (s, SiMe$_3$). ESI-MS (negative ion, MeOH) *m/z*: 940.2149 [M – Na]$^-$ (calcd 940.2100) 6.2%; 862.1970 [M – Na – dmso]$^-$ (calcd 862.1961) 3.7%; 419.6040 [M – 2Na – dmso]$^{2-}$ (calcd 419.6034) 53%; 774.1884 [M – 2Na –dmso + CH$_3$OH – CCSiMe$_3$]$^-$ (calcd 774.1857) 40%; 368.5608 [M – 2Na – dmso – HCCSiMe$_3$ – 2H$_2$]$^{2-}$ (calcd 368.5602) 100%.

Complex **6** was obtained from phenylacetylene (20 µL, 0.180 mmol) after 3 h of reaction as a yellow solid (81.3 mg, 93%). IR (cm^{-1}): *ν* (C≡C) 2105 (m). ^{1}H NMR (500 MHz, dmso-d$_6$): δ 7.73 (s, 2H, Imz); 7.56 (s, 4H, Ar); 7.07 (m, 5H, Ph); 2.86 (hept, $^{3}J_{HH}$ = 7.0, 4H, C*H*Me$_2$); 1.28 (d, $^{3}J_{HH}$ = 6.5, 12H, CH*Me*$_2$); 1.07 (d, $^{3}J_{H\text{-}H}$ = 6.5, 12H, CH*Me*$_2$); –12.07 (s with ^{195}Pt satellites, $^{1}J_{H\text{-}Pt}$ = 1398.0, 1H, PtH). ^{1}H NMR (300 MHz, D$_2$O): δ 7.71 (s, 4H, Ar); 7.55 (s, 2H, Imz); 7.09 (m, 5H, Ph); 2.79 (hept, $^{3}J_{H\text{-}H}$ = 6.9, 4H, C*H*Me$_2$); 1.28 (d, $^{3}J_{H\text{-}H}$ = 6.4, 12H, CH*Me*$_2$); 1.03 (d, $^{3}J_{H\text{-}H}$ = 6.9, 12H, CH*Me*$_2$); –12.14 (s with ^{195}Pt satellites, $^{1}J_{H\text{-}Pt}$ = 1392.0, 1H, PtH). ^{13}C{^{1}H} NMR (75 MHz, dmso-d$_6$): δ 175.4 (s, Imz-C^2), 148.7 (s, Ar-C^4), 144.9 (s, Ar-C^2), 135.1 (s, Ar-C^1), 130.0, 129.9 and 127.2 (3 × s, Ph), 127.6 (s, Ph-C^1), 124.1 (s, Imz-C^{4,5}), 120.4 (s, Ar-C^3), 111.7 (s, *C*≡CPh), 105.9 (s, C≡*C*Ph), 41.7 (s, Me$_2$SO), 27.6 (s, *C*HMe$_2$), 25.1 (s, CH*Me*$_2$), 22.2 (s, CH*Me*$_2$). ESI-MS (negative ion, MeOH) *m/z*: 866.1791 [M – Na – dmso]$^-$ (calcd 866.1879) 3.5%; 844.1931 [M – 2Na + H – dmso]$^-$ (calcd 844.2059) 2.4%; 421.5913 [M – 2Na – dmso]$^{2-}$ (calcd 421.5993) 29%; 368.5526 [M – 2Na –dmso – HCCPh – 2H$_2$]$^{2-}$ (calcd 368.5602) 100%.

Synthesis of [{1,3-bis(2,6-diisopropyl-4-sodiumsulfonatophenyl)imidazol-2-ylidene}{bis(methylacrylate)}platinum(0)] (7), and complex 1. Methyl acrylate (for **7**) (7,5 µL, 0.083 mmol) or 1,3-divinyltetramethyldisiloxane (for **1**) (10 µL, 0.043 mmol) was added to a solution of complex **5** or **6** (0.020 mmol) in H$_2$O (2 mL). The mixture was stirred at room temperature for the time indicated below, then the solvent was removed under high vacuum at 50 °C to dryness. The powdery solid thus obtained was dried under vacuum at 50 ºC and 4 mbar of pressure for 12 h.

Complex **7** was obtained as a beige solid after 1 h of reaction (18.8 mg, 98%). Ratio of diastereoisomers: 70:30. Major (enantiomers *re*/*re* and *si*/*si*): ^{1}H NMR (500 MHz, D$_2$O): δ 7.70 (d, $^{3}J_{H\text{-}H}$ = 2.5, 2H, Ar); 7.64 (s, 2H, Imz); 7.57 (d, $^{3}J_{H\text{-}H}$ = 2.5, 2H, Ar); 3.17 (s, 3H, CO$_2$Me); 2.82 (m, 2H, C*H*Me$_2$); 2.63 (m, 2H, C*H*Me$_2$); 2.61 (m, 2H, CH$_2$=C*H*CO$_2$Me), 2.13 (dd with

^{195}Pt satellites, $^{2}J_{H\text{-}Pt}$ = 46.5, $^{3}J_{H\text{-}H}$ = 8.2, $^{2}J_{H\text{-}H}$ = 2.0, 2H, C*H*$_2$=CHCO$_2$Me); 1.97 (dd with ^{195}Pt satellites, $^{2}J_{H\text{-}Pt}$ = 51.0, $^{3}J_{H\text{-}H}$ = 11.0, $^{2}J_{H\text{-}H}$ = 2.0, 2H, C*H*$_2$=CHCO$_2$Me); 1.36 (d, $^{3}J_{H\text{-}H}$ = 7.0, 6H, CH*Me*$_2$); 1.23 (d, $^{3}J_{H\text{-}H}$ = 7.0, 6H, CH*Me*$_2$); 0.94 (d, $^{3}J_{H\text{-}H}$ = 7.0, 6H, CH*Me*$_2$); 0.88 (d, $^{3}J_{H\text{-}H}$ = 7.0, 6H, CH*Me*$_2$). ^{13}C{^{1}H} NMR (75 MHz, D$_2$O): δ 176.2 (s, *C*O$_2$Me), 173.3 (s, Imz-C^2), 147.5 (s, Ar-C^2), 146.7 (s, Ar-C^2), 143.76 (s, Ar-C^4), 137.4 (s, Ar-C^1), 125.3 (s, Imz-C^{4,5}), 121.0 (s, Ar-C^3), 121.1 (s, Ar-C^3), 51.0 (s with ^{195}Pt satellites, $^{3}J_{H\text{-}Pt}$ = 39.6, CO$_2$*Me*), 44.0 (s with ^{195}Pt satellites, $^{1}J_{H\text{-}Pt}$ = 144.1, CH$_2$=*C*HCO$_2$Me), 42.6 (s with ^{195}Pt satellites, $^{1}J_{H\text{-}Pt}$ = 154.4, *C*H$_2$=CHCO$_2$Me), 28.8 (s, *C*HMe$_2$), 28.3 (s, *C*HMe$_2$), 25.6 (s, CH*Me*$_2$), 24.0 (s, CH*Me*$_2$), 21.9 (s, CH*Me*$_2$), 20.5 (s, CH*Me*$_2$). Minor (mesomeric form: *re*/*si* = *si*/*re*): ^{1}H NMR (500 MHz, D$_2$O): δ 7.65 (s, 2H, Imz); 7.62 (s, 4H, Ar); 3.21 (s, 3H, CO$_2$Me); 2.86 (m, 2H, CH$_2$=C*H*CO$_2$Me); 2.82 (m, 2H, C*H*Me$_2$); 2.63 (m, 2H, C*H*Me$_2$); 2.21 (dd with ^{195}Pt satellites, $^{2}J_{H\text{-}Pt}$ = 48.5, $^{3}J_{H\text{-}H}$ = 10.5, $^{2}J_{H\text{-}H}$ = 1.5, 2H, C*H*$_2$=CHCO$_2$Me); 1.90 (dd with ^{195}Pt satellites, $^{2}J_{H\text{-}Pt}$ = 47.0, $^{3}J_{H\text{-}H}$ = 8.5, $^{2}J_{H\text{-}H}$ = 2.0, 2H, C*H*$_2$=CHCO$_2$Me); 1.19 (d, $^{3}J_{H\text{-}H}$ = 7.0, 6H, CH*Me*$_2$); 1.08 (d, $^{3}J_{H\text{-}H}$ = 7.0, 6H, CH*Me*$_2$). ^{13}C{^{1}H} NMR (75 MHz, D$_2$O): δ 176.1 (s, *C*O$_2$Me), 172.1 (s, Imz-C^2), 147.1 (s, Ar-C^2), 143.82 (s, Ar-C^4), 137.6 (s, Ar-C^1), 125.6 (s, Imz-C^{4,5}), 121.0 (s, Ar-C^3), 50.7 (s, CO$_2$*Me*), 41.6 (s, *C*H$_2$=CHCO$_2$Me), 38.6 (s, CH$_2$=*C*HCO$_2$Me), 28.6 (s, *C*HMe$_2$), 24.8 (s, CH*Me*$_2$), 21.2 (s, CH*Me*$_2$). ESI-MS (positive ion, H$_2$O) *m*/*z*: 916.2559 [M – 2Na + 3H]$^+$ (calcd 916.2471) 13%; 830.2119 [M – 2Na + 3H – CH$_2$CHCO$_2$Me]$^+$ (calcd 830.2103) 100%; 852.1893 [M – Na + 2H – CH$_2$CHCO$_2$Me]$^+$ (calcd 852.1923) 40%. ESI-MS (negative ion, H$_2$O) *m*/*z*: 828.1995 [M – 2Na + H – CH$_2$CHCO$_2$Me]$^-$ (calcd 828.1958) 3.3%; 413.5968 [M – 2Na – CH$_2$CHCO$_2$Me]$^{2-}$ (calcd 413.5942) 100%.

Complex **1** was obtained as a yellow solid after 3 h of reaction (18.5 mg, 95%). Complex **1** was characterized by comparison with their previously reported NMR data.[9]

ASSOCIATED CONTENT

Supporting Information

NMR spectra of complexes **4**–**7**. This material is available free of charge via the Internet at http://pubs.acs.org.

AUTHOR INFORMATION

Corresponding Authors

*Email: juanc.flores@uah.es (J.C.F.), ernesto.dejesus@uah.es (E.d.J).

ACKNOWLEDGMENT

This work was supported by the Spanish Ministerio de Economía y Competitividad (project CTQ2011-24096). E.A.B. is grateful to the Universidad de Alcalá for an FPI Doctoral Fellowship. G.F.S. is grateful to the Spanish Ministerio de Educación for a Postdoctoral Fellowship.

REFERENCES

(1) a) J. R. Berenguer, M. Bernechea, E. Lalinde, *Organometallics* **2007**, *26*, 1161-1172; b) S. Crementieri, P. Leoni, F. Marchetti, L. Marchetti, M. Pasquali, *Organometallics* **2002**, *21*, 2575-2577; c) J. R. Berenguer, M. Bernechea, J. Fornies, E. Lalinde, J. Torroba, *Organometallics* **2005**, *24*, 431-438; d) I. Ara, L. R. Falvello, J. Fornies, E. Lalinde, A. Martin, F. Martinez, M. T. Moreno, *Organometallics* **1997**, *16*, 5392-5405; e) A. L. Bandini, G. Banditelli, M. Manassero, A. Albinati, D. Colognesi, J. Eckert, *Eur. J. Inorg. Chem.* **2003**, 3958-3967; f) S. Reinartz, M.-H. Baik, P. S. White, M. Brookhart, J. L. Templeton, *Inorg. Chem.* **2001**, *40*, 4726-4732.

(2) in *N-Heterocyclic Carbenes: From Laboratory Curiosities to Efficient Synthetic Tools* (Ed.: S. Diez-Gonzalez), RSC Catalysis Series; The Royal Society of Chemistry, **2011**.

(3) G. L. Petretto, M. Wang, A. Zucca, J. P. Rourke, *Dalton Trans.* **2010**, *39*, 7822-7825.

(4) a) O. Rivada-Wheelaghan, M. A. Ortuno, J. Diez, A. Lledos, S. Conejero, *Angew. Chem., Int. Ed.* **2012**, *51*, 3936-3939; b) O. Rivada-Wheelaghan, B. Donnadieu, C. Maya, S. Conejero, *Chem. Eur. J.* **2010**, *16*, 10323-10326; c) G. C. Fortman, N. M. Scott, A. Linden, E. D. Stevens, R. Dorta, S. P. Nolan, *Chem. Commun.* **2010**, *46*, 1050-1052.

(5) a) D. S. McGuinness, K. J. Cavell, B. F. Yates, B. W. Skelton, A. H. White, *J. Am. Chem. Soc.* **2001**, *123*, 8317-8328; b) B. Pan, S. Pierre, M. W. Bezpalko, J. W. Napoline, B. M. Foxman, C. M. Thomas, *Organometallics* **2013**, *32*, 704-710.

(6) a) M. A. Duin, N. D. Clement, K. J. Cavell, C. J. Elsevier, *Chem. Commun.* **2003**, 400-401; b) D. Bacciu, K. J. Cavell, I. A. Fallis, L.-l. Ooi, *Angew. Chem., Int. Ed.* **2005**, *44*, 5282-5284.

(7) a) J. A. Labinger, J. E. Bercaw, *Top. Organomet. Chem.* **2011**, *35*, 29-60; b) M. Lersch, M. Tilset, *Chem. Rev.* **2005**, *105*, 2471-2526; c) R. J. Puddephatt, *Coord. Chem. Rev.* **2001**, *219-221*, 157-185; d) J. L. Look, D. D. Wick, J. M. Mayer, K. I. Goldberg, *Inorg. Chem.* **2009**, *48*, 1356-1369; e) G. Minghetti, S. Stoccoro, M. A. Cinellu, G. L. Petretto, A. Zucca, *Organometallics* **2008**, *27*, 3415-3421; f) M. Kirchmann, K. Eichele, L. Wesemann, *Organometallics* **2008**, *27*, 6029-6031; g) A. Zucca, S. Stoccoro, M. A. Cinellu, G. L. Petretto, G. Minghetti, *Organometallics* **2007**, *26*, 5621-5626; h) C. Gallego, M. Martinez, V. Sixte Safont, *Organometallics* **2007**, *26*, 527-537; i) U. Fekl, K. I. Goldberg, *J. Am. Chem. Soc.* **2002**, *124*, 6804-6805.

(8) a) A. E. Shilov, G. B. Shul'pin, *Chem. Rev.* **1997**, *97*, 2879-2932; b) J. A. M. Simoes, J. L. Beauchamp, *Chem. Rev.* **1990**, *90*, 629-688; c) A. N. Vedernikov, J. C. Fettinger, F. Mohr, *J.*

Am. Chem. Soc. **2004**, *126*, 11160-11161; d) A. J. Canty, S. D. Fritsche, H. Jin, J. Patel, B. W. Skelton, A. H. White, *Organometallics* **1997**, *16*, 2175-2182; e) A. Haskel, E. Keinan, *Organometallics* **1999**, *18*, 4677-4680; f) H. C. Clark, K. R. Dixon, W. J. Jacobs, *Chem. Commun.* **1968**, 548.

(9) G. F. Silbestri, J. C. Flores, E. de Jesús, *Organometallics* **2012**, *31*, 3355-3360.

(10) a) E. A. Baquero, G. F. Silbestri, P. Gómez-Sal, J. C. Flores, E. de Jesús, *Organometallics* **2013**, *32*, 2814-2826; b) E. A. Baquero, J. C. Flores, J. Perles, P. Gomez-Sal, E. de Jesus, *Organometallics* **2014**, *33*, 5470-5482.

(11) E. A. Baquero, S. Tricard, J. C. Flores, E. de Jesus, B. Chaudret, *Angew. Chem. Int. Ed.* **2014**, 13220-13224.

(12) A. Ruiz-Varilla, E. A. Baquero, G. F. Silbestri, E. de Jesus, C. Gonzalez-Arellano, J. C. Flores, *Manuscript under preparation* **2015**.

(13) E. A. Baquero, J. Gonzalez, M. Temprado, J. Davalos, J. C. Flores, E. de Jesús, *Manuscript under preparation* **2015**.

(14) a) B. M. Still, P. G. A. Kumar, J. R. Aldrich-Wright, W. S. Price, *Chem. Soc. Rev.* **2007**, *36*, 665-686; b) J. Y. Lallemand, J. Soulie, J. C. Chottard, *J. Chem. Soc., Chem. Commun.* **1980**, 436-438.

(15) C. P. Newman, R. J. Deeth, G. J. Clarkson, J. P. Rourke, *Organometallics* **2007**, *26*, 6225-6233.

(16) a) J. R. Berenguer, J. Fornies, F. Martinez, J. C. Cubero, E. Lalinde, M. T. Moreno, A. J. Welch, *Polyhedron* **1993**, *12*, 1797-1804; b) I. Ara, J. R. Berenguer, E. Eguizabal, J. Fornies, J. Gomez, E. Lalinde, J. M. Saez-Rocher, *Organometallics* **2000**, *19*, 4385-4397.

(17) a) N. D. Clement, K. J. Cavell, L.-l. Ooi, *Organometallics* **2006**, *25*, 4155-4165; b) M. A. Duin, M. Lutz, A. L. Spek, C. J. Elsevier, *J. Organomet. Chem.* **2005**, *690*, 5804-5815; c) C. Martin, F. Molina, E. Alvarez, T. R. Belderrain, *Chem. Eur. J.* **2011**, *17*, 14885-14895.

(18) C. Fleckenstein, S. Roy, S. Leuthaeusser, H. Plenio, *Chem. Commun.* **2007**, 2870-2872.

(19) A. V. Zhukhovitskiy, M. G. Mavros, T. Van Voorhis, J. A. Johnson, *J. Am. Chem. Soc.* **2013**, *135*, 7418-7421.

Supporting Information

Synthesis of Water-Soluble Hydride(NHC)platinum(II) Complexes by Reversible Oxidative Addition of Alkynes to Pt(0) Complexes

Edwin A. Baquero, Gustavo F. Silbestri, Juan C. Flores,* and Ernesto de Jesús*

Departamento de Química Orgánica y Química Inorgánica, Campus Universitario, Universidad de Alcalá, 28871 Alcalá de Henares, Madrid, Spain.

Email: juanc.flores@uah.es, ernesto.dejesus@uah.es

Table of Contents

1. ^{1}H and $^{13}C\{^{1}H\}$ NMR spectra of the new compounds

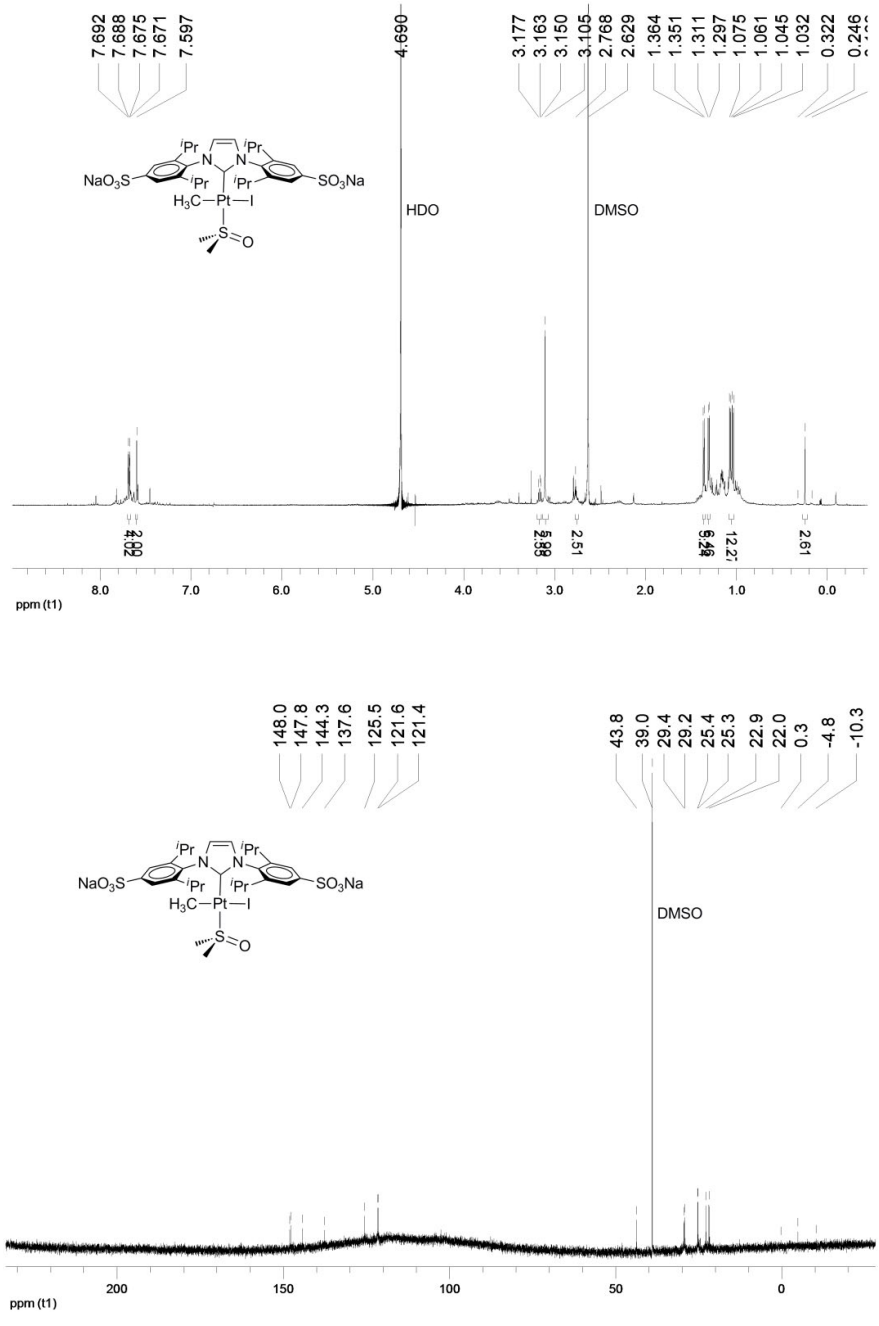

Figure S1. ^{1}H (500 MHz, D_2O) and $^{13}C\{^{1}H\}$ (125 MHz, D_2O) NMR spectra for **4**.

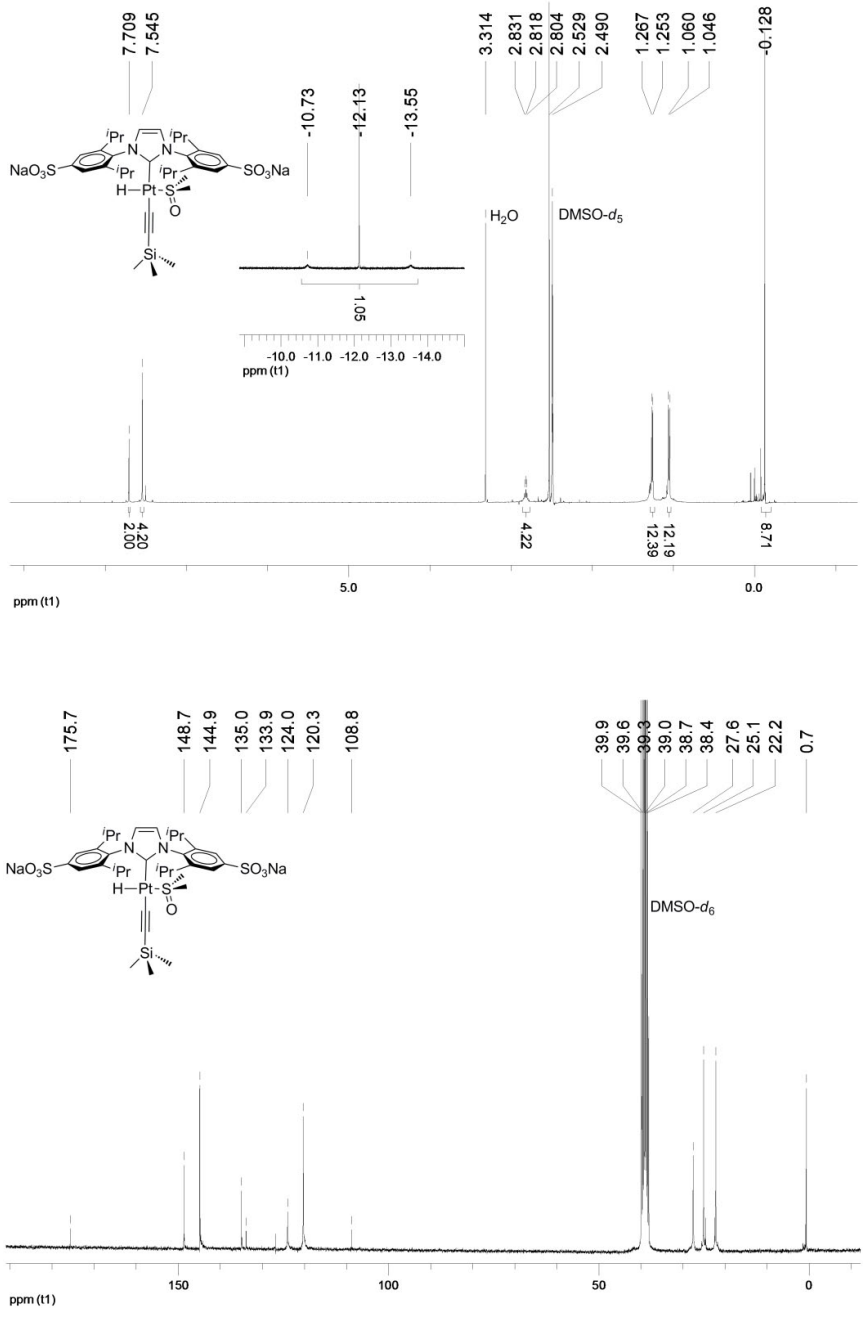

Figure S2. ^{1}H (500 MHz, dmso-d_6) and $^{13}C\{^{1}H\}$ (75 MHz, dmso-d_6) NMR spectra for **5**.

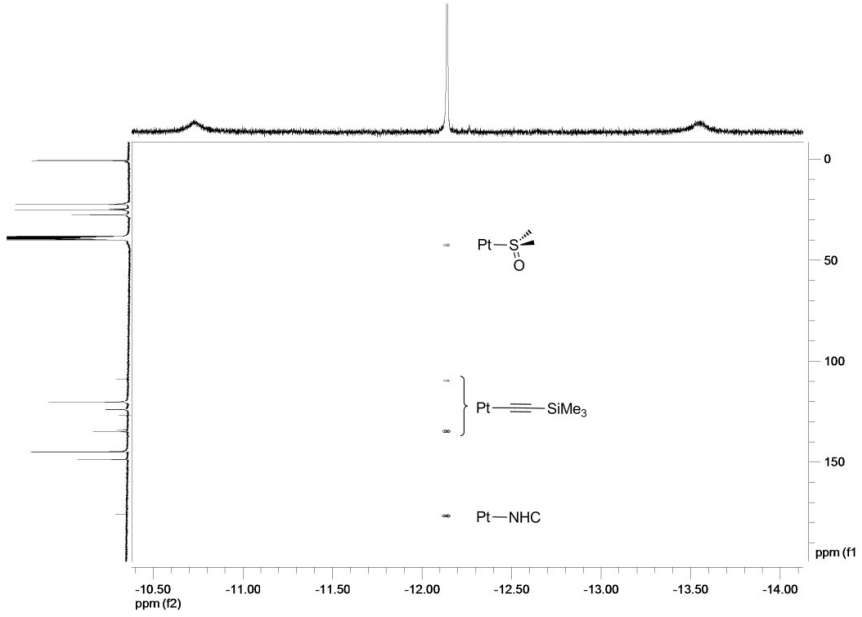

Figure S3. ^{1}H–^{13}C HMBC spectrum in the region of Pt–H moiety for complex **5**.

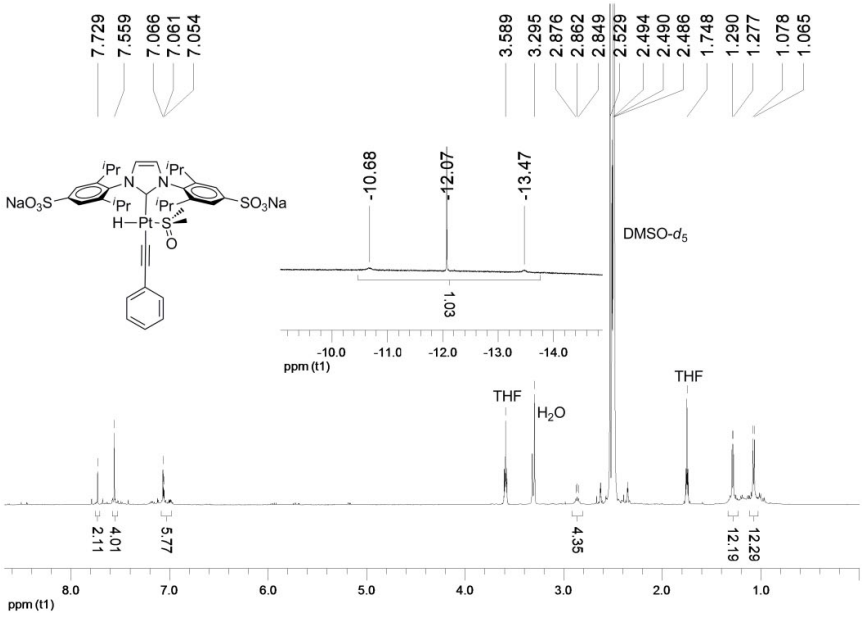

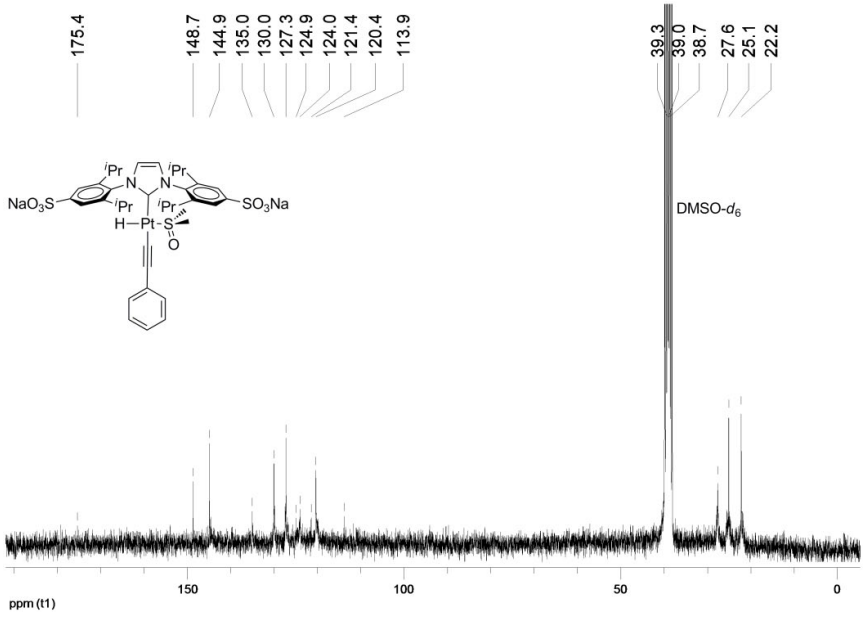

Figure S4. ^{1}H (500 MHz, dmso-d_6) and ^{13}C{^{1}H} (75 MHz, dmso-d_6) NMR spectra for **6**.

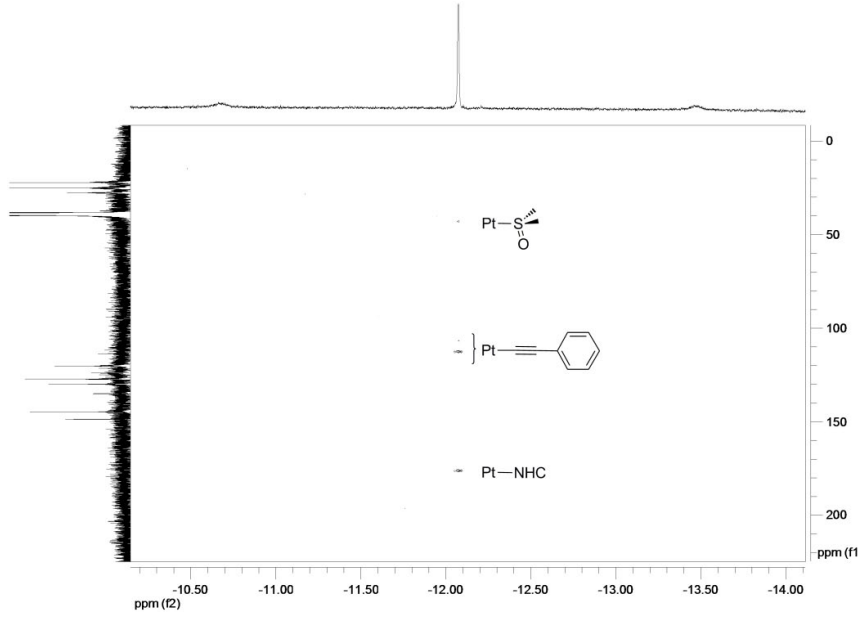

Figure S5. ^{1}H–^{13}C HMBC spectrum in the region of Pt–H moiety for complex **6**.

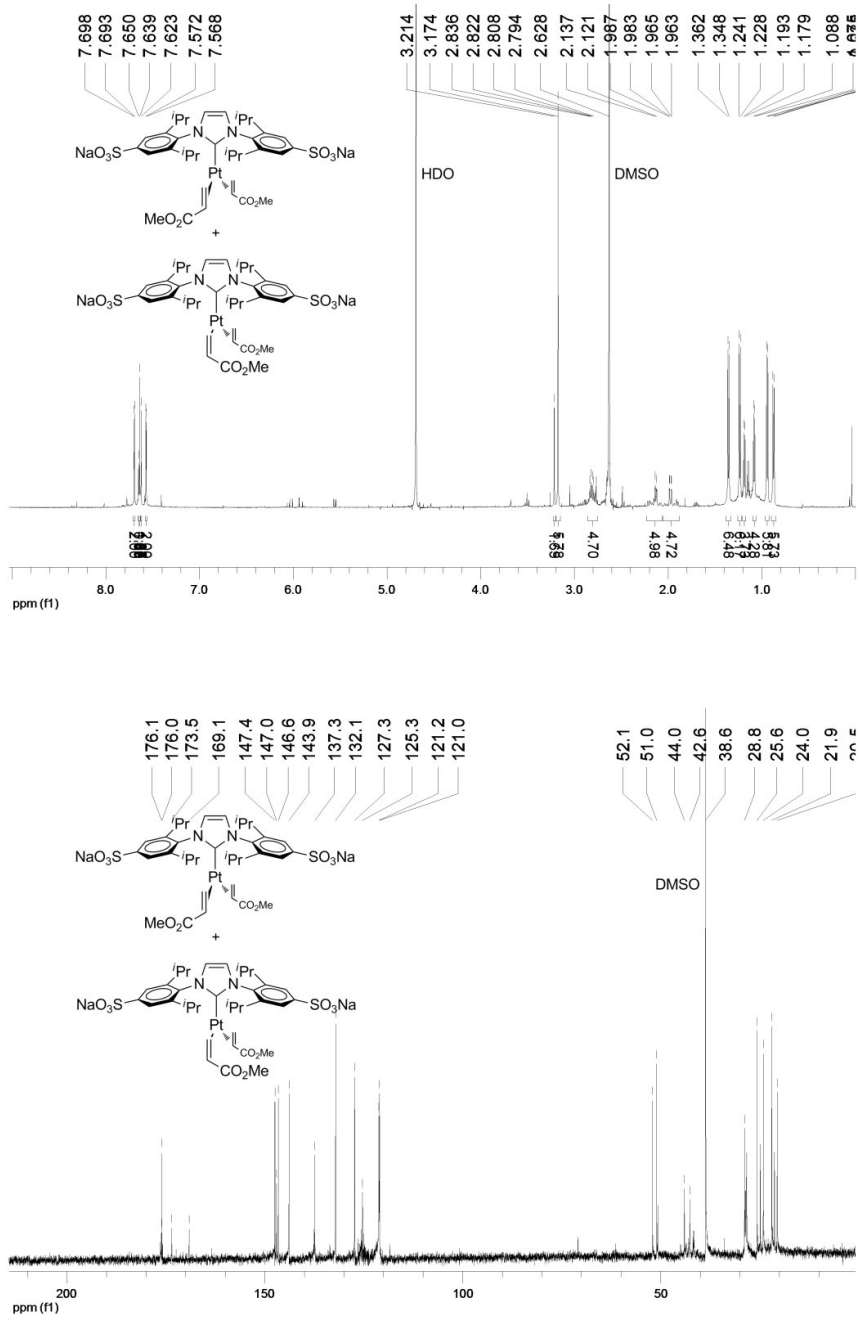

Figure S6. ^{1}H (500 MHz, D_2O) and $^{13}C\{^{1}H\}$ (75 MHz, D_2O) NMR spectra for **7**.

Chapter VI. Highly Stable Water-Soluble Platinum Nanoparticles Stabilized by Hydrophilic N-Heterocyclic Carbenes

Edwin A. Baquero, Simon Tricard, Juan C. Flores, Ernesto de Jesús, and Bruno Chaudret, *Angew. Chem. Int. Ed.*, **2014**, 13220–13224. *Selected as Hot-Topics of Wiley-VCH on Surfaces and Interfaces.*

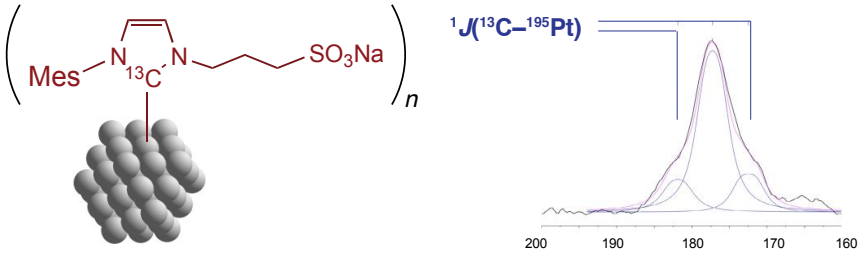

Highly Stable Water-Soluble Platinum Nanoparticles Stabilized by Hydrophilic N-Heterocyclic Carbenes

Edwin A. Baquero,[†] *Simon Tricard,*[‡] *Juan C. Flores,**[†] *Ernesto de Jesús,**[†] *and Bruno Chaudret**[‡]

[†]Departamento de Química Orgánica y Química Inorgánica, Campus Universitario, Universidad de Alcalá, 28871 Alcalá de Henares, Madrid, Spain

[‡]LPCNO; Laboratoire de Physique et Chimie de Nano-Objets. 135, Avenue de Rangueil, 31077 Toulouse, France

ABSTRACT

Controlling the synthesis of stable metal nanoparticles in water is a current challenge in nanochemistry. The strategy presented herein uses sulfonated N-heterocyclic carbene (NHC) ligands to stabilize platinum nanoparticles (PtNPs) in water, under air, for an indefinite time period. The particles were prepared by thermal decomposition of a preformed molecular Pt complex containing the NHC ligand, and were then purified by dialysis, and characterized by TEM, high-resolution TEM, and spectroscopic techniques. Solid-state NMR studies showed coordination of the carbene ligands to the nanoparticle surface and allowed the determination of a $^{13}C–^{195}Pt$ coupling constant for the first time in a nanosystem (940 Hz). Additionally, in one case a novel structure was formed in which platinum(II) NHC complexes form a second coordination sphere around the nanoparticle.

INTRODUCTION

Although the synthesis and applications of metal nanoparticles (MNPs) have been widely studied, their surface chemistry after modification with organic ligands remains relatively unexplored.[1] The agglomeration of MNPs can be avoided by coordinating ligands to their surface.[2] N-heterocyclic carbenes (NHCs) have been shown to form fairly robust transition metal complexes, which are excellent candidates for a large number of homogenous catalytic processes.[3] Surprisingly, the stabilization of MNPs with NHC ligands and, more specifically, the interaction between the metal surface and the NHC ligand, have rarely been studied.[4-13] Some of us have characterized the coordination of such ligands to ruthenium nanoparticles by solid-state NMR spectroscopy.[4] Furthermore, Pleixats and co-workers[6] and Glorius et al.[7,8] have reported the coordination of NHCs to Pd nanoparticles, which were subsequently employed as catalysts. Additionally, NHCs have been used to synthesize Au[9,10] and Ag[11] MNPs

as model systems for the formation of either conglomerates or 3D networks. We recently described the behavior of RuNPs as catalysts for the hydrogenation of arenes[5] and the synthesis of PtNPs as chemoselective catalysts for the hydrogenation of aromatic nitro compounds,[12] both stabilized by bulky NHCs. Although all of these studies involved organic solvents, the alternative use of water is very attractive for a wide range of applications of MNPs. After reporting the synthesis of Pt complexes with sulfonated NHC ligands in which the NHC–Pt bond was shown to be hydrolytically stable,[14,15] we reasoned that the dimethyl complexes depicted in the Scheme 1 could potentially be suitable precursors for the synthesis of NHC-PtNPs by thermally activated ethane elimination.

Herein, and to our knowledge, we describe the first example of water-soluble MNPs supported by NHC ligands. The synthesized PtNPs were stable in water for months and could accommodate coordinated carbene ligands, as evidenced, for the first time, by the determination of a ^{13}C–^{195}Pt coupling between the ligand and the PtNP by NMR spectroscopy. As a test of the reactivity of these MNPs we also studied the hydrogenation of styrene in water.

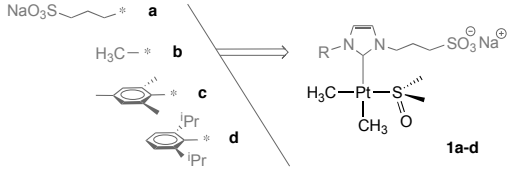

Scheme 1. Dimethyl (NHC)Pt^{II} complexes **1a–d**. R group on complexes **1a–d** given by the functional groups on the left.

RESULTS AND DISCUSSION

Aqueous solutions of complexes **1a–d** decompose at 80 °C with formation of the Pt nanoparticles **2a–d**, which gave a black, ink-like appearance to the solutions (Scheme 2). The PtNPs were purified by dialysis using a regular cellulose membrane. Although the colloidal solutions became neutral after work-up, the pH measured before dialysis was higher than 9, as would be expected because of hydrolysis of some of the carbene ligands released during MNP formation. The colloidal suspensions of **2a–d** in water were homogeneous and highly stable in air, remaining totally dispersed without agglomeration or Pt^0 precipitation for at least six months. The PtNPs were obtained in notable yields (57–82% based on metal content determined by inductively coupled plasma mass spectrometry (ICP-MS) after purification).

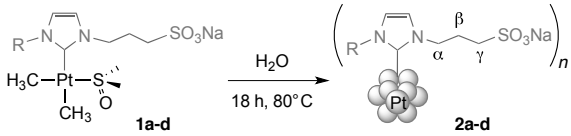

Scheme 2. Synthesis of PtNPs **2a–d** from Pt^{II} complexes **1a–d**.

Transmission electron microscopy (TEM) showed the formation of non-agglomerated, spherical nanoparticles with a fairly uniform size and diameters in the range 1.3–2.0 ± 0.4 nm depending on the ligand (Figure 1a and Figures S3–S5 in the Supporting Information). Use of the bulkiest ligands (**c** and **d)** provided the smallest PtNPs (1.3 ± 0.4 nm). High-resolution TEM (HRTEM) analyses unambiguously showed the highly crystalline character and face-centered cubic structure of PtNPs **2a**–**d**. Fast Fourier transformation (FFT) studies revealed reflections corresponding to the (111) and (002) atomic planes in all cases (Figure 1b and Figures S3–S5).

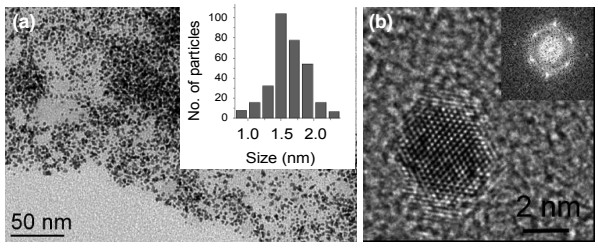

Figure 1. (a) TEM image and size distribution, and (b) HRTEM image with its corresponding FFT picture for the PtNPs **2a**. Scale bar in (b) = 2 nm.

The PtNPs were characterized by attenuated total reflection Fourier transform infrared spectroscopy (ATR-FTIR) and ^{1}H NMR spectroscopy to confirm the presence of the NHC ligands (Figures S7–S10 and S13–S16). Only broad resonance signals were evident in the ^{1}H NMR spectra in D_2O of MNPs **2b**–**d**, whereas additional sharp signals were measured in the case of **2a** (see below). The ^{1}H resonance signals for the protons on the imidazole group and the propylsulfonate β- and γ-methylenes (labels assigned in Scheme 2) displayed chemical shifts comparable to the precursor **1** (δ = 7.4–7.1, 2.2 and 2.9 ppm, respectively), as did those for the methyl protons of the aryl groups in **2c** and **2d** (2.1–1.8 ppm for **2c**, and 1.3–0.9 ppm for **2d**). However, the signals corresponding to the α-methylene, the C*H* isopropyl (in **2d**), and the C*H* aryl (in **2c** and **2d**) were not detected. These protons are expected to be located close to the MNP surface and the absence of resonance signal is caused by the combined effect of an increased rigidity in the coordinated ligands after formation of the MNPs, slow tumbling of the particles which leads to rapid T_2 relaxation times, and the heterogeneity of the surface. [16] Similar effects have been observed in NHC-stabilized Au,[10] Pd,[8] or Ru nanoparticles.[4] Furthermore, the close proximity of the phenyl rings to the nanoparticle surface in **2c** and **2d** suggested by the ^{1}H NMR results reinforces the possibility of NHC-PtNP bonding by agostic or π interactions, as we previously reported for NHC and 4-(3-phenylpropyl)pyridine ligands stabilizing RuNPs.[4,17] In contrast, the observation of resonance signals attributable to protons on the flexible propylsulfonate groups suggests that these chains point away from the particle, thus meaning that their ionic moieties are hydrated by the polar solvent. This interaction explains both the solubility and the high stability of PtNPs **2** in water.

We also investigated the coordination of the carbene ligands to the NPs by solid-state ^{1}H–^{13}C cross-polarization magic angle spinning (CP-MAS) NMR measurements (Figure 2). No resonance signals are detected attributable to carbons on the Pt–CH_3 and Pt–DMSO moieties in the spectra of the PtNPs (Figure 2c for PtNP **2b**). These signals would be expected at circa δ = –5 and 40 ppm, respectively, considering the spectra of complexes **1a–d** (Figure 2 and Figures S17–S19). It appears that NHCs are the only ligands to remain attached to the nanoparticle surface (not counting water molecules), thus resulting in broad ^{13}C resonances in the expected regions for the imidazolic methine carbon centers (δ = 124–122 ppm), the α, β and γ-methylenes (δ = 49, 26 and 49 ppm), the methyl groups in **2c–d** (δ = 22–18 ppm), and the *C*H isopropyl carbon in **2d** (δ = 28 ppm). Coordination of the NHC ligand through the carbenic carbon center is supported by the appearance of a resonance signal at approximately δ = 166–172 ppm (not detected for **2c**) together with the absence of signal where signals for the carbenic carbon atoms of the imidazolium salts appeared (δ = 145–139 ppm). The signal for the carbenic carbon center is slightly shifted to higher field with respect to that found in **1** (δ = 185–182 ppm) or in related [(NHC)Pt(0)(dvtms)] complexes (δ = 200–180 ppm; dvtms = divinyltetramethyldisiloxane).[14,18] We have previously observed the same effect in Pt/PVP/^{13}CO and Pt/dppb/^{13}CO nanoparticles (PVP = poly(*N*-vinyl-2-pyrrolidone); dppb = 1,4-bis(diphenylphosphino)butane) and proposed that it could be related to the Knight shift.[19]

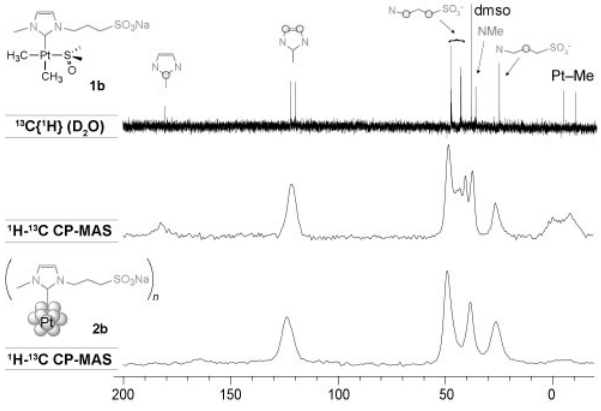

Figure 2. From top to bottom: $^{13}C\{^{1}H\}$ NMR spectrum for complex **1b** in solution in D_2O and ^{1}H–^{13}C CP-MAS NMR spectra for **1b** and **2b** in the solid state.

The carbenic carbon resonance signal was very weak in the case of **2a**, **2b** and **2d**, and undetectable for **2c**. To clear up uncertainties, we prepared nanoparticles **^{13}C-2c** containing a ^{13}C-labeled carbon in the C^2 position (i.e. the carbenic carbon atom) of the imidazolic ring (see Supporting Information for details). The size distribution of these labeled PtNPs was similar to that found for their nonlabeled analogues (1.3 ± 0.3 nm, Figure S6). The CP-MAS spectrum showed a clear resonance at the expected shift of δ = 177 ppm (Figure 3c and Figure S20).

Moreover, the observation of a $^{13}C–^{195}Pt$ coupling involving a direct ligand-MNP interaction confirmed the attachment of the carbenic carbon center to the Pt surface. Line-shape deconvolution of the peak gave a coupling value equal to 940 ± 20 Hz. As expected, the carbene carbon atom is less strongly coupled to ^{195}Pt center in **^{13}C–2c** than in molecular (NHC)Pt^0 complexes (around 1365 Hz),[18] although the interaction is still more intense than in the precursor **^{13}C-1c** (767 Hz), in which the oxidation state of the metal (+2) helps to decrease the magnitude of the coupling.[18,20] This coupling is an unambiguous indication of the carbene nature of the ligand coordinated to the Pt surface.

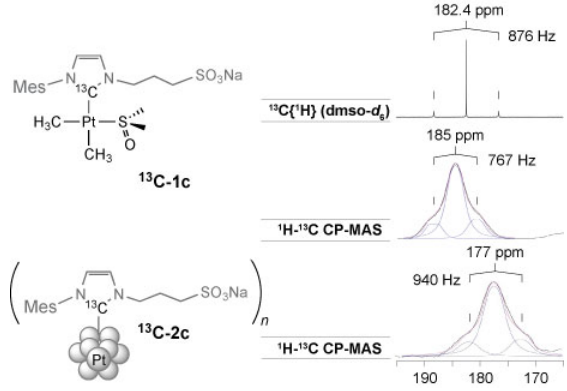

Figure 3. From top to bottom: resonance signals attributable to the Pt-bonded carbenic carbons in the $^{13}C\{^1H\}$ NMR spectrum of **^{13}C-1c** and the $^1H–^{13}C$ CP-MAS NMR spectra of **^{13}C-1c** and **^{13}C-2c**, displaying their corresponding deconvolution curves.

To determine the free sites on the surface, solid samples of **^{13}C-2c** were treated with ^{13}CO under mild conditions (room temperature, 1 bar). Unfortunately, the CP-MAS spectra of the resulting MNPs did not show any ^{13}CO coordination, although the IR spectra of samples recorded immediately after ^{13}CO treatment (within 5 min of removal of the gas) showed a band corresponding to CO adsorbed with a terminal mode of coordination (2010 cm^{-1}). However, this CO desorbed quite quickly and the band disappeared completely after 1 h (Figure S12). The lability of CO as a ligand contrasts with the stability showed by the NHC coordination.

Even after 72 h of dialysis, the ^1H NMR spectrum of nanoparticles **2a** showed the presence of sharp resonance signals in addition to the typical broad signals of the surface-coordinated NHC ligands (Figure S13). These sharp resonances are assigned to a bis(carbene) complex of formula $Na_3[PtMe(OH_2)(NHC)_2]$ (**3a**) based on the chemical shifts and integrals measured by ^1H NMR spectroscopy and the detection of the fragment [**3a**–Na–H_2O]$^-$ in the ESI-MS spectrum of MNPs **2a** (Figure S23). Their persistence after dialysis is ascribed to the association, presumably by electrostatic interactions, of complex **3a** in a second coordination sphere around nanoparticle **2a** (nano-object **2a**/**3a**, Scheme 3). This interpretation is

supported by diffusion ordered NMR spectroscopy (DOSY), which gave almost the same diffusion coefficients for the nano-object components **2a** (broad signals, 2.5 ± 0.3 × 10^{-10} m^2/s) and **3a** (sharp signals, 2.8 ± 0.3 × 10^{-10} m^2/s), whereas those for the imidazolium salt (**aH**, Scheme 1) and complex **1a** were higher (5.4 and 4.2 ± 0.3 × 10^{-10} m^2/s, respectively). DLS measurements consistently indicated a hydrodynamic diameter of 5.9 ± 1.8 nm for **2a** (*i.e.*, the nano-object **2a/3a**) and of 2.2 ± 0.5, 1.6 ± 0.6 and 1.6 ± 0.7 nm for **2b-d**, respectively. These values are in good agreement with the sizes measured by TEM for **2b**-**d** (2.0 ± 0.3, 1.3 ± 0.4 and 1.3 ± 0.4 nm, respectively) but not for **2a** (1.6 ± 0.4 nm). As no saturation transfer was detected by 2D–NMR exchange spectroscopy (EXSY), complex **3a** does not exchange with the NHC ligands on the PtNP surface.

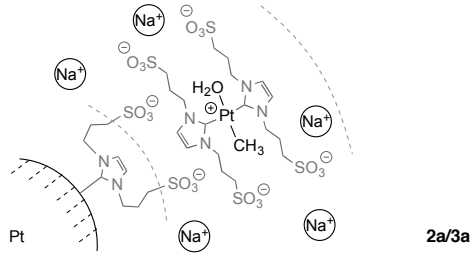

Scheme 3. Second coordination sphere in the nano-object **2a**/**3a**.

Further support for the formulation proposed for complex **3a** was obtained from treatment of the nano-object **2a/3a** with ^{13}CO at 3 bars in D_2O. Under these conditions, the complex *trans*-$Na_3[PtMe(^{13}CO)(NHC)_2]$ (**4a**) was formed (Scheme S1). The structure proposed for **4a** is supported by detection of the ion [**4a** – Na]$^-$ in the ESI-MS spectrum of the resulting solution, the resonance signal in the ^{13}C NMR spectrum for the coordinated ^{13}CO ligand at δ = 175 ppm, and a cross peak in the ^1H–^{13}C HMBC spectrum between this ^{13}CO resonance signal and that of the protons on the Pt–CH_3 moiety (Figures S24–S27). Additionally, the ^1H–^{13}C coupling of 1.6 Hz between the signals attributable to the CH_3 and CO ligands is in agreement with a *trans* stereochemistry. Complex **4a** must remain attached to the MNP (nano-object **2a**/**4a**) as the DOSY measurements showed similar diffusion coefficients for this complex (2.9 ± 0.4 × 10^{-10} m^2/s) and the nano-object **2a**/**3a** (2.8 ± 0.3 × 10^{-10} m^2/s). A biscarbene complex (**3b**) was also detected by ^1H NMR spectroscopy during the formation of PtNPs from complex **1b** but not in the case of complexes with the more sterically demanding NHC ligands **1c** or **1d**. The ^{13}C(NHC)–^{195}Pt coupling in complex **3b** (1042 Hz) is in accordance with reported values for bis(NHC)platinum(II) complexes (see the Supporting Information for other characterization data).[21] In contrast to **3a**, complex **3b** was washed away during dialysis, suggesting that the two flexible and anionic propylsulfonate groups are important for formation of the second coordination sphere in the nano-object **2a**/**3a**.

The PtNPs catalyzed the chemoselective hydrogenation of styrene to ethylbenzene at room temperature in water at 1 bar of H_2 (Table S1). The reactions were almost complete after 1 hour with Pt loadings of 0.4–0.6 mol%, except in the case of the nano-object **2a**/**3a**, where the second coordination sphere might hinder mass transfer to the reactive metal surface. The mono(NHC) Pt^{II} complexes **1** were much less active than their corresponding PtNPs even at higher catalyst loadings (Supporting Information). After extraction of the organic components with toluene, aqueous solutions containing MNPs **2d** were reused in nine consecutive recovery cycles with no noticeable modification of the catalytic performance (Figure S29) and with only a 0.44% loss of the starting Pt metal in the overall process (determined by ICP-MS analysis). TEM imaging showed that the MNPs retained their morphologies after the ninth recycling series (Figure S30).

CONCLUSIONS

In conclusion, unprecedented water-soluble PtNPs stabilized by NHC ligands can be obtained by thermal decomposition of dimethylplatinum(II) precursors containing sulfonated NHC ligands in water. Solution NMR spectroscopy studies, including diffusion measurements, revealed that the high stability and solubility of these MNPs in water is a consequence of the strong and inert coordination of the hydrophilic NHC ligand to the Pt surface. Unambiguous evidence for ligand coordination has been obtained by ^{13}C isotopic labeling of the carbenic carbon center, thus allowing observation of the first coupling (^{13}C–^{195}Pt) between ligands and PtNPs. Additionally, we have demonstrated the formation of a novel system involving the association of a nanoparticle with a molecular complex that remains coordinated to the particle but can still react with CO. This interesting finding may find a use in the design of associations between nanoparticles and molecular complexes with a view to, for example, cascade catalytic reactions. The results herein open up new routes towards catalytically active and water-stable metal nanoparticles.

ASSOCIATED CONTENT

Supporting Information

Procedures, NMR spectra of labeled compounds, TEM images and other characterization data. This material is available free of charge on the WWW under http://dx.doi.org/10.1002/anie.201407758.

AUTHOR INFORMATION

Corresponding Authors

*Email: juanc.flores@uah.es (J.C.F.), ernesto.dejesus@uah.es (E.d.J), chaudret@insa-toulouse.fr (B.C.).

ACKNOWLEDGMENT

This work was supported by the Spanish Ministerio de Economía y Competitividad (project CTQ2011-24096) and CNRS and ANR (Siderus project ANR-08-BLAN-0010-03). We thank Y. Coppel (LCC) and P.F. Fazzini (LPCNO) for NMR and TEM/HR-TEM measurements, respectively. E.A.B. is grateful to the Universidad de Alcalá for a FPI Doctoral Fellowship and S.T. to the European Commission for a postdoctoral grant (PCIG11-GA-2012-317692).

EXPERIMENTAL SECTION

Synthesis of nanoparticles: The corresponding Pt complex **1** (0.945 mmol) was introduced into a 50 mL Schlenk flask and dissolved in deionized water (5 mL). The resulting colorless to pale-yellow solutions were stirred at 1000 rpm and heated at 80 ºC for 18 h. The resulting black solutions were left to reach room temperature slowly, filtered through a PTFE 0.2 μm filter, and dialyzed for 36 h in water using a cellulose membrane (MWCO = 14000 Dalton).

REFERENCES

(1) a) *Clusters and Colloids: From Theory to Applications* (Ed.: G. Schmid), Wiley-VCH, Weinheim, Germany, **1994**; b) *Nanoparticles. From Theory to Application* (Ed.: G. Schmid), Wiley-VCH, Weinheim, Germany, **2004**; c) A. Roucoux, K. Philippot, in *Handbook of Homogeneous Hydrogenations* (Eds.: J. G. de Vries, C. J. Elsevier), Wiley-VCH, Weinheim, **2008**, pp. 217-256; d) *Nanoparticles and Catalysis* (Ed.: D. Astruc), Wiley-Interscience, New York, **2008**.

(2) L. S. Ott, R. G. Finke, *Coord. Chem. Rev.* **2007**, *251*, 1075-1100.

(3) a) *N-Heterocyclic Carbenes: From Laboratory Curiosities to Efficient Synthetic Tools* (Ed.: S. Diez-Gonzalez), The Royal Society of Chemistry, Cambridge, UK, **2011**; b) M. C. Jahnke, F. E. Hahn, in *Transition Metal Complexes of Neutral h^1-Carbon Ligands* (Eds.: R. Chauvin, Y. Canac), Topics in Organometallic Chemistry 30; Springer, Berlin Heidelberg, **2010**, pp. 95-129; c) F. E. Hahn, M. C. Jahnke, *Angew. Chem. Int. Ed.* **2008**, *47*, 3122-3172; d) O. Kühl, *Chem. Soc. Rev.* **2007**, *36*, 592-607.

(4) P. Lara, O. Rivada-Wheelaghan, S. Conejero, R. Poteau, K. Philippot, B. Chaudret, *Angew. Chem. Int. Ed.* **2011**, *50*, 12080-12084.

(5) D. Gonzalez-Galvez, P. Lara, O. Rivada-Wheelaghan, S. Conejero, B. Chaudret, K. Philippot, P. W. N. M. van Leeuwen, *Catal. Sci. Tech.* **2013**, *3*, 99-105.

(6) M. Planellas, R. Pleixats, A. Shafir, *Adv. Synth. Catal.* **2012**, *354*, 651-662.

(7) K. V. S. Ranganath, J. Kloesges, A. H. Schäfer, F. Glorius, *Angew. Chem. Int. Ed.* **2010**, *49*, 7786-7789.

(8) C. Richter, K. Schaepe, F. Glorius, B. J. Ravoo, *Chem. Commun.* **2014**, *50*, 3204-3207.

(9) E. C. Hurst, K. Wilson, I. J. S. Fairlamb, V. Chechik, *New J. Chem.* **2009**, *33*, 1837-1840.

(10) J. Vignolle, T. D. Tilley, *Chem. Commun.* **2009**, 7230-7232.

(11) X. Ling, N. Schaeffer, S. Roland, M.-P. Pileni, *Langmuir* **2013**, *29*, 12647-12656.

(12) P. Lara, A. Suárez, V. Collière, K. Philippot, B. Chaudret, *ChemCatChem* **2014**, *6*, 87-90.

(13) The coating of planar metal surfaces with NHCs has been studied in a) T. Weidner, J. E. Baio, A. Mundstock, C. Große, S. Karthäuser, C. Bruhn, U. Siemeling, *Aust. J. Chem.* **2011**, *64*, 1177-1179; b) A. V. Zhukhovitskiy, M. G. Mavros, T. Van Voorhis, J. A. Johnson, *J Am. Chem. Soc.* **2013**, *135*, 7418-7421; c) C. M. Crudden, J. H. Horton, I. I. Ebralidze, O. V. Zenkina, A. B. McLean, B. Drevniok, Z. She, H.-B. Kraatz, N. J. Mosey, T. Seki, E. C. Keske, J. D. Leake, A. Rousina-Webb, G. Wu, *Nat. Chem.* **2014**, *6*, 409-414.

(14) a) G. F. Silbestri, J. C. Flores, E. de Jesús, *Organometallics* **2012**, *31*, 3355-3360; b) E. A. Baquero, J. C. Flores, J. Perles, P. Gomez-Sal, E. de Jesús, **2014**, 5470-5482.

(15) E. A. Baquero, G. F. Silbestri, P. Gómez-Sal, J. C. Flores, E. de Jesús, *Organometallics* **2013**, *32*, 2814-2826.

(16) a) E. Ramirez, L. Eradès, K. Philippot, P. Lecante, B. Chaudret, *Adv. Func. Mater.* **2007**, *17*, 2219-2228; b) E. Ramirez, S. Jansat, K. Philippot, P. Lecante, M. Gomez, A. M. Masdeu-Bultó, B. Chaudret, *J. Organomet. Chem.* **2004**, *689*, 4601-4610.

(17) I. Favier, S. Massou, E. Teuma, K. Philippot, B. Chaudret, M. Gomez, *Chem. Commun.* **2008**, 3296-3298.

(18) G. Berthon-Gelloz, O. Buisine, J.-F. Brière, G. Michaud, S. Stérin, G. Mignani, B. Tinant, J.-P. Declercq, D. Chapon, I. E. Markó, *J. Organomet. Chem.* **2005**, *690*, 6156-6168.

(19) S. Kinayyigit, P. Lara, P. Lecante, K. Philippot, B. Chaudret, *Nanoscale* **2014**, *6*, 539-546.

(20) a) D. Tapu, D. A. Dixon, C. Roe, *Chem. Rev.* **2009**, *109*, 3385-3407; b) B. M. Still, P. G. A. Kumar, J. R. Aldrich-Wright, W. S. Price, *Chem. Soc. Rev.* **2007**, *36*, 665-686; c) K. A. Netland, A. Krivokapic, M. Tilset, *J. Coord. Chem.* **2010**, *63*, 2909-2927.

(21) a) O. Rivada-Wheelaghan, B. Donnadieu, C. Maya, S. Conejero, *Chem. Eur. J.* **2010**, *16*, 10323-10326; b) O. Rivada-Wheelaghan, M. A. Ortuño, J. Díez, A. Lledós, S. Conejero, *Angew. Chem. Int. Ed.* **2012**, *51*, 3936-3939; c) O. Rivada-Wheelaghan, M. Roselló-Merino, M. A. Ortuño, P. Vidossich, E. Gutiérrez-Puebla, A. Lledós, S. Conejero, *Inorg. Chem.* **2014**, *53*, 4257-4268.

Angewandte Chemie
Eine Zeitschrift der Gesellschaft Deutscher Chemiker

Supporting Information

69451 Weinheim, Germany

Highly Stable Water–Soluble Platinum Nanoparticles Stabilized by Hydrophilic N-Heterocyclic Carbenes

Edwin A. Baquero,[1] Simon Tricard,[2] Juan C. Flores,[1] Ernesto de Jesús,[1]* and Bruno Chaudret[2]**

[1] Departamento de Química Orgánica y Química Inorgánica, Campus Universitario, Universidad de Alcalá, 28871 Alcalá de Henares, Madrid, Spain.

[2] Laboratoire de Physique et Chimie de Nano–Objets, CNRS, INSA, Université de Toulouse, 135, Avenue de Rangueil, 31077 Toulouse, France.

anie_201407758_sm_miscellaneous_information.pdf

Table of Contents

1. General procedures and characterization techniques

All operations were carried out under argon atmosphere using standard Schlenk tube or Fischer-Porter bottle techniques. Unless otherwise stated, reagents and solvents were used as received from commercial sources. Argon, N_2 and H_2 were purchased from Air Liquide, ^{13}CO (^{13}C, 99.14%) from Eurisotop, styrene (>99%) and dodecane (>99%) from Acros Organics, formaldehyde-^{13}C (20% wt in water, atom 99% ^{13}C), 1,3-propanesultone and dialysis tubing cellulose membrane (average flat width 25mm, molecular weight cut-off = 14000 Dalton) from Sigma-Aldrich. Deionized water (type II quality) was obtained using a Millipore Elix 10 UV Water Purification System. Dimethyl sulfoxide was distilled under argon over calcium hydride. Complexes *cis*-[$Pt(CH_3)_2$(dmso)(NHC)] **1**,[1] ^{13}C-labeled *N*–mesitylimidazole,[2] and *cis*-dimethylbis(dimethyl sulfoxide)platinum(II),[3] were synthesized as described in the literature.

Samples for TEM and HRTEM were prepared by deposition after evaporation on a covered holey copper grid of three drops of the nanoparticles in water (0.5 mL) dispersed in EtOH (2 mL), or a drop of the crude aqueous colloidal solution. TEM analyses were performed at the "Service Commun de Microscopie Electronique de l'Université Paul Sabatier" (TEMSCAN-UPS) by using a JEOL JEM 1011 CX-T electron microscope operating at 100 kV with a point resolution of 4.5 Å. The approximation of the particles mean size was made through a manual analysis of enlarged micrographs by measuring a large number of particles (> 250) using ImageJ software to analyse the images. HRTEM observations were carried out with a JEOL JEM 2010 electron microscope, working at 200 kV with a resolution point of 2.35 Å. FFT treatments have been carried out with Digital Micrograph Version 1.80.70.

Solid state NMR with ^{1}H-^{13}C cross polarization (CP-MAS NMR) were performed at the LCC (Toulouse) on a Bruker Avance 400WB instrument equipped with a 2.5 mm probe with the sample rotation frequency being set at 12 kHz. Measurements were carried out in a 4 mm ZrO_2 rotor. ^{1}H-, ^{13}C-, and ^{195}Pt-NMR spectra in liquid phase were recorded on a Bruker AMX 500 NMR, Bruker Avance 400 MHz, Varian Mercury 300 or Unity 300 MHz spectrometers. Chemical shifts (δ, parts per million) are quoted relative to $SiMe_4$ (^{1}H, ^{13}C) and K_2PtCl_6 in water (^{195}Pt). They were measured by internal referencing to the ^{13}C or residual ^{1}H resonances of the deuterated solvents (D_2O ^{1}H δ 4.69; dmso–d_6 ^{1}H δ 2.49, ^{13}C δ 39.0; respectively) or by the substitution method in the case of ^{195}Pt. Coupling constants (*J*) are given in Hertz.

Gas chromatography was performed using a GC Perkin Elmer–Clarus 500 Gas Chromatograph with an Agilent S&W HP-5 non polar (5%-Phenyl)-methylpolysiloxane capillary column of 30 m × 0.32 mm × 0.25 μm (GC setting for the assessment of styrene hydrogenation catalyses: 0 min at 50 °C, and a ramp of 8 °C/min until 260 °C). IR spectra were

recorded on a Thermo Scientific Nicolet 6700 FT-IR spectrometer in the range 4000–500 cm^{-1}, using a Smart Orbit ATR platform. ICP-MS analyses were performed in the Center for Applied Chemistry and Biotechnology at the Universidad de Alcalá. The C, H, and N analyses were made by the Analytical Services of the Universidad de Alcalá using a Heraeus CHN-O-Rapid microanalyzer elemental analysis. The ESI mass spectra were performed in the analytical services of the Université de Toulouse using an a Xevo G2 QTof (Waters) mass spectrometer. DLS were measured with a Nanotrac Ultra instrument.

2. Synthesis and characterization data for water-soluble Pt nanoparticles (2a-d)

The corresponding platinum complex **1** (0.945 mmol) was introduced in a 50 mL Schlenk flask and dissolved in deionized water (5 mL). The resulting colorless to pale-yellow solutions were stirred at 1000 rpm, and heated at 80 ºC for 18 h. The black solutions formed were left to reach room temperature slowly, filtered through a PTFE 0.2 μm filter in order to remove any eventual suspended solid, and the resulting solutions were dialysed in water using a cellulose membrane (MWCO = 14000 Dalton) for 36 h. The dialyses were monitored taking aliquots of the nanoparticle solutions and analyzing by ^{1}H-NMR the disappearance of dmso and molecular species (*e.g.*, **3b** or free imidazolium salts). Subsequent solvent removal under vacuum (50 °C, 100 mbar, 3 h) afforded black solids that were dried overnight under vacuum (room temperature, 10 mbar). The platinum nanoparticles were found to be stable in water under air, without precipitation over the time (> 6 months).

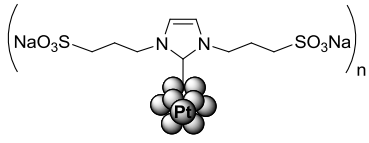

PtNPs 2a: The platinum nanoparticles **2a** were obtained from **1a** (0.623 g, 0.945 mmol) as a black powder (0.275 g, 65 % based on Pt). **TEM**: NP mean size, 1.6 ± 0.4 nm. **DLS**: 5.9 ± 1.8 nm. **HRTEM**: fcc Pt nanoparticles. **Elemental Analysis**: C, 15.27%; H, 2.770%; N, 4.434%. **ICP-MS**: Pt, 43.4%. **^{1}H-^{13}C CP-MAS NMR**: δ 172.0 (broad s, Imz-C^2), 122.5 (s, Imz-$C^{4,5}$), 49.3 (s, NCH_2 and CH_2S overlapping), 26.8 (s, $CH_2CH_2CH_2$).

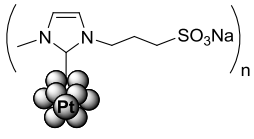

PtNPs 2b: The platinum nanoparticles **2b** were obtained from **1b** (0,500 g, 0.945 mmol) as a black powder (0.185 g, 57 % based on Pt). **TEM**: NP mean size, 2.0 ± 0.3 nm. **DLS**: 2.3 ± 0.7 nm. **HRTEM**: fcc Pt nanoparticles. **Elemental Analysis**: C, 11.97%; H, 2.314%; N, 4.073%. **ICP-MS**: Pt, 56.6%. **^{1}H-^{13}C CP-MAS NMR**: δ 166.4 (broad s, Imz-C^2), 124.0 (s, Imz-C^4 and Imz-C^5 overlapping), 49.1 (s, NCH_2 and CH_2S overlapping), 38.3 (s, NCH_3), 26.4 (s, $CH_2CH_2CH_2$).

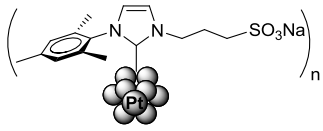

PtNPs 2c: The platinum nanoparticles **2c** were obtained from **1c** (0.599 g, 0.945 mmol) as a black powder (0.236 g, 81 % based on Pt). **TEM**: NP mean size, 1.3 ± 0.4 nm. **DLS**: 1.6 ± 0.6 nm. **HRTEM**: fcc Pt nanoparticles. **Elemental Analysis**: C, 14.78%; H, 1.826%; N, 2.580%. **ICP-MS**: Pt, 63.2%. **^{1}H-^{13}C CP-MAS NMR**: δ 135.2 (s, Ar-C^4, Ar-C^2 and Ar-C^1 overlapping), 128.9 (s, Ar-C^3), 122.1 (s, Imz-C^4 and Imz-C^5 overlapping), 48.4 (s, NCH_2 and CH_2S overlapping), 28.1 (s, $CH_2CH_2CH_2$), 18.0 (s, Ar-*p-Me* and Ar-*o-Me* overlapping), Imz-C^2 not observed.

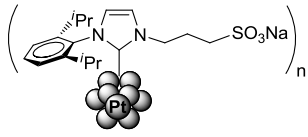

PtNPs 2d: The platinum nanoparticles **2d** were obtained from **1d** (0.639 g, 0.945 mmol) as a black powder (0.244 g, 82 % based on Pt). **TEM**: NP mean size, 1.3 ± 0.4 nm. **DLS**: 1.6 ± 0.7 nm. **HRTEM**: fcc Pt nanoparticles. **Elemental Analysis**: C, 32.13%; H, 4.140%; N, 4.436%. **ICP-MS**: Pt, 61.6%. **^{1}H-^{13}C CP-MAS NMR**: δ 172.0 (broad s, Imz-C^2), 146.3 (s, Ar-C^2), 134.5 (s, Ar-C^1), 128.5 (s, Ar-C^4), 123.9 (s, Ar-C^3, Imz-C^4 and Imz-C^5 overlapping), 48.3 (s, NCH_2 and CH_2S overlapping), 27.9 (s, $CHMe_2$, $CH_2CH_2CH_2$ overlapping), 22.5 (s, $CHMe_2$).

3. Synthesis of ^{13}C-labeled compounds and nanoparticles (^{13}C-cH, ^{13}C-1c and ^{13}C-2c)

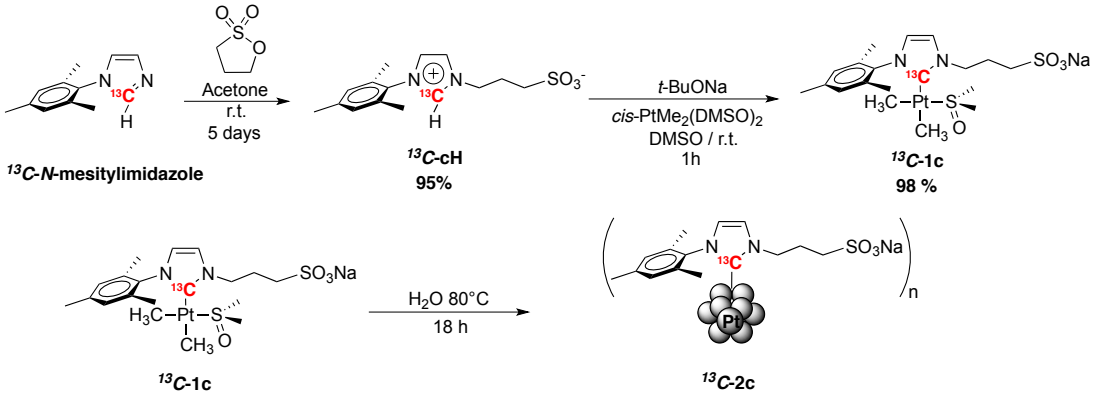

***^{13}C-N*-mesitylimidazole**

***^{13}C*-cH**
95%

***^{13}C*-1c**
98 %

***^{13}C*-1c**

***^{13}C*-2c**

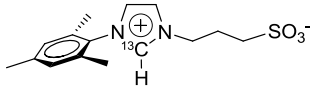

1-(3-sodiumsulfonatepropyl)-3-(2,4,6-trimethylphenyl)-2-^{13}C-imidazolium (^{13}C-cH, NMR spectra in Figure S1): A solution of 1,3-propanesultone (1.50 mL, 17.1 mmol) in acetone (5 mL) was added dropwise to a 100 mL Schlenck Flask containing another solution of ^{13}C-*N*-mesitylimidazole (0.956 g, 5.11 mmol) in the same solvent (15 mL). The resulting brown solution was stirred at room temperature for 5 days. After this period of time, the precipitate was filtered, washed with acetone (3 × 20 mL), and

dried under vacuum (2 h, 25 °C, 10 mbar). The imidazolium salt was thus obtained as a beige powder (1.502 g, 95%). ^{1}H-NMR (300 MHz, dmso-d_6): δ 9.36 (d, $^{2}J(^{1}\text{H-}^{13}\text{C})$ = 223.2, 1H, Imz-H^{2}), 8.10 (d, $^{3}J(^{1}\text{H-}^{13}\text{C})$ = 5.1, 1H, Imz-H^{5}), 7.91 (d, $^{3}J(^{1}\text{H-}^{13}\text{C})$ = 4.5, 1H, Imz-H^{4}), 7.13 (s, 2H, Ar), 4.40 (m, 2H, NCH_2), 2.43 (t, $^{3}J_{HH}$ = 7.0, 2H, CH_2S), 2.31 (s, 3H, Ar-*p*-Me), 2.18 (m, 2H, $CH_2CH_2CH_2$), 2.01 (s, 6H, Ar-*o*-Me). ^{13}C{^{1}H}-NMR (75 MHz, dmso-d_6): δ 139.7 (s, Ar-C^{4}), 137.0 (s, Imz-C^{2}), 133.8 (s, Ar-C^{2}), 130.7 (d, $^{2}J(^{13}\text{C-}^{13}\text{C})$ = 1.5, Ar-C^{1}), 128.7 (s, Ar-C^{3}), 123.3 (d, $^{2}J(^{13}\text{C-}^{13}\text{C})$ = 2.5, Imz-C^{4}), 122.7 (s, Imz-C^{5}), 47.8 (d, $^{2}J(^{13}\text{C-}^{13}\text{C})$ = 1.8, NCH_2), 46.8 (s, CH_2S), 25.5 (s, $CH_2CH_2CH_2$), 20.1 (s, Ar-*p*-Me), 16.8 (s, Ar-*o*-Me). ESI-MS (negative ion, MeOH): *m*/*z* 308.1145 [M – H]$^-$ (calcd 308.1155) 100%. ESI-MS (positive ion, MeOH): *m*/*z* 310.1305 [M + H]$^+$ (calcd 310.1301) 100%. The ^{13}C content of the imidazolium C2 carbon was estimated in 92%. This value was determined by integration of the doublet and singlet resonances corresponding, respectively, to the protons bonded to this C2 carbon in the ^{13}C– or ^{12}C–containing imidazolium salt.

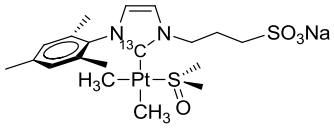

C*is*-dimethyl(dimethyl sulfoxide)[1-(3-sodiumsulfonatepropyl)-3-(2,4,6-trimethylphenyl)imidazol-2-^{13}C-ylidene]platinum(II) (^{13}C-1c, NMR spectra in Figure S2): Sodium *tert*-butoxide (0.126 g, 1.31 mmol) was added to a solution of *cis*-[$PtMe_2(dmso)_2$] (0.500 g, 1.31 mmol) and the imidazolium salt **^{13}C-cH** (0.405 g, 1.31 mmol) in dimethyl sulfoxide (10 mL). The mixture was stirred for 1 h at room temperature, and filtered through a plug of kieselguhr. After complete evaporation of the solvent (90 °C, 4 mbar), the resulting solid was dried under vacuum (12 h, 90 ºC, 4 mbar) to afford the platinum complex **^{13}C-1c** as a pale orange solid (0.815 g, 98%). ^{1}H-NMR (300 MHz, dmso-d_6): δ 7.49 (dd, $^{3}J_{HH}$ = 2.1, $^{3}J(^{1}\text{H-}^{13}\text{C})$ = 2.4, 1H, Imz), 7.13 (dd, $^{3}J_{HH}$ = 2.1, $^{3}J(^{1}\text{H-}^{13}\text{C})$ = 2.4, 1H, Imz), 6.95 (s, 2H, Ar), 4.37 (m, 1H, NCH_2), 4.26 (m, 1H, NCH_2), 2.84 (s br, 6H, Me_2SO), 2.46 (m, 2H, CH_2S), 2.27 (s, 3H, Ar-*p*-Me), 2.16 (m, 2H, $CH_2CH_2CH_2$), 2.07 (s, 3H, Ar-*o*-Me), 1.99 (s, 3H, Ar-*o*-Me), 0.10 (d with ^{195}Pt satellites, $^{2}J(^{1}\text{H-}^{195}\text{Pt})$ = 80.7, $^{3}J(^{1}\text{H-}^{13}\text{C})$ = 1.8, 3H, PtMe *cis* to NHC), -0.36 (d with ^{195}Pt satellites, $^{2}J(^{1}\text{H-}^{195}\text{Pt})$ = 60.9, $^{3}J(^{1}\text{H-}^{13}\text{C})$ = 1.8, 3H, PtMe *trans* to NHC). ^{13}C{^{1}H}-NMR (75 MHz, dmso-d_6): δ 182.4 (s with ^{195}Pt satellites, $^{1}J(^{13}\text{C-}^{195}\text{Pt})$ = 876, Imz-C^{2}), 136.7 (s, Ar-C^{4}), 135.9 (d, $^{3}J(^{13}\text{C-}^{13}\text{C})$ = 5.4, Ar-C^{2}), 134.9 (d, $^{2}J(^{13}\text{C-}^{13}\text{C})$ = 36.9, Ar-C^{1}), 128.0 (d, $^{4}J(^{13}\text{C-}^{13}\text{C})$ = 4.3, Ar-C^{3}), 121.8 (s, Imz-C^{4}), 120.0 (s, Imz-C^{5}), 48.2 (d, $^{2}J(^{13}\text{C-}^{13}\text{C})$ = 7.0, NCH_2), 48.0 (s, CH_2S), 25.9 (s, $CH_2CH_2CH_2$), 20.1 (s, Ar-*p*-Me), 17.8 (s, Ar-*o*-Me), 17.7 (s, Ar-*o*-Me), -0.83 (d, $^{2}J(^{13}\text{C-}^{13}\text{C})$ = 31.6, PtMe *trans* to NHC), -8.5 (s, PtMe *cis* to NHC). ^{195}Pt-NMR (64 MHz, dmso-d_6): δ –3985 (d, $^{1}J(^{195}\text{Pt-}^{13}\text{C})$ = 882). ESI-MS (negative ion, H_2O): *m*/*z* 611.1352 [M – Na]$^-$ (calcd 611.1412)

3%; 533.1262 [M – Na – DMSO]$^-$ (calcd 533.1273) 4%; 517.0956 [M – Na – DMSO – CH_4]$^-$ (calcd 517.0960) 100%; 501.0647 [M – Na – DMSO – $2CH_4$]$^-$ (calcd 501.0647) 12%. Anal. Calcd (%) for $C_{18}{}^{13}CH_{31}N_2NaO_4PtS_2(5{\cdot}H_2O)$: C, 31.62; H, 5.70; N, 3.87. Found (%): C, 31.86; H, 5.20; N, 4.29.

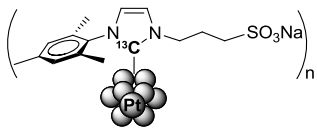

^{13}C-Labeled platinum nanoparticles (^{13}C-2c): The platinum complex **^{13}C-1c** (0.600 g, 0.945 mmol) was introduced into a 50 mL Schlenck flask and dissolved in deionized water (5 mL). The resulting pale orange solution was stirred at 1000 rpm, and heated at 80 ºC during 18 h. After this period of time, the black solution was left to reach room temperature slowly and then filtered through a PTFE 0.2 μm filter in order to remove any particle in suspension. The resulting solution was dialyzed against water using a cellulose membrane (MWCT = 14000 Dalton) for 36 h. The dialyses were monitored taking aliquots of the nanoparticle solutions and analyzing by ^{1}H-NMR the disappearance of dmso and molecular species. Subsequent removal of the solvent under vacuum (3h, 50 ºC, 100 mBar) gave a black solid that was dried overnight under vacuum (25 ºC, 10 mBar). The platinum nanoparticles **^{13}C-2c** were obtained as a black powder (0.235 g, 83% based on Pt). They were found to be stable in water under air, without precipitation after several months. **TEM**: NP mean size, 1.3 ± 0.4 nm. **DLS**: 1.6 ± 0.6 nm. **ICP-MS**: Pt, 65.2%. **^{1}H-^{13}C CP-MAS NMR**: δ 177.2 (s with ^{195}Pt satellites, $^1J(^{13}C\text{-}^{195}Pt)$ = 940 ± 20, Imz-C^2), 138.3 (s, Ar-C^4, Ar-C^2, and Ar-C^1 overlapping), 130.4 (s, Ar-C^3), 122.5 (s, Imz-C^4 and Imz-C^5 overlapping), 47.9 (s, NCH_2 and CH_2S overlapping), 26.5 (s, $CH_2CH_2CH_2$), 20.3 (s, Ar-*p*-*Me*), 18.0 (s, Ar-*o*-*Me*).

4. ^{1}H- and ^{13}C-NMR spectra for ^{13}C-labeled compounds (^{13}C-cH and ^{13}C-1c)

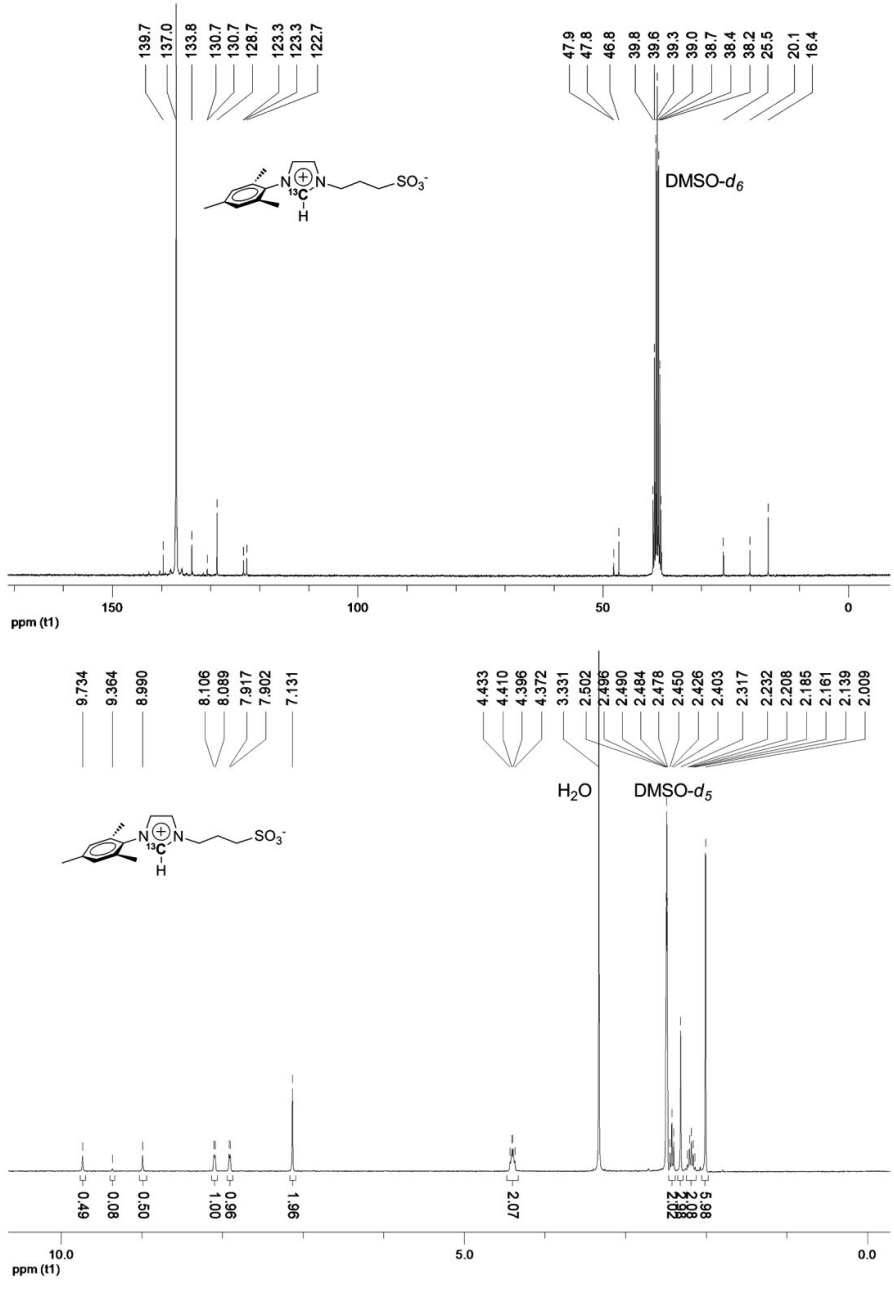

Figure S1. ^{1}H- (300 MHz) and ^{13}C-NMR (75 MHz) spectra for **^{13}C-cH**.

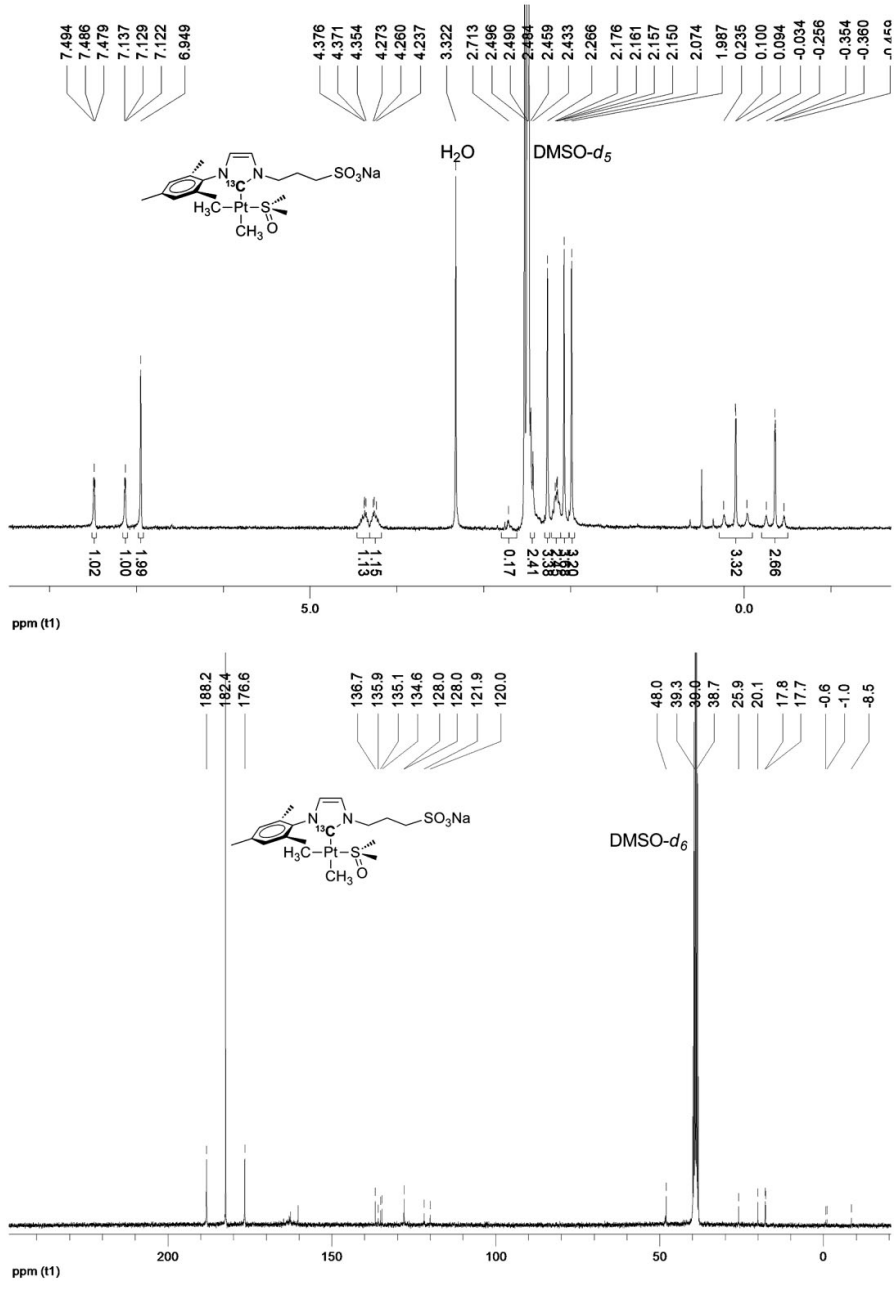

Figure S2. ^{1}H- (300 MHz) and ^{13}C-NMR (75 MHz) spectra for **^{13}C-1c**.

5. TEM and HRTEM images for the Pt nanoparticles

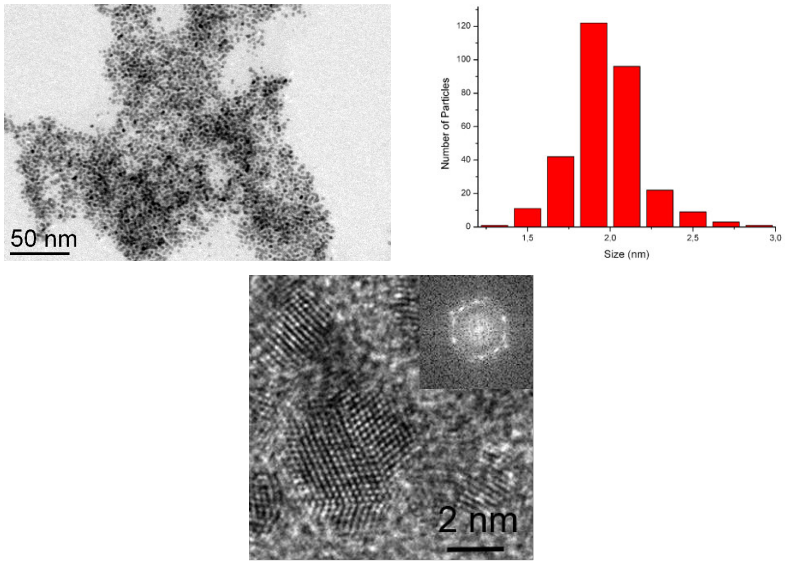

Figure S3. TEM and HRTEM images with the corresponding size distribution and FFT picture obtained for PtNPs **2b**.

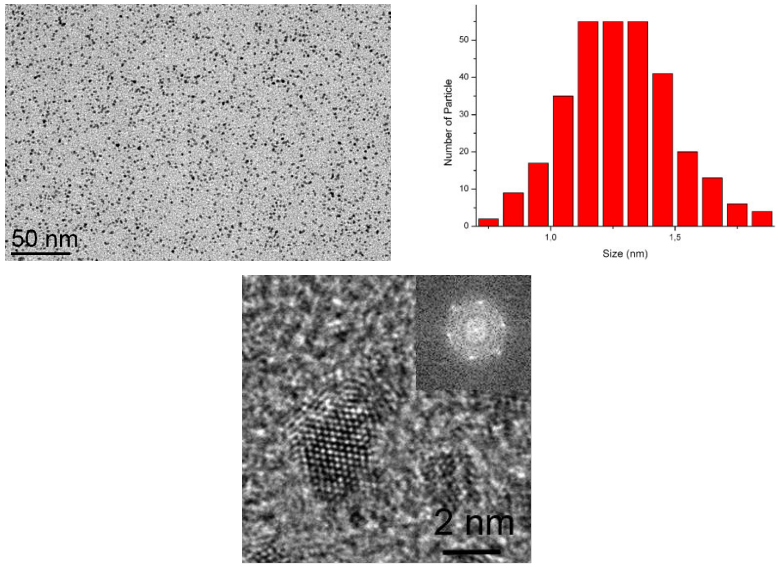

Figure S4. TEM and HRTEM images with the corresponding size distribution and FFT picture obtained for PtNPs **2c**.

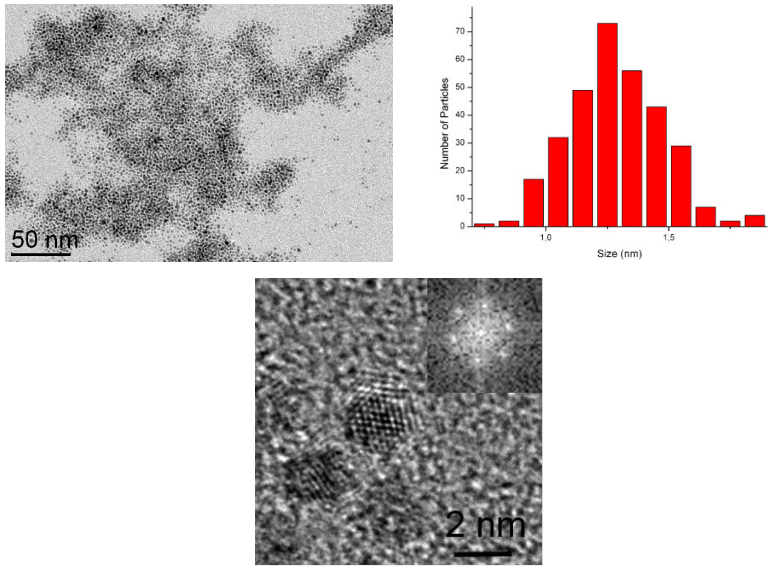

Figure S5. TEM and HRTEM images with the corresponding size distribution and FFT picture obtained for PtNPs **2d**.

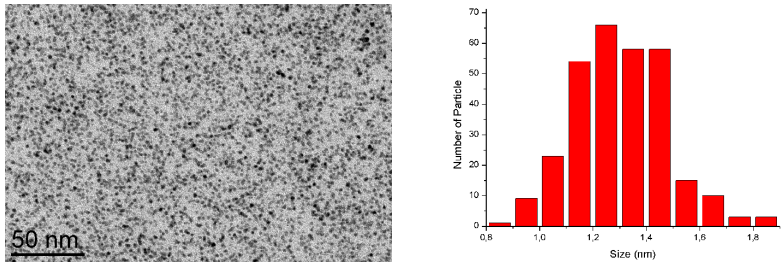

Figure S6. TEM image with the corresponding size distribution obtained for PtNPs ^{13}**C-2c**.

6. ATR-FTIR spectra of the imidazolium salts, Pt complexes and Pt nanoparticles

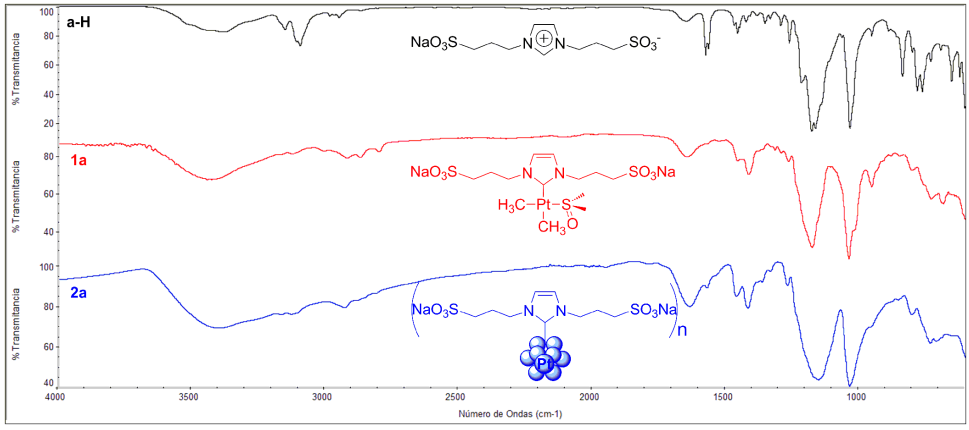

Figure S7. ATR-FTIR spectra of **aH**, **1a** and **2a**.

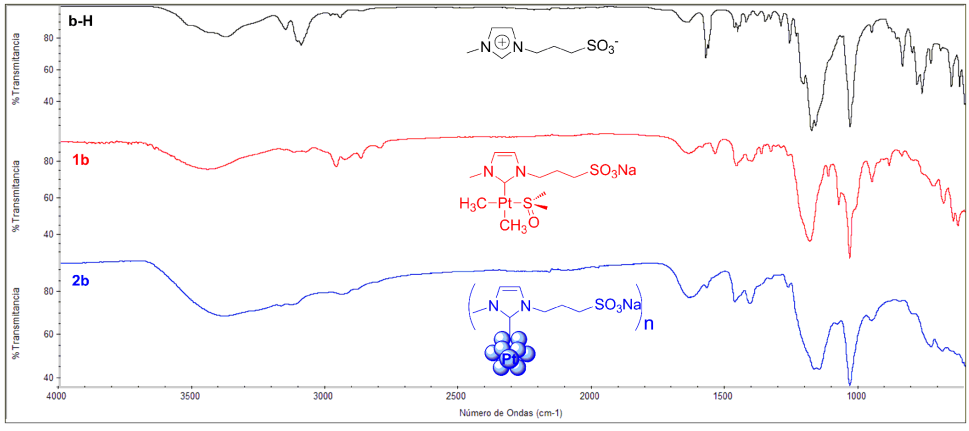

Figure S8. ATR-FTIR spectra of **bH**, **1b** and **2b**.

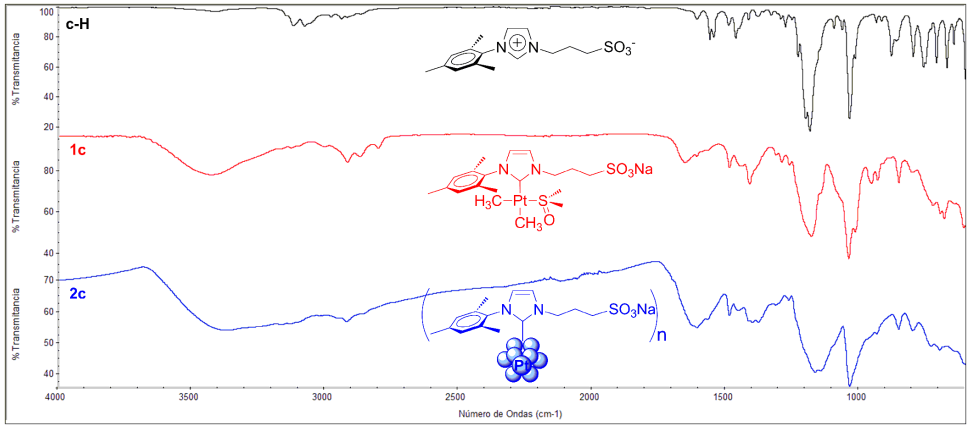

Figure S9. ATR-FTIR spectra of **cH**, **1c** and **2c**.

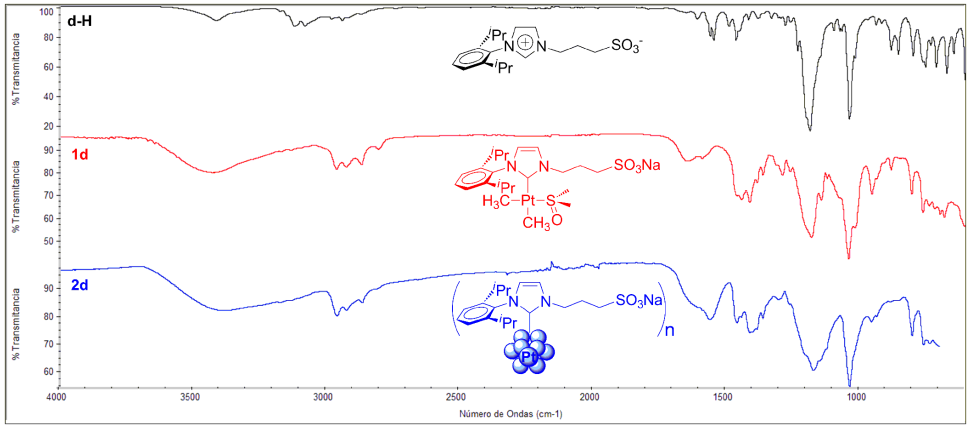

Figure S10. ATR-FTIR spectra of **dH**, **1d** and **2d**.

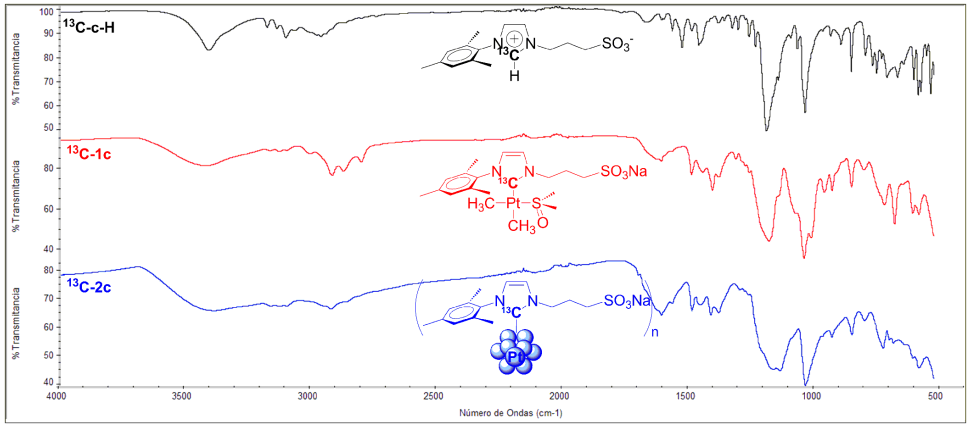

Figure S11. ATR-FTIR spectra of **^{13}C-cH**, **^{13}C-1c** and **^{13}C-2c**.

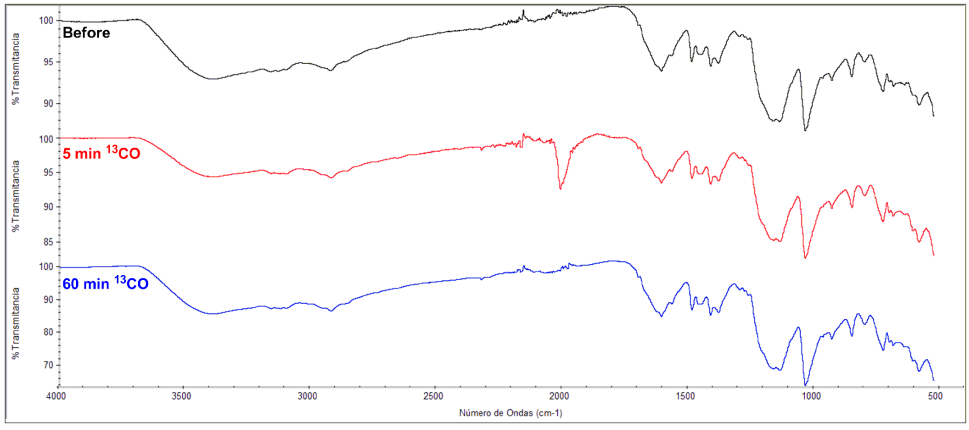

Figure S12. ATR-FTIR spectra of **^{13}C-2c** before treatment with ^{13}CO, 5 min after treatment with ^{13}CO, and 1 hour after treatment with ^{13}CO.

7. ^{1}H-NMR spectra for Pt nanoparticles

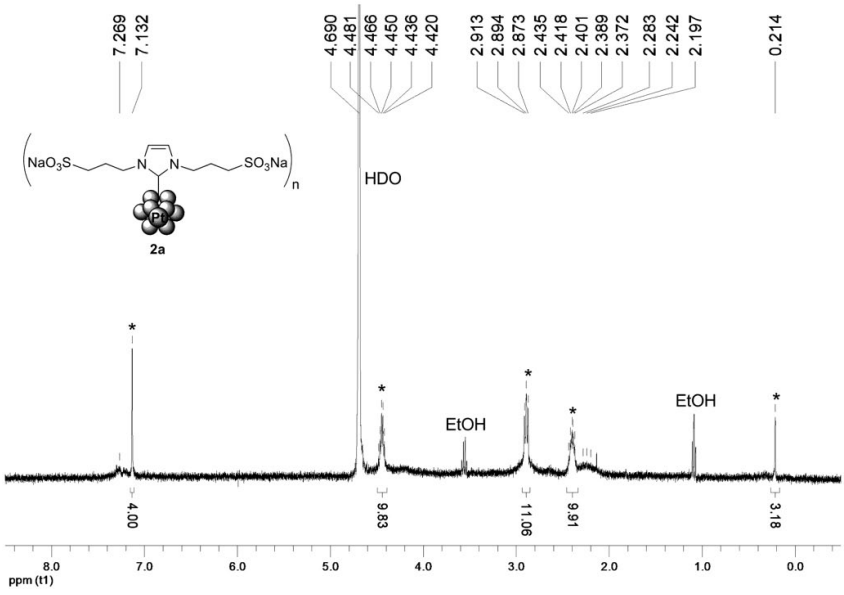

Figure S13. ^{1}H-NMR (400 MHz) for PtNPs **2a** (*i.e.*, pair **2a/3a**) in D_2O. Resonances marked with an asterisk correspond to the bis(carbene) complex **3a**, which is located in a second coordination sphere around NPs **2a**.

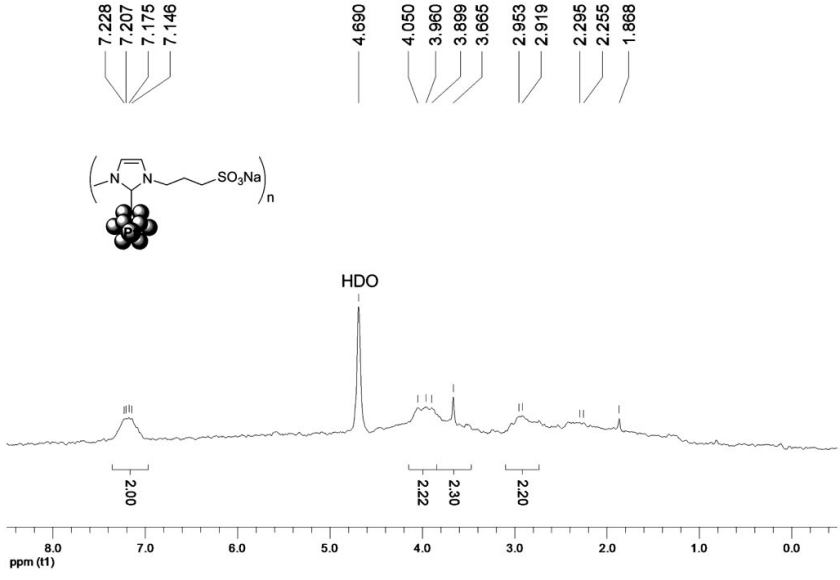

Figure S14. ^{1}H-NMR (400 MHz) for PtNPs **2b** in D_2O, recorded with solvent suppression.

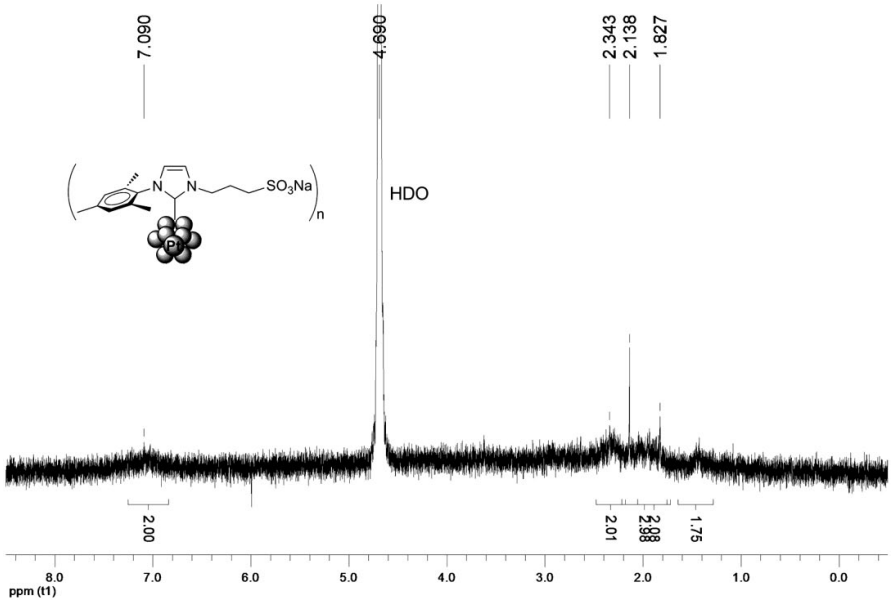

Figure S15. ^{1}H-NMR (400 MHz) for PtNPs **2c** in D_2O.

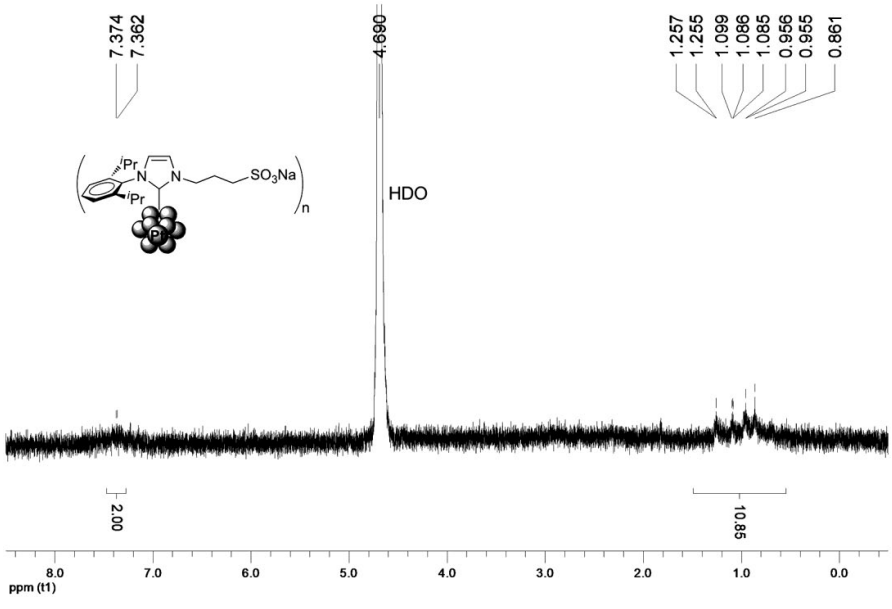

Figure S16. ^{1}H-NMR (400 MHz) for PtNPs **2d** in D_2O.

8. ^{1}H-^{13}C CP-MAS NMR spectra for imidazolium salts, Pt complexes and Pt nanoparticles

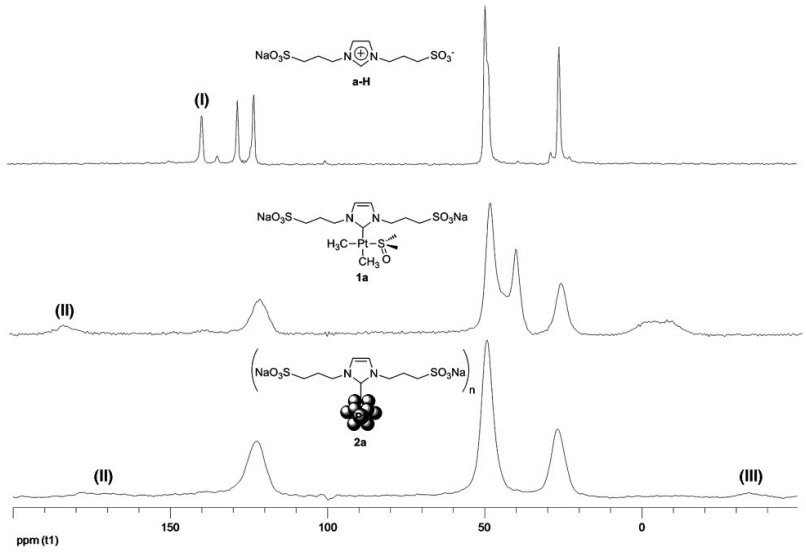

Figure S17. ^{1}H-^{13}C CP-MAS NMR spectra for **aH**, **1a** and **2a** (*i.e.*, pair **2a/3a**). Resonances (I) and (II) correspond to C^{2}_{Imz}–H and Pt–C^{2}_{NHC} carbons, respectively, and (III) to the Pt–CH_3 group in complex **3a**.

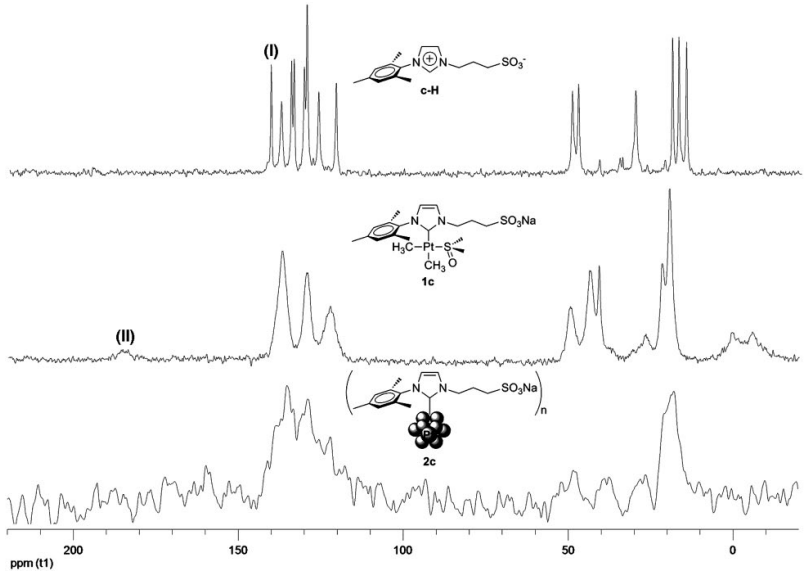

Figure S18. ^{1}H-^{13}C CP-MAS NMR spectra for **cH**, **1c** and **2c**. Resonances (I) and (II) correspond to C^{2}_{Imz}–H and Pt–C^{2}_{NHC} carbons, respectively.

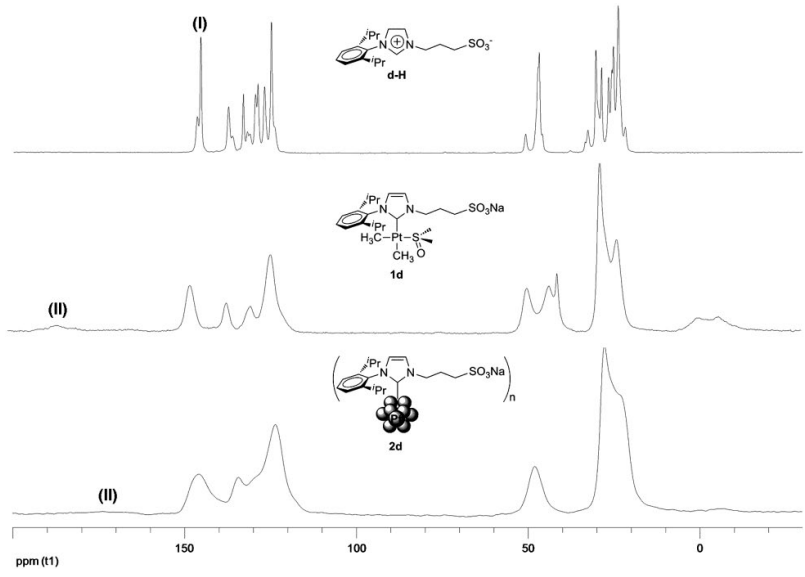

Figure S19. ^{1}H-^{13}C CP-MAS NMR spectra for **dH**, **1d** and **2d**. Resonances (I) and (II) correspond to C^{2}_{Imz}–H and Pt–C^{2}_{NHC} carbons, respectively.

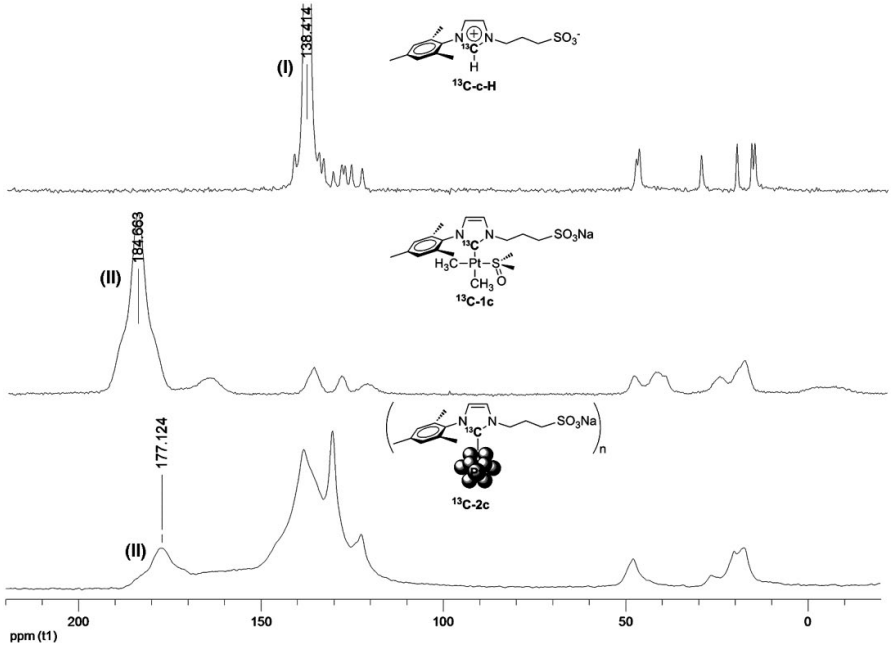

Figure S20. ^{1}H-^{13}C CP-MAS NMR spectra for **^{13}C-cH**, **^{13}C-1c** and **^{13}C-2c**. Resonances (I) and (II) correspond to $^{13}C^{2}_{Imz}$–H and Pt–$^{13}C^{2}_{NHC}$ carbons, respectively.

9. Characterization of nano-object 2a/3a

Reactions with ^{13}CO were carried out in order to get information about the molecular species persistently present in PtNPs **2a** (resonances marked with an asterisk in Figure S13). In these experiments, a solution of the dialyzed nanoparticles **2a** in D_2O (5 mg/mL) was introduced into a Fischer Porter bottle, charged with ^{13}CO at 3 bar, and stirred at room temperature overnight (12 h). The solution was then analyzed by NMR spectroscopy and ESI mass spectrometry. The NMR and MS data corresponding to the complex are given before (**3a**) and after (**4a**) reaction with ^{13}CO.

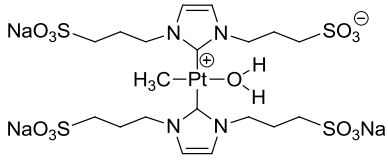

Trisodium *trans*-aquamethylbis[1,3-bis(3-sulfonatepropyl)imidazol-2-ylidene]platinate(3–) (3a): ^{1}H-NMR (400 MHz, D_2O): δ 7.13 (s, 4H, Imz), 4.44 (m, 8H, NCH_2), 2.89 (t, $^3J_{HH}$ = 8.4, 8H, CH_2S), 2.40 (m, 4H, $CH_2CH_2CH_2$), 0.21 (s, 3H, PtMe). $^{13}C\{^1H\}$-NMR (75 MHz, D_2O): δ 169.6 (s, Imz-C^2), 121.9 (s, Imz-$C^{4,5}$), 48.8 (s, NCH_2), 47.9 (s, CH_2S), 25.2 (s, $CH_2CH_2CH_2$), –15.8 (s, PtMe). ESI-MS (negative ion, H_2O/D_2O 2:1): m/z 876.0267 $[M - H_2O - Na]^-$ (calcd 876.0266) 15%; 838.0 $[M - H_2O - 2Na - CH_3]^-$ (calcd 838.0) 36%; 816.0 $[M - H_2O - 3Na - CH_3 + H]^-$ (calcd 816.0) 13%; 504.0 $[M - H_2O - NHC - 3Na - CH_4]^-$ (calcd 504.0) 100%.

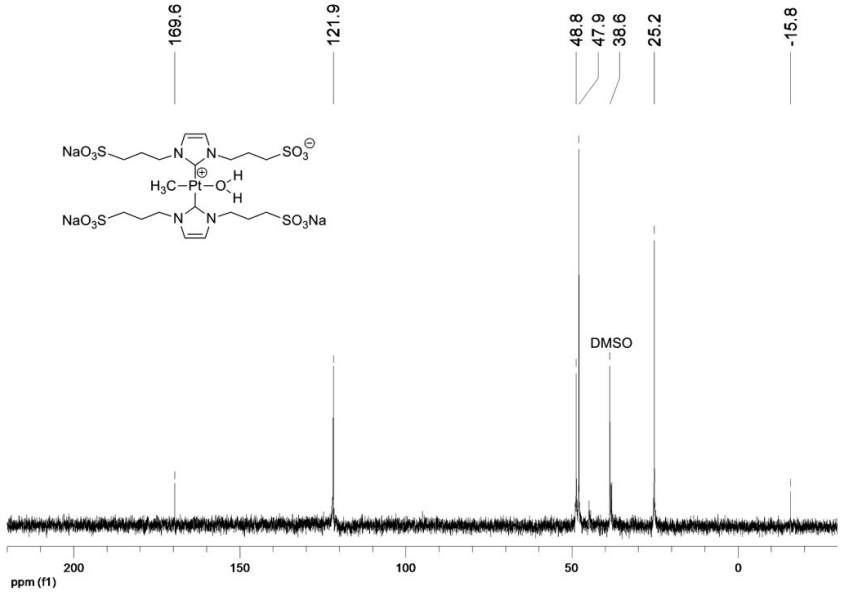

Figure S21. ^{13}C NMR (75 MHz) spectrum for **2a**/**3a**.

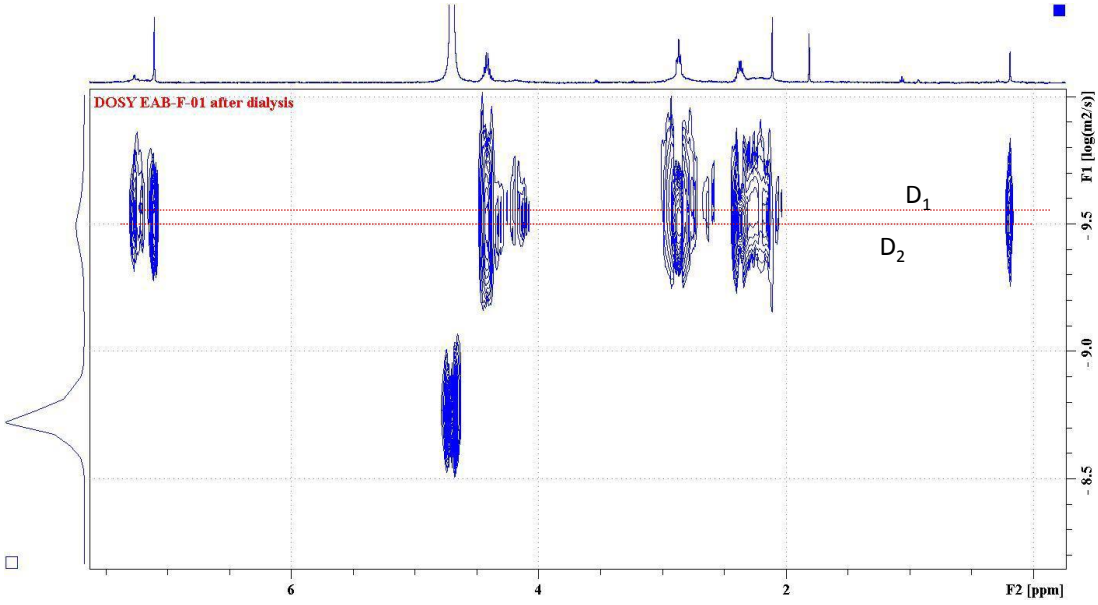

Figure S22. DOSY spectrum for **2a/3a**.

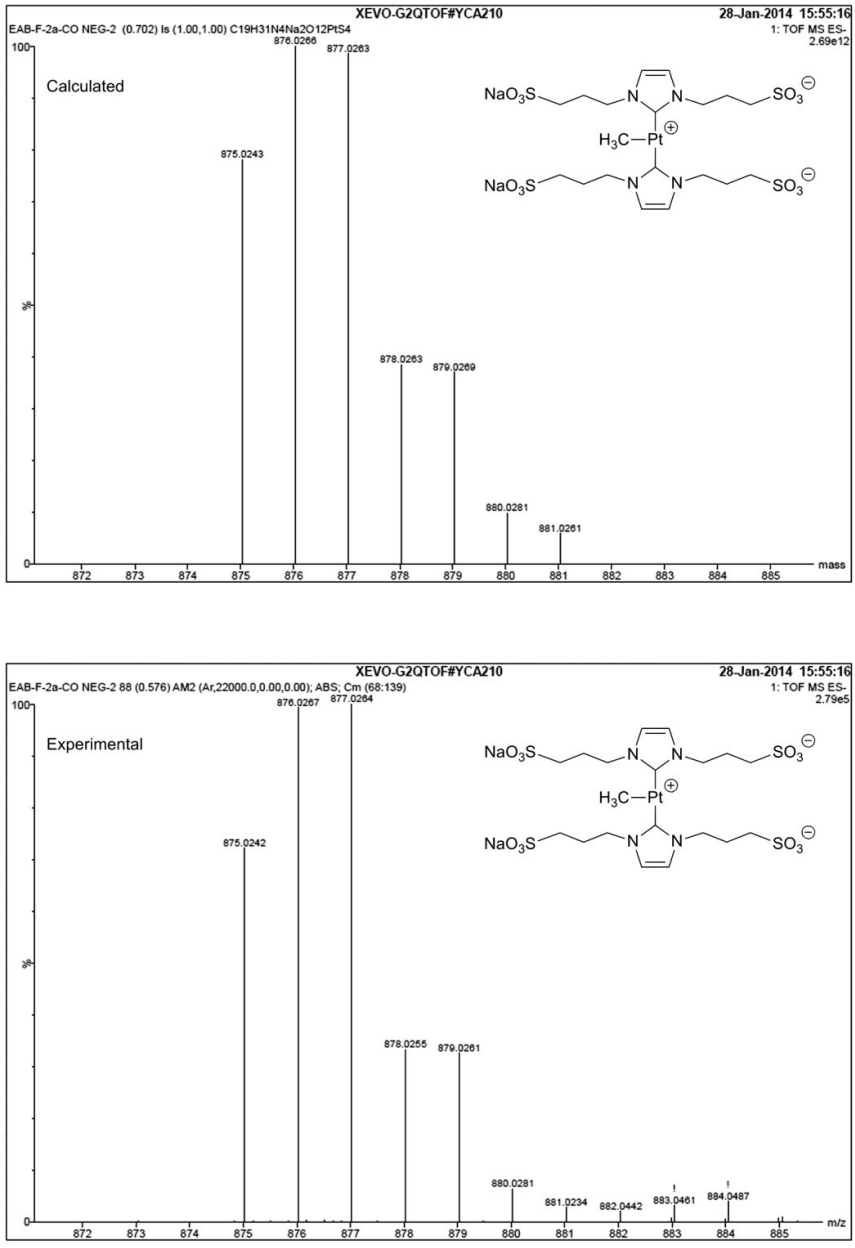

Figure S23. Calculated and experimental isotopic distributions of the molecular fragment [**3a** – Na – H_2O]$^-$ detected in the ESI mass spectra of **2a/3a**.

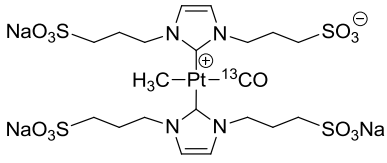

Trisodium *trans*-^{13}C-carbonylmethylbis[1,3-bis(3-sulfonatepropyl)imidazol-2-ylidene]platinate(3–) (4a): ^{1}H-NMR (400 MHz, D_2O): δ 7.27 (s, 4H, Imz), 4.26 (m, 8H, NCH_2), 2.83 (t, $^3J_{HH}$ = 8.4, 8H, CH_2S), 2.27 (m, 8H, $CH_2CH_2CH_2$), 0.19 (d with ^{195}Pt satellites, $^3J(^1H\text{-}^{13}C)$ = 1.6, $^2J(^1H\text{-}^{195}Pt)$ = 55.2, 3H, PtMe). $^{13}C\{^1H\}$-NMR (100 MHz, D_2O): δ 175 (Pt–CO). ESI-MS (negative ion, H_2O/D_2O 2:1): m/z 905.0285 $[M - Na]^-$ (calcd 905.0293) 25%; 876.0 $[M - {}^{13}CO - Na]^-$ (calcd 876.0) 32%; 838.0 $[M - {}^{13}CO - 2Na - CH_3]^-$ (calcd 838.0) 33%; 816.0 $[M - {}^{13}CO - 3Na - CH_3 + H]^-$ (calcd 816.0) 5%; 504.0 $[M - {}^{13}CO - NHC - 3Na - CH_4]^-$ (calcd 504.0) 100%.

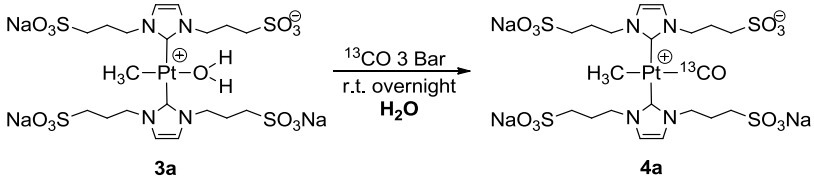

Scheme S1. Synthesis of the nano-object **2a**/**4a** (PtNP **2a** is omitted for clarity)

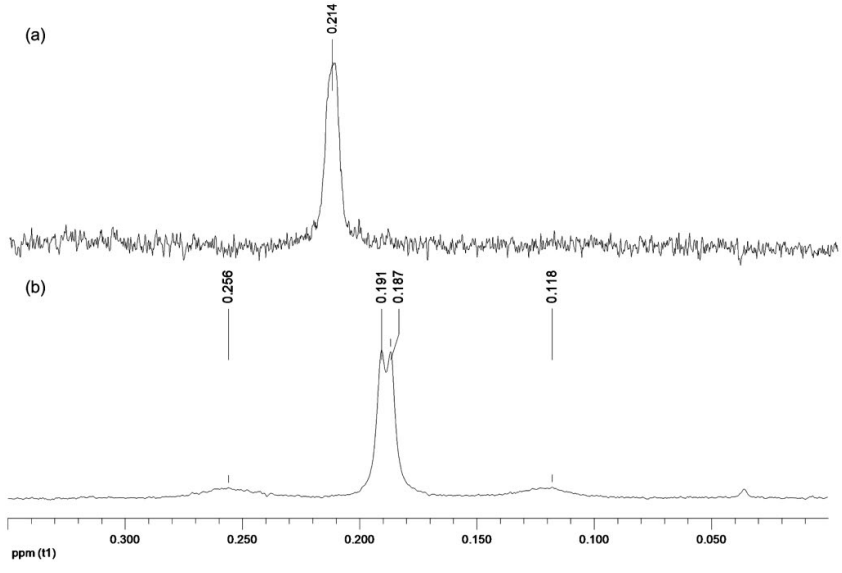

Figure S24. ^{1}H-NMR (400 MHz) spectral region for the Pt–CH_3 group of molecular complex located in a second coordination sphere around PtNPs **2a**, before (a; **2a/3a**) and after (b; **2a/4a**) reaction with ^{13}CO.

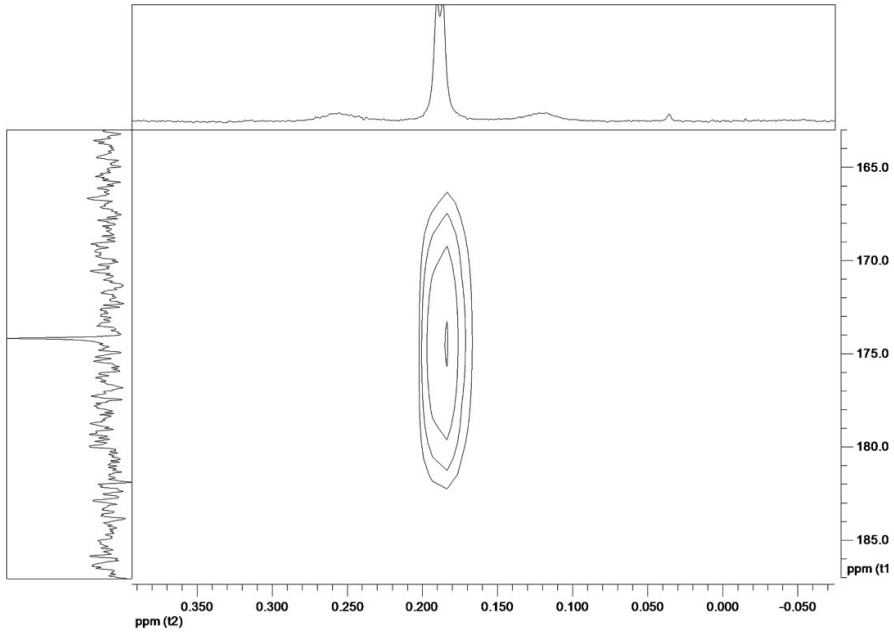

Figure S25. ^{1}H-^{13}C HMBC spectral region showing the cross peak between Pt–CH_3 and Pt–^{13}CO groups after reaction with ^{13}CO (**2a/4a**).

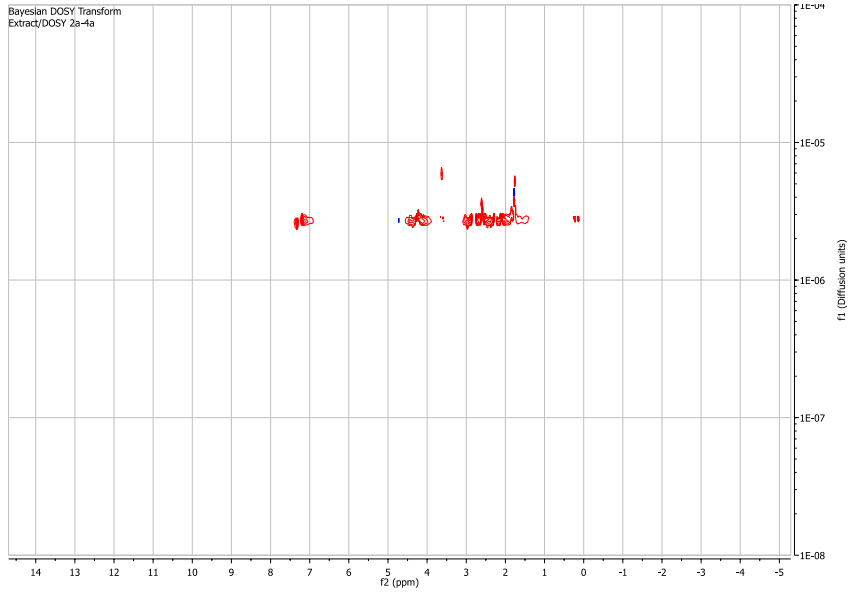

Figure S26. DOSY spectum for **2a/4a**.

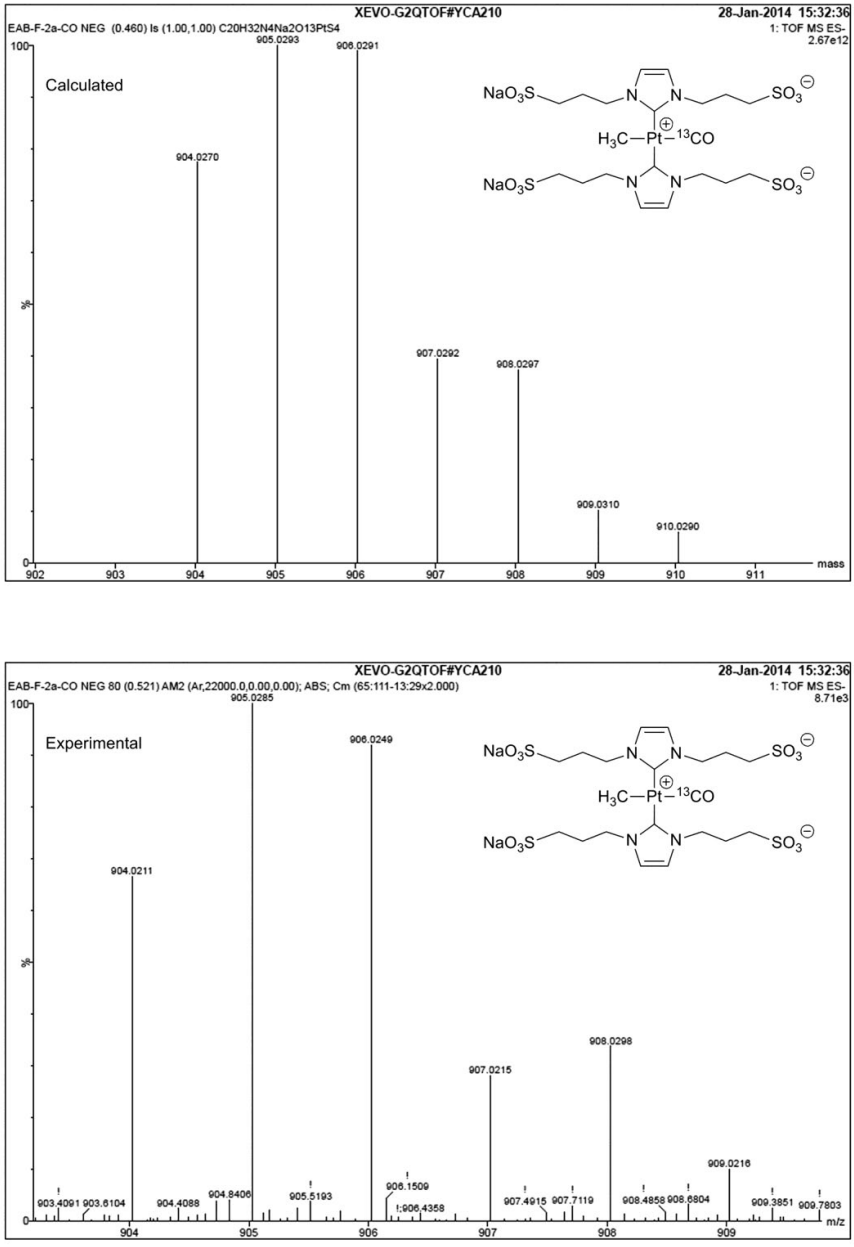

Figure S27. Calculated and experimental isotopic distributions of the molecular fragment [**4a** – Na]$^-$ detected in the ESI mass spectra of **2a/4a** (after reaction of PtNPs **2a** with ^{13}CO).

10. Formation and identification of the bis(carbene) complex 3b

A solution of 20.5 mg (0.0387) mmol of **1b** in 0.6 mL of D_2O was introduced under an argon atmosphere into a NMR tube fitted with a J. Young valve. The tube was heated at 80 °C and changes monitored by ^{1}H–NMR spectroscopy. Complete transformation of mono(carbene) **1b** into the bis(carbene) complex **3b** was observed after 18 h of reaction accompanied by the formation of a black solution of PtNPs **2b**.

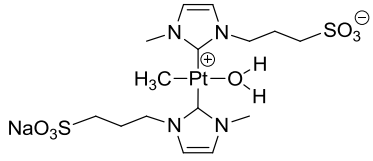

Sodium *trans*-aquamethylbis[1-methyl-(3-sulfonatepropyl)imidazol-2-ylidene]platinum(II) (3b): ^{1}H-NMR (300 MHz, D_2O): δ 7.22 (s, 2H, Imz), 7.21 (s, 2H, Imz), 4.48 (m, 2H, NCH_2), 4.21 (m, 2H, NCH_2), 3.81 (s, 6H, NMe), 2.86 (m, 4H, CH_2S), 2.26 (m, 4H, $CH_2CH_2CH_2$), 0.24 (s, with ^{195}Pt satellites, $^2J(^1H\text{-}^{195}Pt)$ = 77.7, 3H, PtMe). ^{13}C{^{1}H}-NMR (75 MHz, D_2O): δ 169.8 (s, with ^{195}Pt satellites, $^1J(^{13}C\text{-}^{195}Pt)$ = 1042, Imz-C^2), 121.3 (s, Imz-C^5), 121.2 (s, Imz-C^4), 48.5 (s, NCH_2), 48.0 (s, CH_2S), 36.7 (s, NMe), 25.4 (s, $CH_2CH_2CH_2$), –16.8 (s, with ^{195}Pt satellites, $^1J(^{13}C\text{-}^{195}Pt)$ = 605, PtMe). ESI-MS (negative ion, H_2O:D_2O 2:1) m/z: 616.0865 $[M–H_2O–Na]^-$ (calcd 616.0869) 100%.

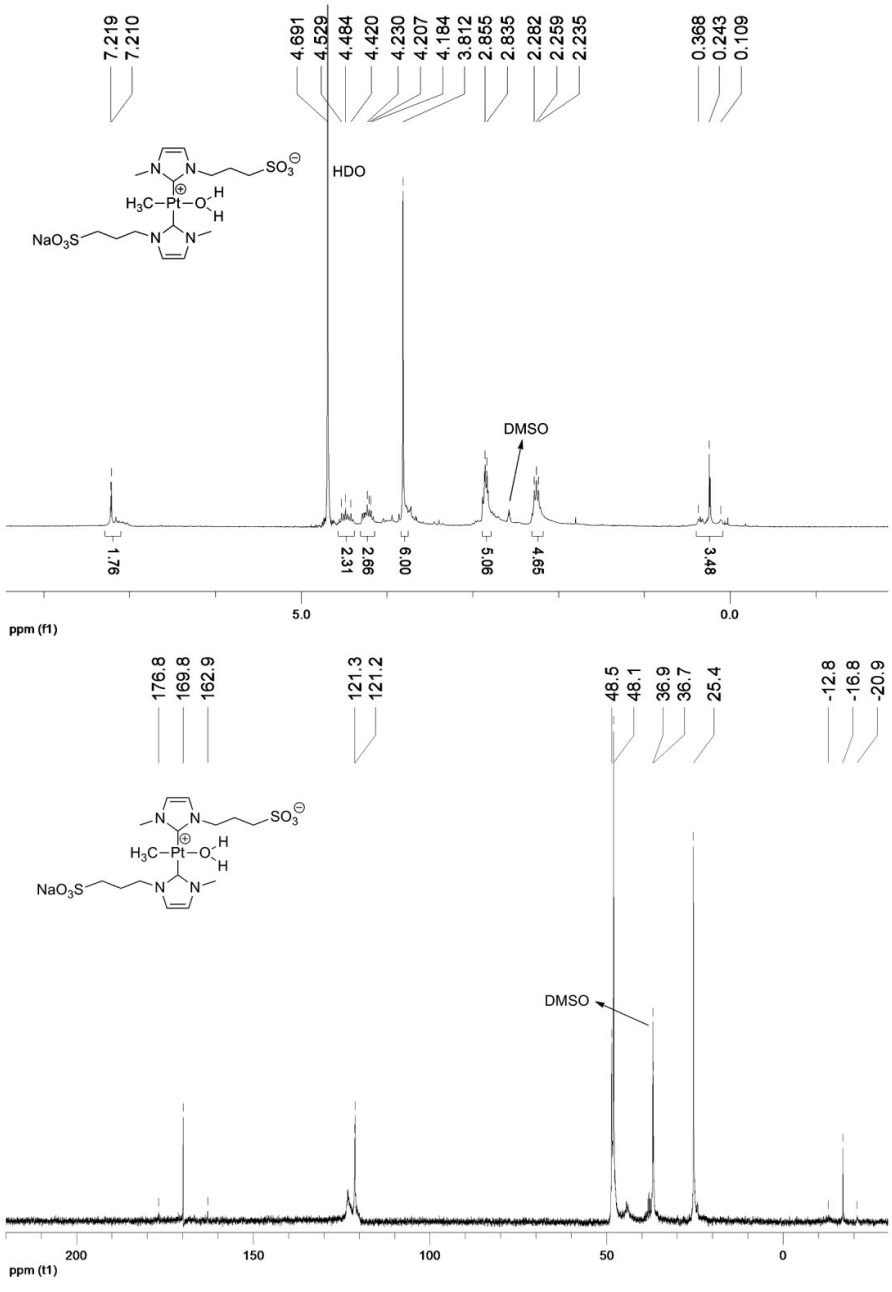

Figure S28. ^{1}H- (300 MHz) and ^{13}C-NMR (75 MHz) spectra for the mixture of PtNPs **2b** and complex **3b**.

11. Hydrogenation of styrene in water

Styrene (200.0 μL, 1.740 mmol) was added into a Fischer Porter bottle to a solution of the corresponding Pt complex **1** (17.4 μmol) or Pt nanoparticles **2** (5.0 mg, 0.7 – 0.9 mol%) in water (5 mL). The system was cooled in a bath of liquid nitrogen and degassed for 15 min. The Fischer Porter bottle was then returned to room temperature and pressurized with H_2 (1 bar). The reaction mixture was stirred at 1500 rpm at room temperature for the time indicated in the Table S1. After addition of the internal standard (dodecane, 395.0 μL, 1.739 mmol), the organics were extracted with toluene (3 × 1.5 mL) and the collected organic phases were combined and dried over $MgSO_4$. Conversions and yields were determined by GC. In the case of the PtNPs, the effective Pt loadings (mol% [Pt]) were calculated taking into account the percentage of Pt determined by ICP-MS and the estimated fraction of metal atoms at the NP surface has been estimated to be 65 ± 3 % for NPs **2**, based on a fcc packing for icosahedral clusters.[4-5]

The decanted aqueous phase containing PtNPs **2d** was reused in nine consecutive recovery cycles (for a graphic representation of conversions and yields in the recycling series, see Figure S27).

Table S1. Styrene Hydrogenation in water catalysed by Pt complexes **1** and NPs **2**.

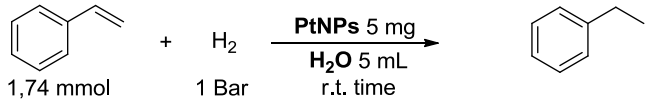

Entry	PtNPs	time (h)	Conv. (%)[a]	Yield (%)[b]
1	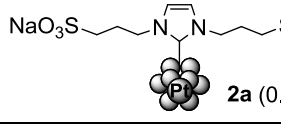 **2a** (0.4 mol%)[d]	0,5	28	28
2		1	69	64
3		2	>99	92
4[c]		2	65	64
5	**1a** (1 mol%)	2	42	38
6	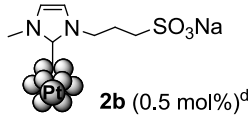 **2b** (0.5 mol%)[d]	0,5	58	44
7		1	98	97
8		2	>99	88
9[c]		2	93	92
10	**1b** (1 mol%)	2	16	15
11	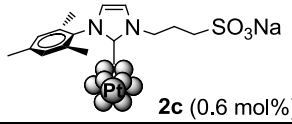 **2c** (0.6 mol%)[d]	0,5	68	58
12		1	97	86
13		2	>99	92
14[c]		2	92	90
15	**1c** (1 mol%)	2	36	30
16	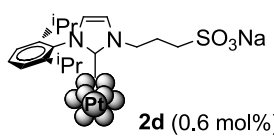 **2d** (0.6 mol%)[d]	0,5	62	59
17		1	97	93
18		2	>99	90
19[c]		2	85	83
20[e]		24	>99	89
21	**1d** (1 mol%)	2	46	39

[a] Determined by GC
[b] Determined by GC using dodecane as internal standard
[c] 2,5 mg of PtNPs
[d] The effective Pt loadings are given in parenthesis
[e] 5 Bar of H_2

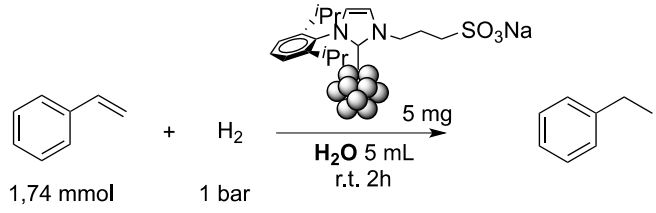

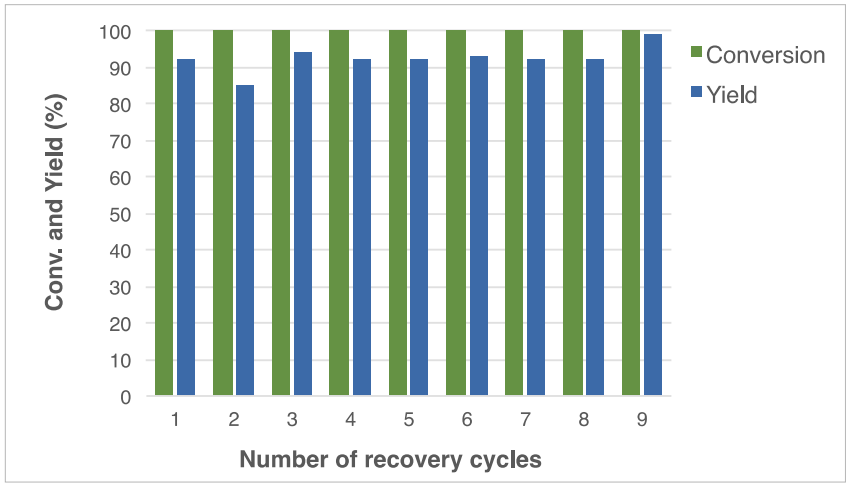

Figure S29. Catalyst recycling experiments for the hydrogenation of styrene in water using PtNPs **2d** as catalyst.

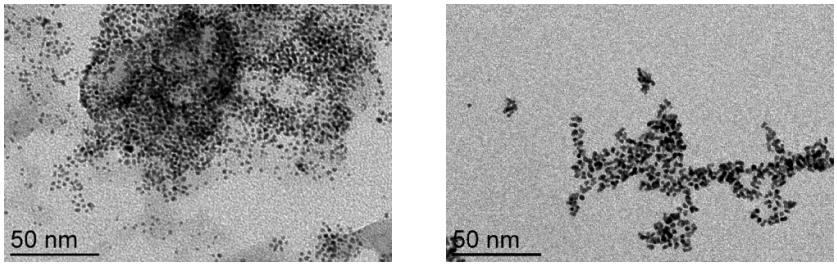

Figure S30. TEM images for PtNPs **2d** after the 1st (left) and 9th (rigth) recovery cycle (see **Figure S5** for an image before any use in catalysis).

12. References

(1) E. A. Baquero, J. C. Flores, J. Perles, P. Gómez-Sal, E. de Jesús, *Organometallics* **2014**, *33*, 5470–5482.

(2) H. L. Su, L. M. Pérez, S. J. Lee, J. H. Reibenspies, H. S. Bazzi, D. E. Bergbreiter, *Organometallics*, **2012**, *31*, 4063–4071.

(3) C. Eaborn, K. Kundu, A. Pidcock, *J. Chem. Soc. Dalton Trans*. **1981**, 933–938.

(4) B. K. Teo, H. Zhang, *Magic Numbers in Clusters*, chapter 3 in *Metal Nanoparticles: Synthesis, Characterization, and Applications*, D. L. Fedlheim, C. A. Foss Jr. (Eds.), CRC Press, **2002**.

(5) A. P. Umpierre, E. de Jesús, J. Dupont, *ChemCatChem*, **2011**, *3*, 1413–1418.

Chapter VII. Water-Soluble Platinum Nanoparticles Stabilized by Sulfonated N-Heterocyclic Carbenes: Effect of the Synthetic Approach

Edwin A. Baquero, Simon Tricard, Yannick Coppel, Juan C. Flores, Bruno Chaudret, and Ernesto de Jesús, *Manuscript In Preparation*. **2015**.

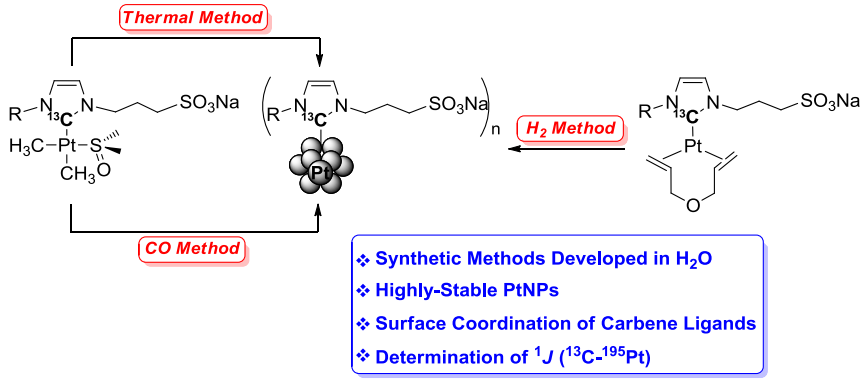

Water-Soluble Platinum Nanoparticles Stabilized by Sulfonated N-Heterocyclic Carbenes: Effect of the Synthetic Approach

Edwin A. Baquero,[1,2] Simon Tricard,[2] Yannick Coppel,[3] Juan C. Flores,[1] Bruno Chaudret*[2] and Ernesto de Jesús*[1]*

[1]Departamento de Química Orgánica y Química Inorgánica, Campus Universitario, Universidad de Alcalá, 28871 Alcalá de Henares, Madrid, Spain.

[2]LPCNO; INSA, CNRS, Université de Toulouse, 135, Avenue de Rangueil, 31077 Toulouse, France.

[3]LCC; CNRS, INPT, Université de Toulouse, 205 Route de Narbonne, 31077 Toulouse, France.

ABSTRACT

The synthesis of metal nanoparticles under controlled conditions in water remains a challenge in nanochemistry. Two different approaches are disclosed here for platinum, which involve the treatment of aqueous solutions of preformed sulfonated (NHC)Pt(II) and (NHC)Pt(0) complexes (NHC = N-heterocyclic carbene) with CO and H_2, respectively. The resulting nanoparticles were found to be water-soluble, and highly stable in this solvent under air for indefinite time period. The particles were characterized by TEM and spectroscopic techniques. The coordination of NHC ligands through the carbenic carbon was corroborated by solid-state NMR studies, where an unambiguous evidence of such a bonding was obtained by the determination of the ^{13}C–^{195}Pt coupling constant (940 Hz) for particles containing a ^{13}C labeled-NHC ligand. The coordination of CO to (NHC)Pt(II) precursors, prior to the formation of the nanoparticles, was also verified by NMR spectroscopy. A second coordination sphere containing bis(NHC)Pt(II) complexes found for a particular type of NHC ligand, is also presented. Although the comparison of the procedure using CO with that previously reported through thermal decomposition of dimethyl precursors, showed only significant differences in the reaction time (faster for the latter), the synthesis of PtNPs by using the hydrogenation method was found to progress even much slower than the decomposition under CO and produced bigger NPs. In addition, the study highlighted the importance of ligand design for the NPs stabilization.

INTRODUCTION

Metal nanoparticles (MNPs) have become a subject at the forefront of research areas such as catalysis, where their large specific surface area and singular electronic properties are beneficial in many instances.[1-5] Nevertheless, the understanding of the surface chemistry of MNPs after modification with organic ligands has been scarcely explored.[6-9] A major challenge in the field is the inhibition of spontaneous agglomeration frequently observed due to poor thermodynamic stability of the particles. Ligands able to coordinate to the MNPs surface, such as thiols, thioethers, disulfides, amines, or phosphanes, have been utilized as stabilizers to overcome the phenomenon.[10,11]

N-heterocyclic carbenes (NHCs) have risen as a leading class of ancillary ligand in organometallic chemistry, mainly because these electron-rich ligands tend to bind strongly to metals, rendering fairly robust complexes useful for a wide range of applications.[12-15] Although NHCs appear to be very attractive ligands for the stabilization of MNPs, surprisingly, their use and, more specifically, their bonding interaction with metal surfaces have rarely been studied.[16-31] NHCs have been involved in the synthesis of MNPs for M = Ru, Au, Ag, Pd, and Pt, more often through formation of the particles from the metal precursor in the presence of the corresponding NHC ligand,[16-18] or by its post-synthetic addition to MNPs aimed to gain stability by substitution of the existing coordinated ligands.[19,21] A different pathway has consisted in the reduction of preformed (NHC)Au(I)[22,28-30] and Ag(I) complexes.[23] It is noteworthy that the mode of coordination of the NHC ligand to the metal surface has been experimentally addressed only for a few cases. Some of us have characterized the coordination of NHCs to RuNPs by solid-state NMR studies.[16] Likewise, Pleixats and co-workers[18] and Glorius et al.[19,20] have disclosed the coordination of NHCs to Pd nanoparticles.

The MNPs containing NHC ligands have been employed as catalysts in Suzuki cross-couplings,[18] selective hydrogenation of alkenes,[20] and in the asymmetric α–arylation of ketones.[19] We have recently described the behavior of RuNPs as catalysts for the hydrogenation of arenes,[17] and the synthesis of PtNPs as chemoselective catalysts for the hydrogenation of aromatic nitro compounds,[24] both stabilized by bulky NHCs. Moreover, NHC ligands have been used to prepare Au[21,22,25-31] and Ag[23] MNPs as model systems for the formation of either conglomerates or 3D networks, or for surface reactivity studies.

Although all of these studies involved organic solvents, the alternative use of water is very attractive for a wide range of applications of MNPs. Water offers exceptional chemical reactivity due to its unique properties, such as high dielectric constant and ability to solvate salts and polar compounds. Nonetheless, water-soluble MNPs stabilized by carbene ligands

were unknown until very recently when we communicate the synthesis in water of PtNPs **2a–d** through a thermal decomposition of dimethyl complexes **1a–d** containing sulfonated NHCs ligands (Scheme 1).[32] Nanoparticles **2a–d** were found to be highly stable in water under air for indefinite time period, revealing a strong and inert coordination of the NHCs to the platinum surface, in an interaction that occurs through the carbenic carbon, as demonstrated by the observation of the corresponding ^{13}C–^{195}Pt coupling constant by solid-state NMR spectroscopy (940 Hz).

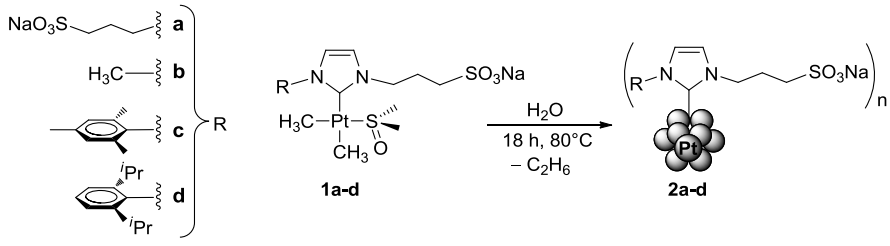

Scheme 1. Synthesis of water-soluble PtNPs **2a–d** stabilized by NHC ligands **a–d**.

The above findings encouraged us to explore diverse methodologies for the formation of PtNPs supported by sulfonated NHC ligands in aqueous-phase and under mild conditions. We wanted to explore the suitability of this type of sulfonated precursors to generate water-stable PtNPs under different synthetic approaches and their effect on the features of the resulting nanoparticles. Herein, we describe the preparation of water-soluble PtNPs containing the NHC ligands depicted in Scheme 2 by reduction of dimethyl complexes **1a–c** with CO, and by hydrogenation of (NHC)Pt(0)(AE) complexes[33] **4a**, **4c**, and **4e** (AE = allyl ether, Scheme 2). The PtNPs were found to be stable in water for months, they could accommodate coordinated carbene ligands as evidenced by NMR spectroscopy, and we confirmed that the nanoparticles mean sizes depend on the approach used for their synthesis, and their stability is also sensible to the ligand design.

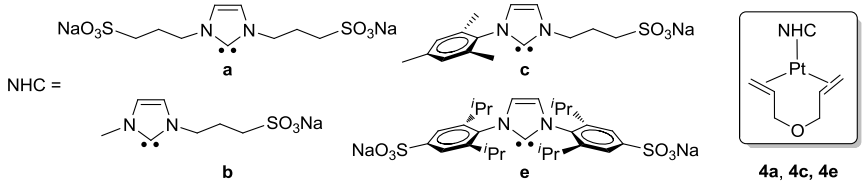

Scheme 2. Water-soluble NHC ligands and (NHC)Pt(0)(AE) complexes used in this work.

RESULTS AND DISCUSSION

Synthesis of PtNPs 3a–c by reduction of Pt(II) precursors with CO. Platinum nanoparticles **3a–c** were synthesized by stirring aqueous solutions of dimethyl complexes **1a–**

c at room temperature under 3 bar of CO (Scheme 3). The PtNPs were purified by dialysis using a regular cellulose membrane. The colloidal solutions were basic before dialysis (pH > 9), as expected from the hydrolysis of some NHC ligands during nanoparticle formation, but they became neutral after the purification process, indicating that hydroxyl ions were effectively removed together with other by-products (*e.g.*, imidazolium salts undetected in the characterization of dialyzed **3a–c**). Aqueous colloidal solutions of PtNPs **3a–c** were homogeneous and highly stable in air, remaining totally dispersed without agglomeration or Pt^0 precipitation for at least one year of observation.

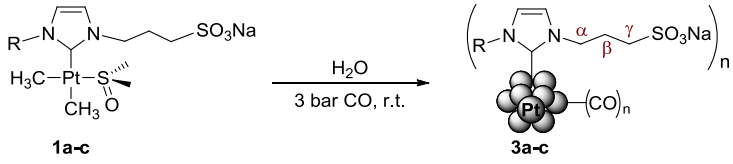

Scheme 3. Synthesis of PtNPs **3a–c** from Pt(II) complexes **1a–c**.

Transmission electron microscopy (TEM) revealed the formation of non-agglomerated, spherical ultra small nanoparticles with a fairly uniform size and diameters in the range 1.0–1.3 ± 0.4 nm (Figure 1 and Figures S2–S3 in the Supporting Information).

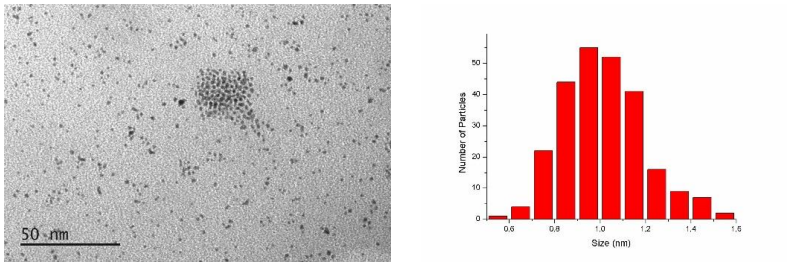

Figure 1. TEM image (left) and size distribution (right) for PtNPs **3a.**

The PtNPs were characterized by attenuated total reflection Fourier transform infrared spectroscopy (ATR-FTIR) and ^{1}H solution NMR spectroscopy in order to corroborate the presence of the NHC ligands on the NPs. In all cases, the ATR-FTIR spectra in the solid-state (Figures S8–S10) showed bands attributable to the NHCs on the PtNPs, but also revealed the coordination of carbonyl groups to the metallic surface in a terminal mode (2075–2065 cm^{-1}). This coordination appeared to be fairly strong, as any desorption of carbonyl ligands was never observed, even after 60 h of dialysis. This result contrasts with that found for PtNPs **2**, for which exposure in the solid-state to CO, resulted in a labile coordination of the ligand that completely desorpted within 1 h after removal of the gas.[32] Analysis by ^{1}H NMR spectroscopy of NPs **3** in D_2O (Figures S16–S18) showed only broad peaks in the expected regions for each NHC ligand, except for **3a** where additional sharp signals were also found (*vide infra*). The ^{1}H resonance signals on the imidazole and

propylsulfonate γ- and β-CH_2 groups (CH_2-tagging in Scheme 3) appeared at typical chemical shifts comparable to precursors **1** (7.3 – 7.1, 2.9 and 2.3 ppm, respectively), as did those for the methyl groups in **3c** (2.0 – 1.8 ppm), whereas the resonance signals for α-CH_2 and aromatic protons in the case of **3c** were not detected. According to our findings for PtNPs **2**,[32] and similar observations for NHC-stabilized Au,[22] Pd,[20] or Ru nanoparticles,[16] peak broadening and absence of some resonance signals are indications of the coordination of NHC ligands to the platinum surface. The effect is assigned to the proximity of the corresponding protons to the nanoparticle surface, which are consequently affected by the combination of not only the general increased rigidity in the coordinated ligands on the MNPs, but also slow tumbling of the particles which leads to rapid T_2 relaxation times, and the heterogeneity of the surface.[34,35] As a result, the spectra are absent of resonances due to the protons of the ligand nearest to the surface, and show broad peaks for the rest of them. Moreover, the close proximity suggested by ^{1}H NMR for the phenyl group to the particle surface in **3c** makes feasible an NHC-PtNPs bonding scheme reinforced by agostic or π interaction, as previously reported for NHC and 4-(3-phenylpropyl)pyridine ligands stabilizing RuNPs.[16,36] On the contrary, the observation by ^{1}H NMR of signals corresponding to protons on the propylsulfonate groups suggest that these flexible chains point to the medium, away from the particles, where their ionic moieties are better hydrated by the solvent (*i.e.*, D_2O), and thus explaining both the solubility and high stability of PtNPs **3** in water.

The coordination mode of NHC ligands on the surface of the NPs was further investigated by solid-state NMR spectroscopy measurements. Solid-state ^{1}H–^{13}C cross-polarization magic angle spinning (CP-MAS) NMR spectra carried out for PtNPs **3** showed no resonance signals attributable to carbons on the Pt–DMSO and Pt–CH_3 moieties (Figure 2c for PtNPs **3a**, and Figures S22–S23 for **3b** and **3c**, respectively). These resonances are expected to occur at around –5 and 40 ppm, respectively, according to the ^{1}H–^{13}C CP-MAS spectra recorded for platinum complexes **1a–c** (Figure 2b and Figures S22–S23). Therefore, according to this and to the ATR-FTIR data, NHC and CO appeared to be the only ligands –not counting water molecules- remaining attached to the surface after the nanoparticle formation. The NHC ligands provided ^{13}C signals at expected chemical shifts (*i.e.*, imidazolic carbons at 124–123 ppm; α, β, and γ methylene groups of the propylsulfonate chain at 49, 26–28, and 49 ppm, respectively; and aromatic and methyl groups for **3c** at 135–129 and 21–18 ppm, respectively). The coordination of the NHC ligands through the carbenic carbon is supported by the observation of a broad peak centered at 164–162 ppm, together with the absence of the resonance signal assignable to that methine carbon in the corresponding imidazolium salt (145–139 ppm). As illustrated in Figure 3 for PtNPs **3a**, the resonance attributable to the carbenic carbon was not observed in the direct ^{13}C-MAS spectra of **3**, but

it was in the $^{1}H–^{13}C$ CP-MAS spectra as a consequence of the signals enhancement caused by the polarization transfer from the protons of the imidazole ring. This resonance is shifted to higher field compared to that found for complexes **1** (185–182 ppm) or in related [(NHC)Pt(0)(dvtms)] complexes (200–180 ppm; dvtms = divinyltetramethyldisiloxane).[37-39] The same effect has been observed previously in Pt/PVP/^{13}CO and Pt/dppb/^{13}CO nanoparticles (PVP = poly(N-vinyl-2-pyrrolidone); dppb = 1,4-bis(diphenylphosphino)butane) and for PtNPs **2**, and it has been proposed that it could be related to the Knight shift.[32,40] Nevertheless, it is remarkable that carbonyl ligands (chemical shift expected at 190–210 ppm)[40] were never detected (Figure 3 for PtNPs **3a**), neither when direct ^{13}C-MAS spectra were recorded, nor by solid-state $^{1}H–^{13}C$ CP-MAS NMR spectroscopy.

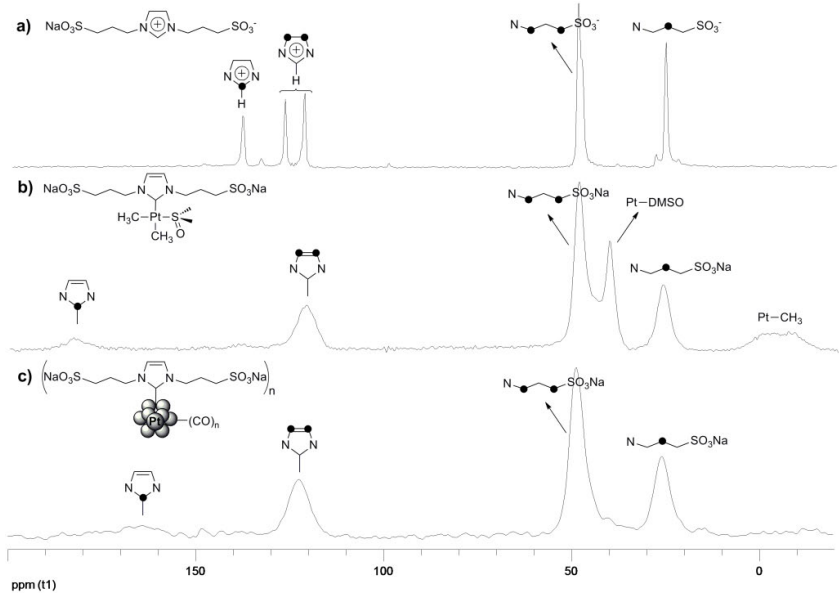

Figure 2. $^{1}H–^{13}C$ CP-MAS spectra of a) **aH**, b) **1a** and c) **3a** in the solid-state.

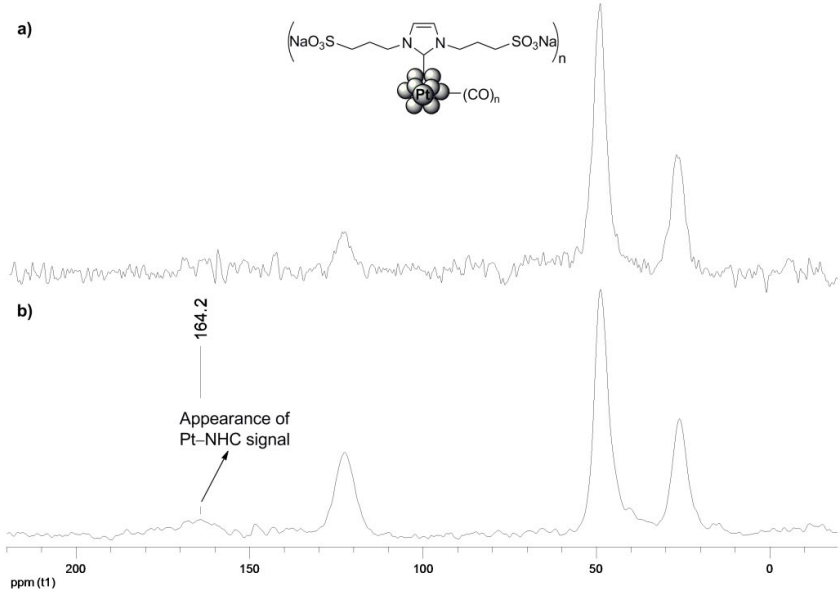

Figure 3. a) ^{13}C-MAS and b) ^{1}H–^{13}C CP-MAS spectra for PtNPs **3a**.

Although the carbenic carbon resonance signal was observed in all cases, the intensity was quite low. With the idea to confirm unambiguously the coordination mode and the strength of the interaction, we prepared platinum nanoparticles **^{13}C-3c** containing NHC ligands labeled with ^{13}C at the C^{2}-position (*i.e.*, the carbenic carbon atom) of the imidazolic ring (see Experimental Section for details). Analysis by TEM displayed PtNPs with a mean size similar to that found for the ^{13}C-unlabeled analogues (1.1 ± 0.4 vs. 1.0 ± 0.3 nm, Figure S4). The ^{1}H–^{13}C CP-MAS spectrum showed an intense resonance signal for the carbenic carbon atom at the expected chemical shift (163 ppm, Figure S24). Additionally, the direct bonding interaction of that C-donor atom with the platinum surface was confirmed by the observation of the ^{13}C–^{195}Pt coupling. Line-shape deconvolution process of the peak rendered a coupling constant of 940 ± 20 Hz (Figure 4). The coupling is weaker than that for molecular (NHC)Pt(0) complexes (around 1365 Hz),[39] but is the same than the one found for PtNPs **^{13}C-2c** (940 ± 20 Hz).[32]

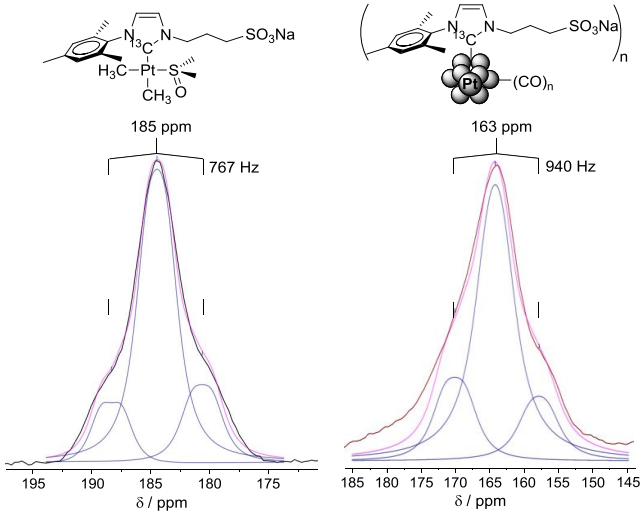

Figure 4. Resonance signals attributable to the Pt-bonded carbenic carbons in the ^{1}H–^{13}C CP-MAS NMR spectra for complex ^{13}**C-1c** (left) and PtNPs ^{13}**C-2c** (right), displaying their corresponding deconvolution curves.

Even after 60 hours of dialysis, the ^{1}H NMR spectrum in D_2O for PtNPs **3a** showed several sharp signals in addition to the broad peaks discussed above for the coordinated NHC ligands (Figure S16). These sharp signals were assigned to the presence of a biscarbene monomethyl complex **3a*** of formula $Na_3[PtMe(CO)(NHC)_2]$ based on: (a) the chemical shifts, splitting patterns, and integration measured by ^{1}H NMR spectroscopy, compatible with the presence of two equivalent NHC ligands per methyl group; (b) the cross peaks found for the Pt–CH_3 moiety and the methylene groups of the propylsulfonate chain in rotating-frame nuclear Overhauser effect spectroscopy (ROESY) experiment (Figure S39), locating the methyl ligand *cis* to the two carbenes; and (c) the detection of the fragment [**3a*** – Na]$^-$ by electrospray ionization mass spectrometry (ESI-MS, Figure S40). We have previously observed the formation of an isotopomer of the complex **3a*** after modification with ^{13}CO of a nano-object obtained during formation of PtNPs **2a**.[32] As it was for PtNPs **2a**, the persistence of this biscarbene complex after dialysis of PtNPs **3a** is ascribed to the association of such specie, most likely through electrostatic interactions, in a second coordination sphere around the nanoparticle (Figure 5).[32] This association was also supported by diffusion ordered spectroscopy (DOSY) experiments performed in D_2O, showing virtually the same diffusion coefficient for the NHCs attached to the PtNPs than for those in the biscarbene complex. Even though, the interaction in nano-object **3a/3a*** must be weaker, because DOSY measurements revealed dissimilar values for each part of the pair ($2.5 \pm 0.4 \times 10^{-10}$ m^2s^{-1} for PtNPs **3a** and $4.0 \pm 0.4 \times 10^{-10}$ m^2s^{-1} for complex **3a***). Both findings, the persistent presence of **3a*** associated to **3a** and the diffusion coefficients found for **3a/3a***, suggest the biscarbene complex residing into the second layer of the PtNP with

a higher mobility in **3a** than in **2a**. The latter can be related to a different surface composition, since competing coordination of CO must result in a lower superficial density of NHC ligands in **3a** (*i.e.*, less charge-dense), at the same time that introduces some degree of lipophilicity at the surface, reducing the affinity for polar or charged groups.

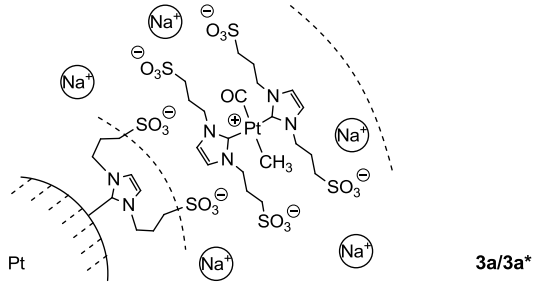

Figure 5. Second coordination sphere in the nano-object **3a/3a***.

Further studies were devoted to elucidate the chemical transformations that occurred on complexes **1** under nanoparticle formation conditions. Thus, solutions of complexes **1** in D_2O were treated at room temperature with ^{13}CO at 3 bar and periodically monitored by NMR spectroscopy. The first event revealed by the ^1H NMR spectra was the substitution of the dmso ligand by ^{13}CO to afford species **[3a-c]** (Scheme 4). The process was completed in 3 h for the bulkiest (**1c**), or in 1 day for the less hindered complexes (**1a,b**). The structural proposal for complexes **[3]** was based on their NMR data (Experimental Section, and Figures S28-S33) and ESI-MS spectra. The coordination of the ^{13}CO ligand in complexes **[3]** was characterized by its intense resonance signal in the ^{13}C NMR spectra (*ca.* 181 – 180 ppm, with platinum satellites $^1J(^{13}C–^{195}Pt)$ = 998 – 1023 Hz). In contrast, DMSO coordinated to Pt atom was undetectable by ^1H NMR after completion of the reactions (silent spectra at 2.95 ppm), observing the presence of free DMSO in the samples (2.63 ppm in D_2O). The chemical nonequivalence of the methyl ligands, unveiled by both the ^1H and ^{13}C NMR spectra, indicated a *cis* configuration of these groups. The chemical shift for carbenic carbon in **[3]** was slightly shifted to up field compared to that found in precursors **1** (177 – 174 vs. 183 – 181 ppm). ESI mass spectrometry experiments performed in negative mode also supported the formation of species **[3]**, with spectra showing the presence of intense ion peaks due to fragments [**[3]** – $Na]^-$, except for **[3b]**, for which biscarbene species were detected instead.

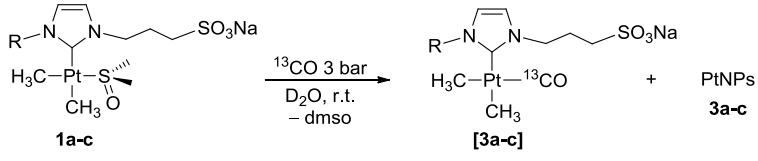

Scheme 4. Formation of intermediates **[3a-c]** under nanoparticle formation conditions.

According to TEM studies subsequently performed on the samples analyzed by NMR, the formation of carbonyl complexes **[3]** was always concurrent with that of PtNPs. Several experiments were carried out to test if species **[3]** are involved as intermediates in the nanoparticle formation process. Complexes **1a** and **1c** were combined with ^{13}CO in D_2O under nanoparticle formation conditions (*vide supra*). After 1 h of reaction, ^{1}H NMR spectra showed a conversion to complex **[3a]** of only 5%, whilst it was 95% for **[3c]**, relative to the unreacted precursor remaining in solution (**1a** and **1c**, respectively). TEM analysis (Figure S37) revealed the formation of PtNPs to be evident only for the sample derived from the reaction of **1c**, suggesting that a high concentration of species **[3]** facilitates the formation of the nanoparticles, and thus pointing them as intermediate precursors of PtNPs **3**. The same reaction was also inspected in two tests which were performed starting from **^{13}C-1c**, namely, complex **1c** containing the heterocycle ^{13}C-enriched at C^2-position. The corresponding product **[^{13}C-3c]** (for NMR data see Experimental Section, and Figures S34 – S36) was the only molecular complex detected in solution (*i.e.*, total conversion of **^{13}C-1c**) after 3 h of reaction. Then, the ^{13}CO atmosphere was replaced by argon gas in one of the test, and kept in the other. After 4 days, ^{1}H NMR spectroscopy revealed that complex **[^{13}C-3c]** was stable under argon, whilst it vanished under ^{13}CO to yield PtNPs **^{13}C-3c** together complex **A** as the only detectable byproduct (Scheme 5). Therefore, the experiences make clear that carbon monoxide is required to form and promote the reductive elimination of intermediates **[3]** and initiate the formation of the particles.

Unlike to the preparation of nanoparticles **^{13}C-3c** described above, the identification by NMR of zwitterionic compound **A** in the latter set of experiments was possible due to the direct analyses of undialyzed reaction mixture in D_2O. According to the ^{1}H and ^{13}C NMR data, species **A** must derived from hydrolysis of one of the methyl ligand in **[^{13}C-3c]** (Scheme 5). Thus, the ^{1}H NMR spectrum showed a resonance signal (*ca.* 0.22 ppm, ^{195}Pt satellites with $J_{H\text{-}Pt}$ = 73 Hz) for a single type of methyl group integrating 1:1 relative to the NHC ligand, and coupled to two ^{13}CO groups (both $J_{H\text{-}C}$ = 2 Hz), whereas the ^{13}C NMR spectrum indicated the presence of two carbonyl ligands (177 and 206 ppm, showing the corresponding satellites with $J_{C\text{-}Pt}$ around 1000 Hz). In addition, cross peaks for the Pt–Me protons with each carbonyl groups and with the carbenic carbon were observed by ^{1}H–^{13}C HMBC (Figure S37).

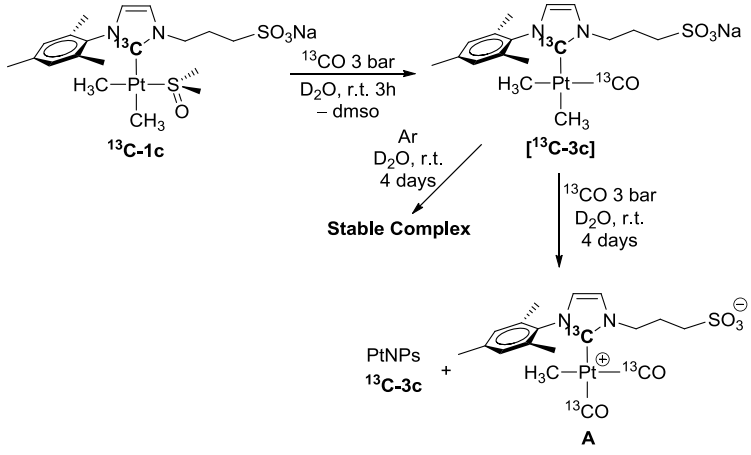

Scheme 5. Transformation of **^{13}C-1c** under ^{13}CO atmosphere in D_2O.

Synthesis of PtNPs 5a, 5c and 5e by hydrogenation of Pt(0) precursors. Platinum nanoparticles **5a**, **5c** and **5e** were synthesized by hydrogenation with H_2 (3 bar) of solutions of diolefin Pt(0) complexes **4a**, **4c** and **4e** in water, and at room temperature (Scheme 6). Under these conditions, the allyl ether ligand is hydrogenated to release "naked" NHC–Pt(0) fragments, which are the source of nucleation seeds to yield nanoparticles **5**. However, the reactions progressed very slowly and complete transformation of precursors **4** was observed to occur after several days by ^{1}H NMR spectroscopy, resulting the lowest rate for the bulkiest complex. Thus, reaction time for **4a**, **4c**, and **4e** was found to be 10, 22, and 42 days, respectively. After purification by dialysis, the aqueous colloidal solutions of PtNPs **5a** and **5c** were homogeneous and highly stable exposed to air, remaining totally dispersed in solution without agglomeration or Pt^0 precipitation for at least one year of observation. However, agglomeration was observed for **5e** after just one day. Aside greater proclivity to reach the agglomeration limit due to larger size of particles **5e**, the poor stability of their colloidal solutions can be attributed to contributions from the NHC ligand, such as structural rigidity. The aromatic rings containing the sulfonated groups in **5e** are directed and close to the NP surface, hindering the suitable stabilizing interaction between those ionic groups and the solvent.

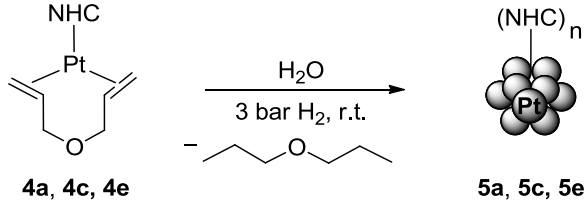

Scheme 6. Synthesis of PtNPs **5** derived from (NHC)Pt(0) complexes **4**.

TEM images analyses showed the presence of spherical and non-agglomerated nanoparticles, with relatively high polydispersity in diameters in all cases. The mean sizes found for PtNPs **5** was strongly dependent on the bulkiness of the NHC ligand and the flexibility of the moieties holding the solubilizing sulfonated groups, with the smallest nanoparticles for **5a** (1.7 ± 0.6 nm; Figure 6), the biggest for **5e** (4.0 ± 0.8 nm; Figure S6), while the mean size for **5c** was intermediate (3 ± 2 nm; Figure S5). The correlation observed between the hydrogenation reaction times and the particles size found by TEM is in accordance with a nucleation/growth process, in which slow decomposition rate of precursors (*i.e.*, higher reaction time) favors growth of particles in greater extent than the nucleation process, hence, leading to particles with higher mean sizes, and vice versa.

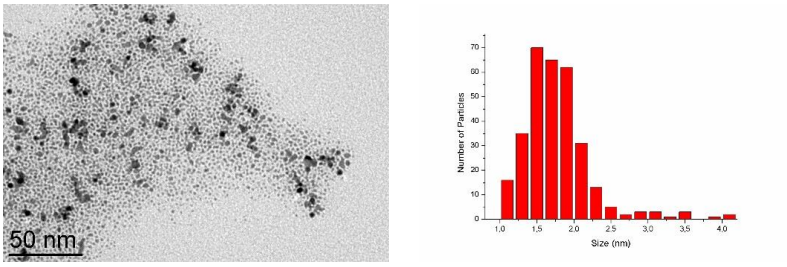

Figure 6. TEM image (left) and size distribution (right) for PtNPs **5a**.

ATR-FTIR spectroscopy performed on platinum nanoparticles **5** evidenced the presence of NHC ligands (Figures S12 – S14). Further characterization by ^{1}H NMR spectroscopy in solution also supported the grafting of the carbene ligands to the surface, with spectra showing broad peaks in the chemical shift regions attributable to NHCs, and the absence of resonances due to protons expected to be in close proximity to the NP surface (*i.e.*, α-methylene groups in **5a** and **5c**, and aromatic protons in **5c** and **5e**) (Figures S19 – S21). The coordination mode of such ligands in nanoparticles **5** was investigated by solid-state ^{1}H–^{13}C CP-MAS NMR spectroscopy. As expected, resonances attributable to carbons of the Pt–(η^2:η^2-allyl ether) moiety (expected at *ca.* 70, 33, and 43 ppm) were never observed (Figure 7c for PtNPs **5a** and Figures S25 – S26 for **5c** and **5e**, respectively), thus indicating that NHC and presumably some hydride are the only ligands coordinated to the surface (not counting water molecules). The ^{13}C resonances for the NHC ligands were observed at expected regions when taking those for precursors **4** as a reference. The coordination of the NHC ligands through the C^2-position of the ring (*i.e.*, carbenic carbon atom) was supported by the absence of resonance signal due to the C^2-atom of the corresponding imidazolium salts (150 – 139 ppm), and the detection of a broad signal at the customary chemical shift (179 – 175 ppm; not observed for **5a**). Again, these signals were slightly shifted to upper field compared with the precursor, in agreement with coordination of NHC ligands to the platinum surface, and with a superior net shielding on the NHC-donor atom exerted by metallic particle than by the Pt(0) atom in the starting molecular complex.[32,40]

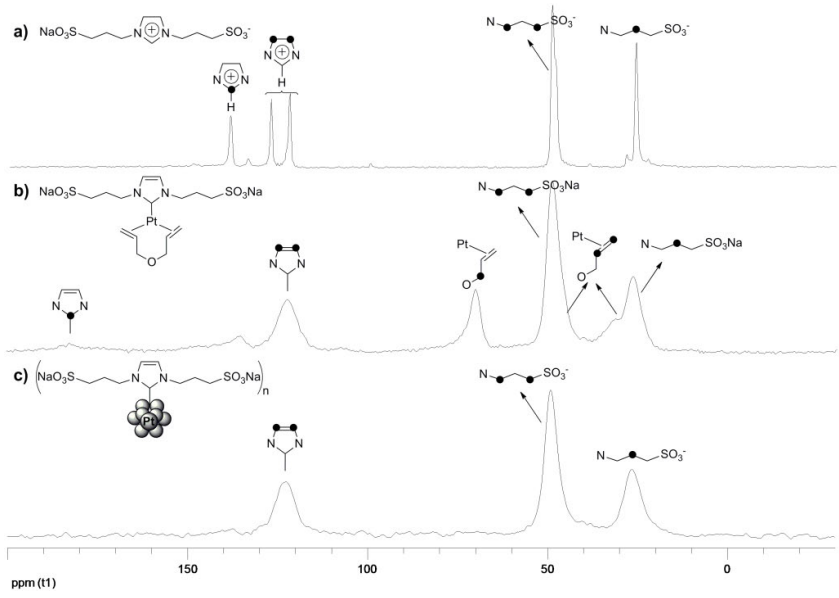

Figure 7. $^{1}H–^{13}C$ CP-MAS spectra of a) **aH**, b) **4a** and c) **5a** in the solid-state.

The carbenic carbon in PtNPs **5** rendered resonance signals from very weak (**5a** and **5c**) to undetectable (**5a**). Thus, in order to get stronger evidence of the coordination mode of NHC ligand in these NPs, we prepared ^{13}C-labeled platinum nanoparticles **^{13}C-5c** (see Experimental Section for details). Analysis by TEM revealed the presence of nanoparticles with similar shape and distribution size than their non-labeled counterparts **5c** (*i.e.*, 3 ± 2 nm; Figures S5 and S7). The ^{1}H-^{13}C CP-MAS spectrum showed a resonance signal at 176 ppm, assigned unequivocally to the carbenic carbon coordinated to the NP surface (Figure S27), although in this case the $^{13}C–^{195}Pt$ coupling constant could not be measured since deconvolution of the signal was unfeasible because of partial overlapping of the satellites with another peak.

CONCLUSIONS

Two synthetic strategies for the preparation in aqueous medium of new water-soluble platinum nanoparticles stabilized by sulfonated NHC ligands, have been developed: *a)* reduction under CO of dimethylplatinum(II), and *b)* hydrogenation of diallyletherplatinum(0) water-soluble NHC complexes. High stability in water have been found for nanoparticles derived from complexes containing propylsulfonate substituents on the carbene ligand, which has been ascribed to inert coordination of NHC ligands to the surface, together suitable flexibility of the sulfonated chains for effective hydration of the ionic groups. Unambiguous evidence for such coordination has been obtained by solid-state NMR spectroscopy with the determination of a $^{13}C–^{195}Pt$ coupling constant (940 Hz) in PtNPs isotopicaly ^{13}C-labeled at the carbenic carbon atom. The characterization of NPs prepared by

method *a)* has revealed that carbonyl ligands are also firmly coordinated to the metallic surface, and experiments aimed to follow the transformation of the dimethylplatinum(II) precursors have disclosed the coordination of CO to Pt(II) before nanoparticle formation. Additionally, a second coordination sphere with bis(NHC)Pt(II) complexes has been observed associated to PtNPs containing NHC ligands symmetrically *N,N'*-substituted with propylsulfonate chains, similar to that we have previously described.[32] On the other hand, NPs size obtained by method *b)* has been found to strongly depend on the NHC bulkiness. Thus, the biggest nanoparticles have been obtained for the bulkiest ligand and vice versa. It is important to note that this method has afforded more polydispersed particles than approach *a)*. Moreover PtNPs **5** revealed that a stability of their colloidal solutions is only possible with flexible sulfonated moieties, which enable the suitable interaction between the sulfonate groups and the aqueous medium.

The results presented here represent the first investigation on mild synthetic methods carried out in water for the development of water-soluble metal nanoparticles stabilized by hydrophilic NHC ligands. This research opens a new perspective to the application and functionalization of metal nanoparticles. For example, further efforts are under way in our laboratories with regard to the functionalization and catalytic applications of nanosystems here obtained.

EXPERIMENTAL SECTION

General Procedures. All operations were carried out under argon atmosphere using standard Schlenk tube or Fischer-Porter bottle techniques. Unless otherwise stated, reagents and solvents were used as received from commercial sources. Argon, CO and H_2 were purchased from Air Liquide, ^{13}CO (^{13}C, 99.14%) from Eurisotop, formaldehyde-^{13}C (20% wt in water, atom 99% ^{13}C), 1,3-propanesultone and dialysis tubing cellulose membrane (average flat width 25mm, molecular weight cut-off = 14000 Dalton) from Sigma-Aldrich. Deionized water (type II quality) was obtained using a Millipore Elix 10 UV Water Purification System. Dimethyl sulfoxide was distilled under argon over calcium hydride. Complexes *cis*-[Pt(CH_3)$_2$(dmso)(NHC)] **1**,[38] [Pt(AE)(NHC)] (AE = diallylether) **4**,[33] ^{13}C-labelled *N*–mesitylimidazole,[41] and *cis*-[Pt(CH_3)$_2$(dmso)(^{13}C-NHC)] **^{13}C-1c**,[32] were synthesized as described in the literature.

Samples for TEM were prepared by deposition after evaporation on a covered holey copper grid of three drops of the nanoparticles in water (0.5 mL) dispersed in EtOH (2 mL), or a drop of the crude aqueous colloidal solution. TEM analyses were performed at the "Service Commun de Microscopie Electronique de l'Université Paul Sabatier" (TEMSCAN-UPS) by using a JEOL JEM 1011 CX-T electron microscope operating at 100 kV with a point resolution of 4.5 Å. The approximation of the particles mean size was made through a

manual analysis of enlarged micrographs by measuring a large number of particles (> 250) using ImageJ software to analyze the images.

Solid-state NMR with ^{1}H-^{13}C cross polarization (CP-MAS NMR) were performed at the LCC (Toulouse) on a Bruker Avance 400WB instrument equipped with a 2.5 mm probe with the sample rotation frequency being set at 12 kHz. Measurements were carried out in a 4 mm ZrO_2 rotor. ^{1}H-, and ^{13}C-NMR spectra in liquid phase were recorded on a Bruker AMX 500 NMR, Bruker Avance 400 MHz, Varian Mercury 300 or Unity 300 MHz spectrometers. Chemical shifts (δ, parts per million) are quoted relative to $SiMe_4$ (^{1}H, ^{13}C). They were measured by internal referencing to the ^{13}C or residual ^{1}H resonances of the deuterated solvents (D_2O ^{1}H δ 4.69; dmso–d_6 ^{1}H δ 2.49, ^{13}C δ 39.0; respectively). Coupling constants (J) are given in Hertz. When required, two dimensional $^{1}H-^{13}C$ HSQC and HMBC experiments were carried out for the unequivocal assignment of ^{1}H and ^{13}C resonances.

IR spectra were recorded on a Thermo Scientific Nicolet 6700 FT-IR spectrometer in the range 4000–500 cm^{-1}, using a Smart Orbit ATR platform. IR absorptions are given in cm^{-1}. The Analytical Services of the Universidad de Alcalá performed the mass spectra in an Agilent G3250AA LC/MSD TOF Multi (MALDI and ESI) mass spectrometer in the electrospray ionization mode, whereas those performed by the analytical services of the Université de Toulouse were made in a Xevo G2 QTof (Waters) mass spectrometer.

Synthesis of water-soluble platinum nanoparticles PtNPs 3 by the CO method. The corresponding platinum complex **1** (1.00 mmol) was introduced into a 100 mL Fischer Porter flask, dissolved in deionized water (10 mL), and the resulting colorless to pale-yellow solutions stirred at 1000 rpm for 5 days at room temperature under CO at 3 bar. The black solutions formed were filtered through a PTFE 0.2 μm filter in order to remove any eventual suspended solid, and then dialyzed in water using a cellulose membrane (MWCO = 14000 Dalton) for 24 h. The dialyses were monitored by taking aliquots of the nanoparticle solutions and analyzing the disappearance of dmso and molecular species (*e.g.*, free imidazolium salts) by ^{1}H-NMR spectroscopy. Subsequent solvent removal under vacuum (50 °C, 100 mbar, 3 h) afforded black solids that were dried under vacuum overnight (room temperature, 10 mbar). The platinum nanoparticles were found to be stable in water under air, without precipitation over the time (> 6 months).

PtNPs 3a: The platinum nanoparticles **3a** were obtained from **1a** (0.660 g, 1.00 mmol) as a black powder. **TEM**: NP mean size, 1.0 ± 0.3 nm. **ATR-FTIR (cm^{-1})**: υ (CO) = 2075 (terminal). **^{1}H-^{13}C CP-MAS NMR**: δ 164.2 (broad s, Imz-C^2), 122.6 (s, Imz-$C^{4,5}$), 48.8 (s, NCH_2 and CH_2S overlapping), 26.0 (s, $CH_2CH_2CH_2$).

PtNPs 3b: The platinum nanoparticles 3**b** were obtained from **1b** (0,530 g, 1.00 mmol) as a black powder. **TEM**: NP mean size, 1.3 ± 0.4 nm. **ATR-FTIR (cm^{-1})**: υ (CO) = 2071 (terminal). **^{1}H-^{13}C CP-MAS NMR**: δ 162.7 (broad s, Imz-C^{2}), 123.1 (s, Imz-C^{4} and Imz-C^{5} overlapping), 48.9 (s, NCH_2 and CH_2S overlapping), 37.6 (s, NCH_3), 26.3 (s, $CH_2CH_2CH_2$).

PtNPs 3c: The platinum nanoparticles **3c** were obtained from **1c** (0.633 g, 1.00 mmol) as a black powder. **TEM**: NP mean size, 1.0 ± 0.3 nm. **ATR-FTIR (cm^{-1})**: υ (CO) = 2065 (terminal). **^{1}H-^{13}C CP-MAS NMR**: δ 162.1 (broad s, Imz-C^{2}), 135.0 (s, Ar-C^{4}, Ar-C^{2} and Ar-C^{1} overlapping), 128.6 (s, Ar-C^{3}), 124.5 (s, Imz-C^{4} and Imz-C^{5} overlapping), 48.7 (s, NCH_2 and CH_2S overlapping), 28.2 (s, $CH_2CH_2CH_2$), 20.9 (s, Ar-*p-Me*), 18.0 (s, Ar-*o-Me*).

Synthesis of ^{13}C-labelled platinum nanoparticles ^{13}C-3c. PtNPs **^{13}C-3c** were prepared starting from platinum complex **^{13}C-1c**[32] (0.501 g, 0.789 mmol) following the general procedure detailed above for nanoparticles **3**. In this case dialysis was kept for 36 h. **TEM**: NP mean size, 1.1 ± 0.4 nm. **ATR-FTIR (cm^{-1})**: υ (CO) = 2065 (terminal). **^{1}H-^{13}C CP-MAS NMR**: δ 162.6 (s with ^{195}Pt satellites, $^{1}J(^{13}C\text{-}^{195}Pt)$ = 1060 ± 20, Imz-C^{2}), 135.1 (s, Ar-C^{4}, Ar-C^{2} and Ar-C^{1} overlapping), 128.6 (s, Ar-C^{3}), 123.1 (s, Imz-C^{4} and Imz-C^{5} overlapping), 48.4 (s, NCH_2 and CH_2S overlapping), 26.7 (s, $CH_2CH_2CH_2$), 19.9 (s, Ar-*p-Me*), 17.4 (s, Ar-*o-Me*).

Formation of intermediates *cis*-[Pt(CH$_3$)$_2$(^{13}CO)(NHC)] ([3]). The corresponding platinum complex **1** (0.0551 mmol) was introduced into a 5 mL Fischer Porter flask, dissolved in D_2O (1.0 mL), and the resulting solution stirred at 1000 rpm at room temperature under 3 bar of ^{13}CO for the time indicated below for each complex. After depressurization, the samples were analyzed by ^{1}H and ^{13}C NMR spectroscopy and ESI mass spectrometry.

Cis-(^{13}*C-carbonyl)[1,3-bis(3-sodiumsulfonatepropyl)imidazol-2-ylidene]dimethylplatinum(ii)* ***([3a])***. Complex **[3a]** was obtained from **1a** (36.3 mg, 0.0551 mmol) after 24 h of reaction. ^{1}H NMR (500 MHz, D_2O): δ 7.18 (s with ^{195}Pt satellites, $^{4}J(^{1}H-^{195}Pt)$ = 6.0, 2H, Imz), 4.17 (m, 4H, NCH_2), 2.80 (m, 4H, CH_2S), 2.16 (m, 4H, $CH_2CH_2CH_2$), 0.41 (d with ^{195}Pt satellites, $^{2}J(^{1}H-^{195}Pt)$ = 67.0, $^{3}J(^{1}H-^{13}C)$ = 2.0, 3H, Me *trans* to NHC), 0.15 (d with ^{195}Pt satellites, $^{2}J(^{1}H-^{195}Pt)$ = 71.0, $^{3}J(^{1}H-^{13}C)$ = 2.5, 3H, Me *cis* to NHC). $^{13}C\{^{1}H\}$ NMR (125 MHz, D_2O): δ 180.2 (s with ^{195}Pt satellites, $^{1}J(^{13}C-^{195}Pt)$ = 998, ^{13}CO), 177.4 (s, Imz C^{2}), 121.4 (s with ^{195}Pt satellites, $^{3}J(^{13}C-^{195}Pt)$ = 20.2, Imz C$^{4\text{-}5}$), 48.2 (s with ^{195}Pt satellites, $^{3}J(^{13}C-^{195}Pt)$ = 29.2, NCH_2), 48.0 (s, CH_2S), 25.4 (s, $CH_2CH_2CH_2$), 0.14 (d with ^{195}Pt satellites, $^{1}J(^{13}C-^{195}Pt)$ = 593.0, $^{2}J(^{13}C-^{13}C)$ = 34.0, PtMe *cis* to NHC), −11.1 (d with ^{195}Pt satellites, $^{1}J(^{13}C-^{195}Pt)$ = 491.0, $^{2}J(^{13}C-^{13}C)$ = 2.5, PtMe *trans* to NHC). ESI-MS (negative ion, H_2O:D_2O 1:1): *m*/*z* 587.0287 $[M - Na]^-$ (calcd 587.0292) 25%; 503.9860 $[M - 2Na + H - {}^{13}CO - 2CH_4]^-$ (calcd 503.9868) 100%.

Cis-(^{13}*C-carbonyl)dimethyl[1-methyl-3-(3-sodiumsulfonatepropyl)imidazol-2-ylidene]platinum(ii)* ***([3b])***. Complex **[3b]** was obtained from **1b** (29.2 mg, 0.0551 mmol) after 24 h of reaction. ^{1}H NMR (500 MHz, D_2O): δ 7.17 (d, $^{3}J_{HH}$ = 2.0, 1H, Imz), 7.11 (d, $^{3}J_{HH}$ = 1.5, 1H, Imz), 4.18 (t, $^{3}J_{HH}$ = 7.0, 2H, NCH_2), 3.64 (s, 3H, NMe), 2.82 (t, $^{3}J_{HH}$ = 8.0, 2H, CH_2S), 2.19 (m, 2H, $CH_2CH_2CH_2$), 0.44 (d with ^{195}Pt satellites, $^{2}J(^{1}H-^{195}Pt)$ = 67.0, $^{3}J(^{1}H-^{13}C)$ = 2.0, 3H, PtMe *trans* to NHC), 0.18 (d with ^{195}Pt satellites, $^{2}J(^{1}H-^{195}Pt)$ = 71.5, $^{3}J(^{1}H-^{13}C)$ = 2.5, 3H, PtMe *cis* to NHC). $^{13}C\{^{1}H\}$ NMR (125 MHz, D_2O): δ 180.3 (s with ^{195}Pt satellites, $^{1}J(^{13}C-^{195}Pt)$ = 995, ^{13}CO), 176.8 (s, Imz-C^2), 122.8 (s with ^{195}Pt satellites, $^{3}J(^{13}C-^{195}Pt)$ = 20.0, Imz-C^5), 120.9 (s with ^{195}Pt satellites, $^{3}J(^{13}C-^{195}Pt)$ = 21.2, Imz-C^4), 48.12 (s, NCH_2), 48.09 (s, CH_2S), 36.7 (s, NMe), 25.5 (s, $CH_2CH_2CH_2$), −0.03 (d, $^{2}J(^{13}C-^{13}C)$ = 34.1, PtMe *cis* to NHC), −11.0 (d, $^{2}J(^{13}C-^{13}C)$ = 2.4, PtMe *trans* to NHC). ESI-MS (negative ion, H_2O:D_2O 1:1): *m*/*z* 645.0848 $[M - Na - CH_3 + NHC]^-$ (calcd 645.0851) 85%; 616.0867 $[M - Na - CH_3 + NHC - {}^{13}CO]^-$ (calcd 616.0869) 100%.

Cis-(^{13}*C-carbonyl)dimethyl[1-(3-sodiumsulfonatepropyl)-3-(2,4,6-trimethylphenyl)imidazol-2-ylidene]platinum(ii)* ***([3c])***. Complex **[3c]** was obtained from **1c** (34.9 mg, 0.0551 mmol) after 2 h of reaction. ^{1}H NMR (500 MHz, D_2O): δ 7.31 (s, 1H, Imz), 6.74 (s, 2H, Ar), 6.73 (s, 1H, Imz), 4.15 (m, 2H, NCH_2), 2.69 (m, 2H, CH_2S), 2.16 (m, 2H, $CH_2CH_2CH_2$), 2.00 (s, 3H, Ar-*p*-Me), 1.80 (s, 6H, Ar-*o*-Me), 0.18 (s with ^{195}Pt satellites, $^{2}J(^{1}H-^{195}Pt)$ = 68.0, 3H, PtMe *trans* to NHC), 0.13 (s with ^{195}Pt satellites, $^{2}J(^{1}H-^{195}Pt)$ = 71.0, 3H, PtMe *cis* to NHC). $^{13}C\{^{1}H\}$ NMR (100 MHz, D_2O): δ 181.0 (s with ^{195}Pt satellites, $^{1}J(^{13}C-^{195}Pt)$ = 1022, ^{13}CO), 174.0 (s, Imz-C^2), 138.7 (s, Ar-C^4), 135.9 (s, Ar-C^2), 134.9 (s, Ar-C^1), 128.9 (s, Ar-C^3), 122.6 (s, Imz-C^4), 121.7 (s, Imz-C^5), 48.1 (s, NCH_2), 48.0 (s, CH_2S), 25.6 (s, $CH_2CH_2CH_2$), 20.6 (s, Ar-*p*-Me), 17.5 (s, Ar-*o*-Me), 2.3 (d, $^{2}J(^{13}C-^{13}C)$ = 34.1, PtMe *cis* to NHC), −9.7 (d, $^{2}J(^{13}C-^{13}C)$ = 2.4, PtMe *trans* to NHC). ESI-MS (negative ion, H_2O:D_2O 1:1): *m*/*z* 561.1223 $[M - Na]^-$ (calcd 561.1218) 100%; 516.0923 $[M - Na - {}^{13}CO - CH_4]^-$ (calcd 516.0926) 6%.

Cis-(^{13}*C-carbonyl)dimethyl[1-(3-sodiumsulfonatepropyl)-3-(2,4,6-trimethylphenyl)imidazol-2-*^{13}*C-ylidene]platinum(ii)* ***([*^{13}***C-3c])***. Complex **[^{13}C-3c]** was obtained from **^{13}C-1c** (26.1 mg, 0.0411 mmol) after 4 h of reaction. ^{1}H NMR (500 MHz, D_2O): δ 7.28 (s, 1H, Imz), 6.76 (s, 2H, Ar), 6.75 (s, 1H, Imz), 4.16 (m, 2H, NCH_2), 2.74 (m, 2H, CH_2S), 2.17 (m, 2H, $CH_2CH_2CH_2$), 2.00 (s, 3H, Ar-*p*-Me), 1.79 (s, 6H, Ar-*o*-Me), 0.16 (s with ^{195}Pt satellites, $^{2}J(^{1}H-^{195}Pt)$ = 67.0, 3H, PtMe *trans* to NHC), 0.12 (s with ^{195}Pt satellites, $^{2}J(^{1}H-^{195}Pt)$ = 71.0, 3H, PtMe *cis* to NHC). $^{13}C\{^{1}H\}$ NMR (125 MHz, D_2O): δ 180.8 (s with ^{195}Pt satellites, $^{1}J(^{13}C-^{195}Pt)$ = 1023, ^{13}CO), 174.0 (s with ^{195}Pt satellites, $^{1}J(^{13}C-^{195}Pt)$ = 810, Imz-C^2), 138.9 (s, Ar-C^4), 135.7 (s, Ar-C^2), 135.0 (s, Ar-C^1), 128.8 (s, Ar-C^3), 122.7 (s, Imz-C^4), 121.6 (s, Imz-C^5), 48.0 (s, NCH_2 and CH_2S overlapping), 25.6 (s, $CH_2CH_2CH_2$), 20.5 (s, Ar-*p*-Me), 17.4 (s, Ar-*o*-Me), 2.1 (d with ^{195}Pt satellites, $^{2}J(^{13}C-^{13}CO)$ = 37.5, $^{1}J(^{13}C-^{195}Pt)$ = 601, PtMe *cis* to NHC), −10.1 (d with ^{195}Pt satellites, $^{2}J(^{13}C-^{13}C_{NHC})$ = 28.9, $^{1}J(^{13}C-^{195}Pt)$ = 486, PtMe *trans* to NHC).

NMR data for cis-di(^{13}*C-carbonyl)methyl[1-(3-sulfonatepropyl)-3-(2,4,6-trimethylphenyl)imidazol-2-*^{13}*C-ylidene]platinum(ii) (**A**).* ^{1}H NMR (300 MHz, D_2O): δ 7.45 (s, 1H, Imz), 7.10 (s, 1H, Imz), 7.02 (s, 2H, Ar), 4.33 (m, 2H, NCH_2), 2.87 (m, 2H, CH_2S), 2.29 (m, 2H, $CH_2CH_2CH_2$), 2.24 (s, 3H, Ar-*p*-Me), 1.90 (s, 6H, Ar-*o*-Me), 0.22 (dd with ^{195}Pt satellites, $^{2}J(^{1}H-^{195}Pt)$ = 72.9, $^{3}J(^{1}H-^{13}C)$ = 2.1, $^{3}J(^{1}H-^{13}C)$ = 2.1, 3H, PtMe). $^{13}C\{^{1}H\}$ NMR (125 MHz, D_2O): δ 206.3 (d with ^{195}Pt satellites, $^{1}J(^{13}C-^{195}Pt)$ = 1006, $^{2}J(^{13}C-^{13}C)$ = 47.5, ^{13}CO *trans* to NHC), 177.3 (s with ^{195}Pt satellites, $^{1}J(^{13}C-^{195}Pt)$ = 1001, ^{13}CO *cis* to NHC), 170.6 (s, Imz-C^2), 140.1 (s, Ar-C^4), 136.4 (s, Ar-C^2), 135.4 (s, Ar-C^1), 129.2 (s, Ar-C^3), 123.2 (s, Imz-C^4), 122.1 (s, Imz-C^5), 48.3 (s, NCH_2), 47.9 (s, CH_2S), 25.6 (s, $CH_2CH_2CH_2$), 20.1 (s, Ar-*p*-Me), 17.0 (s, Ar-*o*-Me), −6.3 (s, PtMe).

Synthesis of water-soluble platinum nanoparticles PtNPs 5 by the H_2 method. The corresponding platinum complex **4** (0.390 mmol) was introduced into a 100 mL Fischer Porter flask, dissolved in deionized water (10 mL), and the resulting colorless to pale-yellow solution stirred at 1000 rpm at room temperature under 3 bar of H_2 for the time indicated below for each complex. The progress of the reaction was monitored by ^{1}H-NMR inspecting the disappearance of the resonances due to the allyl ether ligand. In addition, the formation of propyl ether was confirmed by extracting the hydrogenated product in $CDCl_3$ and subsequent recording of the ^{1}H-NMR spectrum of the solutions. The black solutions formed were filtered through a PTFE 0.2 μm filter, and dialyzed in water using a cellulose membrane (MWCO = 14000 Dalton) for 36 h. The dialyses were also monitored by ^{1}H-NMR spectroscopy. Subsequent removal of the solvent (50 °C, 100 mbar, 3 h) afforded black solids that were dried overnight under vacuum (room temperature, 10 mbar). The platinum nanoparticles were found to be stable in water under air, without precipitation over the time (> 6 months), except for **5e** where a solid was observed after one day, although, the solid can be re-dispersed in the aqueous medium by simply shaking.

PtNPs 5a: The platinum nanoparticles **5a** were obtained from **4a** (0.253 g, 0.390 mmol) after 10 days of reaction as a black powder. **TEM**: NP mean size, 1.7 ± 0.6 nm. **^{1}H-^{13}C CP-MAS NMR**: δ 122.7 (s, Imz-$C^{4,5}$), 49.1 (s, NCH_2 and CH_2S overlapping), 26.6 (s, $CH_2CH_2CH_2$). Imz-C^2 not observed.

PtNPs 5c: The platinum nanoparticles **5c** were obtained from **4c** (0.243 g, 0.390 mmol) after 22 days of reaction as a black powder. **TEM**: NP mean size, 3 ± 2 nm. **^{1}H-^{13}C CP-MAS NMR**: δ 174.9 (broad s, Imz-C^2), 135.4 (s, Ar-C^4, Ar-C^2 and Ar-C^1 overlapping), 129.8 (s, Ar-C^3), 123.8 (s, Imz-C^4 and Imz-C^5 overlapping), 48.8 (s, NCH_2), 41.2 (s, CH_2S), 26.2 (s, $CH_2CH_2CH_2$), 21.0 (s, Ar-*p-Me*) 18.0 (s, Ar-*o-Me*).

PtNPs 5e: The platinum nanoparticles **5e** were obtained from **4d** (0.345 g, 0.390 mmol) after 42 days of reaction as a black powder. **TEM**: NP mean size, 4.0 ± 0.8 nm. **^{1}H-^{13}C CP-MAS NMR**: δ 178.9 (broad s, Imz-C^{2}), 146.7 (s, Ar-C^{4}, and Ar-C^{2} overlapping), 136.2 (s, Ar-C^{1}), 123.0 (s, Imz-C^{4}, Imz-C^{5}, and Ar-C^{3}, overlapping), 29.4 (s, *C*HMe), 24.4 (s, CH*Me*).

Synthesis of ^{13}C-labelled complex ^{13}C-4c. In a Schlenck flask, Pt(norb)$_3$ (0.500 g, 1.05 mmol) was dissolved in diallylether (1.30 mL, 10.6 mmol), and the mixture stirred for 20 min at room temperature. In another Schlenck flask, imidazolium salt **^{13}C-cH**^{41} (0.323g, 1.05 mmol) was combined with sodium tert-butoxide (0.120 g, 1.25 mmol) in DMSO (10 mL), and stirred for 5 min at room temperature. This solution was subsequently transferred under argon to the first one. After stirring for 3 h at room temperature, the resulting mixture was filtered through a pad of kieselguhr, followed by partial removal of the solvent under vacuum –up to a remaining volume of 2–3 mL. The product was then precipitated by the addition of THF (60 mL), separated by filtration, washed with THF (3 × 20 mL), and dried under vacuum (2 h, 90 ºC, 4 mbar) to yield the platinum complex **^{13}C-4c** as a brown solid (0.607 g, 93%). ^{1}H-NMR (300 MHz, dmso-d$_6$): δ 7.64 (dd, $^{3}J_{HH}$ = 2.1, ^{3}J (^{1}H-^{13}C) = 2.4, 1H, Imz); 7.30 (d, $^{3}J_{HH}$ = 2.1, ^{3}J (^{1}H-^{13}C) = 2.4, 1H, Imz); 6.86 (s, 2H, Ar); 4.02 (m, 2H, NCH$_2$); 3.92 (dd with ^{195}Pt satellites, ^{3}J(^{1}H-^{195}Pt) = 44.8, $^{3}J_{HH}$ = 11.4, $^{2}J_{HH}$ = 1.8, 2H, OCH$_2$ eq); 2.44 (m, 2H, CH$_2$S); 2.30 (m, 2H, C*H*=CH$_2$); 2.19 (s, 3H, Ar *p*-Me); 2.00 (m, 2H, CH$_2$C*H*$_2$CH$_2$); 1.94 (s, 6H, Ar *o*-Me); 1.64 (d with ^{195}Pt satellites, ^{2}J(^{1}H-^{195}Pt) = 48.9, $^{3}J_{HH}$ = 8.2, 2H, CH=C*H*$_2$); 1.63 (t, $^{3}J_{HH}$ = 11.1, 2H, OCH$_2$ ax); 1.19 (d with ^{195}Pt satellites, ^{2}J(^{1}H-^{195}Pt) = 58.8, $^{3}J_{HH}$ = 10.8, 2H, CH=C*H*$_2$). ^{13}C{^{1}H}-NMR (75 MHz, dmso-d$_6$): δ 181.9 (s with ^{195}Pt satellites, ^{1}J(^{13}C-^{195}Pt) = 1334, Imz C^{2}), 137.1 (s, Ar C^{4}), 136.7 (s, Ar C^{1}), 134.3 (s, Ar C^{2}), 127.7 (s, Ar C^{3}), 122.3 (s, Imz C^{4}), 121.0 (s, Imz C^{5}), 68.5 (s, OCH$_2$), 48.5 (d, ^{2}J(^{13}C-^{13}C) = 8.2, NCH$_2$), 48.0 (s, CH$_2$S), 45.7 (d, ^{2}J(^{13}C-^{13}C) = 4.7, *C*H=CH$_2$), 30.8 (s with ^{195}Pt satellites, ^{1}J(^{13}C-^{195}Pt) = 191, CH=*C*H$_2$), 26.0 (s, CH$_2$*C*H$_2$CH$_2$), 20.1 (s, Ar *p*-Me), 17.0 (s, Ar *o*-Me). ESI-MS (negative ion, MeOH) *m/z*: 600.1530 [M–Na]$^-$ (calcd 601.1535) 100%. Anal. Calcd (%) for C$_{20}$^{13}CH$_{33}$N$_2$NaO$_6$PtS (**^{13}C-4c**•2H$_2$O): C, 38.33; H, 5.03; N, 4.24. Found (%): C, 38.03; H, 4.781; N, 4.667.

Synthesis of ^{13}C-labelled platinum nanoparticles ^{13}C-5c. PtNPs **^{13}C-5c** were prepared starting from platinum complex **^{13}C-4c** (0.500 g, 0.801 mmol) following the procedure detailed above for nanoparticles **5c**. **TEM**: NP mean size, 3 ± 2 nm. **^{1}H-^{13}C CP-MAS NMR**: δ 175.8 (broad s, Imz-C^{2}), 137.3 (s, Ar-C^{4}, Ar-C^{2} and Ar-C^{1} overlapping), 129.4 (s, Ar-C^{3}), 123.9 (s, Imz-C^{4} and Imz-C^{5} overlapping), 48.3 (s, NCH$_2$), 37.4 (s, CH$_2$S), 26.6 (s, CH$_2$*C*H$_2$CH$_2$), 20.3 (s, Ar-*p-Me*) 17.6 (s, Ar-*o-Me*).

ASSOCIATED CONTENT

Supporting Information

TEM images, ATR-FTIR spectra and NMR spectra for PtNPs, Intermediates **[3a–c]** and [^{13}**C-3c**], complex ^{13}**C-4c**, and characterization data for nano-object **3a/3a***. This material is available free of charge via the Internet at http://pubs.acs.org.

AUTHOR INFORMATION

Corresponding Authors

*Email: juanc.flores@uah.es (J.C.F.), chaudret@insa-toulouse.fr (B.C.), ernesto.dejesus@uah.es (E.d.J).

ACKNOWLEDGMENT

This work was supported by the Spanish Ministerio de Economía y Competitividad (project CTQ2011-24096) and CNRS and ANR (Siderus project ANR-08-BLAN-0010-03). E.A.B. is grateful to the Universidad de Alcalá for a FPI Doctoral Fellowship, and S.T. to the European Commission for a Postdoctoral Grant (PCIG11-GA-2012-317692).

REFERENCES

(1) A. Roucoux, J. Schulz, H. Patin, *Chem. Rev.* **2002**, *102*, 3757-3778.

(2) C. Burda, X. Chen, R. Narayanan, M. A. El-Sayed, *Chem. Rev.* **2005**, *105*, 1025-1102.

(3) D. Astruc, F. Lu, J. R. Aranzaes, *Angew. Chem., Int. Ed.* **2005**, *44*, 7852-7872.

(4) L. Duran Pachon, G. Rothenberg, *Appl. Organomet. Chem.* **2008**, *22*, 288-299.

(5) R. J. White, R. Luque, V. L. Budarin, J. H. Clark, D. J. MacQuarrie, *Chem. Soc. Rev.* **2009**, *38*, 481-494.

(6) *Clusters and Colloids: From Theory to Applications*, Schmid, G. ed., Wiley-VCH, Weinheim, **1994**.

(7) *Nanoparticles. From Theory to Application*, Schmid, G. ed., Wiley-VCH, Weinheim, **2004**.

(8) A. Roucoux, K. Philippot, in *Handbook of Homoge-neous Hydrogenations, Vol. 9* (Eds.: J. G. de Vries, C. J. Elsevier), Wiley-VCH, Weinheim, **2007**, pp. 217 - 255.

(9) *Nanoparticles and Catalysis*, Astruc, D. ed., Wiley-Interscience, New York, **2008**.

(10) L. S. Ott, R. G. Finke, *Coord. Chem. Rev.* **2007**, *251*, 1075-1100.

(11) B. L. Cushing, V. L. Kolesnichenko, C. J. O'Connor, *Chem. Rev.* **2004**, *104*, 3893-3946.

(12) in *N-Heterocyclic Carbenes: From Laboratory Curiosities to Efficient Synthetic Tools* (Ed.: S. Diez-Gonzalez), RSC Catalysis Series; The Royal Society of Chemistry, **2011**.

(13) M. C. Jahnke, F. E. Hahn, *Top. Organomet. Chem.* **2010**, *30*, 95-129.

(14) F. E. Hahn, M. C. Jahnke, *Angew. Chem. Int. Ed.* **2008**, *47*, 3122-3172.

(15) O. Kühl, *Chem. Soc. Rev.* **2007**, *36*, 592-607.

(16) P. Lara, O. Rivada-Wheelaghan, S. Conejero, R. Poteau, K. Philippot, B. Chaudret, *Angew. Chem. Int. Ed.* **2011**, *50*, 12080-12084.

(17) D. Gonzalez-Galvez, P. Lara, O. Rivada-Wheelaghan, S. Conejero, B. Chaudret, K. Philippot, P. W. N. M. van Leeuwen, *Catal. Sci. Tech.* **2013**, *3*, 99-105.

(18) M. Planellas, R. Pleixats, A. Shafir, *Adv. Synth. Catal.* **2012**, *354*, 651-662.

(19) K. V. S. Ranganath, J. Kloesges, A. H. Schäfer, F. Glorius, *Angew. Chem. Int. Ed.* **2010**, *49*, 7786-7789.

(20) C. Richter, K. Schaepe, F. Glorius, B. J. Ravoo, *Chem. Commun.* **2014**, *50*, 3204-3207.

(21) E. C. Hurst, K. Wilson, I. J. S. Fairlamb, V. Chechik, *New J. Chem.* **2009**, *33*, 1837-1840.

(22) J. Vignolle, T. D. Tilley, *Chem. Commun.* **2009**, 7230-7232.

(23) X. Ling, N. Schaeffer, S. Roland, M.-P. Pileni, *Langmuir* **2013**, *29*, 12647-12656.

(24) P. Lara, A. Suárez, V. Collière, K. Philippot, B. Chaudret, *ChemCatChem* **2014**, *6*, 87-90.

(25) T. Weidner, J. E. Baio, A. Mundstock, C. Grosse, S. Karthaeuser, C. Bruhn, U. Siemeling, *Aust. J. Chem.* **2011**, *64*, 1177-1179.

(26) A. V. Zhukhovitskiy, M. G. Mavros, T. Van Voorhis, J. A. Johnson, *J. Am. Chem. Soc.* **2013**, *135*, 7418-7421.

(27) C. M. Crudden, J. H. Horton, I. I. Ebralidze, O. V. Zenkina, A. B. McLean, B. Drevniok, Z. She, H.-B. Kraatz, N. J. Mosey, T. Seki, E. C. Keske, J. D. Leake, A. Rousina-Webb, G. Wu, *Nat. Chem.* **2014**, *6*, 409-414.

(28) S. G. Song, C. Satheeshkumar, J. Park, J. Ahn, T. Premkumar, Y. Lee, C. Song, *Macromolecules* **2014**, *47*, 6566-6571.

(29) M. Rodriguez-Castillo, D. Laurencin, F. Tielens, A. van der Lee, S. Clement, Y. Guari, S. Richeter, *Dalton Trans.* **2014**, *43*, 5978-5982.

(30) J. Crespo, Y. Guari, A. Ibarra, J. Larionova, T. Lasanta, D. Laurencin, J. M. Lopez-de-Luzuriaga, M. Monge, M. E. Olmos, S. Richeter, *Dalton Trans.* **2014**, *43*, 15713-15718.

(31) R. T. W. Huang, W. C. Wang, R. Y. Yang, J. T. Lu, I. J. B. Lin, *Dalton Trans.* **2009**, 7121-7131.

(32) E. A. Baquero, S. Tricard, J. C. Flores, J. E. de, B. Chaudret, *Angew. Chem. Int. Ed.* **2014**, *53*, 13220-13224.

(33) A. Ruiz-Varilla, E. A. Baquero, G. F. Silbestri, E. de Jesus, C. Gonzalez-Arellano, J. C. Flores, Manuscript *under preparation* **2015**.

(34) E. Ramirez, L. Eradès, K. Philippot, P. Lecante, B. Chaudret, *Adv. Func. Mater.* **2007**, *17*, 2219-2228.

(35) E. Ramirez, S. Jansat, K. Philippot, P. Lecante, M. Gomez, A. M. Masdeu-Bultó, B. Chaudret, *J. Organomet. Chem.* **2004**, *689*, 4601-4610.

(36) I. Favier, S. Massou, E. Teuma, K. Philippot, B. Chaudret, M. Gomez, *Chem. Commun.* **2008**, 3296-3298.

(37) G. F. Silbestri, J. C. Flores, E. de Jesús, *Organometallics* **2012**, *31*, 3355-3360.

(38) E. A. Baquero, J. C. Flores, J. Perles, P. Gomez-Sal, E. de Jesus, *Organometallics* **2014**, *33*, 5470-5482.

(39) G. Berthon-Gelloz, O. Buisine, J.-F. Brière, G. Michaud, S. Stérin, G. Mignani, B. Tinant, J.-P. Declercq, D. Chapon, I. E. Markó, *J. Organomet. Chem.* **2005**, *690*, 6156-6168.

(40) S. Kinayyigit, P. Lara, P. Lecante, K. Philippot, B. Chaudret, *Nanoscale* **2014**, *6*, 539-546.

(41) H.-L. Su, L. M. Perez, S.-J. Lee, J. H. Reibenspies, H. S. Bazzi, D. E. Bergbreiter, *Organometallics* **2012**, *31*, 4063-4071.

Supporting Information

Water–Soluble Platinum Nanoparticles Stabilized by Sulfonated N-Heterocyclic Carbenes: Effect of the Synthetic Approach

Edwin A. Baquero,[1,2] Simon Tricard,[2] Yannick Coppel,[3] Juan C. Flores,[1*] Bruno Chaudret,[2*] and Ernesto de Jesús[1*]

[1]*Departamento de Química Orgánica y Química Inorgánica, Campus Universitario, Universidad de Alcalá, 28871 Alcalá de Henares, Madrid, Spain.*

[2]*LPCNO; INSA, CNRS, Université de Toulouse, 135, Avenue de Rangueil, 31077 Toulouse, France.*

[3]*LCC; CNRS, INPT, Université de Toulouse, 205 Route de Narbonne, 31077 Toulouse, France.*

Email: juanc.flores@uah.es, chaudret@insa-toulouse.fr, ernesto.dejesus@uah.es

Table of Contents

1. ^{1}H- and ^{13}C-NMR spectra for ^{13}C-labelled compound (^{13}C-5c)

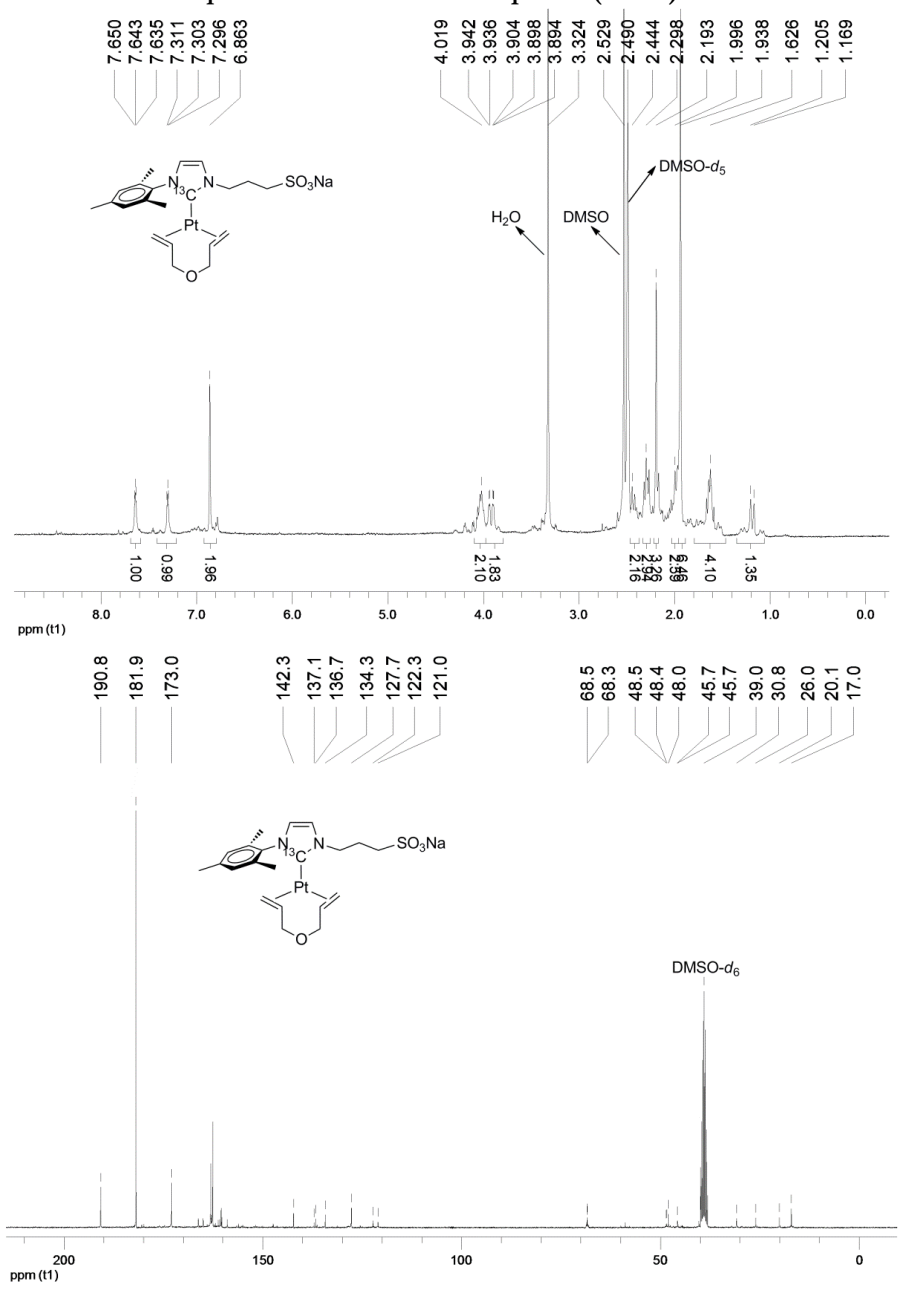

Figure S1. [1] H-NMR (300 MHz) and ^{13}C-NMR (75 MHz) spectra for **^{13}C-5c** in DMSO-d_6.

2. TEM images for the Pt nanoparticles

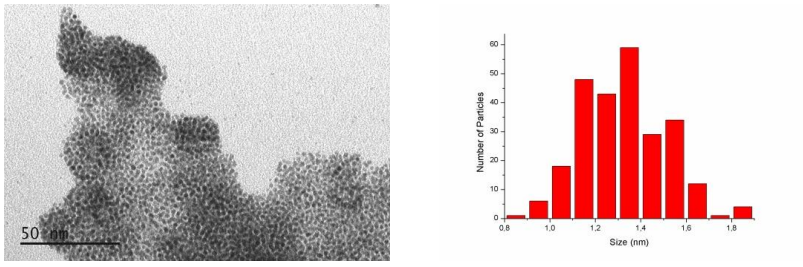

Figure S2. TEM image with the corresponding size distribution obtained for PtNPs **3b**.

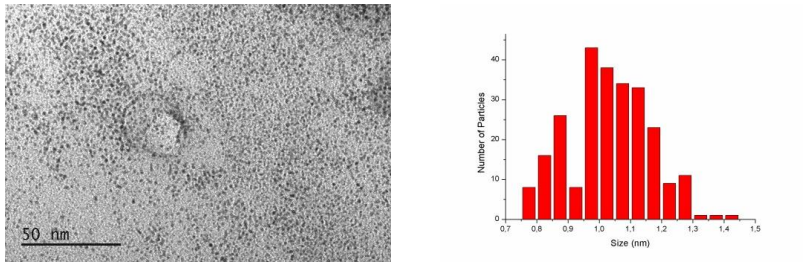

Figure S3. TEM image with the corresponding size distribution obtained for PtNPs **3c**.

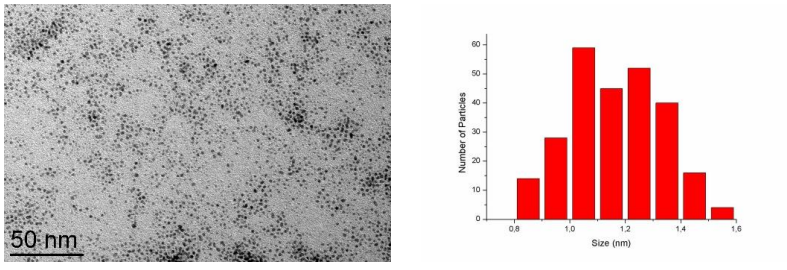

Figure S4. TEM image with the corresponding size distribution obtained for PtNPs **^{13}C-3c**.

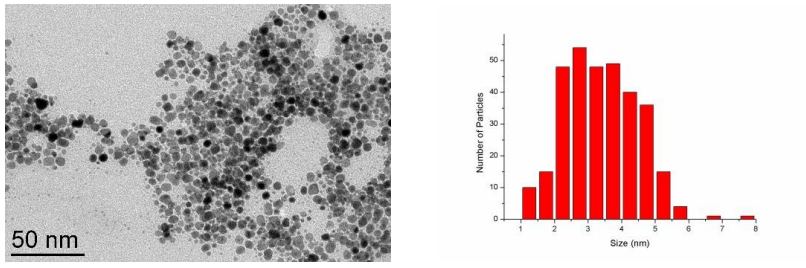

Figure S5. TEM image with the corresponding size distribution obtained for PtNPs **5c**.

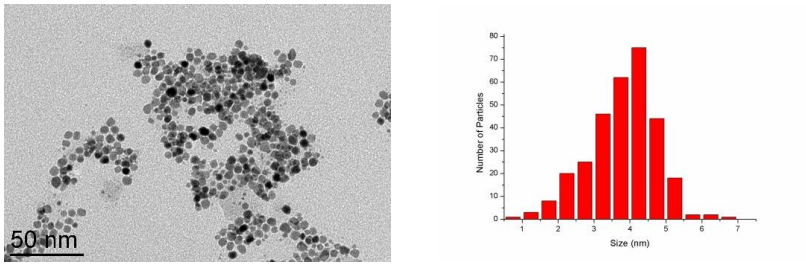

Figure S6. TEM image with the corresponding size distribution obtained for PtNPs **5e**.

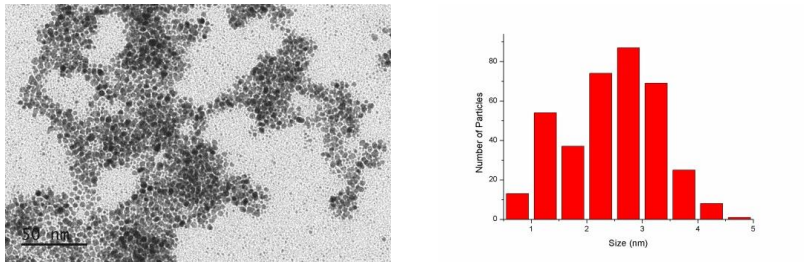

Figure S7. TEM image with the corresponding size distribution obtained for PtNPs **^{13}C-5c**.

3. ATR-FTIR spectra of the imidazolium salts, Pt complexes and Pt nanoparticles

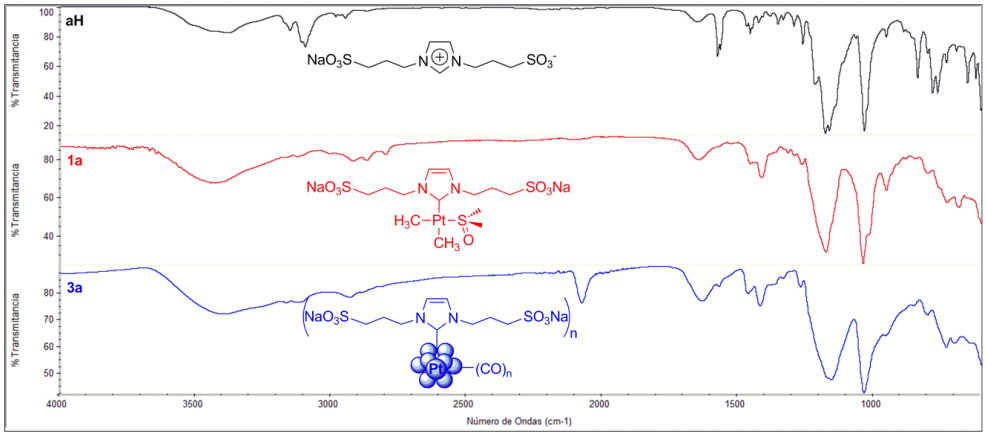

Figure S8. ATR-FTIR spectra of **aH**, **1a** and **3a**.

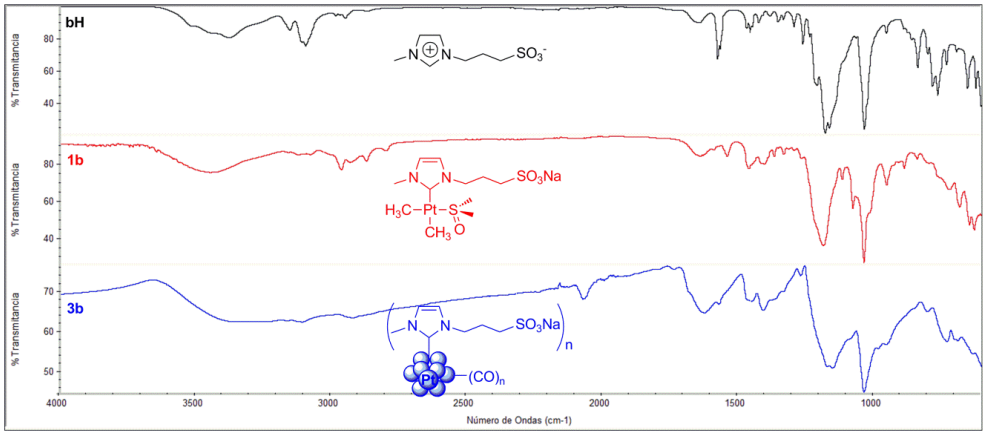

Figure S9. ATR-FTIR spectra of **bH**, **1b** and **3b**.

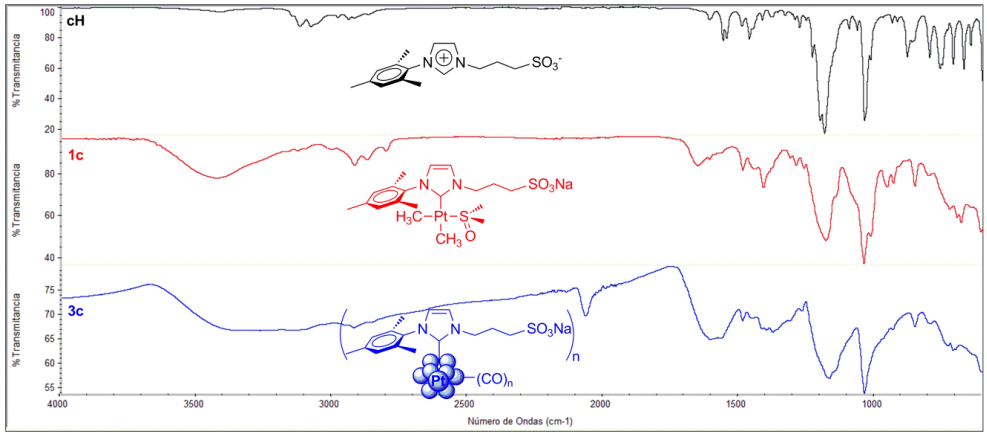

Figure S10. ATR-FTIR spectra of **cH**, **1c** and **3c**.

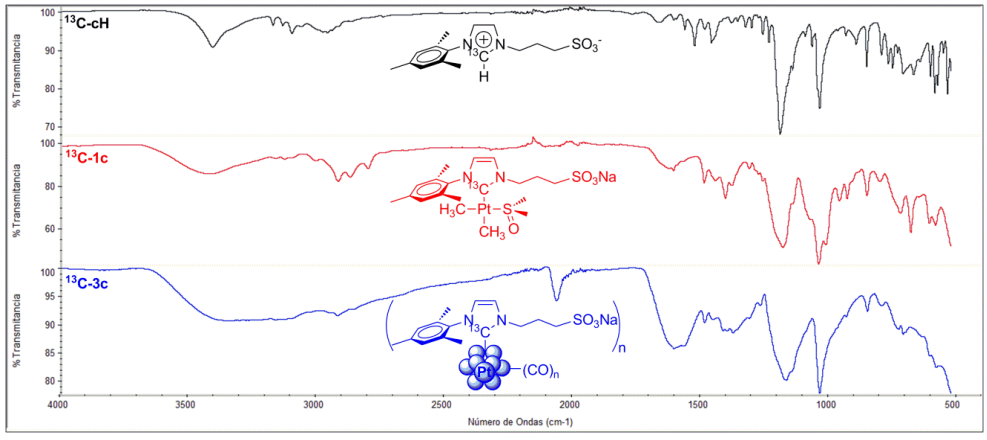

Figure S11. ATR-FTIR spectra of **^{13}C-cH**, **^{13}C-1c** and **^{13}C-3c**.

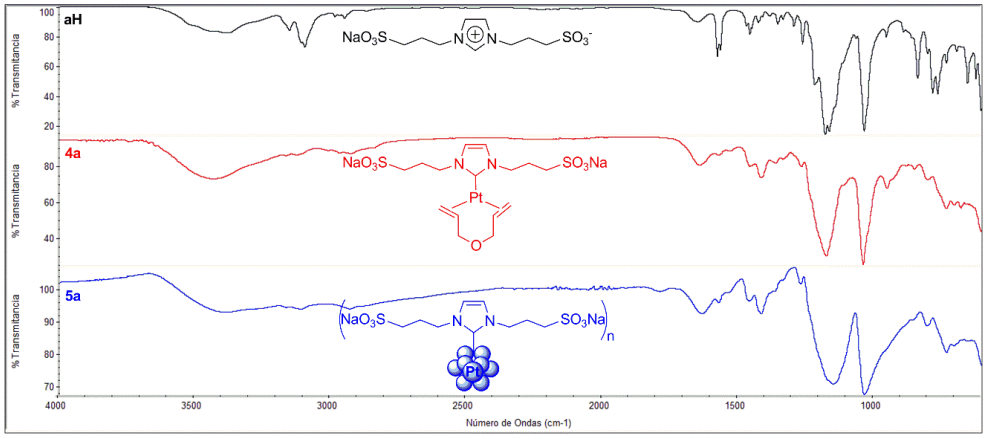

Figure S12. ATR-FTIR spectra of **aH**, **4a** and **5a**.

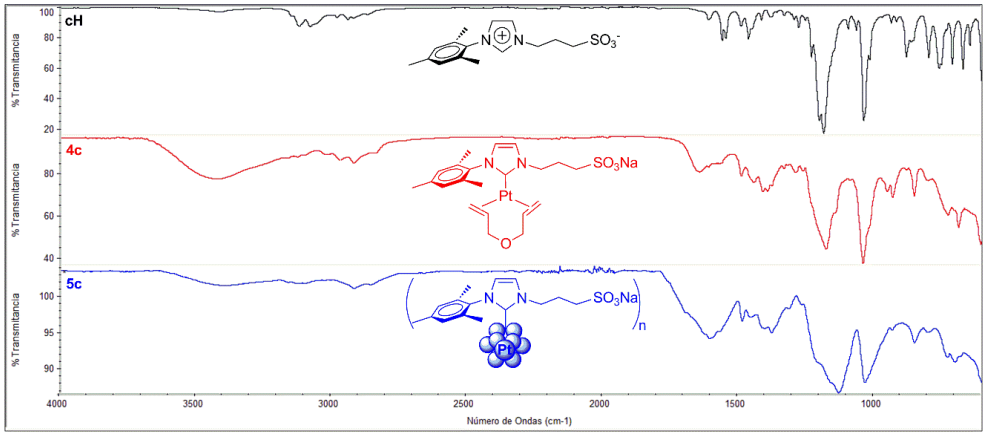

Figure S13. ATR-FTIR spectra of **cH**, **4c** and **5c**.

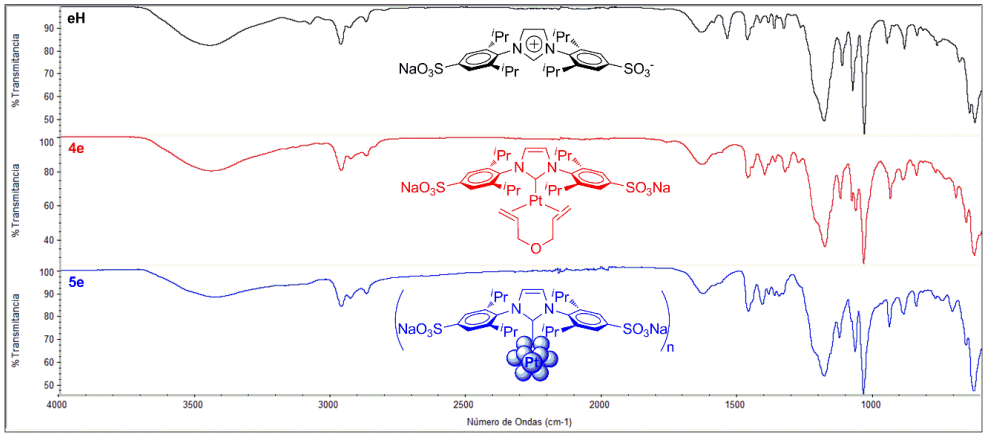

Figure S14. ATR-FTIR spectra of **eH**, **4e** and **5e**.

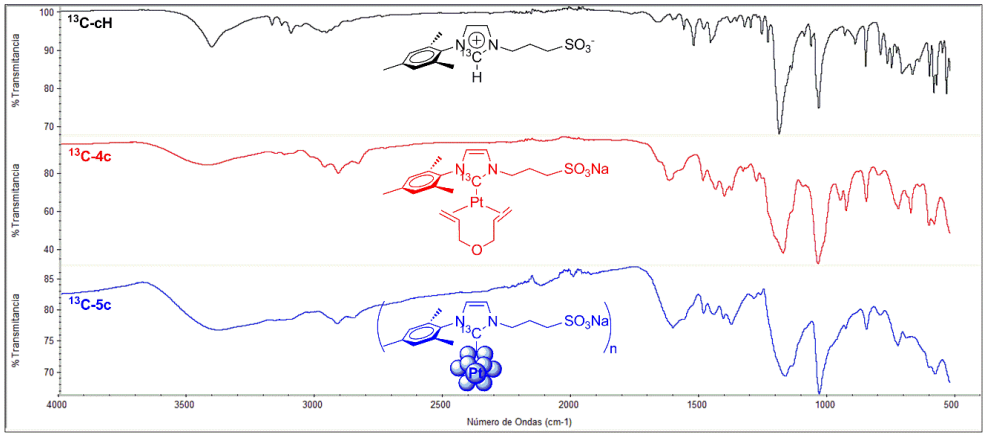

Figure S15. ATR-FTIR spectra of ^{13}**C-cH**, ^{13}**C-4c** and ^{13}**C-5c**.

4. ^{1}H-NMR spectra for Pt nanoparticles

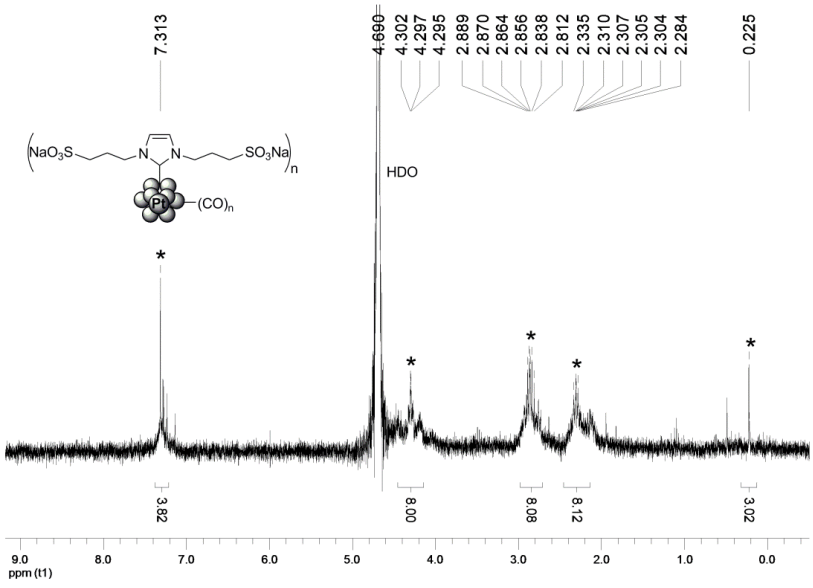

Figure S16. ^{1}H-NMR (300 MHz) for PtNPs **3a** (*i.e.*, pair **3a/3a***) in D_2O. Resonances marked with an asterisk correspond to the bis(carbene) complex **3a***, which is located in a second coordination sphere around NPs **3a**.

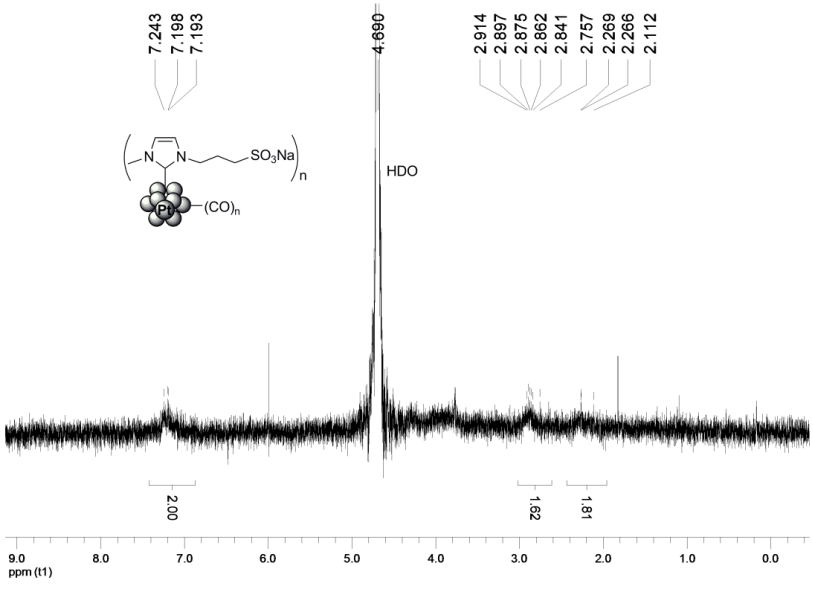

Figure S17. ^{1}H-NMR (300 MHz) for PtNPs **3b** in D_2O.

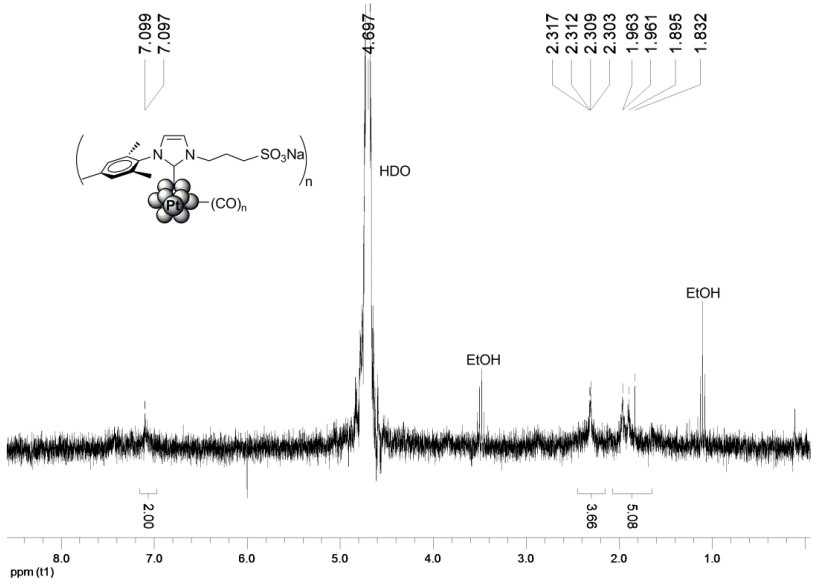

Figure S18. ^{1}H-NMR (300 MHz) for PtNPs **3c** in D_2O.

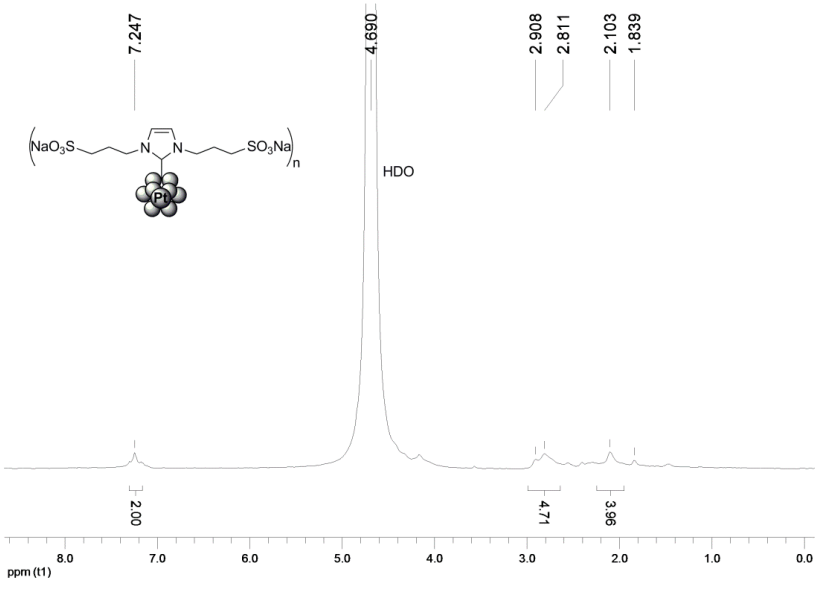

Figure S19. ^{1}H-NMR (500 MHz) for PtNPs **5a** in D_2O.

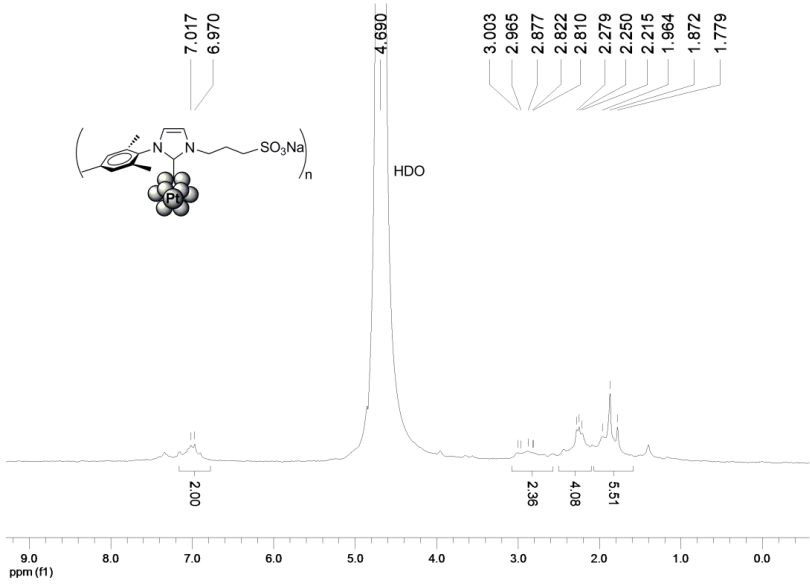

Figure S20. ^{1}H-NMR (500 MHz) for PtNPs **5c** in D_2O.

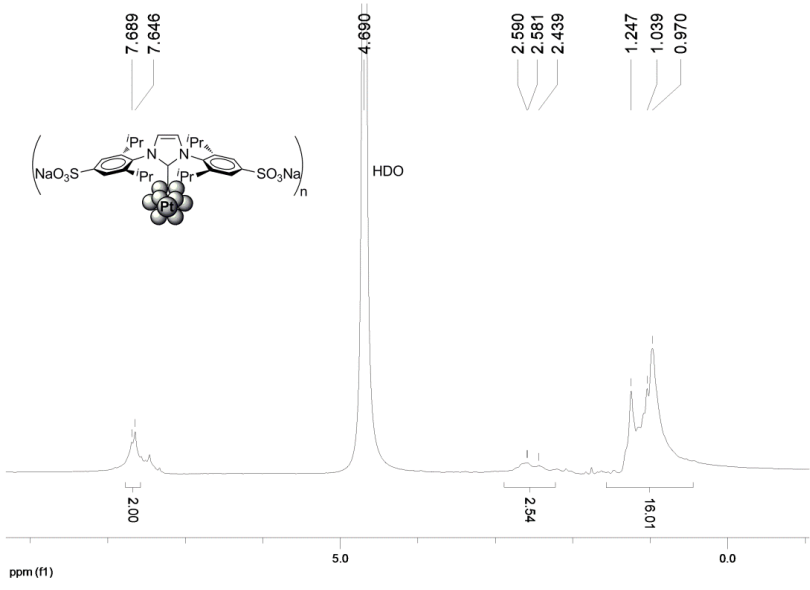

Figure S21. ^{1}H-NMR (500 MHz) for PtNPs **5e** in D_2O.

5. ^{1}H-^{13}C CP-MAS NMR spectra for imidazolium salts, Pt complexes and Pt nanoparticles

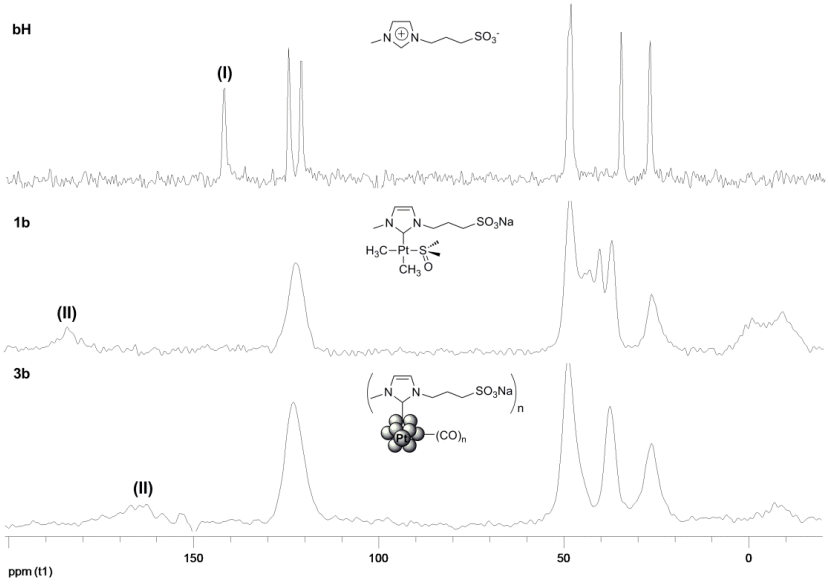

Figure S22. ^{1}H-^{13}C CP-MAS NMR spectra for **bH**, **1b** and **3b**. Resonances (I) and (II) correspond to C^{2}_{Imz}–H and Pt–C^{2}_{NHC} carbons, respectively.

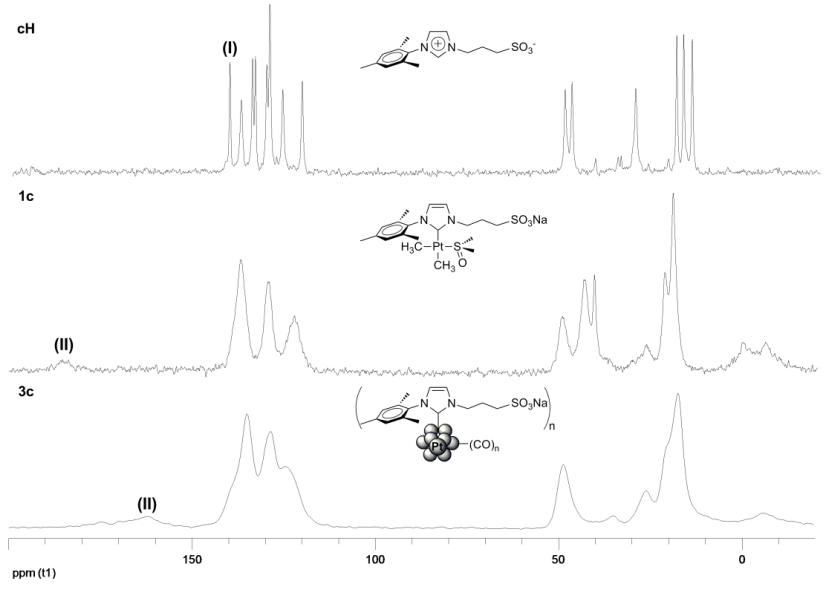

Figure S23. ^{1}H-^{13}C CP-MAS NMR spectra for **cH**, **1c** and **3c**. Resonances (I) and (II) correspond to C^{2}_{Imz}–H and Pt–C^{2}_{NHC} carbons, respectively.

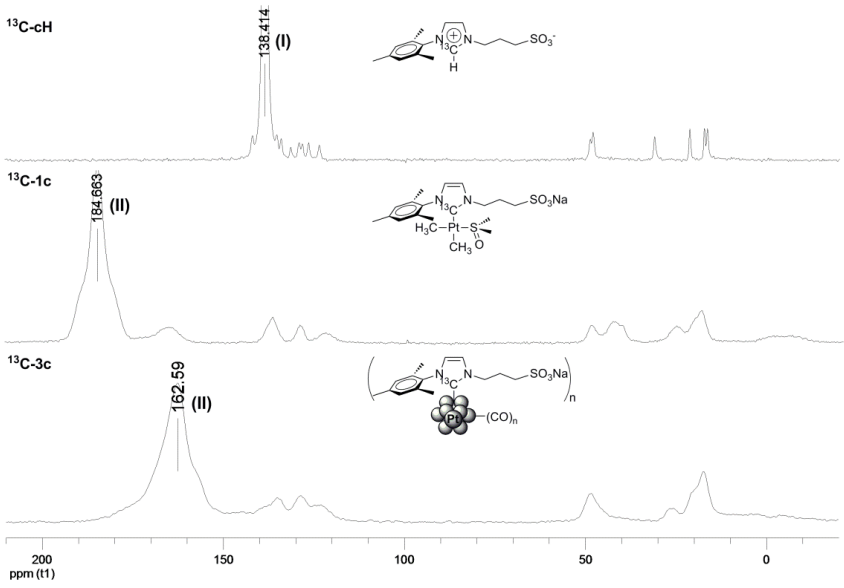

Figure S24. ^{1}H-^{13}C CP-MAS NMR spectra for **^{13}C-cH**, **^{13}C-1c** and **^{13}C-3c**. Resonances (I) and (II) correspond to $^{13}C^{2}_{Imz}$–H and Pt–$^{13}C^{2}_{NHC}$ carbons, respectively.

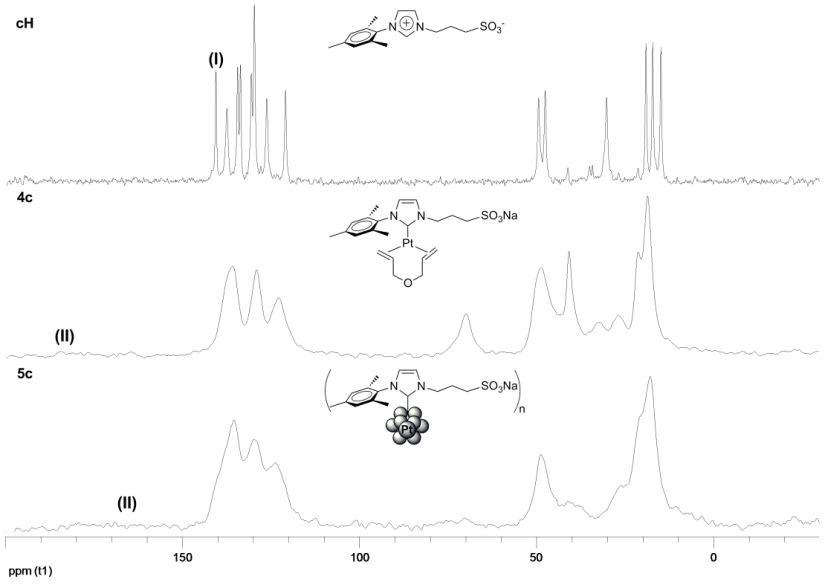

Figure S25. ^{1}H-^{13}C CP-MAS NMR spectra for **cH**, **4c** and **5c**. Resonances (I) and (II) correspond to C^{2}_{Imz}–H and Pt–C^{2}_{NHC} carbons, respectively.

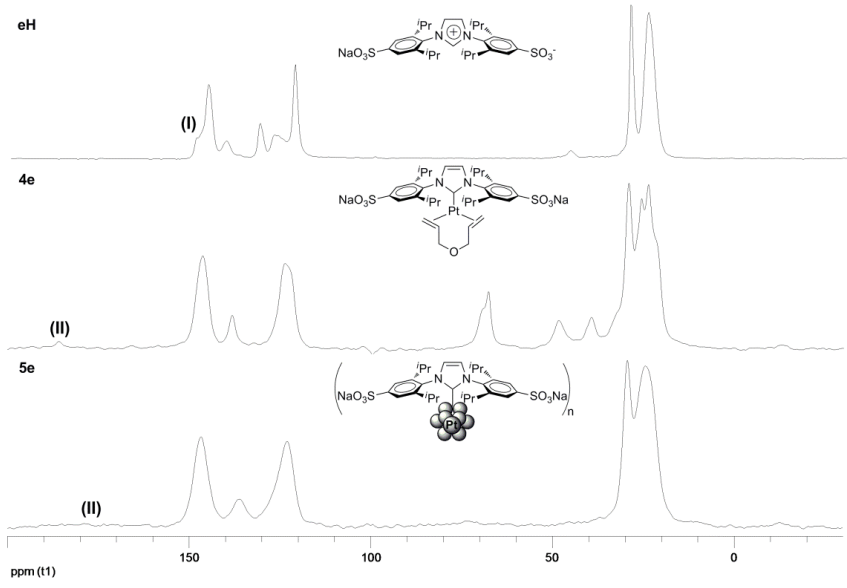

Figure S26. ^{1}H-^{13}C CP-MAS NMR spectra for **eH**, **4e** and **5e**. Resonances (I) and (II) correspond to C^{2}_{Imz}–H and Pt–C^{2}_{NHC} carbons, respectively.

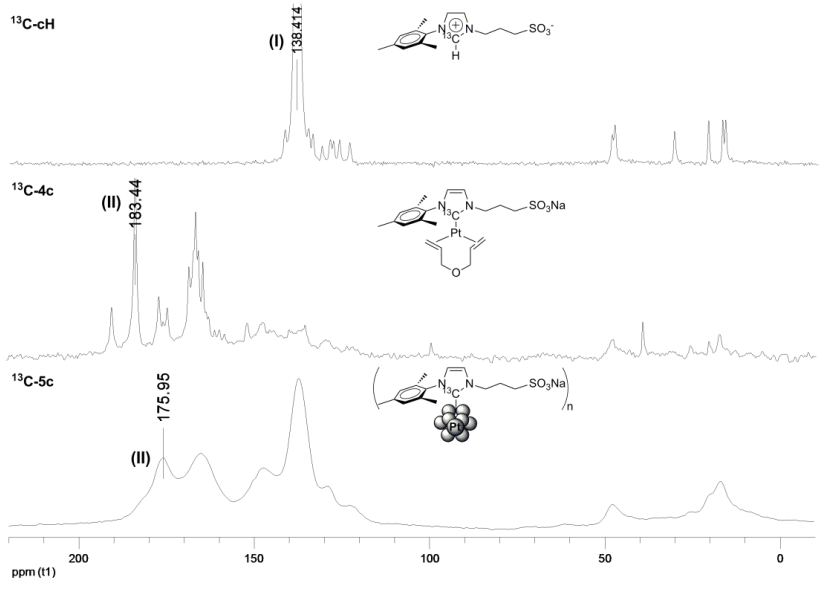

Figure S27. ^{1}H-^{13}C CP-MAS NMR spectra for **^{13}C-cH**, **^{13}C-4c** and **^{13}C-5c**. Resonances (I) and (II) correspond to $^{13}C^{2}_{\mathrm{Imz}}$–H and Pt–$^{13}C^{2}_{\mathrm{NHC}}$ carbons, respectively.

6. ^{1}H- and ^{13}C-NMR spectra for Intermediates [3a] – [3c] and [^{13}C-3c]

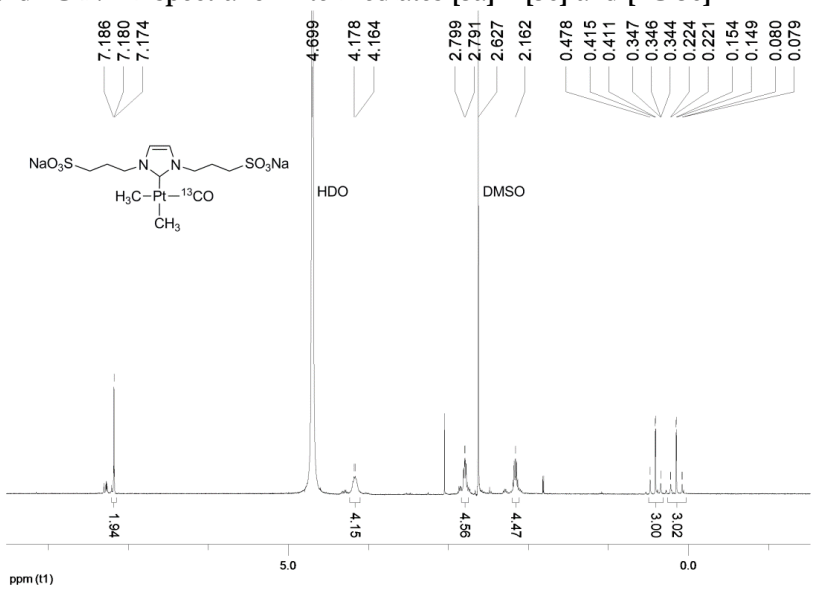

Figure S28. ^{1}H-NMR (500 MHz) for Intermediate [**3a]** in D_2O.

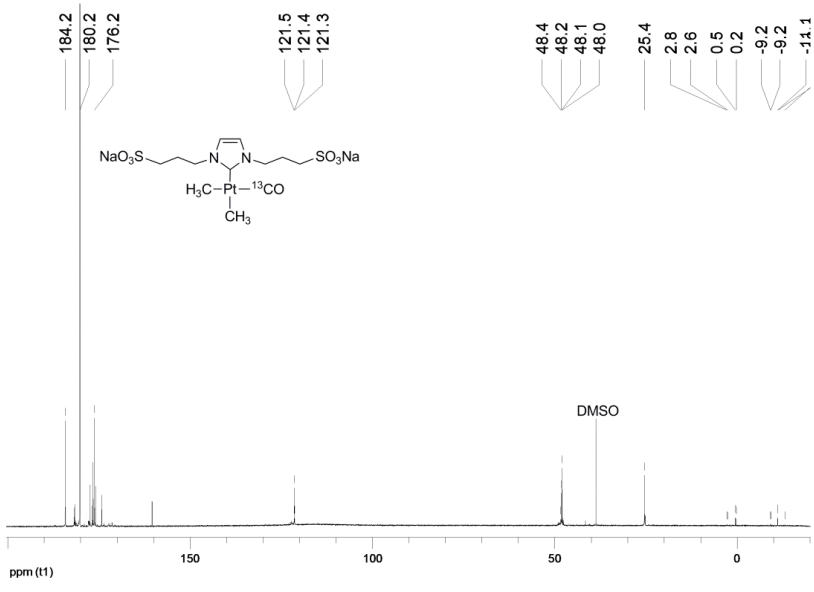

Figure S29. ^{13}C-NMR (125 MHz) for Intermediate [**3a]** in D_2O.

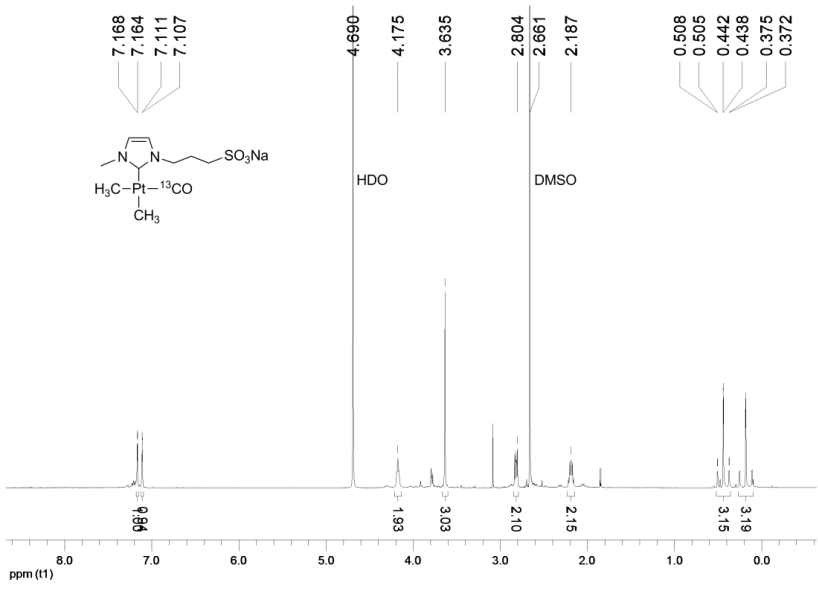

Figure S30. ^{1}H-NMR (500 MHz) for Intermediate [**3b]** in D_2O.

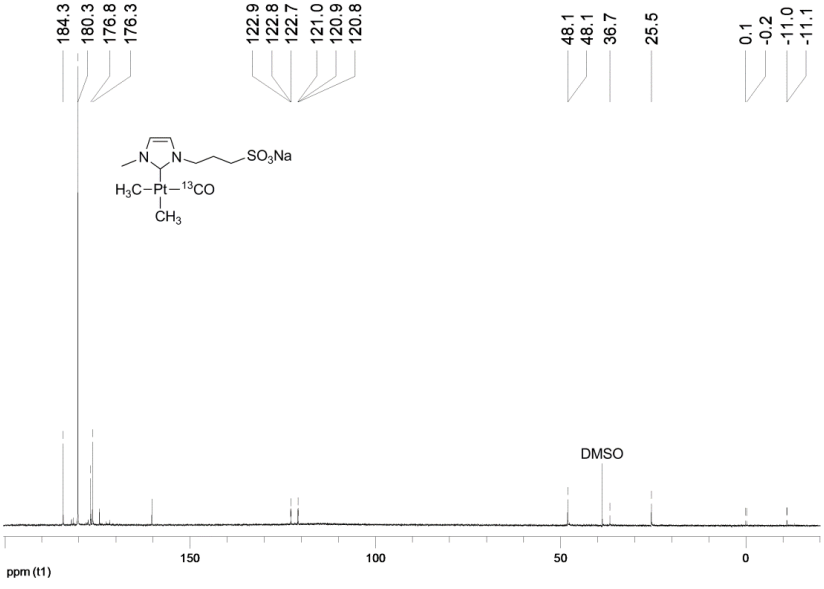

Figure S31. ^{13}C-NMR (125 MHz) for Intermediate [**3b]** in D_2O.

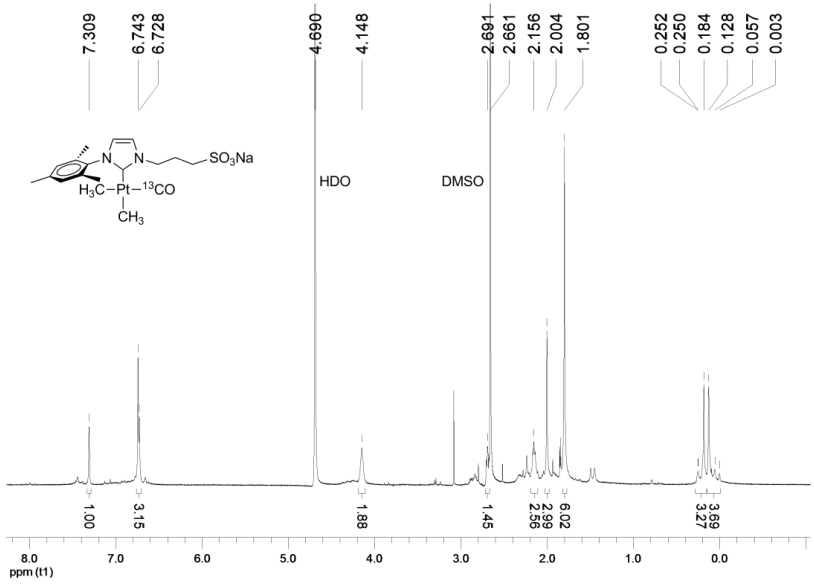

Figure S32. ^{1}H-NMR (500 MHz) for Intermediate **[3c]** in D_2O.

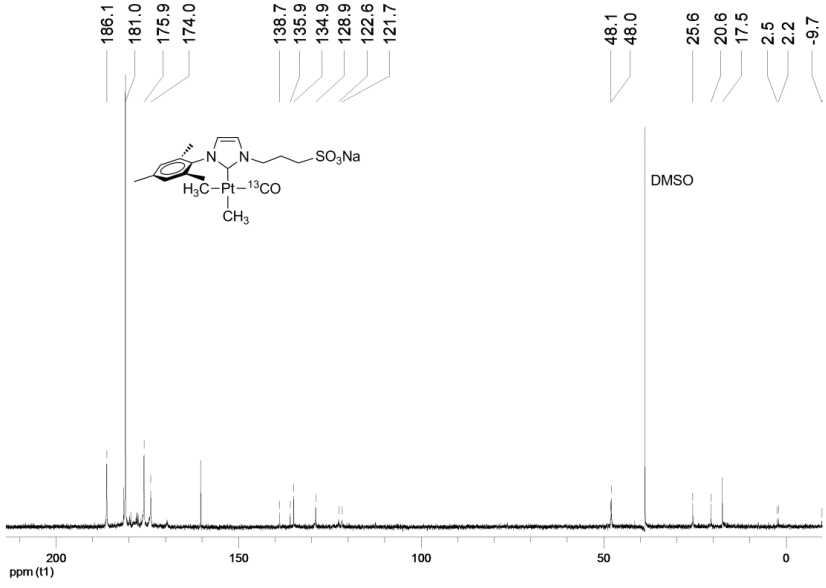

Figure S33. ^{13}C-NMR (125 MHz) for Intermediate **[3c]** in D_2O.

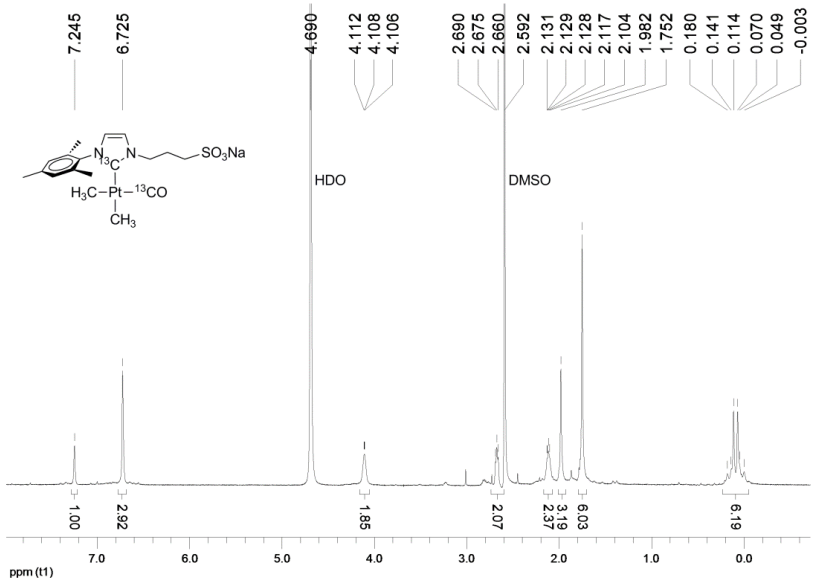

Figure S34. ^{1}H-NMR (500 MHz) for Intermediate [**^{13}C-3c]** in D_2O.

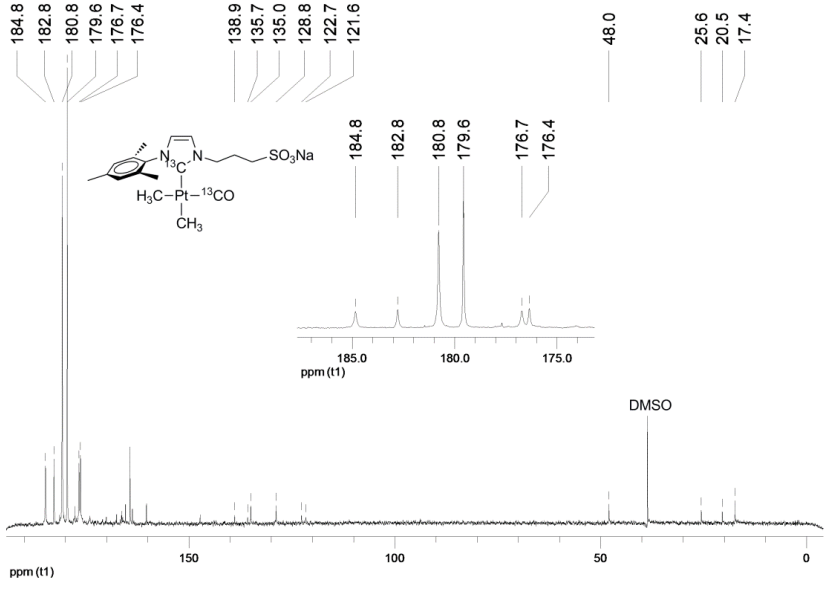

Figure S35. ^{13}C-NMR (125 MHz) for Intermediate [**^{13}C-3c]** in D_2O.

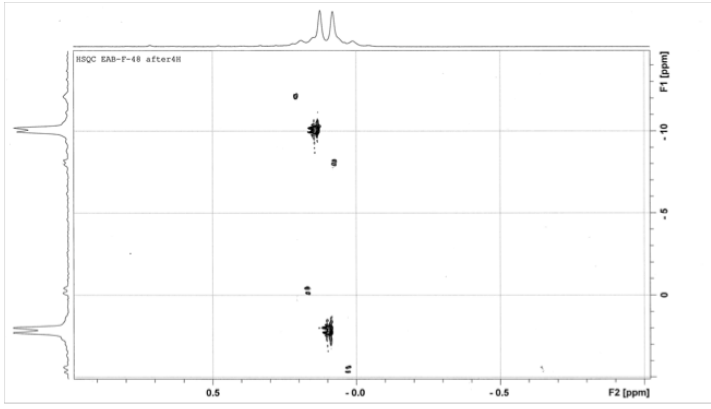

Figure S36. ^{1}H-^{13}C HSQC for Pt–CH_3 moieties in Intermediate [**^{13}C-3c]** in D_2O.

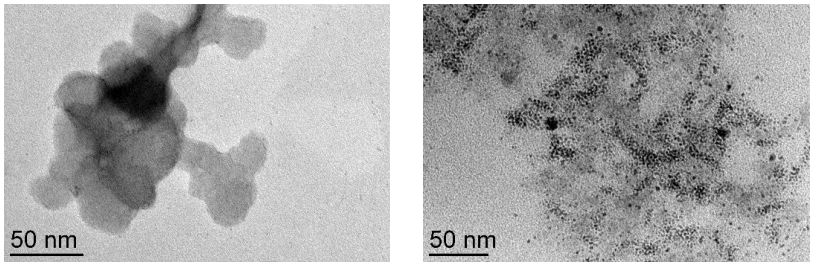

Figure S37. TEM images for **1a** (left) and **1c** (right) after 1 hour of reaction with ^{13}CO in D_2O.

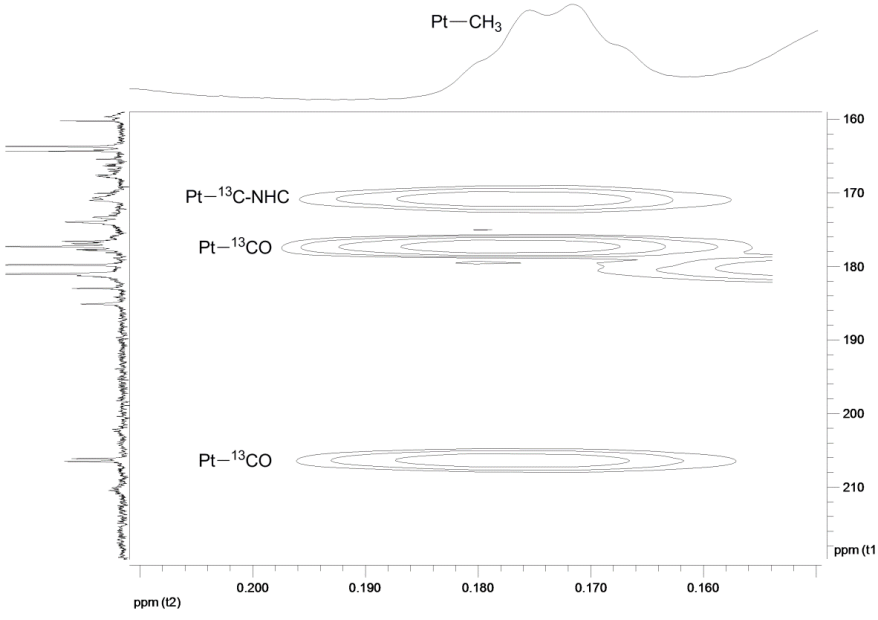

Figure S38. ^{1}H-^{13}C HMBC in the region of Pt–CH_3 moiety for byproduct **A**.

7. Characterization of nano-object 3a/3a*

The complex **3a*** was found in a second coordination sphere in PtNPs **3a** (resonances marked with an asterisk in Figure S18). The solution of PtNPs **3a** was analyzed by NMR spectroscopy and ESI mass spectrometry of samples of the nanoparticles after 36 and 60 h of dialysis, showing that complex **3a*** is still associated to nanoparticle.

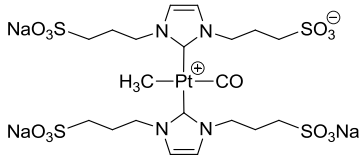

Trisodium *trans*-carbonylmethylbis[1,3-bis(3-sulfonatepropyl)imidazol-2-ylidene]platinate(3–) (3a*): ^{1}H-NMR (300 MHz, D_2O): δ 7.31 (s, 4H, Imz), 4.30 (m, 8H, NCH_2), 2.87 (t, $^{3}J_{HH}$ = 8.4, 8H, CH_2S), 2.31 (m, 8H, $CH_2CH_2CH_2$), 0.22 (s with ^{195}Pt satellites, $^{2}J(^{1}H-^{195}Pt)$ = 63.0, 3H, PtMe). ESI-MS (negative ion, H_2O): m/z 904.0237 [M – Na]$^-$ (calcd 904.0215) 6%; 503.9850 [M – CO – NHC – 3Na – CH_4]$^-$ (calcd 503.9868) 100%.

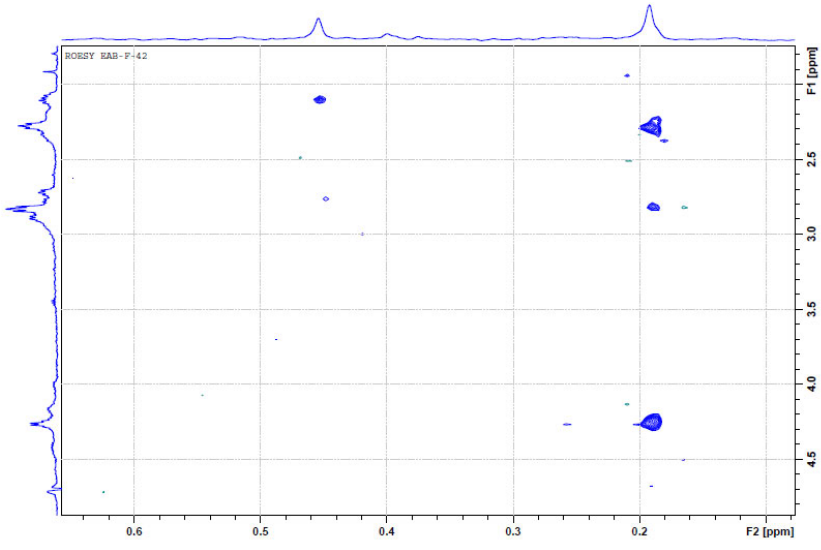

Figure S39. ROESY spectral region showing the cross peaks between Pt–CH_3 and methylene groups of the propylsulfonate chain in nano-object **3a/3a***.

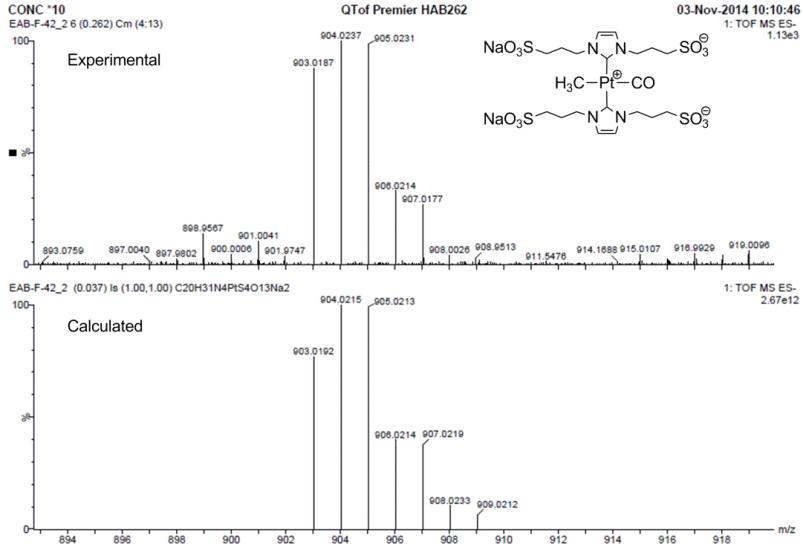

Figure S40. Calculated and experimental isotopic distributions of the molecular fragment [**3a*** – Na]$^-$ detected in the ESI mass spectra of **3a/3a***.

Chapter VIII. Intramolecular Base Assisted C(sp^3)–H Bond Activations in Sulfonated NHC Platinum Complexes in the Gas-Phase

Edwin A. Baquero, Javier González, Manuel Temprado, Juan Z. Dávalos, Juan C. Flores, and Ernesto de Jesús, *Manuscript In Preparation*. **2015**.

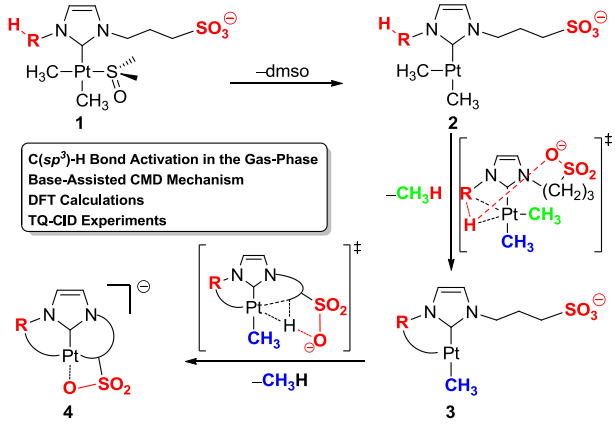

Intramolecular Base Assisted C(sp^3)–H Bond Activations in Sulfonated NHC Platinum Complexes in the Gas-Phase

Edwin A. Baquero,[1] Javier González,[2] Manuel Temprado,[3] Juan Z. Dávalos,[2] Juan C. Flores,[1] and Ernesto de Jesús[1]**

[1]Departamento de Química Orgánica y Química Inorgánica, Campus Universitario, Universidad de Alcalá, 28871 Alcalá de Henares, Madrid, Spain.
[2]Instituto de Química Física "Rocasolano", CSIC, C Serrano 119, 28006, Madrid, Spain.
[3]Departamento de Química Analítica, Química Física e Ingeniería Química, Campus Universitario, Universidad de Alcalá, 28871 Alcalá de Henares, Madrid, Spain.

ABSTRACT

The presence of an *N*-(alkylsulfonate)-*N'*-(R)imidazole-2-ylidene anionic ligand in a series of (dmso)dimethylplatinum(II) complexes has enable their study by mass spectrometry in the absence of ionizing agents. Sets of experiments, using techniques and methodologies such as Fourier Transform Ion Cyclotron Resonance or Infrared Multiphoton Dissociation, reveal a similar pattern of transformations for the complexes in the gas phase, by which dissociation of the coordinated dmso is followed by two consecutive intramolecular C(sp^3)–H bond activations with concurrent release of CH_4. DFT calculations agreeing with these findings disclose the sulfonate group promoting an uncommon concerted metalation-deprotonation process by intramolecular assistance in the C–H bond activation, H^+-transfer, and subsequent protonolysis of Pt–Me bonds. However, the theoretical outcomes also concur with a particular sequence -and type- of events depending on the substitution of the carbene ligand. Compared to a classical C–H oxidative addition, the base-assisted pathway operating here is estimated to lessen the Gibbs energy of activation by 5-7 kcal mol^{-1}, which means a 10^4–10^6-fold increase in the reaction rate.

INTRODUCTION

The activation of C(sp^3)-H bonds by single-site metal complexes stands as a field of current research interest, owing to its potential utility for the selective transformation of inexpensive hydrocarbon feedstocks into value-added products.[1] These reactions are known to occur through diverse mechanisms.[2] Categorizations of the C–H activation processes have been proposed according to a variety of criteria, such as the stoichiometry, possible reaction

mechanism, nature of the transition state, etc. Sometimes, these classifications are rather unclear either, because of the existence of intermediate situations,[2c,2d] or due to different terms in use to refer to similar mechanistic scenarios.[2c] Nonetheless, the main operative mechanisms for the activation of alkanes reported in the literature can be summarized as in Scheme 1.

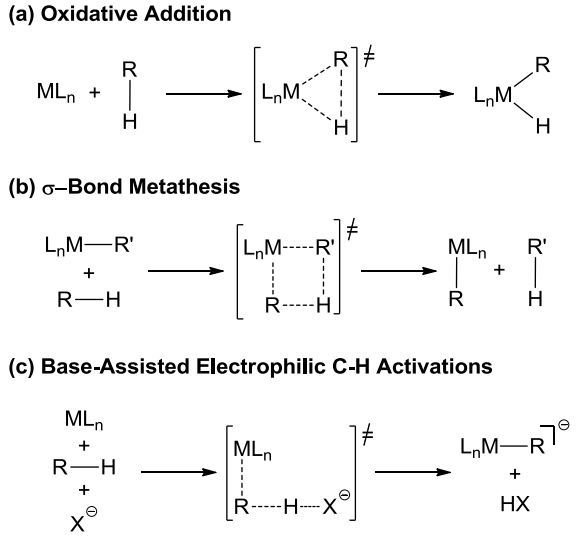

Scheme 1. Mechanisms for C–H bond activation mediated by metal complexes.

The preference for a certain pathway over the others is strongly dependent on the nature of the metal, ancillary ligands, solvent effects, or the presence and strength of basic groups in the complex or in the reaction media. The oxidative addition (OA, (a) in Scheme 1) mechanism[3] is typical for electron-rich, low valent complexes of late transition metals, whereas electrophilic early metal centers use to follow a σ-bond metathesis (SBM, (b) in Scheme 1) pathway.[2d] In OA reactions, the C–H bond adds to the metal through a three-center four-electron transition state, in a process that increases two units the formal oxidation state of the metal center. Conversely, SBM is a concerted reaction, by which two σ-bonds are broken (R–H and M–R') and two new ones are formed (R'–H and M–R) through a four-center four-electron transition state, but without change in the oxidation state of the metal. For both pathways OA and SBM, activations are facilitated by weakening of the C–H bond by σ-alkane complexation in intermolecular activations,[2b,4] or by establishment of an agostic interaction in the case of intramolecular cyclometalations.[5]

Furthermore, the reaction can be assisted by a base, strong enough to cause the heterolytic scission of a C–H bond in the presence of the electrophilic metal center ((c) in Scheme 1). The role as a proton acceptor can be exerted by a coordinated ligand or by an external base. Once the σ-alkane complex or the agostic interaction is present, the C–M and X–H bonds are

formed in a concerted fashion. Concerted metalation-deprotonation (CMD) is commonly used to refer to this kind of activations,[6] whereas Davies, Macgregor and coworkers coined the term ambiphilic metal ligand activation (AMLA)[2c] to emphasize the synergic effect of the metal and a coordinated basic ligand in the heterolytic cleavage of a C–H bond. Likewise, arene C–H bond activations in electrophilic aromatic substitution reactions, can occur through a concerted mechanism, although a stepwise process with formation of stable Wheland intermediates is also possible. The base-assisted electrophilic reactions are common for the activation of a C–H bond of arenes by complexes of late transition metals such as Pd, Ru and Ir.[7]

Many transition metal complexes are able to facilitate C–H bond cleavage.[1] However, since the seminal reports from Shilov and co-workers on the catalytic conversion of alkanes to alcohols under mild conditions,[8] platinum compounds have received a particular attention,[9] mainly thanks to the natural ability they have shown to form Pt–H and Pt–R bonds[10] through the mechanisms described above.[2b] As for C–H bond activation leading to the formation of such bonds, in most instances the process involves an associative mechanism in Pt(II) species.[2b] Nevertheless, there are several examples where a dissociative mechanism has been evidenced in good agreement with formation of transient T-shaped 14-electron Pt(II) complexes.[2c,11]

Although NHCs (NHC = *N*-Heterocyclic Carbene ligand) have proven to be an outstanding class of ligands in modern day organometallic chemistry,[12] (NHC)Pt complexes have been scarcely explored in C–H bond cleavage processes. For example, theoretical studies in the conversion of methane to methanol have been reported,[13] or Pt(0) complexes have been found to activate C–H bonds of imidazolium rings to yield either mono(NHC)[14] or bis(NHC)Pt(II) compounds.[15] Most relevant to our present contribution are a few reports given theoretical and experimental evidences of intramolecular activation of either C(sp^2)–H bonds in mono(NHC)Pt[16] or C(sp^3)–H bonds in unsaturated bis(NHC)Pt(CH_3) cationic T-shaped complexes.[11d,17]

We have recently reported that platinum salts **Na[1a–d]** (Figure 1) are stable and soluble in water, but they undergo processes, such as formation of nanoparticles and release of gases, upon heating of their solutions. Thus, we have observed that complexes **Na[1a–d]** in D_2O at 80 ºC liberate CDH_3, C_2H_6, and CH_4 (*ca.* 1:2:1 molar ratio), and assigned the evolution of the former gases to competing deuterolysis and reductive elimination involving Pt–Me bonds, whereas the nondeuterated methane was proposed to proceed from intramolecular C–H bond activations taking place as well.[18] Motivated by these results, we have conducted further research aiming to bring light onto that assumption. Here, we describe a study on the intramolecular C(sp^3)–H bond activation in these sulfonated NHC Pt(II) complexes using Fourier Transform Ion Cyclotron Resonance Mass Spectrometry (FT-ICR MS) and DFT

calculations. Our findings in the gas phase indicate that the methane release is a consequence of C(*sp*³)–H bond activations at the *N*-substituents of the NHC ligands, in processes where the remote sulfonate group plays a major role as a base intramolecularly assisting singular CMD pathways.

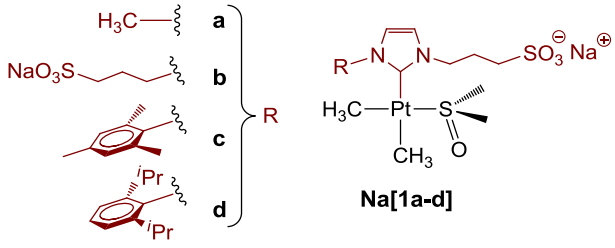

Figure 1. (NHC)Pt(II) complexes used for this study.

RESULTS AND DISCUSSION

Prior to our experimental and theoretical studies in the gas phase, we have found that the evolution of methane from complexes **Na[1a–d]** is also observed in the solid state above 100 °C by Termogravimetric Analysis coupled to Mass Spectrometry (TGA–MS). This fact complements our previous observations in hot aqueous solutions, again suggesting that these complexes tend to undertake some kind of C–H bond activations.

Adventitiously, the ionic nature of the complexes enables their study by electrospray mass spectrometry (ESI) using solutions in plain water in the absence of ionizing agents. In the gas-phase, the complexes undergo the sequence of transformations outlined in Scheme 2. The ESI-TOF spectra found in negative mode show the starting anions **1** only for **1a–b** with low intensities (< 5%), whereas ion-peaks matching to fragments after the loss of the dmso ligand (anions **2**), and subsequent release of one or two methane molecules (**3** and **4**, respectively), are more noticeable. In fact, those corresponding to ions **2** or **3** are the most intense peaks for complexes with alkyl (**2a–b**) or aryl (**3c–d**) substituted NHCs, respectively.

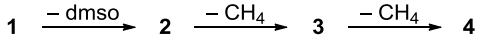

Scheme 2. Transformations observed by ESI(–) MS experiments for the anion in salts **Na[1a–d]**.

Ion assignments are supported by sharp concordances found between experimental and calculated isotopic distribution patterns, and the corresponding measured accurate and calculated exact masses (deviations < 8 ppm; Figures S4–S11 in the Supplementary Information). In addition, the identity for anions **2–4** were verified by fragmentation studies performed by Infrared Multiphoton Dissociation (IRMPD) methods, and isotopic labeling in

the case of **1a–4a**. The IRMPD studies were carried out in a FT-ICR mass spectrometer coupled to a TQ equipped with an ESI source. The anion of interest was isolated in a TQ and fragmented into the cyclotron chamber by the action of a pulsed CO_2-laser. The succession of transformations depicted in Scheme 2 is corroborated by the collected data, because of experiments for particular ions always allow the detection of the same group of fragments derived from **4**, together all respective successor compounds (*e.g*, **3**, and **4** are detected starting from **2**; or **4** from **3**). DFT studies discussed below also support this pathway of transformations occurring in the gas-phase. The theoretical and experimental results point to the series of changes shown in Scheme 3 for the formation of **4b-d** from **1b-d**, whereas the process leading to **4a** from **1a** appears slightly different, and is discussed separately.

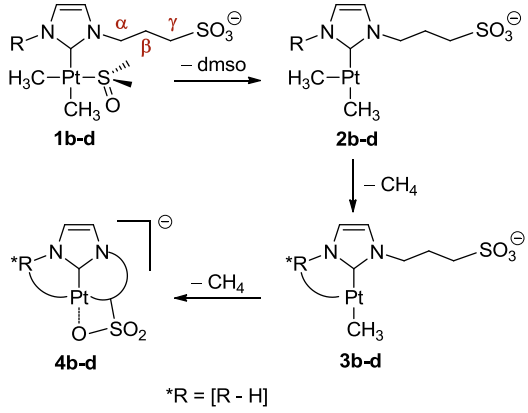

Scheme 3. Sequence proposed for the formation of ions **4b-d** from **1b-d** in the gas-phase.

The structural characterization of ions **4b–d** by IRMPD discloses a common pattern of fragmentations (Scheme 4 and Figures S15–S17). The appearance of product fragments **A** (Figure S18) and **F** (Figure S23) can be explained by the homolytic cleavage of the sulfonated chain and of the *R substituent, respectively, and their detection support that C–H bond activation processes have taken place in both substituents of the NHC ligand. Further fragmentation of **F** must follow to form ion **G** (Figure S24), most likely through concomitant heterolytic Pt–NHC and homolytic N–C(sulfonated chain) bond cleavages, which in turns can render ion fragment **D** (Figure S21) by a plausible β-hydride elimination. Again, the identification of fragment-ions derived from each precursor was based on their corresponding measured accurate masses and isotopic distributions.

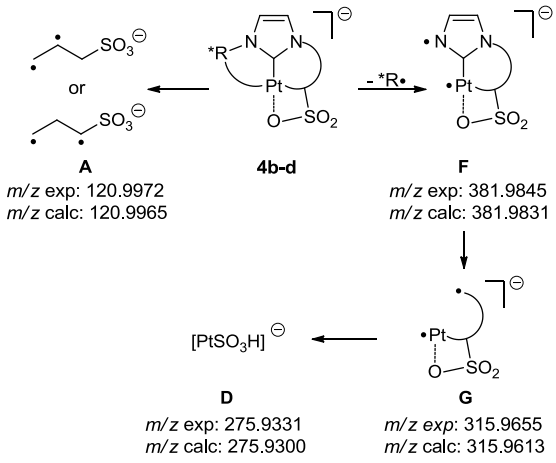

Scheme 4. Ions found and fragmentation pattern proposed from anions **4b–d**.

All these findings concur with C(*sp*³)–H bond activations at the alkyl and aryl NHC-substituents, which at least in the gas-phase must be intramolecular, akin to those reported for bis(NHC) methyl complexes of platinum(II) in solution by the groups of Conejero[11d,17a] and Nolan.[17b] Thus, complexes **Na[1b–d]** must undergo the formation of two platinacycles via consecutive C–H activation processes involving each one of the two *N*-substituents of the NHC ligands in **1b–d**, resulting in anions **4b–d**.

Complex **1a** experiences a different second C–H activation presumably due to the geometrical constrains to form a four-membered platinacycle with the *N*–Me group. In this case, the product of the double C–H activation in the gas-phase is the π-alkeneplatinum(0) complex **4a** (Scheme 5), in which both activations have taken place in the sulfonated chain (formulation based on DFT calculations, *vide infra*). The chain of transformations was also confirmed by IRMPD studies (*i.e.*, successor ions **2a**–**4a**, **3a**–**4a**, or **4a** were detected starting from **1a**, **2a**, or **3a**, respectively). In order to ascertain whether the methane loss to form **4a** involves the *N*-Me or the Pt-Me group of the precursor **3a**, salt **Na[^{13}C1a]** with the *N*-Me group isotopically labeled with ^{13}C was prepared (details in the Supplementary Information).

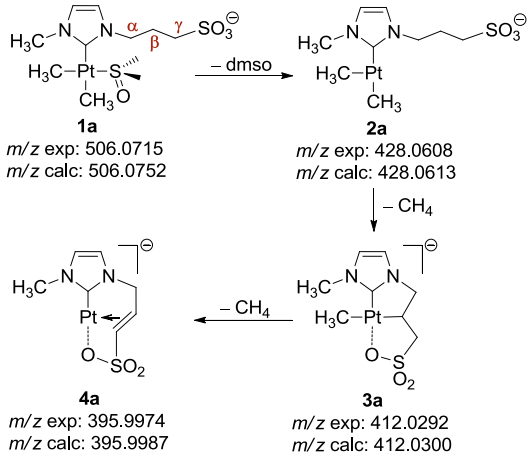

Scheme 5. Proposed sequence for the formation of ion **4a** from **1a** in the gas-phase.

The ESI(–) spectrum for **Na[^{13}C1a]** shows peaks corresponding to anions **^{13}C1a**, **^{13}C2a**, **^{13}C3a**, and **^{13}C4a**, with a similar intensity to that found for the unlabeled analog **Na[1a]**, but at *m*/*z* values consistent with the presence of ^{13}C in all of them (Figure S12), thus demonstrating that the *N*-Me group remains persistently attached in all steps of the process and, consequently, that the liberated molecules of methane derive from the two methyl ligands.

The IRMPD data for **^{13}C4a** support the structural proposal for **4a**. Of those ion-peaks assigned to the type of fragments derived from **4b–d** (*i.e.*, **A**, **D**, **F** or **G**), fragment **D** is the only one detected with relevant intensity in the spectrum for **^{13}C4a**, together with negligible signals for **A**. Instead, new species **B**, **C**, and **E** arise (Scheme 6, and Figures S13 (**^{13}C4a**) and S14 (**4a**)), thus concurring with major differences between **4a** and **4b–d** in their bonding connectivities. In addition, the spectra show the informative fragment **G^{-1H}** (*i.e.*, same pattern of species **G**, but at *m*/*z* 315; see Figure S25) for both **^{13}C4a** and **4a**, in agreement with a double C–H activation at the sulfonated arm in the formation of **4a** (or **^{13}C4a**). At this point it is noteworthy that the IRMPD experiments performed with **4b–d** never revealed ions matching to doubly activated chains. Ion **B** (experimental and calculated isotopic patterns in Figure S19) must result from the release of a molecule of SO_2 from **^{13}C4a**. Fragment **C** (Figure S20) might also derive from **^{13}C4a** by elimination of a propylene diradical, ensuing with the loss of SO_2 to form fragment **E** (Figure S22).

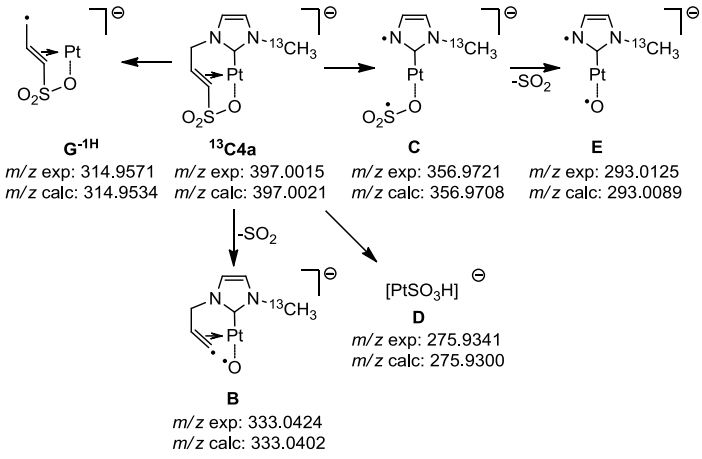

Scheme 6. Ions found and fragmentation sequence proposed for anionic species **^{13}C4a**.

DFT Calculations using the M06 functional[19] were performed in order to discern the operative mechanism for the observed transformations in the gas phase (description of computational method in the Supplementary Information). Since **1a** behaves differently and anions **1b–d** appear to progress in a quite similar manner, the study was focused on the conversion of **1a** to **4a** and **1d** to **4d**.

The first step in both cases involves the dissociation of dmso from **1**(**a** or **d**) to generate a three-coordinate T-shaped Pt(II) intermediate **2**(**a** or **d**),[17c] which is stabilized by an agostic interaction between the unsaturated Pt center and the C–H bond of a methyl group on the diisopropylphenyl ring (**2d**) or a methylene group on the sulfonated chain (**2a**) substituting the NHC ligand (Figure 2). Dissociative mechanism of dmso prior to cyclometalation reactions has been proved for closely related [Pt(Me)$_2$(dmso)(PR$_3$)] complexes in apolar solvents.[20] In keeping with previous studies,[20] no transition state could be found for the dissociation of dmso since the reverse reaction (**2→1**) is barrierless. Thus, the dissociation barrier of dmso for **1** was estimated from ΔG^0(g, 298 K), being 14.4 (**1a**) and 12.5 (**1d**) kcal·mol^{-1} (Figure 2). These data seem to indicate a more stabilizing agostic interaction in the case of **2d**. In fact, the latter is supported by computed structural parameters showing shorter Pt···H and Pt···C contacts for the interaction in **2d** as compared to that in **2a** (**2a**: Pt···H = 2.13 Å, Pt···C = 3.01 Å; **2d**: Pt···H = 2.09 Å, Pt···C = 2.94 Å). The structural features found for **2** (*e.g.*, T-shape and agostic interactions) are in good agreement with those reported for the related species derived from [Pt(Me)$_2$(dmso)(P(*o*-tol)$_3$)], although, in this case, the DFT-calculated ΔG^0(298 K) values for the dissociation of dmso are lower (7.6 and 5.5 kcal·mol^{-1}, in the gas phase and in $CHCl_3$ solution, respectively).[20] Nevertheless, the relative low estimated activation Gibbs energies correlate with the poor (**1a**) or no (**1d**) detection of ion-peaks for the anion of **Na[1]** in their respective ESI(–) spectra.

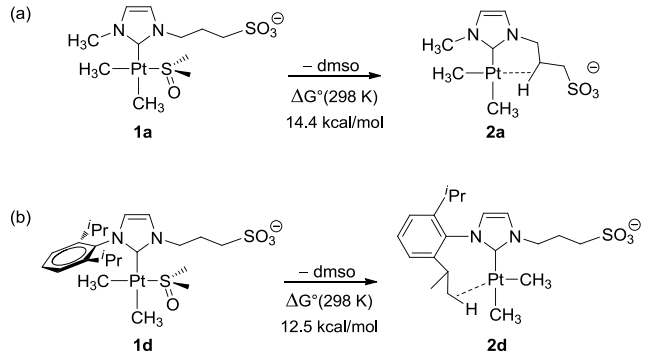

Figure 2. Dissociation of dmso ligand from (a) complex **1a** and (b) complex **1d** with the corresponding ΔG^0(298 K) values.

Once complex **2** is formed, the pathway leading to **4**(**a** or **d**) depends on the substituents at the NHC ligand. The most plausible mechanisms consistent with the experimental observations for the formation of **4d** and **4a** from **2d** and **2a** are discussed below. In the case of **2d**, a first intramolecular C–H bond activation is, in principle, conceivable at the sulfonated chain or at the diisopropylphenyl ring. DFT calculations predict the process at the former as thermodynamically more favorable due to the formation of a Pt–O bond after methane liberation. However, the C–H activation of a methyl group at the diisopropylphenyl substituent is kinetically preferred, in a reversible transformation leading to seven-membered platinacycle **Int[2d-3d]** (Figure 3). The cyclometalation appears to occur via a CMD mechanism,[6] with DFT calculations predicting the hanging sulfonate acting as the proton acceptor, and yielding a $\Delta G^{\ddagger}$(g, 298 K) of 25.3 kcal·mol^{-1}, lower than that for a conventional OA pathway without the participation of the sulfonate group as a base ($\Delta G^{\ddagger}$(g, 298 K) = 30.1 kcal·mol^{-1}). It is noteworthy that a $\Delta G^{\ddagger}$(toluene solution, 298 K) value of 33.2 kcal·mol^{-1} was DFT-calculated for an analogous cyclometalation reaction in $[PtCH_3(I^iPr_2)_2]^+$ (I^iPr_2: 1,3-diisopropylimidazol-2-ylidene), where an OA pathway was assigned as the most feasible mechanism,[21] and that platinacycle **Int[2d-3d]** resembles that previously described as the result of cyclometalation in $[PtCH_3(IPr)_2]^+$ (IPr: 1,3-bis(2,6-diisopropylphenyl)imidazol-2-ylidene).[17a] The fact that DFT calculations predict a CMD pathway predominantly taking place in the intramolecular C–H activation of **2d**, could seem somewhat striking in view of the low basicity of sulfonate groups in water (*e.g.*, the pK_a for CH_3SO_3H is −1.92,[22] much more acidic than for the related carboxylic acid, $pK_a(CH_3COOH)$ = 4.76,[23] both in H_2O at 25 °C). However, the proton affinities (PA) of sulfonate groups are comparable to those of carboxylates (*e.g.*, PA = 182.0 and 187.3 kcal·mol^{-1} for methanesulfonate and acetate respectively).[24] The transition state for this concerted process (**TS1[2d-3d]**) has little Pt(IV) character, as indicated by relatively long Pt···H and Pt···C (2.07 and 2.28 Å respectively) and short C···H and H···O contacts (1.60 and 1.20 Å respectively) in the calculated structure. This set of structural features reflects the synergetic nature of this step, where both H···O and Pt···C interactions reinforce each other to facilitate the C–H bond

heterolytic cleavage. Subsequently, the proton of the sulfonic group present in intermediate **Int[2d-3d]** can be transferred to either methyl ligand, in *trans* or in *cis* position relative to the carbene. Lower activation Gibbs energy is computed for the protonolysis of the Pt–C bond *cis* to the NHC ligand. This stage is accompanied with methane release and formation of unsaturated T-shaped Pt(II) intermediate **3d**, which is again stabilized by an agostic interaction between the 14 e Pt(II) center and one of the C–H bonds in γ-position of the pendant sulfonated chain (Scheme 3), with short Pt···H and Pt···C contacts (2.19 and 2.87 Å respectively). The interaction exhibited by **3d** results in significant weakening of that C–H bond and facilitates the subsequent cyclometalation leading to platinacycle **Int[3d-4d]**, again via a CMD C–H bond activation assisted by the sulfonate group, which in turns undergoes protonolysis of the remaining Pt–CH_3 bond by the sulfonic proton to form **4d**. The activation at the side-chain is kinetically more favorable for the formation of a six- than for a five-membered metallacycle. Unlike **TS1[2d-3d]** (*vide supra*), the transition state for this stage (**TS1[3d-4d]**) corresponds to an oxidatively-added transition state[2d] with high Pt(IV) alkyl hydride character, as it is indicated by the short Pt–H and Pt–C distances (1.57 and 2.19 Å respectively) and a relatively long C···H contact (1.80 Å), showing that the C–H and Pt–C bonds are already greatly broken and formed, respectively, at this point. Moreover, this transition state exhibits a relatively short H···O contact of 2.03 Å, indicative of an extra stabilization. The rate determining step of this second cyclometalation corresponds to the C–H bond activation and occurs with a calculated Gibbs energy of activation of 26.1 kcal·mol^{-1}, a similar value than that computed for the first one (25.3 kcal·mol^{-1}).

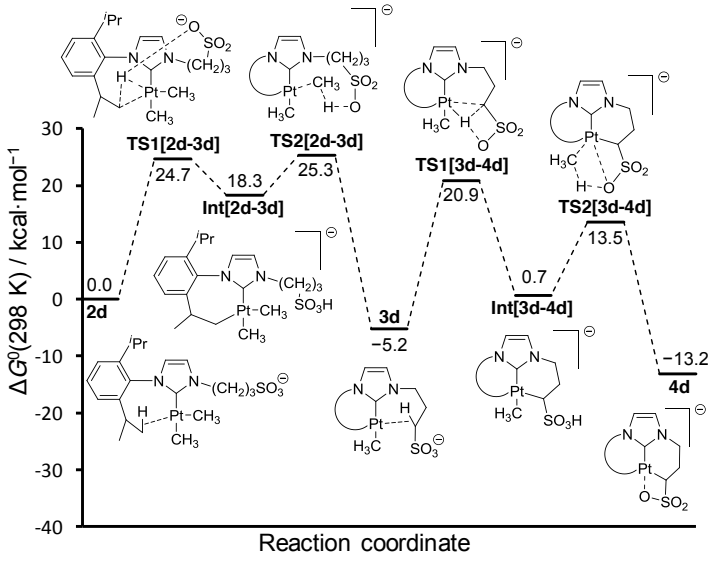

Figure 3. Gibbs energy diagram for the formation of **4d** from **2d** in the gas-phase. Intermediates corresponding to σ-CH_4 complexes[3] omitted for clarity.

As mentioned earlier, the sequence of transformations for the *N*-Me substituted complex **1a** is different. Once **2a** is formed, a reversible intramolecular C–H bond activation takes places at the methylene in β-position on the sulfonated side-arm (Scheme 5). The process goes via a CMD mechanism[6] with the sulfonate group acting as the proton acceptor as well, but in this case a five-membered platinacycle (**Int[2a-3a]** in Figure 4) is kinetically favored (calculated $\Delta G^{\ddagger}$(g, 298 K) = 27.7 kcal·mol^{-1}). Similarly to **TS1[2d-3d]**, **TS1[2a-3a]** (Figure 4) has little Pt(IV) character, (Pt···H = 1.98 Å; Pt···C = 2.31 Å; C···H = 1.51 Å; O···H = 1.32 Å). The alternate classical oxidative addition pathway, without assistance of the sulfonate group, has a calculated activation Gibbs energy 7 kcal·mol^{-1} higher than that corresponding to the CMD C–H activation. Other mechanistic scenarios such as C–H activation of the methyl substituent of the NHC or the methylene in γ-position, both sulfonate-assisted or via an oxidative addition step, were also explored, rendering again higher Gibbs energy barriers. The $\Delta G^{\ddagger}$(g, 298 K) for the transformation **2a→3a** is 2.4 kcal·mol^{-1} higher than the calculated value for the conversion **2d→3d** (Figure 3), which is in agreement with the kinetic preference mentioned above for the activation of a methyl group at the diisopropylphenyl substituent instead that at the sulfonated chain in **2d**. Furthermore, that kinetic effect is supported by the fact that ion **3d** (or **3c**) is the major species in the ESI(–) spectrum of **1d** (or **1c**, also with an *ortho*-substituted aryl ring at the NHC ligand), whereas for complexes lacking of aryl substituents (**1a** and **1b**) the most intense peaks correspond to the ions after the loss of the dmso ligand (**2a** and **2b**).

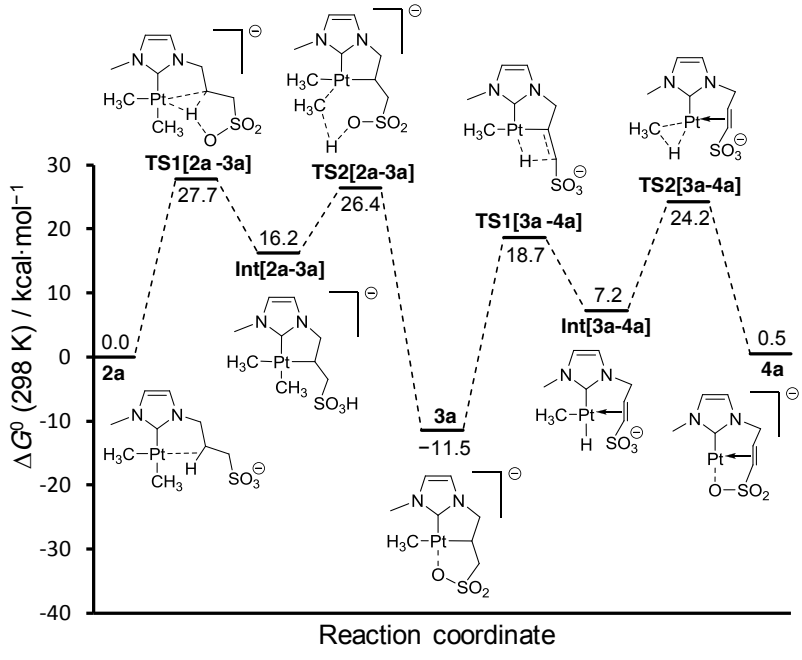

Figure 4. Gibbs energy diagram for the formation of **4a** from **2a** in the gas-phase. Intermediates corresponding to σ-CH_4 complexes[3] omitted for clarity.

The subsequent step corresponds to the intramolecular protonolysis of the Pt–C bond of the methyl *trans* to the NHC with loss of a CH_4 molecule and formation of complex **3a** (see Figure 4) containing a tridentate-chelating NHC-sulfonated ligand. The conversion **2a→3a** is exergonic by −11.5 kcal·mol^{-1} due to the formation of an ancillary stabilizing Pt–O bond in **3a** along with the entropy gain in this dissociative process. Finally, a second C–H bond activation of the sulfonated chain via β-hydride elimination yield the π-alkene hydride complex **Int[3a-4a]** that after a reductive elimination process losses another CH_4 molecule forming the three-coordinate T-shaped Pt(0) final product **4a**. The conversion **3a** to **4a** is endergonic by 12.0 kcal·mol^{-1} and occurs with a considerably high Gibbs energy of activation of 35.7 kcal·mol^{-1}. Thus, this reversible transformation should be expected to occur only in the gas phase where the produced CH_4 is removed under the experimental conditions. An alternative process through protonolysis of the remaining Pt–CH_3 bond with the methyl substituent of the NHC as the proton source, was calculated to have a higher Gibbs energy barrier (39.3 kcal·mol^{-1}).

Furthermore, TQ-CID experiments, aimed to determine the activation energy for the C–H bond activation process (details in the Supplementary Information), were informative in the case of the conversion of **3c** to **4c**. The activation energy experimentally found for this process was 27.9 kcal·mol^{-1}, close to the value calculated for the transformation of **3d** to **4d** (26.1 kcal·mol^{-1}), which must follow a very similar energy profile (*vide infra*) (Figure 5). The same determination was attempted for the conversion of **3a** to **4a**. However, the higher energy required for the reaction (calculated $\Delta G^{\ddagger}$(g, 298 K) = 35.7 kcal·mol^{-1}) resulted in an unclear transformation because of the formation of fragmentation products, fatally complicating the experiment.

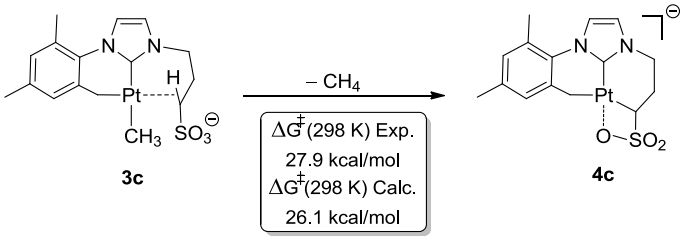

Figure 5. Experimental Gibbs energy of activation for the transformation of **3c** to **4c**. (The calculated Gibbs energy is for the analogue transformation **3d** to **4d**).

The mechanisms proposed in Figures 3 and 4 are consistent with the experimental data collected for the transformation of **1a–d** leading to **4a–d** in the gas phase. Thus, after the dissociation of dmso, the reaction profile for the *N*-Mesityl substituted complex **1c** must be similar to that shown in Figure 3 for **1d**. In contrast, it is reasonable that **1b** must follow the sequence described in Figure 4 for **1a** up to the formation of **3b** (*i.e.*, first C–H activation at

the hanging chain resulting in a five-membered platinacycle), which driven by the conformational constrains imposed by the existing metallacycle, must evolve to **4b** as depicted in Figure 3 for **3d→4d**.

CONCLUSIONS

Base-assisted C−H bond activation through a CMD mechanism is a type of process well-known in the functionalization of arenes and alkenes.[7] However it has been rarely observed for C(sp^3)−H bonds, with the description of only a couple of very recent examples of intermolecular reactions with Ir(III) complexes,[25] and other two intramolecular with Rh(III) or Ru(II) compounds,[26] in all cases assisted by a coordinated carboxylate ligand of the complex. In this work, we have shown that a sulfonate group, acting as a remote base hanging from an *N*-(alkylsulfonate)-*N'*-(R)imidazole-2-ylidene ligand, can promote intramolecular C(sp^3)−H bond activations in (dmso)dimethylplatinum(II) complexes in a concerted manner decreasing the Gibbs energy of activation by 5-7 kcal mol^{-1} as compared to the classical OA pathway. This reduction of the activation barrier implies a considerable acceleration of the reactions with a 10^4–10^6-fold increase in the reaction rate. The presence of the *N*-propylsulfonated substituent of the carbene ligand has also been essential to study these reactions in the gas phase by MS, where all complexes studied undergo a common pattern of transformations, consisting in dissociation of the coordinated dmso, followed by two consecutive C(sp^3)–H bond activations with concurrent release of CH_4 molecules. DFT calculations support this pattern, and the sulfonate-assisted CMD pathway, but also disclose that the particular sequence -and type- of events depends on the substitution of the carbene. Thus, C(sp^3)–H activation at an *ortho*-group in an *N'*-aryl substituent is kinetically favored over that at a C–H bond of the *N*-alkylsulfonated chain, which in turn activates in a second CMD process forming a six-membered platinacycle. The latter, taking place first in the absence of *N'*-aryl substituent, results in a five-membered metallacycle due to higher conformational flexibility in the complex. Finally, the presence of an *N'*-methyl group –with geometrical constrains to be cyclometallated, drives both C-H bond activations to the sulfonated chain, but with the second one occurring via a more conventional β-hydride elimination. These results highlights the concept of "ligand design" as a chemists' tool, since it has been shown that the presence of a basic group linked by a flexible chain to a coordinated ligand can greatly affect the mechanism and rates of C–H bond activation reactions. This effect can in principle serve to reduce the harsh reaction conditions often required for this kind of processes, thus enabling a better control on their selectivity and the catalysts lifetimes and productivities, and probably increasing the substrate scope and functional group tolerances. Due to the interest of the type of process involve here, further work are currently underway in our lab trying to detect products of the C–H activation in aqueous solution.

ASSOCIATED CONTENT

Supporting Information

Experimental procedures and characterization techniques, ESI-MS spectra for anionic species **1–4** and their related fragments, and NMR spectra for labeled compounds **^{13}C-MeIMz**, **^{13}CaH**, and **^{13}C1a**. This material is available free of charge via the Internet at http://pubs.acs.org.

AUTHOR INFORMATION

Corresponding Authors

*Email: juanc.flores@uah.es (J.C.F.), ernesto.dejesus@uah.es (E.d.J).

ACKNOWLEDGMENT

This work was supported by the Spanish Ministerio de Economía y Competitividad (projects CTQ2011-24096 (J. C. F. and E. d. J.) and CTQ2012-36966 (M. T.). E.A.B. is grateful to the Universidad de Alcalá for an FPI Doctoral Fellowship.

REFERENCES

(1) P. J. Perez, *Alkane C-H Activation by Single-Site Metal Catalysis.*, Springer, **2012**.

(2) a) D. Balcells, E. Clot, O. Eisenstein, *Chem. Rev.* **2010**, *110*, 749-823; b) M. Lersch, M. Tilset, *Chem. Rev.* **2005**, *105*, 2471-2526; c) D. H. Ess, W. A. Goddard, III, R. A. Periana, *Organometallics* **2010**, *29*, 6459-6472; d) Z. Lin, *Coord. Chem. Rev.* **2007**, *251*, 2280-2291; e) Y. Boutadla, D. L. Davies, S. A. Macgregor, A. I. Poblador-Bahamonde, *Dalton Trans.* **2009**, 5820-5831.

(3) S. Sakaki, *Top. Organomet. Chem.* **2005**, *12*, 31-78.

(4) R. N. Perutz, S. Sabo-Etienne, *Angew. Chem., Int. Ed.* **2007**, *46*, 2578-2592.

(5) a) M. Brookhart, M. L. H. Green, G. Parkin, *Proc. Natl. Acad. Sci.* **2007**, *104*, 6908-6914; b) I. Omae, *J. Organomet. Chem.* **2011**, *696*, 1128-1145.

(6) S. I. Gorelsky, D. Lapointe, K. Fagnou, *J. Am. Chem. Soc.* **2008**, *130*, 10848-10849.

(7) a) L. Ackermann, *Acc. Chem. Res.* **2014**, *47*, 281-295; b) D. G. Musaev, T. M. Figg, A. L. Kaledin, *Chem. Soc. Rev.* **2014**, *43*, 5009-5031; c) S. I. Gorelsky, *Coord. Chem. Rev.* **2013**, *257*, 153-164.

(8) A. E. Shilov, G. B. Shul'pin, *Chem. Rev.* **1997**, *97*, 2879-2932.

(9) J. A. Labinger, J. E. Bercaw, *Top. Organomet. Chem.* **2011**, *35*, 29-60.

(10) a) J. A. M. Simoes, J. L. Beauchamp, *Chem. Rev.* **1990**, *90*, 629-688; b) G. A. Takhin, H. A. Skinner, A. A. Zaki, *J. Chem. Soc., Dalton Trans.* **1984**, 371-378; c) A. Miedaner, J. W. Raebiger,

C. J. Curtis, S. M. Miller, D. L. DuBois, *Organometallics* **2004**, *23*, 2670-2679; d) C. T. Mortimer, *Rev. Inorg. Chem.* **1984**, *6*, 233-257.

(11) a) A. Paul, C. B. Musgrave, *Organometallics* **2007**, *26*, 793-809; b) M. R. Plutino, L. M. Scolaro, A. Albinati, R. Romeo, *J. Am. Chem. Soc.* **2004**, *126*, 6470-6484; c) R. L. Brainard, W. R. Nutt, T. R. Lee, G. M. Whitesides, *Organometallics* **1988**, *7*, 2379-2386; d) O. Rivada-Wheelaghan, M. A. Ortuno, J. Diez, A. Lledos, S. Conejero, *Angew. Chem., Int. Ed.* **2012**, *51*, 3936-3939.

(12) in *N-Heterocyclic Carbenes: From Laboratory Curiosities to Efficient Synthetic Tools* (Ed.: S. Diez-Gonzalez), RSC Catalysis Series; The Royal Society of Chemistry, **2011**.

(13) B. M. Prince, T. R. Cundari, *Organometallics* **2012**, *31*, 1042-1048.

(14) a) D. S. McGuinness, K. J. Cavell, B. F. Yates, B. W. Skelton, A. H. White, *J. Am. Chem. Soc.* **2001**, *123*, 8317-8328; b) B. Pan, S. Pierre, M. W. Bezpalko, J. W. Napoline, B. M. Foxman, C. M. Thomas, *Organometallics* **2013**, *32*, 704-710.

(15) M. A. Duin, N. D. Clement, K. J. Cavell, C. J. Elsevier, *Chem. Commun.* **2003**, 400-401.

(16) G. L. Petretto, M. Wang, A. Zucca, J. P. Rourke, *Dalton Trans.* **2010**, *39*, 7822-7825.

(17) a) O. Rivada-Wheelaghan, B. Donnadieu, C. Maya, S. Conejero, *Chem. Eur. J.* **2010**, *16*, 10323-10326; b) G. C. Fortman, N. M. Scott, A. Linden, E. D. Stevens, R. Dorta, S. P. Nolan, *Chem. Commun.* **2010**, *46*, 1050-1052; c) M. A. Ortuno, S. Conejero, A. Lledos, *Beilstein J. Org. Chem.* **2013**, *9*, 1352-1382, 1331 pp.

(18) a) E. A. Baquero, J. C. Flores, J. Perles, P. Gomez-Sal, E. de Jesus, *Organometallics* **2014**, *33*, 5470-5482; b) E. A. Baquero, S. Tricard, J. C. Flores, E. de Jesus, B. Chaudret, *Angew. Chem. Int. Ed.* **2014**, 13220-13224.

(19) Y. Zhao, D. G. Truhlar, *Theor. Chem. Acc.* **2008**, *120*, 215-241.

(20) A. Marrone, N. Re, R. Romeo, *Organometallics* **2008**, *27*, 2215-2222.

(21) M. Rosello-Merino, O. Rivada-Wheelaghan, M. A. Ortuno, P. Vidossich, J. Diez, A. Lledos, S. Conejero, *Organometallics* **2014**, *33*, 3746-3756.

(22) J. P. Guthrie, *Can. J. Chem.* **1978**, *56*, 2342-2354.

(23) J. F. J. Dippy, S. R. C. Hughes, A. Rozanski, *J. Chem. Soc.* **1959**, 2492-2498.

(24) E. P. L. Hunter, S. G. Lias, *J. Phys. Chem. Ref. Data* **1998**, *27*, 413-656.

(25) a) D. R. Pahls, K. E. Allen, K. I. Goldberg, T. R. Cundari, *Organometallics* **2014**, *33*, 6413-6419; b) J.-i. Ito, T. Kaneda, H. Nishiyama, *Organometallics* **2012**, *31*, 4442-4449.

(26) a) M. E. O'Reilly, R. Fu, R. J. Nielsen, M. Sabat, W. A. Goddard, III, T. B. Gunnoe, *J. Am. Chem. Soc.* **2014**, *136*, 14690-14693; b) J. S. Cannon, L. Zou, P. Liu, Y. Lan, D. J. O'Leary, K. N. Houk, R. H. Grubbs, *J. Am. Chem. Soc.* **2014**, *136*, 6733-6743.

Supporting Information

Intramolecular Base Assisted C(sp^3)–H Bond Activations in Sulfonated NHC Platinum Complexes in the Gas-Phase

Edwin A. Baquero,[1] Javier González,[2] Manuel Temprado,[3] Juan Z. Dávalos,[2] Juan C. Flores,[1]* and Ernesto de Jesús[1]*

[1]*Departamento de Química Orgánica y Química Inorgánica, Campus Universitario, Universidad de Alcalá, 28871 Alcalá de Henares, Madrid, Spain.*

[2]*Instituto de Química Física "Rocasolano", CSIC, C Serrano 119, 28006, Madrid, Spain.*

[3]*Departamento de Química Analítica, Química Física e Ingeniería Química, Campus Universitario, Universidad de Alcalá, 28871 Alcalá de Henares, Madrid, Spain.*

Email: juanc.flores@uah.es, ernesto.dejesus@uah.es

Table of Contents

1. General Procedures and Characterization Techniques

All reactions were performed under an argon atmosphere using standard Schlenk techniques. Unless otherwise stated, reagents and solvents were used as received from commercial sources. The complexes *cis*-[Pt(CH_3)$_2$(dmso)(NHC)] (**1**),[1] and *cis*-dimethylbis(dimethyl sulfoxide)platinum(II),[2] were prepared as described in the literature. All solvents were deoxygenated prior to use. Dimethyl sulfoxide was distilled under argon over calcium hydride. Deionized water (type II quality) was obtained using a Millipore Elix 10 UV Water Purification System. ^{1}H, ^{13}C, and ^{195}Pt NMR spectra were recorded with Varian Mercury 300, Unity 300, or Unity 500 Plus spectrometer. Chemical shifts (δ) are quoted in ppm relative to $SiMe_4$ (^{1}H, ^{13}C) and K_2PtCl_6 in water (^{195}Pt). They were measured by internal referencing to the ^{13}C or residual ^{1}H resonances of the deuterated solvents, or by the substitution method in the case of ^{195}Pt. Coupling constants (J) are given in Hz. When required, two-dimensional ^{1}H-^{13}C HSQC and HMBC experiments were carried out for the unequivocal assignment of ^{1}H and ^{13}C resonances. Elemental analyses and mass spectra of the ^{13}C-labelled compounds synthesis for this study were performed by the Analytical Services of the Universidad de Alcalá on a LECO CHNS-932 microanalyzer, and on an Agilent G3250AA LC/MSD TOF Multi (MALDI-TOF and ESI-TOF) mass spectrometer, respectively.

ESI-Mass Spectrometry. Mass spectrometry studies were performed on a triple-quadrupole (TQ) Agilent/Varian-320 MS equipped with an electrospray ionization (ESI) source in line with a high resolution and sensitivity mass spectrometer FT-ICR ("Fourier Transform Ion Cyclotron Resonance") Agilent/Varian-920 MS, provided with a 7.0 T actively shielded superconducting magnet. The complexes studied were diluted in water (aprox. 5×10^{-5} m) and very fresh solutions were directly infused into the ESI source, in the negative mode, at a flow rate of 20 μL/min. The temperature of the drying gas was 250 °C.

FT-ICR high-resolution MS measurements: The anions, generated in the ESI source under the conditions already described, were allowed to cross the TQ-MS without filtering them, and were diverted to the FT-ICR-MS, whose conditions such as hexapole ion guides, accumulation ion hexapole and the other key components were optimized in order to maximize the detection in m/z ranges within 100-750 Da. Commercially beer malto-oligosaccharides were used as mass calibrants and tuning standards in the negative ion mode.[3] Fragmentation by IRMPD (Infrared Multiphoton Dissociation) experiments was performed pulsing a 10.6 μm-CO_2 laser (Synrad Model 48-2, Mukilteo-WA-USA). Product ion formation was optimized by varying IRMPD laser pulse total power (25 W).

IRMPD-Fragmentation Study for Anionic Species 4. Fragmentation of selected anionic species were performed in FT-ICR mass spectrometer as described above. The anionic part in complexes **Na[1a-d]** (*i.e.*, **1a-d**) were isolated, and their fragmentation pattern was followed until formation of the bicyclometalated complexes **4**, establishing the product ion for each precursor ion.

TQ-CID Experiments. The dissociation experiments performed in TQ-spectrometer were performed by isolating the desired anions in the first quadrupole (Q_1) with a peak-width enough to include the signal of its main ionic isotopes. The isolated ions were allowed to undergo collision induced dissociation (CID) with argon gas leaked into a curved (90°) collision chamber (Q_2) at a pressure of 1.4 mTorr. The geometry of Q_2 reduces the background noise and increases the signal-to-noise ratio. The dissociation product ions were finally analyzed with a third quadrupole (Q_3).

2. Synthesis of ^{13}C labelled compounds

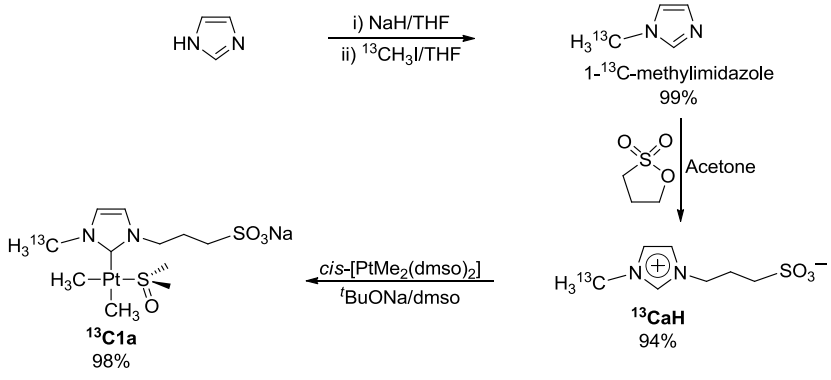

Scheme S1. Synthesis of **^{13}C1a**

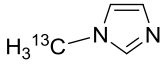

1-^{13}C-methylimidazole. A solution of imidazole (0.404 g, 5.93 mmol) in THF (10 mL) was added dropwise (15 min), from a funnel connected to a bubbler, into a 100 mL Schlenck flask containing a suspension of NaH (0.242 g, 10.1 mmol) in the same solvent (30 mL) at room temperature. The reaction mixture was stirred during 30-45 min until hydrogen evolution ceased completely. Subsequently, $^{13}CH_3I$ (370 μL, 5.93 mmol) was added to the freshly prepared solution of sodium imidazolide, and the stirring was kept at 1100 rpm for further 15 h. After removal of the volatiles (1 h, 25 °C, 10 mbar) the product was extracted in CH_2Cl_2 (3 × 20 mL, each time filtering *via* cannula). The extraction-solvent was evaporated and the residue dried under vacuum (3 h, 35 °C, 800 mbar) to afford 1-^{13}C-methylimidazole as a colorless oil (0.487 g, 99%) spectroscopically pure (NMR spectra in Figure S1). ^{1}H-NMR (300 MHz, $CDCl_3$): δ 7.40 (s, 1H, Imz-H^2); 7.02 (s, 1H, Imz-H^4); 6.85 (s,

1H, Imz-H^5); 3.66 (d, $^1J_{H\text{-}C}$) = 139.8, 3H, $^{13}CH_3$). $^{13}C\{^1H\}$-NMR (75 MHz, $CDCl_3$): δ 137.8 (s, Imz-C^2); 129.5 (d, $^2J_{C\text{-}C}$ = 3.0, Imz-C^5); 120.0 (s, Imz C^4); 33.2 (s, $^{13}CH_3$). ESI-MS (positive ion, $CHCl_3/NH_4HCOO$): m/z 84.0669 $[M + H]^+$ (calcd 84.0637) 100%.

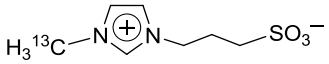

1-^{13}C-methyl-3-(3-sulfonatepropyl)imidazolium ^{13}CaH. A solution of 1,3-propanesultone (1.00 mL, 11.4 mmol) in acetone (5 mL) was added dropwise into a 100 mL Schlenck Flask containing another solution of 1-^{13}C-methylimidazole (0,480 g, 5.78 mmol) in the same solvent (15 mL). The resulting colorless solution was stirred at room temperature for 8 days. During this period of time the product precipitated as a white solid, and was then filtered, washed with acetone (3 × 20 mL), and dried under vacuum (2 h, 25 °C, 10 mbar) to obtain the imidazolium salt **^{13}CaH** (1.117 g, 94%) spectroscopically pure (NMR spectra in Figure S2). ^{1}H-NMR (300 MHz, D_2O): δ 8.63 (s, 1H, Imz-H^2); 7.39 (d, $^3J_{HH}$ = 1.3, 1H, Imz-H^4); 7.32 (d, $^3J_{H\text{-}H}$ = 1.5, 1H, Imz-H^5); 4.24 (t, $^3J_{H\text{-}H}$ = 6.9, 2H, NCH_2); 3.76 (d, $^1J_{H\text{-}C}$ = 144.1, 3H, $^{13}CH_3$); 2.79 (t, 2H, $^3J_{H\text{-}H}$ = 7.7, CH_2S); 2.19 (q, $^3J_{H\text{-}H}$ = 7.2, 2H, $CH_2CH_2CH_2$). $^{13}C\{^1H\}$-NMR (75 MHz, D_2O): δ 136.1 (d, $^2J_{C\text{-}C}$ = 1.1, Imz-C^2); 123.6 (s, Imz-C^5); 122.1 (s, Imz-C^4); 47.6 (s, NCH_2); 47.0 (s, CH_2S); 35.6 (s, $^{13}CH_3$). 25.0 (s, $CH_2CH_2CH_2$). ESI-MS (positive ion, H_2O): m/z 206.0708 $[M + H]^+$ (calcd 206.0675) 100%.

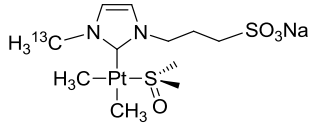

Cis-dimethyl(dimethyl sulfoxide)[1-^{13}C-methyl-3-(3-sodiumsulfonate-propyl)imidazol-2-ylidene] platinum(II) Na[^{13}C1a]. Sodium *tert*-butoxide (93.7 mg, 0.976 mmol) was added to a solution of *cis*-[$PtMe_2(dmso)_2$] (0.3722 g, 0.9758 mmol) and the imidazolium salt **^{13}CaH** (0.2003 g, 0.9759 mmol) in dimethyl sulfoxide (10 mL). The mixture was stirred for 2 h at room temperature, filtered through a plug of kieselguhr, and the solvent was completely removed. The platinum complex **Na[^{13}C1a]** was dried under vacuum (12 h, 90 ºC, 4 mbar) and isolated as a pale yellow solid (0.510 g, 98%) analytically pure (NMR spectra in Figure S3) without further workup. ^{1}H-NMR (300 MHz, D_2O): δ 7.07 (d, $^3J_{H\text{-}H}$ = 2.1, 1H, Imz); 7.01 (d, $^3J_{HH}$ = 1.8, 1H, Imz); 4.28 (m, 1H, NCH_2); 4.10 (m, 1H, NCH_2); 3.63 (d, $^1J_{H\text{-}C}$ = 140.2, 3H, $^{13}CH_3$); 2.93 (s with ^{195}Pt satellites, $^3J_{H\text{-}Pt}$ = 11.5, 3H, Me_2SO); 2.92 (s with ^{195}Pt satellites, $^3J_{H\text{-}Pt}$ = 11.5, 3H, Me_2SO); 2.80 (m, 2H, CH_2S); 2.15 (m, 2H, $CH_2CH_2CH_2$); 0.34 (s with ^{195}Pt satellites, $^2J_{H\text{-}Pt}$ = 81.0, 3H, *cis*-NHC-Pt-*Me*); 0.032 (s with ^{195}Pt satellites, $^2J_{H\text{-}Pt}$ = 61.0, 3H, *trans*-NHC-Pt-*Me*). $^{13}C\{^1H\}$-NMR (75 MHz, D_2O): δ 181.3 (d with ^{195}Pt satellites, $^1J_{C\text{-}Pt}$ = 852.7, $^2J_{C\text{-}C}$ = 7.8, Imz-C^2), 122.7 (d with ^{195}Pt satellites, $^3J_{C\text{-}Pt}$ = 19.7, $^2J_{C\text{-}C}$ = 3.0, Imz-C^5), 120.6 (s with ^{195}Pt satellites, $^3J_{C\text{-}Pt}$ = 22.8, Imz-C^4), 48.4 (s, CH_2S), 48.3 (s with ^{195}Pt satellites, $^3J_{C\text{-}Pt}$ = 28.7, NCH_2), 43.9 (s with ^{195}Pt satellites, $^2J_{C\text{-}Pt}$ = 31.7, Me_2SO), 43.6

(s with ^{195}Pt satellites, $^{2}J_{C\text{-}Pt}$ = 29.9, Me_2SO), 36.8 (s with ^{195}Pt satellites, $^{3}J_{C\text{-}Pt}$ = 34.7, $^{13}CH_3$), 25.8 (s, $CH_2CH_2CH_2$), –3.9 (s with ^{195}Pt satellites, $^{1}J_{C\text{-}Pt}$ = 541.0, *trans*-NHC-Pt-*Me*), –9.6 (s with ^{195}Pt satellites, $^{1}J_{C\text{-}Pt}$ = 674.4, *cis*-NHC-Pt-*Me*). ^{195}Pt-NMR (64 MHz, dmso-d_6): δ –4020. ESI-MS (negative ion, MeOH TOF): m/z 429.0614 $[M - Na - dmso]^-$ (calcd 429.0647) 100%; 413.0281 $[M - Na - dmso - CH_4]^-$ (calcd 413.0334) 36%; 396.9993 $[M - Na - dmso - 2CH_4]^-$ (calcd 397.0021) 14%. ESI-MS (negative ion, MeOH FT-ICR): m/z 507.0786 $[M - Na]^-$ (calcd 507.0786) 1.7%; 429.0636 $[M - Na - dmso]^-$ (calcd 429.0647) 100%; 413.0327 $[M - Na - dmso - CH_4]^-$ (calcd 413.0334) 13%; 397.0018 $[M - Na - dmso - 2CH_4]^-$ (calcd 397.0021) 2.6%. Anal. Calcd (%) for $^{13}CC_{10}H_{29}N_2NaO_7PtS_2$ (**[^{13}C1a]Na**·$3H_2O$): C, 22.77; H, 5.00; N, 4.79. Found (%): C, 22.54; H, 4.68; N, 4.86.

3. ^{1}H- and ^{13}C-NMR spectra for ^{13}C-labelled compounds

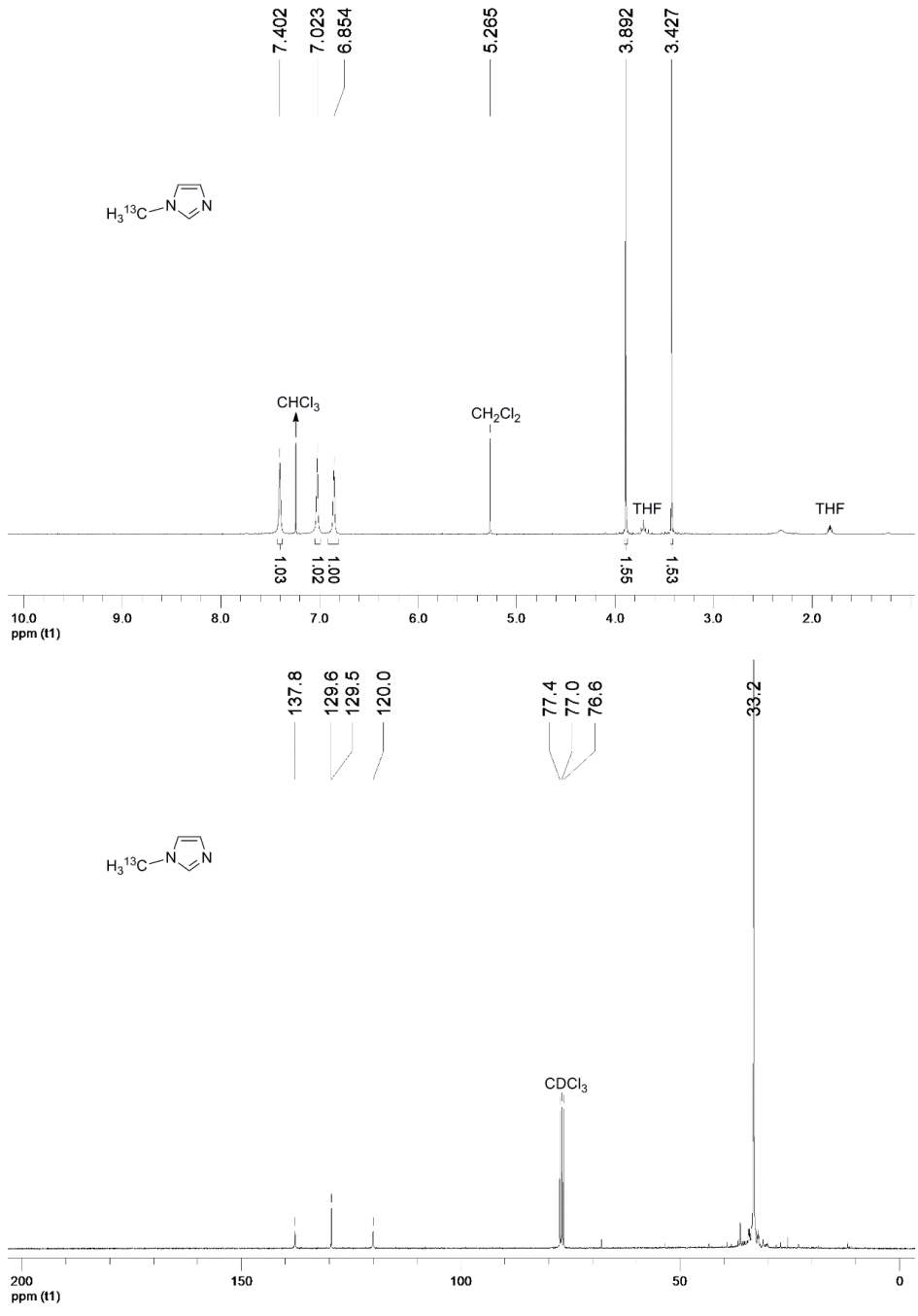

Figure S1. ^{1}H (300 MHz, $CDCl_3$) and $^{13}C\{^{1}H\}$ (75 MHz, $CDCl_3$) NMR Spectra for 1-^{13}C-methylimidazole.

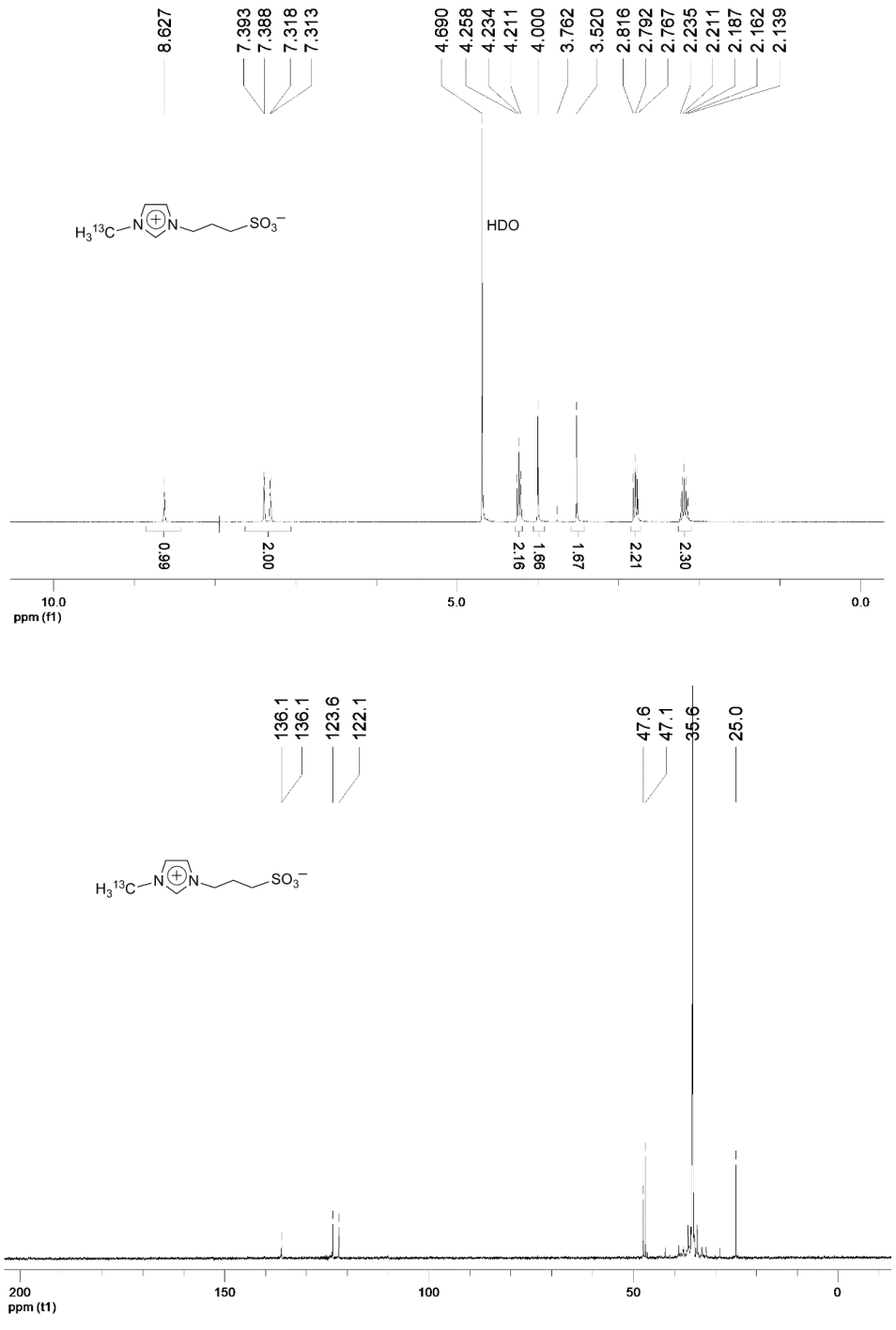

Figure S2. ^{1}H (300 MHz, D_2O) and $^{13}C\{^{1}H\}$ (75 MHz, D_2O) NMR Spectra for **^{13}CaH**.

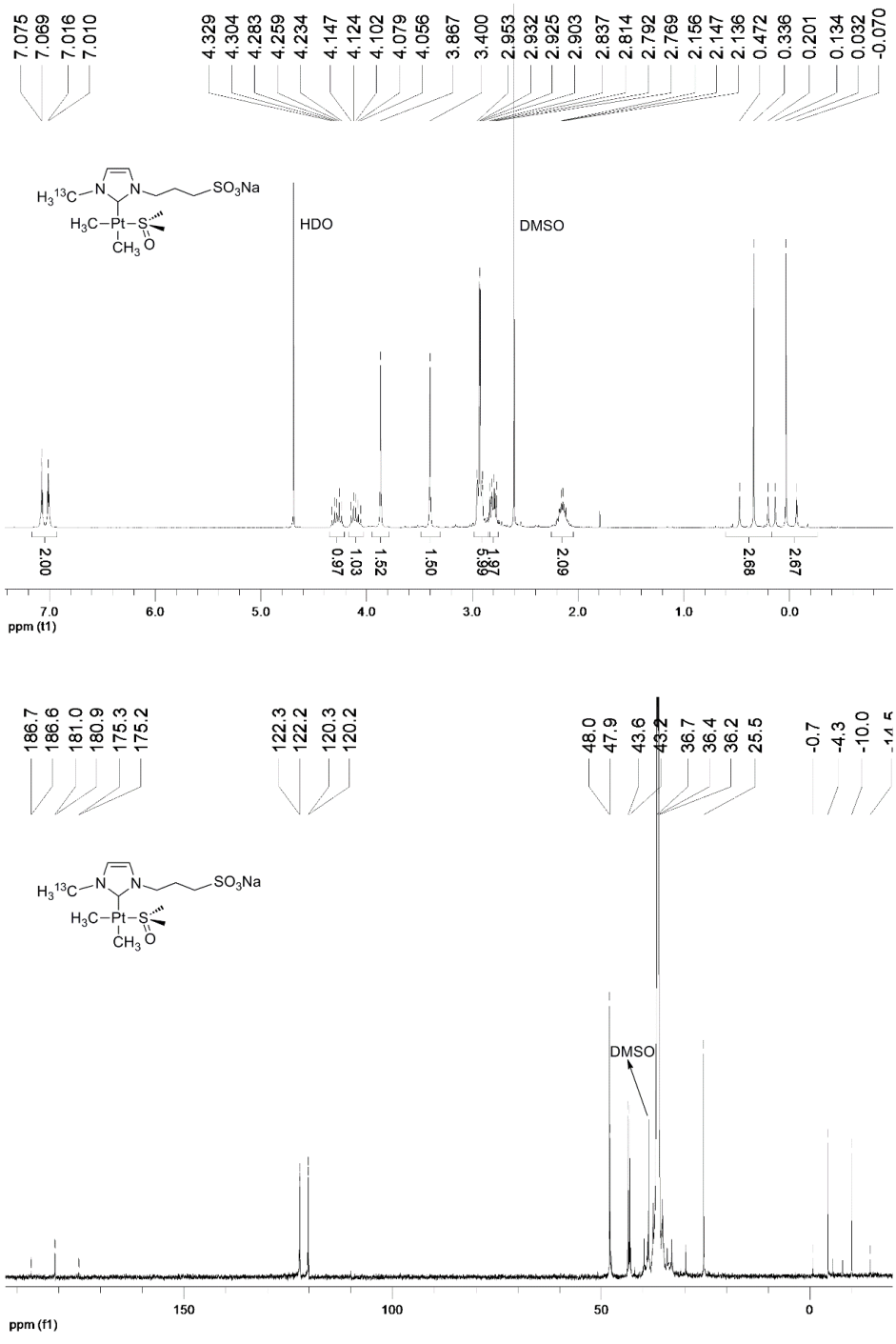

Figure S3. ^{1}H (300 MHz, D_2O) and $^{13}C\{^{1}H\}$ (75 MHz, D_2O) NMR Spectra for **Na[^{13}C1a]**.

4. Mass Spectra for Complexes Na[1a-d]

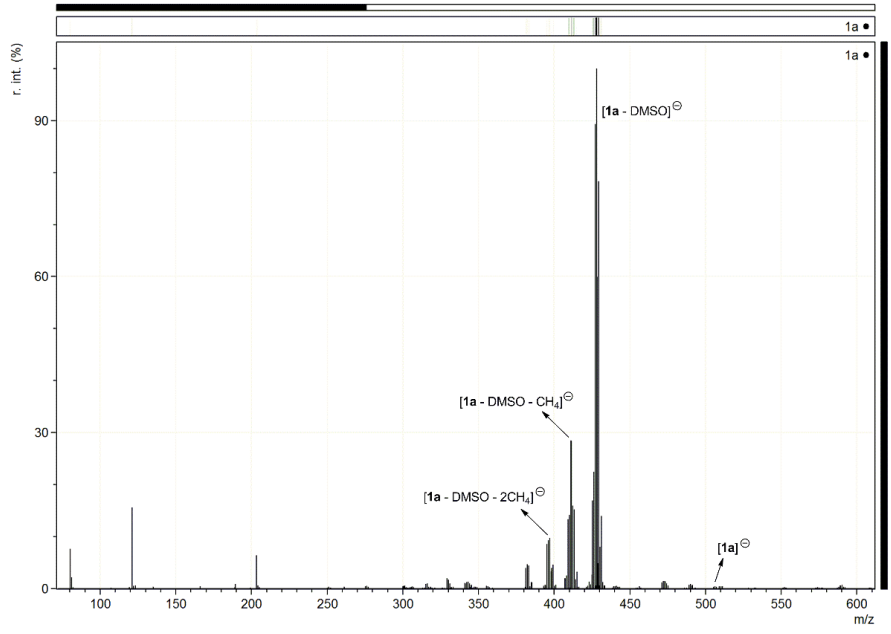

Figure S4. ESI-TOF Mass Spectrum in negative mode for **Na[1a]**.

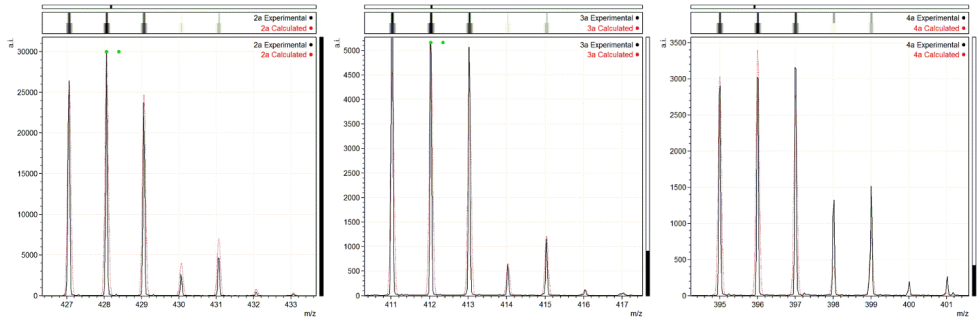

Figure S5. Experimental and calculated isotope patterns of **2a**, **3a** and **4a**.

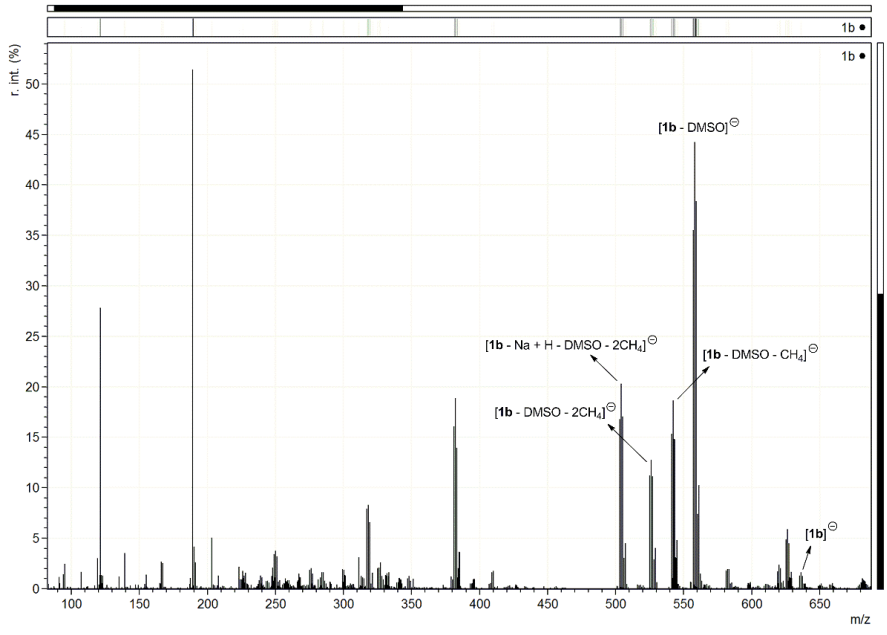

Figure S6. ESI-TOF Mass Spectrum in negative mode for **Na[1b]**.

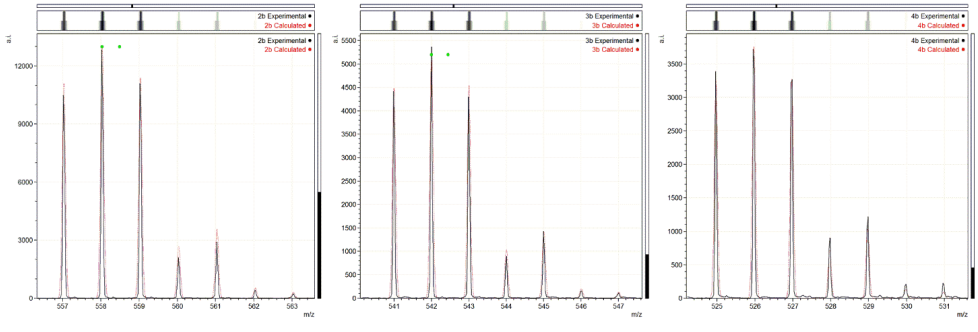

Figure S7. Experimental and calculated isotope patterns of **2b**, **3b** and **4b**.

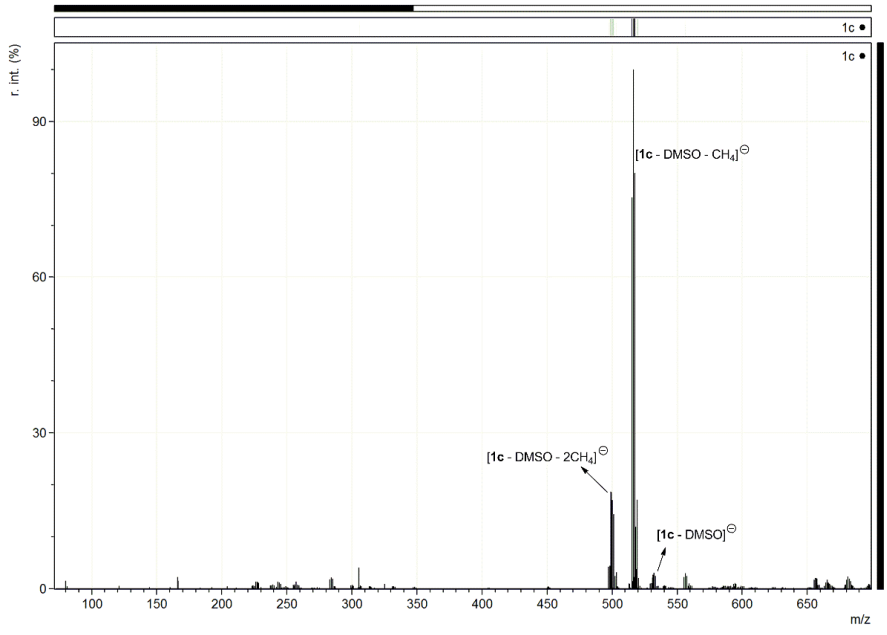

Figure S8. ESI-TOF Mass Spectrum in negative mode for **Na[1c]**.

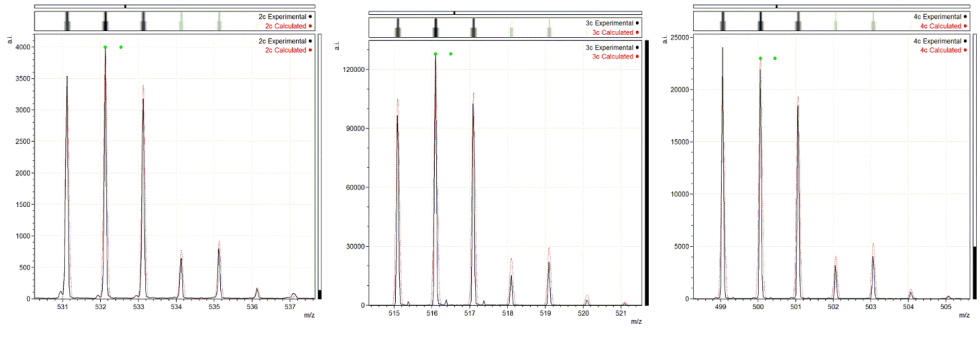

Figure S9. Experimental and calculated isotope patterns of **2c**, **3c** and **4c**.

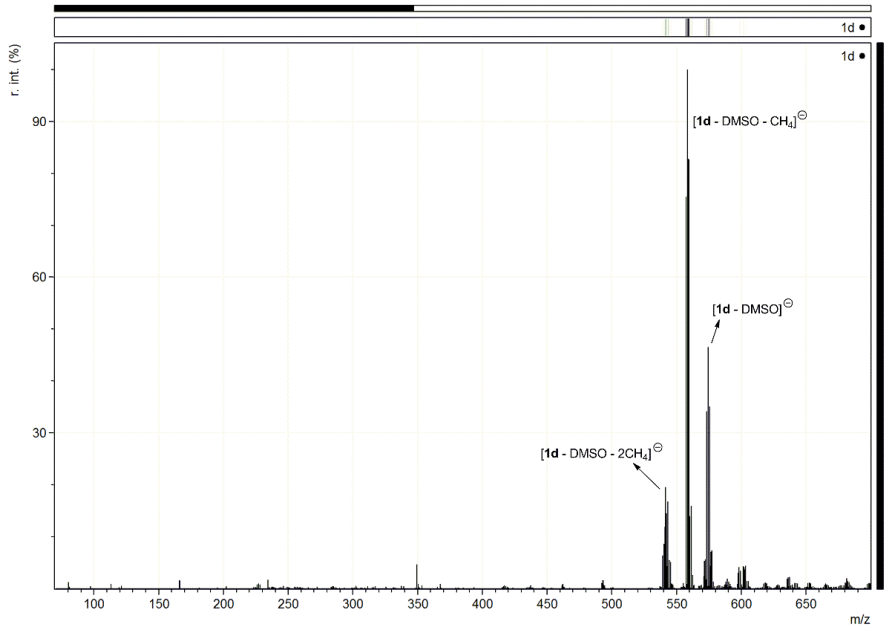

Figure S10. ESI-TOF Mass Spectrum in negative mode for **Na[1d]**.

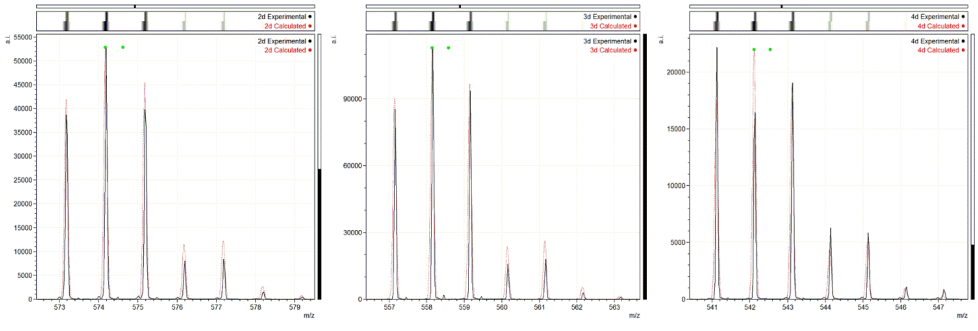

Figure S11. Experimental and calculated isotope patterns of **2d**, **3d** and **4d**.

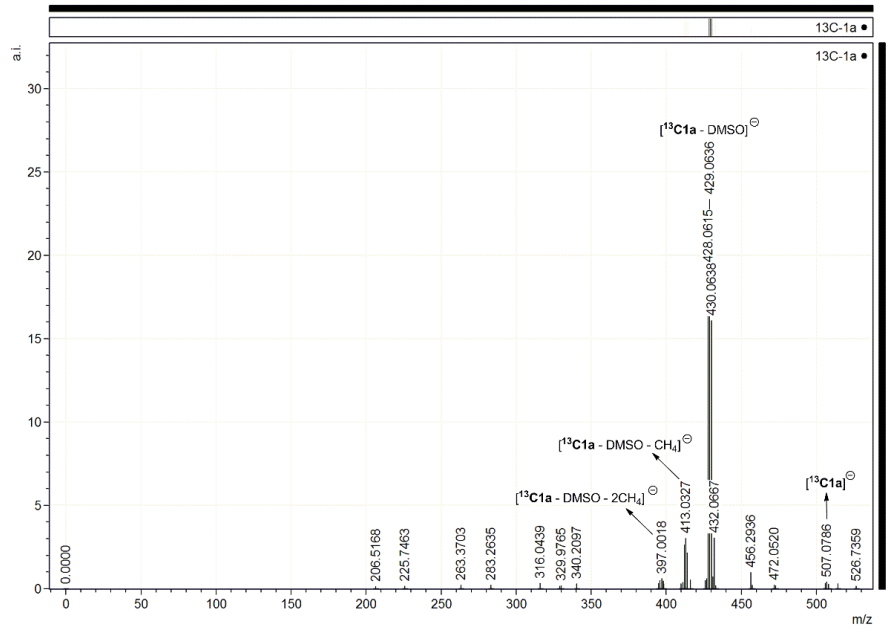

Figure S12. ESI-TOF Mass Spectrum in negative mode for **Na[^{13}C1a]**.

5. Mass Spectra from IRMPD-Fragmentation Studies for Anionic Species 4

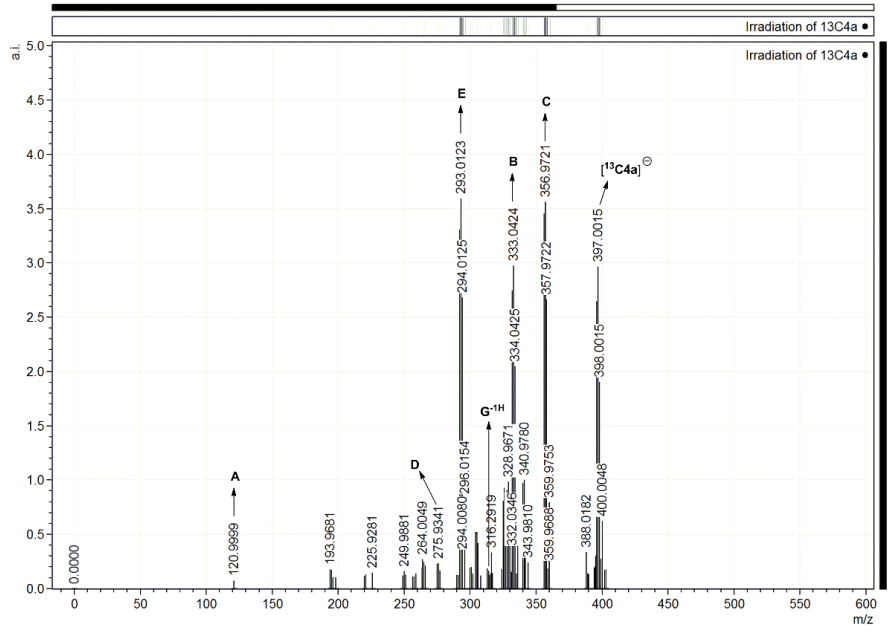

Figure S13. ESI-FT-ICR mass spectrum for the anionic species after IRMPD-fragmentation of **^{13}C4a**.

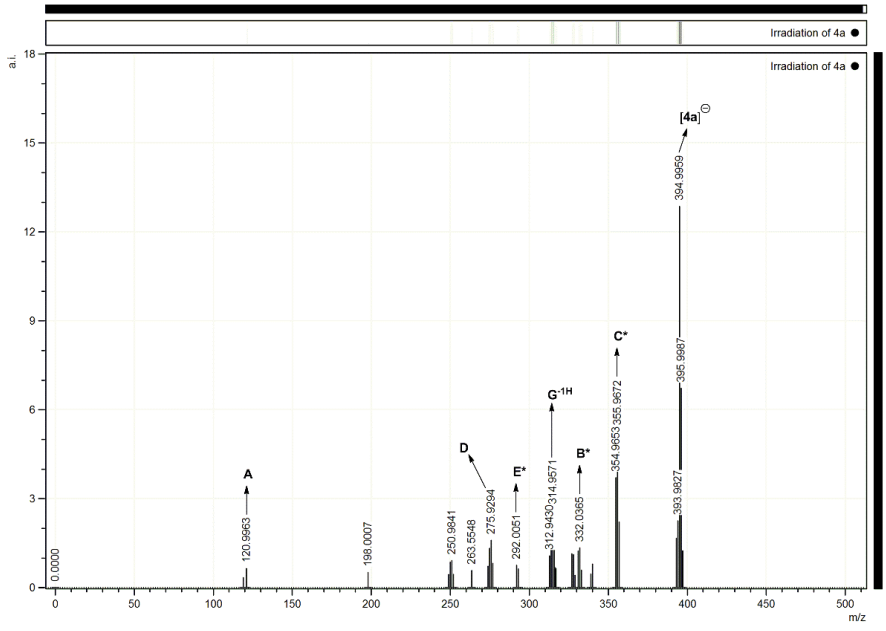

Figure S14. ESI-FT-ICR mass spectrum for the anionic species after IRMPD-fragmentation of **4a** (The species **B***, **C***, and **E*** correspond to species **B**, **C**, and **E** found in **^{13}C4a** without ^{13}C enrichment).

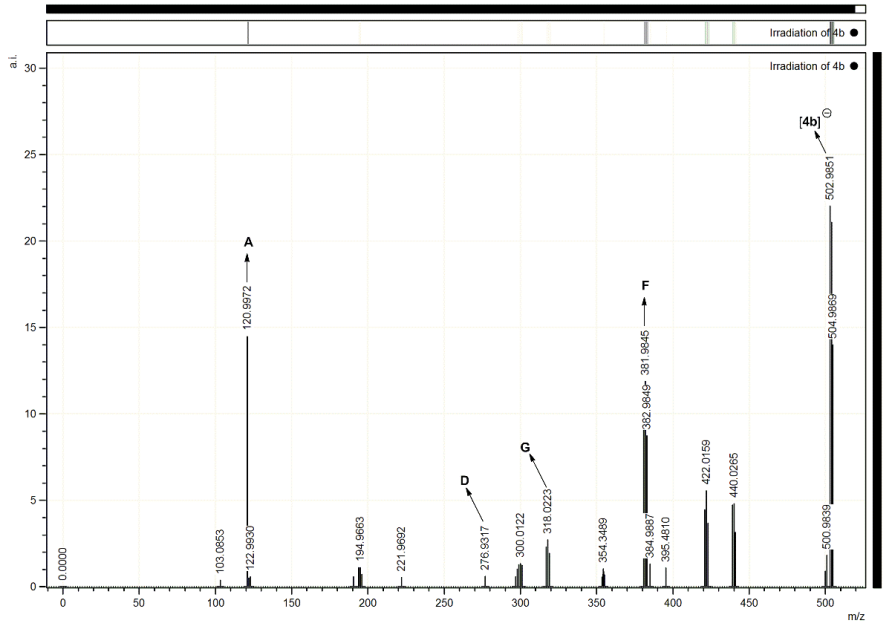

Figure S15. ESI-FT-ICR mass spectrum for the anionic species **4b** after IRMPD-fragmentation.

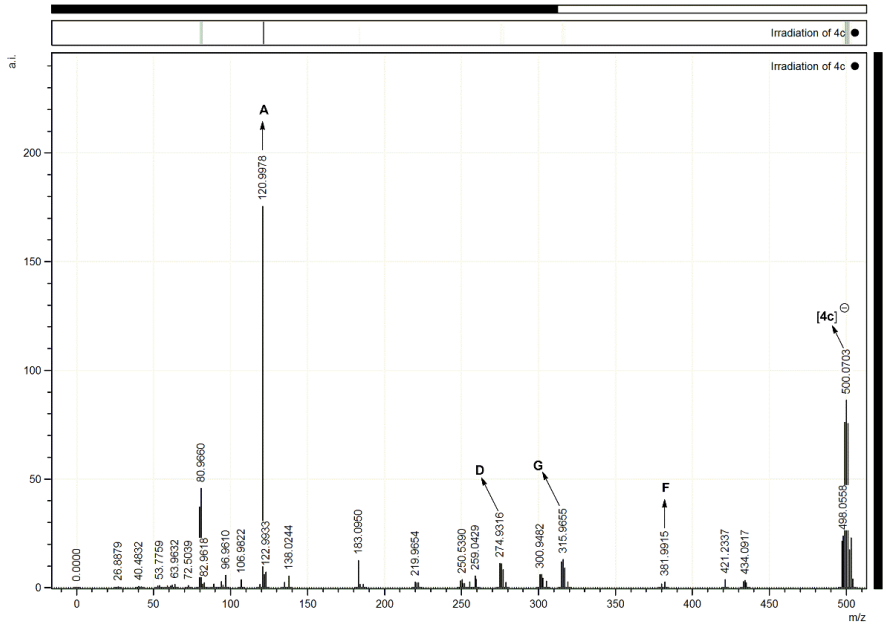

Figure S16. ESI-FT-ICR mass spectrum for the anionic species **4c** after IRMPD-fragmentation.

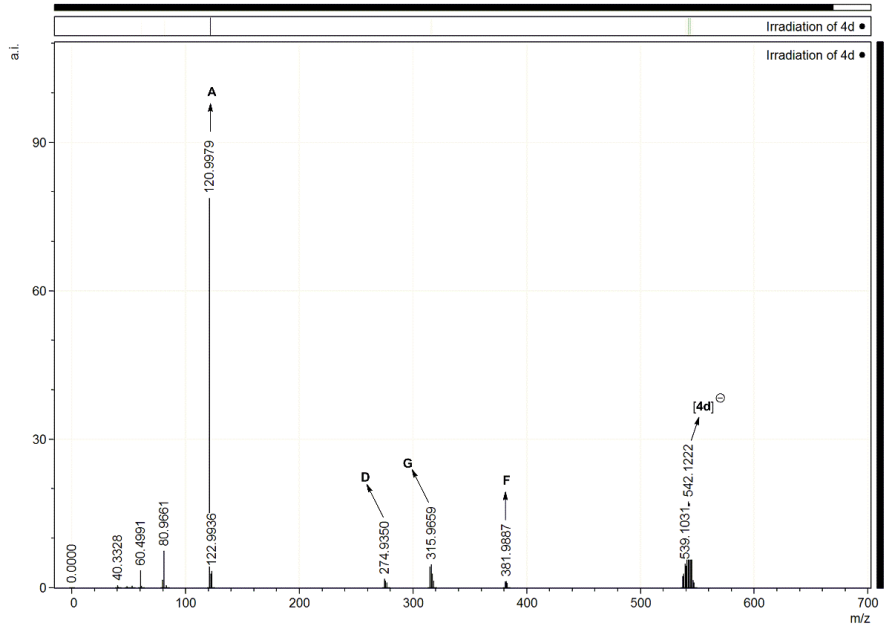

Figure S17. ESI-FT-ICR mass spectrum for the anionic species **4d** after IRMPD-fragmentation.

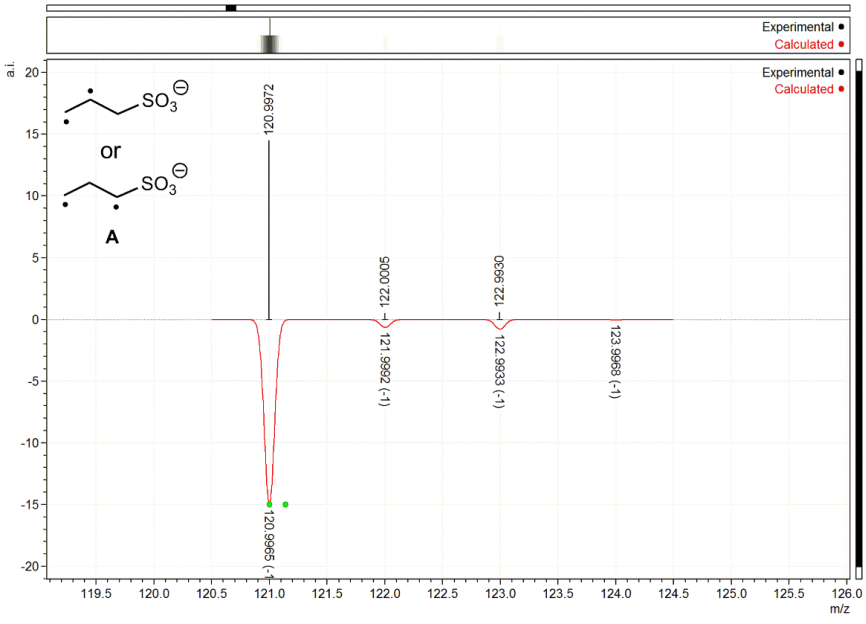

Figure S18. Experimental (up) and calculated (down) isotopic distribution for anion **A** detected by IRMPD (FT-ICR) fragmentation of ions **4b-d**.

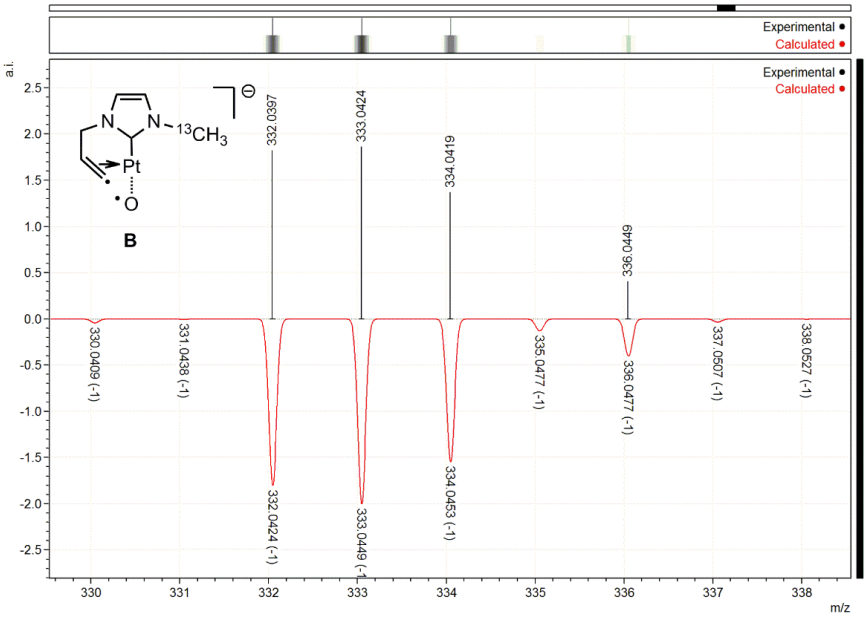

Figure S19. Experimental (up) and calculated (down) isotopic distribution for anion **B** detected by IRMPD (FT-ICR-MS) fragmentation of ion **^{13}C4a**.

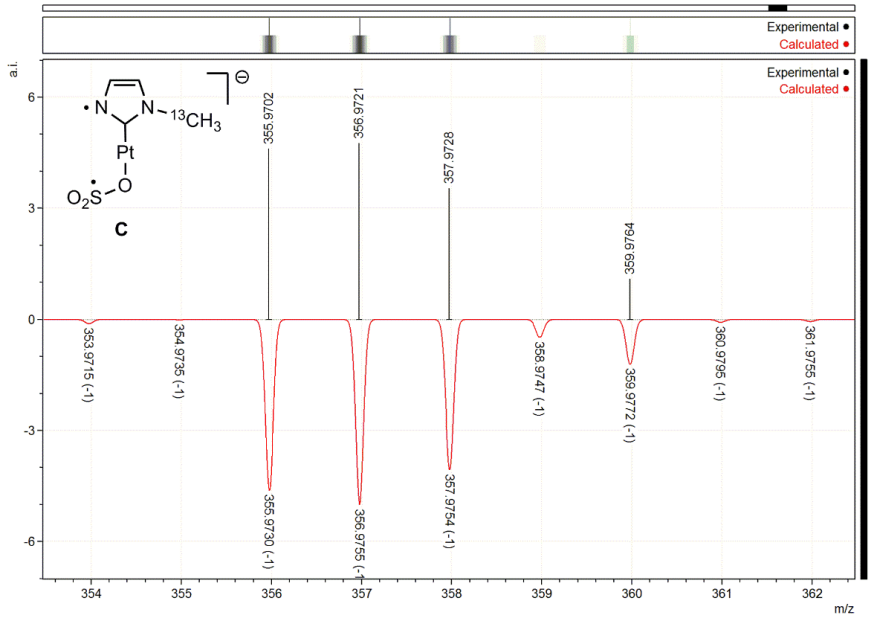

Figure S20. Experimental (up) and calculated (down) isotopic distribution for anion **C** detected by IRMPD (FT-ICR) fragmentation of ion **^{13}C4a**.

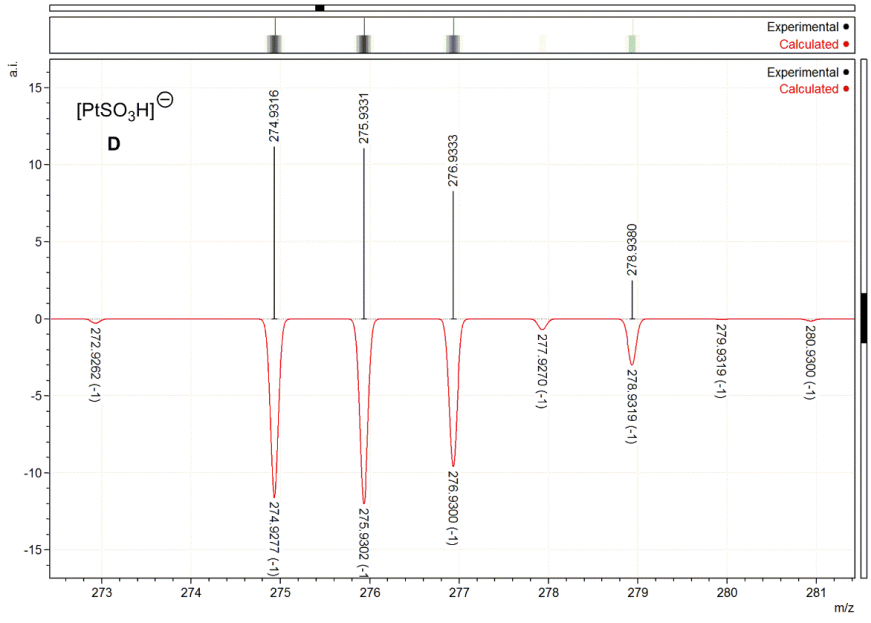

Figure S21. Experimental (up) and calculated (down) isotopic distribution for anion **D** detected by IRMPD (FT-ICR) fragmentation of ions **4a-d**.

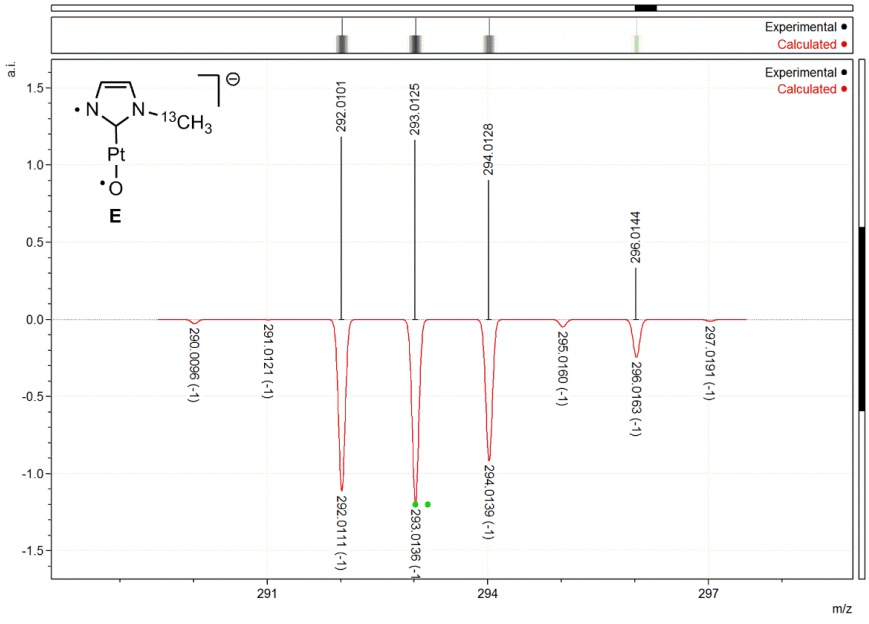

Figure S22. Experimental (up) and calculated (down) isotopic distribution for anion **E** detected by IRMPD (FT-ICR) fragmentation of ion **^{13}C4a**.

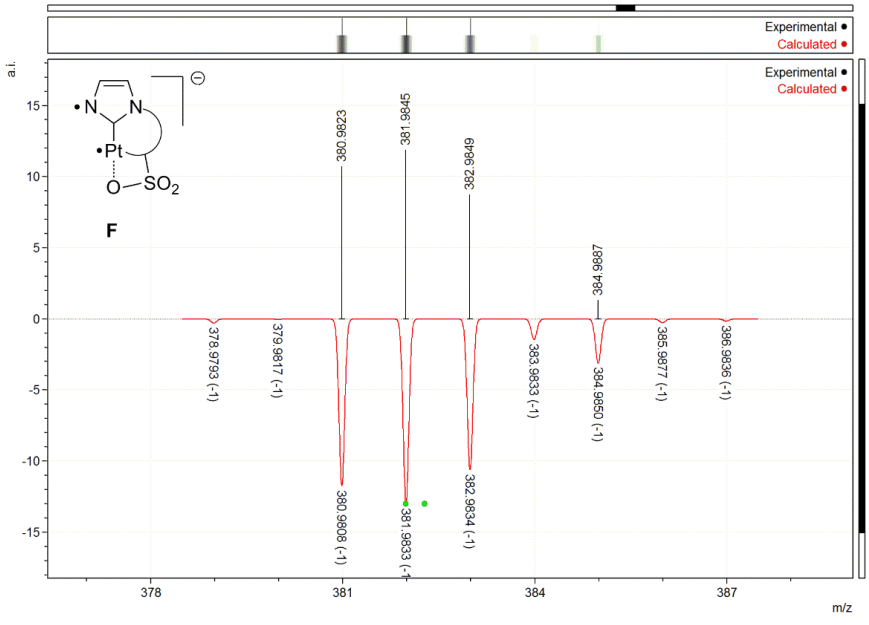

Figure S23. Experimental (up) and calculated (down) isotopic distribution for anion **F** detected by IRMPD (FT-ICR) fragmentation of ions **4b-d**.

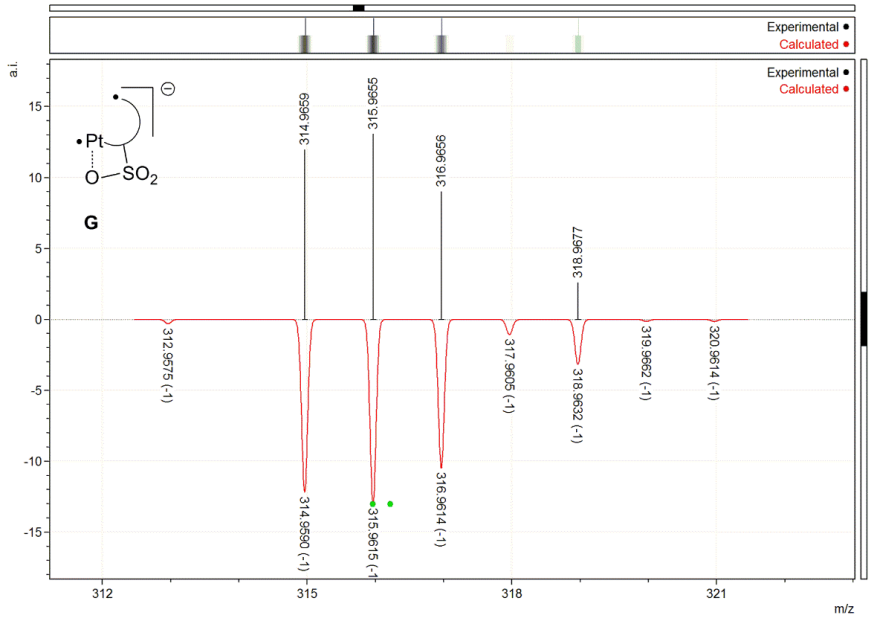

Figure S24. Experimental (up) and calculated (down) isotopic distribution for anion **G** detected by IRMPD (FT-ICR) fragmentation of ions **4b-d**.

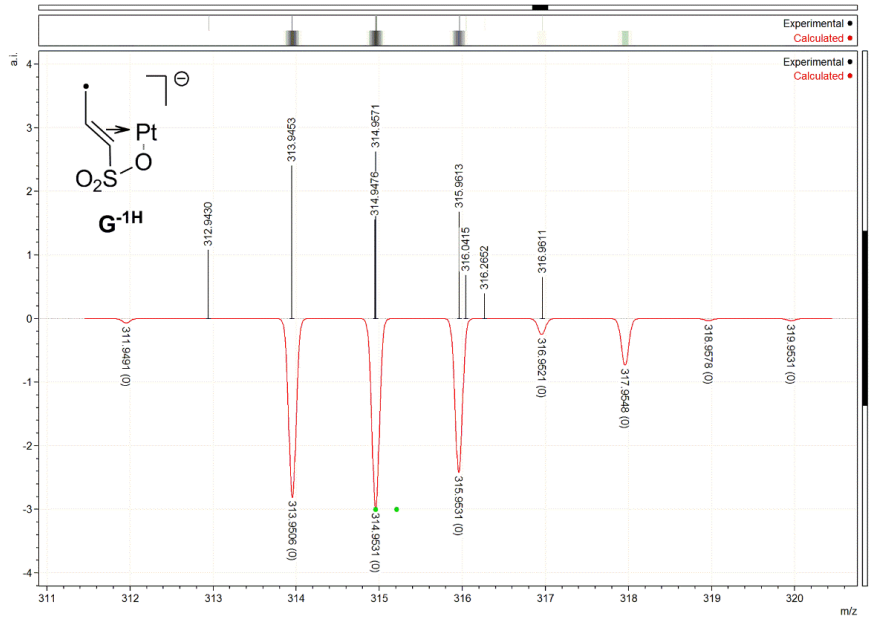

Figure S25. Experimental (up) and calculated (down) isotopic distribution for anion **G**$^{-1H}$ detected by IRMPD (FT-ICR) fragmentation of ions **4a** and ^{13}**C4a**.

6. Energy Resolved TQ-CID Experiments

The TQ-CID experiments were performed at 21 different collision energies, corresponding to the center-of-mass energies (E_{cm}) of 0-1.8 eV. The center-of-mass energy was calculated using the equation:

$$E_{cm} = E_{lab}[m/(M + m)]$$

Where E_{lab} is the ion kinetic energy in the laboratory frame, m is the mass of the collision gas (argon), and M is the mass of the anion under study. The final intensities of the dissociation product ions were determined as the average of 100 measurements of one second of detection.

The bond dissociation energy (BDE) of the complex **3c** was obtained from the corresponding dissociation energy threshold, E_0, in the reaction:

$$[\mathbf{3}\boldsymbol{c}]^- \rightarrow [\mathbf{4}\boldsymbol{c}]^- + CH_4 \qquad (E_0) \qquad \textbf{(1)}$$

The experimental total reaction cross section, σ, was determined using the relation $I_R = I_{tot} \cdot e^{-\sigma \cdot \varrho \cdot l}$, where I_{tot} and I_R are the total ion intensity and fragment ion intensity, respectively, both measured after the dissociation, ϱ is the collision gas density, and l is the path length (18.5 cm) of the collision cell. It was assumed that all fragment ions formed during the dissociation were detected and that the effect of multiple collisions was not relevant. The relative intensities of the precursor (**3c** m/z 516) and product (**4c** m/z 500) anions were plotted as a breakdown diagram in function of the E_{cm} (Figure S26).

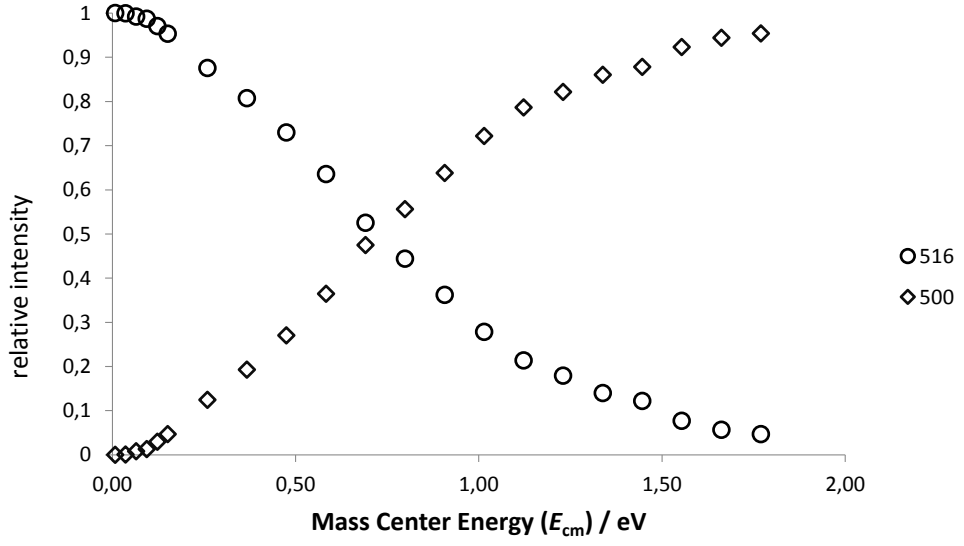

Figure S26. Experimental breakdown diagram for anion **3c**.

A simulation of σ for reaction (**1**) as a function of E_{cm} is shown in Figure S27. It was obtained with L-CID operational simpler method developed by Chen and co-workers.[4] The threshold energy extracted was E_0 = 1.21 ± 0.09 eV. This energy corresponds to the highest energy along the reaction coordinate for dissociation without reverse activation barrier in a "loose transition state".[5] The corresponding uncertainty was obtained by checking the flexibility of the fit upon variations in the adjustable parameters, such as fwhm (full-width at half maximun) of kinetic ion distribution (Figure S28), temperature, and number of ions in the simulation. The error limits in E_0 were then established by noting its value when the fit to the data became significantly worse. The obtained experimental value of E_0 is in good agreement with the computed change of total energy at 0 K for reaction (**1**), $\Delta E_{(0\,K)}$ = 1.21 eV.

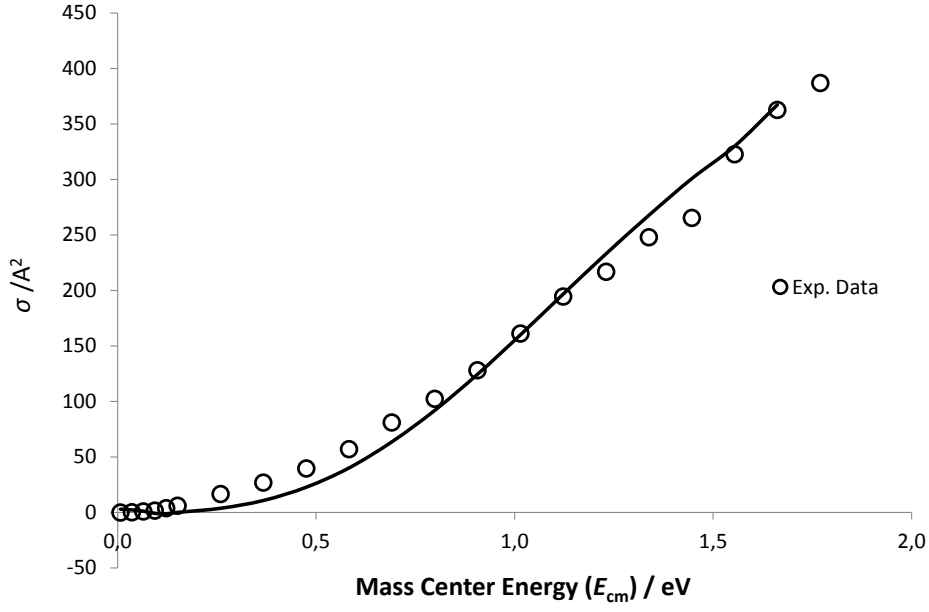

Figure S27. L-CID simulation of cross section σ versus E_{cm} for reaction (**1**).

Thus, a well-defined near-Gaussian distribution of the ions kinetic and, presumably, internal energies is achieved (Figure S28). The ion kinetic energy for one specific ion can be determined by retarding the potential measurements after the so-called Q_0 pole ion guide. Thus, a well-defined near-Gaussian distribution of the ions kinetic and, presumably, internal energies is achieved (Figure S28). This Gaussian fit (red line) has a full width at half-maximum of 0.89 eV. The theoretical fit was done using OriginPro, Origin (OriginLab, Northampton, MA).

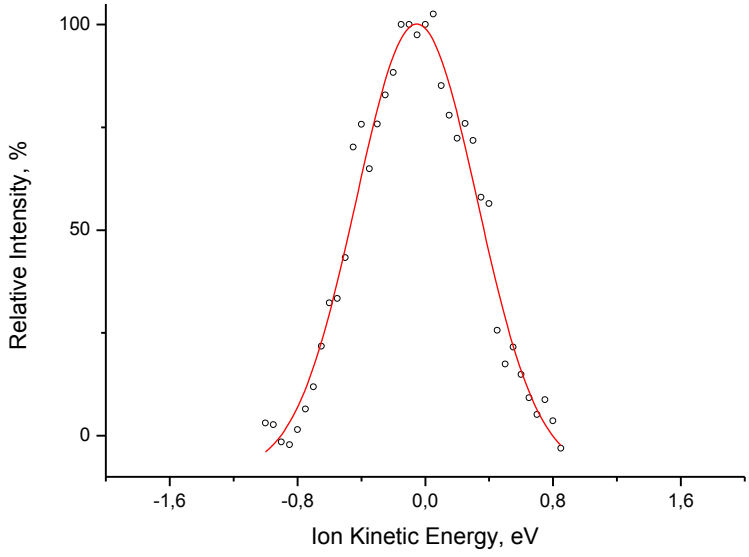

Figure S28. Distribution of ion kinetic energies in the laboratory frame, determined for ion **4c**.

7. DFT Calculations

Electronic structure calculations were carried out using the M06[6] density functional with the Stuttgart-Dresden MWB60 effective core potential and basis[7] including a set of additional f functions for Pt and the triple zeta quality basis 6-311+G(d, p) for other elements. This basis set combination will be referred to as BS1. Minimum energy and transition state structures were optimized by computing analytical energy gradients. The obtained stationary points were characterized by performing energy second derivatives, confirming them as minima or first order saddle points by the number of negative eigenvalues of the hessian matrix of the energy (zero and one negative eigenvalues respectively). To further refine the energies obtained from the M06/BS1 calculations, single-point calculations on the previously optimized structures were performed using the same pseudopotential and basis set for Pt and the larger basis set 6-311++G(3df, 2p) for all the remaining atoms. Computed electronic energies were corrected for zero-point energy, thermal energy, and entropic effects to obtain the corresponding thermodynamic properties H^0 and G^0. All calculations were carried out with the Gaussian 09 suite of programs.[8]

8. References

(1) E. A. Baquero, J. C. Flores, J. Perles, P. Gomez-Sal, E. de Jesús, *Organometallics* **2014**, *33*, 5470-5482.

(2) a) C. Eaborn, K. Kundu, A. Pidcock, *J. Organomet. Chem.* **1979**, *170*, C18-C20; b) C. Eaborn, K. Kundu, A. Pidcock, *J. Chem. Soc., Dalton Trans.* **1981**, 933-938.

(3) B. H. Clowers, E. D. Dodds, R. R. Seipert, C. B. Lebrilla, *Anal. Biochem.* **2008**, *381*, 205-213.

(4) S. Narancic, A. Bach, P. Chen, *J. Phys. Chem. A* **2007**, *111*, 7006-7013.

(5) a) P. B. Armentrout, in *Modern Mass Spectrometry, Vol. 225* (Ed.: C. Schalley), Springer Berlin Heidelberg, **2003**, pp. 233-262; b) T. Baer, P. M. Mayer, *J. Am. Soc. Mass Spectrom.* **1997**, *8*, 103-115.

(6) Y. Zhao, D. G. Truhlar, *Theor. Chem. Acc.* **2008**, *120*, 215-241.

(7) a) D. Andrae, U. Haeussermann, M. Dolg, H. Stoll, H. Preuss, *Theor. Chim. Acta* **1990**, *77*, 123-141; b) J. M. L. Martin, A. Sundermann, *J. Chem. Phys.* **2001**, *114*, 3408-3420.

(8) Frisch, M.J. *et al.* Gaussian 09, revision C.01; Gaussian, Inc.: Wallingford, CT, **2010**.

Capítulo IX. Resumen y Conclusiones (Chapter IX. Summary and Conclusions)

Química de Complejos Carbeno N-Heterocíclico de Platino Hidrosolubles (Chemistry of Water-Soluble N-Heterocyclic Carbene Platinum Complexes)

INTRODUCCIÓN Y ANTECEDENTES

Los carbenos N-heterocíclico (NHC) se han consolidado durante las últimas dos décadas como una clase de ligandos excepcionales en la química organometálica debido, principalmente, a su capacidad para estabilizar diferentes especies metálicas y las implicaciones que eso conlleva en aplicaciones clave como la catálisis.[1] Si bien la gran mayoría de procesos han sido desarrollados en disolventes orgánicos,[1a] el interés por el empleo de agua en estas aplicaciones, incluida la catálisis, es evidente. De hecho, las publicaciones que describen la síntesis de complejos organometálicos hidrosolubles con ligandos NHC con grupos hidrofílicos (iónicos o no-iónicos) han aumentado considerablemente durante los últimos 10 años.[2] Sin embargo, la utilización de tales complejos en procesos catalíticos en un medio acuoso es un campo mucho menos estudiado.[2] En este contexto, nuestro grupo de investigación ha sido pionero en el empleo de complejos NHC hidrosolubles de Pt(0) como catalizadores reciclables en la reacción de hidrosililación de alquinos terminales en agua (Esquema 1).[3]

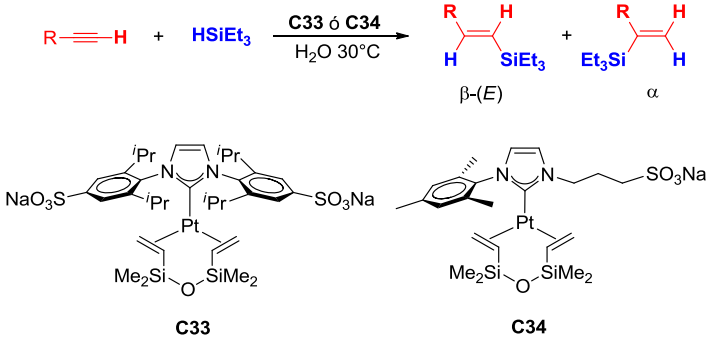

Esquema 1. Complejos hidrosolubles (NHC)Pt(0) para la hidrosililación de alquinos terminales en agua.[3]

Una conclusión importante a destacar de ese trabajo (Esquema 1) fue la estabilidad e inercia mostrada por el enlace NHC–Pt en medio acuoso bajo las condiciones catalíticas empleadas. Lo anterior nos llevó a interesarnos por estudios fundamentales sobre el comportamiento químico de esta clase de especies en agua; que es un tema relativamente

poco explorado en química organometálica. En el caso de complejos hidrosolubles con ligandos NHC, los trabajos que han aparecido en la bibliografía han tratado esencialmente aspectos sintéticos y aplicaciones catalíticas.[2] Por ello, decidimos abordar una investigación sobre la reactividad en fase acuosa de complejos hidrosolubles de Pt con ligandos NHC sulfonados, con un especial énfasis en la estabilidad hidrolítica de los enlaces NHC–Pt u otros enlaces Pt–C presentes.

El trabajo de tesis doctoral que aquí se presenta comprende la síntesis y estudios del comportamiento químico de las familias de nuevos complejos hidrosolubles de Pt(II) y Pt(0) representados en la Figura 1. Además de la información obtenida en el estudio de la preparación de estos carbenos metálicos, su estabilidad y determinadas reacciones de sustitución, en esta memoria se recogen los resultados obtenidos con los complejos de tipo **2** en procesos de activación C(sp^3)–H intramoleculares en fase gas, así como su empleo en la síntesis en agua de nanopartículas estables e hidrosolubles de Pt. Igualmente, se recogen estudios preliminares sobre la reactividad de los complejos **3** en reacciones de adición oxidante dirigidos a la síntesis de complejos hidruro de Pt(II) solubles en agua.

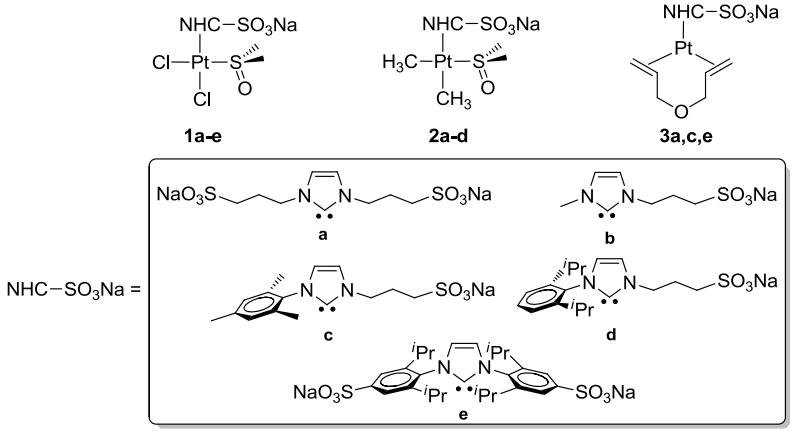

Figura 1. Familias de complejos objeto de estudio en esta tesis doctoral.

Síntesis Mejorada de *cis*-[Pt(dmso)$_2$Me$_2$] y *trans*-[Pt(dmso)$_2$MeCl] (CAPÍTULO II)

Los complejos metálicos *cis*-[Pt(dmso)$_2$Me$_2$] (**1**) y *trans*-[Pt(dmso)$_2$MeCl] (**2**), se utilizan con frecuencia como precursores para la introducción de fragmentos PtMe$_2$ y PtMeCl en variedad de complejos de coordinación.[6] El método descrito por Eaborn[7] y posteriormente por Romeo y Scolaro[8] para el derivado monometilo **2**, partiendo de *cis*-[Pt(dmso)$_2$Cl$_2$] y SnMe$_4$ en dmso a 80 ºC durante 24 h, es la metodología más habitual para su preparación (Esquema 2). Desafortunadamente, en el curso de nuestras investigaciones siguiendo los protocolos para la obtención de **2**, la reacción o no tuvo lugar o condujo a rendimientos muy

bajos (≤ 9%). Este bajo rendimiento puede ser debido a la volatilidad del $SnMe_4$ cuyo punto de ebullición es varios grados inferior a la temperatura de trabajo.

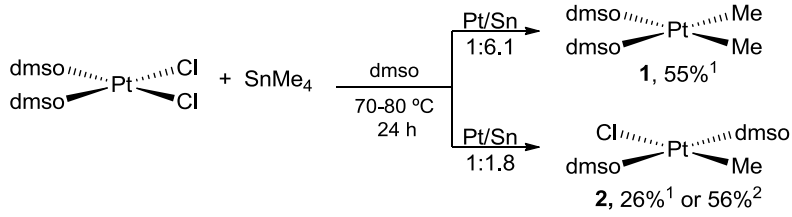

Esquema 2. Síntesis descrita para los complejos **1** y **2** partiendo de *cis*-$[Pt(dmso)_2Cl_2]$ y $SnMe_4$.[7-8]

Hemos comprobado que al cambiar las condiciones de trabajo a un sistema cerrado y con relaciones molares Pt:$SnMe_4$ de 1:2,5, la reacción transcurre en menor tiempo (3 h), pero inesperadamente hacia el complejo **1** como producto único con un 82% de rendimiento (55% en el procedimiento descrito para **1**, después de 24 h y a Pt:$SnMe_4$ 1:6.1). Incluso utilizando una relación Pt:$SnMe_4$ 1:1 se obtiene **1** como único complejo metilado, aunque con un rendimiento de aproximadamente el 50%. Entendiendo que la formación de **1** es cinéticamente más rápida que la de **2**, tal y como se muestra en el Esquema 3, hemos podido acceder a este último mediante la reacción de redistribución de ligandos entre el producto **1** y el de partida *cis*-$[Pt(dmso)_2Cl_2]$ en CH_2Cl_2, obteniendo **2** con un 65% de rendimiento (56% en el procedimiento descrito para **2**, en dmso y a Pt:$SnMe_4$ 1:1.8).

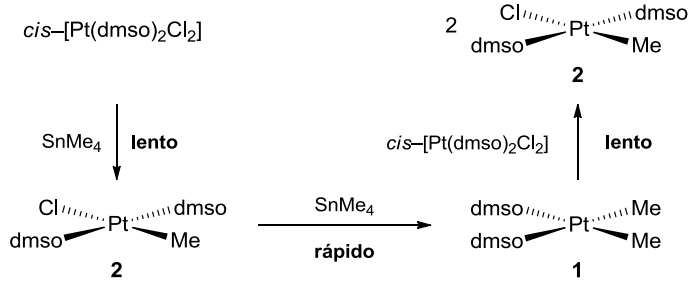

Esquema 3. Formación de **2** por medio de un intercambio metil-cloro entre **1** formado *in situ* y *cis*-$[Pt(dmso)_2Cl_2]$.

Los complejos di y monometilo **1** y **2**, junto a su precursor *cis*-$[Pt(dmso)_2Cl_2]$, han sido utilizados como productos de partida en la síntesis de la mayoría de los complejos NHC sulfonados preparados y estudiados en este trabajo de tesis doctoral.

Complejos Hidrosolubles de Plata(I) con Ligandos Carbeno N-Heterocíclico Sulfonados: Comportamiento en Medio Acuoso y como Agentes de Transferencia a Platino(II) (CAPÍTULO III)

El tratamiento de las sales de imidazolio **1a–e** con óxido de plata en medio acuoso genera los complejos correspondientes de tipo bis(carbeno) sulfonados de Ag(I) $\mathbf{2^{Ag+}}$ (Esquema 4b), que tratados con NaCl dan lugar a los derivados **2**, a los que también se puede acceder directamente si la reacción se lleva a cabo en presencia de cloruro de sodio (Esquema 4a). El resultado cambia en un disolvente polar aprótico, como dmso (dimetilsulfóxido), puesto que en este caso se forman los complejos mono(carbeno) **3** (Esquema 4c). Todos los complejos se obtienen con buenos rendimientos (> 80%) y han sido caracterizados por diferentes técnicas tales como, RMN de ^{1}H y ^{13}C, espectrometría de masas y difracción de rayos X en el caso de $\mathbf{2e^{Ag+}}$, **2e** y **3e** (Figura 2).

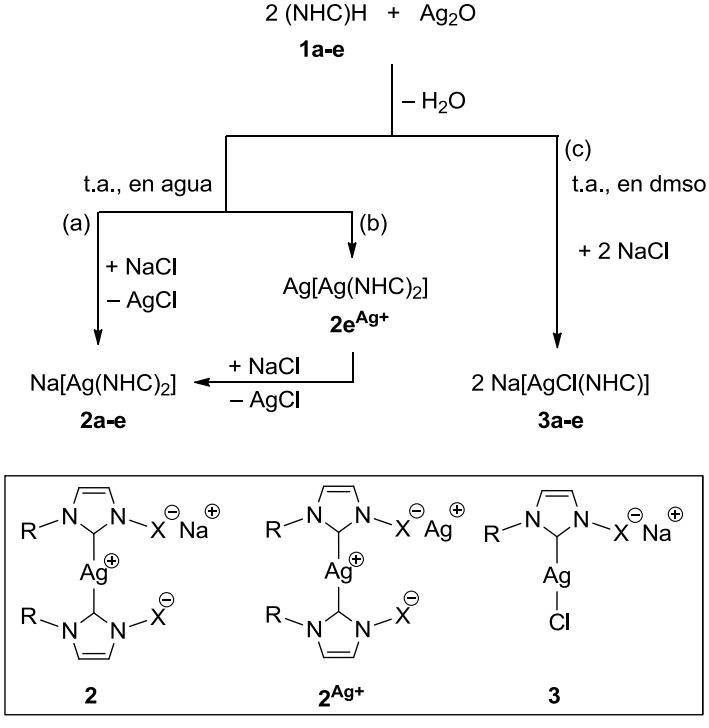

Esquema 4. Síntesis de complejos bis (**2**) y mono(carbeno) (**3**) de plata(I) con ligandos NHC sulfonados.

El papel desempeñado por el disolvente en la formación de las especies mono (**3**) o bis(carbeno) (**2**) lo hemos relacionado con el equilibrio recogido en el Esquema 5 entre las especies mono(carbeno) **I** y las bis(carbeno) **II**, pero en el que también hay que considerar la eliminación del haluro de plata (AgX) para dar los complejos bis(carbeno) **III**. En

disolventes polares próticos, como MeOH o agua, se produce la precipitación del haluro de plata como consecuencia de la inestabilidad del anión $[AgX_2]^-$, lo que justifica la formación de especies bis(carbeno) en estos disolventes. En dichos disolventes próticos, hemos podido comprobar además que se promueve la hidrólisis de los enlaces Ag–NHC. Por otra parte, el desplazamiento del equilibrio hacia las especies mono(carbeno), se ve favorecido en disolventes polares apróticos como CH_3CN o dmso.

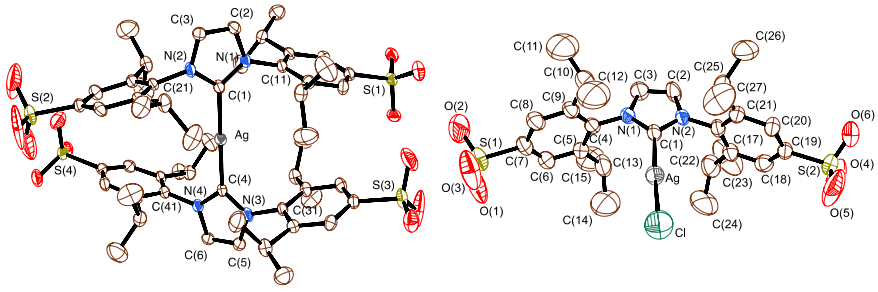

Figura 2. Diagramas ORTEP para las estructuras moleculares de los complejos **2e** (izquierda) y **3e** (derecha). Se omiten los hidrógenos e iones Na^+ por claridad.

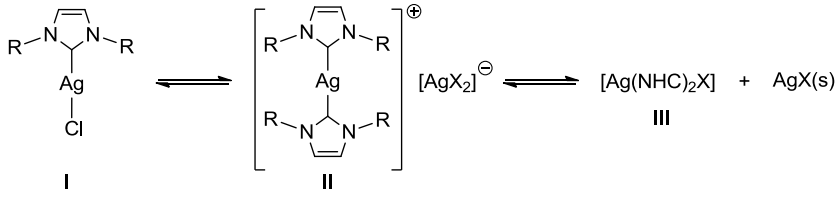

Esquema 5. Especies en equilibrio para complejos NHC de plata(I).

Los derivados de plata(I) han sido ensayados como agente de transferencia de carbeno[4] en la síntesis de complejos de Pt(II). La reacción no se verifica al tratar el precursor metálico *cis*-$[PtCl_2(dmso)_2]$ con los bis(carbeno) de plata **2** (Esquema 5a), mientras que el uso de las especies **3** conduce a la formación de los compuestos de fórmula *cis*-$[PtCl_2(dmso)(NHC)]$. En estas síntesis se observa la concurrencia de procesos de hidrólisis competitivos que no han podido ser sorteados (Esquema 5b), encontrando que la metodología más conveniente para acceder a los complejos **4** con rendimientos aceptables (60–90%), comprende la generación *in situ* del carbeno libre correspondiente por tratamiento con $NaHCO_3$ como base desprotonante, en presencia del precursor metálico en dmso a 90 °C (Esquema 5c).

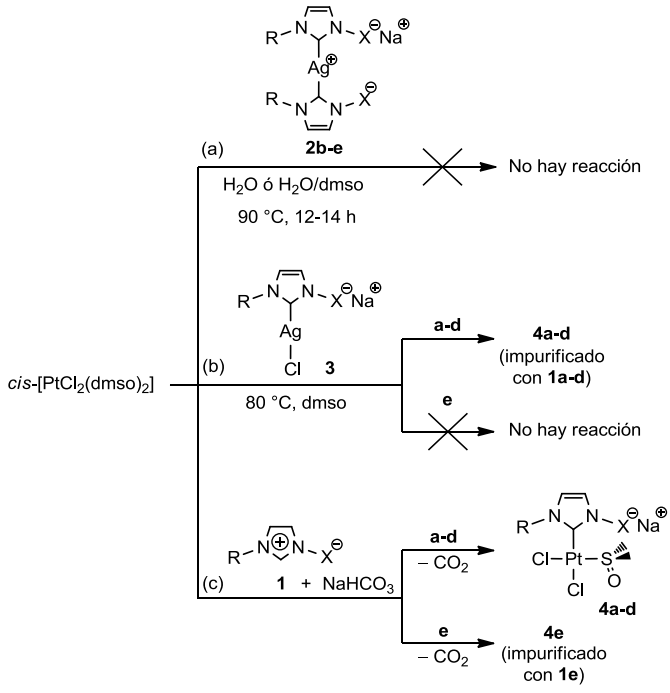

Esquema 5. Síntesis de los complejos NHC de platino(II) *cis*-[$PtCl_2$(dmso)(NHC)] (**4**).

Los complejos **4** han sido caracterizados por RMN de ^{1}H, ^{13}C y ^{195}Pt, así como análisis elemental, espectrometría de masas y difracción de rayos X en el caso de **4a** (Figura 3).

Estos complejos han sido empleados en la hidratación catalítica de alquinos terminales e internos,[5] en reacciones que se llevan a cabo con complejos hidrosolubles de Pt(II) en agua pura. Los complejos **4** permiten transformar alquinos como fenilacetileno y derivados, con conversiones totales en algunos casos en menos de 1 h, con cargas metálicas ≤ 2 mol%, en agua a 80 ºC y sin la necesidad de adicionar co-catalizadores ácidos o agentes de transferencia de fase.

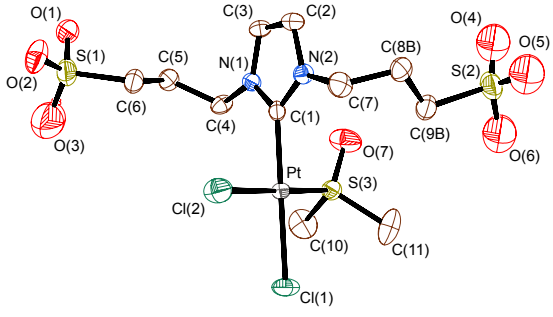

Figura 3. Estructura molecular encontrada para **4a**. Se omiten los hidrógenos e iones Na^{+} por claridad.

Complejos Hidrosolubles Mono- y Dimetilo de Platino(II) con Ligandos Carbeno N-Heterocíclico: Síntesis y Reactividad (CAPÍTULO IV)

Los complejos **2a–d** se han obtenido como sólidos analíticamente puros y con rendimientos elevados (> 90%) a través del tratamiento de las respectivas sales de imidazolio **1a–d** con el precursor metálico *cis*-[Pt(dmso)$_2$Me$_2$] y ^{t}BuONa como base en dmso a temperatura ambiente (Esquema 6).

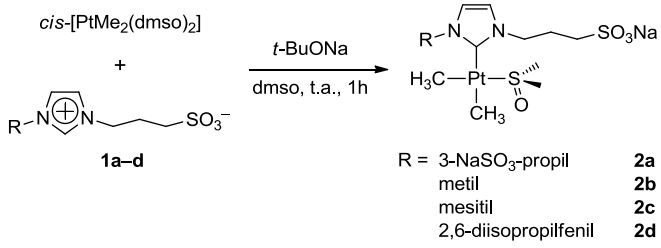

Esquema 6. Síntesis de los complejos *cis*-[PtMe$_2$(dmso)(NHC)] (**2**).

Los complejos han sido caracterizados por espectroscopías de RMN de ^{1}H, ^{13}C y ^{195}Pt, así como espectrometría de masas, análisis elemental y en el caso de **2a**, por difracción de rayos X (Figura 4).

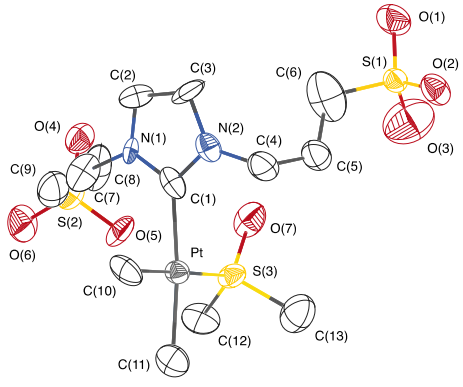

Figura 4. Estructura molecular encontrada para 2**a**. Se omiten los hidrógenos e iones Na^+ por claridad.

Los complejos **2** son estables en agua a pHs neutro y básicos (estudios realizados en D_2O y 0,1 M NaOD) a temperatura ambiente. En cambio, la calefacción a 80 °C de disoluciones neutras en agua deuterada produce la descomposición lenta de los complejos generando CH_3D, CH_4 y C_2H_6 en proporciones aproximadamente de 1:1:2, respectivamente. La formación de metano-d_1 se justifica, lógicamente, por la hidrólisis de algunos enlaces Pt–CH_3, mientras que el desprendimiento de etano es debido a un proceso de eliminación reductora

sufrido por los complejos **2** para generar especies (NHC)Pt(0) y el de metano es causado por procesos de activación C(sp^3)–H del ligando carbeno en los que se ven involucrados otros enlaces Pt–CH_3, generando probablemente especies ciclometaladas de Pt(II) y que se tratan con mayor detalle en el Capítulo VIII.[9] En estos estudios destaca que no se observa la formación de sal de imidazolio, lo que indica que el enlace NHC–Pt es inerte en todas las condiciones estudiadas.

Se ha evaluado el comportamiento de los complejos **2** frente a diferentes ácidos de Brønsted en agua. Con un equivalente de HCl se obtienen los complejos de fórmula [PtMeCl(dmso)(NHC)] (**3**) como una mezcla de estereoisómeros *SP*-4-3 y *SP*-4-4 (Esquema 7a). La adición de un segundo equivalente conduce a la formación de los complejos dicloruro **4** previamente descritos en el Capítulo III (Esquema 7b). También hemos comprobado que se puede acceder a los complejos **3** mediante reacciones de sustitución de dmso por el ligando carbeno en *trans*-[PtClMe(dmso)$_2$] (Esquema 7c). Hay que remarcar que los complejos **4** no sufren cambio alguno en presencia de más HCl, indicando que el enlace NHC–Pt es muy robusto. Por otro lado, con un equivalente de HBF_4 los carbenos de platino **2** generan los complejos metilaquo **5** como una mezcla de diastereoisómeros (Esquema 7d), que aislados y redisueltos en dmso-d_6 dan lugar a los complejos **6**, pero como un único isómero (Esquema 7e). Con otro equivalente de HBF_4 los complejos zwitteriónicos **5** evolucionan a los complejos diaquo **7** (Esquema 7f), que en presencia de NaCl en exceso termina formando los derivados dicloruro **4** (Esquema 7g).

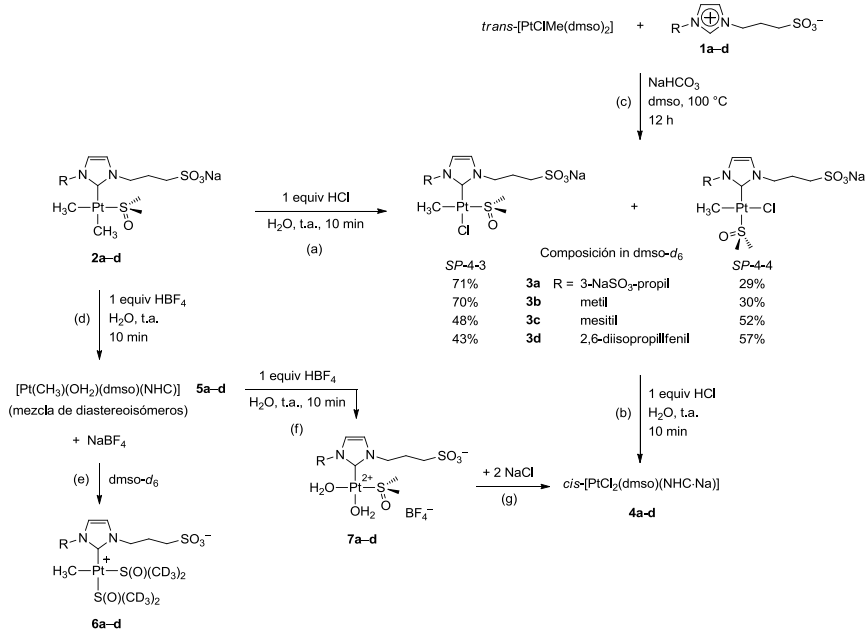

Esquema 7. Secuencias de reacciones de **2** con HCl y HBF_4.

Los complejos **3**, **5–7** han sido caracterizados por RMN de ^{1}H, ^{13}C y ^{195}Pt, espectrometría de masas y para el caso del estereoisómero *SP*-4-3-**3a**, fue posible obtener su estructura cristalina mediante difracción de Rayos X (Figura 5).

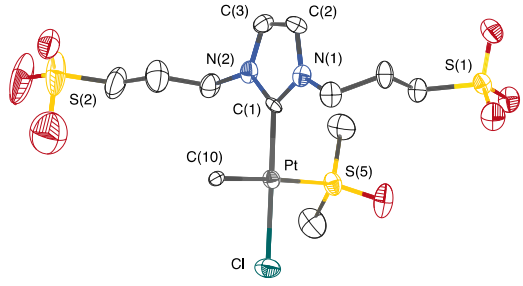

Figura 5. Estructura molecular del complejo *SP*-4-3-**3a**. Se omiten los hidrógenos e iones Na^{+} por claridad.

Con el objetivo de profundizar en el estudio de la estabilidad hidrolítica de los complejos dimetilo **2**, se han llevado a cabo reacciones frente a nucleófilos tales como cianuro. La adición de un equivalente de KCN a disoluciones de los complejos **2** en agua, causa lentamente la formación de los productos de sustitución *cis*-[$PtMe_2$(CN)(NHC)] (**8**), aunque la reacción no llega a completarse y es acompañada de la evolución de los complejos ciano hacia la formación de los complejos **9** (Esquema 8a). Lo anterior sugiere que la adición de CN^{-} a **2** promueve la hidrólisis del enlace Pt–CH_3 *trans* al ligando NHC en **8**, aspecto que se ve respaldado por el hecho de que la reacción en presencia de dos equivalentes de KCN es mucho más rápida hacia la formación casi cuantitativa de **9** (Esquema 8b). La notable aceleración de la transformación **2** → **8** → **9** con el incremento de la concentración de CN^{-} es propio de un mecanismo de sustitución asociativo para complejos plano-cuadrados de Pt(II). La facilidad con que ahora se produce la hidrólisis del enlace Pt–CH_3 puede ser debido a que la naturaleza aniónica del intermediario **8** incrementa la nucleofilia del ligando metilo. En relación con esta hipótesis, hemos comprobado que la reacción de **2** con un ligando isocianato con un grupo electroatractor, concretamente el $CNCH_2COOK$, conduce a los complejos **10** en los que la hidrólisis se inhibe hasta tal punto que son estables en disolución acuosa por más de 3 días a temperatura ambiente (Esquema 8c).

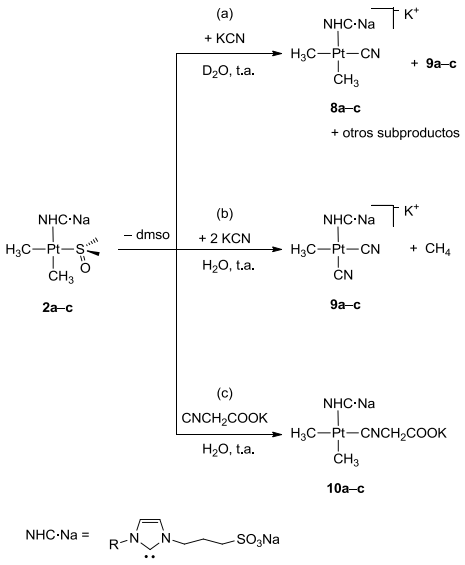

Esquema 8. Reacciones de los complejos dimetilo **2** con KCN y $CNCH_2COOK$ en agua.

Los complejos **9–10** han sido caracterizados por RMN de ^{1}H y ^{13}C, espectroscopía IR, espectrometría de masas y en el caso de **9a**, fue posible obtener su estructura cristalina por medio de difracción de rayos X (Figura 6a). En la estructura de **9a** en estado sólido destaca una disposición tridimensional particular, puesto que se ordena en forma de panal con celdas de simetría tetragonal y canales con diámetros internos de 6 Å decorados con átomos de Pt (Figura 6b).

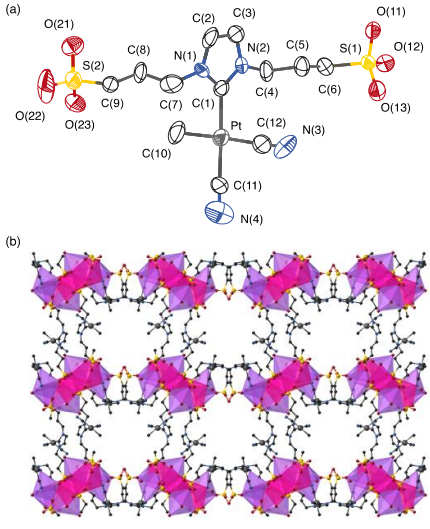

Figura 6. (a) Estructura molecular de **9a**. Los hidrógenos e iones Na+ son omitidos por claridad. (b) Vista de la estructura cristalina de **9a** a lo largo del eje cristalográfico *c*. Las esferas de coordinación de los cations Na^+ y K^+ son representados como poliedros.

Síntesis de Complejos Hidruro NHC de Platino(II) Hidrosolubles Mediante la Adición Oxidante Reversible de Alquinos a Complejos de Pt(0) (CAPÍTULO V)

En un ensayo prototipo para comprobar la propensión de complejos NHC de Pt(0) hidrosolubles a sufrir reacciones de adición oxidante, se ha comprobado que el derivado diolefínico **2** frente a CH_3I en dmso a 50 °C, genera fácilmente el complejo [PtMeI(dmso)(NHC)] **4** como único estereoisómero (*SP*-4-4) en alto rendimiento (90%) (Esquema 9). Consideramos que el resultado puede tener interés sintético debido a que el procedimiento utilizado anteriormente para acceder a complejos haloalquilo de este tipo (ver Capítulo IV), no es estereoselectivo y conduce a mezcla de estereoisómeros.[10]

Esquema 9. Síntesis del complejo **4** mediante adición oxidante.

La reacción de adición oxidante de alquinos terminales en el complejo **2** con la intención de sintetizar derivados hidruro de platino, también ha sido de nuestro interés. Se ha encontrado que el complejo adiciona trimetilsililacetileno y fenilacetileno generando los hidruros de Pt(II) **5** y **6** con rendimientos altos (> 90%) (Esquema 10).

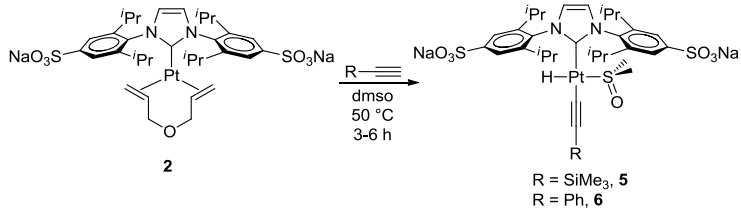

Esquema 10. Síntesis de los complejos hidrosolubles hidruro NHC de Pt(II) **5** y **6**.

Los nuevos complejos son solubles en agua y moderadamente estables en este disolvente. En estudios sobre su estabilidad llevados a cabo en D_2O mediante RMN de ^1H, se observa que **5** y **6** liberan lentamente el alquino precursor al medio, en un proceso de descomposición que parece completarse en aproximadamente 10 días a temperatura ambiente. Entendiendo que el resultado es un indicio de la tendencia de estos derivados hidrurolaquinilo a sufrir una eliminación reductora en agua, se diseñaron nuevas experiencias tanto a escala de tubo de RMN como preparativa. Por ejemplo, en las disoluciones acuosas de los complejos en presencia de alil éter se regenera el complejo de Pt(0) **2** en conversiones prácticamente cuantitativas en tan solo unas 3 h. La reacción ha sido ensayada con otras olefinas (acrilato de metilo y diviniltetrametildisiloxano) con el mismo resultado, es decir, la eliminación del

alquino terminal con formación del complejo diolefina de Pt(0) correspondiente. Por lo tanto, el proceso de adición oxidante se ve favorecido en un disolvente como dmso, mientras que la reacción inversa es la que ocurre en agua (Esquema 11), ilustrando una vez más que el agua como disolvente puede producir cambios importantes en la reactividad de estas especies. También consideramos que la tendencia de los complejos hidruroalquinilo a sufrir la eliminación reductora en agua, puede ser de valor sintético porque se trata de una metodología sin precedentes en la preparación de complejos NHC de Pt(0) hidrosolubles.

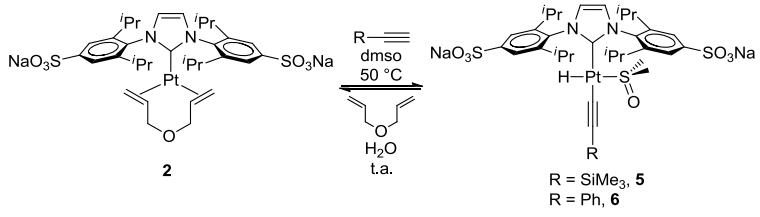

Esquema 11. Dependencia del disolvente para el comportamiento reversible de la adición oxidante para **2** y la eliminación reductora de **5** y **6**.

Nanopartículas Hidrosolubles de Platino Altamente Estabilizadas por Ligandos Hidrofílicos de Tipo Carbeno N-Heterocíclico (CAPÍTULO VI)

Como se ha avanzado en el Capítulo IV, la descomposición térmica de las disoluciones acuosas de los complejos de tipo *cis*-[$PtMe_2$(dmso)(NHC)] liberaba etano como gas más abundante, observándose además el oscurecimiento de las disoluciones. En consecuencia, hemos abordado el estudio de los complejos dimetilo **1a–d** como precursores de nanopartículas hidrosolubles de platino (NPsPt) **2a–d** (Esquema 12). Las nanopartículas se obtuvieron con buenos rendimientos (57–82%, basado en el contenido de metal determinado por espectrometría de masas inductivamente acoplado a plasma, ICP-MS) después de ser purificadas mediante técnicas de diálisis con una membrana de celulosa. Las nanopartículas **2** resultan ser muy estables en disolución acuosa por tiempo indefinido sin observarse la precipitación o aglomeración de las mismas.

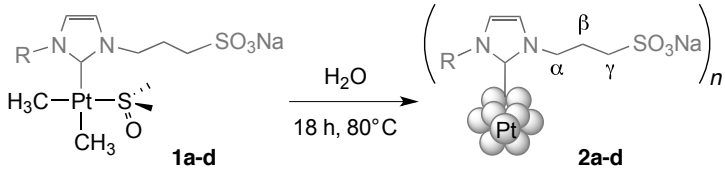

Esquema 12. Síntesis de nanopartículas de platino **2a–d** partiendo de los complejos **1a–d**.

Las nanopartículas de platino **2** se han caracterizado mediante TEM y TEM de alta resolución (Figura 7), dispersión de luz dinámica (DLS), ICP-MS, análisis elemental, IR,

RMN ^{1}H en disolución y ^{13}C en estado sólido usando la técnica de polarización cruzada con giro de ángulo mágico (CP-MAS). Los tamaños medios de las partículas encontrados por microscopía electrónica son de 1,3–2,0 ± 0,4 nm. Los estudios de RMN en disolución indican que los ligandos NHC se encuentran coordinados a la superficie de las nanopartículas a través del carbono carbénico con las cadenas sulfonadas dispuestas alejándose de la superficie hacia el seno de la disolución acuosa, facilitando una interacción eficiente de los grupos iónicos con el disolvente que justifica tanto la estabilidad como la solubilidad de las nanopartículas.

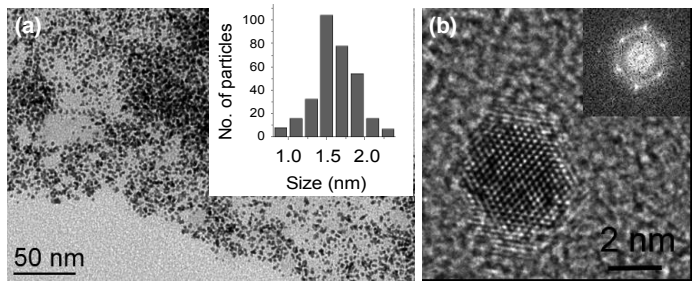

Figura 7. (a) Imagen TEM y distribución de tamaños y (b) imagen TEM de alta resolución con su correspondiente figura de transformación rápida de Fourier (FFT) para las NPsPt **2a**. Escala de la barra en (b) = 2 nm.

Para confirmar la presencia y modo de coordinación de los ligandos NHC a la superficie, se ha realizado la síntesis de las nanopartículas **2c** con el carbono carbénico marcado con ^{13}C (**^{13}C-2c**). Por RMN de ^{13}C en estado sólido mediante CP-MAS, se constata inequívocamente la coordinación del carbono carbénico a la superficie de las NPsPt, no solo por su frecuencia de resonancia (177 ppm), sino porque se ha podido determinar por primera vez una constante de acoplamiento ^{13}C–^{195}Pt en un nano-sistema (940 Hz) (Figura 8).

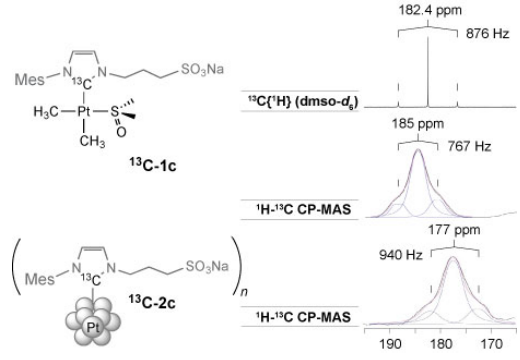

Figura 8. De arriba a abajo: frecuencia de resonancia atribuida a los carbonos carbénicos enlazados a Pt en el espectro de RMN de $^{13}C\{^{1}H\}$ **^{13}C-1c** y los espectros ^{1}H–^{13}C CP-MAS de **^{13}C-1c** y **^{13}C-2c**, mostrando sus respectivas curvas de deconvolución.

A modo de ensayo testigo de sus posibles aplicaciones, las nanopartículas sintetizadas **2** han sido utilizadas en la reacción de hidrogenación catalítica de estireno en agua en condiciones suaves (temperatura ambiente, presión de 1 bar de H_2). Las NPsPt **2** se muestran activas con cargas de 0,4–0,6 mol%, transformando el 100% del estireno selectivamente a etilbenceno en tan solo 2 h de reacción. En una serie de reacciones con **2d** se ha reciclado el catalizador un total de nueve veces sin muestras de agotamiento del mismo (pérdida de actividad o selectividad), encontrando que el nivel de lixiviado en las operaciones de separación de los productos es tan solo un 0,44% del contenido de Pt inicial al finalizar la última reacción catalítica de la serie.

Nanopartículas Hidrosolubles de Platino Estabilizadas por Ligandos Carbeno N-Heterocíclico Sulfonados: Efecto de la Metodología Sintética (CAPÍTULO VII)

Tras los resultados obtenidos en la síntesis de nanopartículas de Pt mediante descomposición térmica de la familia de complejos organometálicos *cis*-[$PtMe_2$(dmso)(NHC)], se han diseñado nuevos experimentos con el objeto de ampliar las metodologías sintéticas para este tipo de partículas y explorar el efecto de las condiciones de obtención sobre las mismas.

Una primera aproximación ha consistido en la preparación de las nanopartículas **3** mediante descomposición de las disoluciones acuosas de complejos dimetilo **1** a temperatura ambiente en presencia de una atmósfera de CO (3 bar) (Esquema 13).

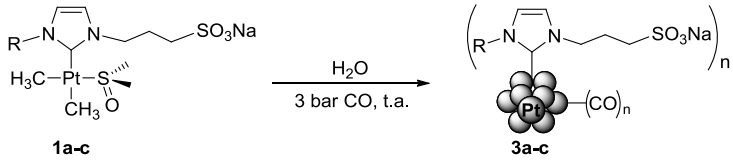

1a-c **3a-c**

Esquema 13. Síntesis de las nanopartículas **3a–c** partiendo de los complejos dimetilo **1a–c**.

Las nanopartículas **3** han sido caracterizadas por TEM, IR, RMN en disolución de ^{1}H y en estado sólido de ^{13}C mediante CP-MAS, y se han mostrado estables dispersadas en agua por tiempo indefinido, presentando tamaños medios de partícula entre 1,0–1,3 ± 0,3 nm. Se ha podido comprobar por espectroscopía IR la presencia de grupos carbonilo coordinados a su superficie en modo terminal, mientras que los resultados obtenidos por RMN en disolución y en estado sólido demuestran inequívocamente la coordinación del ligando NHC a través del carbono carbénico. Por ejemplo, en las nanopartículas **^{13}C-3c**, marcadas con ^{13}C en esa posición, el desplazamiento químico para ese carbono es de 163 ppm y se ha podido determinar una constante de acoplamiento $^{1}J_{C\text{-}Pt}$ de 940 Hz.

Se han llevado a cabo seguimientos por RMN en disolución de la formación de las nanopartículas, con la idea de poder desvelar información sobre el papel que juega el monóxido de carbono en el proceso. La imagen que proporcionan los resultados obtenidos (Esquema 14) está de acuerdo con que en las etapas tempranas del mismo se produce la sustitución del ligando dmso por CO dando lugar a los intermediarios **[3a–c]**, y con que éstos son los verdaderos precursores de las NPs, puesto que si se elimina la atmósfera de CO se detiene completamente la formación de las partículas y los intermedios permanecen inalterados, estables, en la disolución.

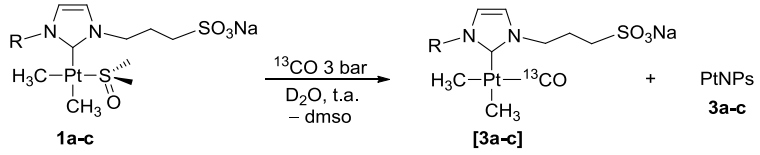

Esquema 14. Formación de los intermediarios **[3a-c]** bajo las condiciones de formación de nanopartículas.

Una metodología sintética que también ha sido explorada es la que se basa en la hidrogenación de ligandos olefínicos, como alil éter, de complejos NHC de Pt(0) en disolución acuosa, con el fin de generar especies "desnudas" NHC–Pt(0) que pueden servir tanto a modo de semillas de nucleación como de fuente de unidades de construcción en el proceso de crecimiento de las nanopartículas. Siguiendo este procedimiento, los complejos de Pt(0) **4a**, **4c** y **4e**, sometidos a una presión de H_2 de 3 bar en agua y a temperatura ambiente, dan lugar a las nanopartículas **5a**, **5c** y **5e** (Esquema 15). Estas nanopartículas también se muestran estables en disolución acuosa por tiempo indefinido, con la excepción de las **5e** en las que se observa precipitación después de un día, aunque se redispersan con facilidad por simple agitación manual. Esta falta de estabilidad se atribuye a la disposición de los grupos sulfonato, que en este caso se encuentran apuntando hacia la superficie de la nanopartícula en un ligando con escasa flexibilidad, de manera que no se dan las condiciones adecuadas para una solvatación eficiente de estos grupos iónicos en el medio acuoso.

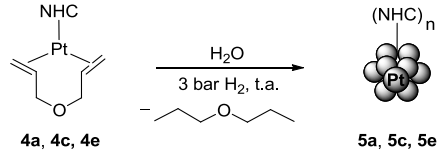

Esquema 15. Síntesis de las nanopartículas **5** derivadas de los complejos NHC de Pt(0) **4**.

El tiempo de la reacción de formación depende significativamente del impedimento estérico impuesto por los ligandos NHC sobre el metal. Con el ligando menos voluminoso (**a**) la reacción se completa en 10 días, mientras que con los más voluminosos (**c** y **e**) el proceso requiere periodos más largos (23 y 42 días, respectivamente). El efecto puede estar

relacionado con la cinética del proceso de hidrogenación, pero la capacidad de los ligandos más impedidos de estabilizar especies metálicas intermedias entorpeciendo la etapa de nucleación, debe jugar un papel importante. De hecho, la velocidad de formación de **5** conlleva diferencias importantes en la distribución de tamaños determinada por TEM para las nanopartículas, encontrando una correlación entre sus tamaños y el tiempo necesario para completar su formación (1,7 ± 0,6; 3 ± 2 y 4,0 ± 0,8 nm para **5a**, **5c** y **5e**, respectivamente). Es decir, con ligandos más voluminosos se dificulta la nucleación, permitiendo un crecimiento que, aunque sea más lento que con ligandos menos impedidos, resulta en nanopartículas de mayores tamaños.

Las nanopartículas **5** también han sido caracterizadas por IR y RMN de ^{1}H en disolución y de ^{13}C en estado sólido mediante CP-MAS. La coordinación del ligando NHC a la superficie de la nanopartícula a través del carbono carbénico se evidencia con la frecuencia de resonancia a 176 ppm observada en el espectro de ^{1}H-^{13}C CP-MAS para las nanopartículas **^{13}C-4c** marcadas con ^{13}C en esa posición del heterociclo.

Activaciones Intramoleculares Asistidas por la Base de Enlaces C(sp^3)–H en Complejos (NHC)Pt(II) Sulfonados en Fase Gas (CAPÍTULO VIII)

A raíz de los resultados de descomposición térmica comentados para los complejos *cis*-[$PtMe_2$(dmso)(NHC)] en D_2O a 80 °C (ver Capítulo IV), se decidió investigar este tipo de procesos en fase gas. La naturaleza aniónica de estos complejos posibilita su estudio por espectrometría de masas en condiciones de electroespray sin la necesidad de aditivo ionizante alguno. En estas condiciones los complejos dimetilo **1a–d** sufren la serie de transformaciones que se muestra en el Esquema 16. Inicialmente tiene lugar la descoordinación del ligando dmso para generar las especies tricoordinadas en forma de "T" **2a**–**d**, que posteriormente son susceptibles de sufrir una activación intramolecular C(sp^3)–H de los sustituyentes del grupo R del ligando NHC en **1a**, **1c** y **1d**, liberando una molécula de metano y generando las especies ciclometaladas **3**. Finalmente, se forma una segunda molécula de metano del mismo modo, pero activando la cadena propil sulfonato, dando los iones diciclometalados **4**. Para **1b**, las dos activaciones C(sp^3)–H tienen lugar en la cadena sulfonada generando una especie **π-**alqueno de platino(0). Los picos que corresponden a las especies **2** son las más intensas en sus respectivos espectros de masas cuando el sustituyente R era un grupo alquilo (**2a** y **2b**), mientras que las debidas a las especies **3** son las más intensas cuando el sustituyente es arilo (**3c** y **3d**). Esto parece indicar que la primera activación C(sp^3)–H está más favorecida cinéticamente cuando hay un sustituyente arilo, lo que podría deberse a que los grupos metilo de los anillos aromáticos se disponen en las proximidades del centro metálico y a que estadísticamente (*i.e.*, mayor número de enlace C–H en disposición de ser activados) también se espera una mayor facilidad en este tipo de activaciones.

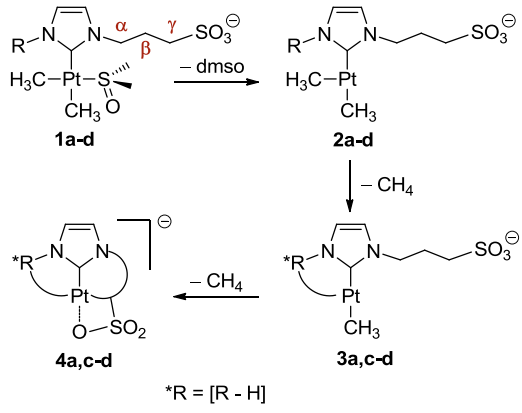

Esquema 16. Secuencia propuesta en la formación en fase gas de los iones **4a**, **c-d** partiendo de **1a, c-d**.

Los iones generados fueron estudiados por espectrometría de masas de resonancia ciclotrónica de iones con transformada de Fourier (FT-ICR MS). La secuencia de transformaciones, así como su estructura fue corroborada mediante estudios de fragmentación por disociación multifotónica de infrarrojo (IRMPD) llevadas a cabo sobre cada uno de los respectivos iones previamente aislados en la celda del ciclotrón. Por ejemplo, los iones **3** y **4** se detectan cuando se aísla y fragmenta **2**, del mismo modo que se detectan las especies **4** cuando los iones de partida en los estudios de fragmentación son los **3**.

Se han realizado cálculos DFT para discernir el mecanismo que opera en estos procesos de activación de enlaces C(sp^3)–H. Se encuentra que el grupo sulfonato juega un papel muy importante en el proceso de activación C–H, participando como base abstractora del protón del enlace involucrado en la activación (**TS1[2d-3d]** Figura 9), lo que supone un descenso de la barrera de energía de formación de, por ejemplo, **3d** comparado con otros mecanismos típicos de activación C–H evaluados (*e.g.*, 5-7 kcal/mol menos que en la adición oxidante con formación de un intermediario de Pt(IV)). El grupo sulfonato también asiste la segunda activación C–H sobre el metileno γ de la cadena propilsulfonato (ver asignación de metilenos en Esquema 16), dando lugar al producto final **4d**. Los cálculos realizados para el complejo con R = Me (**1b**) están de acuerdo con una primera activación (**2b** → **3b**) sobre la cadena, pero ahora en posición β, aunque también asistida por la base, mientras que la segunda consiste en un proceso más convencional de β-eliminación de hidruro sobre la misma cadena, que termina dando un complejo π-alqueno de platino(0) tras eliminar metano (**3b** → **4b**). Se han llevado a cabo estudios de disociación inducida por colisión en un triple cuadrupolo (TQ-CID) con el fin determinar la energía de activación de la transformación de **3c** → **4c**, encontrando que la energía obtenida teóricamente (26.1 kcal/mol para **3d** → **4d**)

está en concordancia la obtenida experimentalmente en los ensayos de colisión (27.9 kcal/mol).

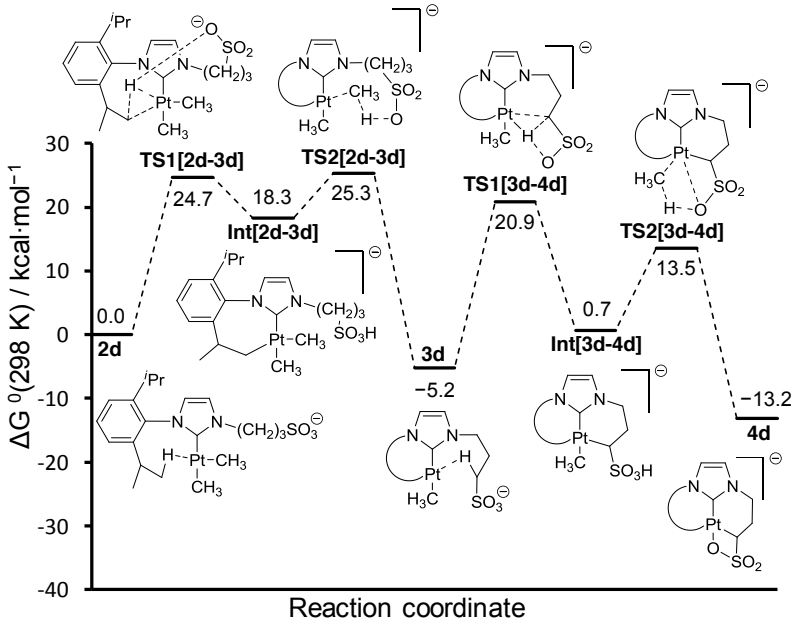

Figura 9. Diagrama de energía de Gibbs para la formación en fase gas de **4d** partiendo de **2d**.

CONCLUSIONES

El trabajo acá presentado abarca la síntesis de complejos organometálicos de metales de transición solubles en agua, el estudio de su comportamiento químico en este disolvente, así como de sus aplicaciones. La investigación se ha centrado en complejos hidrosolubles de platino con ligandos carbeno N-heterocíclico (NHC) sulfonados. El número escaso de ejemplos descritos en la bibliografía englobando aspectos fundamentales de la reactividad organometálica en fase acuosa de esta clase de sistemas, ha condicionado la necesidad de llevar a cabo tanto estudios básicos orientados a la comprensión de las limitaciones sintéticas que operan en este disolvente, como al análisis de la resistencia térmica o a la hidrólisis de enlaces Pt–C, o sobre diversidad de otros procesos (reacciones de sustitución, adición oxidante/eliminación reductora, síntesis de nanopartículas estables y solubles en agua, activaciones de enlaces C–H, etc) incluidos algunos ejemplos de reacciones catalizadas en agua.

Más concretamente, los aspectos más destacados del trabajo realizado para esta tesis doctoral, son los que se relacionan a continuación:

- La mejora de las síntesis de los complejos de partida *cis*-[Pt(dmso)$_2$Me$_2$] y *trans*-[Pt(dmso)$_2$MeCl] ha facilitado la realización de gran parte de este trabajo.

- Se ha podido acceder a nuevos complejos hidrosolubles mono y bis(NHC) de Ag(I). De ellos se ha estudiado el efecto de disolventes polares próticos (H_2O y MeOH) y polares apróticos (dmso y CH_3CN) en el desplazamiento del equilibrio que se establece entre especies mono(NHC)–bis(NHC) en disolución, encontrándose que en medios próticos se ve favorecida la formación de especies bis(NHC)Ag(I), mientras que en disolventes apróticos se promueve la formación de complejos mono(NHC)Ag(I). Además, se ha comprobado que sólo los últimos se comportan como agentes de transferencia de carbeno en la síntesis de complejos de platino(II), pero en ausencia de agua porque en ese medio se transforman en derivados bis(NHC)Ag(I).

- También se han podido preparar de manera eficiente (rendimientos > 90%) nuevos complejos hidrosolubles de Pt con ligandos NHC sulfonados de tipo *cis*-[Pt(II)X$_2$(dmso)(NHC)] (X = Cl y/o Me) y [Pt(0)(AE)(NHC)] (AE = alil éter), mediante síntesis directa por generación del carbeno *in situ* en presencia del precursor metálico correspondiente.

- Los complejos de tipo *cis*-[Pt(II)Cl$_2$(dmso)(NHC)] son bastante activos en la reacción de hidratación catalítica de alquinos en agua, sin la necesidad de otros aditivos y en condiciones relativamente suaves (≤ 2 mol% [Pt], 80 ºC).

- El estudio realizado en fase acuosa con los derivados *cis*-[PtMe$_2$(dmso)(NHC)] frente a ácidos de Brønsted (HCl y HBF_4) y nucleófilos (KCN y $CNCH_2COOK$), ha desvelado información sobre la estabilidad hidrolítica de los enlaces Pt–NHC y Pt–C. Los complejos dimetilo son estables en medios neutro o alcalino (0,1 M NaOD), mientras que a 80 °C los complejos sufren tres tipos de transformaciones competitivas: (a) hidrólisis de enlaces Pt–CH_3, (b) eliminación reductora de etano y (c) activaciones de enlaces C(sp^3)–H de los sustituyentes del ligando NHC. La protonólisis controlada de enlaces Pt–CH_3 con ácidos ha dado lugar a nuevas familias de compuestos ([PtMeCl(dmso)(NHC)], [PtMe(H_2O)(dmso)(NHC)], *cis*-[Pt(H_2O)$_2$(dmso)(NHC)] y *cis*-[PtMe(dmso-d_6)$_2$(NHC)]) de naturaleza diversa, al igual que las reacciones de sustitución de ligandos por nucleófilos en medio neutro, en ocasiones acompañada de procesos de hidrólisis de enlaces Pt–CH_3 (*cis*-[PtMe$_2$(CN)(NHC)], *cis*-[PtMe(CN)$_2$(NHC)] y *cis*-[PtMe$_2$($CNCH_2COOK$)(NHC)]). Todos ellos han sido sintetizados al examinar la reactividad de los complejos de partida en agua, pero el hecho más sobresaliente que pone de manifiesto este

estudio es la gran robustez de los enlaces NHC–Pt(II), cuya inercia queda probada incluso en medios ácidos.

- El complejo [Pt(0)(AE)(NHC)] (NHC = versión sulfonada de IPr) en dmso y a 50 ºC, sufre con facilidad reacciones de adición oxidante de CH_3I y de alquinos terminales. Este procedimiento tiene valor sintético para preparar complejos hidrosolubles mono(NHC)-haloalquilo e -hidruroalquinilo de Pt(II), respectivamente, porque en ambos casos la reacción es esteroselectiva dando diasteroisómeros únicos con un elevado rendimiento. Los nuevos complejos hidruro son moderadamente estables en agua, donde muestran tendencia a revertir la adición del alquino (*i.e.*, su eliminación reductora), en un hecho que también tiene provecho con fines sintéticos, dado que la adición de olefinas a la disolución acuosa de estos hidruros provoca la formación de complejos [Pt(0)((di)olefina)(NHC)].

- La descomposición térmica de los complejos *cis*-[$PtMe_2$(dmso)(NHC)] se constituye como la primera ruta sintética desarrollada en agua para la preparación de nanopartículas hidrosolubles de platino altamente estabilizadas por ligandos NHC. Las nanopartículas son estables en disolución acuosa por tiempo indefinido y presentan tamaños entre 1,3–2,0 nm, en síntesis que son completamente reproducibles. Esta estabilidad es debida a la coordinación de los ligandos carbeno a la superficie mediante enlaces, fuertes e inertes, cuya existencia ha sido demostrada con la determinación, por primera vez en un nano-sistema, de la constante de acoplamiento $^{195}Pt–^{13}C$ (940 Hz). Las nanopartículas sintetizadas son activas en la hidrogenación catalítica de estireno en agua en condiciones suaves (temperatura ambiente, 1 bar de H_2), se separan muy fácilmente de los productos de la reacción y se pueden reutilizar sin pérdida de sus propiedades catalíticas ni degradación aparente.

- Se han estudiado otras dos metodologías químicas para sintetizar nanopartículas de platino en agua, que consisten en la reducción de precursores de Pt(II) *cis*-[$PtMe_2$(dmso)(NHC)] con CO o la hidrogenación de precursores de Pt(0) con olefinas coordinadas a temperatura ambiente en disolución acuosa. Las nanopartículas sintetizadas presentan propiedades similares a las obtenidas por el método "térmico" en cuanto a la estabilidad en agua y la coordinación de los ligandos NHC a su superficie ($^1J_{C–Pt}$ = 940 Hz). Sin embargo, el procedimiento de preparación afecta al tamaño de las mismas, encontrando, además, que éste depende claramente del ligando cuando son sintetizadas por la ruta del H_2 (*i.e.*, mayor tamaño de nanopartícula a mayor impedimento estérico del NHC).

- Los procesos de activación C(sp^3)–H de los ligandos NHC en los complejos *cis*-[$PtMe_2$(dmso)(NHC)] siguen un patrón muy característico. Los estudios realizados en fase gas muestran que la secuencia común para todos ellos implica la descoordinación del ligando dmso y la liberación consecutiva de dos moléculas de metano. Los cálculos teóricos realizados para complementar los resultados de estas experiencias, desvelan que en la cadena de sucesos se ven involucrados los enlaces C(sp^3)–H de los sustituyentes del carbeno, primero estabilizando las especies mediante interacciones agósticas tras la liberación del dmso y, después, participando en procesos sucesivos de ciclometalación intramolecular que conllevan la liberación de las dos moléculas de metano. Sin embargo, la secuencia particular y tipo de activación depende de la sustitución del ligando carbeno, encontrando que está cinéticamente más favorecida sobre los enlaces C(sp^3)–H de grupos en *orto* de arilos, seguida de una activación en posición γ de la cadena propilsulfonato presente como el otro sustituyente. La primera ciclometalación ocurre a través de la posición β de esa cadena en ausencia de grupos arílicos y cuando el segundo sustituyente presenta restricciones geométricas para ser activado (*e.g.*, un grupo metilo), la segunda activación también se verifica, pero sobre la misma cadena y a través de un proceso de β-eliminación de hidruro, dando un complejo π-alqueno de Pt(0).

- Un aspecto relevante encontrado en el estudio teórico-experimental realizado sobre las activaciones de enlaces C(sp^3)–H, es que ocurren a través de un mecanismo singular por el que se produce la desprotonación del enlace C–H, de forma concertada con el metal, asistido intramolecularmente por la base remota (*i.e.*, el grupo sulfonato). Esta asistencia reduce la energía de Gibbs de activación del proceso en 5-7 kcal/mol comparada con la que correspondería a una reacción clásica de adición oxidante C–H, lo que se corresponde con un incremento relativo de la velocidad de esta reacción de 4 a 6 órdenes de magnitud. Este hecho evidencia que la presencia del sulfonato, introducido a modo de grupo hidrosolubilizante, no resulta inocua en la reactividad de estos complejos, llegando a modificar o facilitar determinados comportamientos de los mismos.

Estos resultados constituyen una aportación modesta, pero sólida, al cuerpo de conocimiento sobre la química organometálica en agua, en el que el interés por su crecimiento se sustenta en perspectivas como, por ejemplo, permitir el diseño racional de catalizadores funcionales y recuperables capaces de operar en fase acuosa en condiciones suaves sin degradación, o identificar comportamientos y desarrollar procesos químicos novedosos en este disolvente y que están aún por desvelar.

BIBLIOGRAFÍA

(1) a) *N-Heterocyclic Carbenes in Synthesis*, Nolan, S. P., ed., Wiley-VCH, Weinheim, **2006**; b) *N-Heterocyclic Carbenes in Transition Metal Catalysis*, Glorius, F., ed., Topics in Organometallic Chemistry 21; Springer, Berlin Heidelberg, **2007**; c) in *N-Heterocyclic Carbenes: From Laboratory Curiosities to Efficient Synthetic Tools* (Ed.: S. Diez-Gonzalez), RSC Catalysis Series; The Royal Society of Chemistry, **2011**.

(2) a) H. D. Velazquez, F. Verpoort, *Chem. Soc. Rev.* **2012**, *41*, 7032-7060; b) L.-A. Schaper, S. J. Hock, W. A. Herrmann, F. E. Kühn, *Angew. Chem. Int. Ed.* **2013**, *52*, 270-289.

(3) G. F. Silbestri, J. C. Flores, E. de Jesús, *Organometallics* **2012**, *31*, 3355-3360.

(4) I. J. B. Lin, C. S. Vasam, *Coord. Chem. Rev.* **2007**, *251*, 642-670.

(5) a) F. Alonso, I. P. Beletskaya, M. Yus, *Chem. Rev.* **2004**, *104*, 3079-3159; b) L. Hintermann, A. Labonne, *Synthesis* **2007**, 1121-1150.

(6) a) G. L. Petretto, M. Wang, A. Zucca, J. P. Rourke, *Dalton Trans.* **2010**, *39*, 7822-7825; b) V. Khlebnikov, M. Heckenroth, H. Mueller-Bunz, M. Albrecht, *Dalton Trans.* **2013**, *42*, 4197-4207; c) R. Romeo, G. D'Amico, *Organometallics* **2006**, *25*, 3435-3446; d) S. Lanza, F. Nicolo, G. Tresoldi, *Eur. J. Inorg. Chem.* **2002**, 1049-1055; e) A. Zucca, G. L. Petretto, S. Stoccoro, M. A. Cinellu, M. Manassero, C. Manassero, G. Minghetti, *Organometallics* **2009**, *28*, 2150-2159; f) A. Zucca, D. Cordeschi, S. Stoccoro, M. A. Cinellu, G. Minghetti, G. Chelucci, M. Manassero, *Organometallics* **2011**, *30*, 3064-3074; g) L. Maidich, G. Zuri, S. Stoccoro, M. A. Cinellu, M. Masia, A. Zucca, *Organometallics* **2013**, *32*, 438-448.

(7) a) C. Eaborn, K. Kundu, A. Pidcock, *J. Organomet. Chem.* **1979**, *170*, C18-C20; b) C. Eaborn, K. Kundu, A. Pidcock, *J. Chem. Soc., Dalton Trans.* **1981**, 933-938.

(8) R. Romeo, L. M. Scolaro, *Inorg. Synth.* **1998**, *32*, 153-158.

(9) a) G. C. Fortman, N. M. Scott, A. Linden, E. D. Stevens, R. Dorta, S. P. Nolan, *Chem. Commun.* **2010**, *46*, 1050-1052; b) O. Rivada-Wheelaghan, B. Donnadieu, C. Maya, S. Conejero, *Chem. Eur. J.* **2010**, *16*, 10323-10326; c) O. Rivada-Wheelaghan, M. A. Ortuno, J. Diez, A. Lledos, S. Conejero, *Angew. Chem., Int. Ed.* **2012**, *51*, 3936-3939.

(10) E. A. Baquero, J. C. Flores, J. Perles, P. Gomez-Sal, E. de Jesus, *Organometallics* **2014**, *33*, 5470-5482.

SCIENTIFIC PRODUCTION

The list of contributions which has led the work presented here and the status of some of them at the time of printing this PhD dissertation, are related below.

ARTICLES

- **Edwin A. Baquero**, Simon Tricard, Juan C. Flores,* Ernesto de Jesús,* and Bruno Chaudret.* "Highly Stable Water–Soluble Platinum Nanoparticles Stabilized by Hydrophilic N–Heterocyclic Carbene". *Angew. Chem. Int. Ed.,* **2014**, *53*, 13220-13224.

- **Edwin A. Baquero**, Juan Carlos Flores,* Josefina Perles, Pilar Gómez-Sal, and Ernesto de Jesús.* "Water–Soluble Mono– and Dimethyl N–Heterocyclic Carbene Platinum(II) Complexes: Synthesis and Reactivity". *Organometallics*, **2014**, *33*, 5470–5482.

- **Edwin A. Baquero**, Gustavo Silbestri, Pilar Gómez-Sal, Juan Carlos Flores,* and Ernesto de Jesús.* "Sulfonated Water–Soluble N–Heterocyclic Carbene Silver(I) Complexes: Behavior in Aqueous Medium and as NHC–Transfer Agents to Platinum(II)". *Organometallics*, **2013**, *32*, 2814–2826.

- **Edwin A. Baquero**, Juan C. Flores,* and Ernesto de Jesús.* "Improved synthesis of *cis*-[Pt(dmso)$_2$Me$_2$] and *trans*-[Pt(dmso)$_2$MeCl] through the understanding of their formation reactions". **2015**. *In Preparation*.

- **Edwin A. Baquero**, Javier González, Manuel Temprado, Juan Z. Dávalos, Juan C. Flores,* and Ernesto de Jesús.* "Intramolecular Base Assisted C(sp^3)–H Bond Activations in Sulfonated NHC Platinum Complexes in the Gas-Phase". **2015**. *In preparation*.

- **Edwin A. Baquero**, Simon Tricard, Yannick Coppel, Juan C. Flores,* Bruno Chaudret,* and Ernesto de Jesús.* "Water-Soluble Platinum Nanoparticles Stabilized by Sulfonated N-Heterocyclic Carbenes: Effect of the Synthetic Approach". **2015**. *In preparation*.

- **Edwin A. Baquero**, Gustavo F. Silbestri, Juan C. Flores,* and Ernesto de Jesús.* "Water-Soluble Hydride(NHC)platinum(II) Complexes: Synthesis through Oxidative Addition of Alkynes and Reactivity in Water towards Reductive Elimination". **2015**. *In preparation*.

- Andrea Ruiz-Varilla, **Edwin A. Baquero**, Gustavo F. Silbestri, Ernesto de Jesús, Camino González-Arellano,* and Juan C. Flores.* "Synthesis of Water-Soluble NHC Pt(0) Complexes and their Application in the Hydrosilylation of Phenylacetylene". **2015**. *In preparation*.

CONGRESS CONTRIBUTIONS

- Andrea Ruiz-Varilla, **Edwin A. Baquero**, Camino González-Arellano, Juan C. Flores, Ernesto de Jesús. "Synthesis of water-soluble NHC Pt(0) complexes and their application in the hydrosilylation of phenylacetylene". "XXXII Reunión del Grupo Especializado de Química Organometálica". Tarragona, Spain. **2014**.

- **Edwin A. Baquero**, Juan C. Flores, Ernesto de Jesús, Manuel Temprado, Javier González, Juan Dávalos, Simon Tricard, Bruno Chaudret. "Synthesis and applications of water-soluble dimethyl NHC platinum(II) complexes". "XXXII Reunión del Grupo Especializado de Química Organometálica". Tarragona, Spain. **2014**.

- **Edwin A. Baquero**, Javier González, Manuel Temprado, Juan Dávalos, Juan C. Flores, Ernesto de Jesús. "On the C(sp^3)-H bond activation of sulfonated (NHC)Pt(II) complexes in gas-phase: Experimental and DFT study". "2nd International Symposium on C-H Activation". Rennes, France. **2014.**

- **Edwin A. Baquero**, Javier González, Juan Dávalos, Juan C. Flores, Ernesto de Jesús. "C(sp^3)-H bond activation on sulfonated (NHC)Pt(II) complexes: A gas-phase study using FT-ICR mass spectroscopy". "ICIQ-UniCat Summer School". Tarragona, Spain. **2013**.

- **Edwin A. Baquero**, Juan C. Flores, Ernesto de Jesús. "Complejos hidrosolubles (NHC)Pt(II): Síntesis y Aplicación Catalítica en Fase Acuosa". "XXX Reunión del Grupo Especializado en Química Organometálica GEQO". Castellon de la Plana, Spain. **2012**.

- **Edwin A. Baquero**, Juan C. Flores, Ernesto de Jesús. "Hydration of Alkynes in water based on (NHC)Pt(II) catalysts". "9th Green Chemistry Conference. An International Event.". Alcalá de Henares, Spain. **2011**.

- **Edwin A. Baquero**, Juan C. Flores, Ernesto de Jesús. "Nuevos complejos de Pt(II) con ligandos Carbeno N-Heterocíclico (NHC) sulfonados". "3er Simposio Latinoamericano de Química de Coordinación y Organometálica (SILQCOM 2011)". La Serena, Chile. **2011**.

- **Edwin A. Baquero**, Juan C. Flores, Ernesto de Jesús, Pilar Gómez-Sal. "Síntesis y caracterización de nuevos biscarbenos de Ag hidrosolubles en agua". "XXVIII Reunión del grupo Especializado de Química Organometálica". Punta Umbría, Spain. **2010**.

- **Edwin A. Baquero**, Juan C. Flores, Ernesto de Jesús. "Synthesis and Characterization of New Water-Soluble Ag(I) N-Heterocyclic Carbene Complexes". "International School on Polymer Synthesis and Characterization (ISOPSC-2010)". Fisciano-Salerno, Italy. **2010**.

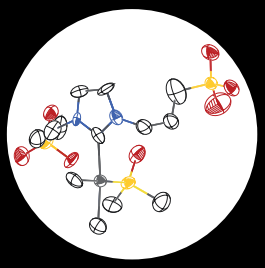

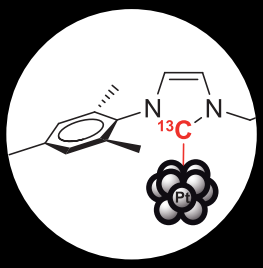
N
N
13C
Pt

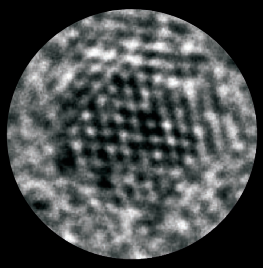

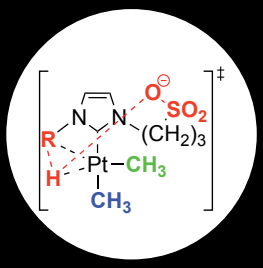
O
SO2
(CH2)3
N
N
R
H
Pt
CH3
CH3
‡